Simulation and Analysis of a Middle Vessel Batch Distillation Column

by

Weiyang Cheong

Submitted to the Department of Chemical Engineering
in partial fulfillment of the requirements for the degree of

Bachelor of Science in Chemical Engineering

at the

MASSACHUSETTS INSTITUTE OF TECHNOLOGY

June 1998

Author .....
Department of Chemical Engineering
May 22, 1998

Certified by .....
Paul I. Barton
Assistant Professor, Department of Chemical Engineering
Thesis Supervisor

Accepted by .....
Charles M. Mohr
Undergraduate Officer

Simulation and Analysis of a Middle Vessel Batch Distillation Column

by

Weiyang Cheong

Submitted to the Department of Chemical Engineering
on May 22, 1998, in partial fulfillment of the
requirements for the degree of
Bachelor of Science in Chemical Engineering

Abstract

In this thesis, a batch distillation column with the holdup vessel feed in the middle of the column was modelled and simulated. This distillation configuration, termed as a "Middle Vessel Column (MVC)" by various researchers, was first proposed by Robinson and Gilliland, but has only been analyzed in detail recently. It is in contrast to the traditional batch distillation configurations of batch rectifiers (with feed from the holdup pot at the bottom of the column) and batch strippers (with feed from the holdup pot at the top of the column).

A mathematical model was developed for the MVC, and a theoretical analysis of the model conducted. For validation purposes, simulations were conducted with the model using ABACUSS (Advanced Batch and Continuous Unsteady State Simulator, a program developed for simulation and optmization of dynamic models). The results compared favorably with the theoretical analysis. A theoretical analysis was also conducted on the exploitation of curved separatrices to separate azeotropic mixtures into the complete set of pure components in a *single* middle vessel column. Feasible separation schemes were formulated and simulated with the ABACUSS model to affirm their validity. Finally, the model was extended to that of a "Multi-Vessel Column (MuVC)", where there are several trays in the column with substantial amounts of holdup, and from which product streams may be drawn. The traditional batch rectifiers, strippers and the recently suggested MVC can all be considered as special cases of the MuVC.

The results of this thesis also suggests substantial environmental benefits to speciality chemical and pharmaceutical manufacturers due to the ability of the MVC to break azeotropes in a single multi-purpose unit operation, thereby removing the hazard of chemical spillage associated with transfers between unit operations. The MVC thus represents the ultimate multi-purpose solvent recovery technology for batch processes.

Thesis Supervisor: Paul I. Barton
Title: Assistant Professor, Department of Chemical Engineering

Acknowledgments

I would like to thank my thesis supervisor, Professor Paul Barton for his undying patience with me and his invaluable guidance. I would also like to thank John Tolsma, Santos Galán, Wade Martinson, and Arvind Mallik in the Barton-Group who have helped in many ways to make my work a reality. Certainly, I would also like to extend my deepest, heart-felt gratitude to my friends Pitiporn Phanaphat, Wanwipa Siriwatwechakul, Michael Sy, and Tseh-Hwan Yong for their enlightening moral support in my darkest days prior to the completion of my Bachelor's Thesis. Last but not least, I would like to thank my beloved family for their moral support in whatever little way possible, all the way from the other side of the earth in sunny Singapore.

Contents

List of Figures

List of Tables

Chapter 1

Introduction

Distillation is the most common unit operation used for the separation of liquid mixtures in many industries. There are two major modes of operation, namely batch distillation and continuous distillation. Although it has long been recognized that continuous distillation is much more energy efficient and less labor intensive than batch distillation [18], batch distillation has continued to be an important technology due to the greater operational flexibility that it offers. This operational flexibility of batch distillation columns make them particularly suitable for smaller, multiproduct or multi-purpose operations.

Manufacturing in the pharmaceutical and speciality chemical industries are examples of such small, multiproduct operations, where products are typically required in small volumes, and subject to short product cycles and fluctuating demand. With the advancement of chemistry and biotechnology, the pharmaceutical and speciality chemical industries have grown in importance in recent years, resulting in a renewed academic interest in batch distillation processes. In particular, research has been focused on two main areas: 1) optimal operational/control policies for batch distillation columns and 2) feasibility of product sequences and optimal sequencing of columns. A survey of this research will be conducted in more detail in Chapter 2.

1.1 The "Middle Vessel Column"

Traditionally, the most common type of batch distillation columns were the rectifiers or "regular" columns, for which the feed is charged into a large reboiler at the bottom of the rectifying column and the lighter components are removed from the top of the column. Less frequently used are batch strippers or "inverted" columns, where the feed is charged into a holdup tray at the top of the stripping column, and the heavier components are withdrawn from the bottom of the column.

The batch stripper is usually used when a small amount of the heavier component (product) has to be separated from a large amount of light components (solvents). In this situation, use of a batch stripper rather than a batch rectifier, optimizes the operation duration, as the product is removed immediately. This is in contrast to a rectifier where the products are left in the pot only after all the light components have been boiled off. There are however, disadvantages associated with the use of a batch stripper over a batch rectifier, which include that 1) the highest temperature occurs at the beginning of the operation, which may result in thermal decomposition reactions, and 2) solids in the feed will get into the column, resulting in clogging and the need for frequent servicing of the column.

The location of the feed (from the holdup vessel) at the top of the batch stripper column does not pose a structural problem if we employ a simple pumping line as suggested by Hasebe [17]. As shown in Figure 1-1, the holdup vessel can be located on ground level with the liquid pumped from the vessel to the top of the column, and the vapor from the top of the column condensed and added to the liquid in the holdup vessel.

Recently, beginning with Hasebe in 1992 [17], study on the feasibility of product sequences and optimal sequencing of columns has led researchers to reconsider a column configuration first proposed by Gilliland and Robinson in 1950 [31]. In this "novel" configuration, the feed from the vessel with large holdup is introduced in the middle of the column. Thus in a way, there is both a stripping section and a rectifying section in this column. Structurally, the configuration proposed was similar to that

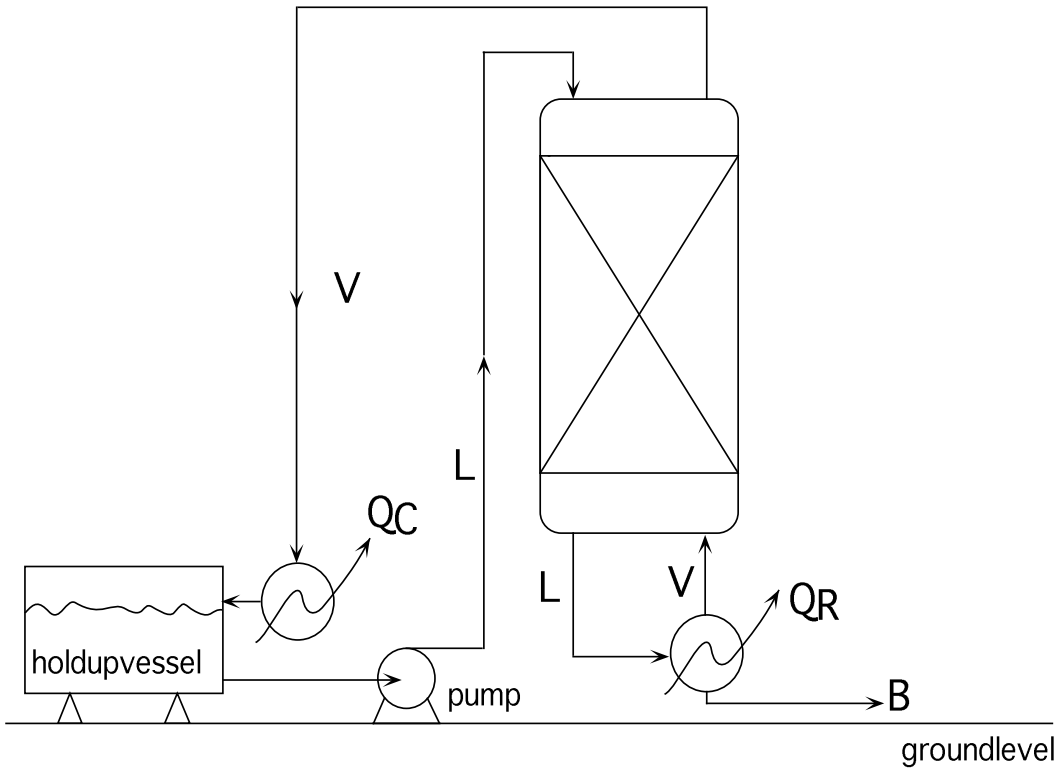

Figure 1-1: Structural Configuration of a Batch Stripper

of the batch stripper in Figure 1-1, with the holdup vessel at ground level. Two variations have been proposed by Hasebe [17] and Davidyan *et al.* [7] r espectively, as shown in Figure 1-2. Hasebe proposed having 2 batch rectifiers, with the distillate vapor outlet and liquid inlet in the first column (which acts as the stripping section) fed into/from the bottoms holdup vessel of the second batch rectifier which serves as the rectifying section of the middle vessel column. Alternatively, Davidyan *et al.* proposed introducing the liquid feed from the holdup tank into the middle of a column with a reboiler and a condenser, and with an option of introducing and removing heat from the holdup tank. Hasebe's configuration is helpful in a plant that already has existing batch rectifiers. Davidyan *et al.*'s configuration on the other hand, can easily be applied to a modified continuous distillation column, as attempted by Barolo [4, 3]. Various names have been given to this column configuration, including "complex batch distillation column" and the more definitive "middle vessel column (MVC)". Much research work has been conducted on this novel column in recent

years, and a summary of this work is provided in Chapter 2.

Despite the large number of papers published on the middle vessel column, there has yet to be an all-encompassing paper which satisfactorily explains and characterizes the middle vessel column completely. Most papers had stopped short of developing the model fully: ideal mixtures were assumed [7], or the possibility of azeotropes neglected [27]. The use of entrainers with the middle vessel column has also been explored [35, 34], despite the less than satisfactory understanding of middle vessel columns. There have been some attempts, however, to characterize the product sequences of the middle vessel column [33, 32], but they stopped short of fully characterizing the middle vessel column both mathematically and graphically. It is thus the aim of this thesis to bridge this gap; to gather the current work on the middle vessel column, build on it and form a satisfactory model of the middle vessel column. This will then allow us to characterize and hence better understand the behavior of the middle vessel column.

1.2 A Road Map

This thesis is in 8 chapters. Chapter 2 surveys the current work to date on batch distillation columns and middle vessel columns. A survey of the shortcomings associated with the work done thus far on middle vessel columns is also provided.

Chapter 3 develops a relatively simple model of the middle vessel column. The concept of warped time, as used extensively in the analysis of traditional batch distillation columns (rectifiers), is employed.

Next, Chapter 4 explores the implications of the model developed. The limiting behaviour of the column (at infinite reflux and infinite trays) are explored, and compared to the predictions made by other researchers.

Chapter 5 explores some of the implications of separatrix curvature for novel operations that can break azeotropes, and the effect on the behavior of middle vessel batch distillation columns.

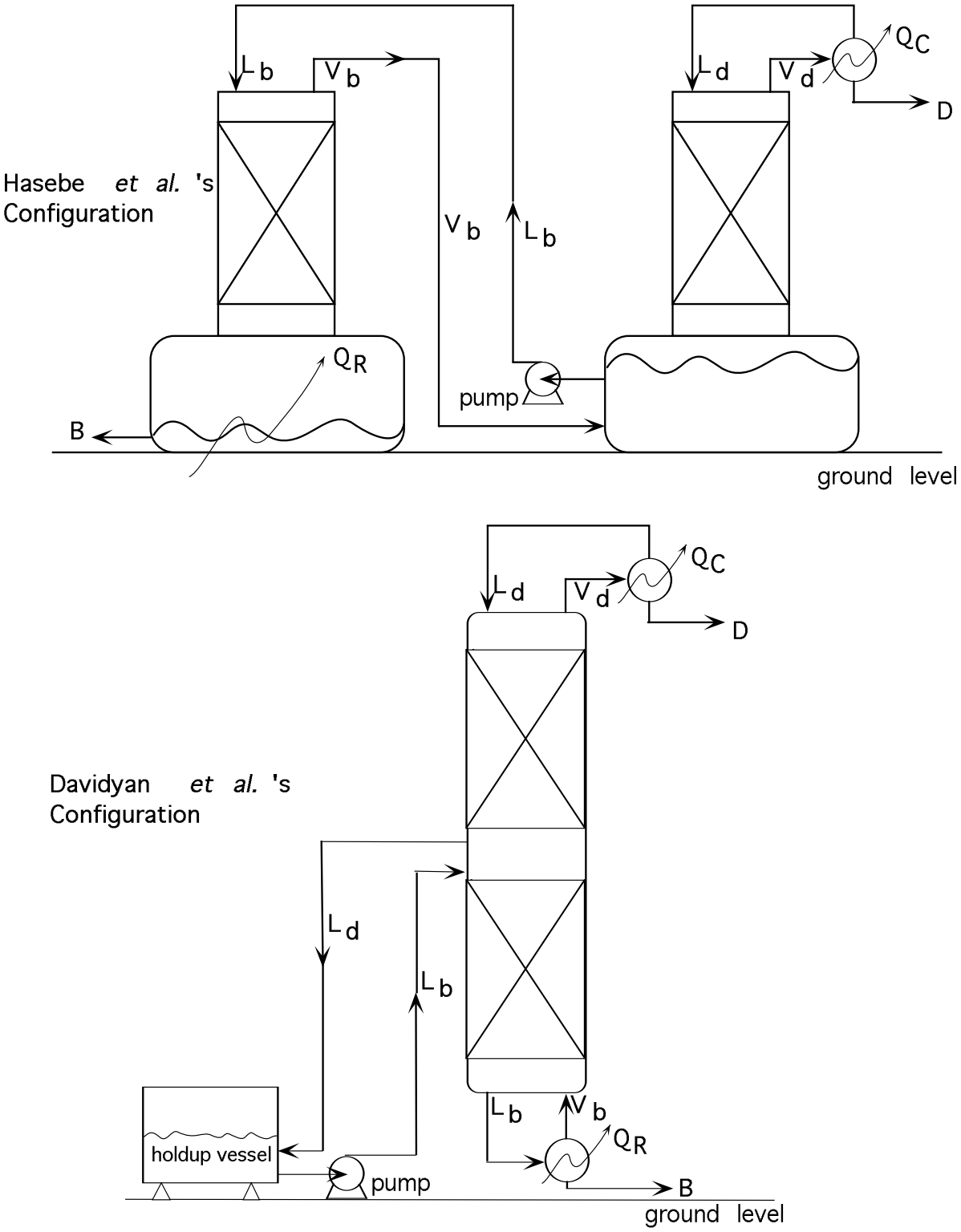

Figure 1-2: Proposed Structural Configurations of a Middle Vessel Column

In Chapter 6, the mathematical model is tested by simulation, using ABACUSS[1] The extensively studied ternary mixture of acetone, chloroform, and methanol is tested, assuming non-ideal vapor liquid equilibria. The results are compared to the theoretical predictions made in Chapter 4.

In Chapter 7, we simulate an operating procedure in the middle vessel column which breaks the maximum-boiling azeotrope of acetone and chloroform, using benzene as an entrainer. Such a separation is possible due to the implications of separatrix curvature explored in Chapter 5.

Finally, Chapter 8 summarizes our work. Suggestions for further work in this area are also furnished.

[1]ABACUSS (Advanced Batch And Continuous Unsteady-State Simulator) process modelling software, a derivative work of gPROMS software, ©1992 by Imperial College of Science, Technology and Medicine.

Chapter 2

Background

In this chapter, a brief survey is conducted of recent advances in subjects related to the middle vessel column. This puts our work in perspective with respect to the rest of the literature.

2.1 Batch Distillation

Traditionally, batch distillation has been of interest to chemical engineers because of the need for optimal control strategies that would give rise to the shortest possible distillation time or the minimum cost of operation, etc.. Textbooks have been written specifically on this topic [9]. A problem statement such as: "given a feed composition and a product specification, what should be the optimal reflux profile and product cut schedule as a function of time?", is a question that would be classified in the field of optimal control and systems engineering.

There has also been research in the area of product sequences in distillation columns and the feasibility of product sequences, which leads to the question of optimal sequencing of columns to achieve a given product separation. This has included attempts to characterize the basic distillation regions for n-component mixtures with and without azeotropes. We define the basic distillation regions as the points in a simple distillation residue curve map which belong in the same family of residue curves, i.e., those possessing the same alpha limit set and omega limit set [1]. Simple

distillation residue curve maps are the phase portrait diagrams of the residue (liquid) in a simple distillation process, with the dynamics of the simple distillation given by $\frac{d\mathbf{x}}{dt} = \mathbf{x} - \mathbf{y}(\mathbf{x})$, where $\mathbf{x}$ is the vector of liquid residue mole fractions and $\mathbf{y}(\mathbf{x})$ is the vector of vapor mole fractions in equilibrium with the liquid. Serafimov, Petlyuk, and Aleksandrov [36], Petlyuk, Kievskii, and Serafimov [29]j, and Petlyuk [28] all worked on algorithms for characterizing n-component residue curve maps. Matsuyama and Nishimura [26] enumerated all of the possible 3-component residue curve maps and Baburina, Paltonov, and Slin'ko [2] also generated and classified them. Doherty and Caldarola [11] and Doherty [10] generated 3 component residue curve maps based on topological relationships between fixed points (pure components and azeotropes). The behaviour of these basic distillation regions was studied by Doherty and Perkins [12, 13].

Much work has also been conducted on batch distillation regions, first defined by Ewell and Welch [16] as the "set of compositions which will produce the same product sequence when they are separated in a batch distillation column". Malenko [23, 24, 25] did some work where he introduced the concept of MTS (maximum temperature surfaces), as he thought that the separatrices of residue curve maps corresponded to temperature ridges. Van Dongen and Doherty [14] disproved that theory and extended their own theory on separatrices. Van Dongen and Doherty [14, 15], and Bernot, Doherty and Malone [5, 6] did some definitive work in finding the still and product paths for batch distillation using both a rectifier and a stripper. Their analysis was however mostly graphical, and was thus restricted to 3-component and 4-component systems. Ahmad and Barton [1] extended this analysis by presenting an algorithm for finding the batch distillation regions of arbitrary multi-component systems. This algorithm, backed by a series of formal proofs, was shown to work extremely well on 3-component systems but has not been exhaustively tested on higher dimensional systems due to the large number of possible 4-component residue curve map structures. The study also assumed straight line separatrices. Safrit and Westerberg [33, 32] offered another similar algorithm based on the work of Ahmad and Barton [1] but they again assumed straight line (ideal) separating boundaries and presented no new

insight on the subject.

2.2 The "Middle Vessel Column"

First proposed by Gilliland and Robinson in 1950 [31], this "novel" configuration has the holdup vessel located in the middle of the column.

Since Hasebe "rediscovered" it in 1992 [17], there has been a flurry of work in this area. This includes a rigorous mathematical analysis of the middle vessel column by Davidyan *et al.* [7], where a model assuming constant relative volativity was used to characterize the dynamic behaviour of the middle vessel column. Meski and Morari [27] then provided a limiting analysis of a mathematical model for the middle vessel column, assuming no holdup and constant molar overflow. Their work was based on the model proposed by Devyatikh [8], who proposed the use of the middle vessel column to achieve separations of higher purity. The possibility of azeotropes as stable nodes and unstable nodes was however neglected in their analysis.

The use of entrainers with the middle vessel column was explored by Safrit and Westerberg [35], who showed that it was possible to "break" an azeotrope using a suitable entrainer added continuously over the entire operation to a middle vessel column. In particular, they mentioned that it was possible to "steer" the still pot composition of the middle vessel column. Unfortunately, they stopped short of quantifying and qualifying the direction of this steerage. They also mentioned that the middle vessel column had a characteristic distillation region which is a combination of the rectifying batch distillation region and the stripping batch distillation region, but it was not specified as to how these regions were related. We will attempt to fill the gaps left by their work. In their more recent work, Safrit and Westerberg [33, 32] also included the middle vessel column in their algorithm for determining the optimal sequencing of batch distillation columns, but again stopped short of fully characterizing the middle vessel column both mathematically and graphically.

Finally, Barolo *et al.* [4, 3] attempted an experimental characterization of a middle vessel column using a holdup tank fed into an existing continuous distillation column

(which usually has both a rectifying and a stripping section). Their results appear to be in good agreement with the theorectical models proposed thus far.

2.3 The "Multi-Vessel Column"

In an extension of the middle vessel column, the "Multi-Vessel Column" was also proposed by Hasebe in 1995 [18]. The multi-vessel column is just an extension of the middle vessel column, with vessels (which have significant holdup) feeding material at several points distributed along the length of the column. Wittgens *et al.* [42] considered the limiting case of total reflux operation in this column, and conducted both a simulation and an experimental analysis of this batch configuration. They also explored the control aspects of this novel column configuration in a recent paper [37].

Chapter 3

Basic Model of the Middle Vessel Column

In this chapter, a coherent mathematical model for the middle vessel column is developed. Our model was developed independently, but it is similar to previous work published on this subject by Davidyan *et al.* [7], and Meski and Morari [27]. It can thus be treated as an extension of the model developed by them. However, they made some assumptions and simplifications which our model will not use. Davidyan *et al.* built a mathematical model for the middle vessel column, and then assumed ideal mixtures with constant relative volatility, obtaining the solutions of the model for ideal mixtures. Meski and Morari included in their specifications: 1) the removal of only pure components as products, 2) specific analysis of only 2 component and 3 component mixtures, and 3) the assumption of non-azeotropic mixtures. It was mentioned briefly in their paper [27] that their analysis should extend to azeotropic mixtures where every distillation region of an azeotropic mixture is similar to an ideal mixture. Unfortunately, they did not quantify this statement mathematically, and provided only a vague graphical representation of their idea for a 3 component azeotropic mixture. Our model does however retain some of the assumptions made by Davidyan *et al.*, and Meski and Morari, including constant molar overflow (CMO) and negligible liquid and vapor holdup on all column trays apart from the middle vessel.

This chapter is in four sections: the first section describes the model, the second section provides a graphical interpretation of the results of the model, the third section explores the equivalency of a middle vessel column to the combined operation of a stripper and a rectifier, and the fourth section examines the major differences between our analysis versus Davidyan *et al.*'s model as well as Meski and Morari's analysis, and highlights the shortcomings in their analysis.

3.1 Development of Model

Our model of the middle vessel column was inspired by the work of Bernot *et al.* [5] on a mathematical model of the batch rectifier, and subsequently a mathematical model of the batch stripper [6]. A schematic configuration of the middle vessel column is shown in Figure 3-1. As explained in Chapter 1, the middle vessel is actually located on ground level to avoid unnecessary structural difficulties in supporting a heavy vessel in mid-air. The schematic with the middle vessel suspended between the stripping and rectifying sections is only used for ease of representation. However, it should be noted that to maintain symmetry of the middle vessel column, we specify that vapor from the stripping section of the column is bubbled into the holdup vessel, where it is equilibrated with the liquid in the holdup vessel, before it is fed into the rectifying section of the column. This is in contrast to the middle vessel column configurations proposed by Hasebe [17] and Davidyan *et al.* [7], where the vapor stream from the stripping section bypassed the holdup vessel, and is introduced directly into the rectifying section of the column (see Figure 1-2). This results in differences in the column composition profile between our middle vessel column configuration and that of Hasebe and Davidyan *et al.*, but would not affect the overall behavior of the column.

As with Bernot *et al.*, Davidyan *et al.*, and Meski and Morari, our model assumes 1) constant molar overflow (CMO) and 2) quasi-steady state (QSS) in the column due to negligible holdup of liquid and vapor in the stages, and is based on a differential model of the rate of composition change in the middle vessel. We also ignore all heat

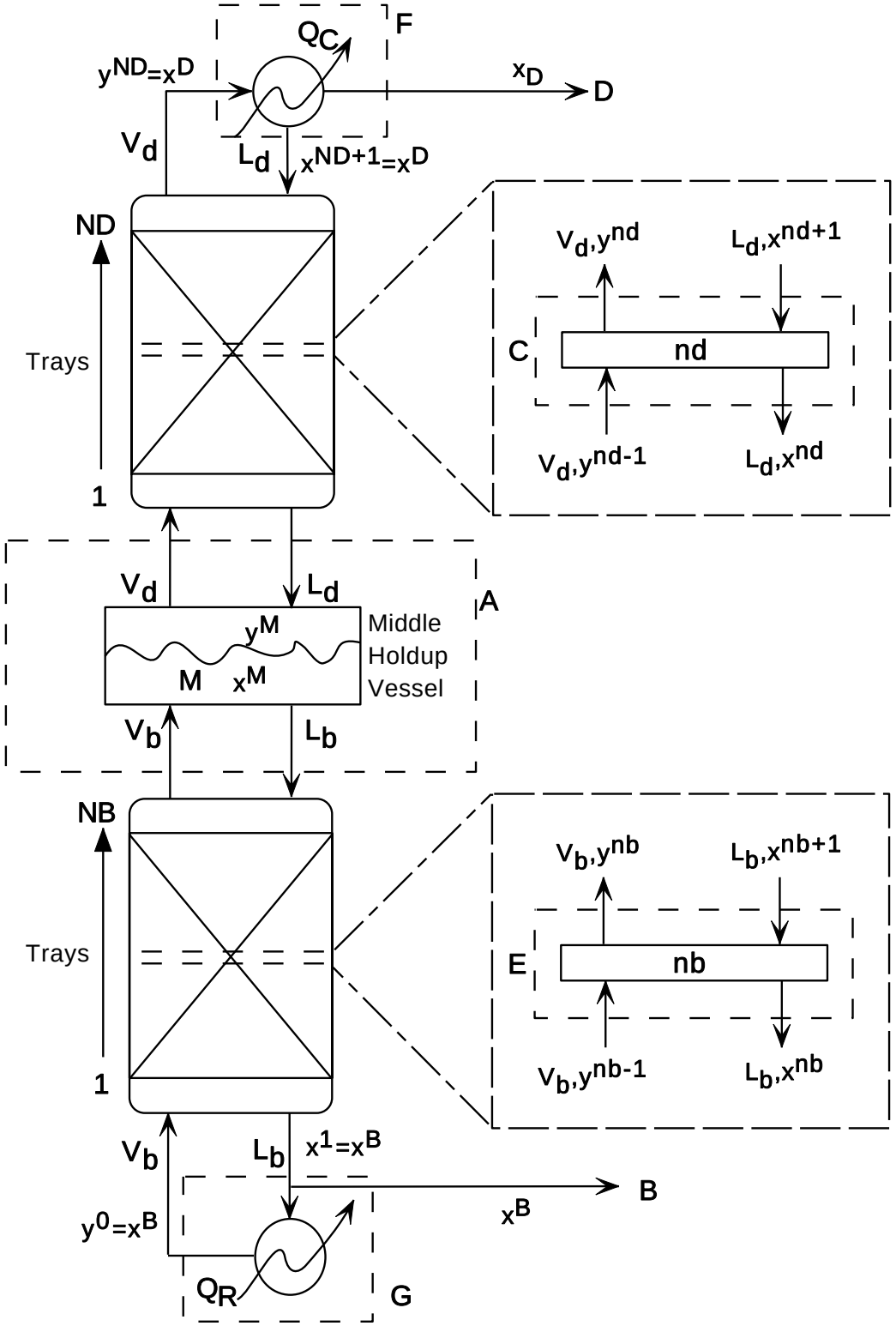

Figure 3-1: Typical Schematic Configurations of a Middle Vessel Column

effects by using the CMO assumption. These assumptions made in our model are relatively reasonable, and help simplify the model into one that is easily analyzed. A simplified model will allow us to predict the basic pattern of composition change in 1) the still, 2) the trays and 3) in the product stream with time, but at the same time remain computationally tractable for many repeated simulations, even for highly non-ideal thermodynamic mixtures.

We consider a column that has ND trays and a total condenser in the rectifying section, NB trays and a total reboiler in the stripping section. A total reboiler is not usually used in industry, but for the purpose of symmetry in the model, we will assume the use of a total reboiler. The use of a typical kettle reboiler/partial reboiler will result in the equivalent of one extra stage of separation in the stripping section, (as shown in Figure 3-2) but will not affect the nature of our results. The mixture to be distilled has NC components, and is characterized with non-ideal VLE models such as the NRTL and Wilson local composition activity coefficient models.

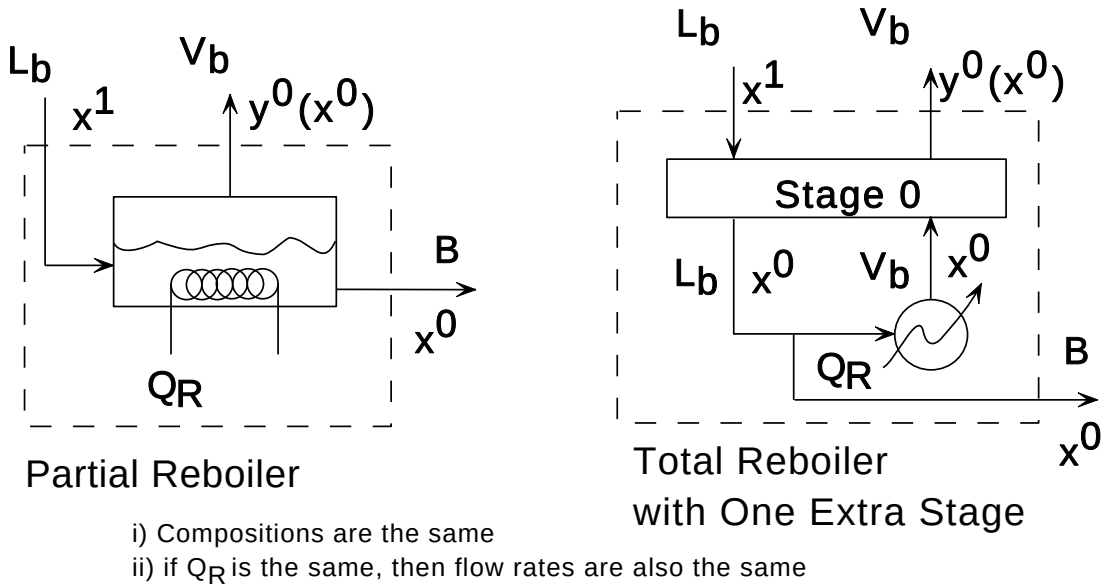

Figure 3-2: Equivalence of a Partial Reboiler to a Total Reboiler with One Stage

Total molar holdup in the middle vessel is M, and two different vapor and liquid rates exist respectively in the stripping and rectifying sections. In the rectifying section, the vapor and liquid flow rates are V_d and L_d respectively, while in the stripping

section, the corresponding vapor and liquid flow rates are V_b and L_b respectively. Distillate is drawn at a flow rate of D from the total condenser, and a bottoms product is drawn at a flow rate of B from the total reboiler. Finally, we complete the preliminaries by defining our dimensionless "middle vessel parameter" as $\lambda \in [0, 1]$, where:

$$\lambda = \frac{D}{D+B} \tag{3.1}$$

Considering the mass balance around the whole column (see envelope A in Figure 3-1), since there is negligible holdup in the trays, the only changes in mass occurs in the still pot. The overall mole balance equation can then be written as:

$$\frac{dM}{dt} = -(D+B) \tag{3.2}$$

and the component mole balance given for $i = (1, \ldots, NC)$ by:

$$\frac{d(Mx_i^M)}{dt} = -(Dx_i^D + Bx_i^B) \tag{3.3}$$

where superscripts indicate location of the composition, M for middle vessel, D for distillate product, and B for bottoms product. Alternatively, in vector notation, where $\mathbf{x}$s are the NC vectors of composition:

$$\frac{d(M\mathbf{x}^M)}{dt} = -(D\mathbf{x}^D + B\mathbf{x}^B) \tag{3.4}$$

In the spirit of Bernot *et al.*, we introduce a dimensionless "warped" time factor ξ defined as:

$$d\xi = (\frac{D+B}{M})dt \tag{3.5}$$

and transform the set of equations above for $i = (1, \ldots, NC)$ into:

$$\frac{dx_i^M}{d\xi} = x_i^M - \lambda x_i^D - (1-\lambda)x_i^B \tag{3.6}$$

or in vector notation:

$$\frac{d\mathbf{x}^M}{d\xi} = \mathbf{x}^M - \lambda\mathbf{x}^D - (1-\lambda)\mathbf{x}^B \tag{3.7}$$

and where the warped time is given by:

$$d\xi = -d(lnM) \tag{3.8}$$

The detailed derivation of these equations is provided in Appendix A. As shown by Bernot *et al.* [5], equation (3.8), can then be manipulated to obtain an expression of the proportion of initial charge that has been drawn off as products, $\Pi/M(0)$, where Π is the cumulative amount of distillate and bottoms removed from time $\xi = 0$ to any given time $\xi > 0$, and $M(0)$ is the initial molar holdup in the still pot. Using the initial conditions of $\xi = 0$ at $M = M(0)$, equation (3.8) is solved as:

$$\frac{\Pi(\xi)}{M(0)} = \frac{M(0) - M(\xi)}{M(0)} = 1 - exp(-\xi) \tag{3.9}$$

where Π is given by:

$$\Pi(\xi) = M(0) - M(\xi) = \int_0^{\xi} (B + D)d\xi \tag{3.10}$$

which can be re-expressed with a change of variables using equations (3.2),(3.5) and (3.8), to obtain the following:

$$\Pi(\xi) = \int_0^{ln[\frac{M(0)}{M(t[\xi])}]} Md\xi \tag{3.11}$$

Note that we make no assumptions about the actual composition of the products drawn from the distillate, $\mathbf{x}^D$ or the bottoms, $\mathbf{x}^B$. Based on the QSS assumption, the instantaneous compositions of these products are a function of the operating parameters of the column (number of trays ND, NB; pressure, P in the column which may or may not be a function of ξ) and is related to the composition of the still pot at a given warped time ξ by static mass balance relationships which involve the vapor and liquid flow rates in both sections of the column, $V_d(\xi)$, $L_d(\xi)$, $V_b(\xi)$,

and $L_b(\xi)$. $\mathbf{x}^D$ and $\mathbf{x}^B$ can thus be expressed in a simplified form as the composite functions:

$$\mathbf{x}^D(\xi) = \mathbf{x}^D(P(\xi), ND, NB, V_d(\xi), L_d(\xi), V_b(\xi), L_b(\xi), \mathbf{x}^M(\xi)) \tag{3.12}$$

and

$$\mathbf{x}^B(\xi) = \mathbf{x}^B(P(\xi), ND, NB, V_d(\xi), L_d(\xi), V_b(\xi), L_b(\xi), \mathbf{x}^M(\xi)) \tag{3.13}$$

In the presence of finite reflux and reboil ratios, and due to the quasi-steady state assumption in the equilibrium trays in the column, equations (3.12) and (3.13) can be further simplified by introducing a reflux ratio $R_d(\xi)$ for the rectifying section and a reboil ratio $R_b(\xi)$ for the stripping section. $\mathbf{x}^D$ and $\mathbf{x}^B$ can then be re-expressed as:

$$\mathbf{x}^D(\xi) = \mathbf{x}^D(P(\xi), ND, NB, R_d(\xi), R_b(\xi), \mathbf{x}^M(\xi)) \tag{3.14}$$

and

$$\mathbf{x}^B(\xi) = \mathbf{x}^B(P(\xi), ND, NB, R_d(\xi), R_b(\xi), \mathbf{x}^M(\xi)) \tag{3.15}$$

The details of the formulation for the set of equations (3.12) and (3.13) or for the set of equations (3.14) and (3.15) are encapsulated in the algebraic mass balances which can be written for the column. Based on the QSS assumptions, given that these mass balances are valid instantaneously at any point in time, accumulation of the variables is omitted. Considering the rectifying section of the column, the total mole balance around the condenser (envelope F in Figure 3-1) gives:

$$V_d = L_d + D \tag{3.16}$$

Component mole balances on each stage of the column (assuming CMO, envelope C in Figure 3-1) then yields the following operating line relationships:

$$-L_d\mathbf{x}^{nd} - V_d\mathbf{y}^{nd} + L_d\mathbf{x}^{nd+1} + V_d\mathbf{y}^{nd-1} = 0, \quad \forall \quad 1 \leq nd \leq ND \tag{3.17}$$

where $\mathbf{y}^0 = \mathbf{y}^M$ is the middle vessel vapor composition, and due to the total condenser assumption $\mathbf{x}^{ND+1} = \mathbf{y}^{ND} = \mathbf{x}^D$.

The vapor liquid equilibrium (VLE) relationship on each tray and in the middle vessel can also be written as:

$$\mathbf{y}^i = \mathbf{y}^i(\mathbf{x}^i, T(\mathbf{x}^i, P), P), \quad i \in \{nd\}, \{nb\}, M \tag{3.18}$$

These equations (3.16), (3.17), and (3.18) define the value of $\mathbf{x}^D$ as expressed by equation (3.12) for a given value of $\mathbf{x}^M$. A similar set of equations can also be obtained for the stripping section of the column, as given by considering envelope G in Figure 3-1:

$$L_b = V_b + B \tag{3.19}$$

and by considering mass balance envelope E in Figure 3-1:

$$-L_b\mathbf{x}^{nb} - V_b\mathbf{y}^{nb} + L_b\mathbf{x}^{nb+1} + V_b\mathbf{y}^{nb-1} = 0, \quad \forall \quad 1 \leq nb \leq NB \tag{3.20}$$

where $\mathbf{x}^{NB+1} = \mathbf{x}^M$ is the still pot liquid composition, and due to the total reboiler assumption $\mathbf{y}^0 = \mathbf{x}^1 = \mathbf{x}^B$. The VLE relationships given by equation (3.18) also hold as before in the stripper trays. Equations (3.19), (3.20), and (3.18) then combine to define $\mathbf{x}^B$ given $\mathbf{x}^M$ as expressed by equation (3.13).

Encapsulating all the mass balance relationships given by equations (3.16) through (3.20) into composite functions (3.12) and (3.13), equations (3.7), (3.8), (3.12) and (3.13) then characterize completely the behavior of the still pot composition in the middle vessel column.

In the presence of finite reboil and reflux ratios, with our assumption of quasi-steady state, a reflux ratio (R_d) and reboil ratio (R_b) can be defined accordingly and the equations (3.16) through (3.20) modified to obtain a set of mass balance relationships based on R_d and R_b. Firstly, the reflux ratio as defined for conventional batch rectifiers, is given by:

$$R_d = \frac{L_d}{D} \tag{3.21}$$

while the reboil ratio can be defined as:

$$R_b = \frac{V_b}{B} \tag{3.22}$$

Next, substituting the definition of the reflux ratio as given by equation (3.21) into (3.17), a new operating line equation is obtained for the rectifying section of the column:

$$-R_d\mathbf{x}^{nd} - (R_d+1)\mathbf{y}^{nd} + R_d\mathbf{x}^{nd+1} + (R_d+1)\mathbf{y}^{nd-1} = 0, \quad \forall \quad 1 \leq nd \leq ND \tag{3.23}$$

where, as before, $\mathbf{y}^0 = \mathbf{y}^M$ is the middle vessel vapor composition, and due to the total condenser assumption $\mathbf{x}^{ND+1} = \mathbf{y}^{ND} = \mathbf{x}^D$.

By a similar procedure, (3.22) can also be substituted into (3.20), to obtain a new operating line equation for the stripping section of the column:

$$-(R_b+1)\mathbf{x}^{nb} - R_b\mathbf{y}^{nb} + (R_b+1)\mathbf{x}^{nb+1} + R_b\mathbf{y}^{nb-1} = 0, \quad \forall \quad 1 \leq nb \leq NB \tag{3.24}$$

where $\mathbf{x}^{NB+1} = \mathbf{x}^M$ is the still pot liquid composition, and as before, due to the total reboiler assumption, $\mathbf{y}^0 = \mathbf{x}^1 = \mathbf{x}^B$.

The vapor liquid equilibrium (VLE) relationship on each tray and in the middle vessel is unchanged and still given by equation (3.18). Equations (3.23) and (3.24) combined with (3.18) then define the distillate product $\mathbf{x}_D$ and the bottoms product $\mathbf{x}_B$ with respect to the reflux ratio R_d and the reboil ratio R_b in the formulation as given by equations (3.14) and (3.15) respectively. An analytical intepretation of this system of equations is given in the next section.

It should be noted that the model described in this section is a generalization of previous batch distillation models, since it contains both the batch rectifier ($\lambda = 1$) and the batch stripper ($\lambda = 0$) as special cases.

3.2 A Graphical Interpretation of the Model

An interpretation of the equations (3.7), (3.8), (3.12) and (3.13) is as follows:

> The still pot composition in the middle vessel column moves away from the instantaneous top and bottom product compositions, in a direction that lies in a vector cone swept out by two vectors: one connecting the distillate composition $\mathbf{x}^D$ to the still pot composition $\mathbf{x}^M$, and one connecting the bottoms composition $\mathbf{x}^B$ to the still pot composition $\mathbf{x}^M$.

The actual direction is given by the relative weights on these vectors, given by λ and $1-\lambda$ respectively. This concept is illustrated in Figure 3-3.

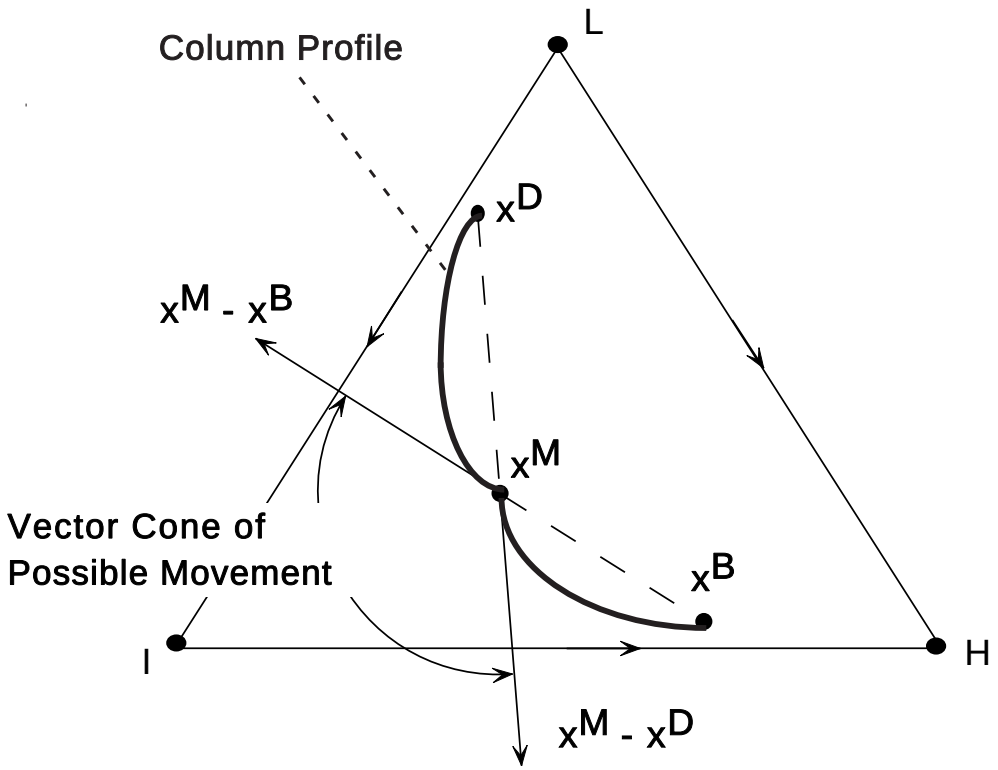

Figure 3-3: Vector Cone of Possible Still Pot Composition Movement

This interpretation is easily obtained via an elementary rearrangement of equation (3.7), which gives:

$$\frac{d\mathbf{x}^M}{d\xi} = (\lambda)(\mathbf{x}^M - \mathbf{x}^D) + (1-\lambda)(\mathbf{x}^M - \mathbf{x}^B) \tag{3.25}$$

where the direction of change in the pot composition $d\mathbf{x}^M/dt$, is given by the direction of vector $(\mathbf{x}^M - \mathbf{x}^D)$ (which points in the direction away from the distillate product composition towards the still pot composition) proportionally weighted with λ, and the vector $(\mathbf{x}^M - \mathbf{x}^B)$ (which points in the direction away from the bottoms product composition towards the still pot composition) proportionally weighted with $1 - \lambda$. This means that the still pot composition moves in a direction that is opposite from that of the distillate product, weighted by λ, and in a direction that is opposite to that of the bottoms product composition, weighted by $1 - \lambda$.

Hence, the still pot composition moves in a direction, given by the vector which is a weighted average of the two vectors which point from the still pot composition away from the product compositions. This concept is graphically illustrated in Figure 3-4 in three forms. In Figure 3-4a, the appropriate weight is applied to each of the vectors, $(\mathbf{x}^M - \mathbf{x}^D)$ (with weight λ) and $(\mathbf{x}^M - \mathbf{x}^D)$ (with weight $(1 - \lambda)$), and then the two weighted vectors added vectorially to obtain the direction and magnitude of motion for the still pot composition.

In an alternative representation, Figure 3-4b shows the application of the ratio theorem to the vector cone given by $(\mathbf{x}^M - \mathbf{x}^D)$ and $(\mathbf{x}^M - \mathbf{x}^B)$ both emanating from $\mathbf{x}^M$. The direction of motion is then given by the appropriate division of the line connecting the heads of the two vectors emanating from the still pot composition, as shown by the division of the line segment $\alpha\beta$ in the ratio of λ and $1 - \lambda$ at the point γ. γ-$\mathbf{x}^M$ then gives the direction of motion of the still pot.

Finally, in Figure 3-4c, a third interpretation that is based on the form of equation (3.7) is shown. The still pot composition $\mathbf{x}^M$ moves directly away from the net product composition point $\mathbf{x}^P$ given by the weighted average of the two product compositions as $\mathbf{x}^P = \lambda\mathbf{x}^D + (1 - \lambda)\mathbf{x}^B$. Equivalently, $\mathbf{x}^P$ gives the instantaneous composition of the combined product (distillate and bottoms) drawn from the column.

Thus, by varying the value of λ (the middle vessel column parameter) a whole range of possible still pot composition paths, as swept out by the vector cone between $\mathbf{x}^M - \mathbf{x}^D$ and $\mathbf{x}^M - \mathbf{x}^B$, is possible. By varying the value of λ with time, we are also able to "steer" the composition in the still pot in different directions as we progress in

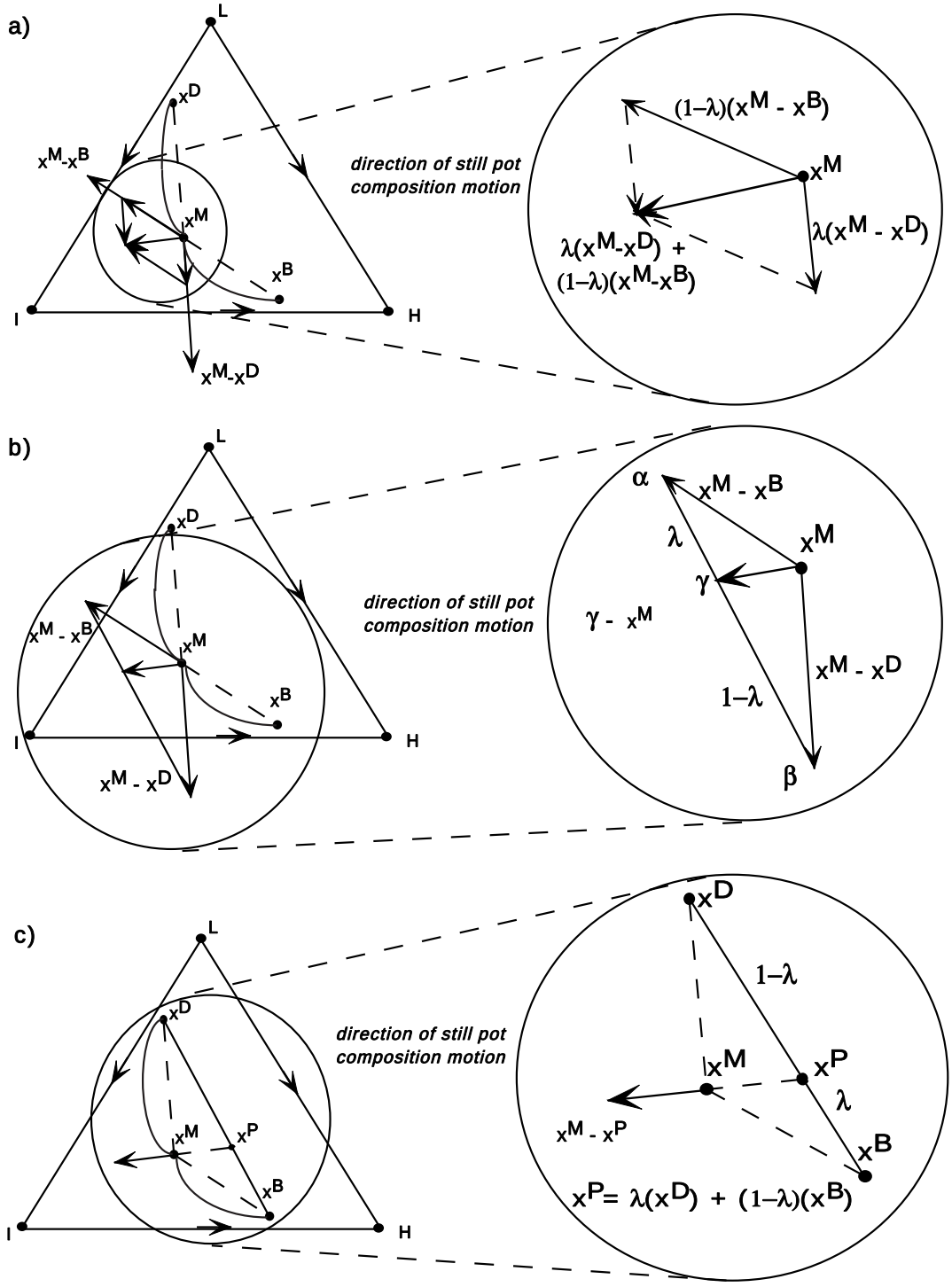

Figure 3-4: Three Ways of Representing the Weighted Average Notion

time. This was an idea first mentioned by Safrit and Westerberg [35, 33, 32, 34], but it was not elucidated how this steering could be achieved. A graphical intepretation of the behavior described above is shown in Figure 3-5. We should note that $\mathbf{x}^D$ and $\mathbf{x}^B$ both also vary with time when there are finite number of trays and finite "reflux" and "reboil" ratios. Thus, a clever manipulation of $\lambda(\xi)$, keeping in mind the variation of $\mathbf{x}^D(\xi)$ and $\mathbf{x}^B(\xi)$, would result in the ability to steer the still pot composition in a desired manner as shown in Figure 3-5.

Determining the operating profile of $\lambda(t)$ to obtain the desired still pot composition path in a column with a finite number of trays and finite "reflux/reboil" ratios poses a challenging open loop optimal control problem, and will not be covered in detail in this thesis. However, an extension of this analysis to the limiting behavior in the presence of an infinite number of trays and an infinite "reflux"/"reboil" ratio, will be presented in Chapter 4.

Although the above analysis was illustrated using a ternary system which contained no azeotropes, it is also applicable to higher dimensional systems and systems with azeotropes. To illustrate this point, Figures 3-3, 3-4, and 3-5 are reproduced for a generic quaternary system with azeotropes, in Figures 3-6, 3-7, and 3-8.

As we can see from Figure 3-6, the concept of the vector cone between $(\mathbf{x}^M - \mathbf{x}^D)$ and $(\mathbf{x}^M - \mathbf{x}^D)$ is unaffected by the presence of separatrices in the composition space. As before, the still pot composition can move in any direction within the vector cone. However, bundles of these separatrices form the boundaries of the basic distillation regions and in some cases these boundaries may be the pot composition boundaries of a stripper, rectifier or middle vessel column. In the presence of linear boundaries, this results in a limited variety of separations as the movement of the still pot composition is restricted to lie within the region bounded by the pot composition barrier [1]. These pot composition boundaries and barriers were defined by Ahmad and Barton, and the characteristics of these pot composition barriers was explained in detail in their work [1], thus, they will not be explored further in this thesis.

The concept of the actual direction of motion being the weighted average of the two vectors $\mathbf{x}^M - \mathbf{x}^D$ and $\mathbf{x}^M - \mathbf{x}^B$ also remains unchanged with the move to a higher

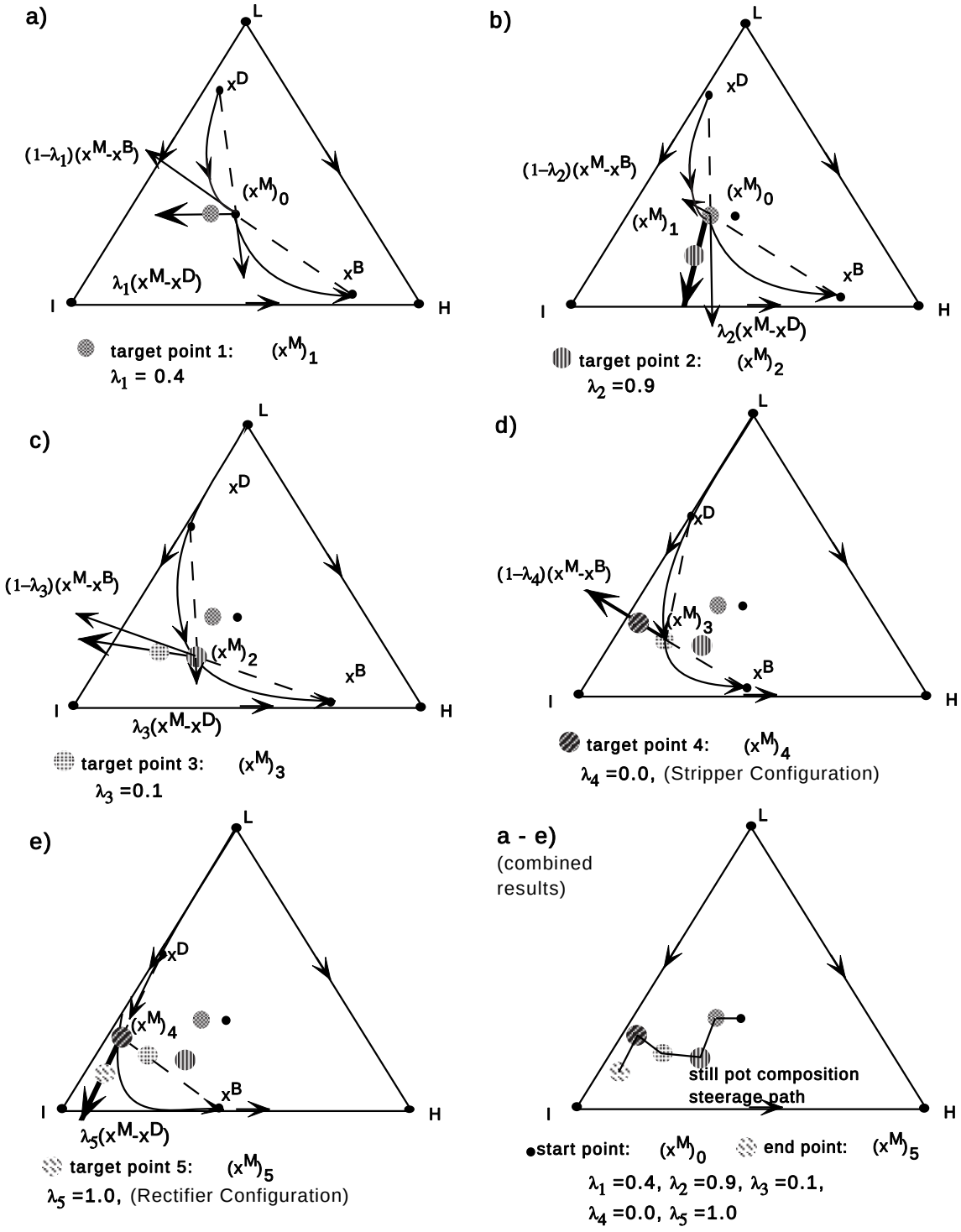

Figure 3-5: Dynamic Steerage of Still Pot Composition by Varying $\lambda(t)$

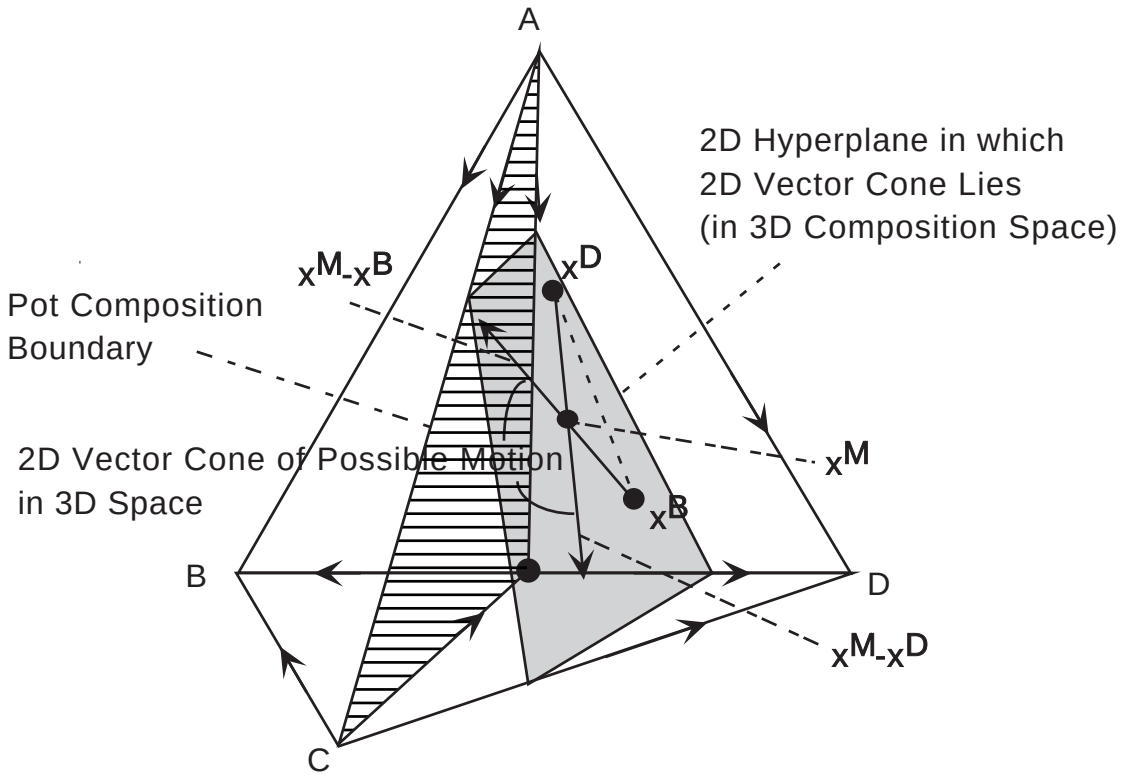

Figure 3-6: Vector Cone of Possible Still Pot Composition Movement, 4 Component System

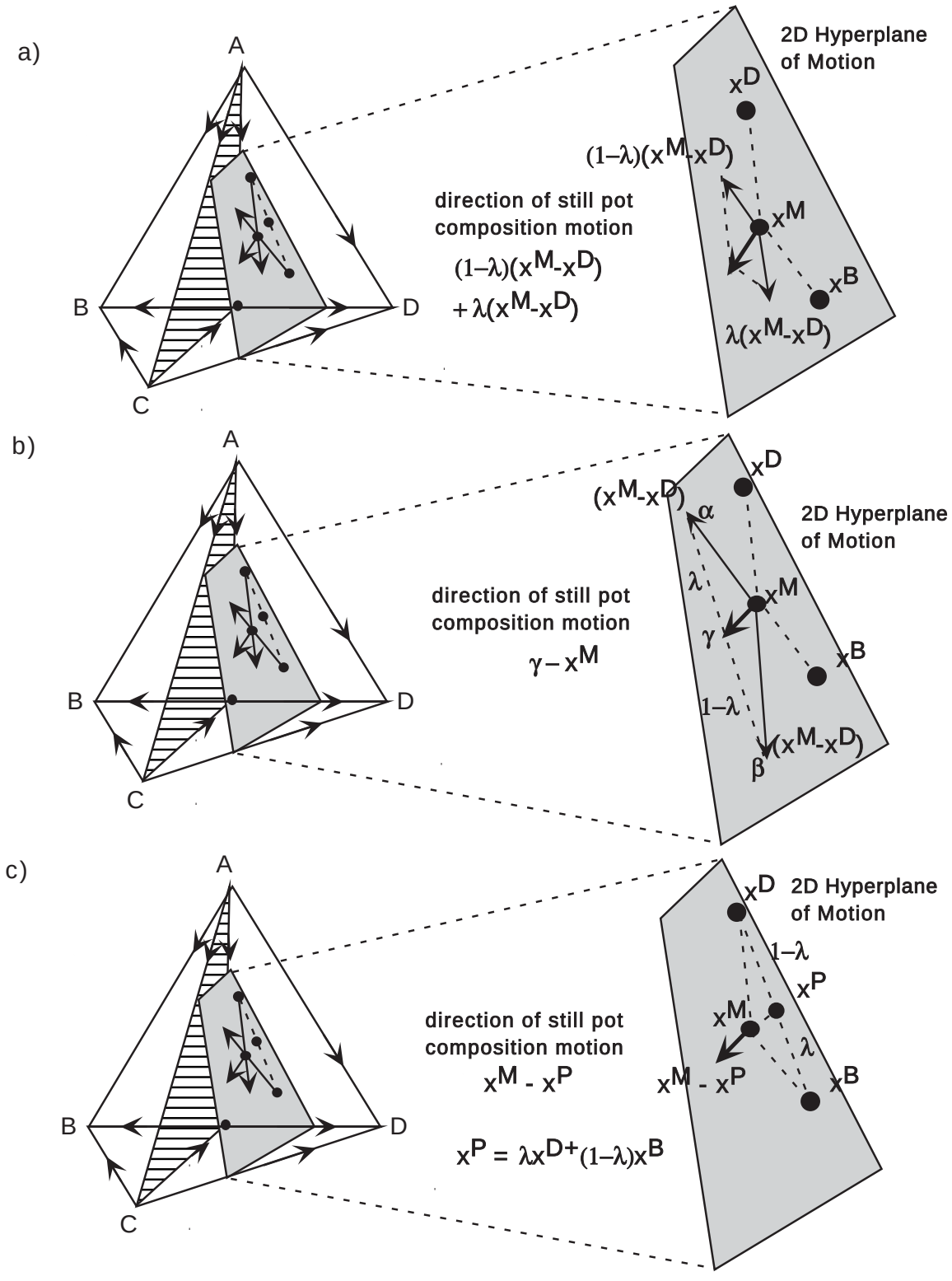

Figure 3-7: Three Ways of Representing the Weighted Average Notion, 4 Component System

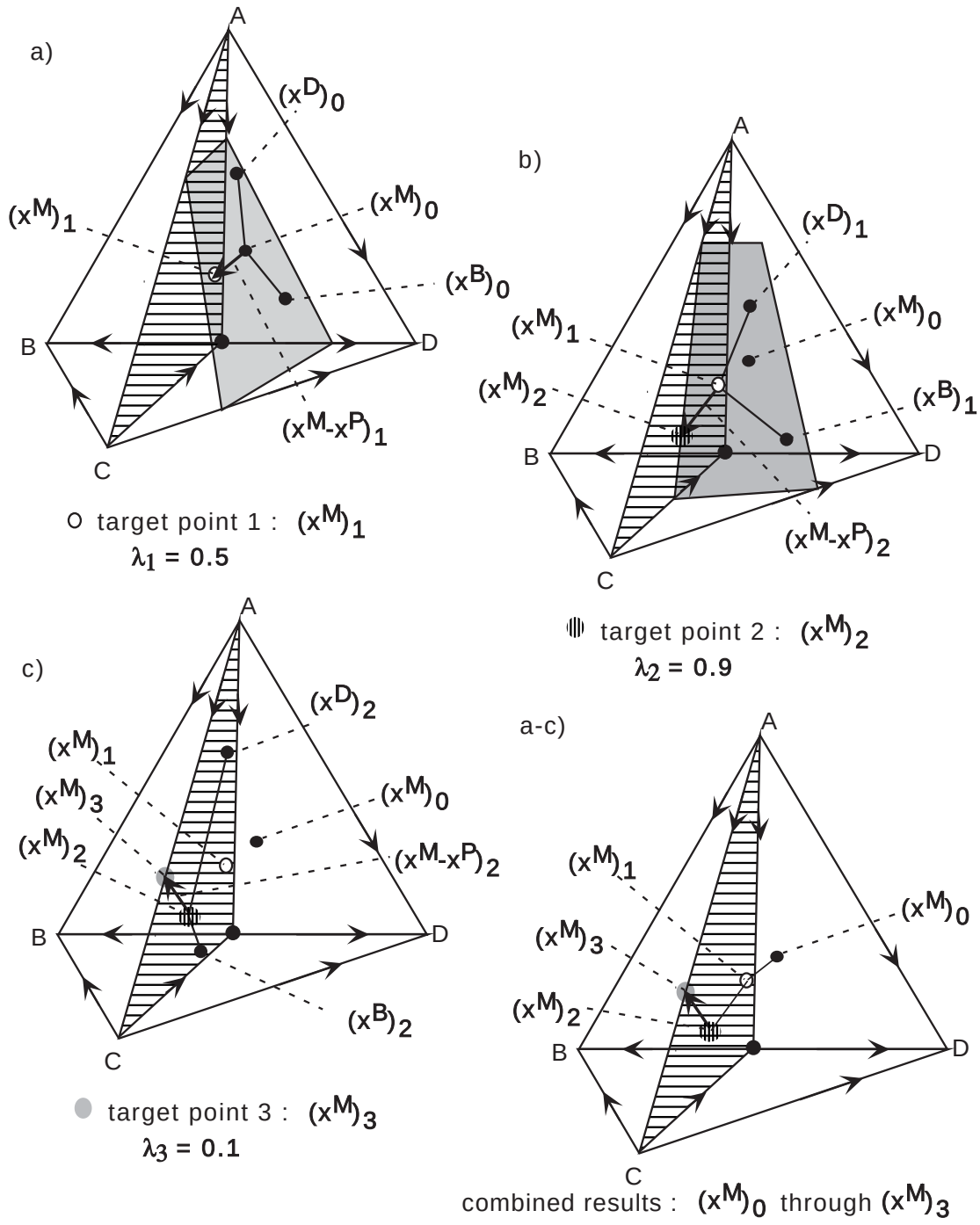

Figure 3-8: Dynamic Steerage of Still Pot Composition by Varying $\lambda(t)$, 4 Component System

dimension system, and is unaffected by the presence of azeotropes, as illustrated in Figure 3-7. The presence of azeotropes only serve to distort the residue curve map by introducing pot composition boundaries (composed of bundles of separatrices) into the composition space, which affect the range of possible values of $\mathbf{x}^D$ and $\mathbf{x}^B$, but once these values are determined, the direction of motion of the still pot is dictated by equation (3.25). The concept of steering the still pot composition is also unaffected by the move to a higher dimensional system and the presence of azeotropes, as seen in Figure 3-8.

Finally, following the argument presented above, this analysis should also apply to n-component systems for $n > 4$, but due to difficulties in representing this on two dimensional paper, systems of higher dimension are not represented geometrically in this thesis.

It should be noted, however, that there is one major difference in the analysis of a quarternary system compared to a ternary system; the vector cone of possible motion in the quartenary system remains as a two-dimesional cone, despite a 3-dimensional composition space for a quaternary mixture (as was illustrated in Figure 3-8). Whereas the motion of the middle vessel composition was initially restricted to lie in the plane $x_1 + x_2 + x_3 = 1$ in the ternary case, the motion of the middle vessel composition in higher dimensions is not restricted to a 2-dimensional plane. However, as only 2 products are drawn at any time, there are only 2 degrees of freedom for the motion of the middle vessel composition, and that results in only a 2 dimensional vector cone. Thus, the possible directions of motion for the middle vessel composition lies in a 2 dimensional plane, as defined by the three points: $\mathbf{x}^B$, $\mathbf{x}^D$, and $\mathbf{x}^M$. In the ternary case, this plane is redundant with the summation of mole fractions.

From this analysis, we can conjecture that it would be useful to have a third product stream drawn from the column in a quarternary system, which would result in a 3 dimensional vector cone of possible motion for the still pot composition, thereby removing any restrictions in the dimensionality of the motion. This was the impetus for recognizing the usefulness of a multi-vessel column, for systems of higher dimension, where the composition space is $(n-1)$-dimensional $(n > 4)$, and restrictions

in the dimensionality of the motion can be removed by drawing $n-1$ streams from each of the $n-1$ holdup trays in the multi-vessel column. A brief note regarding the multi-vessel column will be presented in Chapter 8.

3.3 Equivalence of Middle Vessel Column with Infinitessimal Rectifiers and Strippers

Prior to this section, we have emphasized the difference between a middle vessel batch distillation column and that of a batch rectifier or a batch stripper. In this section, we shall explore the concept that separating a mixture in a middle vessel column can be thought of as being equivalent to an operating schedule in which the still pot holdup is continuously transfered between a batch rectifier and a batch stripper, and operated for infinitessimally short periods of time in each of the rectifier and the stripper.

To illustrate this idea, consider the ternary residue curve map with no azeotropes as given in Figure 3-9a, with the middle vessel composition path given by a value of $\lambda = 0.5$ (which implies that the amount of product drawn off from the stripping section of the middle vessel column as bottoms product is the same as that drawn off from the rectifying section of the middle vessel column as distillate product) resulting in the instantaneous direction given by the vector $(\lambda)(\mathbf{x}^M - \mathbf{x}^D) + (1-\lambda)(\mathbf{x}^M - \mathbf{x}^B)$. As explained in Section 3.2, this vector can be thought of as being one of the vectors swept out by the vector cone as given by the directional vectors $(\mathbf{x}^M - \mathbf{x}^D)$ and $(\mathbf{x}^M - \mathbf{x}^B)$, with the relative weights for each vector set at 0.5 each. However, the direction vector of a mixture being distilled in a rectifier would have been given by $(\mathbf{x}^M - \mathbf{x}^D)$, while the direction vector of a mixture distilled from the still pot of a stripper would been given by $(\mathbf{x}^M - \mathbf{x}^B)$.

Thus, the still pot in the middle vessel is fractionally ($\lambda = 0.5$ times) behaving like a rectifier with ND trays and fractionally ($1 - \lambda = 0.5$ times) behaving like a stripper with NB trays. Therefore,we could intepret the motion of the middle vessel composition in the direction of $(\lambda)(\mathbf{x}^M - \mathbf{x}^D) + (1-\lambda)(\mathbf{x}^M - \mathbf{x}^B)$ as being an

infinitessimal move in the direction of $\mathbf{x}^M - \mathbf{x}^D$ (i.e., acting as a rectifier with ND trays) followed by an infinitessimal move in the direction of $\mathbf{x}^M - \mathbf{x}^B$ (i.e., acting as a stripper with NB trays), with the weights of each move given by λ and $1 - \lambda$ respectively. This representation is shown in Figure 3-9b. It should be noted that after the initial infinitessimal batch rectification, the composition of the still pot will be on a new residue curve, thus the product composition of the infinitessimal batch stripping will be slightly different from the bottoms product obtained from the middle vessel column, but since the initial recitification move is infinitessimal, the bottoms product from the middle vessel column will be equivalent to the product from the batch stripping operation to a first approximation. As the size of this infinitessimal move approaches zero, the composition of the product drawn from the stripping operation will be exactly that of the bottoms product in the middle vessel column.

Equivalently, the order of the infinitessimal moves could be reversed (distillation in a stripper, followed by distillation in a rectifier) with no loss of generality. The two-step operation will still be equivalent to that of a middle vessel column, with the composition of the product drawn from the distillation operation approaching that of the distillate product drawn from the middle vessel column as the infinitessimal move approaches zero.

We should note that this problem of having a slightly different product in the second operation (of the equivalent two-step operation) will not occur as the reflux/reboil ratio and the number of stages approaches infinity. This is because as $ND \to \infty$ and R_d, $R_b \to \infty$, the composition of the products drawn as distillate from the middle vessel column approaches that of the alpha limit set (as defined by Ahmad and Barton [1]) for the current basic distillation region. Similarly, as $NB \to \infty$ and R_d, $R_b \to \infty$, the composition of products drawn from the bottom of the middle vessel column approaches that of the omega limit set (Ahmad and Barton [1]). These product compositions remain unchanged as the middle vessel composition/still pot composition changes within the same basic distillation region. Thus, the product drawn for the second stage of the operation (rectification/stripping) will be exactly that of the product drawn from the equivalent position (distillate/bottoms) in the

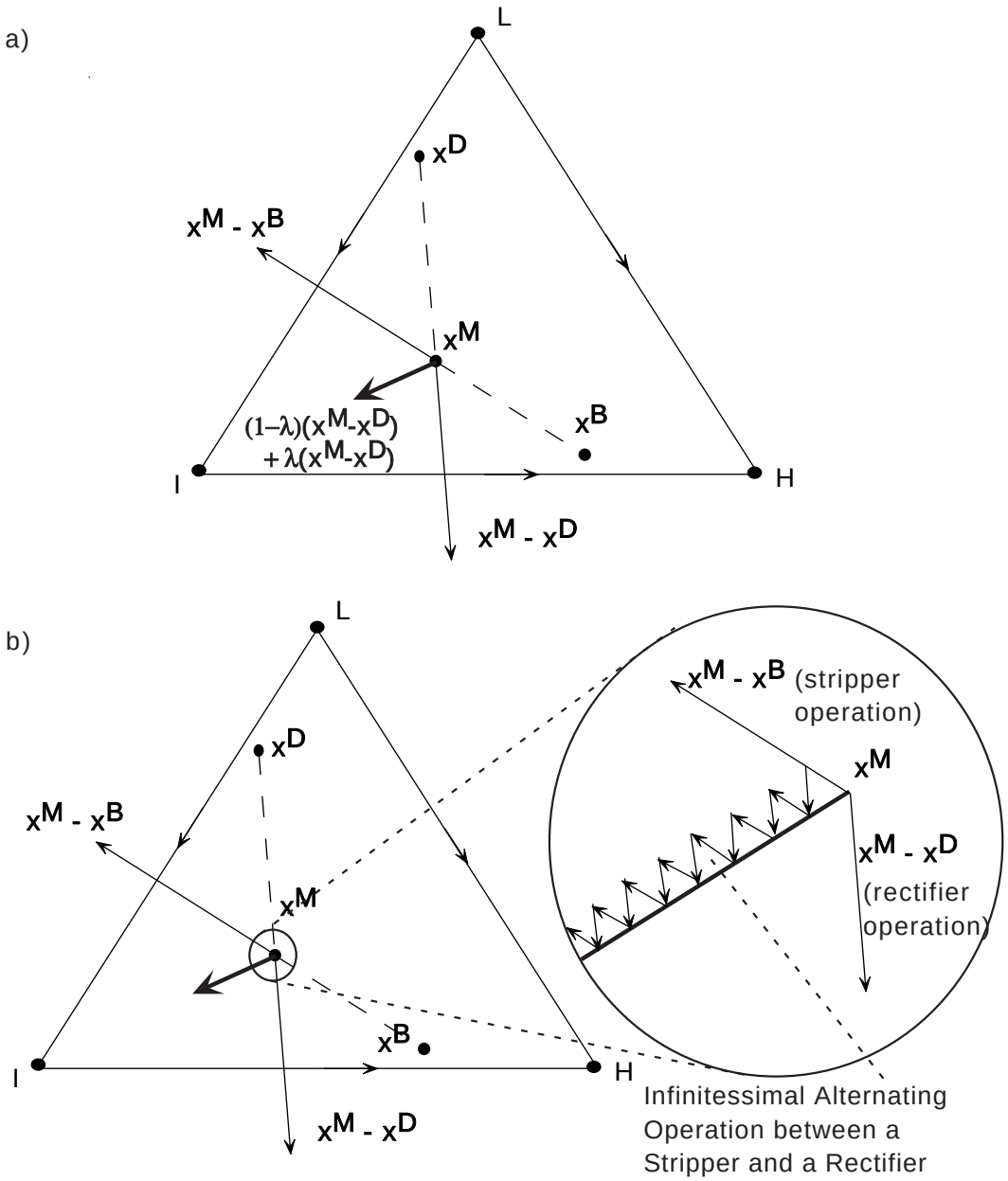

Figure 3-9: Pot Composition Path Using a Middle Vessel Column vs a Stripper and a Rectifier

middle vessel column. Details regarding the behavior of the middle vessel column at the limiting conditions of infinite number of stages and infinite reflux/reboil ratios will be explored in greater detail in Section 4.5.

In fact, this equivalency between the middle vessel column and the combined operation of a batch rectifier and a batch stripper is best illustrated by the fact that Hasebe's original design of the middle vessel column was exactly that: a batch rectifier with the contents of its still pot mixed with the contents of the still pot of a batch stripper such that there is no need to transfer the still pot contents between the stripper and the rectifier (see Figure 1-2a).

With this theoretical equivalency of the middle vessel column and the combined operation of the batch stripper/batch rectifier, it appears that the middle vessel column is perhaps irrelevant. However, this is not the case, as there appears to be advantages (increased separation possibilities) with operating a column at finite reflux/reboil ratios and finite number of trays, the middle vessel column would be needed to avoid and infinity of transfers. The advantages and disadvantages of using a middle vessel column will also be explored in greater detail in Section 4.5 of Chapter 4.

3.4 A Contrast with Davidyan *et al.* (1994) and Meski and Morari (1995)

Finally, in this section, we would also like to give due credit to the work of Davidyan, Valerii, Meski and Morari [7, 27]. Although our model was developed independently, it is somewhat similar to the models developed by Davidyan *et al.* in their 1994 paper [7]. They made the same assumptions on the column of 1) constant molal overflow, ignoring heat effects and 2) negligible holdup on all other trays other than the middle vessel holdup tray. Thus, they obtained the same mathematical equation for the dynamics of the column as given by equation (3.7). Their equation was given

as follows:

$$\begin{aligned} & V\mathbf{y}(\mathbf{x}_{j+1}) - L\mathbf{x}_j - D\mathbf{y}(\mathbf{x}_1) = 0, \qquad j = 1, \ldots, (mv-1) \\ & \dot{\mathbf{x}}_{mv} = \mathbf{x}_{mv} - \tfrac{D}{D+W}\mathbf{y}(\mathbf{x}_1) - \tfrac{W}{D+W}\mathbf{x}_N \\ & L'\mathbf{x}_{j-1} - V'\mathbf{y}(\mathbf{x}_j) - W\mathbf{x}_N = 0, \qquad j = (mv+1), \ldots, N \end{aligned} \tag{3.26}$$

where V and L are the vapor and liquid flow rates in the rectifying section and V' and L' are the vapor and liquid flow rates in the stripping section. The indices $j = 1, \ldots, N$ are the tray numbers, and $\mathbf{y}$ and $\mathbf{x}$ are the vapor and liquid compositions respectively. D is the distillate flow rate, W is the bottoms flow rate and index mv is the location of the middle vessel.

The mass balance (operating line) equations in equations (3.26) are identical to our model, except that the equations were arranged with the presumption that the bottoms and distillate product composition are known, and hence can be used to calculate the individual tray compositions. This formulation serves the purpose of their paper well, as Davidyan *et al.* then proceeded to model the behavior of the column for an ideal mixture with constant relative volatilities. They also assumed the limiting conditions of total reflux and infinite trays, which allowed them to predict the composition of the bottoms and distillate products (which will be pure products, since the mixture is ideal with constant relative volatilities) as a function of the composition of the middle vessel, and the time elapsed.

This is in contrast to our model, where we presumed that the bottoms and distillate compositions are unknown. They are found instead by stepping up stage by stage, from the the composition at the middle vessel feed, using the mass balance and phase equilibrium equations on each tray. Our formulation of the equations thus provide a more robust analysis which can be easily applied to finite models, where the bottoms and distillate product compositions are continually changing.

Davidyan *et al.* obtained much more specific results for the model, but did so based on a model assuming constant relative volatilities. They also assumed limiting conditions, which sharpened the analysis, but also resulted in the lost of generality in their analysis. It is hoped that our i nterpretation of the model, assuming nothing

concerning the operating conditions, and applying it to mixtures with azeotropes, will result in a better understanding of the general behaviour of a middle vessel column.

Meski and Morari then followed up this work with a much less mathematically intense paper, where they revisited the model of the middle vessel column as given by Davidyan *et al.*, and provided a graphical analysis of the model in the limiting conditions of total reflux and infinite number of trays. However, they conducted their analysis for the distillation of a binary non-azeotropic mixture, and hence expected only pure products under infinite separation to give the following equation:

$$\frac{dx_{mv}}{d\tau} = \begin{cases} 0, & x_{mv} = 0 \\ x_{mv} - \frac{D}{D+B}, & 0 < x_{mv} < 1, \quad \tau = -ln\frac{H(t)}{H(0)} \\ 0, & x_{mv} = 1 \end{cases} \tag{3.27}$$

where x is the mole fraction of the light component (for a binary mixture, the composition is completely defined, with the heavier component having mole fraction $1-x$), x_{mv} is the mole fraction of the light component in the middle vessel, and D is the distillate rate, B is the bottoms rate and H is the total holdup in the middle vessel.

From their analysis, it is clear that they were expecting a pure product, as would be expected for a non-azeotropic binary mixture distilled under limiting conditions. We can also see that their equation is a special case of equation (3.7), where $\mathbf{x}_D = 1$ and $\mathbf{x}_B = 0$, and $\mathbf{x}$ is a scalar, and τ is equivalent to ξ.

They then extended their analysis to a 3 component non-azeotropic mixture, and provided the following equation:

$$\frac{d\mathbf{x}_{mv}}{d\tau} = \mathbf{x}_{mv} - \begin{bmatrix} \frac{B}{D+B} \\ \frac{D}{D+B} \end{bmatrix}; \tau = -ln\frac{H(t)}{H(0)} \tag{3.28}$$

This is also a specific case of equation (3.7). As they were investigating a non-

azeotropic mixture, pure products were expected and hence:

$$\mathbf{x}_D = \begin{bmatrix} 0 \\ 0 \\ 1 \end{bmatrix} \tag{3.29}$$

$$\mathbf{x}_B = \begin{bmatrix} 1 \\ 0 \\ 0 \end{bmatrix} \tag{3.30}$$

where the first component is heaviest, and the third component lightest. Substituting this into equation (3.7), we obtain:

$$\frac{d\mathbf{x}^M}{d\xi} = \mathbf{x}^M - \lambda \begin{bmatrix} 0 \\ 0 \\ 1 \end{bmatrix} - (1-\lambda) \begin{bmatrix} 1 \\ 0 \\ 0 \end{bmatrix} \tag{3.31}$$

Given that compositions sum to unity ($\sum_{i=1}^{NC} x_i = 1$), the second (intermediate) composition is then a dependent variable, and can be found via a simple algebraic relation with the first and third compositions. The dynamics of the second composition does not have to be studied if the first and third composition are defined. Reviewing equation (3.1), $\lambda = \frac{D}{D+B}$, which means that $1-\lambda$ is given by:

$$1 - \lambda = \frac{B}{D+B} \tag{3.32}$$

Substituting λ and $1-\lambda$ into equation (3.31), neglecting the intermediate composition, equation(3.31) is rewritten as:

$$\frac{d\mathbf{x}^M}{d\xi} = \mathbf{x}^M - \frac{D}{D+B} \begin{bmatrix} 0 \\ 1 \end{bmatrix} - \frac{B}{D+B} \begin{bmatrix} 1 \\ 0 \end{bmatrix} = \mathbf{x}^M - \begin{bmatrix} \frac{B}{D+B} \\ \frac{B}{D+B} \end{bmatrix} \tag{3.33}$$

which is exactly the equation provided by Meski and Morari. However, note that equations (3.33) only holds up to the point where second component (intermediate

weight) begins to break through in either the top and/or bottoms products. The time at which this occurs and the location at which it occurs (either in the distillate or in the bottom product or both simultaneously) depends on the choice of the value of λ and the composition of the initial charge to the holdup vessel.

Meski and Morari then went on to mention that the above analysis also applies to ternary azeotropic systems, and provided a diagram for a ternary system with a binary azeotrope, but did not explain in depth how it was also applicable, since their analysis had been based completely on the assumption that the products drawn are pure.

Thus, as we can see from this survey of the work by Davidyan *et al.* and Meski and Morari, our analysis is very similar, but in this thesis we will take the analyis one step further, extending it to non-limiting operating conditions and azeotropic mixtures. Although our mathematical model of the mass balance in the middle vessel column is almost identical to that provided by Davidyan *et al.*, we feel that our analysis of the behavior of the still pot composition with respect to 1) time ξ and 2) middle vessel parameter λ, will help provide intuitive insights concerning the evolution of the still pot composition in the middle vessel column. This will then allow us to predict the behavior of the middle vessel column without any intensive calculations.

Chapter 4

Theoretical Analysis of the Limiting Behavior of the MVC Model

In the presence of a finite number of trays and finite operational reflux and reboil ratios, the dynamic variation of the product compositions results in a model that is impossible to analyze theoretically. Thus, analysis of the non-limiting dynamics of the middle vessel still pot composition and products composition is best left to numerical simulations, which are able to solve the large-scale system of differential-algebraic equations (DAEs) describing the middle vessel column model. The equations presented in Chapter 3 can be solved and the dynamics of the column composition simulated using ABACUSS (Advanced Batch and Continuous Unsteady State Simulator).

Based on the model developed in Chapter 3, a theoretical analysis will be conducted on the behavior of the still pot composition in the middle vessel column in the limiting case of infinite reflux and reboil ratios and infinite number of trays. Our analysis builds on work by Van Dongen and Doherty [15], who studied the batch distillation residue curves for a batch rectifier, under the special case of large N (infinite number of trays) and large r (infinite reflux ratio). Bernot *et al.* also examined the dynamics of the holdup vessel composition in both a batch rectifier [5] and a batch

stripper [6] using the same method of analysis.

This chapter is in six sections: the first section clarifies the differences between residue curves and distillation lines (or total reflux column profiles), and justifies the use of a residue curve as an approximation to the column composition profile at high reflux/reboil ratios, as suggested by Van Dongen and Doherty [15]. The second section introduces the basic tools of analysis developed by Van Dongen and Doherty [15], and Bernot *et al.* [5, 6] and provides an analysis of a simple non-azeotropic 3-component system, and a complex 3-component system of Acetone-Chloroform-Methanol which exhibits multiple binary and ternary azeotropes. The third section extends the analysis to higher dimensional systems, with number of components $n \geq 4$, Systems with $n \geq 5$ are hard to represent geometrically on two dimensional paper, but the analysis will extend accordingly to them. The fourth section explores the definition of a "batch distillation region" by Ewell and Welch [16], in the context of a middle vessel column, which will be a function of the middle vessel column parameter λ. A bifurcation analysis is also conducted to identify the transformation of these batch distillation regions, and the nature of these transformations, with the parameter λ. It should be noted that the analysis in the first three sections is based upon the assumption of straight separatrices which greatly simplifies the actual analysis. However, almost all separatrices are almost definitely curved as explained by Reinders and De Minjer [30]. In fact, as shown in Chapters 5 and 7, it is this curvature that gives rise to interesting possibilities in separation of azeotropic mixtures. The fifth section further explores the equivalency between the middle vessel column and the combined operation of rectifier and strippers, and states the limits of this equivalency, and the advantages/disadvantages of each approach. Finally, in the sixth and final section, a comparison is made to the work by Safrit and Westerberg [35, 33, 32, 34] on the following subjects: 1) movement of the still pot composition in middle vessel columns, 2) the concept of steering the still pot composition, and 3) the equivalency of the middle vessel column to a batch stripper combined in operation with a batch rectifier.

4.1 The Non-Equivalence of Residue Curves and Distillation Column Profiles

Van Dongen and Doherty [15] examined the dynamics of the batch distillation process, comparing them with the traditional simple distillation residue curve maps and came to the conclusion that at very high reflux ratios ($r \geq 7$), there is very little error in the approximation that $\mathbf{x}^D$ and $\mathbf{x}^M$ both lie on the same simple distillation residue curve, and that the simple residue curve approximates the distillation composition profile in a packed column.

Since Van Dongen and Doherty's definitive work, many researchers have used the residue curves and the distillation composition profile in distillation columns interchangeably. They often point to the similarity of the equation describing the simple distillation processes:

$$\frac{d\mathbf{x}^M}{d\xi} = \mathbf{x}^M - \mathbf{y}^M(\mathbf{x}^M) \tag{4.1}$$

with that of the batch distillation process:

$$\frac{d\mathbf{x}^M}{d\xi} = \mathbf{x}^M - \mathbf{x}^D \tag{4.2}$$

and claim that at total reflux, the simple distillation residue curve describes the column profile in the column. They then go on to use the residue curves as an approximation of the column composition profile even at high (but not infinite) reflux ratios ($r > 7$).

However, as highlighted by Widagdo and Seider [41], the simple distillation residue curve and the actual composition profile in the column are never equivalent, even if they may asymptotically approach each other under limiting conditions. Widagdo and Seider then clarified the definition of distillation lines as lines which describe the composition profile in a distillation column under total reflux conditions; under total reflux conditions (steady state), the composition of a liquid flowing out of a given slice of the column will have to equal the composition of the vapor flowing into that same slice. (see Figure 4-1)

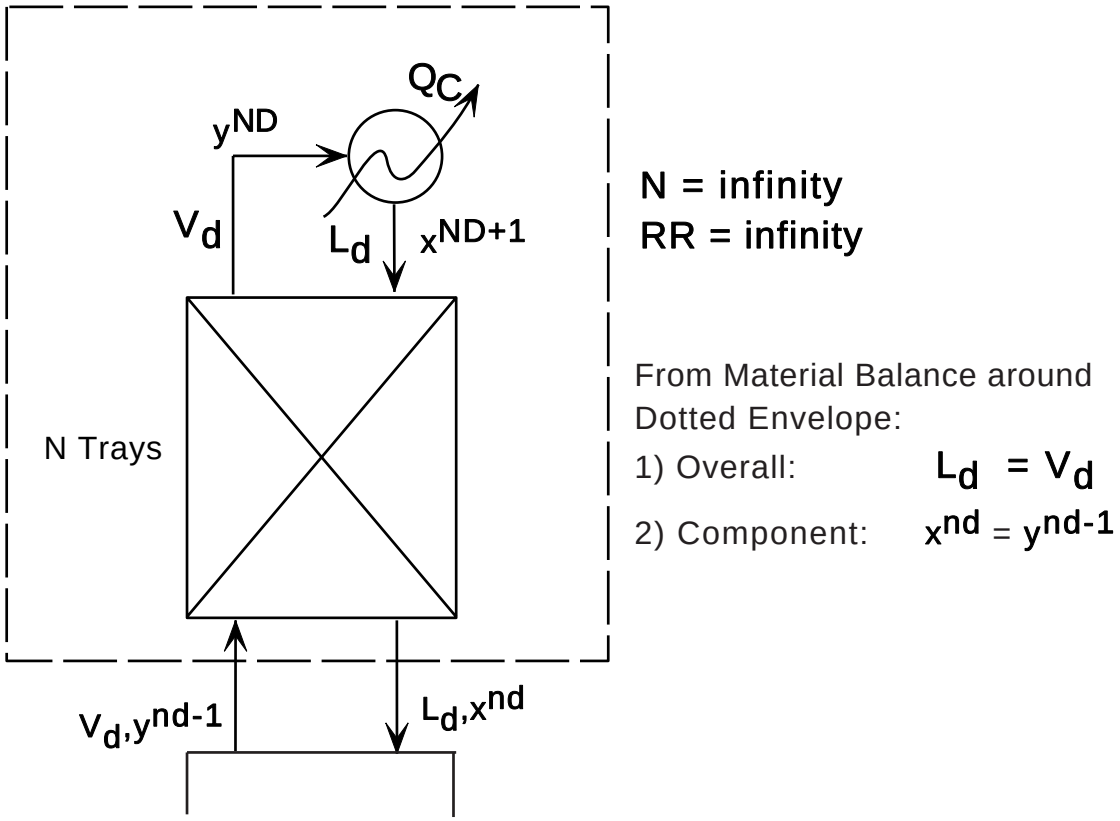

Figure 4-1: Compositions of Vapor In and Liquid Out at Total Reflux

For packed bed columns, the distillation line is then a continuous line (due to the continuous nature of the column) which starts off at the feed composition tray and extends as a function of the height of the column, while for tray columns (for which a discrete composition exists for each tray) the distillation line is a set of discrete points starting at the feed tray composition and each related to the next tray composition by the vapor liquid equilibrium within each tray and mass balance relationship between passing streams. It was then pointed out in their paper, that distillation lines are always more curved than the residue curve that passes through the feed tray composition. The above observation was confirmed by Wahnschafft and Westerberg [40] when they simulated the operation of a continuous column for the separation of a mixture of acetone, benzene and chloroform. A simple calculation of the column profile in a finite reflux column (conducted using the ABACUSS simulation environment) also showed that the distillation lines (or total reflux composition profiles) are more bulged than the residue curves. An example of such a column composition profile with the corresponding residue curve passing through the feed tray/middle vessel composition, is shown in Figure 4-2 for the mixture of acetone, benzene and chloroform, with 100 trays and a reflux/reboil ratio of 5.

A further example is provided in which the curvature of this distillation line causes it to crosses the separatrix of the residue curve map at finite reflux rates. The system is acetone, benzene and chloroform as before, but the residue curve selected now lies right along the stable separatrix of the residue curve map. The column composition profile depicted in Figure 4-3 is for a column with 100 trays, operated at $R_d = R_b = 5$, and due to the extreme curvature of the distillation line, it unambigiously crosses this separatrix into the neighbouring simple distillation region. The residue curve map of the ternary mixture of acetone, benzene and chloroform, with its corresponding separatrix illustrated, is in Appendix B.

However, Widagdo and Seider also point out that as the number of trays $\rightarrow \infty$, the limiting composition in the top and the bottom tray of the column approach the fixed points of the residue curve map. In particular, the limiting composition of the top and the bottom tray in the column will asymptotically approach the alpha and

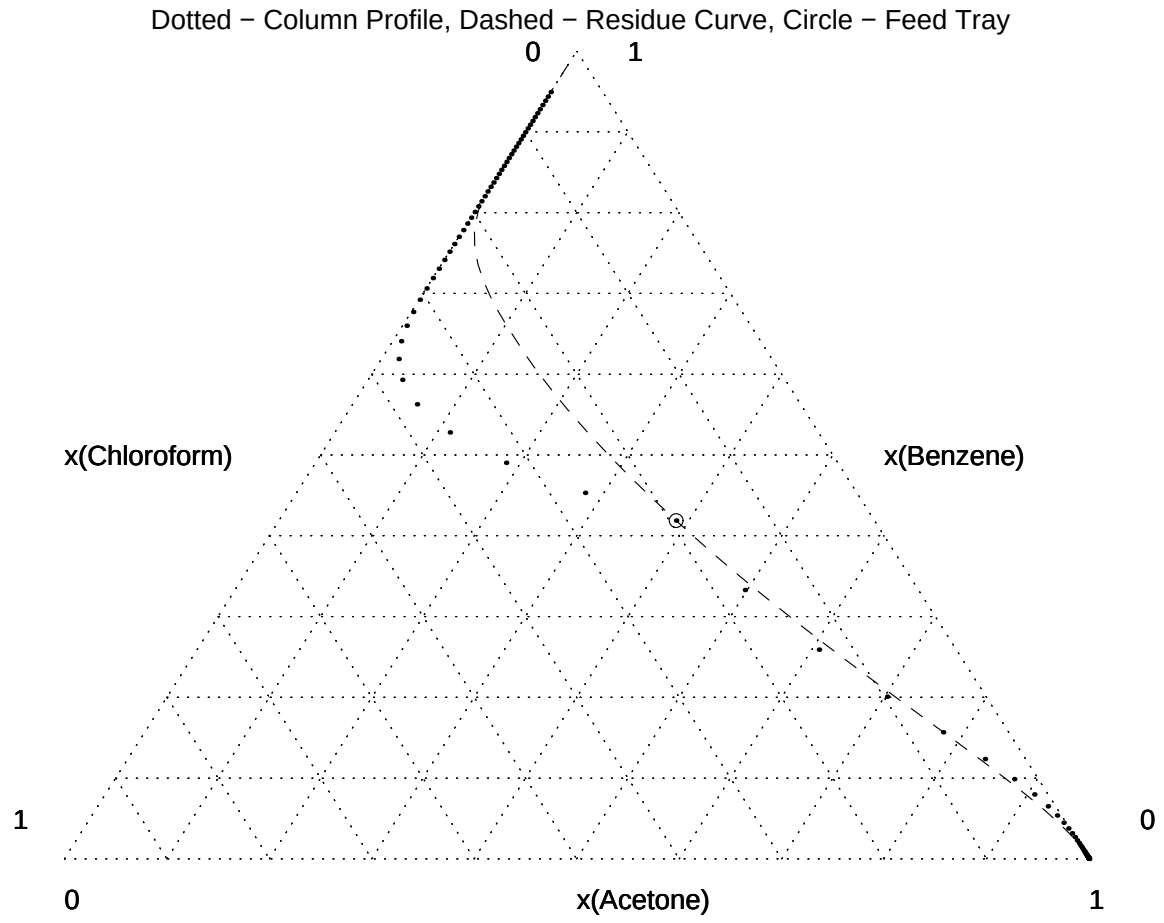

Figure 4-2: Column Composition Profiles Compared to the Corresponding Residue Curve at Finite Reflux

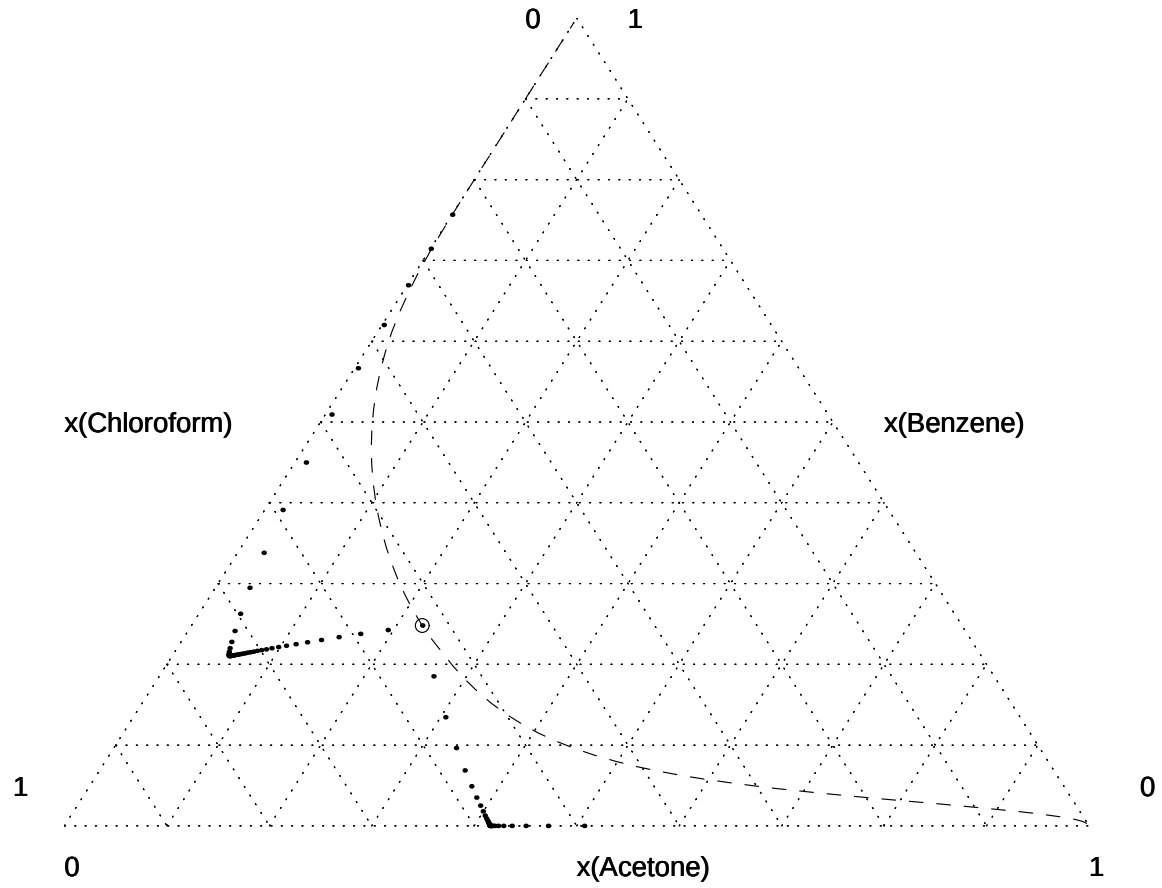

Figure 4-3: Column Composition Profiles Crosses a Separatrix at Finite Reflux

omega limit sets for the residue curves of the basic distillation region in which the feed tray composition resides. As such, for the purposes of a limiting analysis (ND, NB, R_d, $R_b \to \infty$), it is appropriate to use the alpha and omega limit sets of the residue curves to estimate the composition of the top-most and bottom-most tray of a tray column, or to use the alpha and omega limit sets of the residue curve to estimate the composition at the top and the bottom of the packed bed and tray columns.

This is further confirmed by calculating the expected total reflux column profile in a tray column, and comparing this profile to the residue curve that passes through the feed tray composition. As shown in Figures 4-4 and 4-5 for each of the initial still pot compositions illustrated in Figures4-2 and 4-3, there is very little difference between the residue curve and the discrete points that make up the tray composition profile at total reflux. Furthermore, the limit of the distillation line sequence (i.e., the top and bottom composition of the column as the number of trays approach infinity), unambigiously approach the fixed points of the residue curves (i.e., the alpha and omega limit sets of $\varphi(\mathbf{x}^M)$). It is thus reasonable to assume that the top and bottom composition of a distillation column will be given by the alpha and omega limit sets of the residue curve that passes through the feed tray composition.

However, despite the similarities in the fixed points of the distillation lines (as $ND \to \infty$ and $NB \to \infty$) and the fixed points of the residue curve (as $\xi \to \pm\infty$), it should be categorically recognized that they are inherently not equivalent to each other. This applies both to distillation lines for packed and tray columns.

Furthermore, a residue curve is composed of an uncountable infinity of points, and as such is a different mathematical entity as compared to the tray column profile which exists as a countable infinity of points even as $ND \to \infty$ and $NB \to \infty$. A total reflux column profile for a tray column with R_d, $R_b \to \infty$ and ND, $NB \to \infty$ is composed from a countably infinite number of linear line segments which connects each of the tray compositions in the tray column, where the direction of each line segment is equal to the tangent to the residue curve through the composition point defining the beginning of the line segment. As such, it is an entirely different mathematical object from the residue curve which is a continuous curve. The countable sequence

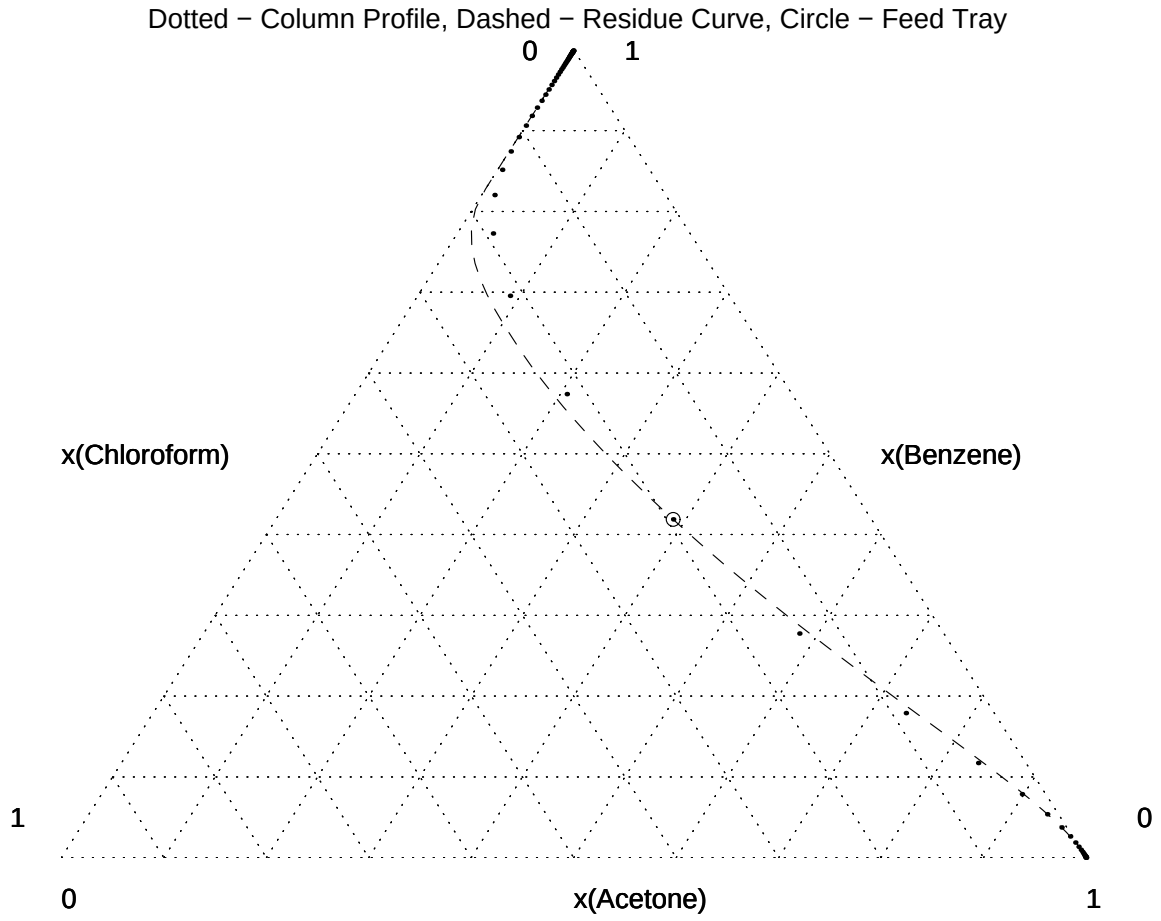

Figure 4-4: Column Composition Profiles For the First Feed Composition Compared to the Corresponding Residue Curve at Infinite Reflux

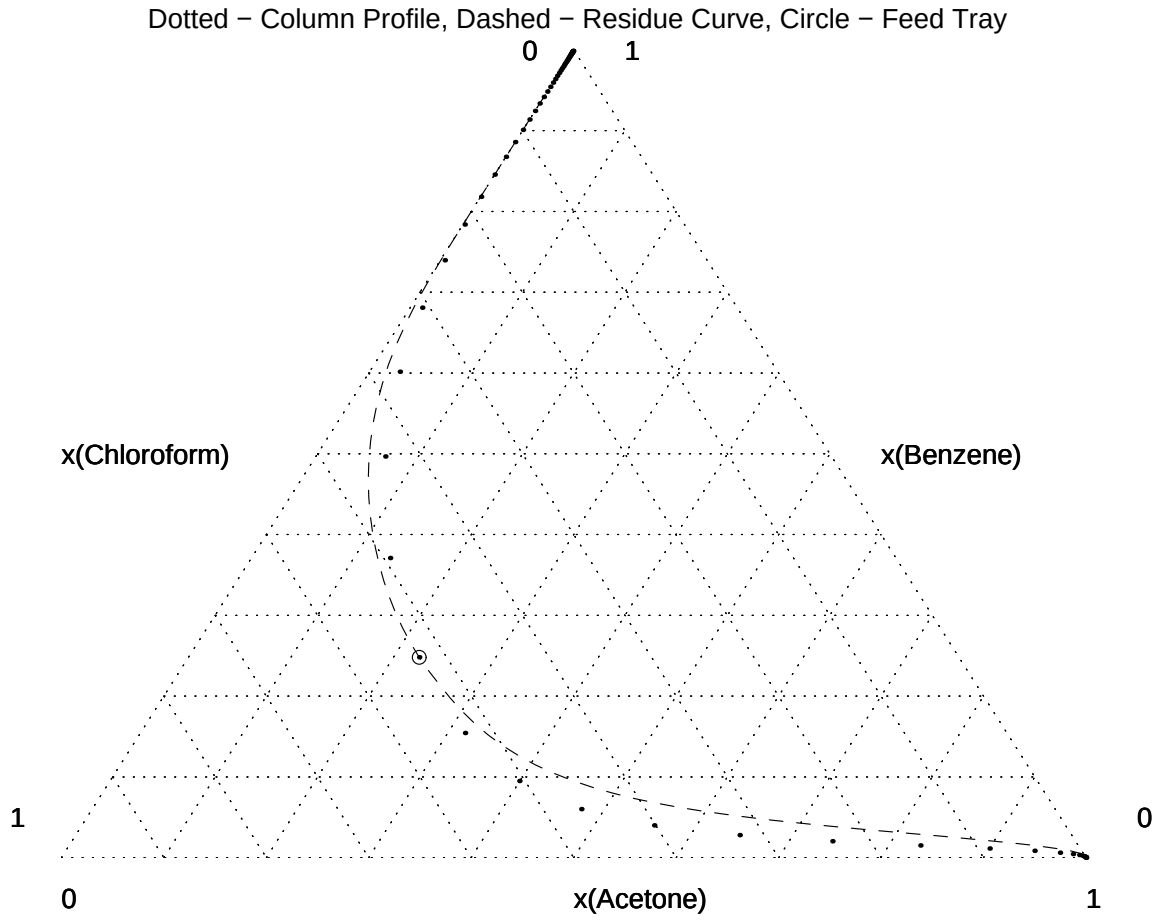

Figure 4-5: Column Composition Profiles For the Second Feed Composition Compared to the Corresponding Residue Curve at Infinite Reflux

of points (which indicate the distillation column composition profiles) thus defined does, however, converge to the alpha limit set of the residue curves in the rectifying section of the column, and the omega limit set of the residue curves in the stripping section of the column. The reason for this behavior being the fact that every line segment in the distillation curve is tangent to a residue curve, and this tangent line segment points into the fixed point of the residue curve map if the tray composition is close enough to the fixed point on that residue curve.

It should also be noted that despite the fact that the composition profile for a packed column is a continuous line (due to the continuous nature of the packed distillation column), it is still not equivalent to the residue curve. However, as R_d, $R_b \to \infty$ and height of the packed distillation column $\to \infty$, the packed column distillation lines will approach the residue curves asymptotically.

4.2 Infinite Reflux, Infinite Trays

Based on their conception that column composition profiles can be approximated by residue curves, Van Dongen and Doherty then went on to analyse the behavior of the pot composition in a batch rectifier. With this approximation, as $R_d \to \infty$, the composition profile in the column will be given by the simple distillation residue curve between $\mathbf{x}^D$ and $\mathbf{x}^M$. It was also found that the value of N, the number of theoretical stages in the column, determined the position of the distillate composition on the simple distillation residue curve. If N was low, the distillate composition $\mathbf{x}^D$ would be relatively near the still pot composition $\mathbf{x}^M$, whereas if N was high, the distillate composition would be further from the still pot composition but still on the same simple distillation residue curve. Finally, in the limit, as $N \to \infty$, the distillate composition will be given by the unstable node of the system (or more generally, the alpha limit set of a given basic distillation region).

It also follows that if these product compositions are drawn from the column, then by a simple mass balance, the still pot composition moves vectorially in the opposite direction, away from the composition of the product. A tie line can be

drawn between the composition of the product withdrawn from the column and the new still pot composition, with the old still pot composition being the lever point. The lengths of the two sections of the tie line are determined by the amount of product drawn from the column as compared to the holdup orginally in the column. These results are illustrated in Figure 4-6 for a) a generic 3-component ideal system, and b) for the Acetone-Chloroform-Methanol system.

Based on the work of Van Dongen and Doherty, Bernot *et al.* conducted a simulation analysis on batch rectifiers [5], extended the above theoretical analysis of batch distillation regions to batch strippers, and also conducted a similar simulation analysis on batch strippers [6]. Following the analysis provided by Van Dongen and Doherty [15], they pointed out that if, at large values of R_d, the distillate composition lies on the same simple distillation residue curve as the still pot composition, it follows that at large values of R_b, the bottoms composition $\mathbf{x}^B$ in a batch stripper also lies on the same simple distillation residue curve as the still pot composition $\mathbf{x}^M$. Equivalently, the column profile of the batch stripper will be given by the simple distillation residue curve between the compositions $\mathbf{x}^M$ to $\mathbf{x}^B$. They also elucidate that at large values of N ($N \to \infty$), the bottoms composition is given by the stable node of the system (or more generally, the omega limit set of a given basic distillation region). As before, the still pot composition moves vectorially away from the composition of the bottoms product withdrawn. A tie line can also be drawn to determine the new still pot composition based on the amount of bottoms product drawn with respect to the amount of holdup originally in the holdup vessel. These results are also illustrated for a) a generic 3-component ideal system, and b) for the Acetone-Chloroform-Methanol system in Figure 4-7.

Following the arguments and analysis presented by Van Dongen and Doherty, and Bernot *et al.*, the middle vessel column at an infinite reflux ratio should exhibit a similar behavior. In Section 4.1, it was concluded that as ND, $NB \to \infty$ and R_d, $R_b \to \infty$, the composition of the top tray of the rectifying section (equivalent to the distillate composition) is the alpha limit set of the residue curve that passes through the current still pot composition, and the composition of the bottom

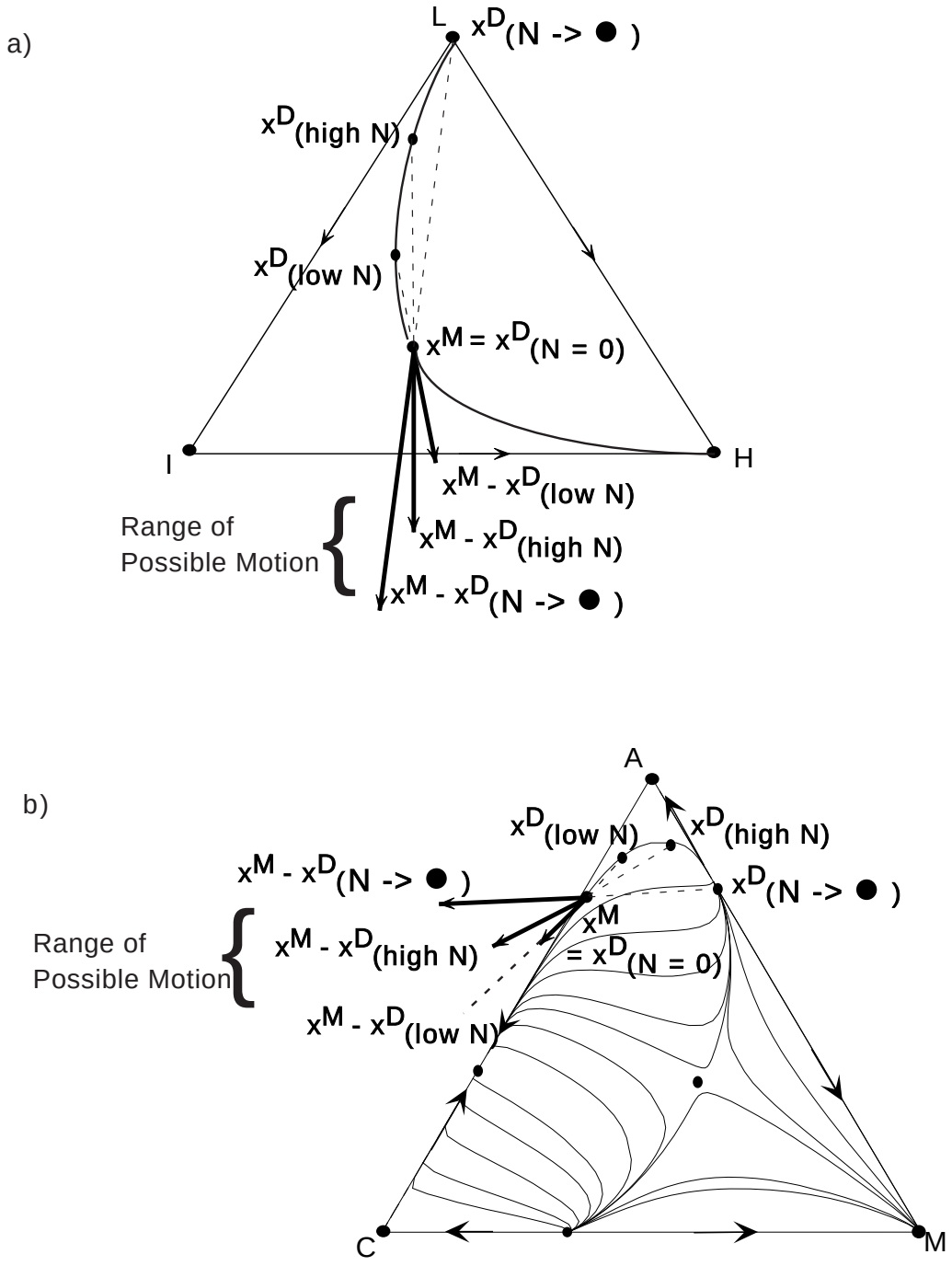

Figure 4-6: Product Composition as a Function of N for a Batch Rectifier

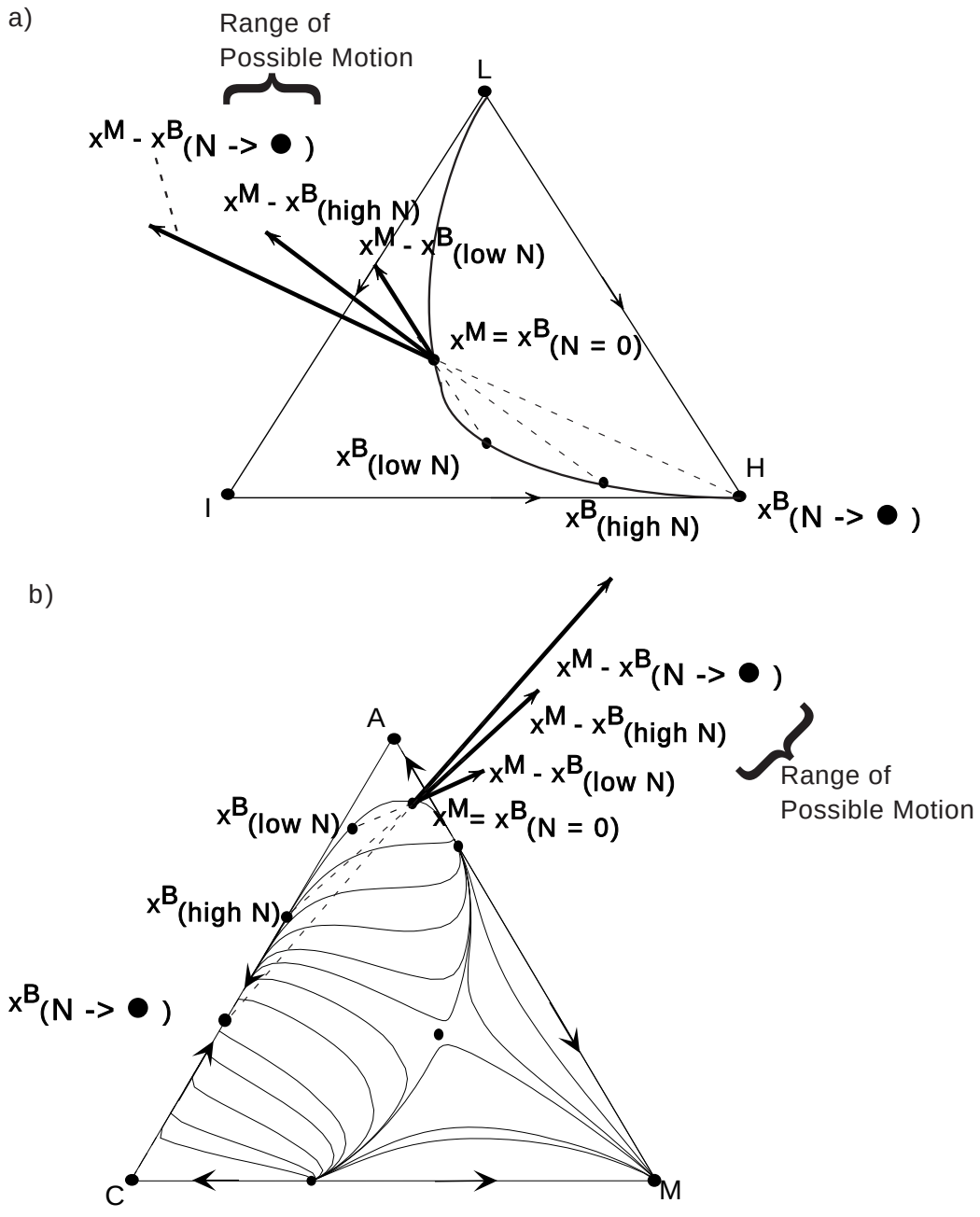

Figure 4-7: Product Composition as a Function of N for a Batch Stripper

tray (equivalent to the bottoms composition) approaches the omega limit set of the residue curve passing through the current still pot composition. The points which mark out the composition of individual trays can then be appoximately traced out by the residue curves under these limiting conditions. It then follows that the column composition profile in the rectifying section will be approximated by points on the simple distillation residue curve running through the still pot composition $\mathbf{x}^M$, between $\mathbf{x}^M$ and the alpha limit set of $\mathbf{x}^M$ ($\alpha(\mathbf{x}^M) = lim_{\xi \to -\infty} \varphi(\xi, \mathbf{x}^M)$) as defined by Ahmad and Barton [1]. The alpha limit set of the residue curves (as given by the functionality φ) approaches a fixed point in the current basic distillation region (either an unstable node or a saddle point). The distillate composition is located close to the curve $\varphi(\xi, \mathbf{x}^M)$, somewhere in the curve segment bounded by $\mathbf{x}^M$ and $\alpha(\mathbf{x}^M)$. The exact location of the distillate composition depends on the number of trays in the rectifying section of the middle vessel column, but with the limits given by:

$$\begin{aligned} &ND \to 0, && \mathbf{x}^D \to \mathbf{x}^M \\ &ND \to \infty, && \mathbf{x}^D \to \alpha(\mathbf{x}^M) \\ &ND \in \{\mathbf{Z}^+\}, && \mathbf{x}^D \in \text{residue curve} : \varphi(\xi, \mathbf{x}^M) \end{aligned} \tag{4.3}$$

It also follows that the column composition profile in the stripping section of the middle vessel column is approximated by points on the simple distillation residue curve running through $\mathbf{x}^M$, between $\mathbf{x}^M$ and the omega limit set of $\mathbf{x}^M$ ($\omega(\mathbf{x}^M) = lim_{\xi \to \infty} \varphi(\xi, \mathbf{x}^M)$) as defined by Ahmad and Barton [1]. As with the distillate, the bottoms composition is located close to this residue curve $\varphi(\xi, \mathbf{x}^M)$ somewhere between $\mathbf{x}^M$ and $\omega(\mathbf{x}^M)$. The exact location of the bottoms composition is then defined by the number of trays in the stripping section of the middle vessel column, with the limits given by:

$$\begin{aligned} &NB \to 0, && \mathbf{x}^B \to \mathbf{x}^M \\ &NB \to \infty, && \mathbf{x}^B \to \omega(\mathbf{x}^M) \\ &NB \in \{\mathbf{Z}^+\}, && \mathbf{x}^B \in \text{residue curve} : \varphi(\xi, \mathbf{x}^M) \end{aligned} \tag{4.4}$$

It thus follows from equations (4.3) and (4.4) that for our limiting analysis of an infinite number of trays in both sections of the column operated at an infinite reflux/reboil ratio, the distillate composition is given by the alpha limit set of the basic distillation region in which the middle vessel pot composition ($\mathbf{x}^M$) lies. Similarly, the bottoms composition is given by the corresponding omega limit set.

A major difference between a column with an infinite number of trays and a finite column, is that in an infinite column the distillate and bottoms product composition are unchanging for long periods of time as compared to the finite column where they are continually changing with time. This is because from the definition of a basic distillation region (Chapter 2), all simple distillation residue curves in the same basic distillation region lead to the same alpha limit set and the same omega limit set [1]. It should be noted that this definition of a basic distillation region takes into account pot composition boundaries, which are, in themselves, basic distillation regions without any volume in the composition space. Hence, while the middle vessel composition remains in the same basic distillation region, and given that the alpha limit set and omega limit set do not change for a given basic distillation region, it follows that if ND and NB remains unchanged at infinity, the same "alpha limit set composition" is always being drawn as the distillate product, and the same "omega limit set composition" always drawn as the bottoms product, irrespective of the instantaneous still pot composition as illustrated in Figure 4-8

The distillate and bottoms composition only change when the still pot composition encounters a separatrix or an edge of the composition simplex in the 3-component system, and thus enters the 2-dimensional line or edge. In this analysis, we shall assume straight line boundaries so as to simplify the analysis. In doing so, we should keep in mind that naturally occuring separatrices tend to be curved [30], which would further complicate our analysis. Upon entering the linear separatrix, the mixture effectively becomes a 2-component system, with a new pair of alpha limit and omega limit sets, and it is these new alpha and omega limit sets which form the new bottoms and distillate products respectively. The still pot compositions in a batch distillation process also cannot cross the separatrices which separate the basic distillation regions

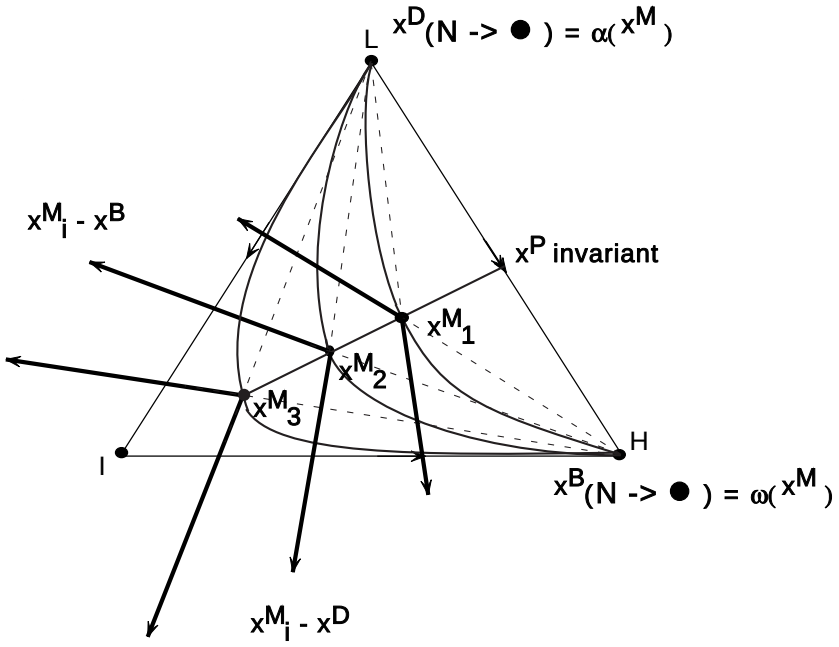

Figure 4-8: Invariance of Product Composition with Infinite Trays and Infinite Reflux and Reboil Ratios

if the separatrices are linear [15], it can only enter them. Separatrices in the 3 component system thus serve as pot composition boundaries, a concept first defined by Ahmad and Barton [1]. This is illustrated in Figure 4-9.

It is thus possible to analyse the dynamics of the still pot composition relatively easily given that the product compositions (both distillate and bottoms) are not continually changing with time, but instead undergo discrete changes only when the still pot composition encounters a separatrix or composition edge, and enters that separatrix or edge. It should be noted that this change in the product compositions can be conveniently expressed as a function of the still pot composition $\mathbf{x}^M$. A sample formulation is:

$$\begin{aligned} &\mathbf{x}^M \in [\text{basic distillation region A } \mathbf{R}^3], \\ &\mathbf{x}^D = \text{alpha limit set(region A)}, \\ &\mathbf{x}^B = \text{omega limit set(region A)} \end{aligned} \tag{4.5}$$

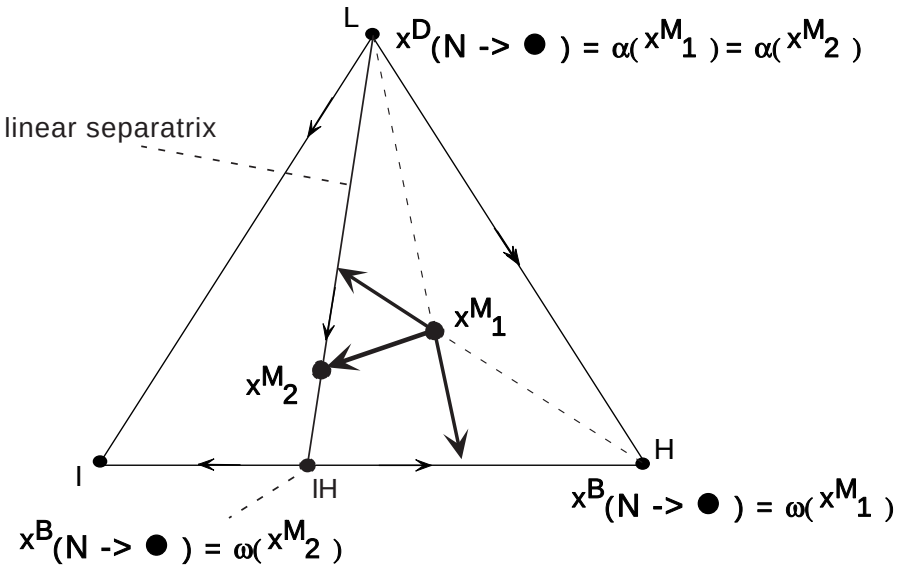

Figure 4-9: Change in the Alpha Limit Set and Omega Limit Set as a Linear Separatrix is Encountered

$$\begin{aligned} \mathbf{x}^M &\in [\text{edge/separatrix of region A, } \mathbf{R}^2], \\ \mathbf{x}^D &= \text{alpha limit set(edge/separatrix of A)}, \\ \mathbf{x}^B &= \text{alpha limit set(edge/separatrix of A)} \end{aligned} \tag{4.6}$$

Hence, the product compositions and consequently the still pot dynamics is completely defined by the location of the current still pot composition with respect to the basic distillation region and separatrices.

Next, a schematic representation of the vector cone which now restricts the motion of the still pot composition is shown in Figure 4-10, again for the two cases: a) a generic 3-component system, and b) for the Acetone-Chloroform-Methanol system.

The direction of motion for the still pot composition will lie within the vector cone, and will be a function of the operating parameter λ which we define for the column. λ may or may not be a function of time, depending on the objective function of the operating procedure. For example, if the objective is efficiency in terms of CAP (capacity factor first defined by Luyben [22]: a measure of the amount of product

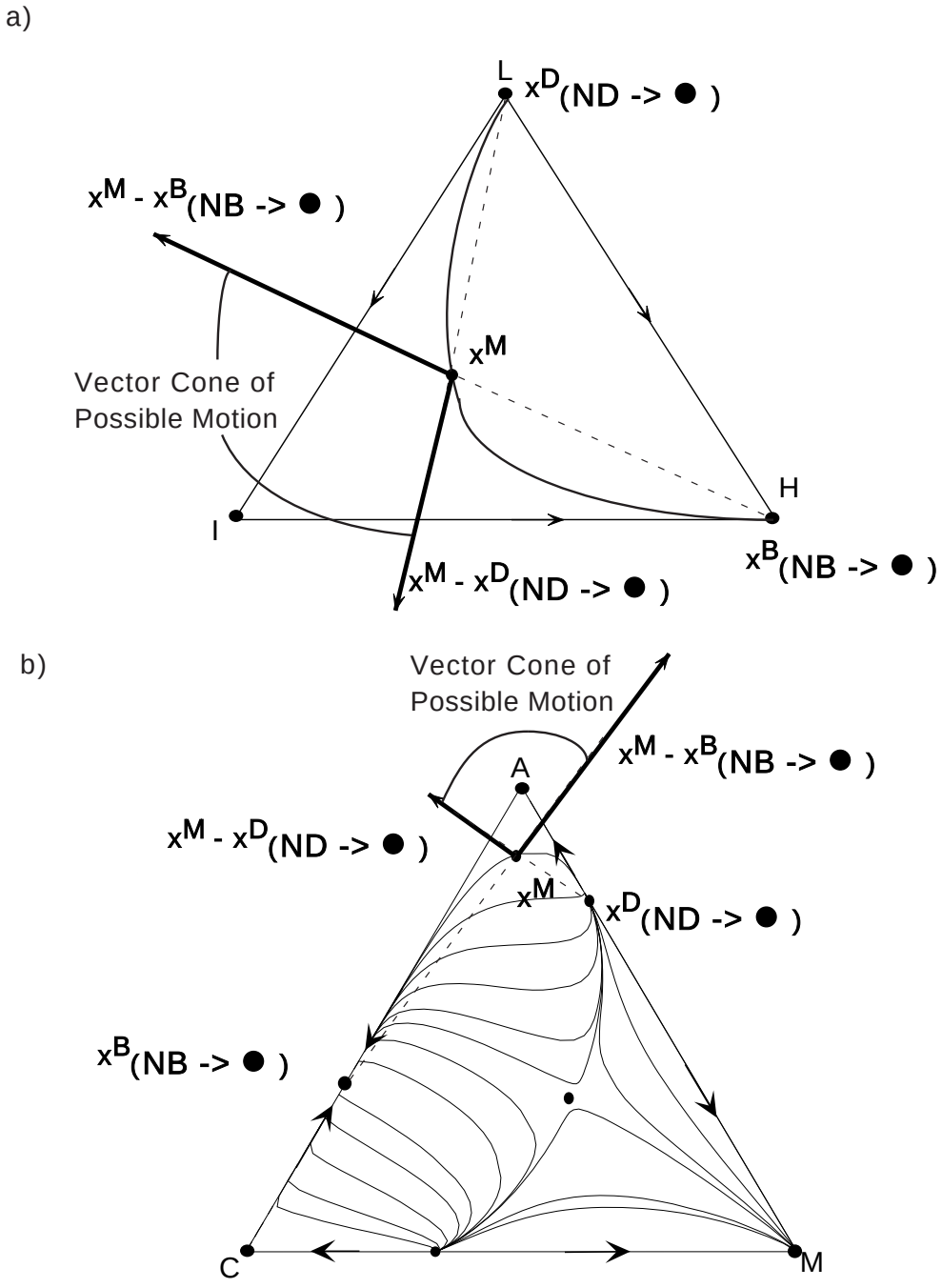

Figure 4-10: Vector Cone of Possible Motion Under Limiting Conditions in a Middle Vessel Column

drawn per unit time), then the best operating procedure for separating a binary ideal mixture will be a constant λ such that net product $\mathbf{x}^P$ is equal to the still pot composition $\mathbf{x}^M$ [27]. As mentioned in Chapter 3, we will not explore the topic of the optimal operating profile for $\lambda(\xi)$ in this thesis.

Revisiting the model in Chapter 3, equations (3.12) and (3.13) can now be written as:

$$\mathbf{x}^D(\xi) = \alpha(\mathbf{x}^M(\xi)) \tag{4.7}$$

and

$$\mathbf{x}^B(\xi) = \omega(\mathbf{x}^M(\xi)) \tag{4.8}$$

Equations (4.7) and (4.8) can then be substituted into equation (3.7) to obtain the following differential equation:

$$\frac{d\mathbf{x}^M}{d\xi} = \mathbf{x}^M - \mathbf{x}^P(\xi) \tag{4.9}$$

where $\mathbf{x}^P$ is defined by:

$$\mathbf{x}^P = \lambda\mathbf{x}^D - (1-\lambda)\mathbf{x}^B \tag{4.10}$$

and $\mathbf{x}^P$ represents the net product drawn from the column, dependent only on warped time ξ through the middle column parameter $\lambda(\xi)$, given that the distillate and bottoms product are invariant with $\mathbf{x}^M$ as long as $\mathbf{x}^M$ remains within the same basic distillation region. The definition of warped time, ξ, remains unchanged as given by (3.8).

Equation (4.9) is easily separable and solved, thus the analytical solution of the equation will depend primarily on the time dependeny of λ. For example, if λ is independent of time, that is:

$$\frac{d\mathbf{x}^P}{d\xi} = 0 \tag{4.11}$$

then, equation (4.9) can be rearranged for each of the components in the mixture, $\forall$

$i \in [1, NC]$:

$$\int_{x_i^M(0)}^{x_i^M(\xi)} \frac{dx_i^M}{x_i^M - x_i^P} = \int_0^{\xi} d\xi, \quad \forall i \in [1, NC] \tag{4.12}$$

with the solution of the equation given by:

$$\ln(\frac{x_i^M(\xi) - x_i^P}{x_i^M(0) - x_i^P}) = \xi, \quad \forall i \in [1, NC] \tag{4.13}$$

or alternatively:

$$\mathbf{x}^M(\xi) = \mathbf{x}^P(1 - \exp(\xi)) + \mathbf{x}^M(0)\exp(\xi), \quad \mathbf{x}^P = \mathbf{x}^P(\lambda) \tag{4.14}$$

Equation (4.14) thus defines the dynamics of the still pot composition as a function of $\mathbf{x}^P$, which remains a function of λ. Thus, for a given value of λ which is invariant, equations (4.7) and (4.8), which define the bottoms and distillate products composition, can be used in conjunction with equation (4.10), which defines the net product drawn from the column, to obtain the value of $\mathbf{x}^P$. The solution as given by equation (4.14) can then be used.

Note however, that the solution as given in equation (4.14) will only apply as long as the alpha limit set and omega limit set of the system remain unchanged (i.e., $\mathbf{x}_M$ remains in the same basic distillation region). As mentioned, the alpha and omega limit set of the system will change when the still pot composition enters a separatrix or pot composition boundary of the current basic distillation region. This consequently results in a change in the net product $\mathbf{x}^P$ withdrawn, and hence a new solution to $\mathbf{x}^M(\xi)$.

For non-trivial formulations of λ as a function of time or warped time ξ, equations (4.9) and (3.8) with the newly defined equations (4.7) and (4.8) will characterize completely the behavior of the middle vessel still pot composition as a function of the parameter $\lambda(\xi)$. Given that $\mathbf{x}^P$ remains only as a function of ξ and not of $\mathbf{x}^M$, equation (4.9) can be solved for $\mathbf{x}^M(\xi)$ with a simple use of integrating factors.

Next, we will explore the graphical implications of this limiting version of the

middle vessel column model. As seen in Figure 4-10, the distillate and bottoms product are invariant in time until the still pot composition encounters a pot composition boundary. Supposing that the parameter λ was kept constant throughout the operation of the column, then the following behavior will be expected:

1. The still pot composition will move away in the opposite direction from the net product composition, as given by $\mathbf{x}^P$ and defined by equation (4.10). This will continue until the still pot composition encounters a pot composition boundary of the basic distillation region.

2. Once the still pot composition encounters the pot composition boundary, it is now restricted in motion by the line which defines the pot composition boundary. A pot composition barrier of a ternary system has dimension one, which means that the motion of the still pot composition is now more restricted than before.

3. Once it enters the hyperplane of the pot composition boundary, the still pot composition obtains new alpha limit and/or new omega limit sets. This results in a new value for $\mathbf{x}^P$, which defines the new net product drawn from the column and a new vector cone of possible motion by the still pot composition. The new vector cone must necessarily lie on the line which defines the pot composition boundary (i.e., a one dimensional vector cone, or equivalently just a normal vector). This requirement that the vector cone lie on the line which defines the pot composition boundary is usually not a problem when the boundaries are not curved, which is our assumption in this analysis.

4. The still pot composition then moves along the pot composition boundary until it enters either the alpha limit set or the omega limit set of the pot composition boundary. Once the still pot composition enters the alpha limit set or the omega limit set, no additional composition change is possible, and the still pot composition remains constant until the still pot runs dry ($\xi \to \infty$).

The above list of events for the operation of the middle vessel column is illustrated in Figure 4-11 as before, for a) a generic 3-component ideal system and for b) the

3-component system of Acetone-Chloroform-Methanol, for ease of understanding.

As an aside, it should be noted that in the presence of curved separatrices, the still pot composition may cross the separatrices and the pot composition boundary and separatrices are no longer equivalent, and as such, the distillate and bottoms product may no longer be the alpha limit set or the omega limit set of the system. The still pot composition *may* be forced to follow the curvature of the separatrix, and the distillate and bottoms product composition are formed accordingly. These product compositions are indicative of the mass balance which must occur as the still pot composition is forced to trace out the curvature of the separatrix, and thus, the distillate or bottoms composition may actually sweep out a line of varying compositions as the still pot composition moves along the curvature of the separatrix. This behaviour is illustrated in Figure 4-12 for the Acetone-Benzene-Chlorofom system, and was first observed by Van Dongen and Doherty [15], and later substantiated by Bernot *et al.* [6].

Based on the analysis presented thus far regarding the product sequences drawn from a middle vessel column, it is appropriate at this point to define the batch distillation region for a middle vessel batch column. Similar to the definition of a batch distillation region for a batch stripper or a batch rectifier, the batch distillation region of a middle vessel column is given by the set of composition points which would result in exactly the same sequence of products in the rectifying and the stripping sections of the column over time. Suppose that the n sequence of cuts from a middle vessel column were given as ([D_1,B_1], [D_2,B_2], ... [D_n,B_n]) for a given initial still pot composition α (where the first term in the square bracket represents the distillate product, the second term in the square bracket represents the bottoms product of that given cut, and each set of terms in square brackets represents different cuts obtained from the middle vessel column). If the sequence of cuts for another initial composition β was given by ([d_1,b_1], [d_2,b_2], ... [d_n,b_n]), then α and β are in the same middle vessel batch distillation region if and only if $\{d_i = D_i \; \forall \; i \in [1, n] \}$ and $\{b_i = B_i \; \forall \; i \in [1, n] \}$. It should be noted that these middle vessel batch distillation regions will vary with λ and are only specified for a given value of λ. To illustrate this idea, the batch

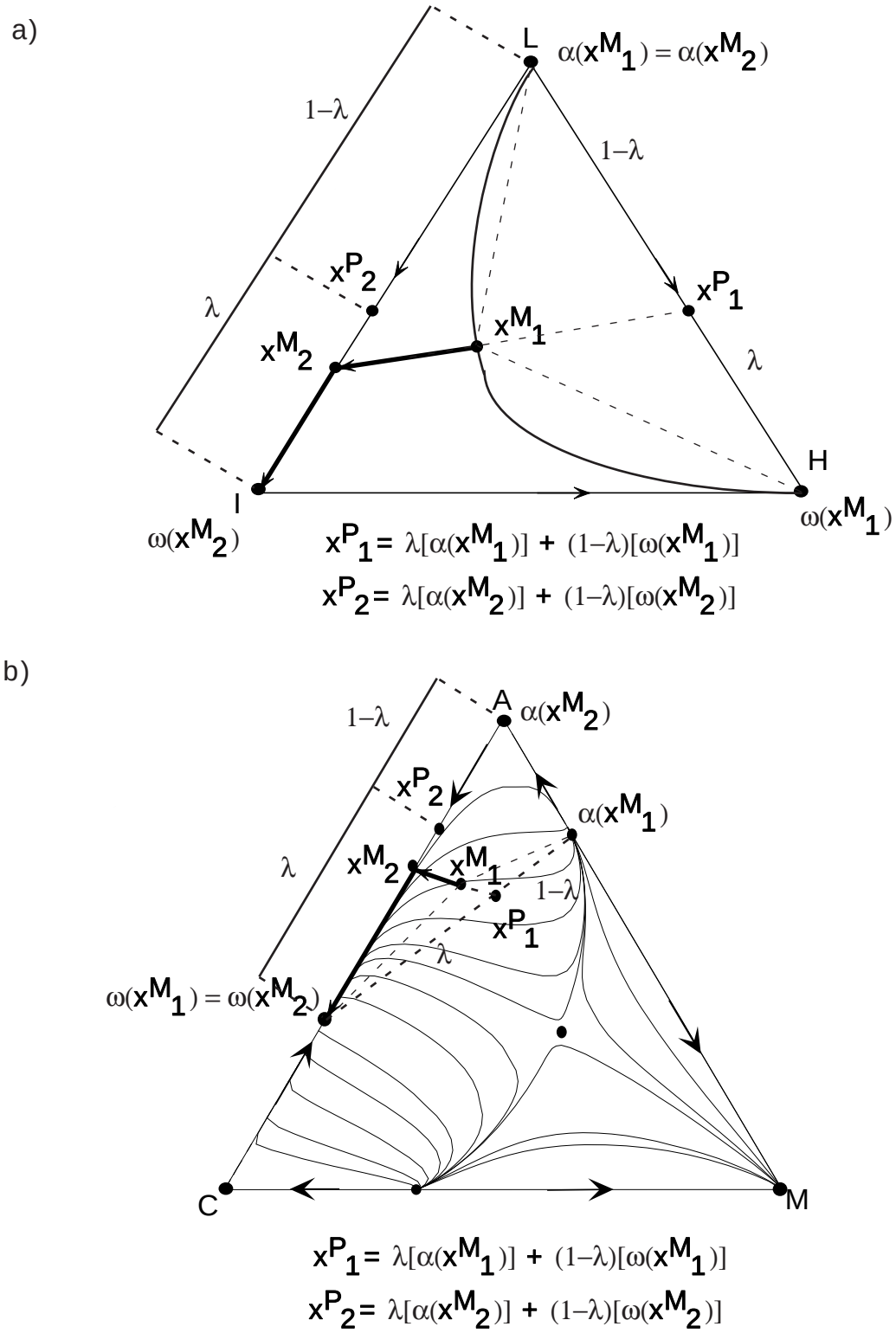

Figure 4-11: Distillate and Bottoms Composition in a Middle Vessel Column

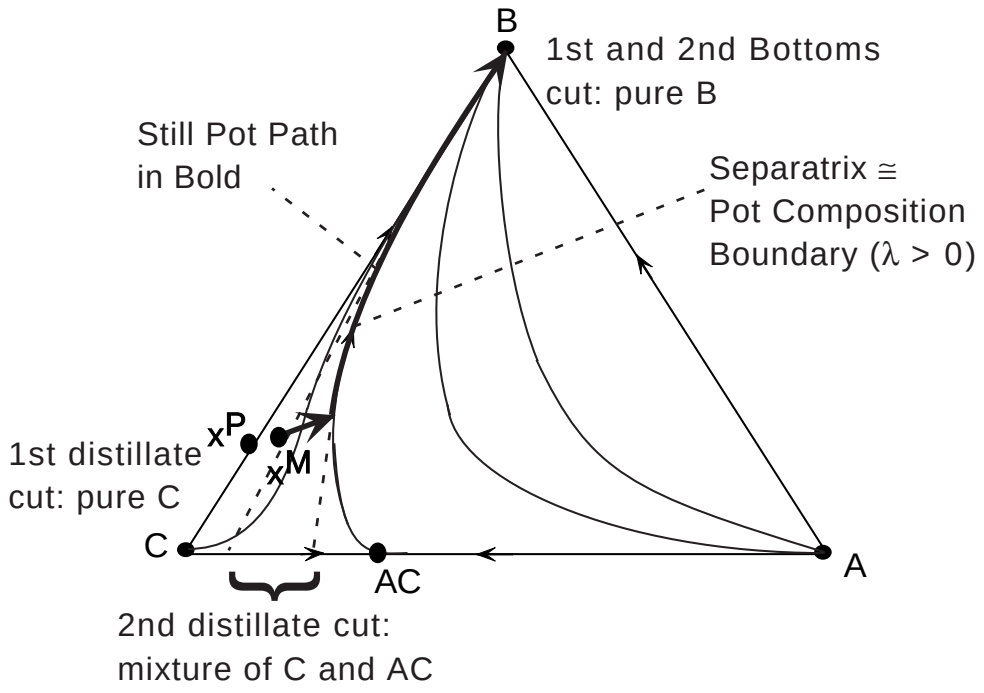

Figure 4-12: Variation of Product Composition in the Presence of Curved Separatrices

distillation regions for a stripper correspond to the middle vessel batch distillation regions when $\lambda = 0$, and the batch distillation regions for a rectifier correspond to the middle vessel batch distillation regions when $\lambda = 1$. These rectifier and stripper batch distillation regions are not necessarily equivalent (Ahmad and Barton [1]). Similarly, batch distillation regions for the middle vessel at different values of λ between 0 and 1 are not necessarily equivalent either.

Finally, the concept of steering the middle vessel composition first introduced in Chapter 3 (Figure 3-5 and 3-8), will also be explored here. As mentioned before, variation of λ with time will result in an ability to steer the still pot composition within the basic distillation region. Since the bottoms and distillate products are much more predictable now (given that they are unchanging within a given simple distillation region), the results of steering (or varying λ) are also much more predictable as a result. A simple illustration is provided in Figure 4-13. As we see in Figure 4-13, suppose that there was a certain composition mix which we would like to avoid (denoted by Regions marked by A), we would be able to steer our still pot composition in such a way that we continue to draw the light (L) and the heavy (H) components

in their pure forms, but at varying rates over time. Calculating the exact values of t_1, t_2, t_3 etc, will only be a matter of conducting an overall material balance, to see how long it would take to draw the required amount of material, before the target points $\mathbf{x}_1^M$, $\mathbf{x}_2^M$, $\mathbf{x}_3^M$ and $\mathbf{x}_4^M$ were reached. We would thus be able to control, with relatively good precision, the path of the still pot composition by varying λ with time (or warped time ξ), without a need for an elaborate feedback control loop.

4.3 Higher Dimensionality Systems

The same concepts used in the earlier section for the analysis of 3 component systems can also be applied to systems of higher dimensionality. To illustrate this, we will attempt to generalize the above description of the behavior of the still pot composition to a generic n-component system. Finally, a graphical analysis will also be presented for the generic 4-component system explored in Chapter 3, to show the applicability of the analysis presented.

As before, the distillate and bottoms composition are unchanging when the still pot composition remains within the same basic distillation region. The distillate and bottoms composition only change when the still pot composition encounters a pot composition boundary in the n-component system, and enters the $n-2$ dimension hyperplane of the pot composition boundary. This is because upon entering the $n-2$ dimension hyperplane, the mixture effectively becomes an $(n-1)$-component system, with new alpha limit and omega limit sets, and it is these alpha and omega limit sets which form the new distillate and bottom product compostions respectively. The hyperplane within which the pot composition boundary lies can also be thought of as a separate distillation region of lower dimension. These pot composition boundaries lie in a $n-2$ dimension hyperplane within the composition simplex, and are thus a subset of that hyperplane restricted by the constraints $\sum_{i=1}^{n} x_i = 1$.

It is thus possible to analyse the dynamics of the still pot composition relatively easily even for a 4-component system, given that the product compositions (both distillate and bottoms) are not continually changing with time, but instead undergo

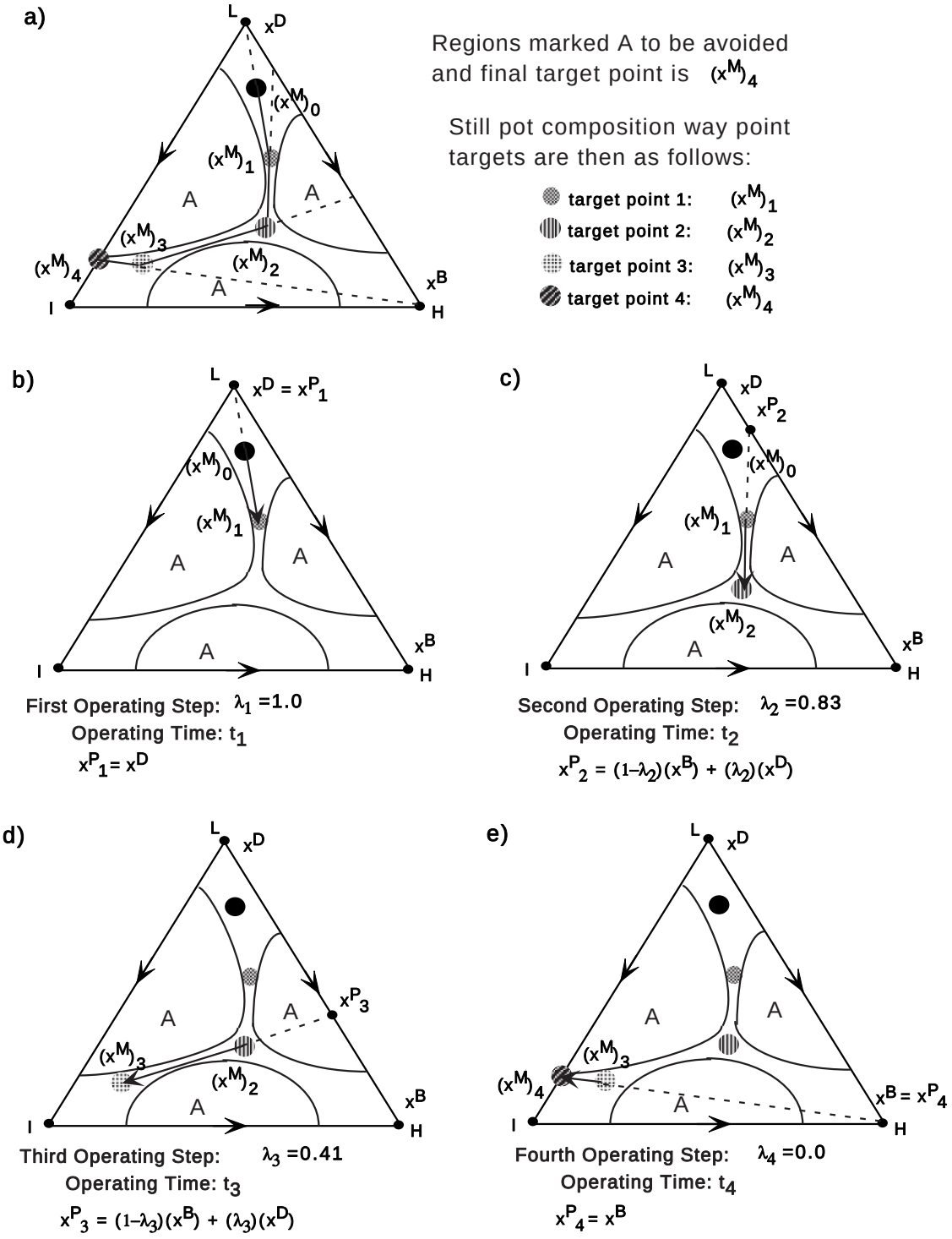

Figure 4-13: Steering the Still Pot Composition for the Limiting Case of Infinite Reflux and Infinite Trays

discrete changes only when the still pot composition encounters a pot composition boundary and enters the hyperplane of the pot composition boundary, which can be thought of as another basic distillation region of lower dimensionality. It should be noted that this change in the product compositions can be expressed as a function of time, but is more conveniently expressed as a function of the still pot composition $\mathbf{x}^M$, as was the case for the ternary system. A sample formulation is given by:

$$\begin{aligned} \mathbf{x}^M &\in [\text{basic distillation region A, } \mathbf{R}^{n-1}], \\ \mathbf{x}^D &= \text{alpha limit set(region A)}, \\ \mathbf{x}^B &= \text{omega limit set(region A)} \end{aligned} \tag{4.15}$$

$$\begin{aligned} \mathbf{x}^M &\in [\text{basic distillation region B, } \mathbf{R}^{n-2}], \\ \mathbf{x}^D &= \text{alpha limit set(region B)}, \\ \mathbf{x}^B &= \text{omega limit set(region B)} \end{aligned} \tag{4.16}$$

where basic distillation region B $\equiv$ pot composition boundary of region A. Hence, the product compositions and consequently the still pot dynamics is still completely defined by the current still pot composition and its location with respect to the basic distillation regions of various dimensionalities.

As in the earlier section, we will explore the graphical implications in this limiting version of the middle vessel column model for 4-component systems. As explained, the distillate and bottoms product are unchanging in time until the still pot composition encounters a pot composition boundary. Supposing that the parameter λ was kept constant throughout the operation of the column, the following behavior will be expected:

1. The still pot composition will move away in the opposite direction from the net product composition, as given by $\mathbf{x}^P$ and defined by equation (4.10). This will continue until the still pot composition encounters a pot composition boundary of the basic distillation region.

2. Once the still pot composition enters a pot composition boundary, it is restricted in motion by the hyperplane within which the pot composition boundary lies. Typically, a pot composition boundary of an n-component system (which was restricted within a $n-1$ dimension hyperplane as defined by $\sum_{i=1}^{n} x_i = 1$) has dimension $n-2$, which means that the motion of the still pot composition is now more restricted than before.

3. Once it enters the pot composition boundary hyperplane, the still pot composition now has a new omega limit set or a new alpha limit set or both. This results in a new value for $\mathbf{x}^P$, which defines the new net product drawn from the column and a new vector cone of possible motion by the still pot composition, which must necessarily lie within the same hyperplane.

4. The process repeats itself 1 through 4, until only the still pot composition finally enters an alpha limit set or an omega limit set and no further composition change of the still pot composition is possible.

The above list of events for the operation of the middle vessel column is illustrated in Figure 4-14 for a generic 4-component system. As mentioned in Chapter 3, the vector cone of possible motion for the still pot composition remains on a plane, despite being in a 3-dimension composition simplex. This is due to the fact that only two products are drawn from the column at any given time, hence the products, the initial still pot composition and the resulting still pot composition must all lie in the same plane.

In the presence of curved boundaries or with a finite reflux/reboil ratio and/or number of trays, the still pot composition may be able to cross the separatrices or pot composition boundaries, due to the topology of the residue curve map. However, more often than not, when a curved boundary is encountered, the still pot is forced to trace a path along the curved boundary. As such, the distillate and bottoms product may no longer be the stable and unstable nodes of the system. As the still pot composition is forced to trace out the curvature of the separatrix, the distillate and bottoms product composition are formed accordingly [15, 6] as explained in the

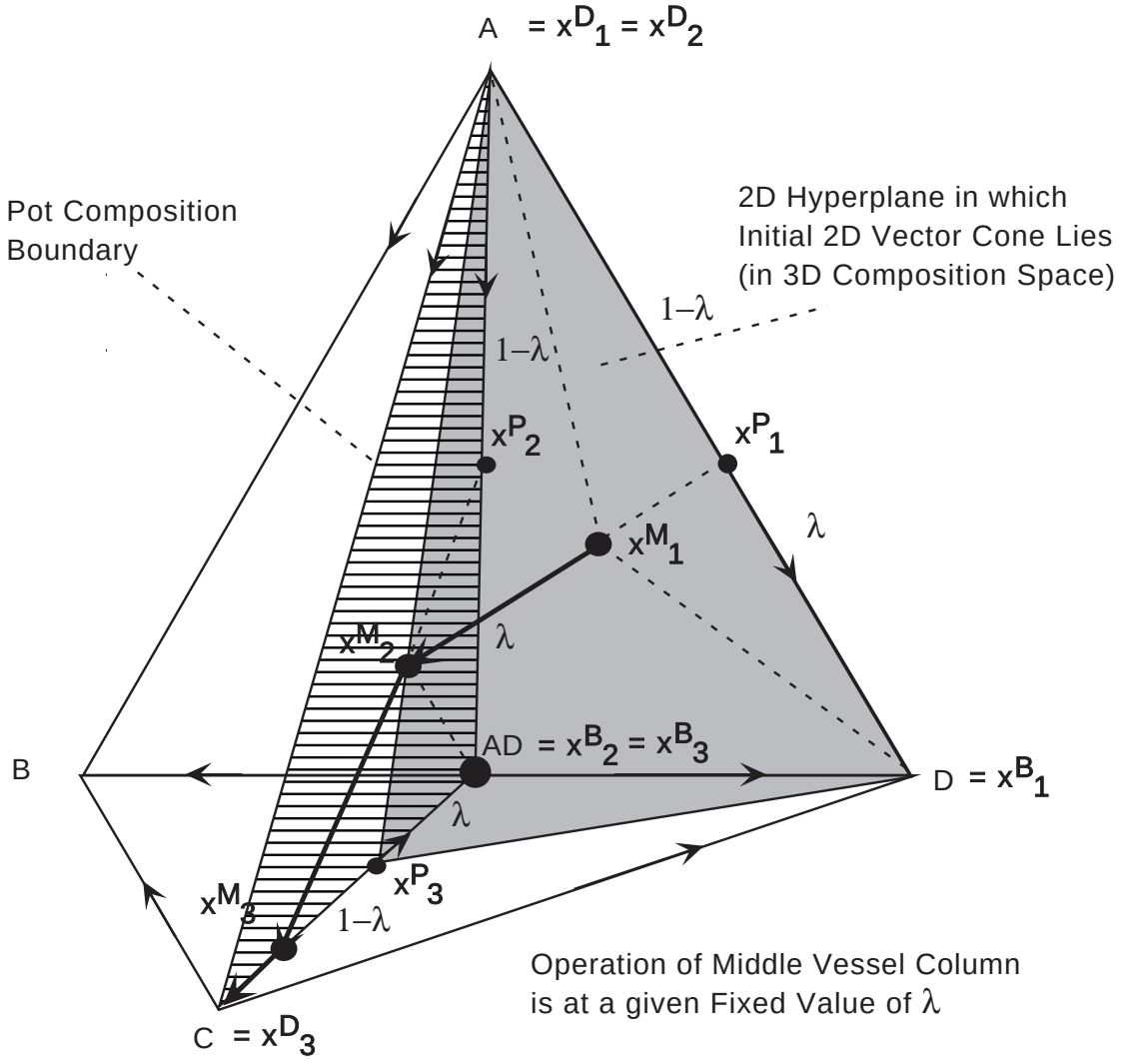

Figure 4-14: Distillate and Bottoms Composition in a Middle Vessel Column for a 4 Component System

earlier section for the 3 component system.

4.4 A Bifurcation Analysis of the MVC Batch Distillation Regions

As mentioned in Section 3.1, the middle vessel column can be thought of as a generalization of previous batch distillation columns (i.e., the rectifier and the stripper), as it encompassed both the batch rectifier ($\lambda = 1$) and the batch stripper ($\lambda = 0$). Given that the middle vessel column actually represents a range of behavior between the two limiting cases of the stripper and rectifier ($0 \leq \lambda \leq 1$), it would be appropriate to consider the behavior of the middle vessel column as a hybrid between the stripper and the rectifier. In particular, for mixtures where the batch distillation regions for the stripper and the rectifier are not the same, we would expect some sort of bifurcation in the behavior of the column and the batch distillation regions of the column from that of the stripper to that of a rectifier as λ varies from 0 to 1. Of particular interest is the transformation that occurs between fixed values of λ for 1) the middle vessel column batch distillation regions and 2) the behavior of the middle vessel column.

To illustrate our analysis in this section, we will consider one of the systems enumerated by Doherty and Caldarola [11] and Matsuyama and Nishimura [26], designated as the 001 system. It is one of the simplest ternary systems enumerated by Doherty, Caldarola, Matsuyama and Nishimura with only one binary azeotrope, but it will suffice for our analysis since the 001 system contains batch rectifying regions which are not equivalent to the batch stripping regions. The residue curves map of the 001 system is illustrated in Figure 4-15.

Using the tools developed by Van Dongen and Doherty, Bernot *et al.* for the analysis of the batch recitifier and batch strippers, the batch distillation regions for the rectifier and stripper (based on the definition of Ewell and Welch [16] of batch distillation regions), were found and labeled accordingly in Figure 4-16. As before,

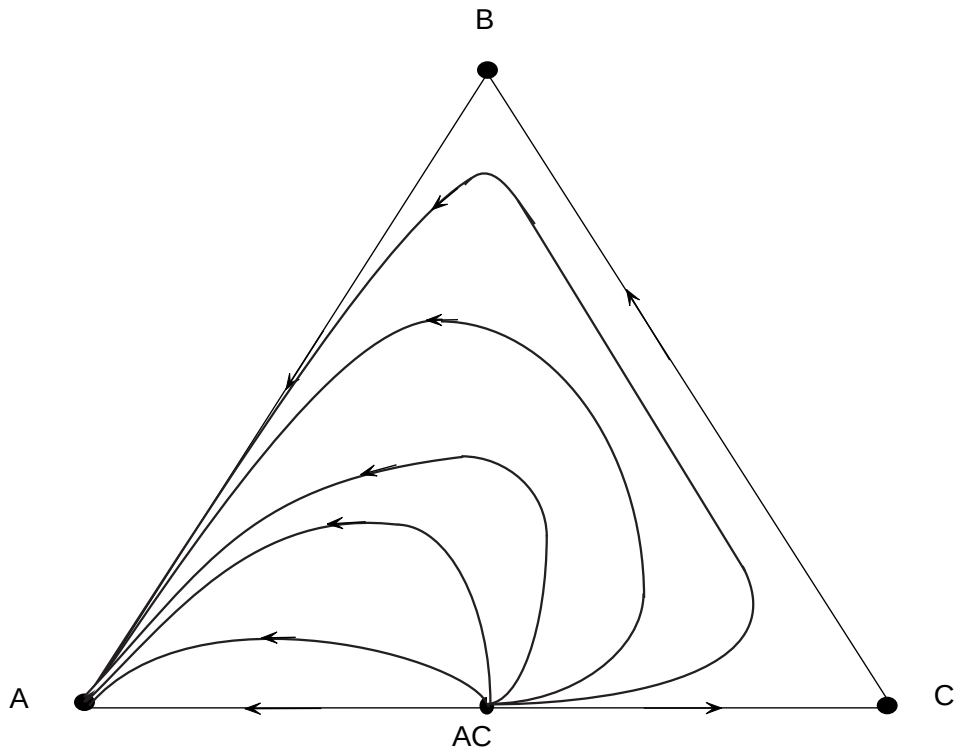

Figure 4-15: Residue Curve Map of the 001 System

we assume the limiting operating conditions of infinite trays and infinite reflux/reboil ratios.

As can be seen from Figure 4-16, there are 2 batch distillation regions (α and β) with non-zero volume for the batch rectifier, but only one batch distillation region with non-zero volume for the batch stripper configuration (γ). It should be noted that each of the A-B and B-C binary edges of the composition simplex, the line segments A-AC, AC-C amd B-AC, and each fixed point of the residue curve map, are individual batch distillation regions of zero volume (one-dimensional for the edges, zero-dimensional for the fixed point), as each of these "regions" will produce a unique sequence of cuts. For an initial still pot composition that lies on one of the binary edges, A-B or B-C or on one of the line segments A-AC and AC-C, each of the two fixed points (alpha and omega limit sets) in that batch distillation "region" will be drawn as distillate and bottoms product respectively, and the pot composition will stay on the edge/line segment. For an initial still pot composition that lies in one of

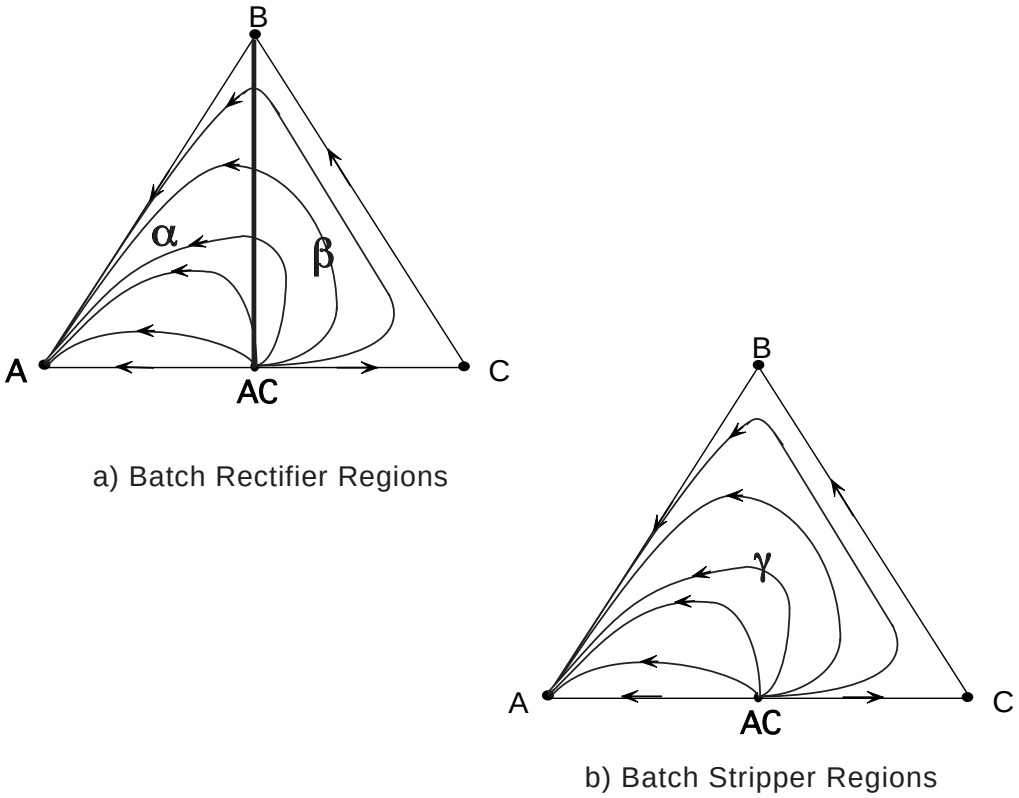

Figure 4-16: Batch Distillation Regions for the Stripper and the Rectifier in the 001 System

the fixed points, it will remain there, with both the distillate and bottoms product being of the same composition as that in the still pot (the alpha and omega limit sets of a fixed point are the fixed point itself). Of greater interest, however, are the non-zero volume batch distillation regions for the batch rectifier (α and β), and the batch stripper (γ); and how these volumes transform as the value of λ varies from $0 \rightarrow 1$ (i.e., as the middle vessel column deforms from being a pure stripper to a pure rectifier).

First, consider the derivation of these batch distillation regions. For the rectifier, any interior point of the composition simplex (i.e., one that does not lie in an edge or a fixed point) would draw azeotrope AC (which is the unstable node in this ternary mixture, and hence the alpha limit set of all the residue curves interior to the simplex) as the distillate product. Hence, any point with composition interior to region α would draw AC as the product until it encounters the A-B edge, where it will enter the batch distillation region of the A-B line segment, draw B, and the finally A as the product. Hence the product sequence is (AC, B, A). Correspondingly, any point with composition in region β would draw AC as the first product until it encounters the B-C edge, where it will enter the batch distillation region of the B-C edge, draw C and finally B as the product. The product sequence associated with β is then (AC, C, B). The product sequences for α and β are not equivalent, hence, they are separate batch distillation regions. For the stripper configuration, any point interior to the composition simplex (i.e., not lying in one of the edges or fixed points) will draw pure A as product, as it is the stable node of the ternary mixture, and hence the omega limit set of the residue curves passing through any point interior of the composition simplex. However, as can be seen from the topology of the residue curve map, any point in the simplex that draws A as a product, will eventually encounter the B-C edge, where it will draw B as the omega limit set of the still pot composition, and finally C as the last product. Hence, there is only one batch stripping region, with the product sequence given by (A, B, C).

Now, consider the operation of the middle vessel column at a given value of λ where $0 < \lambda < 1$. To allow us to better understand the variation of product cuts

with λ, it would be useful to consider the motion of the still pot in terms of it moving away from a "net product" as given by $\mathbf{x}^P$ (see Figure 3-4c and Section 4.2), which is the weighted average of the two products drawn with the weights given by λ (for $\mathbf{x}^D$) and $1-\lambda$ (for $\mathbf{x}^B$) as expressed in equation (4.10). Thus, for a given composition point interior to the composition simplex ($\alpha(\mathbf{x}^M) = AC$ and $\omega(\mathbf{x}^M) = A$), the net product will lie on the line segment AC-A connecting the two products drawn from the column, namely AC and A. Suppose a value of λ which produces a net product in $\mathbf{x}^P(0)$ as shown in Figure 4-17a. Next, draw a line from $\mathbf{x}^P$ to the fixed point of pure B, dividing the residue curve map into 2 regions, δ and ϵ. Further divide region δ into δ_1 and δ_2 by drawing a line from $\mathbf{x}^P$ to $\mathbf{x}^P_\delta$, where $\mathbf{x}^P_\delta$ is given by $\mathbf{x}^P_\delta = \lambda B + (1-\lambda)A$, the net product drawn from the middle vessel column (at this given λ) when the still pot composition is in the A-B binary edge. Region ϵ is also further divided by drawing a line from $\mathbf{x}^P$ to $\mathbf{x}^P_\epsilon$, where $\mathbf{x}^P_\epsilon$ is given by $\mathbf{x}^P_\epsilon = \lambda B + (1-\lambda)C$ and denotes the net product drawn from the column (at the current λ) when the still pot composition lies on the B-C binary edge. There are thus a total of 4 middle vessel batch distillation regions interior to the composition simplex with non-zero volume. It should be noted that each of the lines joining $\mathbf{x}^P$ to $\mathbf{x}^P_\delta$ and $\mathbf{x}^P_\epsilon$ are in themselves a separate middle vessel batch distillation region of zero volume.

Any initial still pot composition that lies within regions δ_i will then draw the net product $\mathbf{x}^P$ and eventually encounter the simplex edge given by line segment A-B. At this point, the alpha limit set for the still pot composition changes to pure B, and the products drawn from the column are now pure A (bottoms) and pure B (distillate), as illustrated in Figure 4-17b. The net product drawn from the middle vessel column is then denoted by $\mathbf{x}^P_\delta$. The middle vessel column will continue to draw this net product such that the still pot composition moves away from $\mathbf{x}^P_\delta$ until it enters the fixed points A (if the initial still pot composition was in δ_1) or B (if the initial still pot composition was in $delta_2$). Once the still pot composition enters one of these fixed points, the top and bottom products will both correspond to the still pot composition. The cuts from the middle vessel column for an initial still pot composition in region δ_1 can thus be characterized as ([AC,A], [B,A], [B,B]), where

Table 4.1: Middle Vessel Batch Distillation Sequence for Regions $\delta_{1,2}$ and $\epsilon_{1,2}$ of Non-Zero Volume

Region	First Cut	Second Cut	Third Cut
δ_1	[AC,A]	[B,A]	[B,B]
δ_2	[AC,A]	[B,A]	[A,A]
ϵ_1	[AC,A]	[C,B]	[B,B]
ϵ_2	[AC,A]	[C,B]	[C,C]

[AC,A] denotes that the distillate product is AC, the bottoms product is A, and the different sets of square brackets denote the different cuts (i.e., first cut is AC in the distillate, A in the bottoms, second cut is B in the distillate, A in the bottoms, and B in both the bottoms and the distillate of the last cut). A similar sequence obtained for δ_2 is then given by ([AC,A], [B,A], [A,A]).

Using a similar analysis for initial still pot composition in regions ϵ_i, recognizing that $\mathbf{x}_\epsilon^P$ is the net product drawn from the middle vessel column once the still pot composition encounters the B-C binary edge, the middle vessel batch distillation sequences are deduced for each of the regions ϵ_1 and ϵ_2 and summarized in Table 4.1.

As such, the δ_1, δ_2, ϵ_1 and ϵ_2 are four different middle vessel column batch distillation regions in the spirit of Ewell and Welch's definition. The pot composition boundaries between these regions are then:

1. The line segment that joins the fixed point B to the initial net product $\mathbf{x}^P(0)$, where $\mathbf{x}^P(0)$ is given by:

$$\mathbf{x}^P(0) = \lambda(\text{composition of } AC) + (1-\lambda)(\text{composition of } A) \tag{4.17}$$

2. The line segment that joins the initial net product $\mathbf{x}^P(0)$ to the net product on the A-B binary edge given by $\mathbf{x}_\delta^P$, where $\mathbf{x}_\delta^P$ is given by:

$$\mathbf{x}_\delta^P = \lambda(\text{composition of } B) + (1-\lambda)(\text{composition of } A) \tag{4.18}$$

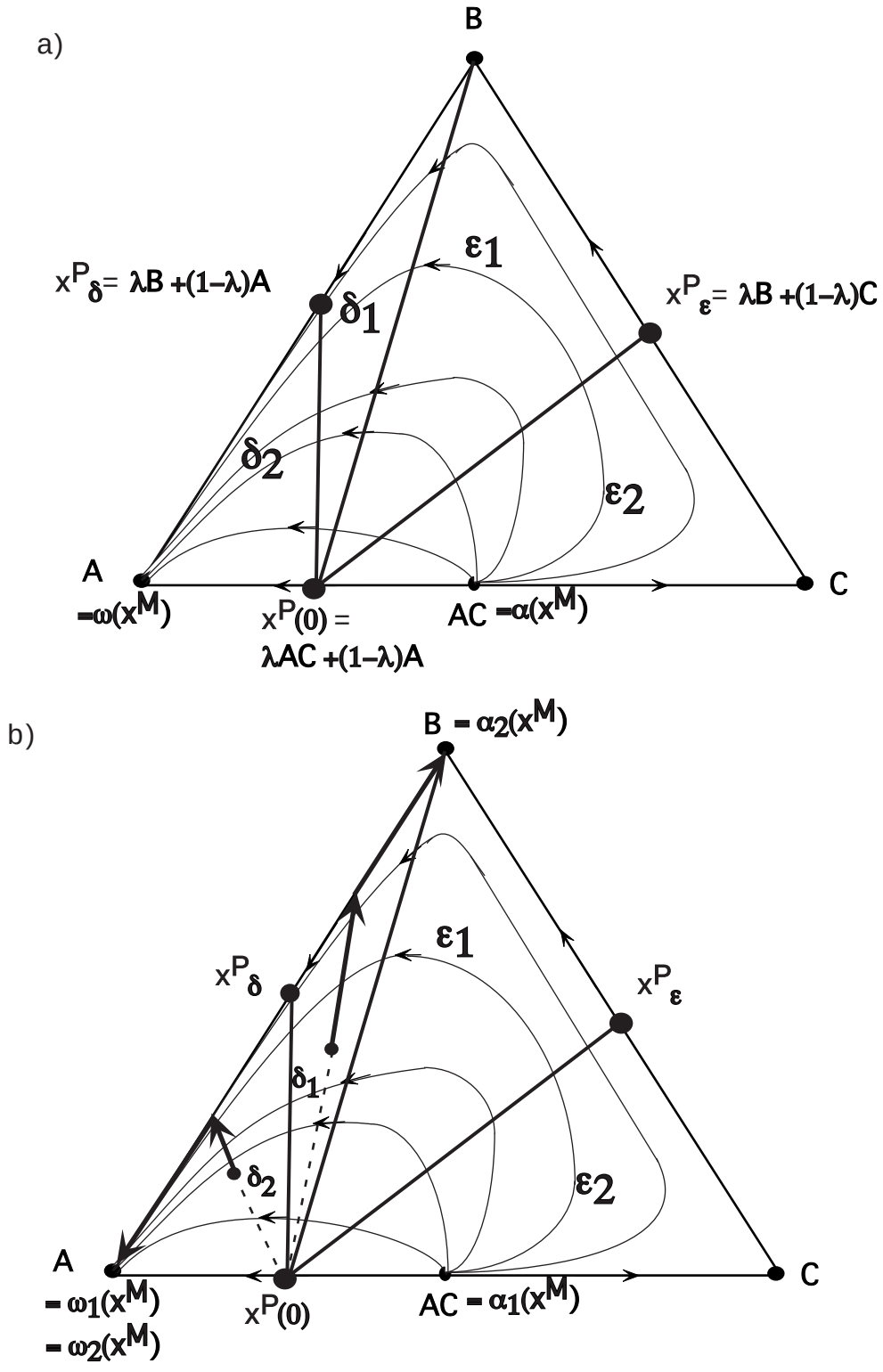

Figure 4-17: Batch Distillation Regions at a given Value of λ

3. The line segment that joins the initial net product $\mathbf{x}^P(0)$ to the net product on the B-C binary edge given by $\mathbf{x}_\epsilon^P$, where $\mathbf{x}_\epsilon^P$ is given by:

$$\mathbf{x}_\epsilon^P = \lambda(\text{composition of } C) + (1-\lambda)(\text{composition of } B) \tag{4.19}$$

As can be seen from our analysis, the motion of the still pot composition is more restricted (at a given λ where $0 < \lambda < 1$) for the middle vessel column, with 4 different distillation regions, as compared to either the batch stripper or the batch rectifier. In fact, if we had explored systems with separatrices, we would note that 1) stable separatrices served as pot composition boundaries for the batch rectifier but not for the stripper, and 2) unstable separatrices served as pot composition boundaries for the batch stripper but not the rectifier, but 3) stable and unstable separatrices both served as pot composition boundaries for a middle vessel column at a given λ. Thus, the still pot composition a middle vessel column is actually more restricted than that of either a stripper or a rectifier if λ is kept constant. However, the flexibility of the middle vessel column lies in the fact that the value of λ is variable during operation of the column. λ could take on any value between 0 and 1 inclusive, which means that it can cross both the stable separatrices (when $\lambda = 0$) and the unstable separatrices (when $\lambda = 1$). Hence, the still pot composition in a middle vessel oclumn is less restricted in motion than either a stripper or a rectifier, when λ is allowed to vary during the operation of the middle vessel column.

It should thus be noted, that these pot composition boundaries enumerated in our analysis only exists for the given value of λ that we had assumed. For a larger value of λ, the initial net product $\mathbf{x}^P(0)$ drawn from the middle vessel column will be nearer to unstable node (AC), while for a smaller value of λ, the initial net product $\mathbf{x}^P(0)$ drawn from the middle vessel column will be nearer to the stable node (A). Correspondingly, varying λ also varies $\mathbf{x}_\delta^P$ and $\mathbf{x}_\epsilon^P$ accordingly. The pot composition boundaries between these four regions will, however, always be from $\mathbf{x}^P(0)$ to the fixed point of pure B, from $\mathbf{x}^P(0)$ to the net product on the A-B edge, $\mathbf{x}_\delta^P$, and from $\mathbf{x}^P(0)$ to the net product on the B-C edge, $\mathbf{x}_\epsilon^P$. Hence, the pot composition boundary

will also shift accordingly with the variation of λ.

In the limit, as $\lambda \to 1$, $\mathbf{x}^P(0) = \mathbf{x}^D = \alpha(\mathbf{x}^M) = AC$, $\mathbf{x}^P_\delta = B$, $\mathbf{x}^P_\epsilon = C$, and the pot composition boundaries are transformed as follows:

$\mathbf{x}^P(0)$-B transforms into AC-B

$\mathbf{x}^P(0)$-$\mathbf{x}^P_\delta$ transforms into AC-B

and

$\mathbf{x}^P(0)$-$\mathbf{x}^P_\epsilon$ transforms into AC-C

Given that the line segment AC-C is along the composition simplex edge, and hence naturally a pot composition boundary, the only remaining pot composition boundary interior to the composition simplex, as $\lambda \to 1$ is thus given by the line segment B-AC, which is exactly the pot composition boundary for a batch rectifier.

Similarly, as $\lambda \to 0$, $\mathbf{x}^P = \mathbf{x}^B = \alpha(\mathbf{x}^M) = A$, $\mathbf{x}^P_\delta = A$, $\mathbf{x}^P_\epsilon = B$, and the pot composition boundaries are transformed as follows:

$\mathbf{x}^P(0)$-B transforms into A-B

$\mathbf{x}^P(0)$-$\mathbf{x}^P_\delta$ transforms into A-A

and

$\mathbf{x}^P(0)$-$\mathbf{x}^P_\epsilon$ transforms into A-B

The A-B line segment and A-A point are all edges of the composition simplex, and as such are naturally occuring pot composition boundaries. Hence, at $\lambda = 0$, we would expect no pot composition boundaries interior to the composition simplex, which is exactly what we would expect for the stripper configuration.

Thus, as λ sweeps out the value between zero and one, the pot composition boundaries transform accordingly as illustrated in Figure 4-18.

The first boundary given by $\mathbf{x}^P(0)$-B starts off as the line segment B-A ($\lambda = 0$) and swivels around point B until it reaches the line segment B-AC at $\lambda = 1$.

The second boundary given by $\mathbf{x}^P(0)$-$\mathbf{x}_\delta^P$ starts off as the fixed point A ($\lambda = 0$), and forms a line which spans the A-B edge and the A-AC edge. The triangle formed by A-B-AC and that formed by A-$\mathbf{x}^P(0)$-$\mathbf{x}_\delta^P$ are similar triangles by construction. This boundary eventually ends up merging with the first boundary into the line segment B-AC at $\lambda = 1$.

and finally,

The last boundary given by $\mathbf{x}^P(0)$-$\mathbf{x}_\epsilon^P$ starts off as the binary edge A-B (at $\lambda = 0$), and forms a line which spans the A-AC edge and the B-C edge. This boundary eventually ends up merging becoming the line segment AC-C, at $\lambda = 1$.

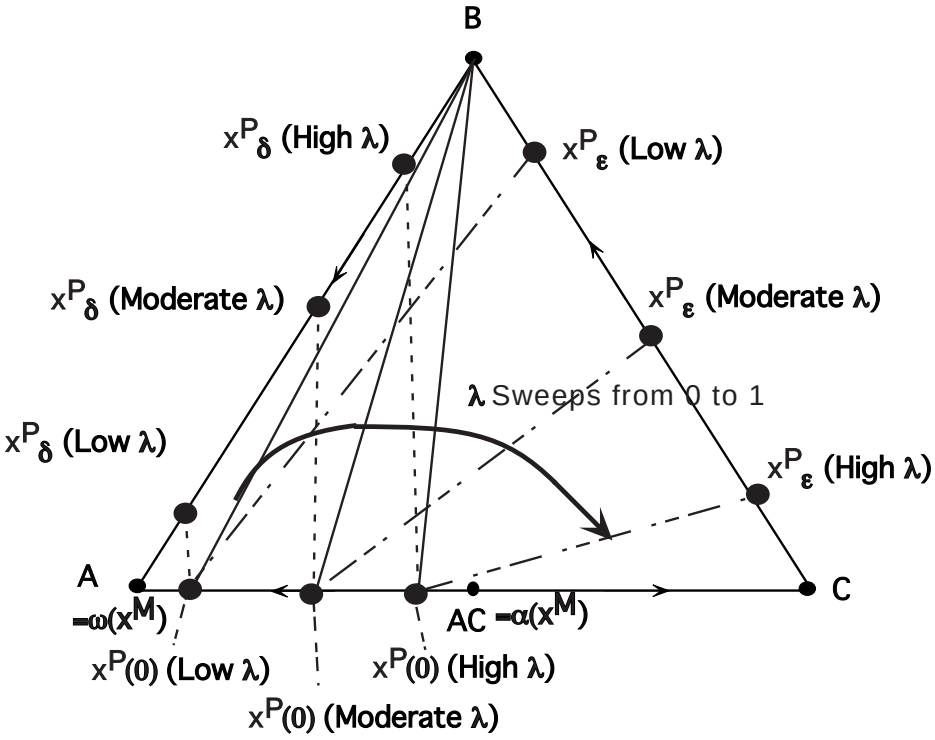

Figure 4-18: Sweep of Pot Composition Boundary as λ Varies Between 0 and 1

Correspondingly, the batch distillation region as given by the region δ_1 in Figure 4-17a starts off at $\lambda = 0$ as a batch distillation region of zero volume along the edge of the line segment B-C. It slowly expands in volume as λ increases, but as λ increases

further, this region than collapses back into a region of zero volume along the line segment B-AC. On the other hand, region δ_2 starts off as the fixed point A, slowly expands as λ increases, and finally becomes the region given by α in Figure 4-16 when $\lambda = 1$. Similarly, the batch distillation region given by the region ϵ_1 starts off at $\lambda = 0$ as a region of zero volume on the edge B-C, and expands as λ increases. It reaches a maxima in volume and then starts shrinking as λ increase further, and finally forms the region given by β in Figure 4-16 at $\lambda = 1$. On the other hand, region ϵ_2 starts off at $\lambda = 0$ as the entire interior of the composition simplex and slowly shrinks as $\lambda \to 1$, until at $\lambda = 1$, it is a distillation region of zero volume given by the line segment AC-C. The batch distillation regions for the rectifier and stripper thus transforms from one to the other as λ is varied in the middle vessel column, and the middle vessel column changes from the limiting case of a stripper (at $\lambda = 0$) into that of a rectifier (at $\lambda = 1$).

To illustrate the validity of this representation of the stripper and rectifier as specific cases of the middle vessel column, consider the product sequence of the stripper and the rectifier in each of the middle vessel batch distillation regions enumerated. We could imagine the stripper as a middle vessel column where no top product is drawn, in which case, it is the bottom product in the middle vessel column sequence that is relevant (i.e., the second term in the ordered pairs [x,y] given for the middle vessel column at each cut). However, we stated that region δ_1 transforms into the line segment A-B when $\lambda \to 0$, but the product sequence for δ_1 was ([AC,A], [B,A], [B,B]), with the relevant product sequence for the stripper being the second terms in each pair, namely (A,A,B) or (A,B). This is indeed the product sequence drawn from the stripper if the inital composition lay on the line segment A-B; pure A is drawn until all the A is exhausted, followed by pure B. Considering also the region δ_2, with the relevant product sequences given by ([AC,A], [B,A], [A,A]). δ_2 is given by the fixed point A at $\lambda = 0$, hence, the only product drawn from the stripper would be pure A. Examining the bottoms product sequence enumerated for region δ_2 in the middle vessel column, we obtain (A,A,A) or (A), which is indeed the behavior of the stripper. Conducting a similar analysis for the middle vessel column batch distillation

Table 4.2: Comparison of Middle Vessel Batch Distillation Sequences for Regions $\delta_{1,2}$ and $\epsilon_{1,2}$ vs Expected Stripper Sequences

MVC Regions	Middle Vessel Product Sequence	Resulting Region at $\lambda = 0$	Expected Stripper Product Sequence
δ_1	([AC,**A**],[B,**A**],[B,**B**])	A-B edge	(A, B)
δ_2	([AC,**A**],[B,**A**],[A,**A**])	Pure A	(A only)
ϵ_1	([AC,**A**],[C,**B**],[B,**B**])	A-B edge	(A, B)
ϵ_2	([AC,**A**],[C,**B**],[C,**C**])	Simplex Interior (γ)	(A, B, C)

regions given by ϵ_1 and ϵ_2, the expected products in a stripper and a middle vessel column is tabulated for each region and compared to each other in Table 4.2. As can be seen from Table 4.2, the bottoms product of the middle vessel column does indeed predict the product obtained from a stripper in the appropriate middle vessel batch distillation region.

Next, consider the case of the batch rectifier. As an inverse of the above analysis, it would be the first term in the square brackets of the middle vessel column product sequence that would be relelvant for a batch rectifier. For the batch distillation region given by δ_1, as $\lambda \to 1$, the region eventually becomes the line segment B-AC. Operation in a rectifier of a composition on the line segment would then yield as products (AC,B), which is completely analogous to the expected distillate product in the middle vessel column product sequence ([AC,A],[B,A],[B,B]). Similarly for region δ_2, as $\lambda \to 1$, the region eventually becomes the region α as given in Figure 4-16. We would then expect the products to be (AC, B, A) for a rectifier with initial still pot composition in region α. This is again analogous to the distillate products of the expected middle vessel product sequence of ([AC,A],[B,A],[A,A]) for δ_2. A similar analysis can also be conducted on the regions ϵ_1 and ϵ_2 and the results are summarized in Table 4.3. As can be seen from Table 4.3, the distillate product of the middle vessel column does indeed predict the product obtained from a rectifier in the appropriate middle vessel batch distillation region.

It seems that the above analysis has been about the deforming of batch distillation regions; the term "bifurcation" does not seem appropriate for describing the

Table 4.3: Comparison of Middle Vessel Batch Distillation Sequences for Regions $\delta_{1,2}$ and $\epsilon_{1,2}$ vs Expected Rectifier Sequences

MVC Regions	Middle Vessel Product Sequence	Resulting Region at $\lambda = 1$	Expected Rectifier Product Sequence
δ_1	([**AC**,A],[**B**,A],[**B**,B])	B-AC line segment	(AC, B)
δ_2	([**AC**,A],[**B**,A],[**A**,A])	Region α	(AC, B, A)
ϵ_1	([**AC**,A],[**C**,B],[**B**,B])	Region β	(AC, C, B)
ϵ_2	([**AC**,A],[**C**,B],[**C**,C])	AC-C line segment	(AC, C)

situation. However, a bifurcation does indeed occur at each composition point within the composition simplex with this deforming of the batch distillation regions. Consider a composition that lies interior to the composition simplex; as an example take the point ϕ in Figure 4-19. Let the initial value of λ be 0 (i.e., the middle vessel column behaves like a stripper). There is only one batch distillation region for the whole interior of the composition simplex (γ in Figure 4-16 or ϵ_2) and ϕ consequently falls within this region, with the corresponding product sequences drawn as given by ([AC,A], [C,B], [C,C]). Now, as λ increases, there would exist values of $\lambda = \lambda_{bifur,i}$, $i = 1 \ldots 3$ at which each of the 3 pot composition boundaries (given by line segments $\mathbf{x}^P(0)$-$\mathbf{x}^P_\epsilon$, B-$\mathbf{x}^P(0)$, and $\mathbf{x}^P(0)$-$\mathbf{x}^P_\delta$) crosses the point ϕ, and ϕ changes its location from one middle vessel batch distillation region to another. $\lambda_{bifur,1}$ represents a switch in behavior for point ϕ from that of region ϵ_2 to that of ϵ_1. $\lambda_{bifur,2}$ represents a switch in behavior for point ϕ from that of region ϵ_1 to that of δ_1, while $\lambda_{bifur,3}$ represents a switch in behavior for point ϕ from that of region δ_1 to that of δ_2.

Based on the above analysis, initial still pot compositions which lie within the region α in Figure 4-16 will exhibit bifurcation behavior at 3 different values of λ as λ varies between 0 and 1, with $\lambda_{bifur,i}$ values characteristic to each initial still pot composition. Initial still pot compositions which lie within the region of β in Figure 4-16 will however exhibit only one bifurcation point, switching in behavior from that of region ϵ_2 to that of region ϵ_1 as λ varies from 0 to 1.

Finally, with this bifurcation behavior in middle vessel columns, it can be seen that the pot composition boundaries of the traditional strippers and rectifiers are no

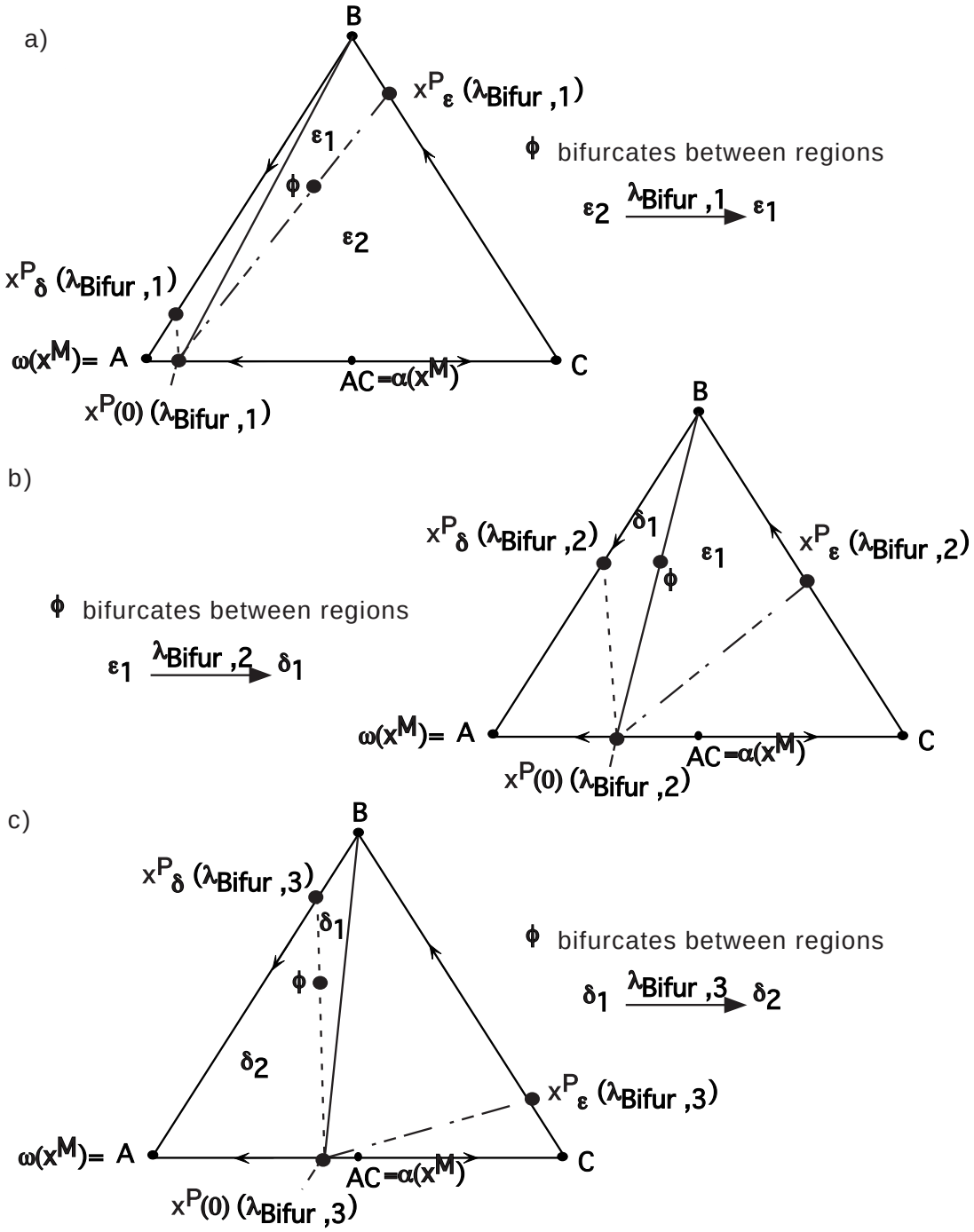

Figure 4-19: Bifurcation Behavior at a Given Point as λ Varies Between 0 and 1

longer valid for the middle vessel column if λ is allowed to vary during the operation of the column. It is only pot composition boundaries that correspond to both the stripper and rectifier configuration which remain as pot composition boundaries for the middle vessel column if λ is allowed to vary during the operation of the middle vessel column. Such a pot composition boundary exists at the same spatial location for all values of λ such that as λ varies from 0 to 1 the boundary exists at all values of λ inclusive of 0 and 1, and is hence common to both rectifier and the stripper.

In our 001 system, consider the pot composition boundary for the batch rectifier (line segment AC-B). Let a point ρ_1 be within the batch rectifier distillation region given by α, as illustrated in Figure 4-20a. An initial composition point such as ρ_1 would be unable to cross the rectifier pot composition boundary as given by line segment AC-B. However, in the middle vessel column, we would be able to vary the value of λ, such that the pot composition boundary given initially by the line segment AC-B will shift, and eventually, with an appropriate value of λ, the point ρ_1 would lie in the middle vessel batch distillation region denoted as ϵ_1 in Figure 4-17. The products from the middle vessel column given the location of ρ_1 in the region ϵ_1 would then be AC (distillate) and A (bottoms), with the still pot composition moving towards the B-C edge. Once the still pot composition crosses the AC-B line segment and arrives at a point such as ρ_2 in Figure 4-20b, the middle vessel can revert to its operation as a batch rectifier, and the pot composition would now be in the batch rectifier distillation region given by β. The still pot composition has thus effectively crossed over from region α into region β. The traditional pot composition boundary for a rectifier (line segment AC-B) is thus, not a pot composition boundary in a middle vessel column. Thus, pot composition boundaries which are not common to both the stripper and rectifier configurations are not pot composition boundaries for the middle vessel column that is allowed to operate at all values of λ. It should be noted however, that separatrices which form pot composition boundaries for either the stripper (unstable separatrices) or the rectifier (stable separatrices), remain as pot composition boundaries for all values of $0 < \lambda < 1$. It is only at $\lambda = 0$ that a stable separatrix is not a pot composition boundary for the middle vessel column,

and at $\lambda = 1$ that an unstable separatrix is not a pot composition boundary for the middle vessel column. However, keeping in mind that a middle vessel column can be operated at all values of $0 \leq \lambda \leq 1$, the middle vessel column is able to cross both the stable and unstable separatrices.

It should be noted that not all pot composition boundaries which are common to both the stripper configuration and the rectifier configuration, remain as pot composition boundaries for the middle vessel column of varying λ. The true criterion for a pot composition boundary being applicable to all values of λ ranging from 0 to 1, is that this particular boundary must not transform in any way as λ varies between 0 and 1. One such example is illustrated in a generic 020 system in Figure 4-21.

As shown in Figure 4-21, the interior of the composition simplex is divided into 8 middle vessel batch distillation regions of non-zero volume, X_1 through X_8, at a given value of $\lambda \neq 0$ or 1. The boundaries that separate this regions are then given by Y_1 through Y_7 as denoted. As $\lambda \to 0$, Y_1 transforms into the fixed point A, Y_2 and Y_3 both tranform into the line segment A-AC, Y_5 and Y_6 transforms into the line segment AC-C, while Y_7 transforms into the fixed point C. The pot composition boundary of Y_4 however remains the same as $\lambda \to 0$. Similarly as $\lambda \to 1$, Y_1 and Y_2 transforms into the line segment B-AC, Y_3 and Y_5 transforms into fixed point B, while Y_6 and Y_7 transform into line segment B-AC. Y_4 is again invariant as $\lambda \to 1$. As such, Y_4, which is a pot composition boundary common to both the stripper ($\lambda = 0$) and the rectifier configuration ($\lambda = 1$), and invariant in λ (i.e., common to all values of λ), will be a pot composition boundary for the middle vessel column. It should be noted that a necessary condition for a middle vessel pot composition boundary is that it must be a boundary that is common to both the stripper and the rectifier configurations, but it is not a sufficient condition. The sufficient condition states that this pot composition boundary common to both the rectifier and the stripper, must remain unchanging as λ varies between 0 and 1.

The removal of pot composition boundaries not common to both the rectifier and the stripper in a middle vessel column capable of operating at all values of λ thus affords a greater degree of freedom to the middle vessel column as compared to

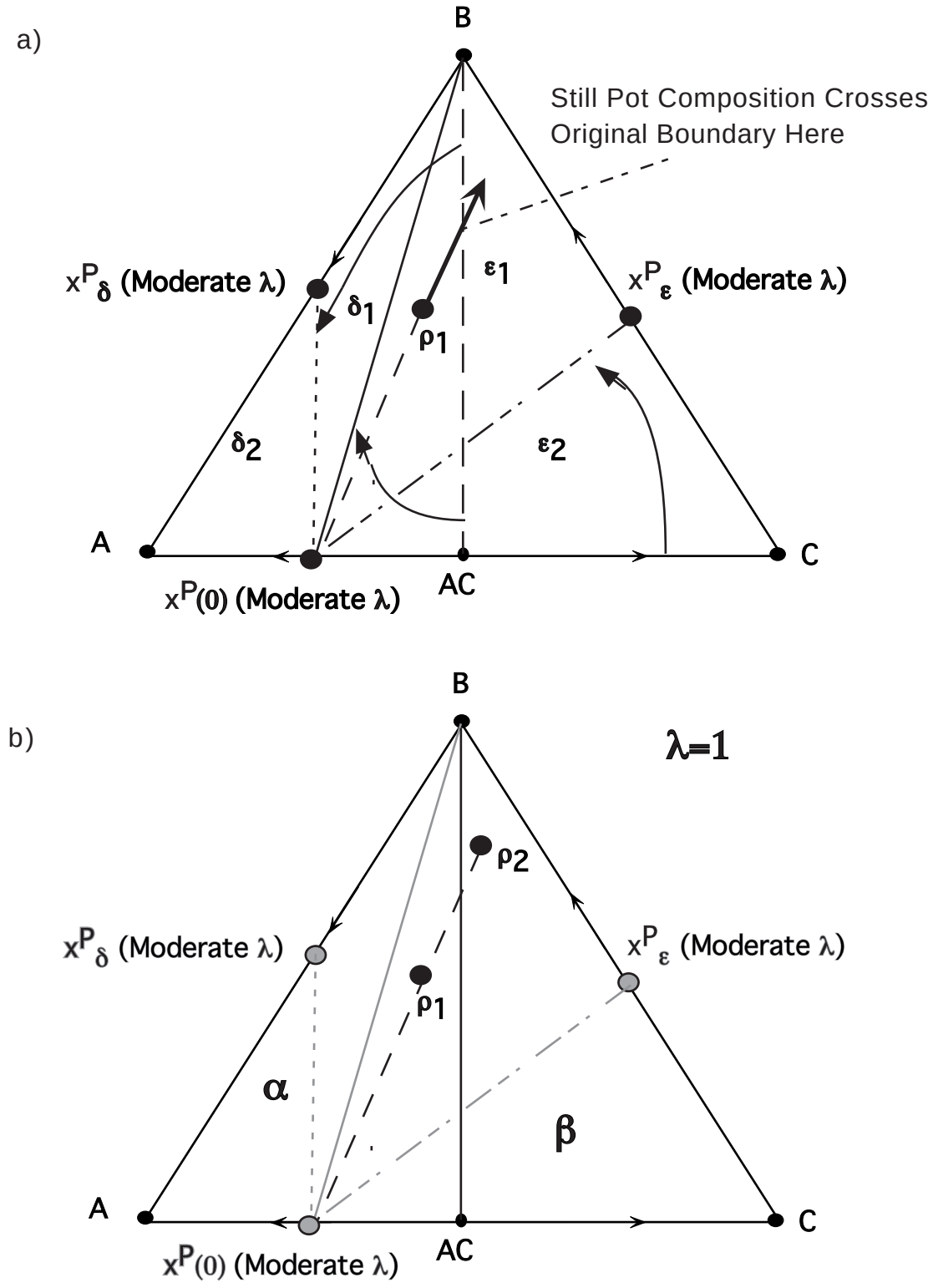

Figure 4-20: Removal of Pot Composition Boundaries that are Not Common to Both Stripper and Rectifier in a Middle Vessel Column

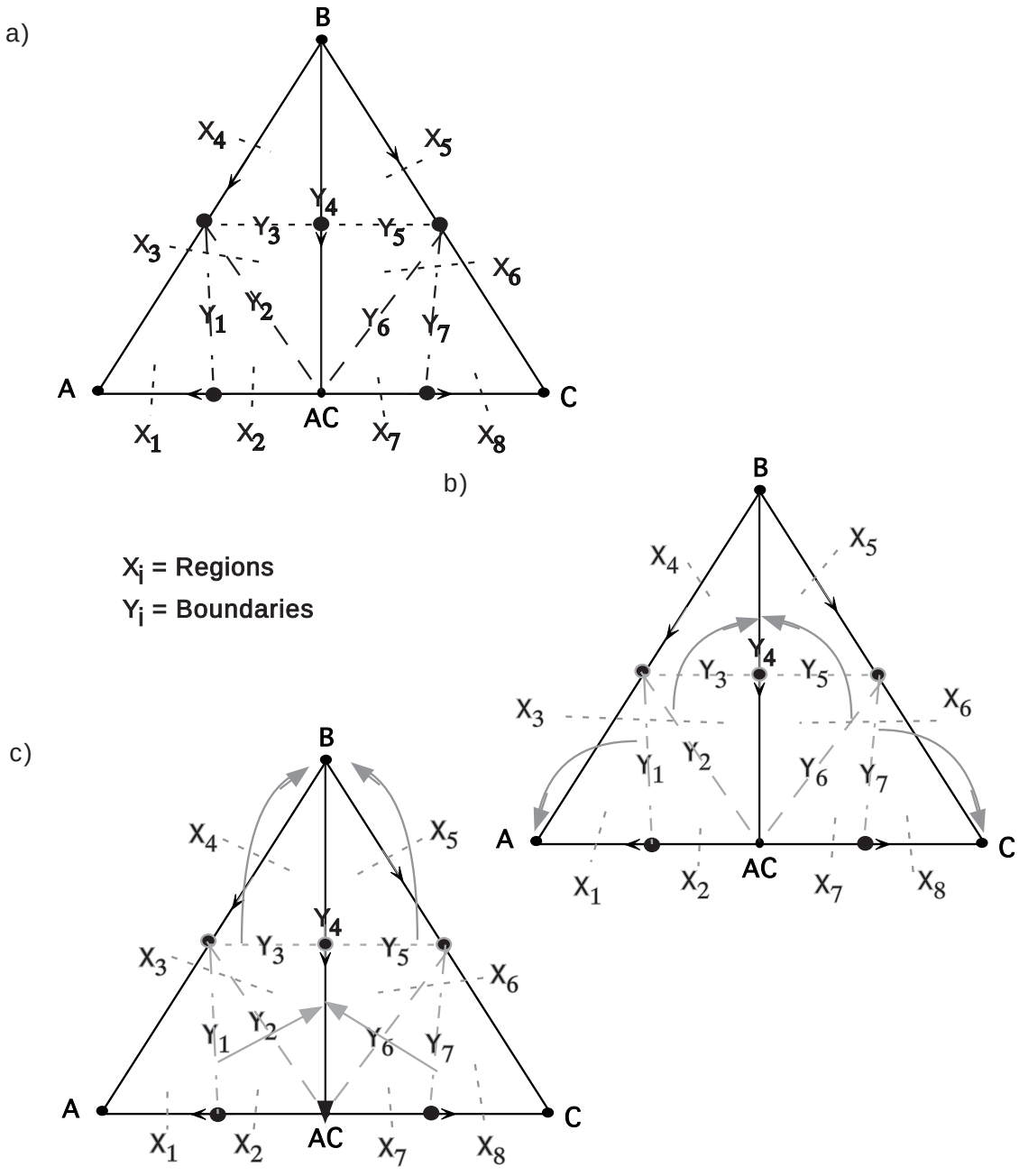

Figure 4-21: Pot Composition Boundary Invariant as λ Varies Between 0 and 1

that of a traditional batch stripper or batch rectifier. It is this non-equivalency of batch distillation regions in the stripper and rectifier, which allows the middle vessel configuration to traverse between batch distillation regions of traditional column configurations. It will also afford a greater variety of possible variations as will be shown in Chapter 5. It should be noted, however, that it might be possible to move from one conventional (stripper or rectifier) region to another, but the reverse movement might not be possible. Taking our example, it was possible to move from region α into region β by operating the middle vessel column cleverly, but it would not have been possible to move from the batch rectifier region of β into the batch rectifier region of α, due to the way in which bifurcation occurs.

In summary, the middle vessel batch distillation region defined for a given λ is actually much more constricted than that of either the traditional stripper or rectifier. However, due to the variability of λ in the operation of a middle vessel column, the batch distillation region for the middle vessel column operated at varying λ thus becomes less restricted than either the stripper or the rectifier, due to its ability to cross pot composition boundaries which are not common to both the stripper and the rectifier. It should also be noted that in our analysis, we have concentrated on "mass-balance" pot composition boundaries, and not separtrix-type pot composition boundaries. Mass-balance boundaries are boundaries that arise due to the fact that the pot composition must move in a straight line away from its net product, and hence, it is restricted in its possible product sequences. Separatrix-type boundaries, however, restrict the motion of the still pot composition due to a change in the alpha or omega limit set of the still pot composition. Separatrix-type boundaries do not transform continuously over varying values of λ, but undergo discrete step changes: from being a boundary to not being a boundary at all. A stable separatrix is a boundary for the middle vessel column for all values of $0 < \lambda \leq 1$, but ceases to be a boundary at $\lambda = 0$. Similarly, an unstable separatrix is a boundary for the middle vessel column for all values of $0 \leq \lambda < 1$, but ceases to be a boundary at $\lambda = 1$. An example is illustrated in Figure 4-22, for the acetone, benzene, chloroform system, where the rectifier pot composition boundary is a separtrix-type boundary, but the

stripper pot composition boundary is a "mass balance" type boundary. Incorporating this insight into the above analysis developed for "mass-balance" type separtrices, bifurcation anaylses can also be conducted on systems with separatrices. It should be noted that these concepts are also applicable to system of higher dimensions, where there are pot composition boundaries made up of bundles of trajectories, some of which are separatrices (separatrix-type boundary) and "mass-balance" pot composition boundaries which are planes indicating the different regions in which product compositions would differ.

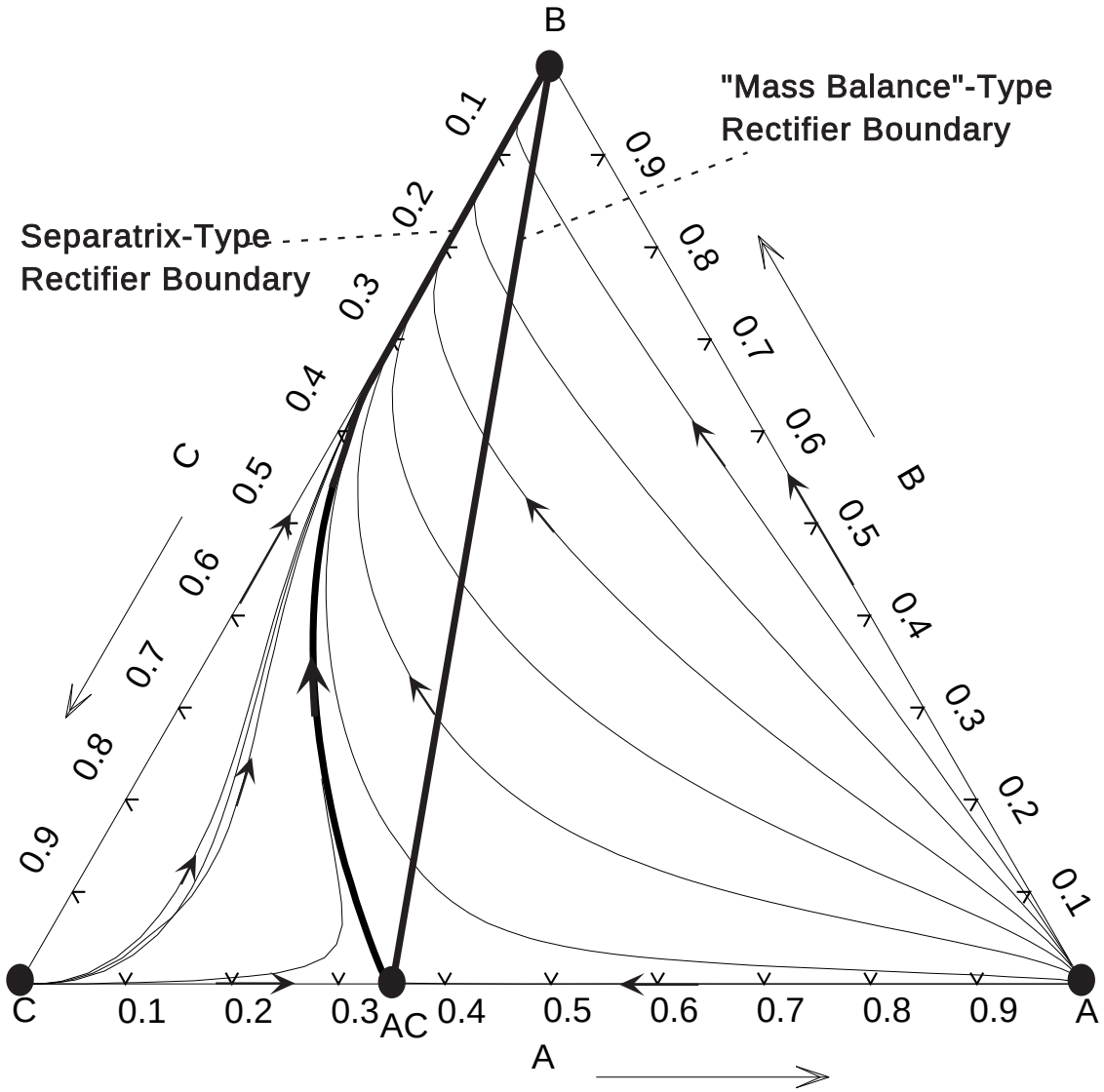

Figure 4-22: Separatrix-type Pot Composition Boundaries versus "Mass-Balance"-type Pot Composition Boundaries

Lastly, it should be noted that a similar analysis to that described in this section can then be extended to all residue curve maps of all dimensions for which the batch stripper regions differ from that of the batch rectifier regions. Bifurcation of these regions as a function of λ can then be characterized appropriately. The consequent removal of batch distillation boundaries due to this bifurcation with the variation of λ can then be used to traverse the pot composition boundaries of the traditional batch stripper and rectifier columns, and possibly afford a richer variety of separation possibilities not possible in traditional stripper or rectifier batch distillation columns.

4.5 More on the Equivalency of the Middle Vessel Column vs a Stripper and a Rectifier

As mentioned in Section 3.3, separation of a mixture in the middle vessel column is theoretically equivalent to distillation for an infinitessimal operating period in a stripper followed by a second infinitessimal operation period in a rectifier, or vice versa.

This theoretical equivalence extends beyond the infinitessimal operation of the rectifier and stripper in the limit of infinite trays and infinite reflux/reboil ratios. Due to the property of product composition invariance for finite periods of time under these limiting conditions, variations in the still pot composition would not affect the composition of the products drawn from the column. Thus, as first briefly explained in Chapter 3, an infinitessimal operating step would not be required for each of the stripper and/or rectifier operating stages, as even a discrete change in the still pot composition will not change the stripper (bottoms) product or the rectifier (distillate) product.

Thus, the equivalence of the rectifier and the stripper to that of the middle vessel column can now be extended to discrete operating steps with the stripper and the rectifier. An example is shown for a generic ternary mixture with no azeotropes in Figure 4-23. Figure 4-23a shows the required still pot composition path with the value

of λ that would allow the middle vessel to achieve the desired path, 4-23b shows the possible operating procedure using infinitessimal rectifier and stripper moves, so as to duplicate the original path achieved by the middle vessel column, and finally in Figure 4-23c, the same final pot composition and product compositions are obtained by using first a rectifier, then followed by a transfer to a stripper, with only one transfer occuring at point α. The equivalent operation can also be achived using a discrete step with a stripper followed by a transfer (at point β) to a rectifier with another discrete operating step, as shown in Figure 4-23d. The need for infinitessimal stripper and rectifier steps in non-limiting columns was due to the changing product compositions which occur with changes in the still pot composition; thus with the limiting column with infinite equilibrium trays this requirement is no longer relevant.

With this equivalency of the rectifier and the stripper versus that of a middle vessel column, it would seem that the middle vessel column is indeed relatively irrelevant. In fact, it is indeed true that the middle vessel column provides negligible advantages over the stripper/rectifier combination during the operational stage of the distillation (i.e., when the products are being drawn). Firstly, energy savings for the production of vapor in the distillation columns may be halved, because in the stripper/rectifier combination there are two operational stages each requiring an approximately equal amount of energy as that supplied to a middle vessel column. However, such energy savings are probably irrelevant in the pharmaceutical or speciality chemical industries, who are the main users of batch distillation technology. Secondly, there are also minimal savings in terms of time as well, provided a relatively large number of batches are to be processed. In the middle vessel column, 2 streams are drawn at the same time, the distillate and the bottoms product, but in the combined operation of the rectifier and the stripper, both columns can be operating at the same time after the initial startup phase where only one column is operating by pursuing an overlapping operation policy of repeated batches. Suppose that we use a rectifier followed by a stripper, then after the first batch of mixture is processed by the rectifier, it is transfered to the stripper, while a second batch of mixture is added to the rectifier.

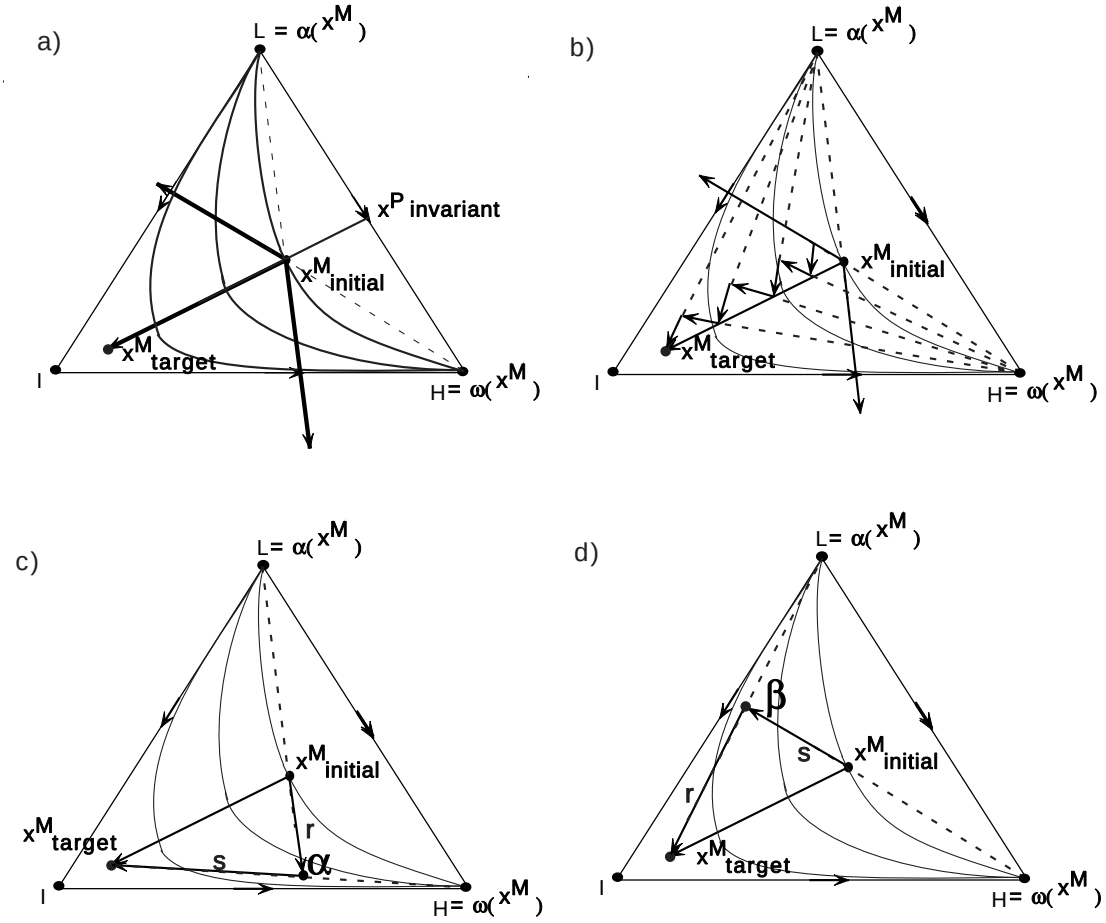

Figure 4-23: Pot Composition Path Using a Middle Vessel Column vs a Stripper and a Rectifier

Hence, at any time after the first batch, there would be the n-th batch in the stripper, and the $(n+1)$-th batch in the rectifier; which implies that at any point in time, both columns are operating, and two product streams are being drawn at any point in time as well. Thus, the middle vessel column does not really afford any time savings in terms of actual column operating time either. Hence, theoretically, there would be no advantage of using a middle vessel column.

However, in the practical operation of any distillation column, there are always overheads involved in processing other than the actual operation of the column. There is usually a startup-stage at total reflux before any products are drawn from the column, as it takes time for the composition profile in the column to reach the desired quasi-steady state such that the desired product can be drawn from the column. There is also processing time required for transfer between the columns. Finally, there is also the shut-down stage, where the contents in the column have to be cooled before they can be safely transfered to another distillation column or storage container. These overheads will actually still be the same for the contending configurations, if there is only one rectification and one stripping stage required (as in Figure 4-23c,d). To see this equivalency, consider the Gantt charts for operating the middle vessel column and the Gantt chart for operating the combined operation of the rectifier and the stripper with overlapping schedules of the columns, as shown in Figure 4-24.

Making reasonable assumptions of equal startup, shutdown and transfer times required for any type of column of 0.5 hours each, we set the operating time in the columns (when product is drawn) to be 5 hours. For the middle vessel column, there is a startup time of 0.5 hours, an operating time of 5 hours, a shutdown time of 0.5 hours and a transfer time of 0.5 hours into the pot and 0.5 hours out of the pot, resulting in a total processing time of 7 hours per batch of product. Compare this to the overlapping operation of the batch rectifier and stripper. Assume that the operating time in each column remains the same at 5 hours (i.e., same number of stages, same rate of product withdrawal). For the first batch, assuming that a rectifier is used first, the mixture is charged into the rectifier over 0.5 hours, followed by a startup time of 0.5 hours, an operating time of 5 hours, and a shutdown time of 0.5

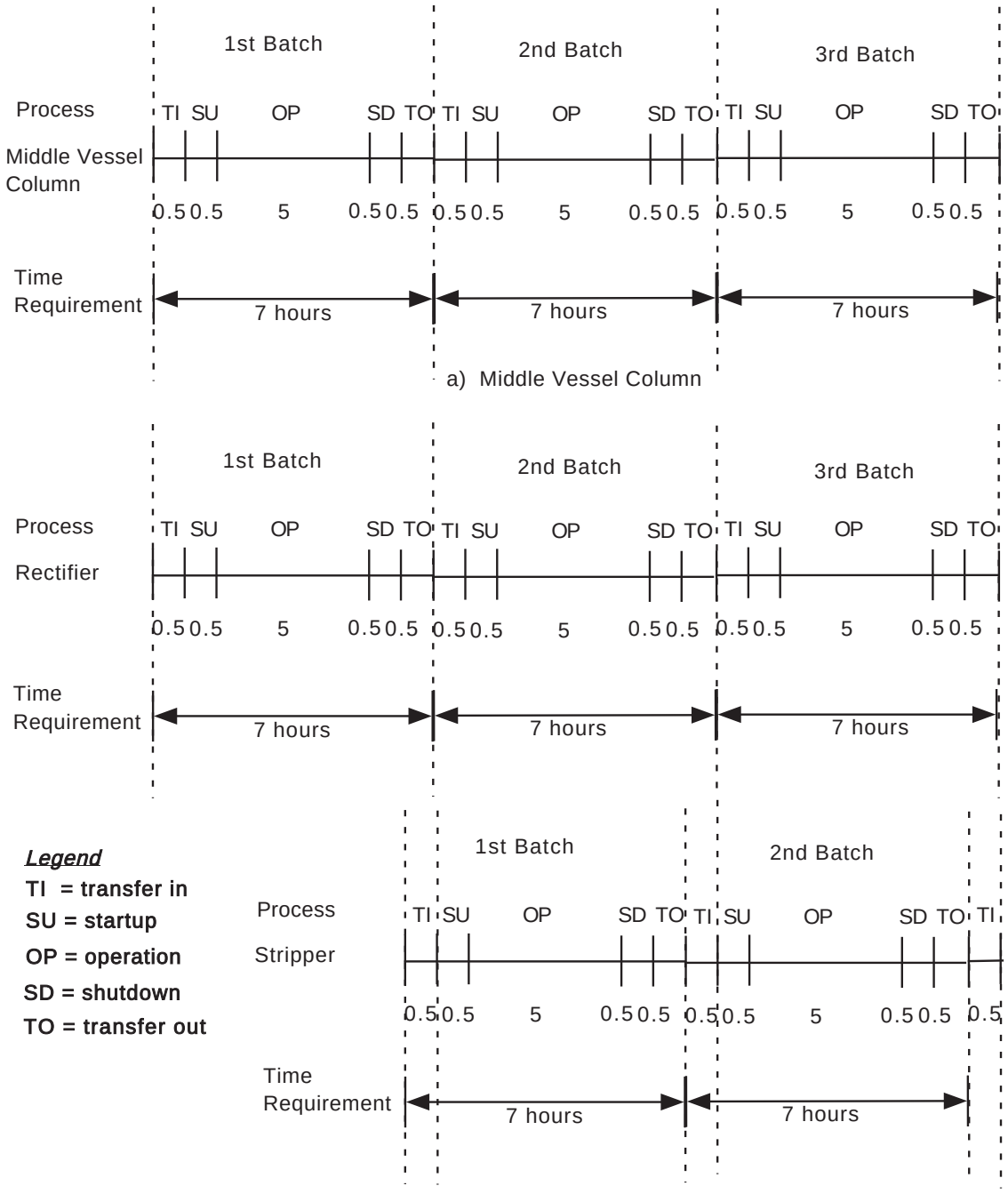

Figure 4-24: Gantt Charts for Operating a) a Middle Vessel Column and b) a Single Set of Stripping-Rectifying Operations

hours and a transfer time of 0.5 hours, for a total cycle time of 7 hours. Immediately after the completion of the transfer from the rectifier to the stripper, startup for the stripper is initiated for 0.5 hours, followed by 5 hours operating time, and 0.5 hours cool down, and finally 0.5 hours to transfer the contents of the still pot into storage, for a total of 6.5 hours cycle time. Meanwhile, the second batch of mixture was also introduced immediately after the rectifier pot has been emptied, and after 6.5 hours (0.5 hours transfer in, 0.5 hours startup, 5 hours operation, 0.5 hours shutdown), the rectifier is ready to transfer its contents to the stripper, just as the stripper is ready to receive the contents of the rectifier. Thus, the total cycle time for each batch is actually still 7 hours, despite using two columns (stripper/rectifier) instead of the middle vessel column, provided that only one stripping operation and one rectifying operation is required. With a similar cycle time, the energy costs involved for total reflux in startup and reboiler vaporization, would also be equivalent.

However, there maybe some constraints on the still pot composition path, other than the initial and the final composition, such as potentially dangerous mixture compositions that should be avoided (Figure 4-25), or any other reason that would require more than one set of stripping and rectifying operations to achieve the equivalent change in the still pot composition as achieved by a single operation of the middle vessel column. This would then result in more than one set of stripping and rectifying operations, which would ultimately mean a longer processing time for the stripping-rectifying combination as the required overhead of 2 hours (0.5 hours transfer in, startup, shutdown, transfer out) would be incurred for each set of stripping-rectifying operations. In the extreme case where the middle vessel path must be strictly adhered to, infinitessimal operation of the rectifier and the stripper would be required (as explored in Chapter 3), which would ultimately result in infinitely many transfers, startups and shutdowns, translating into huge overhead times for the entire process if the combined stripper-rectifier configuration was used rather the middle vessel column.

In summary, there is certainly a theoretical equivalency between the middle vessel column and a combined operation of a batch rectifier and a batch stripper. However,

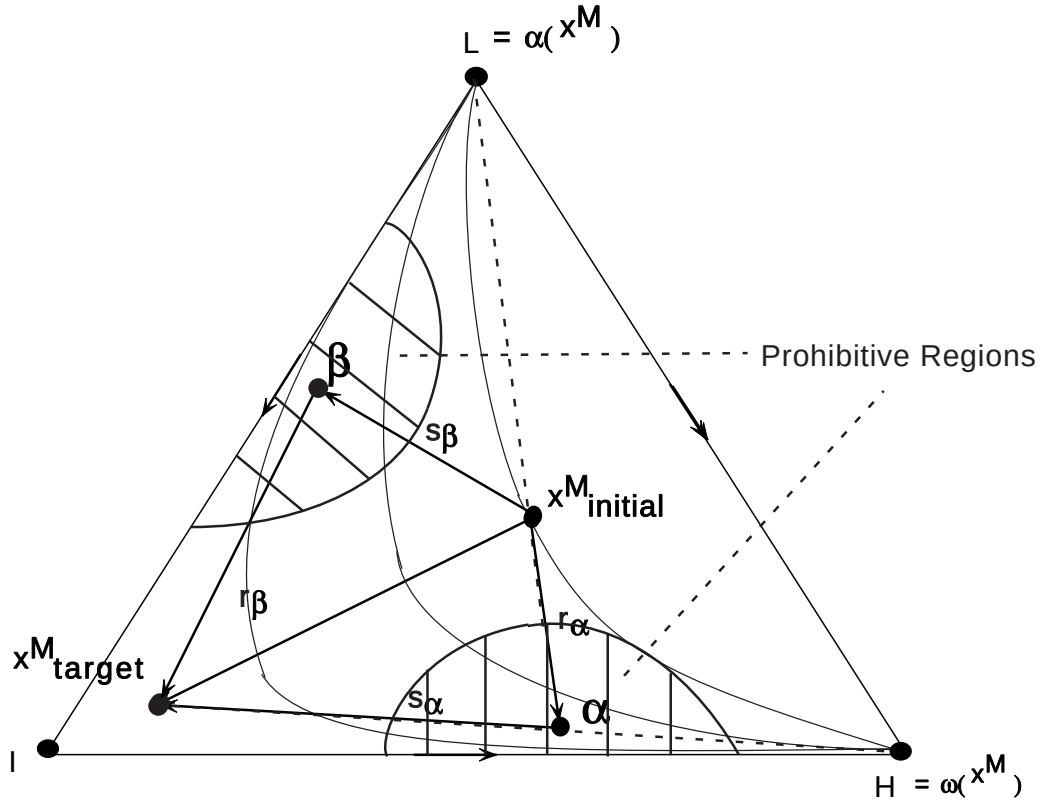

Figure 4-25: Pot Composition Paths in the Presence of Constraints

the final choice between the two different types of configuration would depend on the objective function that has to be maximized (or the cost function that has to be minimized), and also depend on the path constraints imposed on the operation. The ultimate objective of any separation is to move between the initial and final compositions, drawing the required products, in the minimum amount of time and cost, with time and cost weighted appropriately (as determined by the producers' objective functions). If a single set of stripping-rectifying operations is able to achieve the separation required, then perhaps given this equivalency, it would be cheaper to use a stripping-rectifying setup using existing strippers and rectifiers, rather than outfitting a new middle vessel column, thereby incurring capital costs. However, if multiple sets of stripping-rectifying steps are required to achieve the required separation and still pot composition path (see Chapter 7 for examples of such multi-step operations), then perhaps the middle vessel column will be preferable, as it cuts down on overhead times, and reduces energy consumption by requiring less shutdown/startup cycles. Ultimately, it is a trade off between the capital cost of installing a middle vessel column versus the higher operating costs of operating a combined rectifier and stripper column configuration, and a sound financial decision has to be made based on the operating scheme required, the demand for the product, total campaign time expected, and a host of other financial determinants (such as investment rates of return, project beta, credit interest rates, etc.).

Furthermore, with the increased efforts of environmental-friendly organizations to induce the Environmental Protection Agency to put greater emphasis on effluent free processes in chemical manufacturing, the use of a single middle vessel column without transfers of chemicals between unit operations would prove much more attractive. The middle vessel column reduces spillage due to transfers between unit operations (e.g., between a stripper and a rectifier) and reduces the amount of effluent generated from waste/residue remaining in still pots at the end of a batch operation, as only one still pot is required for the entire separation operation.

Another consideration would be that from a safety and operational point of view, one would want to minimize the number of material transfers that occur in the process,

so as to cut down on the possible hazards of leakage/spillage. Such considerations would indicate that the use of a middle vessel column would be preferable to that of the combined stripping-rectifying operations. Also, from the point of view of product quality, less transfers occuring in the process would also decrease the chances of contamination of a batch during transfer, which could lead to extra required processing, possibly reprocessing of the batch, or even discarding of the contaminated batch. Thus, product quality considerations also indicate that a middle vessel column may be preferable to that of the combined stripping-rectifying operations. Thus, the middle vessel column might still prove to be far superior when compared to the analagous combined stripping-rectifying operations when all these factors are taken into consideration and monetized.

4.6 A Comparison to Safrit and Westerberg in Related Topics

Although all of the analysis in the preceding sections was developed independently in our study of the middle vessel column, it was found that some of the ideas explained above in detail had been briefly mentioned by Safrit and Westerberg in their study of the use of entrainers in middle vessel columns [35, 33], and their attempts to formulate an algorithm for generating distillation regions for azeotropic batch distillations [32, 34] based on the work of Ahmad and Barton [1]. However, most of the points which they had touched upon were relatively qualitative, and not rigorously quantified. As such, it is hoped that our work will result in a more quantitative and rigorous understanding of the behavior of the middle vessel column. In this section, we will itemize the contributions made by Safrit and Westerberg, and explain the shortcomings in their analyses.

On the topic of the still pot composition paths, they mentioned that the middle vessel column will produce the unstable node as a distillate product, and the stable node as a bottoms product when the column is at an infinite reflux/reboil ratios

and has an infinite number of trays [35, 34]. The idea behind their statement is valid, in that it is indeed true that the middle vessel column will draw the unstable node as the distillate product and the stable node as the bottoms product, provided that the unstable node is in the alpha limit set and the stable node is in the omega limit set of the basic distillation region which the middle vessel composition currently resides. However, due to the definition of stable nodes and unstable nodes of a simple distillation residue curve map as the fixed points for which the eigenvalues are either all negative (stable node) or all positive (unstable node), there are 2 main objections to their statement. Firstly, a fixed point which may seem like a stable node or unstable node in a system of dimension n might well prove to be a saddle when an additional component is added such that the system is expanded to dimension $n+1$ Figure 4-26 illustrates this idea with the four component system of acetone, benzene, chloroform and ethanol. When the 3 component system of acetone, benzene and chloroform is considered, the fixed point representing pure chloroform exists purely as an unstable node (see Figure 4-26a). However, when ethanol is added to form a quartenary system, pure chloroform becomes a saddle fixed point (as illustrated by Figure 4-26b). Use of the terms "unstable nodes" and "stable nodes" thus seem ambigious and should be substituted with the use of "alpha limit sets" and "omega limit sets" so as to avoid any confusion.

Secondly, even if we are to restrict ourselves to thinking within a system of a given dimensionality (i.e., to refute the first objection as being irrelevant), there will be cases where the product drawn from the middle vessel column is neither the stable node nor the unstable node of the residue curve map. Consider the classic ternary mixture of acetone, chloroform and methanol, with its residue curve map as shown in Figure 4-27a. Suppose we had an initial composition for the still pot at point α, (Figure 4-27b) and drew both the distillate product and the bottoms product, then it would be right to say that the distillate product was the unstable node (the chloroform-methanol azeotrope) and that the bottoms product was the stable node (methanol). However, as we draw these products at a given value of λ, suppose that the still pot composition encounters the pot composition boundary as given by the

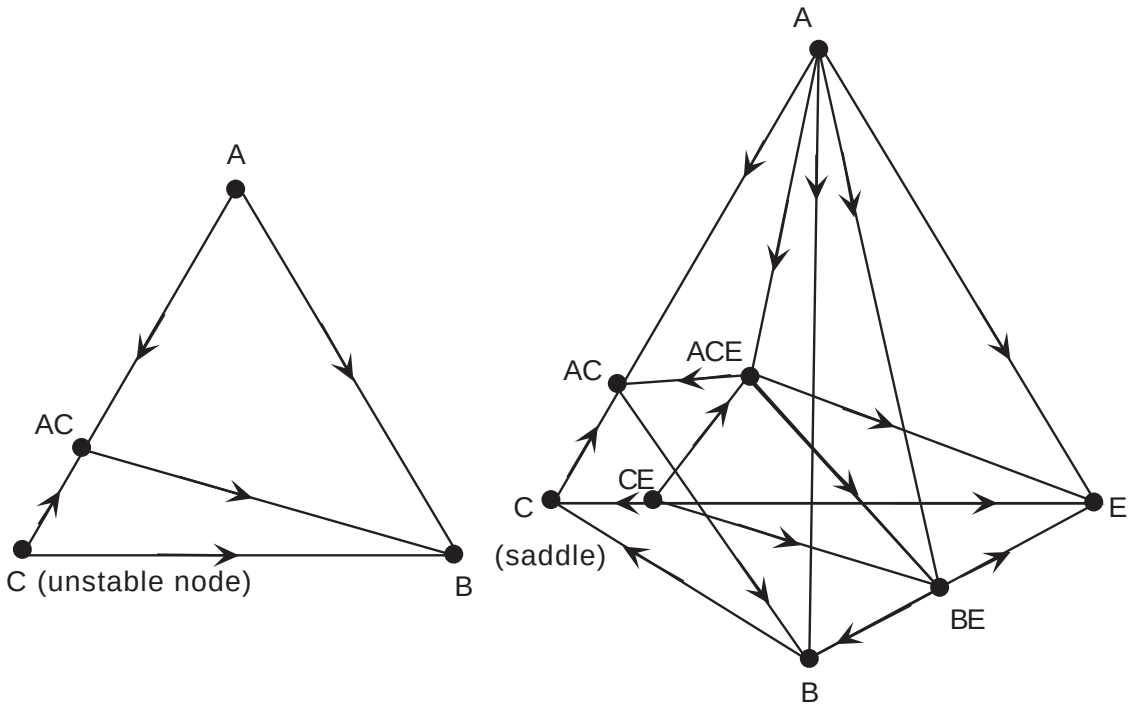

Figure 4-26: Ambigiouity in the Use of Unstable Nodes and Stable Nodes in the Presence of Higher Dimensionalities

line segment ACM-M (Figure 4-27c), the composition profile in the column will start to change, and as the pot composition enters the pot composition boundary at β, the distillate product is now the acetone-chloroform-methanol ternary azeotrope, while the bottoms product remains as pure methanol (Figure 4-27d). However, as we can see from the residue curve map, the acetone-chloroform-methanol ternary azeotrope is not an unstable node; it is actually a saddle point. The azeotrope is however, the alpha limit set of the current still pot composition (with $\varphi(\mathbf{x}^M)$ given by the line segment between ACM and M). Hence, the use of "alpha limit sets" and "omega limit sets" is again preferable to that of using "unstable node" and "stable node".

Next, in their analysis of the middle vessel pot composition path, they also explored the concept of the limiting middle vessel column residue and the middle vessel column residue [34]. However, from their analysis, it appears that they were either mistaken in their understanding of the middle vessel column, or that they were unclear in their explanation. In Safrit and Westerberg's example, in which they explained their concept of the MVC residue, they used the diagram as shown in Figure 4-28.

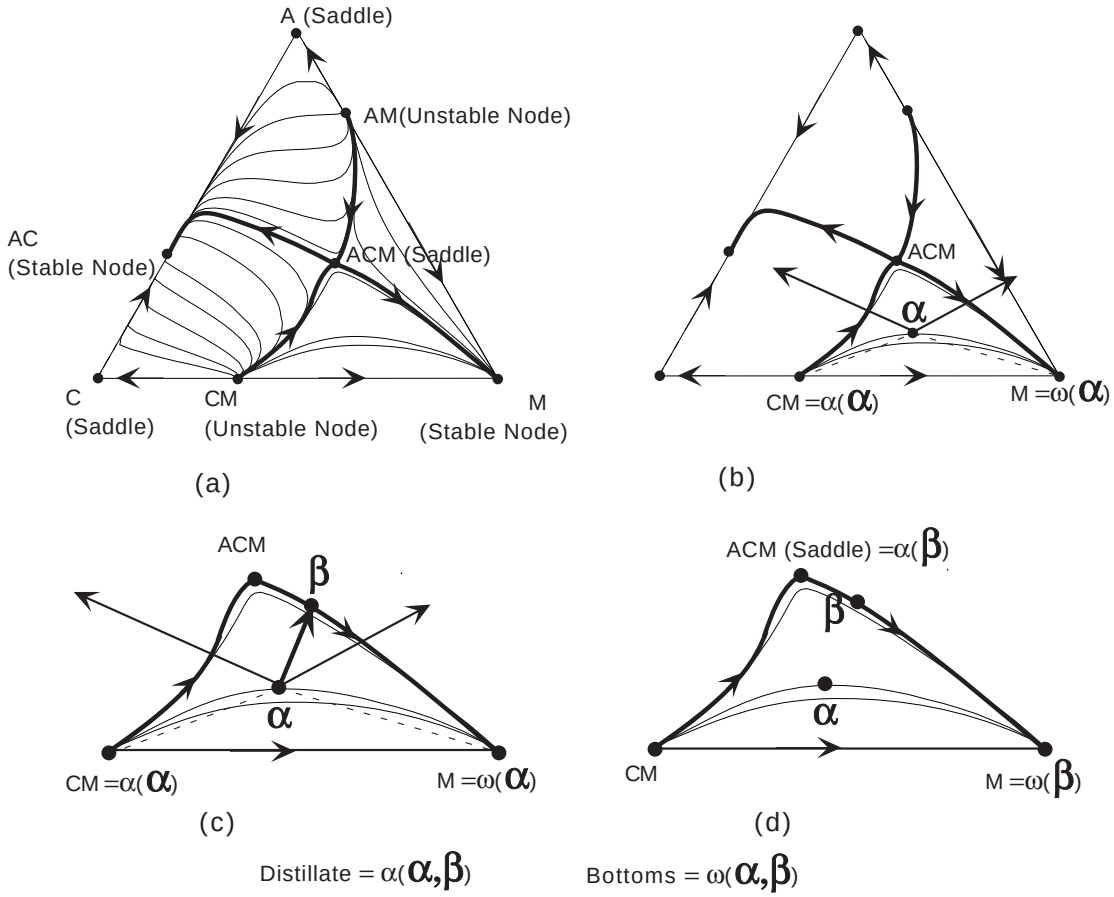

Figure 4-27: Distillate Product of a Middle Vessel Column Need Not be the Unstable Node

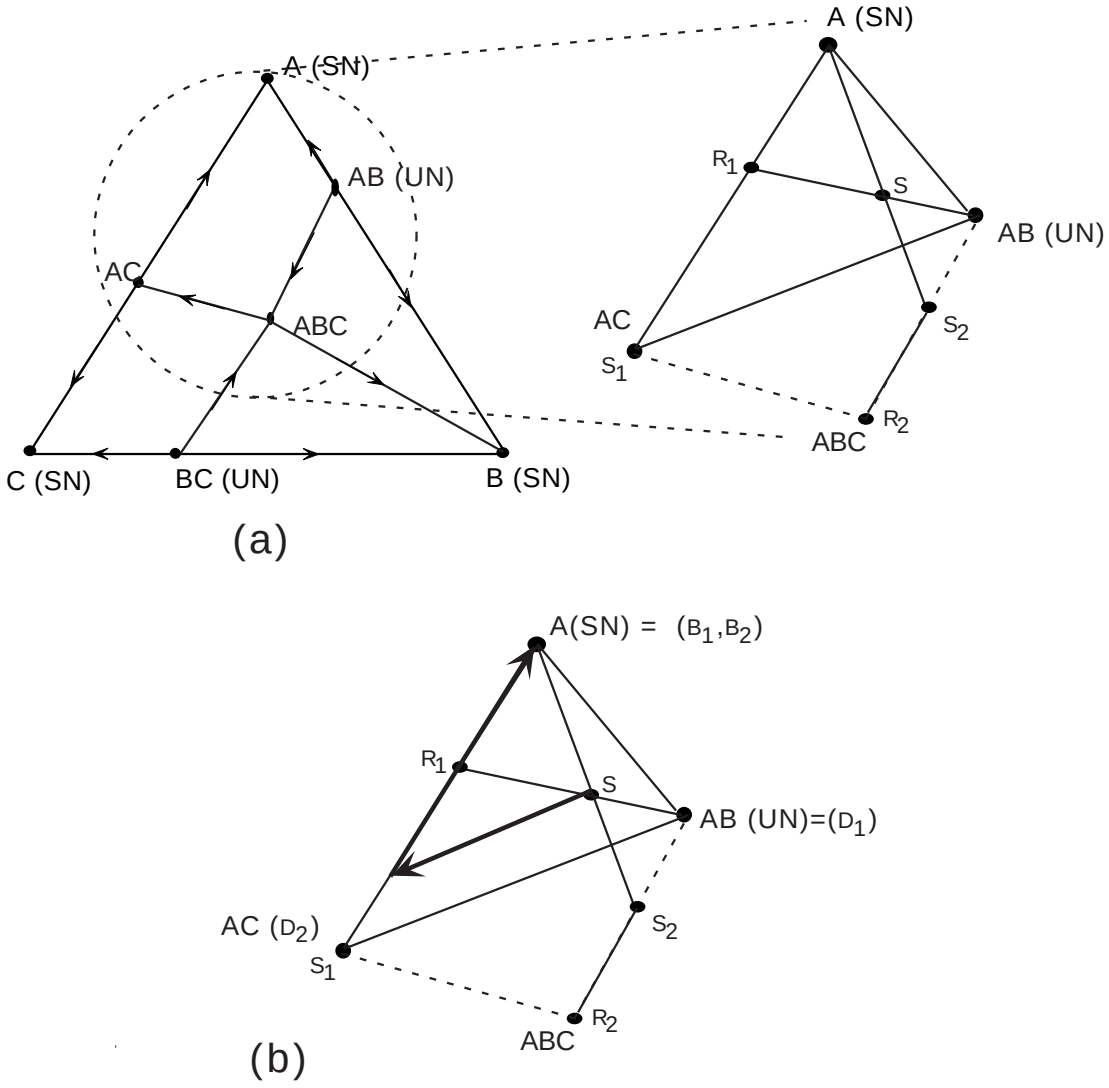

Figure 4-28: Diagram used by Safrit and Westerberg in Explaining the MVC Residue

They then went on to explain:

> The top and bottom products can be taken in different ratios, resulting in several different possible MVC residues. There are two limiting cases for the MVC residue: a rectifier taking all of the UN (unstable node) as a top product followed by a stripper taking all of the remaining SN (stable node) as a bottoms product and a stripper taking all of the SN as a bottoms product, followed by a rectifier taking all of the remaining UN as a top product. In between these two cases, the residue of the MVC will depend on the ratio of the top and bottoms products that are being taken.

They also said that:

> For the inital still composition S, a rectifier would produce a top product of the UN AB resulting in a residue of R_1, followed by a stripper producing a bottoms product of SN A resulting in a residue of S_1. This is one of the limiting MVC residues. The other limiting residue is found by putting S in a stripper rsulting in a residue of S_2 followed by a rectifier resulting in the limiting MVC residue of R_2. From Figure 2, we can see that the MVC residue must lie on the plane defined by the top and bottoms products (AB and A) and the still pot composition (S).

and so on. In other words, they implied that the limiting MVC residues were S_1 and R_2. They go on to explain that any possible MVC residue will lie between the line segment connecting S_1 and R_2 (i.e., line segment AC-ABC).

Firstly, we shall clearly redefine some of the terms used in their analysis, so as to make the analysis easier. The "MVC (middle vessel column) residue" was used by Safrit and Westerberg to describe the composition that remains in the still pot of the middle vessel column after all the stable node and unstable node products had been drawn from the column. They also used the term "limiting MVC residue" to describe the fixed points as given by R_2 and S_1. From their use of the terms, we postulate that the definitions that they really mean to use are as follows. The "MVC

(middle vessel column) residue" describes the composition that remains in the still pot of the middle vessel column when the still pot composition path encounters a pot composition boundary, and exits the current basic distillation region (for which the alpha limit set was the unstable node AB and the omega limit set was the stable node A).

The term "limiting MVC residue" describes the still pot composition that remains unchanging with time as $\xi \to \infty$. However, as long as product continues to be drawn from the middle vessel column, the still pot composition will typically continue to change in time. Given that the alpha limit set composition is always drawn as the distillate product and that the omega limit set composition is always drawn for the bottoms product, the only mechanism for the still pot composition to remain unchanged would be 1) if the alpha limit set approaches the omega limit set ($\alpha(\varphi(\mathbf{x}^M)) \to \omega(\varphi(\mathbf{x}^M))$), which occurs when the still pot composition enters a fixed point, and no further composition change occurs because the alpha limit set equals the omega limit set which equals the current still pot composition, or 2) if the alpha limit set, omega limit set and the still pot composition are colinear, and that the distillate (given by the alpha limit set composition) and the bottoms product (given by the omega limit set composition) are drawn in the appropriate amount such that the still pot composition remains unchanged, i.e.,

$$\frac{D}{D+B}(\mathbf{x}^D) + \frac{B}{D+B}(\mathbf{x}^B) = \mathbf{x}^M \tag{4.20}$$

or in terms of our middle vessel column parameter λ,

$$\lambda(\mathbf{x}^D) + (1-\lambda)(\mathbf{x}^B) = \mathbf{x}^M \tag{4.21}$$

such that the equation for still pot composition change, as given by Equation (3.7) gives:

$$\frac{d\mathbf{x}^M}{d\xi} = \mathbf{x}^M - \lambda\mathbf{x}^D - (1-\lambda)\mathbf{x}^B = 0 \tag{4.22}$$

Strictly speaking, the second mechanism in which the composition remains unchanged

does not really qualify as being a limiting MVC residue, in that any shift in the value of λ would result in a shift in the composition of the MVC still pot. This is in contrast to the first mechanism where, irregardless of the value of λ chosen, the MVC still pot will remain at the fixed point, with both the distillate and the bottoms product drawn being of the same composition as that of the still pot. We would thus propose that the definition of the "limiting MVC residue" be "the composition that finally remains in the still pot as $\xi \to \infty$ and is unchanged as the value of λ is varied in the column".

From Safrit and Westerberg's analysis, the MVC residue was the product that remains in the middle vessel column after all of the stable node and the unstable node products have been drawn. As we have explained in Sections 4.2 and 4.3, it is the alpha and omega limit set compositions that are drawn from the middle vessel column, and when the MVC composition encounters one of the pot composition boundaries (such as line segments A-AC, AB-ABC and AC-ABC in Figure 4-28), the distillate and bottoms products change respectively to the new set of alpha and omega limit sets. For line segment A-AC, the new alpha limit set would be the AC azeotrope, while the omega limit set remains unchanged at pure A; for line segment AB-ABC, the new omega limit set would be ABC, while the alpha limit set remained unchanged at the composition of azeotrope AB; and for line segment AC-ABC, both the limit sets are changed, with the new alpha limit set being the composition of the ABC azeotrope, while the new omega limit set being the compositiong of the AC azeotrope. The fact that Safrit and Westerberg had limited their analysis to the drawing of one type of product from each of the top and the bottom of the column, leads us to think that they have neglected the flexibility involved in operating a MVC batch column, and treated it like a continuous column where only one product composition can be drawn from each of the rectifying and stripping sections. A batch column however has the added flexibility in the number of cuts (any integer from zero to infinity) that can be taken from each of the distillate and bottoms product.

To illustrate this point further using the example given in Figure 4-28, starting at the composition S, we could choose a value of λ, and draw pure A as the bottoms product, and the azeotrope AB as the distillate product, such that the still pot moves

in the direction as shown by the bold arrow. The still pot composition encounters the pot composition boundary of the line segment A-AC at β, and the alpha limit set is changed from the azeotrope AB to the azeotrope AC. Safrit and Westerberg conclude that all that can be done is to continue drawing the stable node product (pure A), such that the still pot composition finally reaches S_1. However, this is not the case, as it is possible to continue operating the column at the given value of λ or at a new value of λ, drawing AC and A as the distillate and bottoms product respectively. With an appropriate value of λ, more AC than A would be drawn out of the column, and the still pot composition will move in the direction of the bold arrow, towards the fixed point of pure A; the final residue in the middle vessel column will then be the fixed point of pure A. A similar exercise can be conducted such that the final residue in the middle vessel column could be either AB, AC or ABC, by varying the value of λ and steering the still pot composition appropriately.

With the above example, it is not difficult to see that if we were to adopt the definitions which Safrit and Westerberg implied for the "MVC residue" and the "limiting MVC residue", the correct delimitation of these entities should be as follows. The "MVC residue" of the initial composition S should be given by any points on the line segments $R_1 - S_1$, $S_1 - R_2$ and $S_2 - R_2$. This is because all the points along these line segments can be reached by the initial composition S, by using an appropriate value of λ. The two extremities given by $\lambda = 0$ (totally stripper configuration) and $\lambda = 1$ (totally rectifier configuration) would result in the pot composition encountering the pot composition boundaries at S_2 and R_1 respectively. Any point on the pot composition barrier between these two points (as given by the line segments $R_1 - S_1$, $S_1 - R_2$ and $S_2 - R_2$) could be the point where the still pot composition encounters a pot composition boundary and exits the current basic distillation region. Hence, any of these points could be the "MVC residue" as defined by Safrit and Westerberg. This is in contrast to their analysis which stated that the "MVC residue" was given only by the line segment $S_1 - R_2$ (see Figure 4-28). Hence, even if their analysis had been limited to the current basic distillation region (A-AB-ABC-AC-A) and not inclusive of the basic distillation boundaries, it is still incorrect.

Furthermore, the correct delimitation of the "limiting MVC residue" should be given by the four fixed points bounding the current basic distillation region (A-AB-ABC-AC-A), since all the fixed points (A, AB, AC, ABC) can be reached by the still pot composition in the middle vessel column with a correct choice of the value of λ. Thus, their analysis which yielded the fixed points AC and ABC as the only "limiting MVC residues" is also incorrect, because they had failed to consider the possibility/flexibility of drawing more than one product from the top or the bottom of the middle vessel column, which is possible as this is a batch process.

It should be noted however, that their statement regarding the coplanarity of the products, the still pot composition and the MVC residue was correct:

> From Figure 2, we can see that the MVC residue must lie on the plane defined by the top and bottoms products (AB and A) and the still pot composition (S).

Although this statement is not very significant in a ternary system where all compositions motion must lie in the composition simplex defined by the plane $x_1 + x_2 + x_3 = 1$ (as is the case in the example in which they presented in Figure 4-28), it is useful in understanding the behavior of the middle vessel column in systems with dimension ≥ 4. This is because in these higher dimensional systems, the composition simplex is not 2-dimensional, and motion need not be restricted to a 2-dimension hyperplane. However, as mentioned in Section 4.3, since only two products are drawn from the middle vessel column at any time (namely the bottoms and the distillate products), there are only 2 degrees of freedom in the motion of the still pot composition which implies that the motion must occur in the 2-dimension hyperplane defined by the still pot composition, the distillate product and the bottoms product. Correspondingly, the MVC residue must lie within this hyperplane.

Safrit and Westerberg also explored the idea of batch distillation boundaries and batch distillation regions for a middle vessel column [32, 34]. They correctly mentioned that the top and bottom sections of the middle vessel column act just like a rectifier and a stripper respectively. They go on to say:

> ...batch boundaries defining the distillate product sequence are the rectifier's boundaries and the batch boundaries defining the bottoms product sequence are the stripper's boundaries. The batch boundaries for the MVC are the boundaries that are common to both the rectifier and the stripper.

and that:

> ...the batch regions for the MVC are a combination of the rectifier and stripper columns. If the rectifier and stripper regions are the same, then the regions for the MVC are the same as the rectifier and the stripper. If they are different, then the rectifying section of the MVC will be constrained to the rectifier region and the stripping section of the MVC will be constrained to the stripper region.

In their analysis of the batch distillation boundaries (which is equivalent to our definition of the pot composition boundaries) and regions, it is clear that there is an implicit equivalency of the middle vessel column with the combined operation of the stripper and rectifier.

It is indeed correct that the pot composition boundaries for the MVC will be the boundaries that are common to both the rectifier and the stripper. However, it is incorrect that the distillate product sequence is bounded by the rectifier's boundaries and that the bottoms product sequence is bounded by the stripper's boundaries. As explored in Section 4.4, using the 001 system [11, 26], varying the middle vessel column parameter λ changes the behavior of the column, and bifurcation occurs for some points in the composition simplex. In the presence of batch rectifier and stripper regions that are not equivalent, the still pot composition is able to traverse between batch distillation regions, because it is only the boundaries that are common to both regions that will form pot composition boundaries for the middle vessel column. Hence, the distillate product need not be limited to the batch rectifier region of the initial still pot composition, neither is the bottoms product necessarily constrained to the batch stripper region of the initial still pot composition. It is true, however, that

the distillate product will be restricted to the batch rectifier region of the *current* still pot composition, and the bottoms product will be restricted to the batch stripper region of the *current* still pot composition.

Finally, in their work regarding the use of entrainers in batch rectifiers to separate azeotropes [35, 33], Safrit and Westerberg mentioned the concept of steering the still pot composition in the middle vessel column by varying the amount of entrainer added, and the amount of bottoms and distillate product drawn from the column. This variation of entrainer flow rate (E), bottoms flow rate (B) and distillate flow rate (D), was used 1) to steer the still pot composition such that it would not encounter the pinch point curves of the distillation process and 2) to steer the still pot composition towards one of the pure product fixed points, so that the final composition in the pot is a pure product, thereby avoiding taking an extra cut from the column (the last cut being the contents of the pot itself). The analysis of pinch point curves was developed by Wahnschafft and Westerberg [39] for the analysis of product composition regions in the distillation of azeotropic mixtures for continuous columns, where a single product composition is drawn at any point in time, and by overall mass balance, the feed, distillate and bottoms product all have to be colinear in the composition simplex. It is not immediately clear that this analysis can be extended to the batch distillation column as the still pot composition, distillate and bottoms product of a batch distillation process need not be colinear in the composition simplex, and the product compositions could change continuously, with more than one cut taken from each product point.

Regardless, they developed an equation for the steering of a middle vessel column in the absence of an entrainer [35], as follows:

$$\frac{d}{dt}(Hx_s) = -(Dx_d + Bx_b) \tag{4.23}$$

where H is the holdup in the middle vessel column, D and B are the respective distillate and bottoms flow rates, x_i denotes the respective compositions, with $i = s, d, b$; s denoting still pot composition, d denoting distillate product composition, and

b denoting bottoms product composition. Equation (4.23) is similar to the equation (3.4) derived in Section 3.1. Hence, they were able to explain that:

> ...the direction of the still path is in a direction opposite to that of the combined directions of x_s to x_d and x_s to x_b, due to the removal of the distillate and bottoms products respectively.

However, Safrit and Westerberg did not attempt to introduce a dimensionless warped time ξ into their equations. As such, they could only explain quantitatively, that:

> ...How these directions are combined is determined by the magnitude of D and B, based on vector addition. So, depending on the magnitude of the product flow rates, it is possible to "steer" the still pot composition in a variety of directions.

They were however, unable to quantify the direction of motion exactly by using the weighted average notion with the middle vessel column parameter of λ which was introduced in Chapter 3.

Safrit and Westerberg also introduced a similar equation in the presence of entrainers, where an entrainer (flow rate E) is introduced into the rectifying section of the middle vessel column [33]. By performing a component mass balance on the entrainer column, they then obtained the following equation describing the behavior of the middle vessel entrainer column:

$$\frac{d}{dt}(Hx_s) = -(Dx_d + Bx_b) + Ex_e \tag{4.24}$$

where H is the column holdup, D, B, and E represent the distillate, bottoms and entrainer flow rates. x_i denotes the respective compositions, with $i = s, d, b, e$; s denoting still pot composition, d denoting distillate product composition, b denoting bottoms product composition, and e denoting entrainer composition. As before, they were unable to quantify the direction of still pot motion because a dimensionless warped time was not introduced into the equation. They were only able to quantitatively explain the following:

> ... The direction of the still path was in a direction opposite to that of the combined directions of x_s to x_d, x_s to x_b, and x_e to x_s. How these directions were combined was determined by the magnitude of D, B, and E, on the basis of vector addition.

From their explanation, the actual direction of still pot composition motion could not be quantified exactly, and only a vague explanation was given regarding the direction of motion of the still pot composition.

To further demonstrate the usefulness of introducing the notion of a dimensionless "warped time" into the analysis of still pot compositions, a dimensionless warped time will be introduced for the equations provided by Safrit and Westerberg for the middle vessel entrainer column to help quantify the direction of still pot motion. From the nature of equation (4.24), the following dimensionless warped time ζ could be introduced, where ζ is defined by:

$$d\zeta = (\frac{D+B-E}{H})dt \tag{4.25}$$

and where 3 relevant parameters, θ_1, θ_2 and θ_3 are defined as:

$$\begin{aligned} \theta_1 &= \tfrac{D}{D+B-E} \\ \theta_2 &= \tfrac{B}{D+B-E} \\ \theta_3 &= -\tfrac{E}{D+B-E} < 0 \end{aligned} \tag{4.26}$$

such that:

$$\theta_1 + \theta_2 + \theta_3 = 1 \tag{4.27}$$

Substituting equations (4.25) and (4.26) into the original equation (4.24) given by Safrit and Westerberg, and rearranging the equation, the following is obtained:

$$\frac{dx_s}{d\zeta} = x_s - \theta_1 x_d - \theta_2 x_b - \theta_3 x_e \tag{4.28}$$

or rearranging it in a form similar to that of equation (3.25), such that it can be easily understood as a weighted average of the difference in the still pot composition with

the other compositions being added to/drawn from the system, we obtain:

$$\frac{dx_s}{d\zeta} = \theta_1(x_s - x_d) + \theta_2(x_s - x_b) + \theta_3(x_s - x_e) \tag{4.29}$$

which states that the motion of the still pot composition, x_s as a function of the dimensionless warped time ζ is given by the weighted average of the 3 directional vectors as given by $x_s - x_d$, $x_s - x_b$, and $x_s - x_e$, with weights of θ_1, θ_2 and θ_3 respectively. Variation of D, B and E will change the parameters θ_1, θ_2, and θ_3 as given by equation (4.26), and hence change the direction of the still pot composition motion accordingly. Thus the effect of varying D, B, and E on the direction of still pot motion, is completely quantified with the use of the dimensionless warped time ζ. Detailed derivation of equation (4.28) and (4.29) is provided in Appendix C.

It should be noted however, that Safrit and Westerberg did mention the concept of a "net product" for a middle vessel column as being the combined distllate and bottoms product drawn from the column. This concept was also used extensively in our analysis of the middle vessel column.

Chapter 5

Insights on the Use of the Middle Vessel Column in Azeotropic Batch Distillations

Using the tools developed in our analysis of the middle vessel column, this chapter explores some interesting insights for the separation of azeotropic systems with curved separatrices, using a middle vessel batch distillation column. For the purpose of this chapter, the ternary mixture of Acetone-Benzene-Chloroform (A-B-C), which is an example of the inverse-020 system [11], will be studied in detail. In the first section, the implications of curved separatrices for pot composition boundaries in a middle vessel batch distillation column are explored, based on the analysis developed in Section 4.4 regarding middle vessel pot composition boundaries.

This then leads to a simple operating procedure for breaking the AC azeotrope detailed in the second section of this chapter, which would allow us to charge the azeotrope or some composition in the ternary mixture composition simplex into a middle vessel batch distillation column, mix it with pure entrainer (in this case benzene) and draw pure products (acetone, chloroform and benzene) from the column without the need for a recycled azeotropic waste cut. This operating procedure is tested via simulations using the ABACUSS model of the middle vessel column, to validate the theory behind such an operating procedure. The results of the simula-

tions are presented in detail in Chapter 7.

Similar ideas to those developed in Section 5.2 were first developed conceptually by Laroche *et al.* [21] in the context of a continuous distillation column. This was further formalized by Wahnschafft *et al* [39, 40], who applied the separation scheme suggested by Laroche *et al.* for an inverse-020 system [11] to the Acetone-Benzene-Chloroform system. In fact, the operating procedures suggested in Section 5.2 can be considered as the time-domain analogs of the space-domain separation sequences suggested by Wahnschafft *et al.* [39, 40], as shown in the third section of this chapter.

Given the above analogies, the fourth section then presents a short discussion about the equivalency of a continuous distillation column to that of a middle vessel batch distillation column. The limitations to this similiarity, however, are also highlighted.

Finally, based on the operating procedure developed for the Acetone-Benzene-Chlorofom mixture, an analysis regarding the perfect entrainer in a middle vessel batch distillation column is then presented in the final section. It should be noted that a complete discussion of feasible entrainers is beyond the scope of this thesis. An analysis of feasible entrainers was conducted by Laroche *et al.* [21] for the separation of homogeneous azeotropes in continuous distillation columns. Some of the insights developed in their work can also be extended to the middle vessel batch distillation columns, keeping in mind the minor differences between a middle vessel batch distillation column and a traditional continuous distillation column, thereby offering an analysis of feasible entrainers for the middle vessel batch distillation column.

5.1 Non-Equivalence of Pot Composition Boundaries for Strippers and Rectifiers in the Presence of Curved Separtrices

The analysis conducted in Chapter 4 was based completely on the assumption of straight line separatrices and planar (or polygonal for higher dimensional systems)

pot composition boundaries. However, as explained by Reinders and De Minjer [30], separatrices can only be linear if the third component added to the first two components (which form the azeotrope) does not affect the relatively volatility of the first two components. This would require a third component that interacts to the same degree with each of the two components. This, however, is unusual physically. Thus, some curvature can always be expected of separatrices and pot composition boundaries formed from a bundle of trajectories (as would be the case in systems of higher dimensions, whre the boundaries are formed by bundles of trajectories, some of which are separatrices).

This non-ideality actually renders some of the previous limiting analysis inaccurate, but as we shall show in this section, it is curvature of the boundaries that allows the derivation of a separation scheme that separates azeotropic mixtures completely and allows us to cross a surface that is theoretically a pot composition boundary under the assumption of linear separatrices. This also leads us to elucidate the characteristics of a perfect entrainer for breaking maximum boiling azeotropes and the corresponding perfect entrainer for breaking minimum boiling azetropes. This is in addition to the entrainers proposed by Bernot *et al.* in their analysis of batch strippers and separating azeotropes [6].

For the purposes of this chapter, we will use the ternary system of Acetone-Benzene-Chloroform to illustrate our ideas. A summary of the azeotropic compositions for this three component mixture, together with the relevant ternary residue curve map is provided in Appendix B. Firstly, let us consider the topological structure of the Acetone-Benzene-Chloroform (A-B-C) residue curves map as given in Figure 5-1.

As calculated by the NRTL model, with parameters and equations provided by Aspen Plus, the separatrix in the Acetone-Benzene-Chloroform system is highly curved and almost hugs the Benezene-Chloroform edge at $x_a \approx 0.0$, $x_b > 0.8$, and $x_c < 0.2$. As will be shown in Chapter 7, using ABACUSS simulations with the model presented in Chapter 3, this extreme curvature of the separatrix does indeed allow us to separate a ternary mixture of acetone, benzene and chloroform into pure components (with

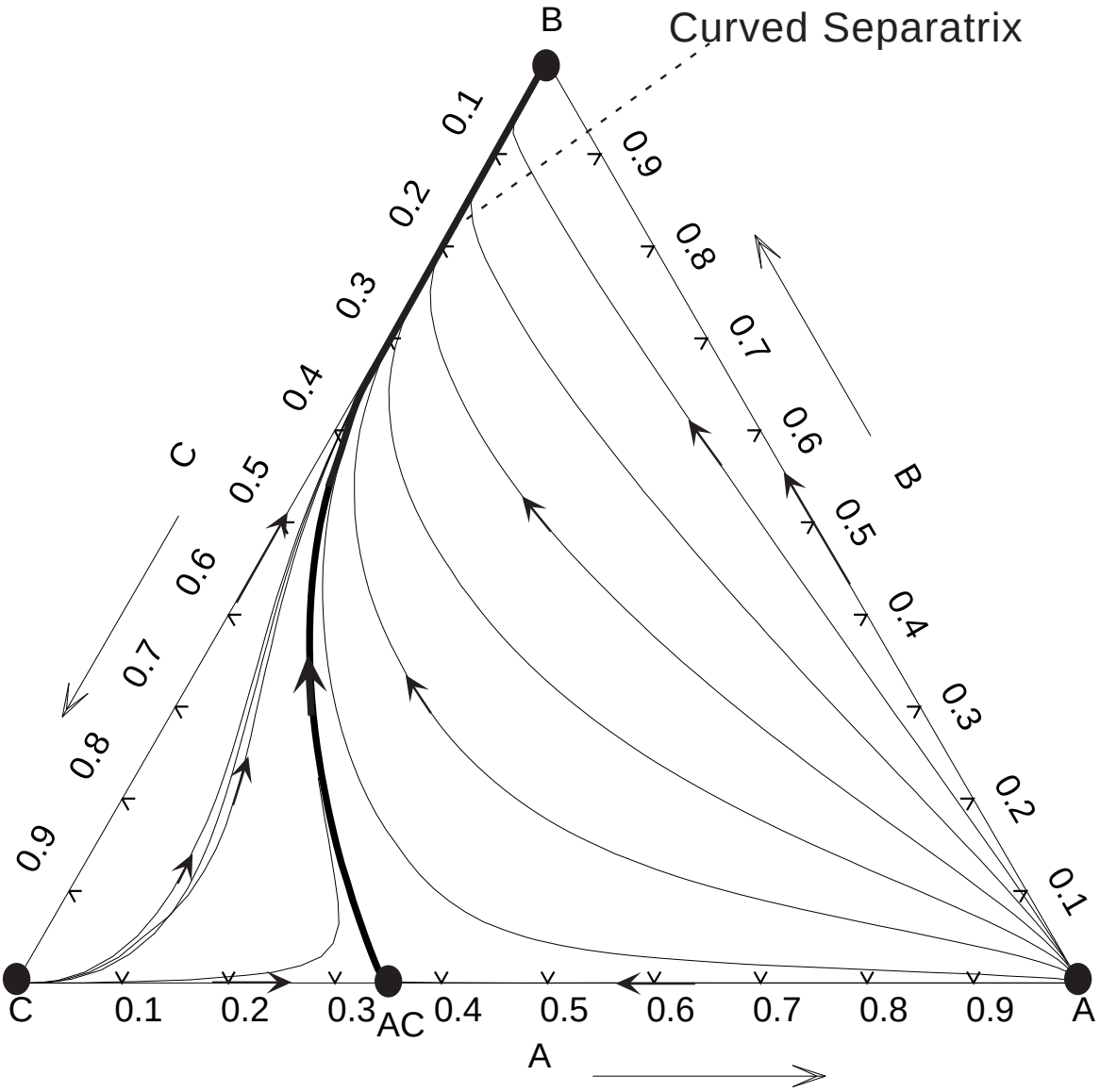

Figure 5-1: Residue Curves Map for Acetone-Benzene-Chloroform System

purities of $> 99\%$), thereby overcoming the binary azeotrope Acetone-Chloroform (AC) ($x_a \approx 0.35$, $x_c \approx 0.65$).

More importantly, in the presence of linear separatrices, the B-AC line segment would have been evaluated as being a pot composition boundary for both the stripper, rectifier and for all values of $0 < \lambda < 1$. Hence, based on our earlier analysis of pot composition boundaries in middle vessel columns (Section 4.4), it would also have been a pot composition boundary of the middle vessel column, as it is a boundary common to both the stripper and the rectifier which exists for all values of λ as λ varies between 0 and 1. It should be noted however, as is the case here, that the boundary that exists at different values of λ need not be the same entity. For $0 < \lambda \leq 1$, the B-AC line segment exists as a boundary because it is a stable separatrix. As explained in Section 4.4, a stable separatrix exists as a pot composition boundary for all values of λ except $\lambda = 0$. However, when $\lambda = 0$ and the "separatrix" pot composition boundary ceases to be a pot composition boundary, a "mass-balance" pot composition boundary moves into the line segment B-AC at exactly $\lambda = 0$. Thus, despite the fact that these pot composition boundaries are not the same entity, because there exists a pot composition boundary at the line segment B-AC for all values of λ, B-AC will be a pot composition boundary for a middle vessel column even if it is free to operate at all values of $0 \leq \lambda \leq 1$.

However, due to the curvature of the separatrix, it turns out that the rectifier boundary and the stripper boundary actually do not coincide. Thus, the line segment B-AC actually does not form a pot composition boundary for the middle vessel column which operates at varying λ, and we are able to cross this "middle vessel pot composition boundary" by a clever manipulation of the operating schedule of the parameter λ.

To illustrate that the stripper and rectifier boundaries are not equivalent, consider the products that will be drawn from the batch stripper and batch rectifier respectively. As mentioned in Section 4.2, for the batch stripper, it is the omega limit set of the current still pot composition that is drawn as product. As can be seen from Figure 5-1, the omega limit set of all points interior to the composition simplex is given

by the stable node of the ternary system, namely pure benzene. Thus, any initial still pot composition interior to the composition simplex would draw pure benzene as the product in a batch stripper. This is as shown in Figure 5-2a, where all initial still pot compositions will move directly away from the fixed point of pure benzene as governed by the equation:

$$\frac{d\mathbf{x}^M}{d\xi} = \mathbf{x}^M - \mathbf{x}^B \tag{5.1}$$

Thus, all the initial still pot compositions interior to the composition simplex will eventually encounter the simplex edge given by the line segment of (A-C), enter the simplex edge and change their omega limit set. The new omega limit set is given by the azeotropic composition of AC. However, if the still pot composition enters the simplex edge in the segment A-AC, the final last cut drawn from the stripper column will be A, whereas if the still pot composition enters the simplex edge in the segment C-AC, the final cut drawn from the stripper will be C. Thus, the interior of the composition simplex is divided into two batch stripper regions, η and κ as shown in Figure 5-2b, with the pot composition boundary given by the straight line connecting fixed point B with fixed point AC. Initial still pot compositions in the region η will draw the product sequence of (B,AC,C), while initial pot compositions in the region κ will draw the sequence of (B,AC,A).

For the case of a batch rectifier, the alpha limit set of the current still pot composition will be drawn as the distillate product, and the direction of motion of the still pot is governed by the following equation:

$$\frac{d\mathbf{x}^M}{d\xi} = \mathbf{x}^M - \mathbf{x}^D \tag{5.2}$$

Thus, for region μ as shown in Figure 5-3a, the distillate product (which is given by the alpha limit set of the region) would be C, and the still pot composition of any initial point in this region would move in a straight line away from the fixed point of pure C.

Thus, the still pot composition will eventually encounter the curved separatrix connecting the fixed points B and AC. When the still pot composition enters the

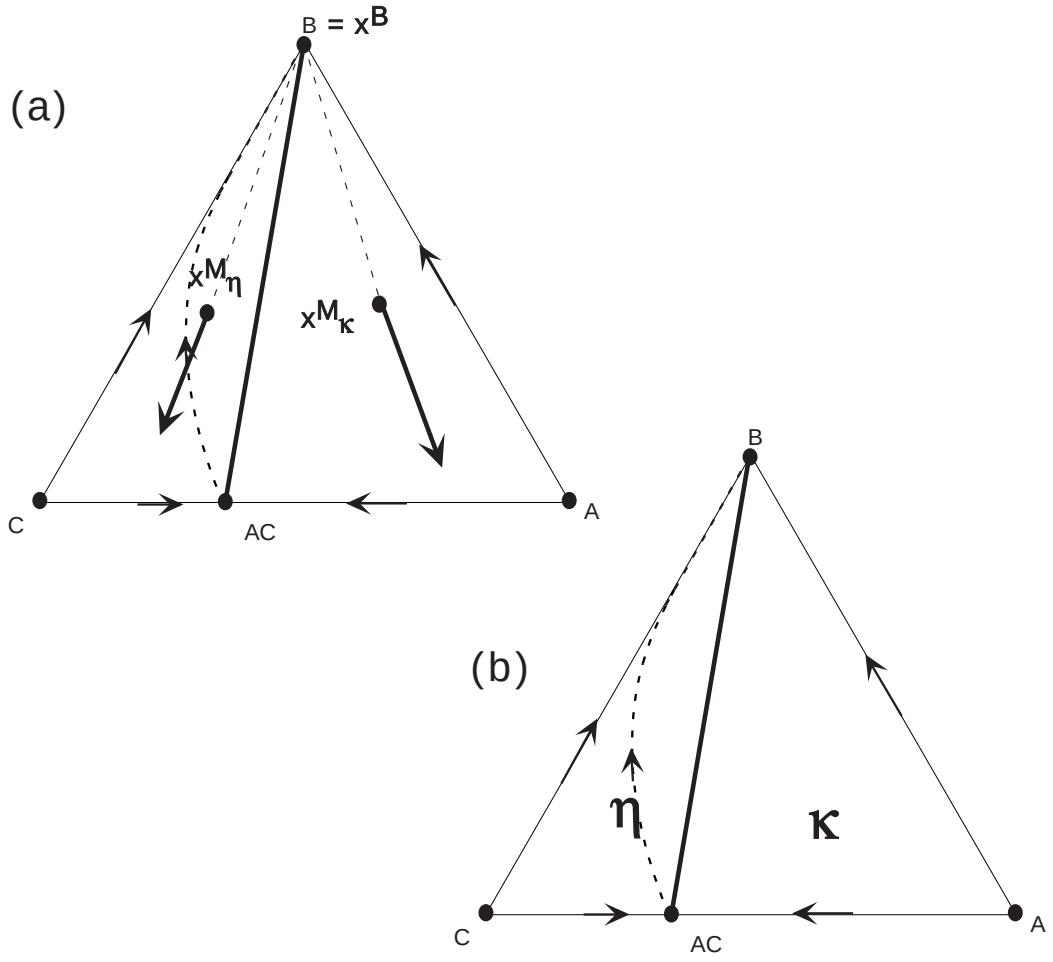

Figure 5-2: Batch Distillation Regions/Pot Composition Boundaries for a Batch Stripper in the Acetone Benzene Chloroform System

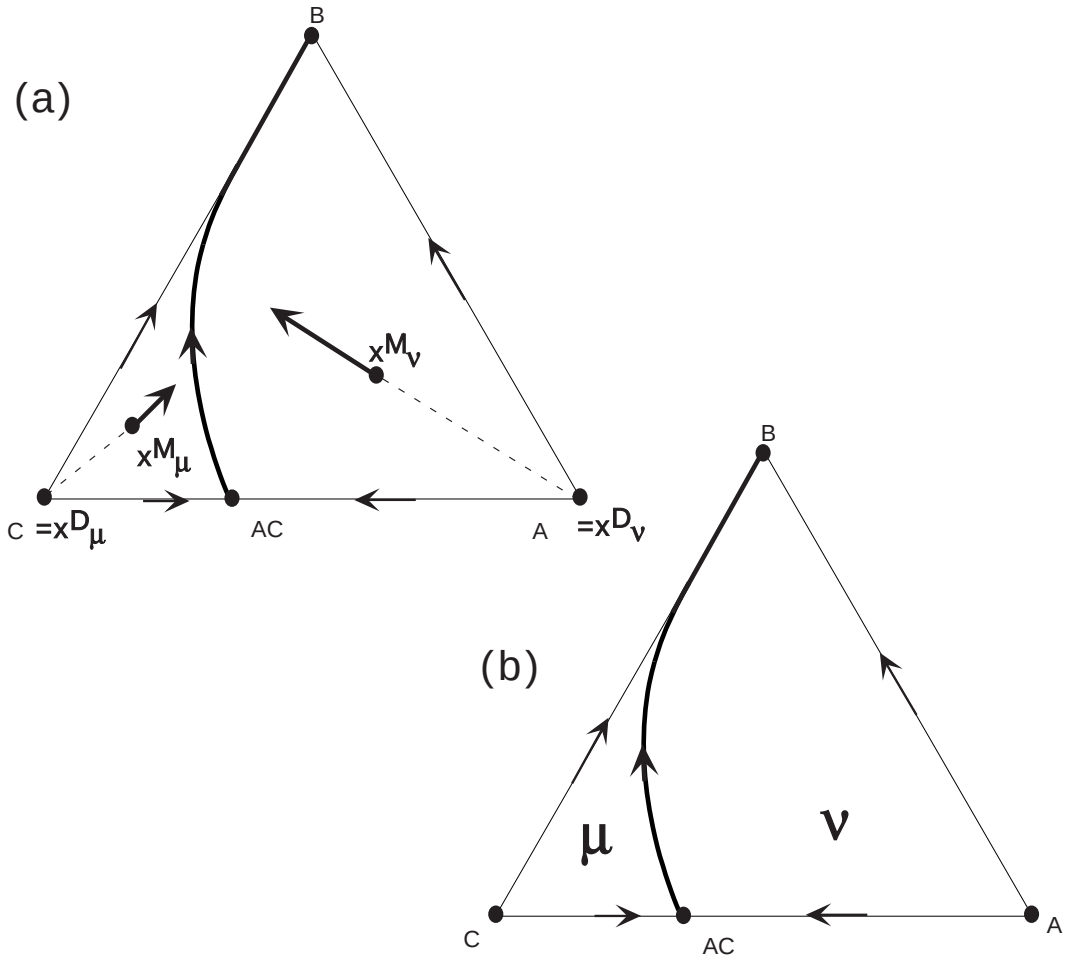

Figure 5-3: Batch Distillation Regions/Pot Composition Boundaries for a Batch Rectifier in the Acetone Benzene Chloroform System

curved separatrix, the rectifier will start drawing the new alpha limit set of the separatrix, which is the fixed point AC. Due to the curvature of the system, drawing of product AC will cause the still pot composition to move off the separatrix back into the region marked μ, and hence change its alpha limit set again, back to pure C. This consequently moves the still pot composition back onto the separatrix, which then changes the alpha limit set back to AC, which in turn pushes the still pot composition back into region μ. This see-sawing of composition of the product drawn as distillate from the rectifier will ensure that the still pot composition stays on the curved separatrix, and follows it to the fixed point B, without ever crossing into region ν. Region μ thus forms a single batch rectifier region with product sequence given by (C, AC-C mixture, B). Compositions originating in region ν, on the other hand, will draw A (its alpha limit set) as the distillate product until it encounters the separatrix between B and AC. The still pot composition will enter the separatrix, change its alpha limit set to AC, and start drawing AC as its distillate product. However, when it draws AC, the still pot composition cross the separatrix again, and a new alpha limit set of pure C will result. Pure C will thus be drawn as a distillate product, but this will force the still pot composition back onto the separatrix, and the see-sawing which had occured around the separatrix for an initial still pot composition in region μ, will also occur here. The still pot composition thus traces out the separatrix to the fixed point of pure B. As before, the separatrix forms the pot composition boundary for the region ν, and any still pot composition that starts in region ν is unable to enter region μ. The product sequence would consequently be given by (A, AC-C mixture, B).

Although the stripper and rectifier pot composition boundaries both serve to separate the interior of the composition simplex into separate batch distillation regions, it should be noted that the nature of these boundaries are qualitatively different. The boundary for the stripper is not really a constraint to motion, in that the still pot composition does not attempt to "cross" this boundary. Rather, it is merely by mass conservation, that an initial still pot composition which starts on one side of the boundary (B-AC straight line), and draws only pure B from the column, does

not cross this B-AC line. This type of pot composition boundary are defined as "mass-balance" pot composition boundaries throughout the thesis. In contrast, the pot composition boundary for the batch rectifier, as given by the separatrix between the fixed points B and AC, constrains the motion, in that a still pot composition does actually enter the pot composition boundary, and is unable to cross the boundary, due to a change in the alpha or omega limit set of the still pot composition as the pot composition boundary (also a separatrix) is entered. This type of pot composition boundaries are defined as "separatrix-type" pot composition boundaries in this thesis. The product sequence switches as the boundary is infinitessimally crossed, and this forces the pot composition back onto the boundary, thereby constraining the motion of the still pot of a batch rectifier within its own batch distillation region.

It should also be noted as an aside that in the presence of straight separatrices (Figure 5-4), the pot composition boundary for the rectifier would have been the same as that for the batch stripper, i.e., given by the straight line segment between the fixed point of pure B and the fixed point of the azeotrope AC. An initial pot composition starting in region μ_s will enter the pot composition boundary given by the straight separatrix, and draw the azeotrope AC as the new alpha limit set. The pot composition will thus stay in the batch distillation region given by the composition boundary of B-AC, draw AC as a distillate product, and finally pure B is left in the still pot. Similary, an initial pot composition starting in region ν_s will draw A as a distillate product, enter the straight sepratrix, and draw AC followed by B. The product sequences for μ_s and ν_s are thus given by (C, AC, B) and (A, AC, B) respectively. This is not significantly different from the product sequence in the presence of curved boundaries. The major difference is that the pot composition boundaries for the stripper (Figure 5-2) and rectifier (Figure 5-4) are both now in common, and the pot composition boundary given by the straight line B-AC will be a pot composition boundary for the middle vessel column.

When the separatrix is straight, the pot composition boundary for a middle vessel column separating the Acetone-Benzene-Chloroform mixture is invariant of λ, such that as λ changes from 0 (stripper configuration) through intermediate values of

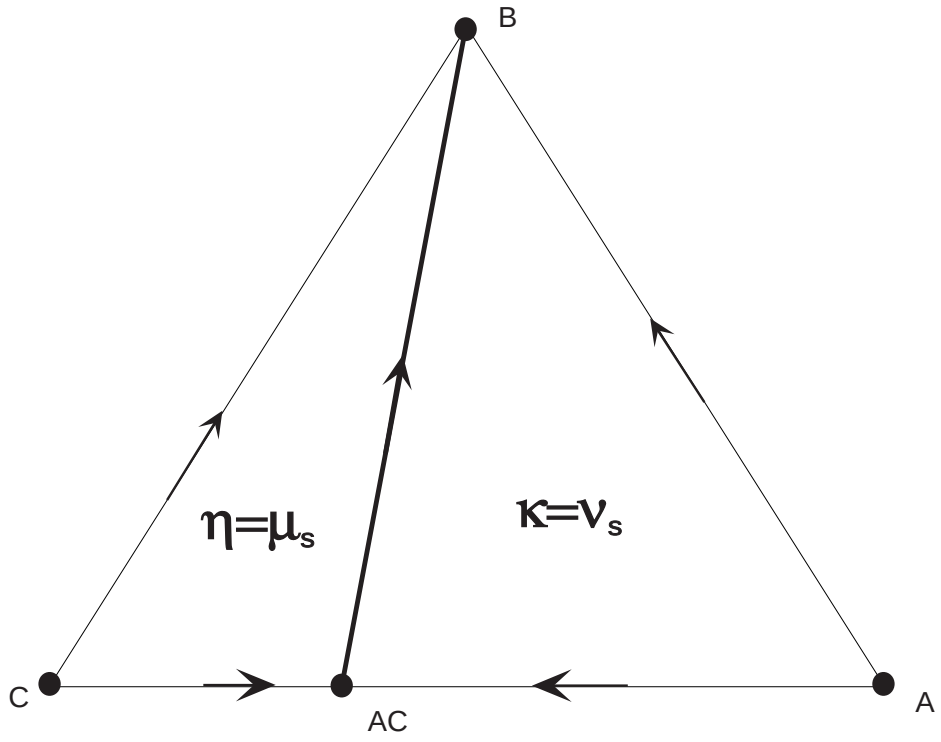

Figure 5-4: Batch Distillation Regions/Pot Composition Boundaries for a Batch Rectifier in the Presence of Straight Separatrices

λ (middle vessel configuration) to 1 (rectifier configuration), the pot composition boundary remains the same. Any pot composition boundary, for a middle vessel column at a fixed λ, which moves as λ varies will not be a pot composition boundary for a middle vessel column free to operate at different λs. This is because, ultimately, in a middle vessel column, there is the operational freedom to choose a value of λ at a given point in time (or warped time ξ), which will allow the shifting of boundaries in the appropriate direction, such that the pot composition barrier which existed at the orginal λ is moved. It should be noted that the pot composition boundary of the middle vessel column for the A-B-C system undergoes a step change, rather than a gradual shift as λ is varied. The pot composition boundary for the middle vessel column exists as the separatrix which connects AC and B for all values of $0 < \lambda \leq 1$, and only switches to the straight line segment between AC and B at $\lambda = 0$.

In summary, the pot composition boundary for the batch stripper is given by the straight line between B and AC, while the pot composition boundary for the batch rectifier is given by the curved separatrix between the fixed points B and AC. The two are not equivalent, hence they do not form a pot composition boundary for the middle vessel column that is free to operate at any chosen value of λ (i.e., it can cross these boundaries with an appropriate choice of λ as a function of time). To illustrate this point, consider the following operating procedure. Starting with a point σ_1 in the region ν, we could operate the middle vessel column as a rectifier drawing pure A as product, and cross the straight line segment B-AC as it is not a pot composition boundary for the rectifier (see Figure 5-5a). After crossing the line segment B-AC under batch rectification, the pot composition is now in the batch stripper region given by η as given by point σ_2 in Figure 5-5b. It is now possible to switch the operation of the column from that of a rectifier ($\lambda = 1$) to that of a stripper ($\lambda = 0$), and move the still pot composition across the separatrix (which does not form a pot composition boundary for the stripper configuration), and enter the batch rectifier region given by μ, to a point such as σ_3 (see Figure 5-5c). Effectively, the still pot composition crossed a batch stripper pot composition boundary given by the straight line between B-AC (moving from σ_1 to σ_2), and it also crossed a batch rectifier pot

composition boundary as given by the curved separatrix between B and AC (moving from σ_2 to σ_3). This follows the prediction in Section 4.4, where it was stated that it would be possible to cross stripper or rectifier pot composition boundaries with a middle vessel column, when the stripper and rectifier regions are not equivalent, as is the case here in the presence of curved separatrices.

Thus, from this simple operating strategy, we see that it is possible to traverse the "pot composition boundary" for the middle vessel column in the presence of curved sepratrices. The key to this result is primarily the fact that in the presence of curved separatrices, the pot composition boundary for one of the conventional (stripper or rectifier) configurations might be straight while the pot composition boundary for the other (rectifier or stripper) configuration is curved. This means that the pot composition boundaries that are common under the assumption of straight line boundaries are no longer common, and these "middle vessel pot composition boundaries" can be crossed by the middle vessel column still pot composition. It should be noted that while it is possible to move from σ_1 via σ_2 to σ_3, it is not possible to move in the reverse direction. This is similar to the case in Section 4.4, where it was possible to cross the batch rectifier boundary from region α into β but it was not possible to move from β into α. In our example of Acetone-Benzene-Chloroform, it is not possible to move the still pot composition from region μ to region ν even though it was possible to move the still pot composition from ν to μ. Similarly, it is not possible to move the still pot composition from region η into κ even though it was possible for the still pot composition to move from κ to η. Thus, even though the differing of stripper and rectifier regions offer some additional separation possibilities in a middle vessel column, the possibilities are not unlimited.

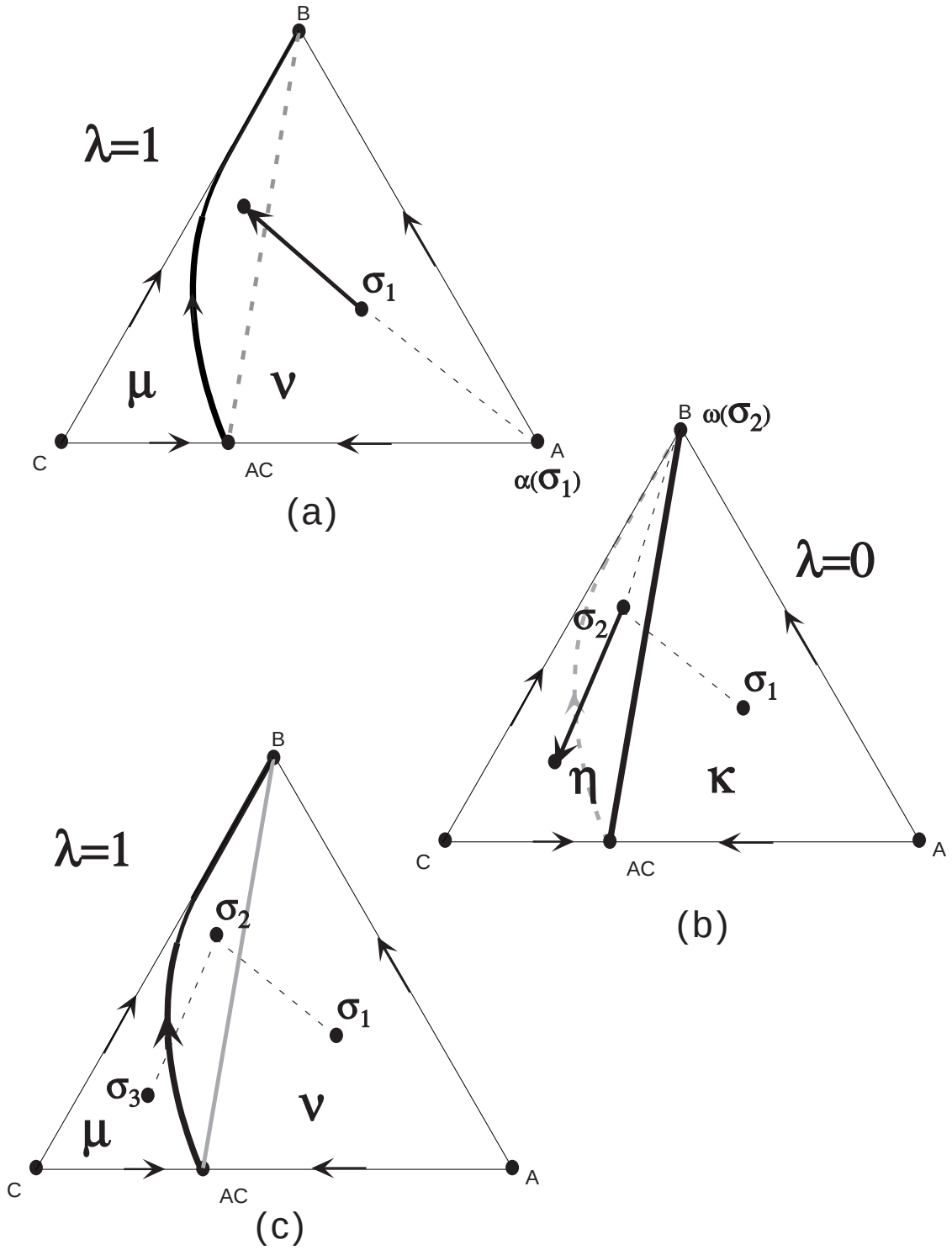

Figure 5-5: Operating Procedure for Crossing the Rectifier and Stripper Pot Compositiong Boundaries in the Presence of Separatrix Curvature

Table 5.1: Product Sequences for Regions μ_i for $i = 1..4$, Straight Line Separatrices

Region	First Cut	Second Cut	Third Cut
μ_1	$[C,B]$	$[AC,B]$	$[B,B]$
μ_2	$[C,B]$	$[AC,B]$	$[AC,AC]$
μ_3	$[C,B]$	$[C,AC]$	$[AC,AC]$
μ_4	$[C,B]$	$[C,AC]$	$[C,C]$

Table 5.2: Product Sequences for Regions ν_i for $i = 1..4$, Straight Line Separatrices

Region	First Cut	Second Cut	Third Cut
ν_1	$[A,B]$	$[AC,B]$	$[B,B]$
ν_2	$[A,B]$	$[AC,B]$	$[AC,AC]$
ν_3	$[A,B]$	$[A,AC]$	$[AC,AC]$
ν_4	$[A,B]$	$[A,AC]$	$[A,A]$

5.2 Operating Procedures Applicable for Breaking Azeotropes

For the analysis in this section, the ternary system of Acetone (A), Benzene (B) and Chloroform (C) will again be used. As explored in section 5.1, it was stated that under the assumption of linear separatrices the pot composition boundary of the rectifier ($\lambda = 1$) and that of the stripper ($\lambda = 0$) would be the same. However, the pot composition boundary for the middle vessel column operating at variable λ are the pot composition boundaries that do not transform as λ varies between 0 and 1. As such, for the A-B-C system, in the presence of straight line separatrices, the line segment B-AC will be a pot composition boundary for the middle vessel column as illustrated in Figure 5-6. This implies that a mixture starting at any point in any of the regions μ_i, (where $i = 1 \ldots 4$) in Figure 5-6, can never draw pure A as one of its products. The sequence of products for each of the regions μ_1 through μ_4 is listed in Table 5.1. Similarly, any initial composition within any of the regions ν_i, (where $i = 1 \ldots 4$) in Figure 5-6, can never draw pure C as one of its products. The corresponding sequence of products is also given in Table 5.2.

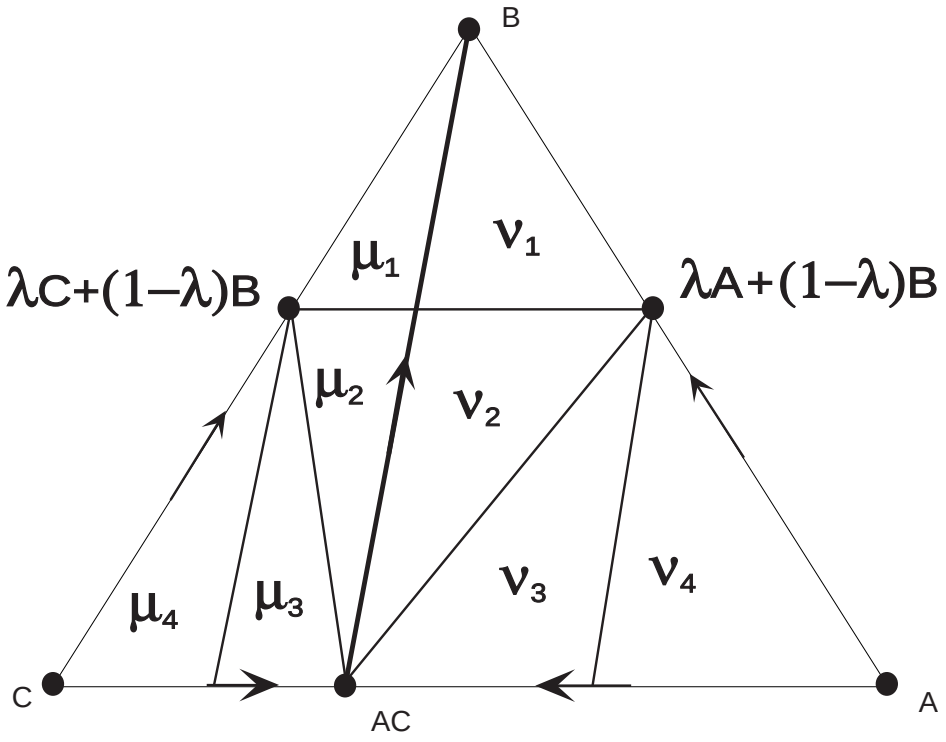

Figure 5-6: Pot Composition Boundary for the Acetone, Benzene and Chloroform System in a Middle Vessel Column

Thus, as illustrated by the sequences in Table 5.1 and 5.2, any initial composition point in the composition simplex of the Acetone-Benzene-Chloroform system, can only either draw (B,C) as pure products or (A,B) as pure products in the presence of straight line separatrices.

However, in the presence of curved separatrices, as is the case for the A-B-C system, the boundaries of the stripper and the rectifier no longer coincide. As explained in Section 5.1, it would thus be possible for the still pot composition to move from the regions given by ν_i ($i = 1 \ldots 4$) in Figure 5-6 to the regions given by μ_i ($i = 1 \ldots 4$). Furthermore, on a closer observation of the curvature of the stable separatrix connecting the fixed points AC to B, we see that the separatrix almost touches the composition simplex edge given by line segment B-C (see Figure 5-7).

Based only on the curved separatrix, it is possible to design an operating procedure (mode A) which involves the recycle of an azeotropic off-cut to the original feed to the still pot, provided that the initial still pot composition lies in the region given by ν.

1. Assume some original composition of the charge to be separated, which is designated as F in Figure 5-8. Mix this with the azeotropic off-cut from the last batch, to obtain a point M in the composition space. This is the initial still pot composition.

2. Operate the middle vessel column as a rectifier (with $\lambda = 1$) such that pure A is drawn, and the still pot composition moves directly away from the fixed point of A. Continue this operation until the still pot composition encounters the separatrix at point D (the separatrix forms a pot composition boundary $\forall\lambda\backslash\{0\}$), and the rectifier product starts changing from pure A to a mixture of AC-C.

3. Since pure cuts are desired, at this point, the operation of the middle vessel column will be switched to that of a pure stripper (with $\lambda = 0$), such that the pot composition boundary is shifted from that of the separatrix to that of the straight line segment between AC and B. The still pot composition is thus

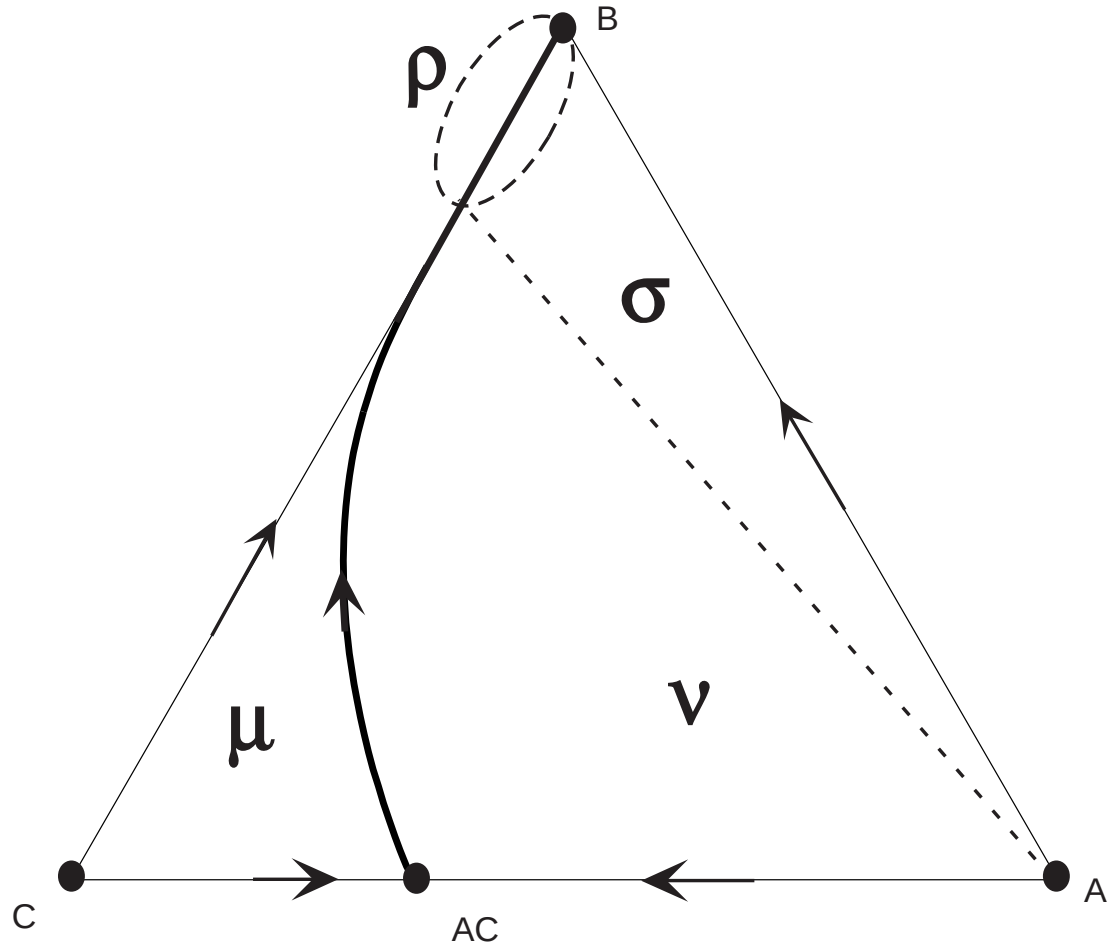

Figure 5-7: Stable Separatrix in the Residue Curves Map of the Acetone, Benzene and Chloroform System

able to cross the separatrix, and the column is operated as a stripper, drawing pure B as the bottoms product of the column. The still pot composition moves directly away from B, and encounters the C-AC edge at point E after all the benzene has been removed from the column.

4. At point E, the alpha and omega limit sets of the still pot composition are given by C and AC respectively. Since the pure products are of interest, the operation of the column will now be switched to that of a rectifier again ($\lambda = 1$), such that pure C is drawn as the distillate product. The azeotropic composition of AC will remain in the still pot after all pure C has been drawn. This still pot residue is then recycled into the next batch of mixture to be separated.

5. Alternatively, at point E (Figure 5-8), instead of using step 4, it is also possible to operate the middle vessel column at a value of $\lambda = \frac{l_2}{l_1+l_2}$ such that the column operates as a *quasi-static* operation, with the column holdup composition, distillate and bottoms product composition all remaining constant until the still pot runs dry (i.e., as $\xi \to \infty$). This operating policy utilizes the full capability of the middle vessel column (its ability to draw up to 2 products at any time). It is not necessarily beneficial, however, as the azeotropic off-cut will be recycled and mixed. The purity of the azeotropic off-cut is therefore not of great importance, and as such, recycling of the still pot residue in step 4 might be sufficient. A detailed analysis of quasi-static operation of the middle vessel column will be conducted in Section 5.4.

Even though the above operating procedures allow us to extract all 3 componenents in the ternary mixture (F) as pure products, it is unsatisfactory for a few reasons. Firstly, it precludes the separation of an original composition that is in the region μ, as any composition that begins in μ cannot be mixed with the azeotropic off-cut to produce an initial still pot composition which lies in region ν. As discussed in Section 5.1, it is impossible to draw pure A with a middle vessel column from a still pot composition starting in region μ, as it is possible to cross from region ν to μ but not the reverse. Hence, separation is not possible for a region (μ) of the com-

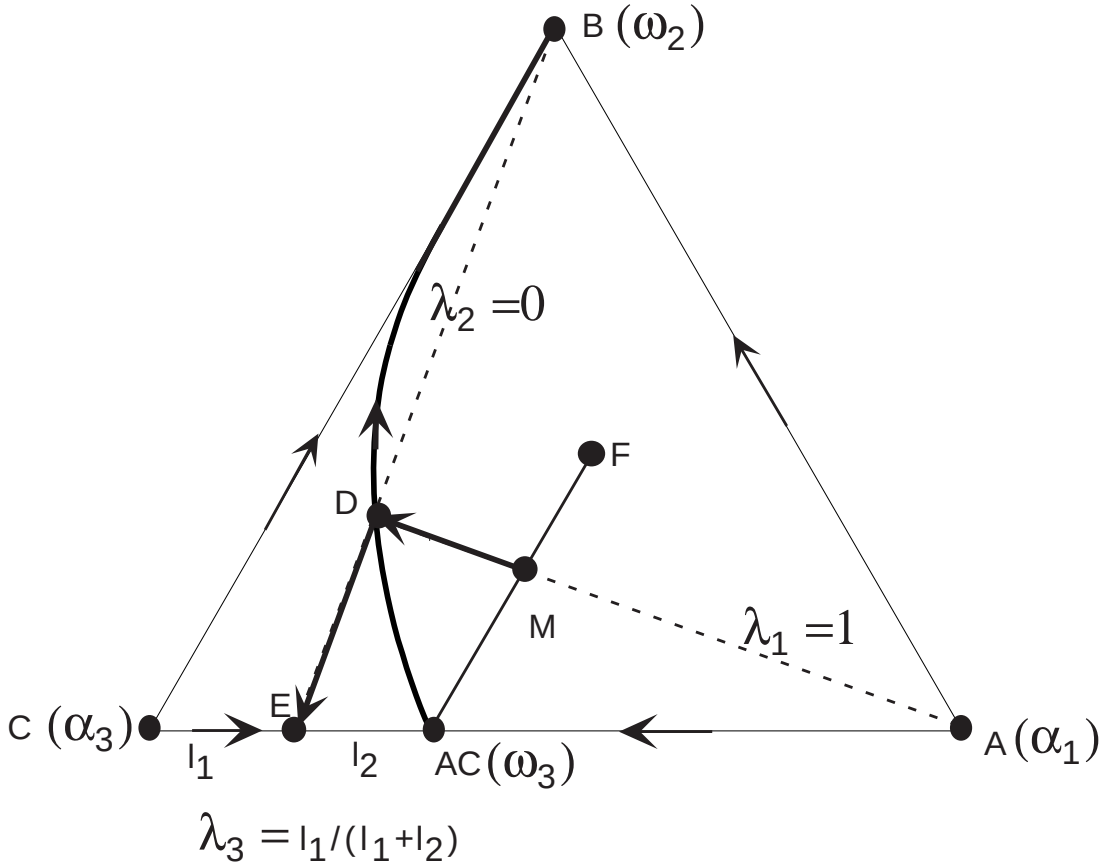

Figure 5-8: Operation Procedure For Separating an Acetone, Benzene and Chloroform Mixure with Recycle of Azeotropic Off-Cut

position simplex. Secondly, a batch distillation system is usually used in preference to a continuous distillation system due to small processing amounts or infrequent or discontinuous processing demands. As such, there might not be a "next batch" in which to mix the azeotropic off-cut into. As such, this azeotropic off-cut may have to be discarded. It would thus be desireable to obtain a separation sequence in which no azeotropic off-cuts are drawn nor recycled to the next batch. Last but not least, it precludes the separation of a mixture that is completely made up of the azeotrope AC, which is the most important mixture within the composition simplex; any point in the composition simplex can theoretically be separated into the pure components and the azeotropic off-cut with a traditional distillation column. Thus, if the azeotropic off-cut can be separated, all cuts can be separated. Furthermore, as the interest is in separating azeotropes, it would seem appropriate that the azeotropic mixture should be separable by the suggested operating strategy.

A better separation scheme for a mixture of acetone, benzene and chloroform which addresses the problems stated above, can then be synthesized based on these observations:

- A still pot composition which lies along the B-C edge of the composition simplex, when separated in a middle vessel column operating as a stripper would thus draw pure B as the product, with pure C as the last cut from the column. However, as observed, the curved separatrix lies so closely to the B-C edge that it is almost on the B-C line segment around the region ρ as shown in Figure 5-7. If it is possible to steer the still pot composition into the separatrix around the region ρ, it would then be possible to separate the remaining B and C in the still pot into pure B and almost pure C. It should be noted that a trickle of A might exist as impurity in the cut for C.

- In order for any mixture of A, B and C to be separated completely, it implies that pure A, pure B and pure C must all be drawn as products from the middle vessel column. Pure A is the alpha limit set of the region ν as shown in Figure 5-7, and can only be drawn as the distillate product of the middle vessel column

if the still pot composition is in the region ν. Pure B being the omega limit set, is drawn as the bottoms product for region ν. If it is possible to steer the still pot composition into the separatrix in the vicinity of ρ, it would then be possible to draw C as the last cut, as mentioned above, without drawing and recycling any azeotrope AC at all.

- However, it should be noted that the movement of the still pot composition is restricted by the vector cone of possible motion for the middle vessel column. In region ν, this is given by the 2 direction vectors, one of which points through the still pot composition away from the omega limit set (pure B), the other which points through the still pot composition away from the alpha limit set (pure A). However, this means that only a limited subset of composition points in the simplex can be steered into the desired location of the separatrix in the vicinity of ρ. This subset of still pot compositions which can be steered into the separatrix in the vicinity of ρ is represented by the region σ in Figure 5-7.

- Furthermore, a composition point in the region μ would not be able to draw pure A, regardless of the operating procedure. As analyzed in Section 5.1, it can only draw pure B, pure C, and a mixture of the azeotrope AC and C (as the still pot composition follows the separatrix). As such, the region μ is of little interest in the attempt to separate a ternary mixture of A, B and C.

- If pure benzene is drawn as one of the cuts, it can be recycled and mixed with the next batch of ternary mixture to be separated. Since pure benzene will again be drawn as pure product in this next batch operation, all the benzene that was added into the system will be recovered as pure benzene without any lost of benzene in the process (i.e., no make-up benzene is necessary).

- Any composition in the Acetone-Benzene-Chloroform composition simplex can be mixed with benzene to obtain a still pot composition for the separation which is different from the original composition of the mixture to be separated. The new initial composition is then related to the original mixture composition

and the pure benzene fixed point by an appropriate tie line. By varying the amount of benzene added, we can manipulate the position of the initial still pot composition, with the limits being:

$$\begin{array}{ll} \text{Amount of Benzene Added} \to 0 & \mathbf{x}^{M}_{initial} \to \mathbf{x}_{original} \\ \text{Amount of Benzene Added} \to \infty & \mathbf{x}^{M}_{initial} \to \text{pure B} \end{array} \tag{5.3}$$

It is thus theoretically possible to move any original composition point in the composition simplex into the region given by σ in Figure 5-7, with an appopriate amount of benzene added to the original mixture to be separated.

The resulting operating procedure (mode B) would then be given by the following steps, and illustrated in Figure 5-9. This can be achieved with any of the 3 categories of original mixture compositions namely that of: 1) a composition in region μ (δ_1 in Figure 5-9), 2) a composition in region ν (δ_2) and 3) the azeotropic composition AC (δ_3).

1. Add an appropriate amount of pure benzene to the original batch of ternary mixture (of A, B, and C) to be separated, such that the initial composition of the mixture to be separated in the middle vessel column is moved into region σ as denoted in Figure 5-9. This moves each of the original still pot compositions (δ_1 through δ_3) to the initial still pot compositions for separation in the middle vessel column, as given by points γ_1 through γ_3 respectively. Note that γ_1 through γ_3 all lie on the edge of region σ because these represents the least amount of benzene added to each of initial compositions δ_1 through δ_3 to move these points into the region σ.

2. With the initial still pot composition in the region of σ, operate the middle vessel column as a rectifier (with $\lambda = 1$) so as to steer the still pot composition to enter the separatrix in region ρ where the separatrix is as near to the B-C edge as possible, so as to minimize the amount of impurity (component A) in the final cut of C from the middle vessel column.

3. After the still pot composition encounters the separatrix at point G (and consequently is very near the B-C edge in the vicinity of ρ), the alpha limit set of the current still pot composition will change to that of the fixed point of AC. However, AC is not a desired product, hence the product flow rate of the rectifying section of the column is shut off at this time. Instead, the product flow rate for the stripping section of the column is turned on, such that the middle vessel column now operates as a stripper. λ has thus changed from 1 to 0 in this operating step, and pure B is now drawn as bottoms product from the column. As mentioned in Section 5.1, the separatrix forms a pot composition boundary for the rectifier only, and as such does not constitute a pot composition boundary for the column operating as a stripper. The still pot composition is thus able to cross the separatrix.

4. Continue to draw pure B as product, until all of the benzene has been removed from the column. The still pot composition will encounter the C-AC edge at this point in time, and the residue in the still pot will be almost pure C with a trickle of A as impurity. If this purity is reasonable, the still pot can be collected as pure C product. This purity should be easily more than 99%.

5. If the purity does not meet the specifications, the middle vessel column can be further operated as a rectifier ($\lambda = 1$) such that the alpha limit set of the still pot composition, namely pure C is drawn as distillate product from the column. The residue that remains will be the azeotrope AC, but it will be a trickle, as determined by the amount of A that remains in the column, which will be significantly less than 1% of the original charge to be separated. Alternatively, the column could also be operated as a stripper for a short period of time to remove the azeotrope off-cut as bottoms product, leaving C in the still pot. The disadvantage of operating the column as a stripper would be that there might be scum which accumulates in the still pot, thereby rendering the C left in the reboiler unpure.

6. Alternatively, we could again subsitute steps 4 and 5 with the following proce-

dure which utilizes the full capability of the column. For this case, the middle vessel column is operated as a stripper such that the still pot composition crosses the separatrix. Once the middle vessel column composition crosses the separatrix, the alpha limit set of the still pot composition will be changed to that of pure C. The column is then operated until a point where the amount of benzene in the column equals the amount of chloroform in the column. It is then possible to employ a quasi-static operation of the column with $\lambda = \frac{l_3}{l_3+l_4} = \frac{1}{2}$ so as to draw the distillate product C and bottoms product B while keeping the pot composition unchanged (and hence the alpha and omega limit sets unchanged, which results in unchaged product compositions). This allows us to draw pure chloroform from the column while benzene is drawn, thereby utilizing the complete capacity of the column to draw two products at a time, while maintaining the required purity of the products (by maintaining the reflux ratio). As the separatrix is not exactly on the B-C edge, some A remains in the system. As such, the final still residue in the pot would be some mixture of A, B and C, which can be discarded, as it is only a trickle.

With the above operation scheme, all the benzene that was added to the system is recovered and can be recycled or resold. The waste cut is negligible, and can be essentially considered as non-existent. The separation scheme above thus essentially allows us to separate any mixture of acetone, chloroform and benzene into its individual components at purities higher than 99%. An actual simulation of each of these operating policies was conducted using the ABACUSS model of a middle vessel column and the results are summarized in Chapter 7.

Finally, it should be noted that ultimately, if there were enough batches of mixture to be separated (such that a recycle of the azeotropic off-cut was feasible) and the original composition was in region ν, there would be a trade-off between the use of the first operating procedure (mode A: recycle of azeotrope, no addition of benzene) against the use of the second operating procedure (mode B: addition of benzene, no recycle of azeotrope). In the mode A operating procedure, without recycle of azeotropic off-cut, a huge portion of the original mixture is recovered as an azeotropic

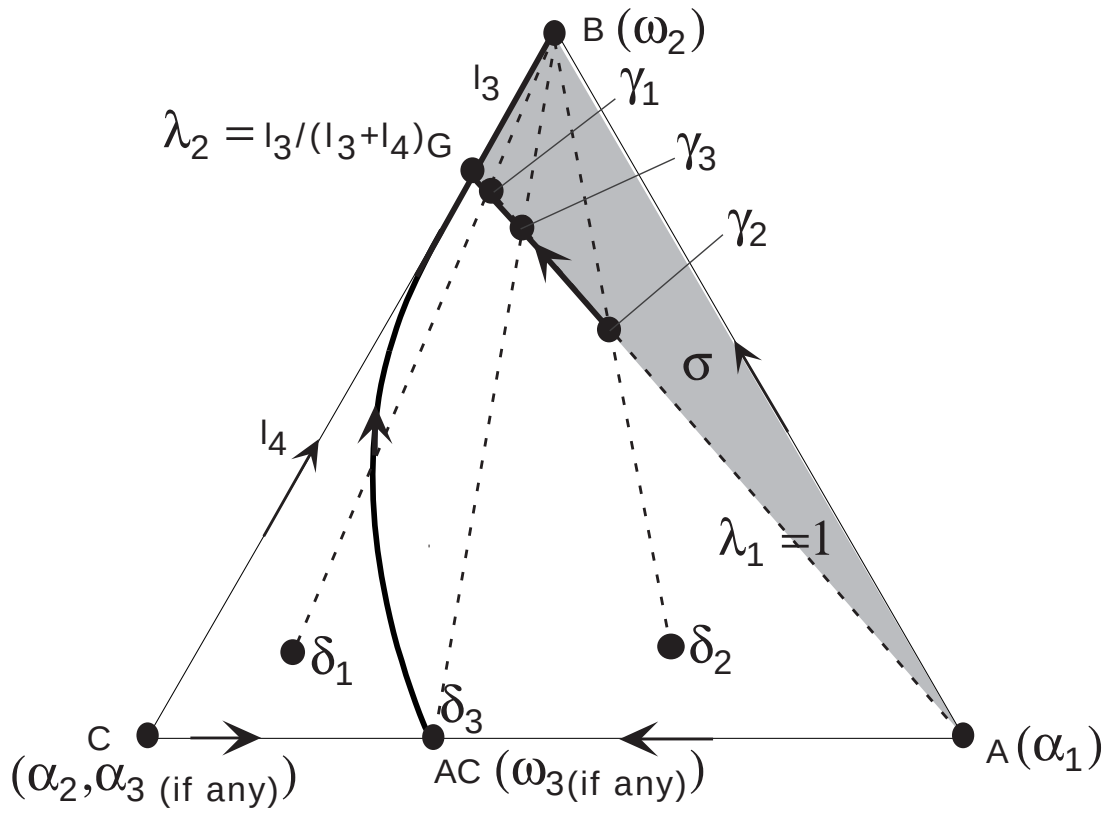

Figure 5-9: Operation Procedure of Separating Acetone, Benzene and Chloroform Mixture with Addition of Benzene as "Entrainer"

off-cut which is undesireable, and represents both a waste disposal cost as well as a raw material cost (due to pure components not recovered). However, the operating load on the column is smaller (i.e., less charge per batch/less batches of charge) and hence, energy costs are lower. Alternatively, following mode A of operation, the azetropic off-cut can be recycled, resulting in larger batches, higher energy costs, but complete recovery of the pure components, with no waste disposal costs and lower raw material costs. Conversely, mode B of operation could be used to recover almost all of the mixture as pure components (or within purity specifications), with a negligible waste cut (and hence minimal lost in revenue). However, the addition of benzene as an entrainer does result in a much larger initial charge into the still pot, which in turn may represent higher energy requirement/cost. Depending on the cost of raw materials, energy and capital equipment rental, the actual objective function of the separation process will vary accordingly. As such, it is not immediately clear which of the 3 suggested operating procedures are preferable. However, with the current emphasis on zero-waste production technologies by speciality chemical and pharmaceutical industries, the use of the second and third procedures would seem more attractive, as they are zero-effluent technologies in which all of the waste cut is recycled to the next batch. Indeed it is possible that a mix of the operating strategies (i.e., mixing with pure benzene coupled with a recycle of an azeotropic off-cut) could be optimal. This is an excercise in optimization which will depend largely on the specification of the problem (such as cost of materials, amount of material, capital cost of operation and energy costs).

It should also be noted that the size of the recycle cut is a direct function of the amount of benzene added, and hence, a choice of the amount of benzene added directly determines the amount of azeotropic off-cut obtained. This is because for a given mixture to be separated, addition of more benzene results in a still pot composition encountering the separatrix (pot composition boundary) at a point nearer to the region ρ (for example H in Figure 5-10), pure benzene is then drawn from the column until the pot composition encouters the point K on the C-AC edge. As can be seen from the diagram, the proportion of C to AC drawn from the still pot is thus given

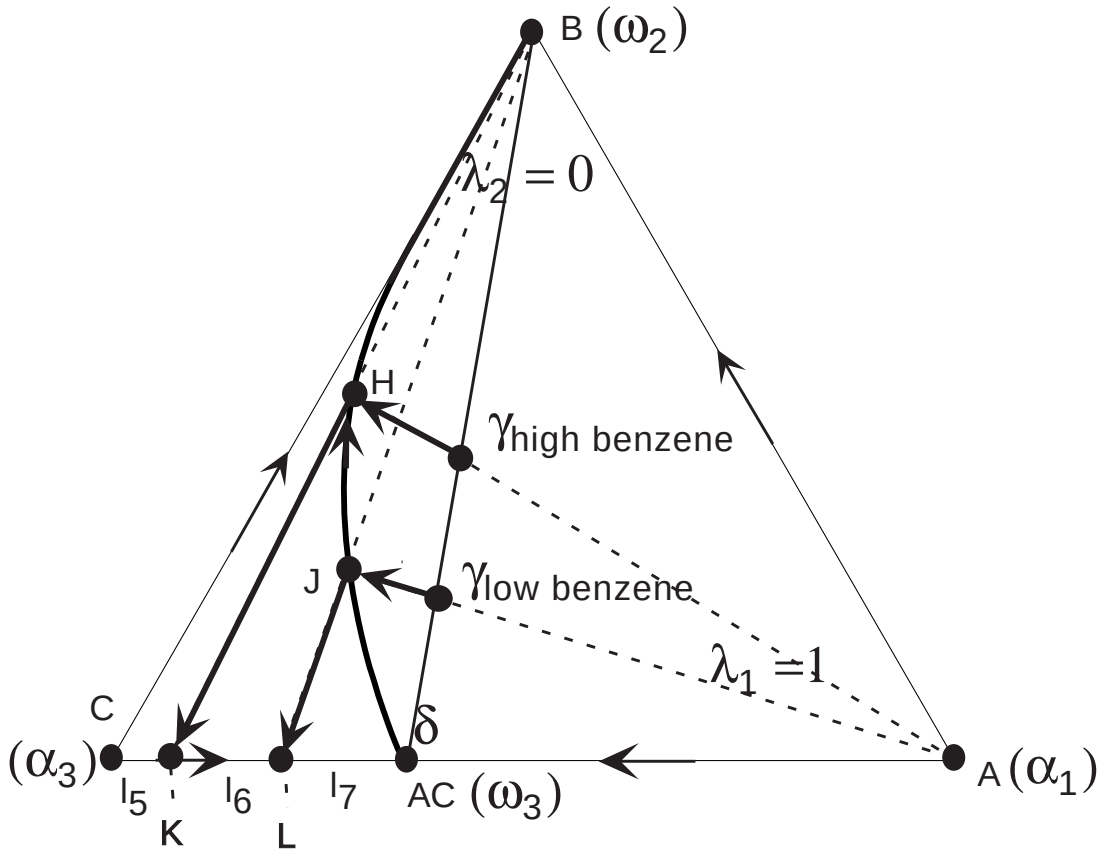

Figure 5-10: Dependency of Recycle Cut Size with the Amount of Benzene Added as "Entrainer"

by the lever ratio of point K between C and AC, which would mean that a fraction $\frac{l_6+l_7}{l_5+l_6+l_7}$ of the C in the mixture, prior to addition of benzene, will be recovered as pure C, while $\frac{l_5}{l_5+l_6+l_7}$ of C has to be recycled or is lost in the AC cut. In comparison, if less benzene were added, and the pot composition encounters the separatrix at a point such as J instead (see Figure 5-10), the resulting interesection of the still pot composition after drawing all the benzene in a stripper configuration, will be at L, and only $\frac{l_7}{l_5+l_6+l_7}$ of the original C can be recovered as pure C, while $\frac{l_5+l_6}{l_5+l_6+l_7}$ of the C is lost as AC. As can be seen, a larger amount of benzene added corresponds to a smaller amount of AC recycled (or discarded), and a direct relationship between the amount of benzene added, the interesection point of the still pot composition with the separatrix B-AC, and correspondingly the fraction of C recovered as pure C or recycled as the azeotropic off-cut AC, can be obtained. There is thus only one degree of freedom in the selection of an optimal policy (i.e., a cost minimization problem with respect to one variable) for this separation process.

5.3 A Comparison to Wahnschafft *et al.*'s Continuous Column Sequences for Separating the Acetone, Benzene and Chloroform Mixture

The above operating procedures for the separation of acetone, benzene, and chloroform in a middle vessel batch distillation column were formulated based on an appreciation of the behavior of a middle vessel column which was developed in our limiting analysis of the middle vessel column. An analog of these operating procedures in a continuous distillation column were, however, first proposed for the separation of the acetone, benzene, and chloroform mixture by Wahnschafft *et al.* in 2 separate papers regarding separability of azeotropes in a continuous distillation column [39], and the synthesis of separation processes with recycle streams (also continuous systems) [40].

An analog to the first operating procedure described in Section 5.2 was proposed in their work on the separability of an azeotrope in a continuous column [39]. Based

on the analysis of Laroche *et al.* [21] who highlighted the separability of an inverse-020 system using multiple columns, Wanschafft *et al.* proposed a similar operating scheme for the Acetone-Benzene-Chloroform system (which is an inverse-020 system). They provided the separation sequence of continuous distillation columns and a depiction of the location of the cuts and recycle streams on the composition simplex as illustrated in Figure 5-11.

From Figure 5-11, we see that their operating procedure is exactly analogous to our first operating procedure (mode A) in the middle vessel batch distillation column in that:

1. The first step involves the mixing of an azeotropic cut (B_3, the bottoms product of their third distillation column) with the original feed F, such that an initial feed composition into the first column is obtained at M, much our initial mixing of the azeotropic cut from the previous batch with a new batch of material with feed composition F to obtain a new initial composition (see Figure 5-8).

2. The first column then draws pure acetone (D_1) as the distillate product, much like the first operating step in our first operating procedure, where pure acetone (D_1) is drawn from the middle vessel column operating as a rectifier ($\lambda = 1$).

3. The second column takes the bottoms product of the first column, which has a composition that lies on the separatrix at B_1, as a feed. B_1 lies colinearly with D_1 and M, an artifact of the mass balance around the column at steady state. This is completely analgous to our operating procedure which draws pure acetone and moves still pot composition in a straight line directly away from the acetone fixed point until it encounters the separatrix, with a still pot composition given by a point such as B_1.

4. With B_1 as its feed, the second continuous column then draws the bottoms product of pure benzene (B_2), and sends the distillate with composition given by D_2 into the third column. This is again exactly analgous to our operation of the middle vessel column as a stripper ($\lambda = 0$) in our second operational step

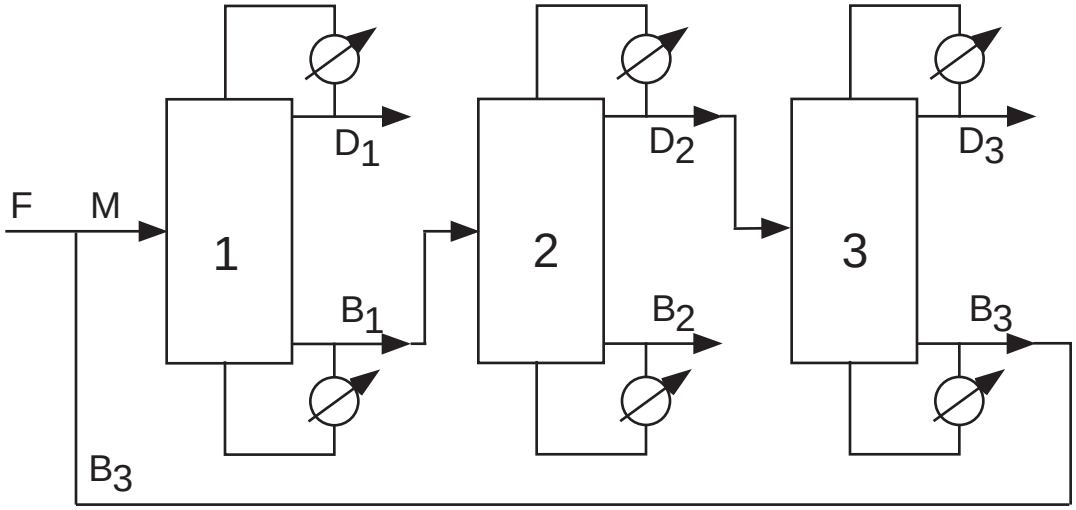

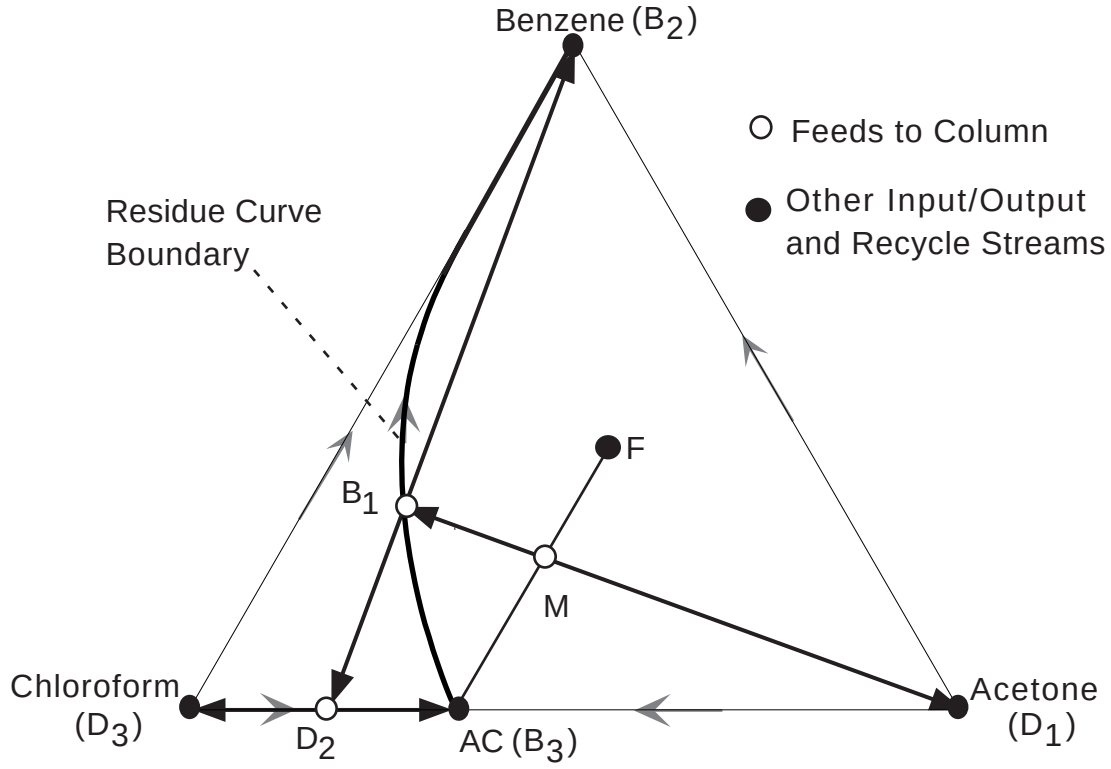

Figure 5-11: Continuous Distillation Analog of First Operating Procedure with No Addition of Benzene and Recycle of Azeotropic Off-Cut

which drew pure benzene as the bottoms product as well. As before, B_2, B_1 and D_2 lie colinearly to each other, which is analogous to the movement of the still pot composition directly away from the fixed point of pure benzene, resulting in a still pot composition such as D_2 at the end of the operating step.

5. Finally, the distillate of the second column D_2 is fed to the third column, where pure chloroform (D_3) is drawn as the distillate product, with the azeotrope of AC (given by B_3) drawn as the bottoms product for recycle back to the first column. This is again analogous to our third operating step, where pure chloroform was drawn from the middle vessel column operating as a pure rectifier ($\lambda = 1$), and the azeotrope is left as the residue in the still pot (step 4, first operating procedure). In fact, it is even more similar to the alternative operating step proposed (step 5, first operating procedure) where pure C was drawn as distillate products, and the azeotrope AC was drawn as bottoms product, to be recycled into the next batch of mixture to be separated. It should be noted that this recycle of the azeotropic off-cut back to the initial column/operating step is also similar across the two columns, continuous and middle vessel batch.

Thus, the main difference between the two processes is that in the continuous column sequence proposed by Wahnschaft *et al.*, the separation was achieved using 3 columns (with 2 sections, rectifying and stripping), at the same point in time (i.e., once the continuous sequence was operating at steady state, pure acetone, benzene and chloroform will all be drawn at the same point in time), whereas for the operating procedure proposed for the middle vessel batch distillation column in Section 5.2, the separation was achieved using one column (again with both a rectifying and a stripping section), but over a period of time with 3 different operating steps. In other words, as mentioned in the introduction of this chapter, the proposed separation scheme by Wahnschafft *et al.* was achieved by spreading out the process in space-domain (spatially distributed into 3 columns), as opposed to our proposed operating procedure in the time-domain (varying the operating procedure over time in the same column).

A spatially distributed operating sequence similar to the second operating procedure (mode B) proposed in Section 5.2 was also proposed by Wahnschaft *et al.* in their discussion of algorithms for synthesizing complex separation processes with recycle [40]. Figure 5-12 illustrates their sequence of continuous distillation columns with the corresponding distillate, feed and bottoms composition on a composition simplex.

As we can see from Figure 5-12, Wahnschafft *et al.* also designated a region of compositions "satisfying mixing goal", similar to the region σ in Figure 5-7. They then went on to specify the operating procedure as follows:

1. As with the first step of our operating procedure proposed in Section 5.2, the first "step" of Wahnschafft *et al.*'s proposed sequence was also the mixing of a benzene recycle flow, from the bottoms product of the second continuous column, with the original feed F to the separation train, so as to obtain a feed composition of M into the first column. As with our analysis in Section 5.2, in order to minimize the amount of benzene recycled (and hence minimize the energy consumption/size requirement of the columns), the feed composition was also moved onto the edge of the shaded region of compositions which "satisfy the mixing goal" (which corresponds to σ).

2. This mixed feed is then introduced into the first continuous column where pure acetone is drawn as the distillate product, while the bottoms product corresponds to a point on the residue curve separatrix in a region where it hugs the B-C edge. As before, the feed to the column M, the distillate (D_1)and bottoms (B_1) product composition are all colinear. This is again similar to the first operational step in our operating procedure in which pure acetone is drawn as the distillate product, resulting in a still pot composition similar to the point B_1 (which is colinear with the initial still pot composition M and the distillate product drawn D_1). This bottoms product in then used as a feed to the next continuous column, much like the still pot residue in the middle vessel column which is separated in the next operational step.

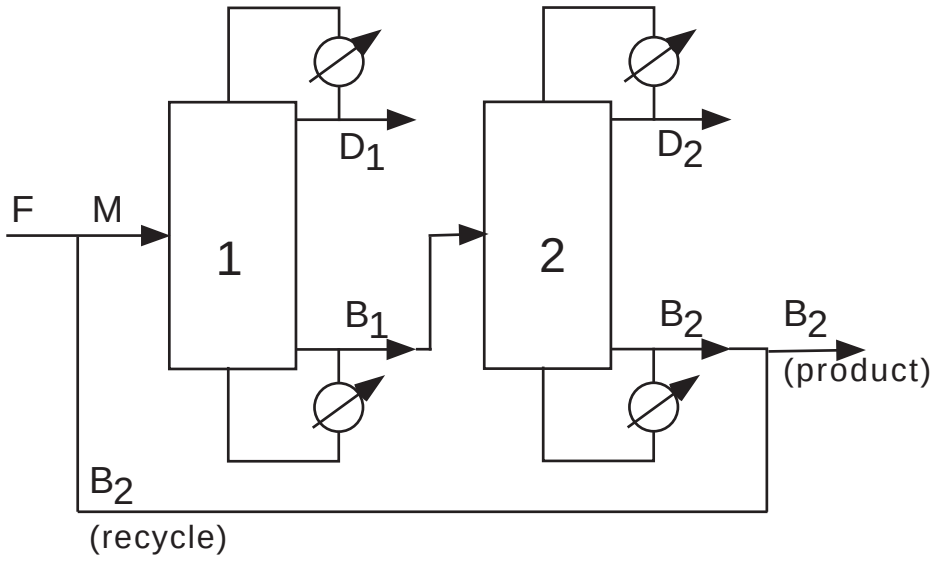

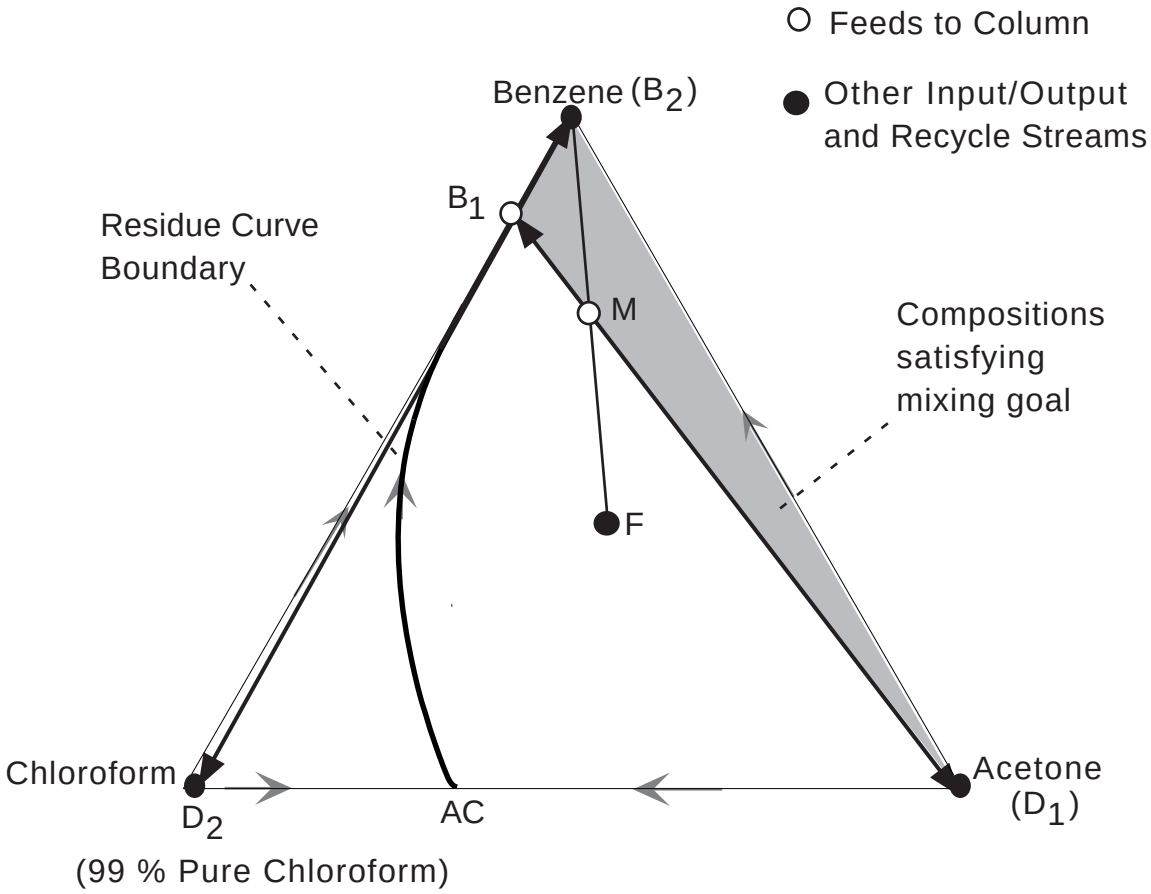

Figure 5-12: Continuous Distillation Analog of Second Operating Procedure with Addition of Benzene and No Recycle of Azeotropic Off-Cut

3. With the feed on a point nearly on the B-C edge, Wahnschafft *et al.* then pointed out that it was possible to draw pure benzene and 99% pure chloroform as products from the second continuous column. This is again analogous to our analysis that it is possible to separate the resulting still pot composition on the separatrix edge and B-C edge, by either operating the column as a stripper (in which case pure benzene is obtained as a distillate product, with the 99% purity chloroform left as the still pot residue) or by operating the column under a quasi-static operation policy, such that pure benzene is drawn as distillate product, pure chloroform is drawn as bottoms product, and the pot composition is (almost) unchanging in time. The residue that remains in the still pot (azeotrope AC) is negligible ($< 1\%$ of the charge) and can be discarded.

Thus, as before, the structure of column sequence proposed by Wahnschafft *et al.* is completely analogous to the time-domain operating policy discussed in Section 5.2 with the middle vessel batch column. In this case, Wahnschafft *et al.*'s 2-column sequence of continuous columns with all 3 pure products drawn at the same point in time is the space-domain analog of the one-column 2-operational step policy in which the products are drawn over different periods of time. A notable difference between the middle vessel batch distillation column operating policy and the continuous distillation column sequences is that the middle vessel column offers the possibility of drawing close to 100% pure chloroform as one of the product cuts and recycle/discard the azeotropic off-cut which is approximately 35% chloroform but of a negligible quantity, whereas by mass balance, the continuous column has to draw chloroform of 99% purity. It is however possible to put this chloroform of 99% purity into another continuous column to obtain chloroform of close to 100% purity, but that would require an additional column for separation. Hence, the fact that the distillate, bottoms and still pot compositions in a middle vessel column need not lie colinear to each other, results in a greater flexibility in separations with a middle vessel column as compared to a continuous column.

From the close parallel of the separation possibilities afforded by the continuous column versus that of the middle vessel batch distillation column, it is not difficult

to realize that the two types of columns are closely related in their behavior. In the next section, we will briefly discuss their similarities and differences.

5.4 A Discussion about the Equivalence of the Middle Vessel Column versus a Continuous Batch Distillation Column

In this section, the similarities and differences are enumerated between a continuous column versus a middle vessel batch distillation column operated in a quasi-static state and a middle vessel column operated with an open loop control policy.

In a continuous column, the distillate and bottoms product compositions must lie colinearly with the feed composition into the column. The distillate and bottoms products must also lie on the same distillation line (which describes the composition profile of the column). As mentioned in Section 4.1, with an infinite reflux/reboil ratio, the composition profile of trays in any column would be traced out by the residue curve that passes through the feed tray composition (i.e., the composition profile of the tray column are discrete points very close to the residue curve), whereas at lower/finite reflux/reboil ratios, the composition profile of the column tends to have a greater curvature as compared to that of the residue curves. Thus, assuming non-limiting conditions, a continuous column processing a feed which is a mixture of acetone, benzene, and chloroform, could have a feed F, bottoms product B_1 and distillate product D_1 as shown in Figure 5-13.

As illustrated in Figure 5-13, the feed composition in a continuous column as given by F need not correspond to that of the feed tray composition (M). The feed composition must be colinear to the other 2 product compositions. This is a fundamental restriction on the operating possibilities of the continuous column that does not exist in the middle vessel column (as illustrated in Section 5.2, where it was pointed out that chloroform of close to 100% purity could be drawn from the middle vessel column but not from the continuous column). To maintain material balance

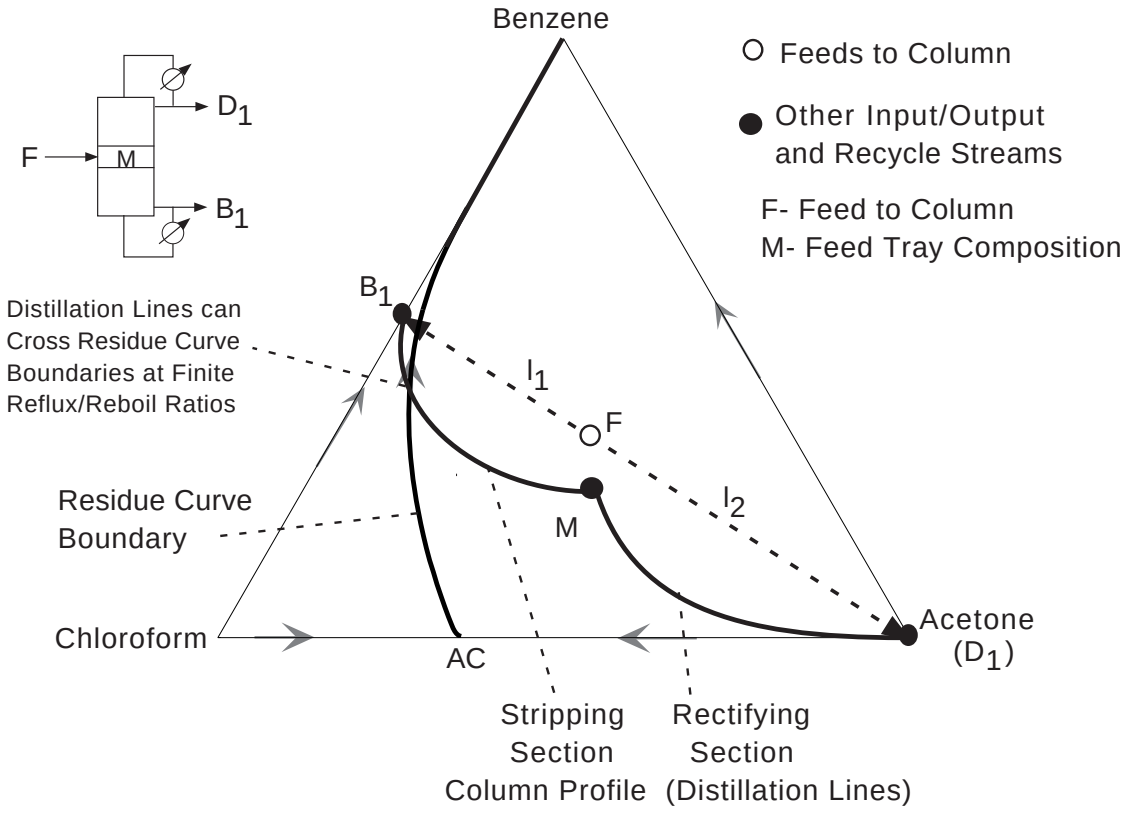

Figure 5-13: Continuous Distillation Column Operating on an ABC Mixture at Non-Limiting Conditions

over the column, the ratio of the D_1 flow rate to the B_1 flow rate drawn from the column is then given by $l_1 : l_2$. The tray composition profile is then given by discrete points along the distillation line of the column.

It is then our claim that a separation such as that illustrated in Figure 5-13 that is achievable at steady state in the continuous column, will also almost always be achievable in a middle vessel column. ("Almost always" is used because it is recognized that intrinsic differences between the two columns will mean that there will be examples in which a separation is achievable by a continuous column but not by a middle vessel batch column.) Using the same feed and product composition points (as that of Figure 5-13), a middle vessel batch column analog of the continuous column separation is illustrated in Figure 5-14.

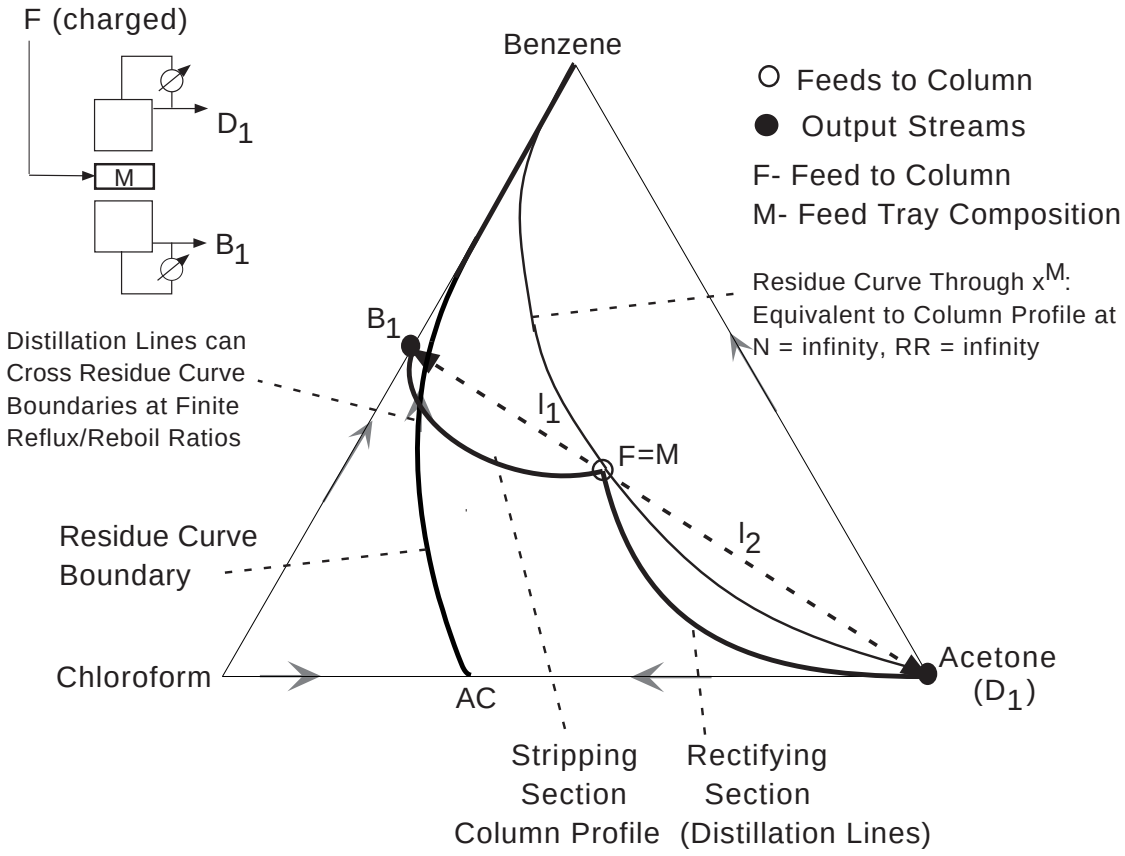

Figure 5-14: Middle Vessel Batch Distillation Column Operating on an ABC Mixture at Non-Limiting Conditions

The first significant restriction on the middle vessel column which does not ap-

ply to a continuous column is that while the feed/charge composition need not lie colinearly on the composition simplex with the bottoms and distillate compositions, they must however lie on the same distillation line (or column profile). It is however possible to vary the number of trays in each of the stripping and rectifying sections of the column, and vary the reflux and reboil ratios for the column, such that the product points of D_1 and B_1 can be achieved as before. Operating the column under a quasi-static operating policy, the ratio of D_1 to B_1 flow rates is again given by $l_1 : l_2$, or in other words, $\lambda = \frac{l_1}{l_1+l_2}$. This quasi-static operating policy completely reproduces the separation achieved by the continuous column, in that 1) with $\lambda = \frac{l_1}{l_1+l_2}$, the net product drawn from the column has effectively been situated at point M. That is to say, the net vector of still pot motion as given by $(\mathbf{x}^M - \mathbf{x}^P)$, is of zero length. The still pot composition will not move as long as λ is unchanging. Conversely, the composition of the products will not vary as long as M remains stationary, and the reflux and reboil ratios are maintained in the rectifying and stripping sections of the column respectively. Thus, with a clever manipulation of the operating parameters of the middle vessel column, a separation that is achievable with a continuous column can also be conducted in a middle vessel column. The only difference is that while the continuous column can operate for $t \to \infty$, the middle vessel batch column can only operate up till just before $\xi \to \infty$. Other than that, the feed/charge and products are of the same composition, and remain at the same composition, throughout the operation of both columns.

Thus the middle vessel column is able to achieve separations which are feasible in a continuous column. This may prove extremely useful for speciality chemical and pharmaceutical industries, where a separation which is currently achievable with a continuous column is not conducted due to the low and infrequent need for this separation. With the possibility of using a middle vessel column to achieve the same separation for batches (rather than a continuous flow of feed), less waste and more recycling of chemicals may be achieved economically by these industries.

Alternatively, given that the crux of separation processes equivalency lies in the composition of the products drawn, the middle vessel column holdup composition

need not be restricted to the same point throughout the duration of the middle vessel column operation, provided the product compositions are not compromised. In that vein, it would be possible to devise an open loop optimal control policy where the distillate product flow rate $D(t)$ and the reboiler heat duty $\dot{Q}_R(t)$ is controlled as illustrated in Figure 5-15, so as to maintain the required distillate and bottoms product composition. The middle vessel still pot composition will then be allowed to move freely in the column, as long as the $D(t)$ and $\dot{Q}_R(t)$ are controlled appropriately. The value of the middle vessel parameter λ at any point in time will be implied by the instantaneous values of $D(t)$ and $\dot{Q}_R(t)$. This operating policy does, however, involve elaborate control system, which is not necessarily desireable. This is balanced by the additional separation possibilities associated with the freedom to move the still pot composition.

Finally, it should be noted that although the middle vessel column offers the added flexibility of still pot composition motion and the added flexibility in that the feed and product compositions need not be colinear, there is also the additional constraint that the feed composition must lie on the same distillation line (or column profile). Thus, while it may offer some additonal operating flexibilities, there may also be additional operating constraints which would normally not apply to continuous column. This could then possibly preclude some of the separations achievable in a continuous column, from being achievable in the middle vessel column. Nevertheless, this quasi-equivalency of the middle vessel column with that of the continuous column would be at least be useful in some cases to industries with low/intermittent-volume of chemical output, in helping them formulate separation policies for their products or wastes.

5.5 A Discussion on the Perfect Entrainer

The characteristics of a perfect entrainer for separating an azeotrope in a middle vessel column can be developed from the above analysis. A perfect entrainer should enable the separation of a given azeotropic feed such that no or negligible azeotropic off-cuts

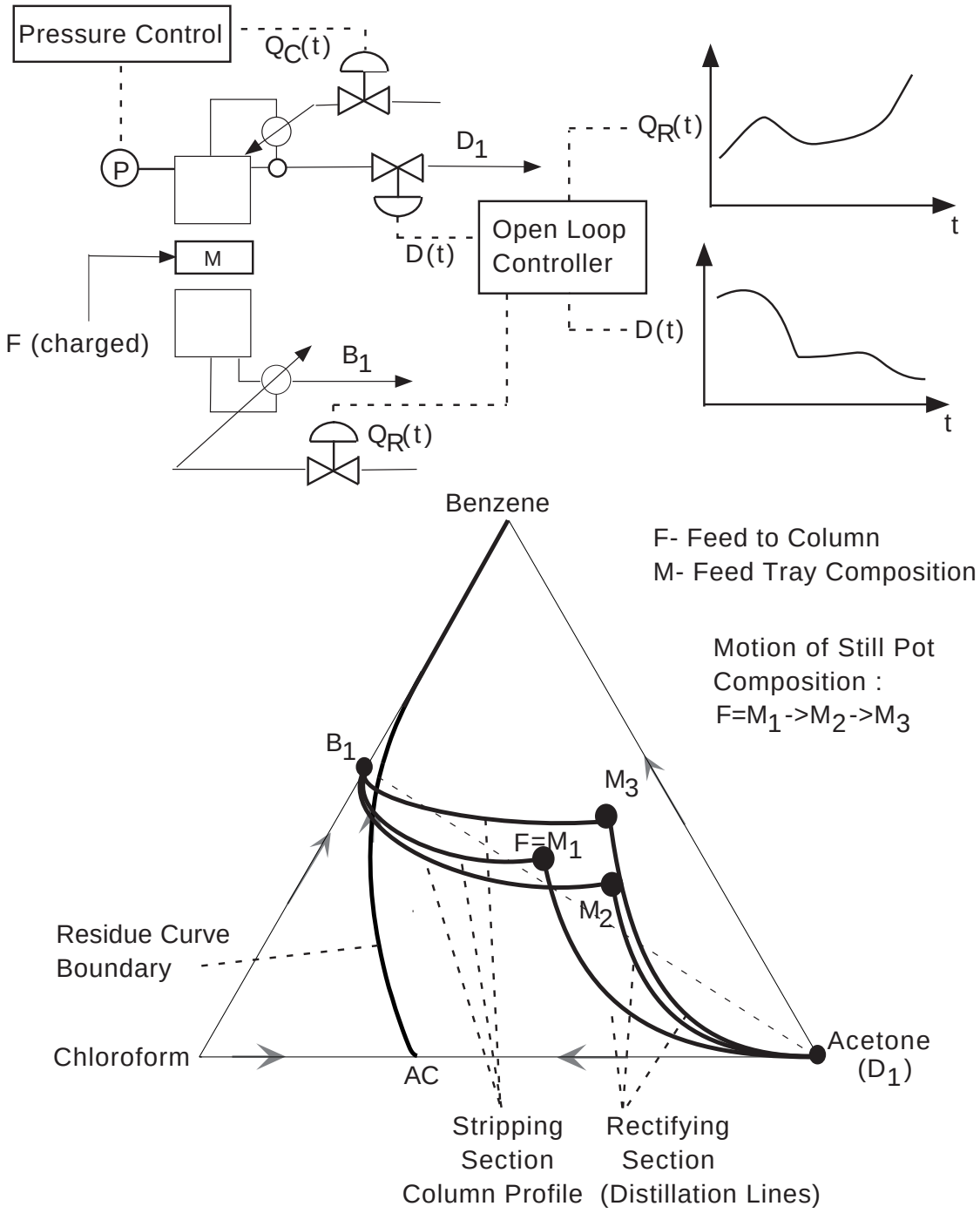

Figure 5-15: Middle Vessel Batch Distillation Column Operating on an ABC Mixture at Non-Limiting Conditions, with an Open Loop Optimal Control Policy

are drawn or recycled, and all products drawn from the middle vessel column have purity that meet reasonable specifications (for example, purity $> 99\%$). As mentioned in Section 5.2, the need for no recycle of the azeotropic off-cuts stem from the fact that there is sometimes no "subsequent" batch to which to recycle the azeotropic cut to, and this azeotropic off-cut would have to discarded.

One such example of a perfect entrainer for a binary azeotrope was provided by Bernot *et al.* in their discussion on the behavior of batch strippers [6]. It was not stated explicitly in their work that such an entrainer was "perfect", but they proposed the addition of an intermediate boiling entrainer to a binary mixture X_i-Y_i which exhibits a binary azeotrope X_iY_i so as to produce either a 001 system (minimum-boiling azeotrope) or an inverse-001 system (maximum-boiling azeotrope). Addition of these entrainers to the azeotrope would then allow us to draw the X_i, Y_i and entrainer E_i using a middle vessel column without the need for recycle of the azeotropic off-cut. In fact, as pointed out by Bernot *et al.*, the minimum-boiling azeotrope X_1Y_1 which forms a 001 system with the entrainer can then be separated completely into its pure components by a stripper (as illustrated in Figure 5-16), while the maximum-boiling azeotrope X_2Y_2 which forms an inverse-001 system can then be separated completely into its pure components by a rectifier (as illustrated in Figure 5-17). The principles behind these separations are based on the fact that a stripper draws as its product the omega limit set of its current pot composition, while a rectifier draws as its product the alpha limit set of its current pot composition (see Section 4.2).

However, entrainers which allow perfect separations of a given azeotrope in a stripper or in a rectifier, would also serve as perfect entrainers for a middle vessel column. This is illustrated in Figures 5-18 and 5-19. For the 001 system in Figure 5-18, after the initial still pot composition of M_1 is obtained via mixing the azeotrope with the entrainer, the column is operated at $\lambda = 0$ as a pure stripper, drawing the first omega limit set (pure X_1) as product until the still pot composition encounters the E_1-Y_1 simplex edge. The column can then be operated at $\lambda = \frac{l_1}{l_1+l_2}$, such that the column draws the new alpha and omega limit sets pure Y_1 and pure E_1 as the distillate and

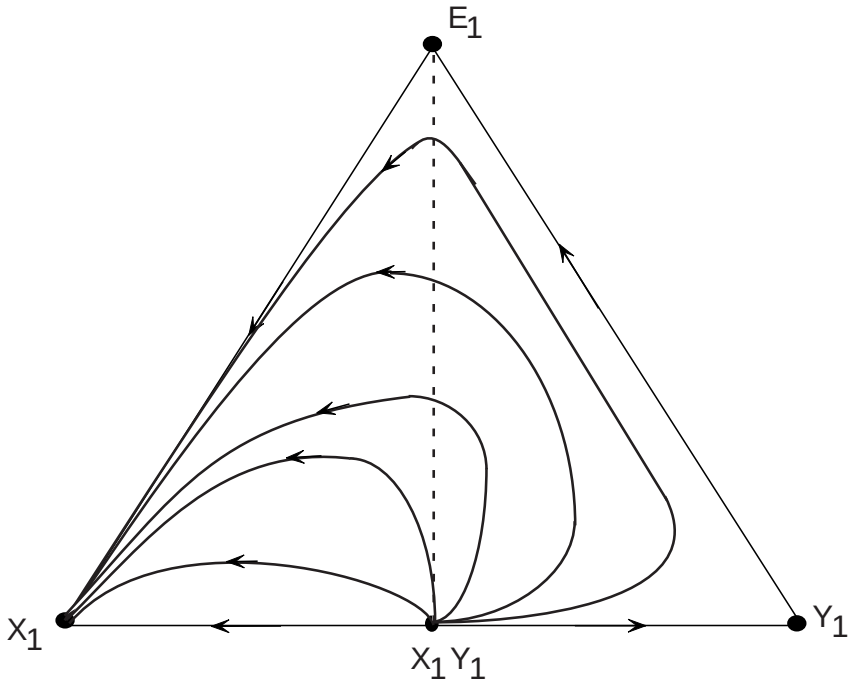

001 System Residue Curves Map

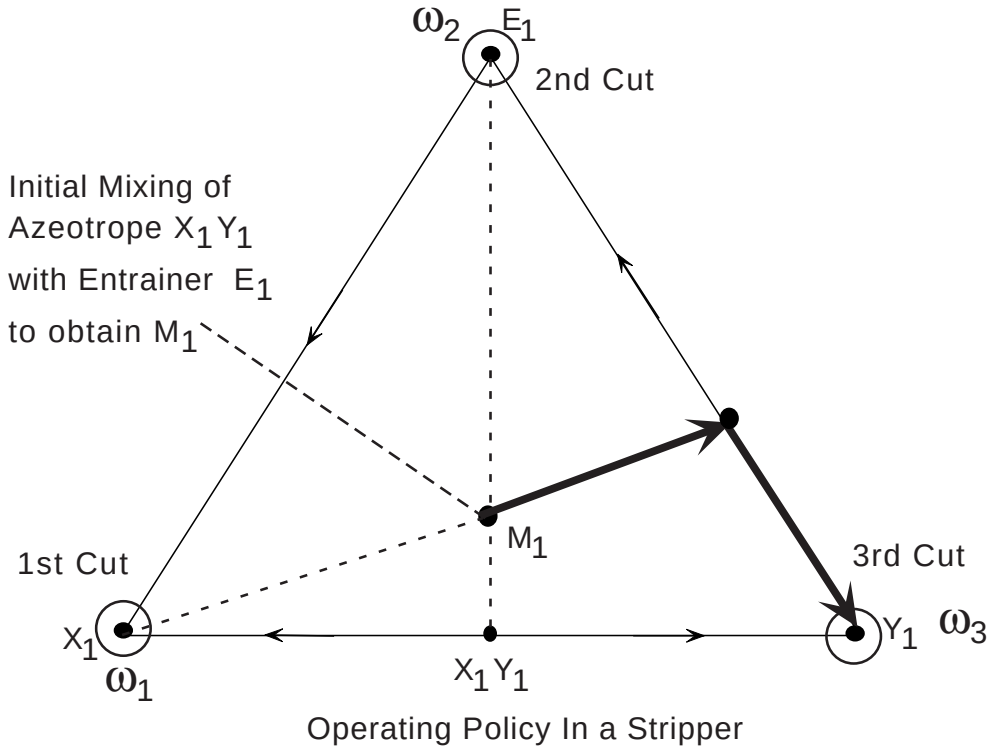

Operating Policy In a Stripper

Figure 5-16: Complete Separation of a Minimum-Boiling Azeotrope in a Batch Stripper Column by Addition of Entrainers to Form a 001 System

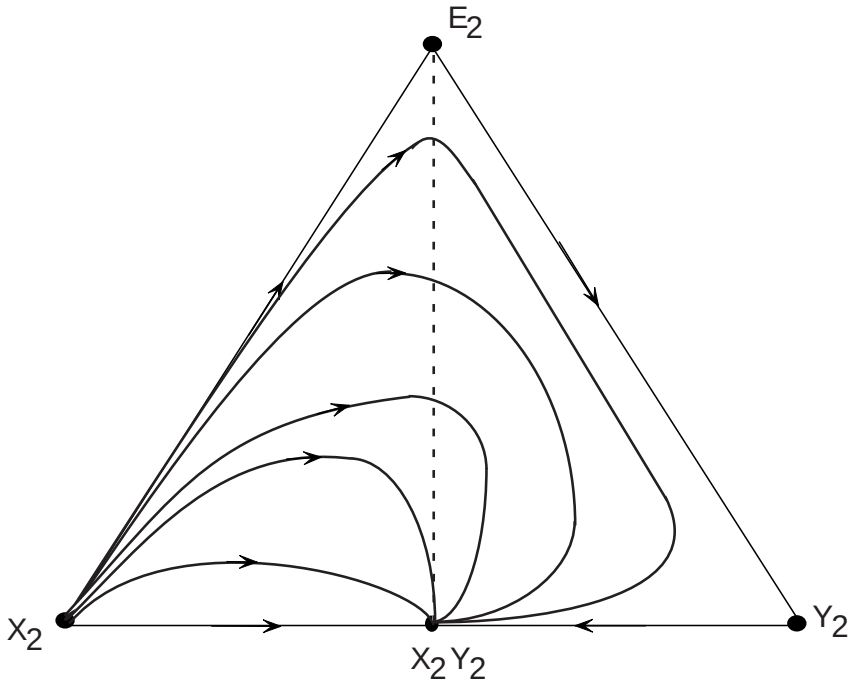

Inverse-001 System Residue Curves Map

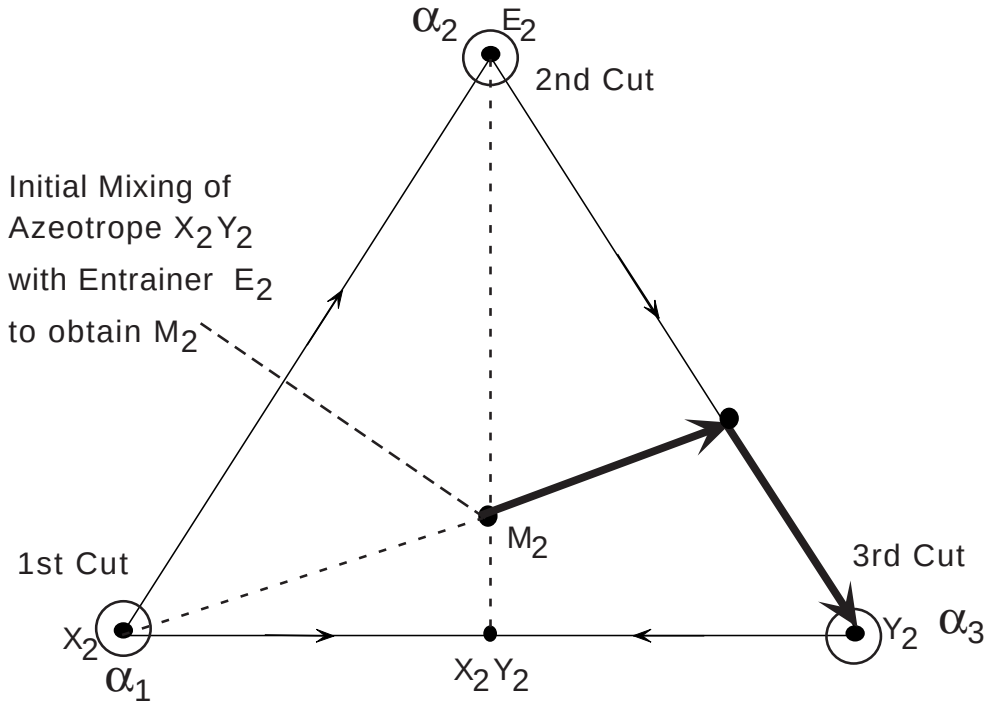

Operating Policy In a Rectifier

Figure 5-17: Complete Separation of a Maximum-Boiling Azeotrope in a Batch Rectifier Column by Addition of Entrainers to Form an inverse-001 System

bottoms product respectively. Thus, entrainer E_1 does indeed allow complete separation of the minimum boiling azeotrope X_1Y_1 in a middle vessel column. Similarly, an analysis of the inverse-001 system in Figure 5-19 shows that it is possible to draw pure X_2 by operating the middle vessel column on the mixed charge M_2 until it encounters the E_2-Y_2 edge. At this point, λ is switched to $\lambda = \frac{l_4}{l_3+l_4}$ such that the column operates in a quasi-static mode, and pure E_2 is drawn as the distillate, while pure Y_2 is drawn as the bottoms product. E_2 is also a perfect entrainer for the separation of the maximum boiling azeotrope X_2Y_2 in a middle vessel column.

It should be noted as an aside that the use of a quasi-static mode of operation might not be optimal in terms of product recovery, because the still pot residue remaining will not be pure at the end of the operation, and the still pot cannot be physically operated until it is empty. This is in contrast to the rectifier/stripper configurations, where the column can be operated until all the light/heavy desired components have been drawn from the column. However, the use of a quasi-static mode of operation results in time-savings, as two products is being drawn at the same time from the column versus the one product drawn at any point in time from the rectifier/stripper configurations. There is thus a trade-off between higher product recovery versus shorter operating time. This trade-off is explored in more detail in Chapter 7, when the middle vessel column operated without a quasi-static step is simulated and compared to the simulation results of an identical operation with a quasi-static step.

The above form of entrainers arise from the fact that by adding an additional dimension to the composition simplex, the pot composition boundary (as represented by the azeotropic point X_iY_i in the original 1-dimensional composition simplex (as represented by line segment X_i-Y_i) does not extend into the 2-dimensional composition simplex ($x_X + x_Y + x_E = 1$), and we are able to go around the boundary (rather than across it). Addition of the Bernot *et al.* "perfect entrainer" has joined the 2 distillation regions (line segments X_i-X_iY_i and X_iY_i-Y_i) via the composition simplex edge E_i-Y_i.

Bernot *et al*'s approach, however, is limited to residue curve map topologies which

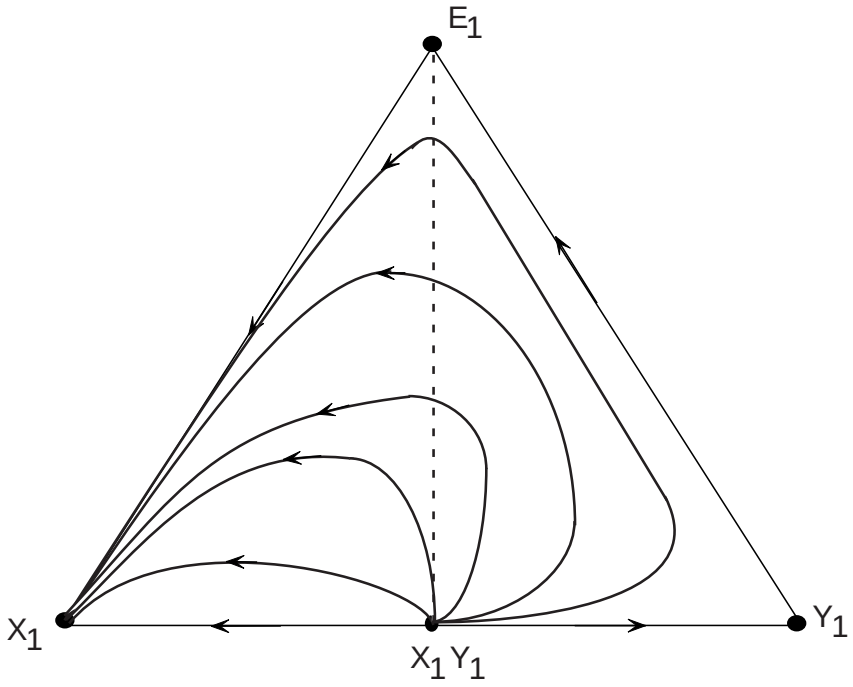

001 System Residue Curves Map

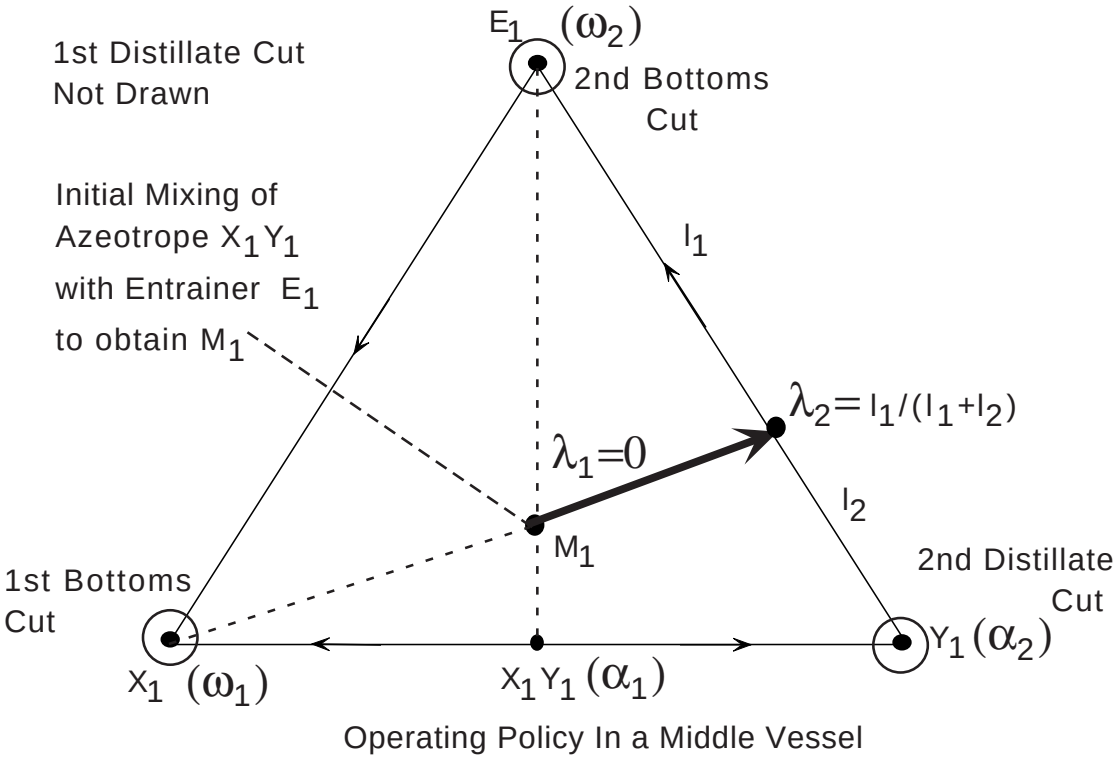

Operating Policy In a Middle Vessel

Figure 5-18: Complete Separation of a Minimum-Boiling Azeotrope in a Middle Vessel Column by Addition of Entrainers to Form a 001 System

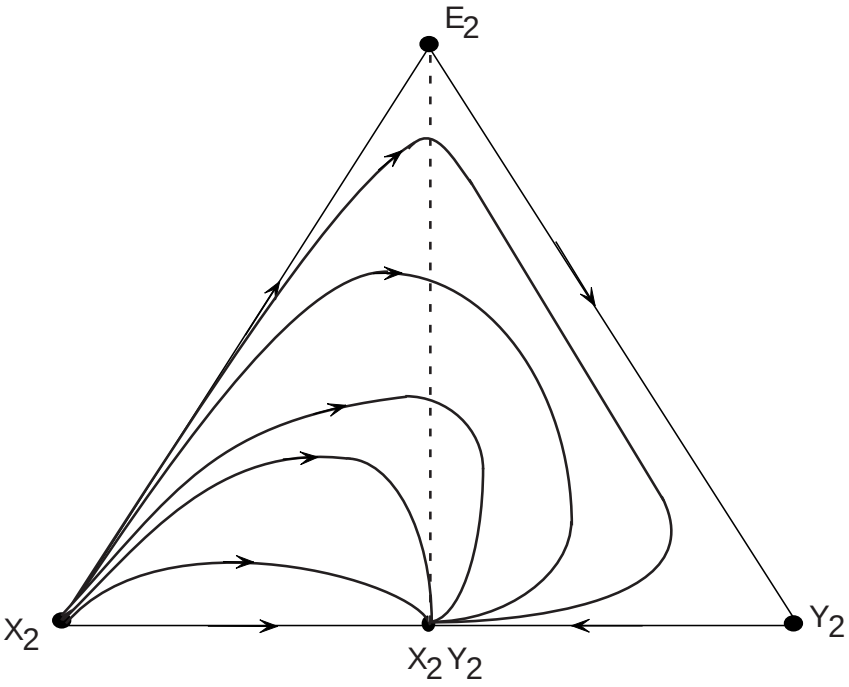

Inverse-001 System Residue Curves Map

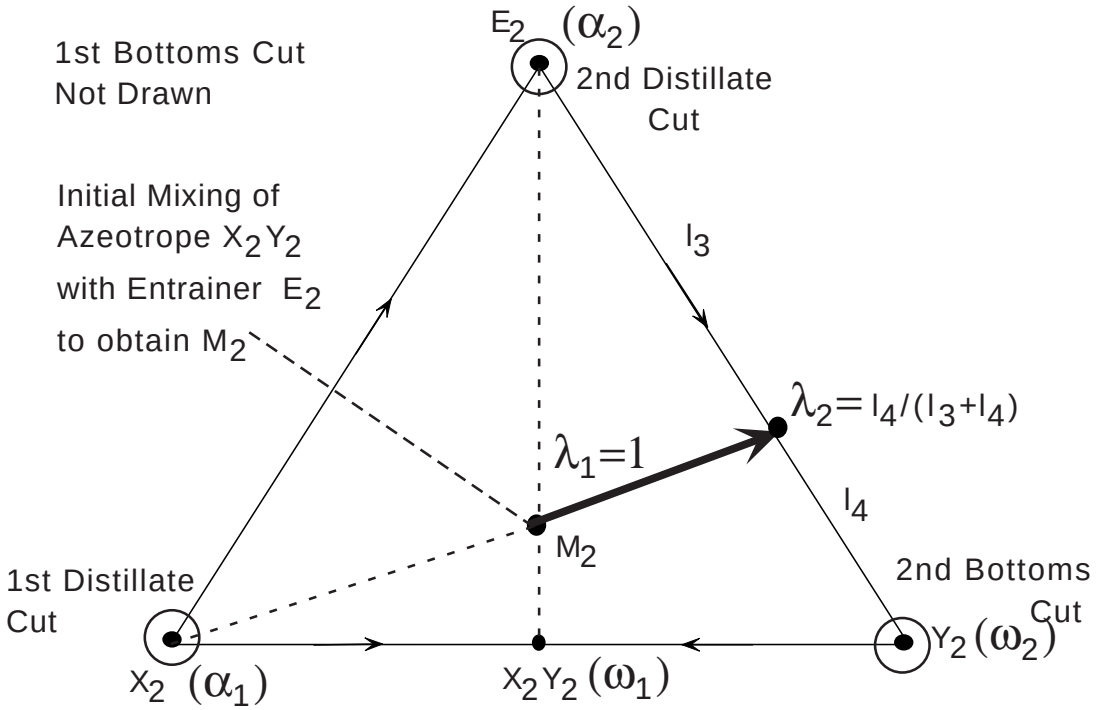

Operating Policy In a Middle Vessel

Figure 5-19: Complete Separation of a Maximum-Boiling Azeotrope in a Middle Vessel Column by Addition of Entrainers to Form an inverse-001 System

do *not* contain separatrices internal to the composition simplex. Physical chances for such intermediate boiling entrainers are low. Thus, we would like to highlight another class of perfect entrainers in which separatrices do exist, but are curved. Since curvature is to be expected of most separatrices [30], it would be much easier to find these perfect entrainers of the second class than compared to the ones suggested by Bernot *et al.*

This other class of perfect entrainers is a higher boiling liquid (than either of the two pure components X_2 or Y_2) which forms an inverse-020 system with the maximum boiling binary azeotrope X_2Y_2 with a very curved stable separatrix as illustrated by the example of the acetone-chloroform azeotrope, with benzene as an entrainer. Alternatively, if the azeotrope was minimum-boiling such as X_1Y_1, the entrainer would have to be a lower boiling liquid (than either X_1 or Y_1) and form a 020-system with a very curved unstable separatrix in order for complete separation to occur. The underlying factor for the usefulness of these entrainers is the curvature of the separatrix formed. Just as the Bernot *et al.* "perfect entrainer" had joined the 2 distillation regions (line segments X_i-X_iY_i and X_iY_i-Y_i) via the composition simplex edge E_i-Y_i, the curved separatrices in the 020 and inverse-020 systems also joins the two regions which contain each of the desired pure products X_i and Y_i via the simplex edge E_i-Y_i. However, due to the presence of the separatrix between E_i and X_iY_i, the still pot composition can only approach the E_i-Y_i edge (it does not quite reach it) in the region where the separatrix hugs the E_i-Y_i edge (region ρ in Figure 5-7). This then allows us to draw pure Y_i from the middle vessel column. The separation scheme for the inverse 020 system was already explained in our example with the acetone, benzene and chloroform system (with benzene as the entrainer). The separation scheme for the 020 system is then the reverse of the operating procedure outlined in Section 5.2. This operating procedure is illustrated in Figure 5-20. A separation scheme for the generic inverse-020 system is shown in Figure 5-21, for ease of comparison to Figure 5-20.

Note that having the separatrix almost hugging the edge allows us to achieve separations with a negligible amount of waste (azeotropic) off-cut, and is thus highly

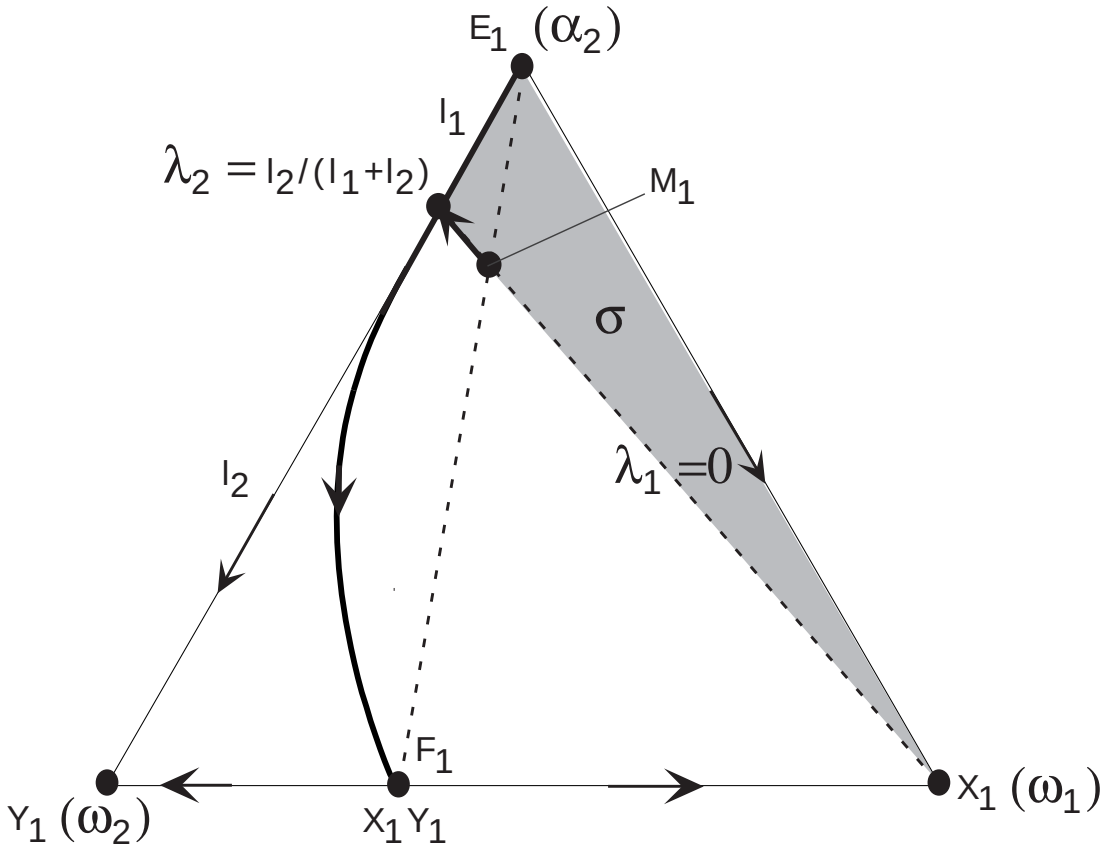

Figure 5-20: Operating Procedure for Separating a Minimum-Boiling Azeotrope by Adding a Lowest Boiling Entrainer which Forms a Highly Curved Unstable Separatrix

desirable. However, it is not absolutely necessary, in that the azeotrope can be broken without the separatrix being extremely close to the composition simplex edge. Separation, however, would be less than perfect.

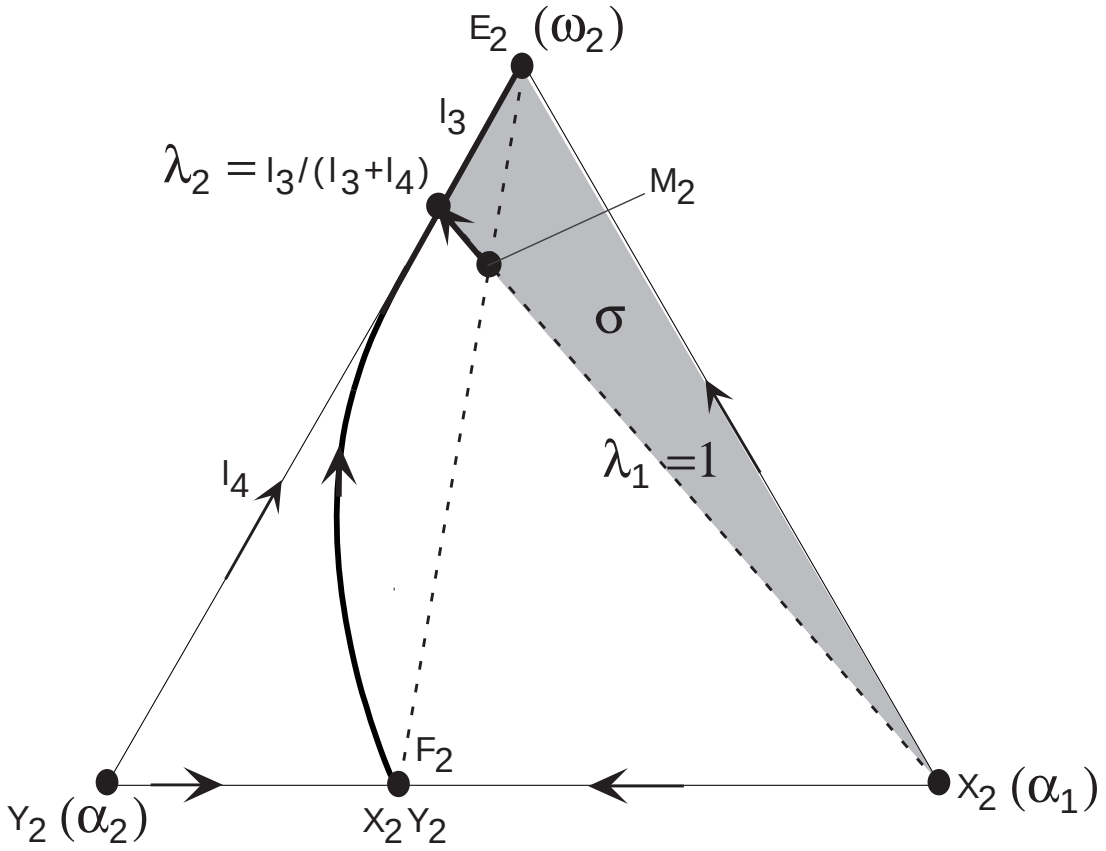

Figure 5-21: Operating Procedure for Separating a Maximum-Boiling Azeotrope by Adding a Highest Boiling Entrainer which Forms a Highly Curved Stable Separatrix

As illustrated in Figure 5-20, the basic operating procedure of the middle vessel column for separating the minimum boiling azeotrope X_1Y_1 with a lowest boiling point entrainer such as E_1 is as follows:

1. Add sufficient entrainer E_1 to the original feed F_1 such that the desired region (σ) is attained at the initial charge composition of M_1.

2. Operate the column as a stripper ($\lambda = 0$) until the E_i-Y_i edge/separatrix is reached, drawing pure X_1 as bottoms product.

3. Then continue the operate the column in a quasi-static operation, by setting

$\lambda = \frac{l_2}{l_1+l_2}$. Thereby drawing almost pure Y_1 as bottoms product and pure E_1 as distillate product until the still pot runs dry ($\xi \to \infty$).

The above examples of perfect entrainers were focused on separation of binary azeotropes. However, the rationale can be applied to azeotropes of higher dimesionality. The characteristics of the perfect entrainer is that it connects the otherwise separate distillation regions which contain the desired pure products that make up the azeotrope. This can be achieved via an entrainer which does not add any new separating boundaries (such as the Bernot *et al.* "perfect entrainer") or an entrainer which forms a separating boundary that is so curved that it is almost touches one of the edges or faces of the composition simplex. This then allows different regions to be joined, and separation of the azeotrope into its constituent pure components is thus achievable. It is conceivable that for azeotropes with a higher number of constituent components might require more than one entrainer for complete separation, and it might require columns which allow more than 2 products to be drawn at a given point in time (such as the multi-vessel column, Chapter 8). The point, however, is to recognise that there is a possibility that the addition of the correct entrainers in appropriate phases of the operating procedure could result in the complete separation of an azeotrope into its constituent pure components without the need for an azeotropic recycle.

Chapter 6

Simulation Analysis of the MVC Model

In this chapter, a simulation analysis is conducted with an ABACUSS model of the middle vessel column, based on the equations derived in Chapter 3. All simulations were conducted on the classic ternary mixture of Acetone-Chloroform-Methanol, which has been studied extensively by various researchers [5, 6, 15].

All simulations were conducted with conditions that approximated the limiting conditions of ND, $NB \to \infty$ and R_d, $R_b \to \infty$. This was achieved by choosing values of $ND = NB = 50$, and $R_d = R_b = 1000$. As will be shown in our simulations, under these conditions, limiting behavior is observed, and it can be said that the results of our simulation validate the limiting behavior of the middle vessel column. All results in this chapter are presented as a function of real time, t, rather than warped time ξ, so as to avoid the inconvenience of an infinite abscissa as $\xi \to \infty$. Sample ABACUSS files used for the simulations in Chapters 6 and 7 are presented in Appendix G.

The simulation analysis is in three parts. Firstly, it shall be validated that the middle vessel column operates exactly like a rectifier when the operating parameter of λ is set to one, and that it operates exactly like a stripper when λ is set to zero. This also serves to validate the soundness of the middle vessel column model that was developed in ABACUSS. Next, simulations were conducted for each of the enumerated middle vessel batch distillation regions in the mixture of acetone, chloroform

and methanol, for the value of λ set at $\frac{1}{2}$. This allows us to obtain a qualitative feel for the behavior of the middle vessel column at a moderate value of λ. It also serves to validate the theoretical limiting behavior developed in Chapters 4 and 5 for middle vessel columns (i.e., ND, $NB \to \infty$, R_d, $R_b \to \infty$). Lastly, a simulation was conducted in which holdup was introduced into each of the individual stages or trays in the column. With a moderate value of holdup in the column (10% of the column charge held up in the trays vs 90% in the still pot), the results obtained were qualitively similar to the results obtained when negligible holdup was assumed.

This chapter is in 4 sections. The first section briefly describes the system of acetone, chloroform and methanol to be studied. The batch distillation regions (in the spirit of Ewell and Welch [16]) for each of the stripper, rectifier and middle vessel column are enumerated and characterized. The expected product sequences for each of these regions are also summarized. The second section describes the simulation analysis of the middle vessel column, operating first as a rectifier ($\lambda = 1$) and then as a stripper ($\lambda = 0$) for one of the regions. The third section describes the simulation analysis of a middle vessel column operated at $\lambda = \frac{1}{2}$. In this section, various regions are studied so as to cover the variety of behavior that is observed in the A-C-M system when operating in a middle vessel column. Finally, the fourth and last section of this chapter presents the simulation results of in which holdup was allowed in the trays. As shown, this does not affect the results significantly, and thus, justifying the assumption of negligible holdup as being valid in the characterization and modelling of the middle vessel column.

6.1 The Acetone-Chloroform-Methanol System

The acetone, chloroform and methanol system is a system that exhibits a total of 3 binary azeotropes (two unstable nodes and one stable node), and a single ternary azeotrope (saddle point); it is a 113-S system, as enumerated by Doherty and Caldarola [11]. The system is characterized by its extrememly curved boundaries, which result is some behavior not encountered in systems with straight boundaries. A sum-

Table 6.1: Composition of Fixed Points in the Acetone, Chloroform and Methanol System

Components Label	$x_{Acetone}$	$x_{Chloroform}$	$x_{Methanol}$	Characteristic Behavior
A	1.0	0.0	0.0	Saddle Point
C	0.0	1.0	0.0	Saddle Point
M	0.0	0.0	1.0	Stable Node
AC	0.3455	0.6545	0.0	Stable Node
AM	0.7780	0.0	0.2220	Unstable Node
CM	0.0	0.6579	0.3421	Unstable Node
ACM	0.3396	0.2322	0.4282	Saddle Point

mary of the fixed points for this three component mixture is provided in Table 6.1. The ternary residue curves map for the system of acetone, chloroform and methanol is provided in Appendix B.

Due to the large number of fixed points in this ternary system, there also exists a large number of batch distillation regions for the system, for each of the stripper, recitifier and middle vessel configurations. These batch distillation regions are shown as follows: in Figure 6-1 for the batch rectifier column, in Figure 6-2 for the batch stripper column and finally, in Figure 6-3 for the middle vessel column.

As seen in Figures 6-1 through 6-3, there are a total of 6 batch distillation regions for the rectifying column, Y_1 through Y_6, 6 batch distillation regions for the stripping column, Z_1 through Z_6, and a grand total of 24 batch distillation regions for the middle vessel column, χ_1 through χ_{24}. Based on the analysis developed by Van Dongen and Doherty [15] and Bernot *et al.* [5, 6] in their anaylsis of the limiting behavior of batch rectifiers and batch strippers, the expected product sequence for each of the enumerated batch distillation regions is tabulated in Table 6.2 (for the rectifier) and Table 6.3 (for the stripper). Furthermore, based on the limiting analysis developed for the middle vessel column in Chapter 4, the expected product sequences for each of the 24 enumerated batch distillation regions of the middle vessel column are also tabulated in Table 6.4.

Note that in the tables, a cut which is followed by a suffix of "mix" indicates a

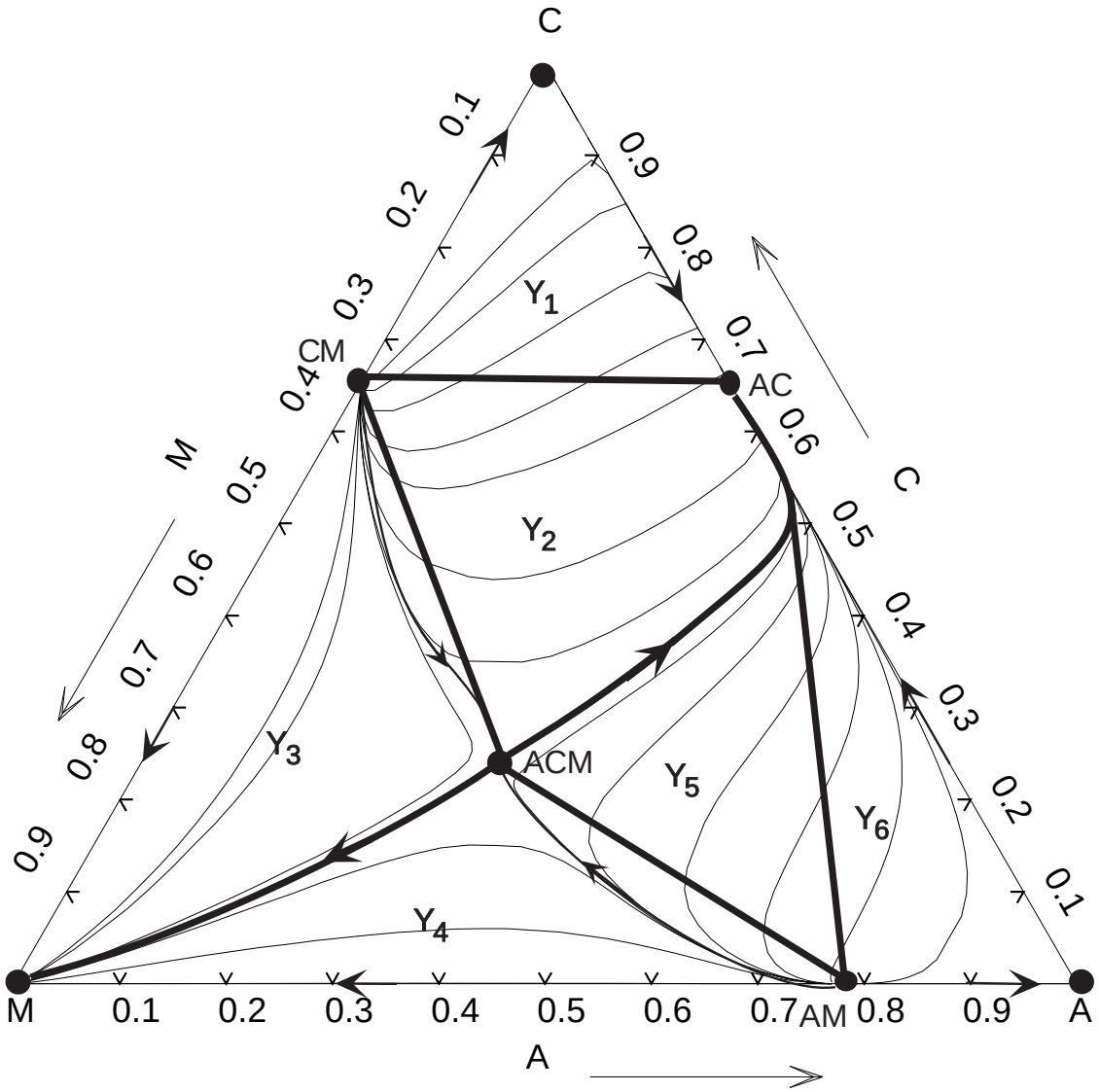

Figure 6-1: Batch Distillation Regions Y_1 through Y_6 in the A-C-M System for the Rectifier Configuration

Table 6.2: Product Sequences for Regions Y_i for $i = 1..6$, in a Batch Rectifier for the A-C-M Mixture

Region	First Cut	Second Cut	Third Cut
Y_1	CM	C	AC
Y_2	CM	ACM-mix	AC
Y_3	CM	ACM	M
Y_4	AM	ACM	M
Y_5	AM	ACM-mix	AC
Y_6	AM	A	AC

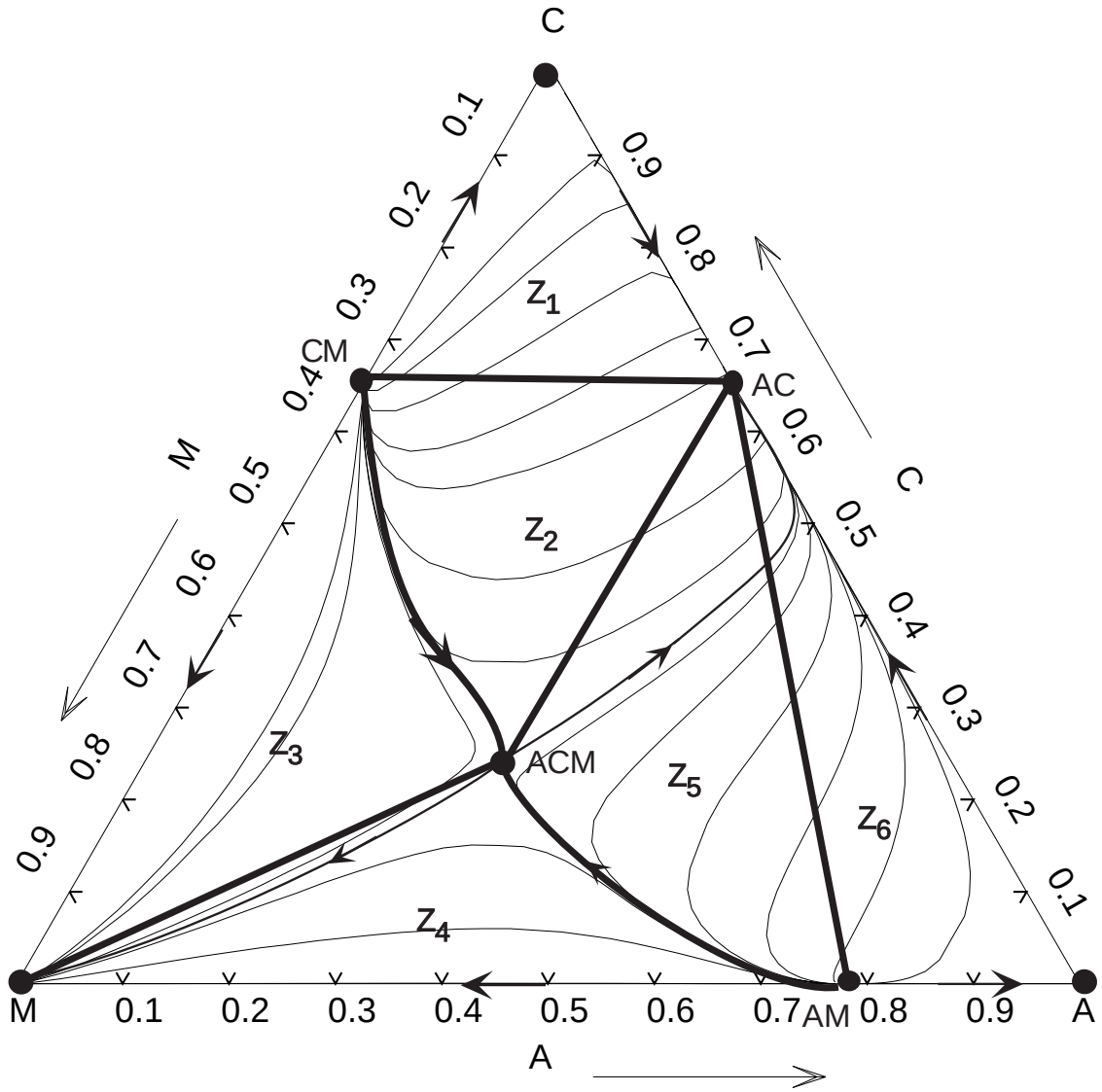

Figure 6-2: Batch Distillation Regions Z_1 through Z_6 in the A-C-M System for the Stripper Configuration

Table 6.3: Product Sequences for Regions Z_i for $i = 1..6$, in a Batch Stripper for the A-C-M Mixture

Region	First Cut	Second Cut	Third Cut
Z_1	AC	C	CM
Z_2	AC	ACM	CM
Z_3	M	ACM	CM
Z_4	M	ACM-mix	M
Z_5	AC	ACM-mix	AM
Z_6	AC	A	AM

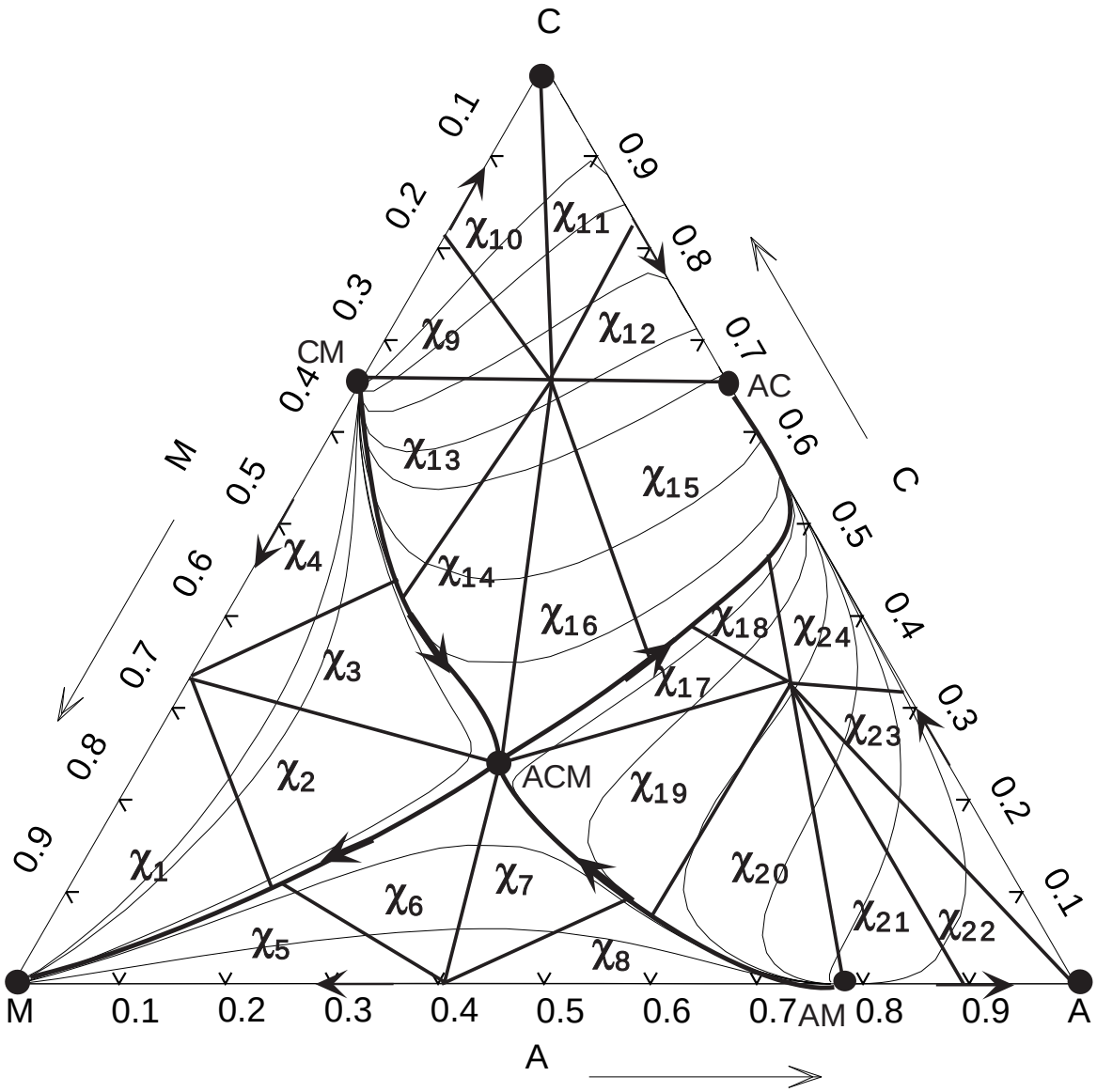

Figure 6-3: Batch Distillation Regions χ_1 through χ_{24} in the A-C-M System for the Middle Vessel Configuration

Table 6.4: Product Sequences Expected For Each Region χ_1 through χ_{24} in the Presence of Curved Boundaries, $\lambda = \frac{1}{2}$

Region	First Cut	Second Cut	Third Cut
χ_1	$[CM,M]$	$[ACM\text{-mix},M]$	$[M,M]$
χ_2	$[CM,M]$	$[ACM\text{-mix},M]$	$[ACM,ACM]$
χ_3	$[CM,M]$	$[CM,ACM\text{-mix}]$	$[ACM,ACM]$
χ_4	$[CM,M]$	$[CM,ACM\text{-mix}]$	$[CM,CM]$
χ_5	$[AM,M]$	$[ACM\text{-mix},M]$	$[M,M]$
χ_6	$[AM,M]$	$[ACM\text{-mix},M]$	$[ACM,ACM]$
χ_7	$[AM,M]$	$[AM,ACM\text{-mix}]$	$[ACM,ACM]$
χ_8	$[AM,M]$	$[AM,ACM\text{-mix}]$	$[AM,AM]$
χ_9	$[CM,AC]$	$[CM,C]$	$[CM,CM]$
χ_{10}	$[CM,AC]$	$[CM,C]$	$[C,C]$
χ_{11}	$[CM,AC]$	$[C,AC]$	$[C,C]$
χ_{12}	$[CM,AC]$	$[C,AC]$	$[AC,AC]$
χ_{13}	$[CM,AC]$	$[CM,ACM\text{-mix}]$	$[CM,CM]$
χ_{14}	$[CM,AC]$	$[CM,ACM\text{-mix}]$	$[ACM,ACM]$
χ_{15}	$[CM,AC]$	$[ACM\text{-mix},AC]$	$[AC,AC]$
χ_{16}	$[CM,AC]$	$[ACM\text{-mix},AC]$	$[ACM,ACM]$
χ_{17}	$[AM,AC]$	$[ACM\text{-mix},AC]$	$[ACM,ACM]$
χ_{18}	$[AM,AC]$	$[ACM\text{-mix},AC]$	$[AC,AC]$
χ_{19}	$[AM,AC]$	$[AM,ACM\text{-mix}]$	$[ACM,ACM]$
χ_{20}	$[AM,AC]$	$[AM,ACM\text{-mix}]$	$[AM,AM]$
χ_{21}	$[AM,AC]$	$[AM,A]$	$[AM,AM]$
χ_{22}	$[AM,AC]$	$[AM,A]$	$[A,A]$
χ_{23}	$[AM,AC]$	$[A,AC]$	$[A,A]$
χ_{24}	$[AM,AC]$	$[A,AC]$	$[AC,AC]$

product cut which is affected in its characteristics by the curvature of the pot composition boundaries in the vicinity of the cut. This results in a varying composition in the cut drawn from the column as the still pot composition is forced to trace out a route along the curved boundary, and the product is formed accordingly as governed by mass-balance. It should be observed that similar to the system of acetone, benzene and chloroform, the curved stable separatrices in the A-C-M system form pot composition boundaries for all values of λ in the middle vessel column other than $\lambda = 0$. Similarly the curved unstable separatrices in the A-C-M system form pot composition boundaries for all values of λ in the middle vessel column other than the value of $\lambda = 1$. Thus, for a generic middle vessel column not operating under special cases of λ at 0 or 1, the separatrices, stable and unstable, form pot composition boundaries for middle vessel column. As explained in Chapter 4, this implies that the middle vessel column's motion is more contrained at a fixed value of λ than either that of the stripper or the rectifier, but when λ is allowed to vary, the motion of the middle vessel column is less contrained than both the stripper and the rectifier.

Finally, it should be noted that the expected product cuts in each middle vessel region, as denoted in Figure 6-3 and Table 6.4, was based on the moderate value of $\lambda = \frac{1}{2}$ and in some sense, is indicative of the behavior of an initial composition in one these regions at all values of λ in between 0 and 1.

6.2 Operation of the Middle Vessel Column as A Stripper ($\lambda = 0$) and A Rectifier ($\lambda = 1$)

In this section, it shall be validated that the middle vessel column operates exactly like a rectifier when the operating parameter of λ is set to one, and that it operates exactly like a stripper when λ is set to zero. This serves as a test to validate the accuracy of the middle vessel column model that was developed with ABACUSS. If the middle vessel column did not behave as expected in the limiting cases of $\lambda = 0$ and 1, it would imply that there was probably something wrong with the ABACUSS

Table 6.5: Operating Conditions for the Rectifier and Stripper Simulations

Operational Parameter	Numerical Value	Units
Initial Still Pot Holdup	100	Moles
Vapor Flow Rate (Stripping Section)	10	Moles/Time
Liquid Flow Rate (Rectifying Section)	10	Moles/Time
Distillate Product Flow Rate	0.01	Moles/Time
Bottoms Product Flow Rate	0.01	Moles/Time
Resulting Reflux Ratio	1000	Dimensionless
Resulting Reboil Ratio	1000	Dimensionless
Number of Trays in the Rectifying Section	50	Dimensionless
Number of Trays in the Stripping Section	50	Dimensionless
Operating Pressure in Column	1	Bar

model developed. As such, testing out the model as a rectifier or a stripper can help identify inconsistencies in the modelling, if any.

Simulations were conducted for a sample point within each of the 6 enumerated regions for both the stripper and the rectifier configuration. The results obtained for each of the sample points were indeed indicative of the batch distillation region in which the sample point belonged to. In this section, the results for the initial composition in region 5 (Y_5 and Z_5) are presented in detail and explained where necessary. The results for the sample points from the other regions are given in Appendix D.

Operating conditions for each simulation were kept constant so as to ensure that the results could be comparable to each other. The pertinent operating parameters used are thus summarized in Table 6.5. The behavior of the column as $N \to \infty$ and the reflux/ratios $\to \infty$, was modelled by using a reflux/reboil ratio of 1000 and 100 trays in the column, with 50 trays in each of the stripping and rectifying sections of the column.

It should be noted at this point that despite the use of the unit "moles" in defining the amount of charge and the product flow rates from the column, it is strictly the molar quantity with respect to the orginal charge into the column that we are

concerned with. A new unit of molar quantity could just as well be redifined as "MITMoles" which would result in a reasonable quantity charged to the column. It is thus the relative vapor, liquid flow rates in the column to product rates which are important (i.e., reflux/reboil ratios). Similarly the definition of a unit of "time" is not important as long as the unit of time is consistently used througout the simulations.

6.2.1 An Analysis of the Results From Region Y_5

These results are representative of the use of a rectifier column to separate the mixture of acetone, chloroform and methanol. The expected product sequence for region Y_5 is (AM, ACM-mix, AC). The initial still pot composition chosen to represent region Y_5 was given by ($X_A = 0.50$, $X_B = 0.25$, $X_C = 0.25$).

As presented in Figure 6-4, the product composition obtained from the middle vessel column operated as a rectifier does indeed correspond to the anticipated cuts of (AM, ACM-mix, AC). Of particular interest is the ACM-mix cut, in which some pure acetone is actually drawn for a period of time, as the still pot composition if forced to trace out the pot composition boundary given by the stable separatrix between ACM and AC. This particular curved separatrix was also highlighted by Bernot *et al.* as giving rise to a varied cut composition, which as can be seen from Figure 6-4, varies from that of a "ACM ternary azeotrope" to that of pure acetone.

The resulting motion of the still pot composition in the composition simplex is also illustrated in Figure 6-5. As can be seen from the diagram, the still pot composition moved directly away from the 1st product cut of region Y_5, given by AM, until it encountered the highly curved stable separatrix between AC and ACM. At this point, a change in the alpha limit set of the still pot occurs, and the new product of the rectifier column becomes that of the ACM azeotrope. However, due to the curvature of the separatrix, the column is unable to draw this ACM azeotrope continuously. Rather, it is forced to trace out the stable separatrix all the way to the fixed point of AC, as shown in Figure 6-5. The product drawn from the column is then a direct result of the mass balance which must occur as the still pot composition traced out the separatrix. This actually gives rise to the unexpected cut of pure acetone in the

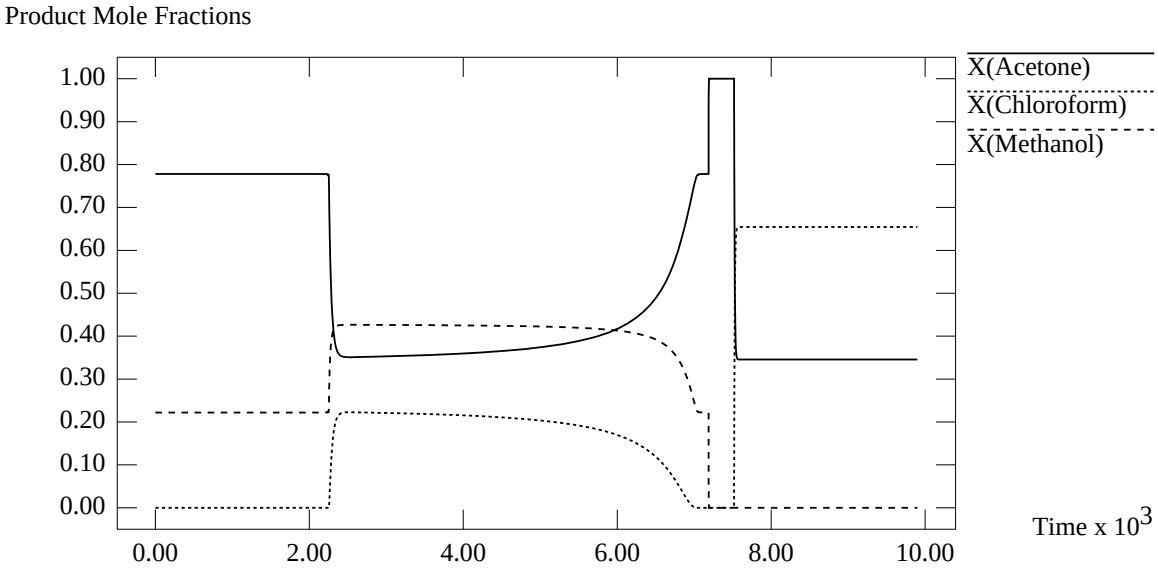

Figure 6-4: Graph of Product Composition against Time

ACM-mix cut, which arises due to the stable separatrix being tangent to the A-C edge as it approaches the AC fixed point for an extended distance. Finally, the still pot composition enters the fixed point of AC, where the rectifier continues to draw AC until the still pot runs dry (i.e., $\xi \to \infty$).

It should be noted that this theme of a "varying cut composition" is characteristic of all systems which exhibit a great degree of curvature in the separatrices (and hence pot composition boundaries) of the simple distillation residue curves map.

6.2.2 An Analysis of the Results From Region Z_5

These results are representative of the use of a stripper column to separate the mixture of acetone, chloroform and methanol. The expected product sequence for region Z_5 is (AC, ACM-mix, AM). The initial still pot composition chosen to represent region Z_5 was given by ($X_A = 0.50$, $X_B = 0.25$, $X_C = 0.25$).

As presented in Figure 6-6, the product composition obtained from the middle vessel column operated as a stripper does indeed correspond to the anticipated cuts of (AC, ACM-mix, AM). As was with the case in the rectifier with region Y_5, an ACM-mix cut shows up in the stripping of the A-C-M mixture in region Z_5.

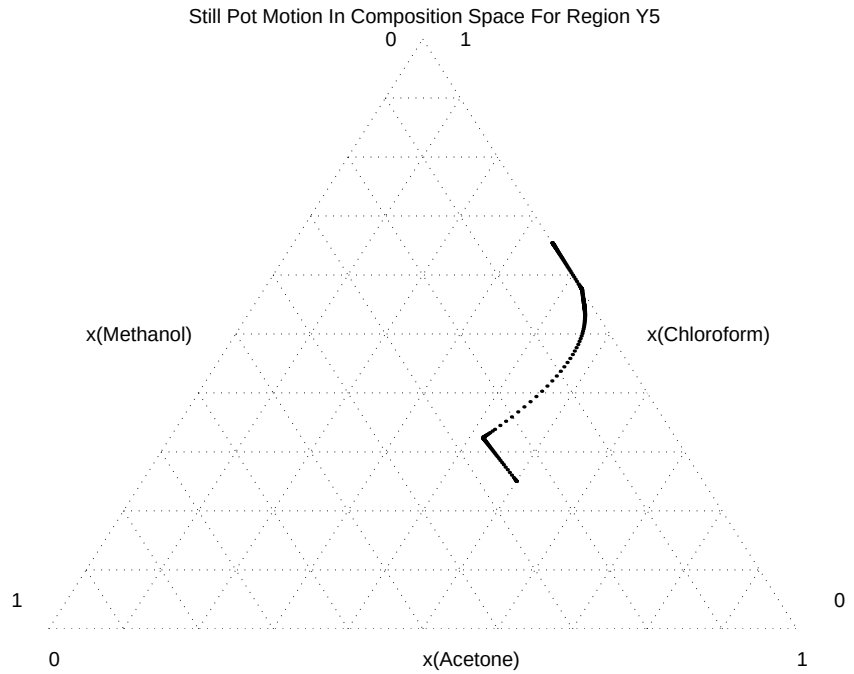

Figure 6-5: Plot of Still Pot Motion in Composition Space

This particular ACM-mix cut arises from the fact that the still pot composition encounters the unstable separatrix between ACM and AM. Again, as with the case of the ACM-AC separatrix, this separatrix is highly curved, and is tangent to the A-M composition simplex edge. However, this tangency is less acute when compared to that of the ACM-AC separatrix, and correspondingly, the "pure methanol cut" obtained as part of the ACM-mix cut does not occur over an extended period of time, as the still pot composition enters the AM fixed point not long after the pure methanol product is drawn. As with Y_5, the ACM-mix cut of Z_5 also varies by a great degree, between that of the "ACM ternary azeotrope" to that of pure methanol.

The resulting motion of the still pot composition in the composition simplex is also illustrated in Figure 6-7. As can be seen from the diagram, the still pot composition moved directly away from the 1st product cut of region Y_5, given by AC, until it encountered the curved unstable separatrix between AM and ACM. At this point, a change in the omega limit set of the still pot occurs, and the new product of the rectifier column becomes that of the ACM azeotrope. However, due to the curvature

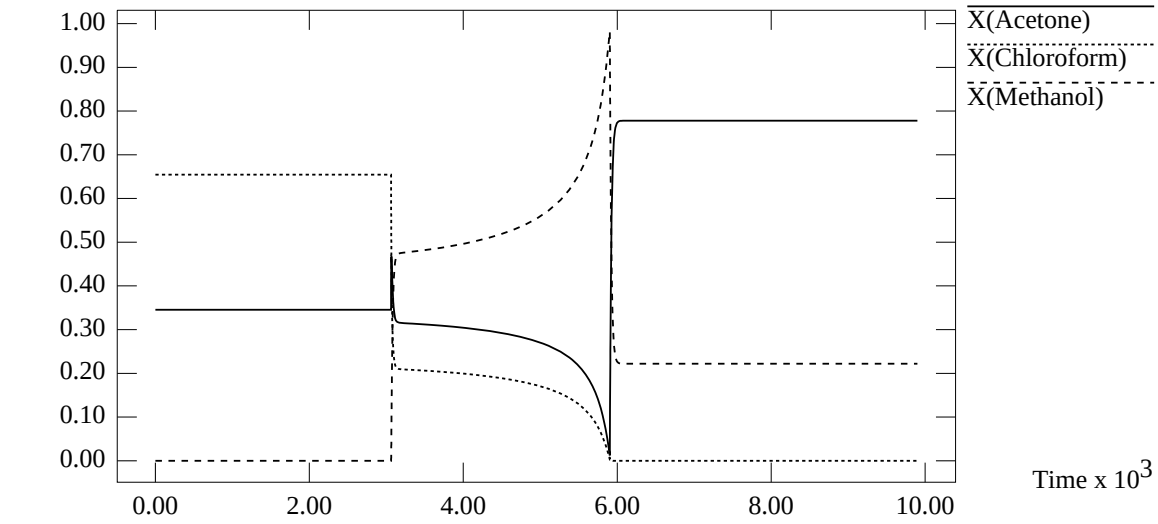

Figure 6-6: Graph of Product Composition against Time

of the separatrix, the column is unable to draw this ACM azeotrope continuously. Rather, it is forced to trace out the unstable separatrix all the way to the fixed point of AM, as shown in Figure 6-7. The product drawn from the column is then a direct result of the mass balance which must occur as the still pot composition traced out the separatrix. This actually gives rise to the unexpected cut of pure methanol in the ACM-mix cut, which arises due to the stable separatrix being tangent to the A-M edge as it approaches the AM fixed point. Finally, the still pot composition enters the fixed point of AM, where the column continues to draw AM until the still pot runs dry (i.e., $\xi \to \infty$).

It should be noted that the unstable separatrix formed a pot composition boundary in the stripper configuration but not in the rectifier configuration, while the stable separatrix formed a pot composition boundary in the rectifier configuration, but not in the stripper configuration. As will be observed, however, both stable and unstable separatrices form pot composition boundaries in the middle vessel column operated at a value of $0 < \lambda < 1$. Hence, separatrices are boundaries for the middle vessel column at all values of λ, except 1) at $\lambda = 0$, the stable separatrix is not a boundary, and 2) at $\lambda = 1$, the unstable separatrix is not a boundary.

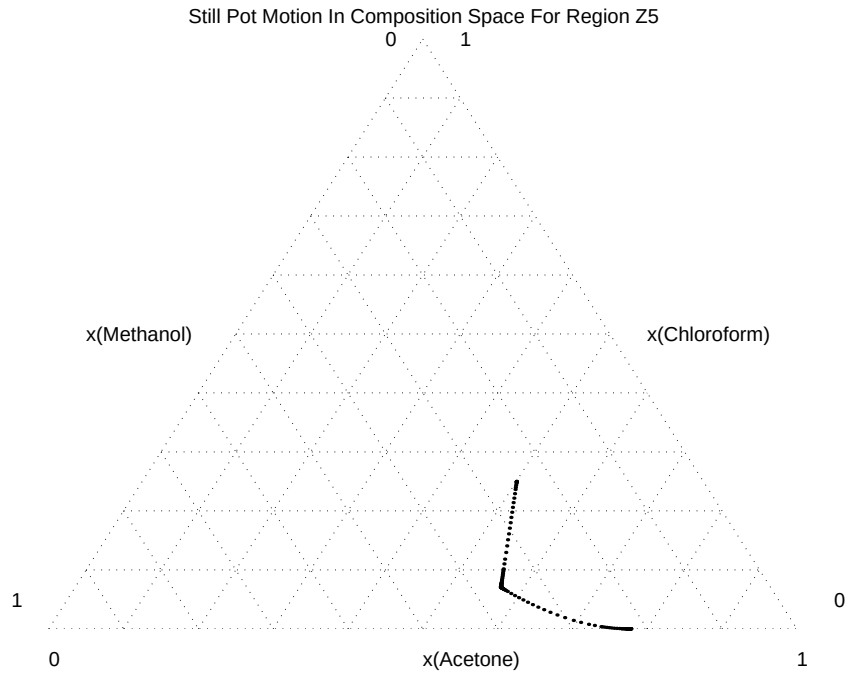

Figure 6-7: Plot of Still Pot Motion in Composition Space

6.3 Operation of the Middle Vessel Column with the Operating Parameter at $\lambda = \frac{1}{2}$

In this section, the middle vessel column is used for processing an initial composition point in each of the 24 middle vessel batch distillation regions, at an operating value of $\lambda = \frac{1}{2}$.

Simulations were conducted for a sample point within each of the 24 enumerated regions, and the results obtained for each of the sample points were indeed indicative of the behavior expected of the batch distillation region in which these sample point belonged (based on the limiting analysis structure developed in Chapter 4 for middle vessel columns). In this section, the results initial compositions in regions χ_1, χ_4, χ_{17}, χ_{21}, χ_{22}, and χ_{24} are presented. These regions were chosen to demonstrate the array of possible behavior to be expected for an initial still pot composition in these regions, when operated with the middle vessel column. The results for the other regions are given in detail in Appendix D.

Operating conditions for each simulation were kept constant so as to ensure that

Table 6.6: Operating Conditions for the Middle Vessel Column Simulations

Operational Parameter	Numerical Value	Units
Initial Still Pot Holdup	100	Moles
Vapor Flow Rate in Column	10	Moles/Time
Liquid Flow Rate in Column	10	Moles/Time
Distillate Product Flow Rate	0.01	Moles/Time
Bottoms Product Flow Rate	0.01	Moles/Time
Resulting Value of λ	$\frac{1}{2}$	Dimensionless
Resulting Reflux Ratio	1000	Dimensionless
Resulting Reboil Ratio	1000	Dimensionless
Number of Trays in the Rectifying Section of Column	50	Dimensionless
Number of Trays in the Stripping Section of Column	50	Dimensionless
Operating Pressure in Column	1	Bar

the results could be comparable to each other. The pertinent operating parameters used are thus summarized in Table 6.6. The behavior of the column as ND, $NB \to \infty$ and the reflux and reboil ratios $\to \infty$, was modelled by using a reflux/reboil ratio of 1000, and up to 100 trays in the entire column.

6.3.1 An Analysis of the Results From Region χ_1

These results are representative of the use of a middle vessel column to separate the mixture of acetone, chloroform and methanol, in which the still pot composition encounters a curved middle vessel batch distillation boundary (stable separatrix in this case) and traces out the stable separatrix to a stable node which forms the final alpha and omega set of the distillation process. The expected product sequence for region χ_1 is ([CM,M], [ACM-mix,M], [M,M]). The initial still pot composition chosen to represent region χ_1 was given by ($X_A = 0.05$, $X_B = 0.22$, $X_C = 0.73$).

As presented in Figure 6-8, the distillate product cut from the middle vessel column was found to be (CM, ACM-mix, M), which was exactly as expected for the region. As before, the slight curvature of the stable separatrix encountered resulted in a slight "mix" in the ACM-mix cut, but when compared to the "mixed" cut

that would be obtained if the still pot composition encountered either the ACM-AC, ACM-AM and ACM-CM separatrices, this "mixing" is almost negligible (see results in Section 6.2).

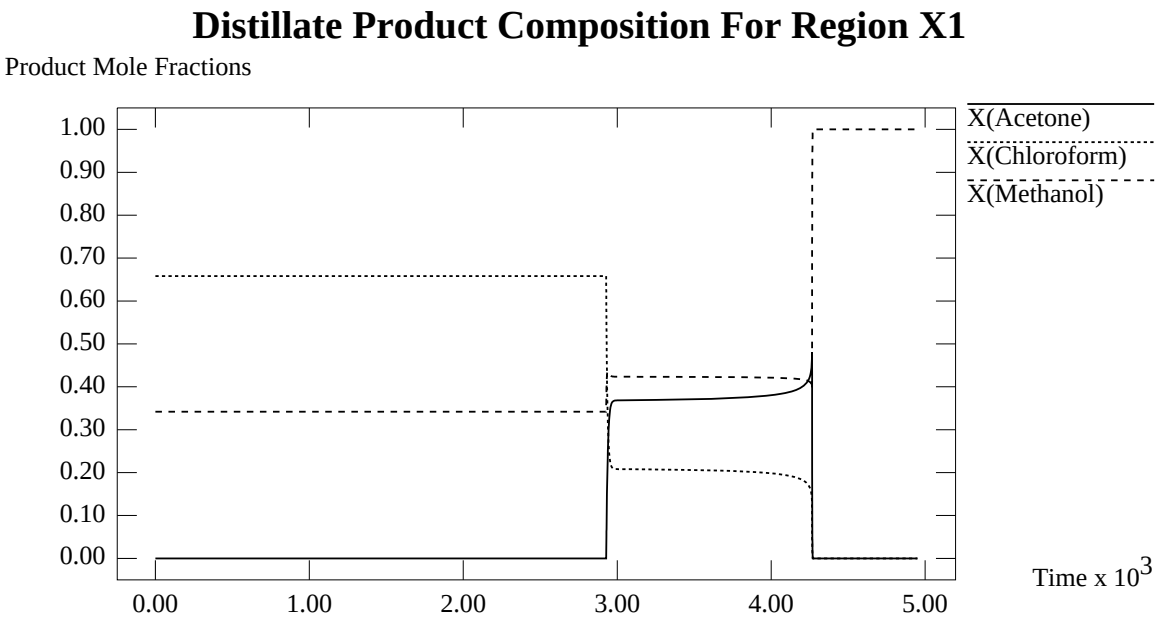

Figure 6-8: Graph of Distillate Product Composition against Time

The bottoms product cut, on the other hand, was predicted to be invariant, as pure M throughout the operation of the column. This is indeed the case as illustrated in Figure 6-9.

The resulting motion of the still pot composition in the composition simplex is also illustrated in Figure 6-10. As can be seen from the diagram, the still pot composition moved directly away from the combined net product given by the midpoint between the fixed points of CM and M, until it encountered the curved stable separatrix between M and ACM. At this point, a change in the alpha limit set of the still pot occurs, and the new products of the rectifying section of the column becomes that of the ACM azeotrope. The bottoms product is unchanging, because the omega limit set of the still pot composition remains as pure B. The still pot then traces out the stable separatrix, instantaneously drawing a net product that is tangent to the separatrix at the point where the still pot composition is instantaneously located, until the still pot composition finally enters the fixed point of pure M. The column

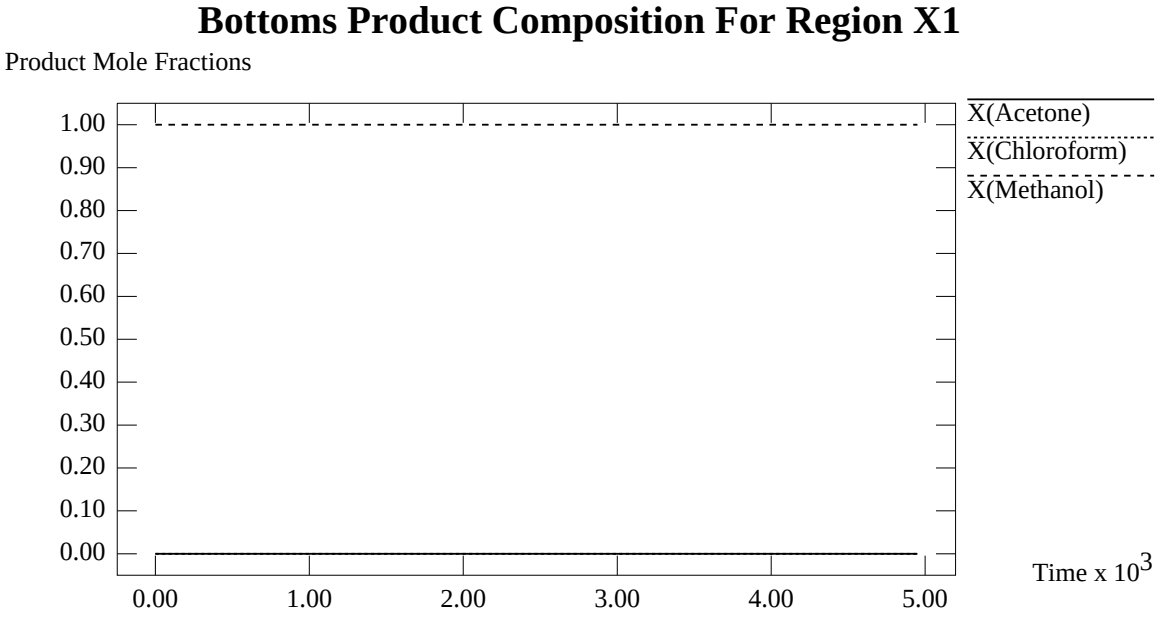

Figure 6-9: Graph of Bottoms Product Composition against Time

thus continues to draw pure M at this point for both the distillate and the bottoms product (since the still pot composition is pure methanol) until the still pot runs dry (i.e., $\xi \to \infty$).

6.3.2 An Analysis of the Results From Region χ_4

These results are representative of the use of a middle vessel column to separate the mixture of acetone, chloroform and methanol, in which the still pot composition encounters a curved middle vessel batch distillation boundary (unstable separatrix in this case) and traces out the unstable separatrix to an unstable node which forms the final alpha and omega set of the distillation process. The expected product sequence for region χ_4 is ([CM,M], [CM,ACM-mix], [CM,CM]). The initial still pot composition chosen to represent region χ_4 was given by ($X_A = 0.05$, $X_B = 0.43$, $X_C = 0.52$).

As presented in Figure 6-11, the bottoms product cut from the middle vessel column was found to be (M, ACM-mix, CM), which was exactly as expected for the region. As before, the curvature of the stable separatrix encountered (ACM-CM) resulted in a slight "mix" in the ACM-mix cut, but as the curvature of this separatrix

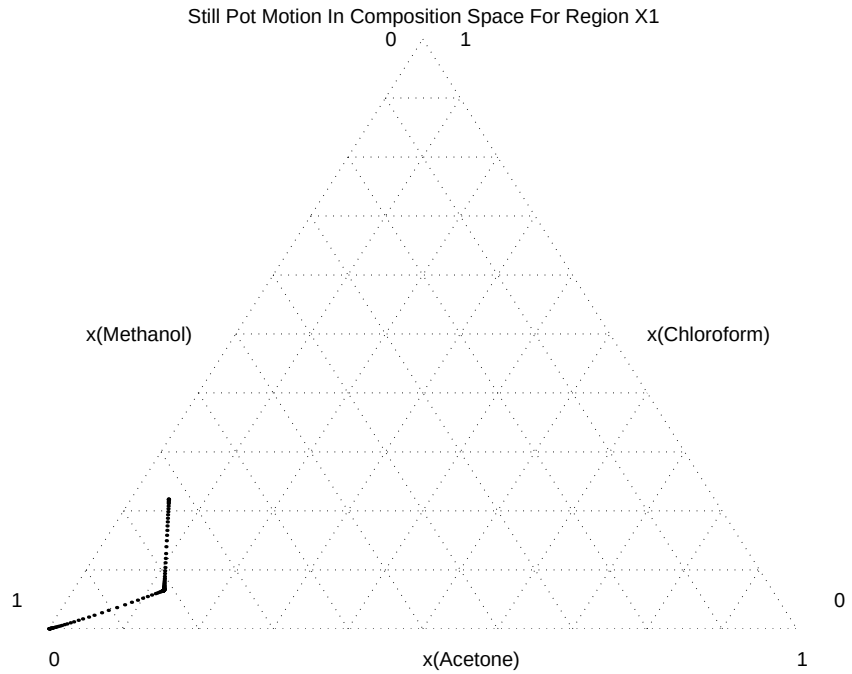

Figure 6-10: Plot of Still Pot Motion in Composition Space

is not as acute as that of the separatrices between ACM-AM and ACM-AC, no pure components are obtained in this mixed cut.

The distillate product cut, on the other hand, was predicted to be invariant, as the azeotrope CM throughout the operation of the column. This is indeed the case as illustrated in Figure 6-12.

The resulting motion of the still pot composition in the composition simplex is illustrated in Figure 6-13. As seen from the diagram, the still pot composition moved directly away from the combined net product given by the midpoint between the fixed points of CM and M, until it encountered the curved unstable separatrix between CM and ACM. At this point, a change in the omega limit set of the still pot occurs, and the new products of the stripping section of the column becomes that of the ACM azeotrope. The distillate product is unchanging, because the alpha limit set of the still pot composition remains as the azeotrope CM. The still pot then traces out the unstable separatrix, instantaneously drawing a net product that is tangent to the separatrix at the point where the still pot composition is instantaneously located, until the still pot composition finally enters the fixed point of azeotrope CM. The

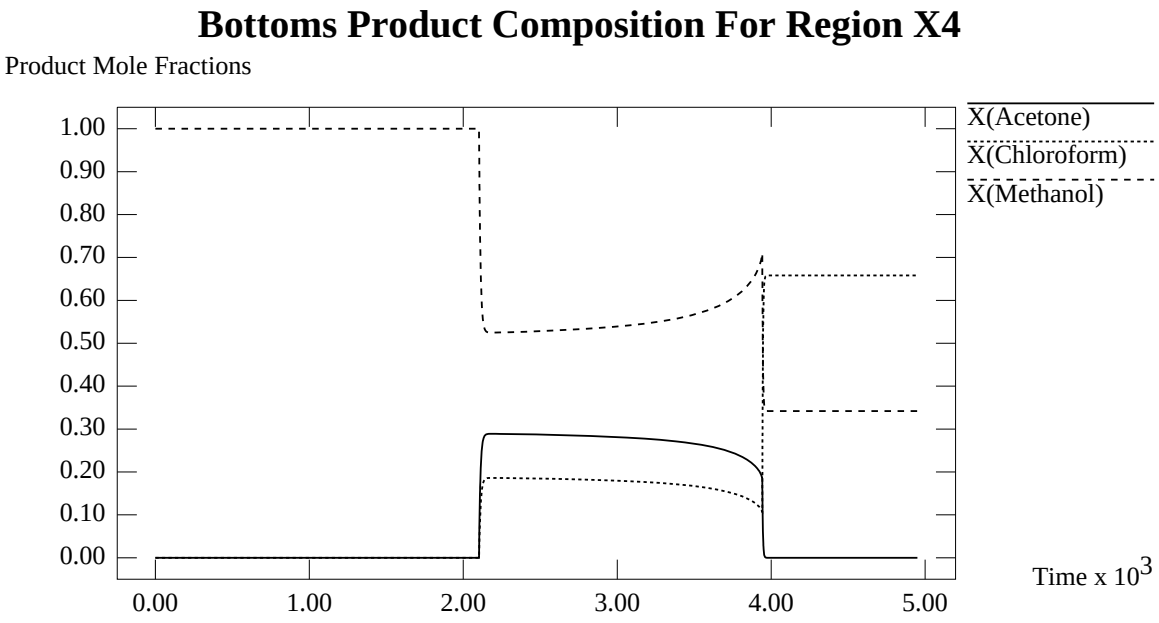

Figure 6-11: Graph of Bottoms Product Composition against Time

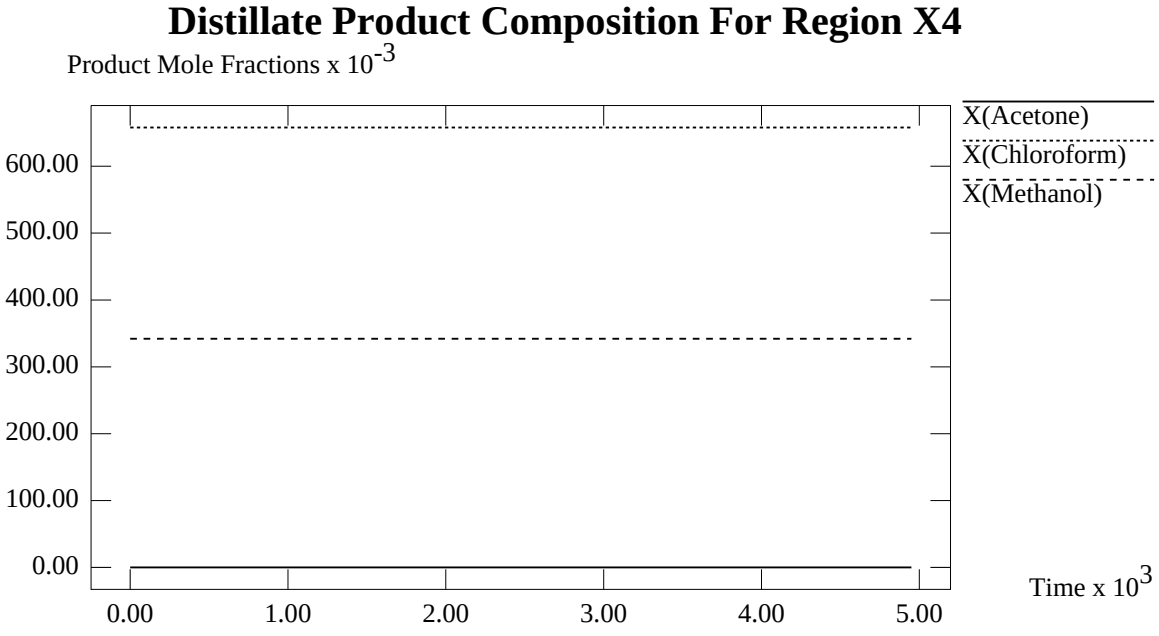

Figure 6-12: Graph of Product Composition against Time

column thus continues to draw CM at this point for both the distillate and the bottoms product (which is the still pot composition) until the still pot runs dry (i.e., $\xi \to \infty$).

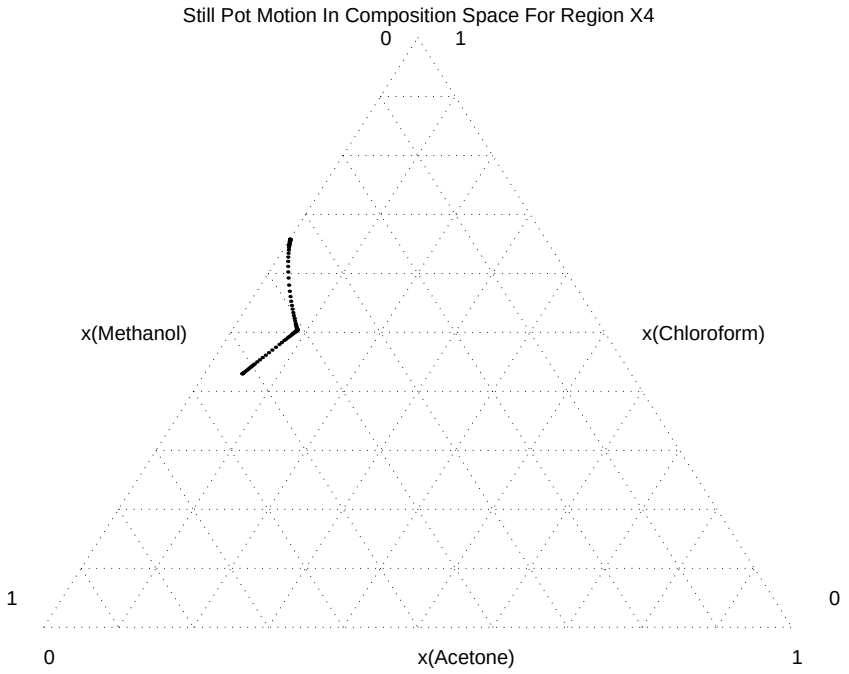

Figure 6-13: Plot of Still Pot Motion in Composition Space

6.3.3 An Analysis of the Results From Region χ_{17}

These results are representative of the use of a middle vessel column to separate the mixture of acetone, chloroform and methanol, in which the still pot composition encounters a curved middle vessel batch distillation boundary (stable separatrix in this case) and traces out the stable separatrix to a saddle point which forms the final alpha and omega set of the distillation process. The expected product sequence for region χ_{17} is ([AM,AC], [ACM-mix,AC], [ACM,ACM]). The initial still pot composition chosen to represent region χ_{17} was given by ($X_A = 0.49$, $X_B = 0.33$, $X_C = 0.18$).

As presented in Figure 6-14, the distillate product cut from the middle vessel column was found to be (AM, ACM-mix, ACM), which was exactly as expected for the region. As before, the curvature of the stable separatrix encountered resulted

in a "mixed" ACM-mix cut, The final composition of the distillate product is that of the ternary azeotropic mixture of ACM (saddle point), which is also the still pot composition at that point in time.

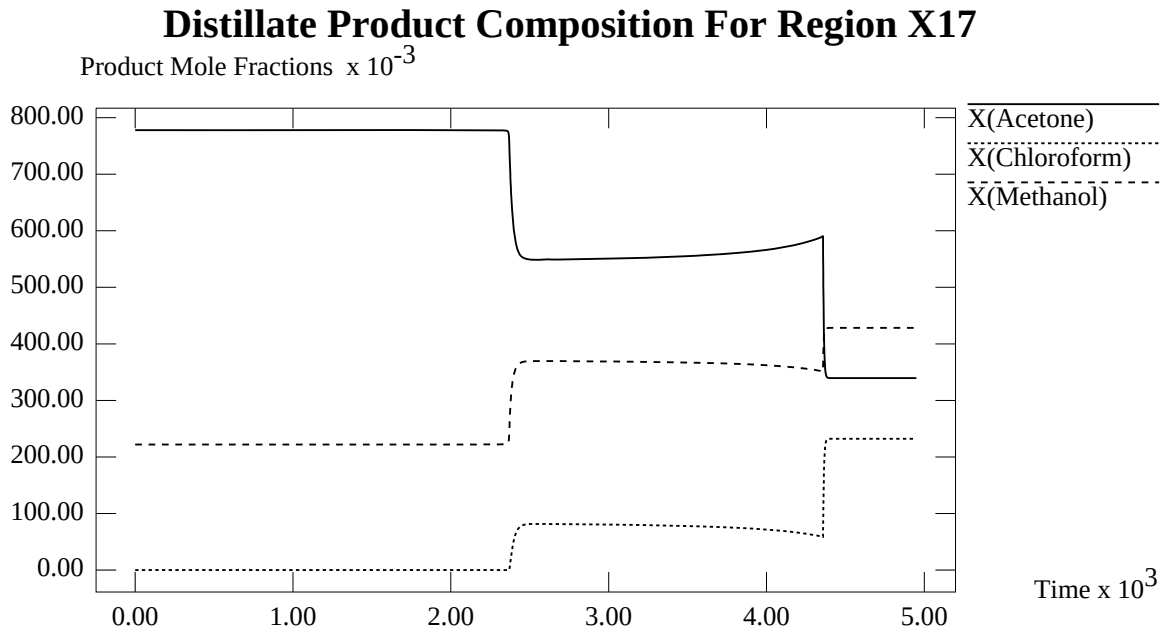

Figure 6-14: Graph of Distillate Product Composition against Time

The bottoms product cut, on the other hand, was predicted to be (AC, AC, ACM), which again corresponded to the results obtained as shown in Figure 6-15. The ACM cut is a result of the still pot composition becoming the azeotropic composition of ACM, resulting in a switch in the omega limit set for the still pot composition to that of saddle point ACM.

The resulting motion of the still pot composition in the composition simplex is also illustrated in Figure 6-16. As can be seen from the diagram, the still pot composition moved directly away from the combined net product given by the midpoint between the fixed points of AM and CM, until it encountered the highly curved stable separatrix between AC and ACM. At this point, a change in the alpha limit set of the still pot occurs, and the new products of the rectifying section of the column becomes that of the ACM azeotrope. The bottoms product is unchanging, because the omega limit set of the still pot composition remains as AC. The still pot then traces out the stable separatrix, instantaneously drawing a net product that is tangent to the

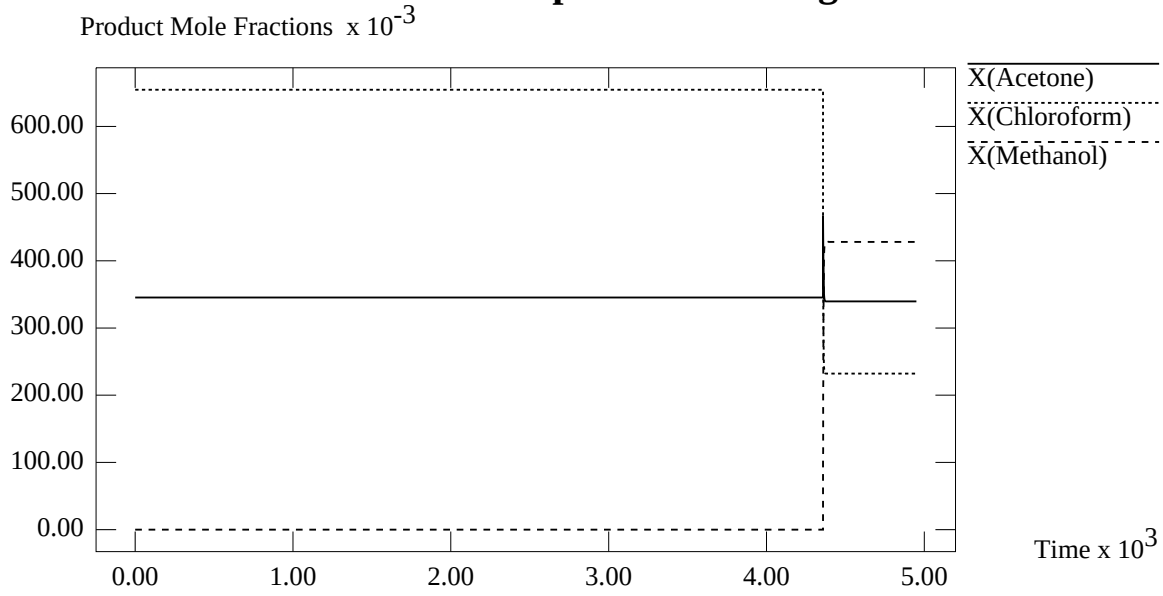

Figure 6-15: Graph of Bottoms Product Composition against Time

separatrix at the point where the still pot composition is instantaneously located, until the still pot composition finally enters the saddle point of ACM. At this point the omega limit set is also changed to that of ACM, and "pure" ACM (rather than ACM-mix) is also drawn as the distillate product. The column thus continues to draw ACM at this point for both the distillate and the bottoms product (since the still pot composition is pure ACM) until the still pot runs dry (i.e., $\xi \to \infty$).

6.3.4 An Analysis of the Results From Region χ_{21}

These results are representative of the use of a middle vessel column to separate the mixture of acetone, chloroform and methanol, in which the still pot composition encounters a straight middle vessel batch distillation boundary (composition simplex edge in this case) and traces out the composition simplex edge to an unstable node which forms the final alpha and omega set of the distillation process. The expected product sequence for region χ_{21} is ([AM,AC], [AM,A], [AM,AM]). The initial still pot composition chosen to represent region χ_{21} was given by ($X_A = 0.71$, $X_B = 0.12$, $X_C = 0.17$).

As presented in Figure 6-17, the bottoms product cut from the middle vessel

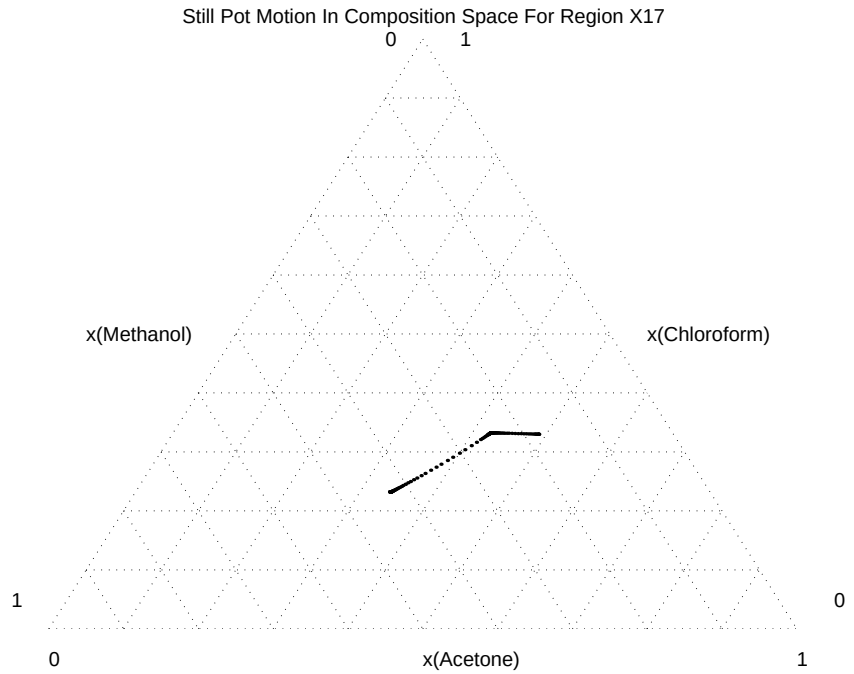

Figure 6-16: Plot of Still Pot Motion in Composition Space

column was found to be (AC, A, AM), which was exactly as expected for the region. In the absence of curved boundaries (as was the case with regions χ_1, χ_4, and χ_{17}), the cuts are much sharper, and the compositions of the cuts are very well defined (due to the limiting operating conditions in both sections of the column).

The distillate product cut, on the other hand, was predicted to be invariant, as the azeotrope AM throughout the operation of the column. This is indeed the case as illustrated in Figure 6-18.

The resulting motion of the still pot composition in the composition simplex is illustrated in Figure 6-19. As seen from the diagram, the still pot composition moved directly away from the combined net product given by the midpoint between the fixed points of AM and AC, until it encountered the composition edge at the line segment between AM and A. At this point, a change in the omega limit set of the still pot occurs, and the new products of the stripping section of the column becomes that of the pure A. The distillate product is unchanging, because the alpha limit set of the still pot composition remains as the azeotrope AM. The still pot then moves along the composition simplex edge, drawing a point between AM and A as the net

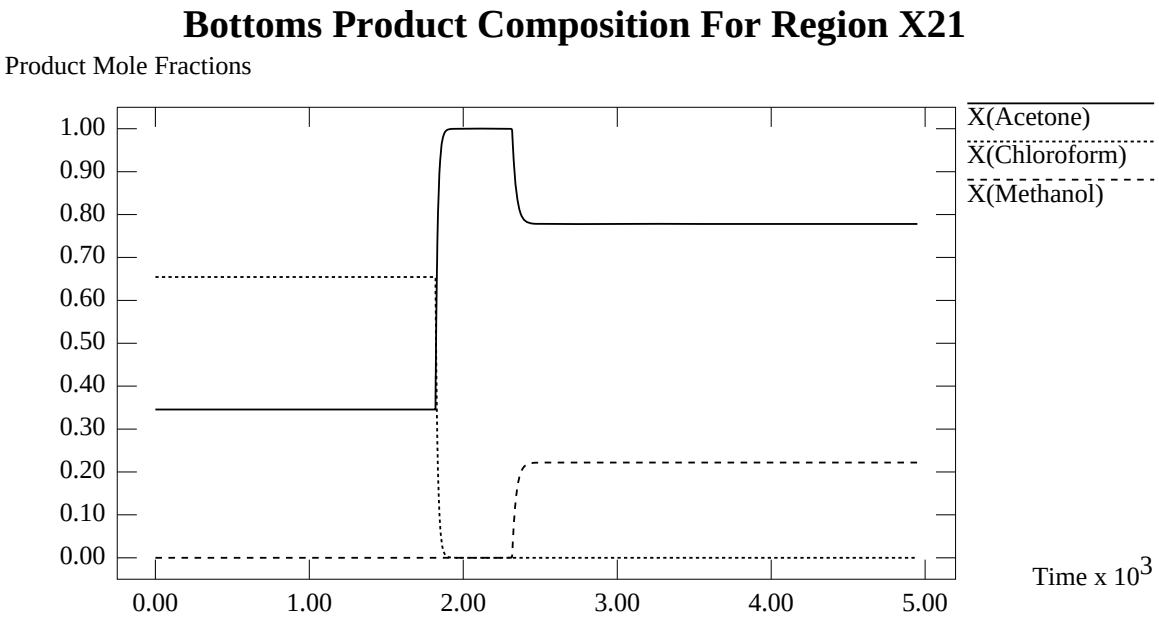

Figure 6-17: Graph of Bottoms Product Composition against Time

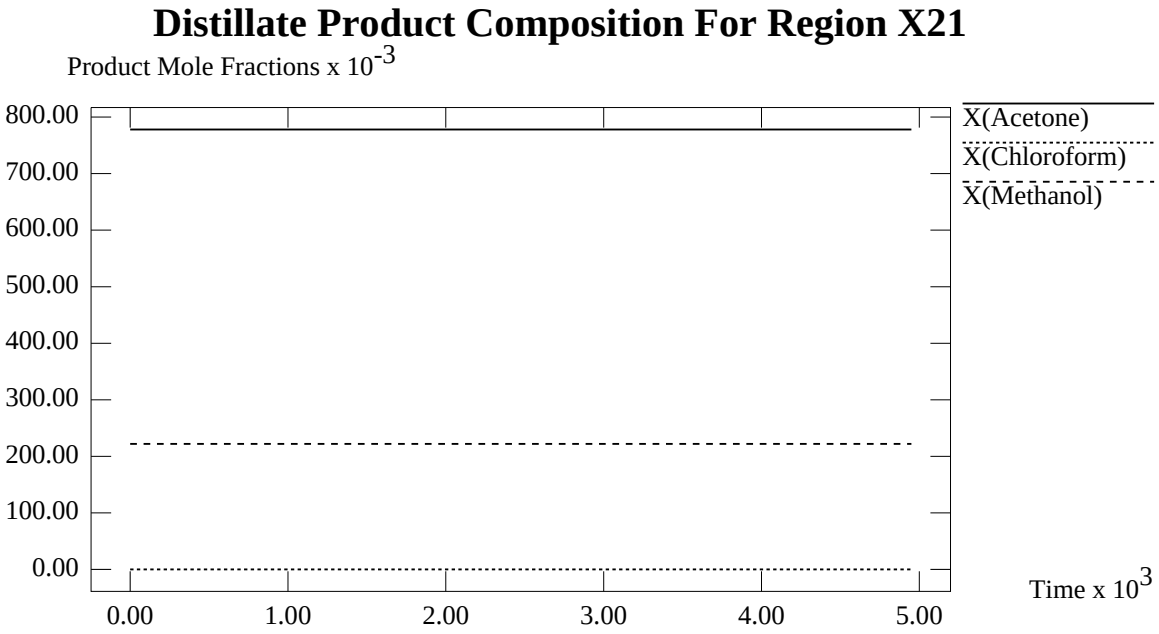

Figure 6-18: Graph of Product Composition against Time

product from the column, until the still pot composition finally enters the unstable node of azeotrope AM. The column thus continues to draw CM at this point for both the distillate and the bottoms product (which is the still pot composition) until the still pot runs dry (i.e., $\xi \to \infty$).

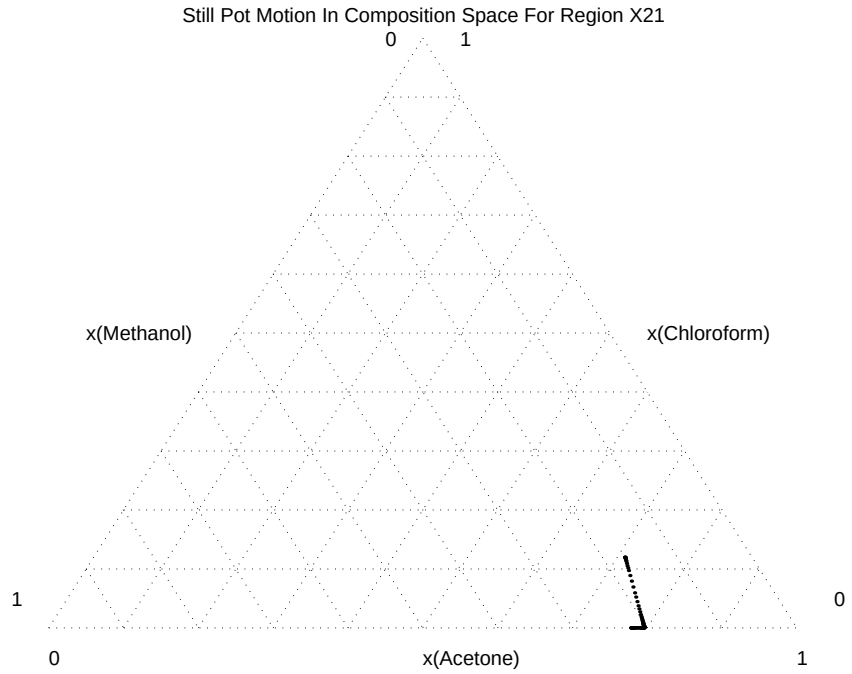

Figure 6-19: Plot of Still Pot Motion in Composition Space

6.3.5 An Analysis of the Results From Region χ_{22}

These results are representative of the use of a middle vessel column to separate the mixture of acetone, chloroform and methanol, in which the still pot composition encounters a straight middle vessel batch distillation boundary (composition edge A-M in this case) and traces out the composition edge to a saddle point which forms the final alpha and omega set of the distillation process. The expected product sequence for region χ_{22} is ([AM,AC], [AM,A], [A,A]). The initial still pot composition chosen to represent region χ_{22} was given by ($X_A = 0.78$, $X_B = 0.15$, $X_C = 0.07$).

As presented in Figure 6-20, the distillate product cut from the middle vessel column was found to be (AM, AM, A), which was exactly as expected for the region. As with the case of χ_{21}, the straight distillation boundaries encountered implied that

the product cuts were sharp, and no "mixed" cuts were obtained. The A cut is a result of the still pot composition becoming that of pure A, such that both the alpha and omega limit sets become pure A.

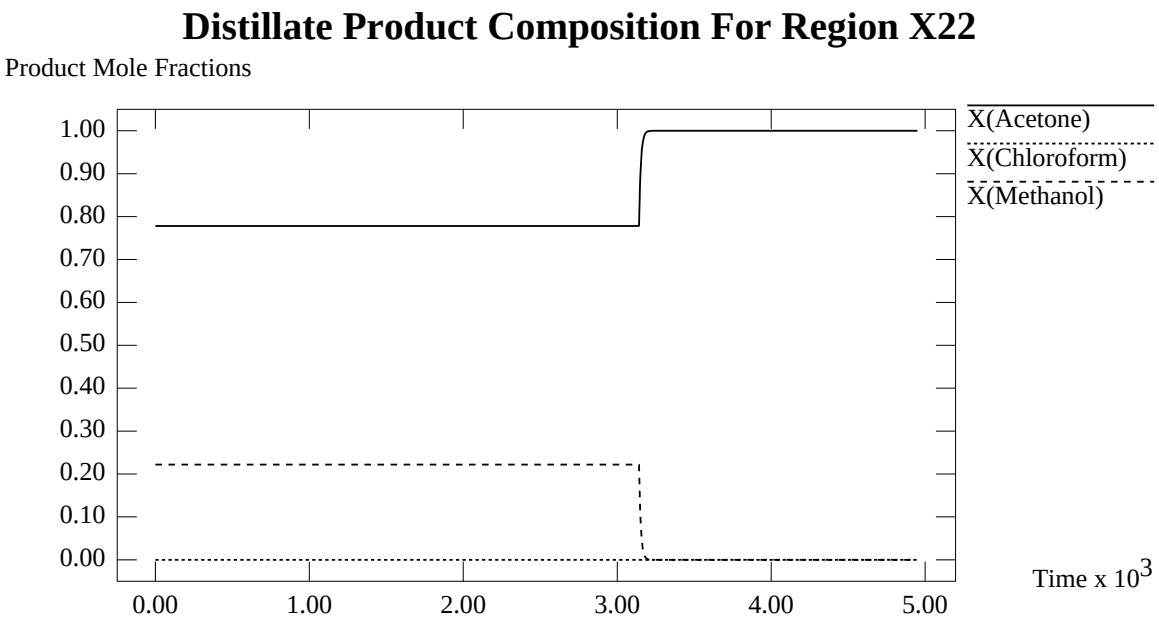

Figure 6-20: Graph of Distillate Product Composition against Time

The bottoms product cut, on the other hand, was predicted to be (AC, A, A), which again corresponded to the results obtained as shown in Figure 6-21. The cut changes to that of pure A when the still pot composition encounters the composition simplex, and the omega limit set of the system is changed from that of the azeotrope AC to that of pure A. The final composition in the pot is also pure A, so the bottoms product remains unchanged.

The resulting motion of the still pot composition in the composition simplex is also illustrated in Figure 6-22. As can be seen from the diagram, the still pot composition moved directly away from the combined net product given by the midpoint between the fixed points of AM and CM, until it encountered the composition simplex edge between A and AM. At this point, a change in the omega limit set of the still pot occurs, and the new products of the stripping section of the column becomes that of pure A. The distillate product is unchanging, because the alpha limit set of the still pot composition remains as AM. The still pot then traces out the composition

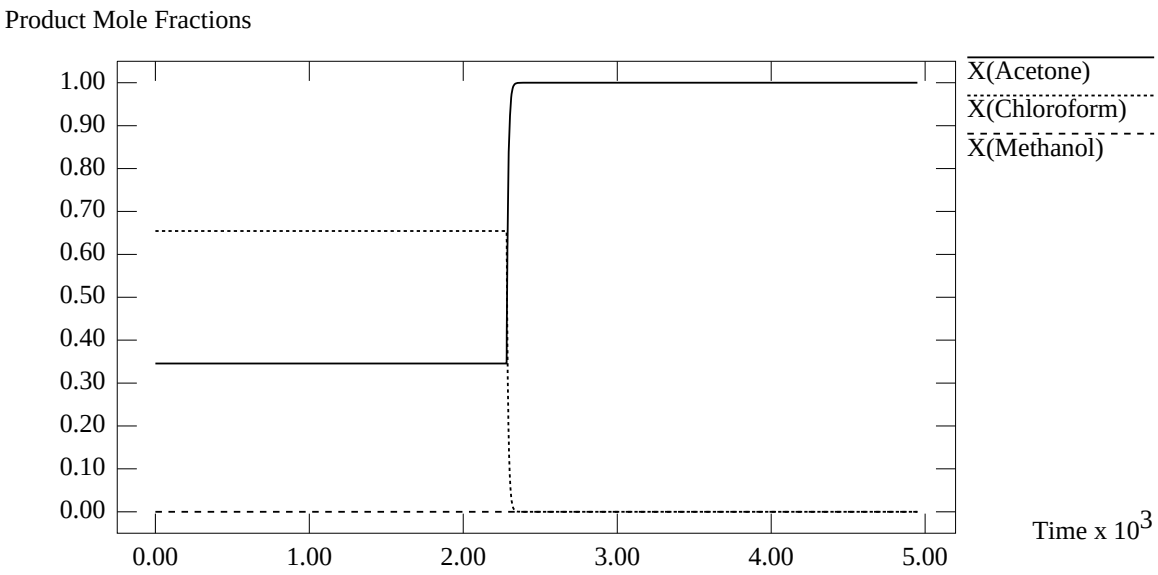

Figure 6-21: Graph of Bottoms Product Composition against Time

simplex edge, away from the net product which is the midpoint between the two products drawn at this point in time (namely AM and A), until the still pot composition finally enters the saddle point of A. At this point the alpha limit set is also changed to that of pure A, which is drawn as the distillate product. This continues until the still pot runs dry (i.e., $\xi \to \infty$).

6.3.6 An Analysis of the Results From Region χ_{24}

These results are representative of the use of a middle vessel column to separate the mixture of acetone, chloroform and methanol, in which the still pot composition encounters a straight middle vessel batch distillation boundary (composition edge A-C in this case) and traces out the composition edge to a stable node which forms the final alpha and omega set of the distillation process. The expected product sequence for region χ_{24} is ([AM,AC], [A,AC], [AC,AC]). The initial still pot composition chosen to represent region χ_{24} was given by ($X_A = 0.55$, $X_B = 0.40$, $X_C = 0.05$).

As presented in Figure 6-23, the distillate product cut from the middle vessel column was found to be (AM, A, AC), which was exactly as expected for the region. As with the case of χ_{21} and χ_{22}, the straight distillation boundaries encountered

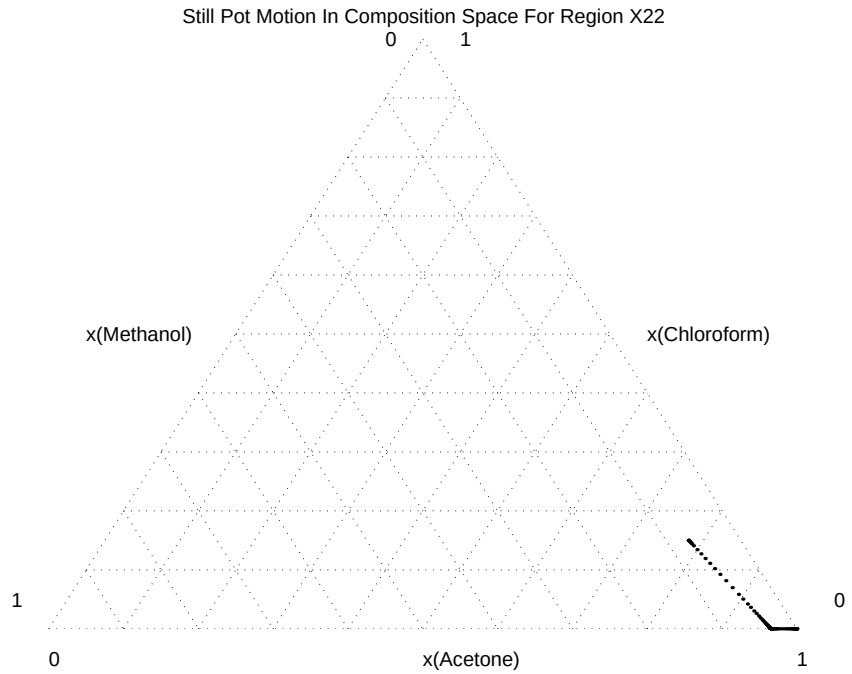

Figure 6-22: Plot of Still Pot Motion in Composition Space

implied that the product cuts were sharp, and no "mixed" cuts were obtained. The A cut is a result of the alpha limit set of the still pot composition becoming that of pure A when the pot composition encountered the A-C edge. Finally, when the still pot composition became AC, AC was drawn as the distillate product as well (i.e., another switch in the alpha limit set occurs).

The bottoms product cut, on the other hand, was predicted to be invariant as AC, which again corresponded to the results obtained as shown in Figure 6-24.

The resulting motion of the still pot composition in the composition simplex is also illustrated in Figure 6-25. As can be seen from the diagram, the still pot composition moved directly away from the combined net product given by the midpoint between the fixed points of AM and CM, until it encountered the composition simplex edge between A and AC. At this point, a change in the alpha limit set of the still pot occurs, and the new products of the rectifying section of the column becomes that of pure A. The bottoms product is unchanging, because the omega limit set of the still pot composition remains as AC. The still pot then traces out the composition simplex edge (A-C), away from the net product which is the midpoint between the

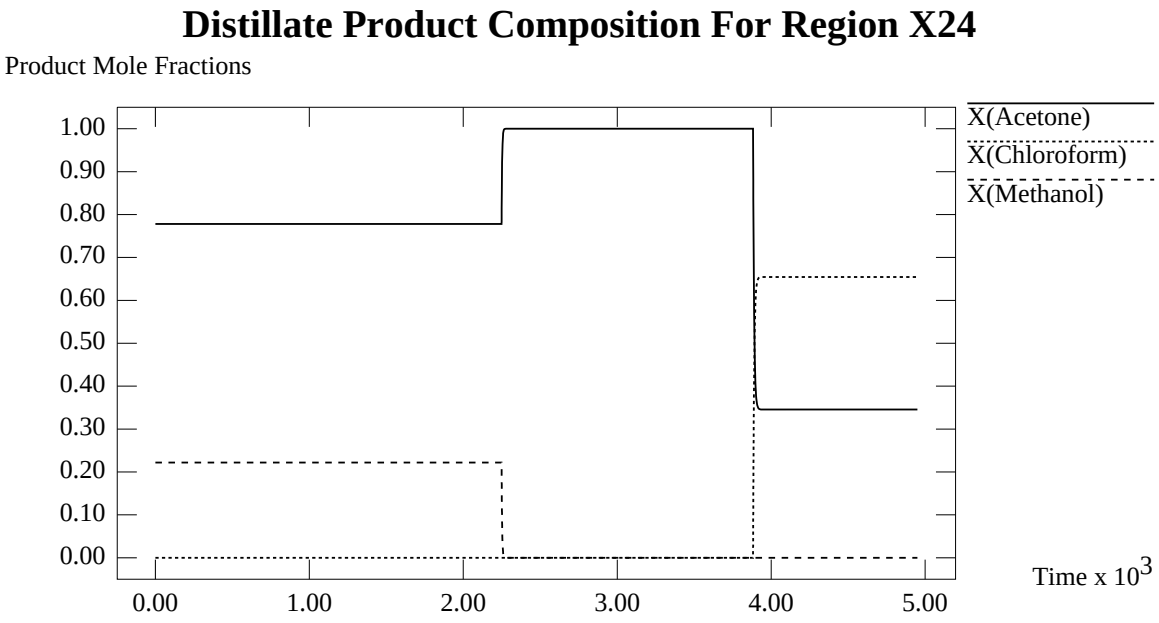

Figure 6-23: Graph of Distillate Product Composition against Time

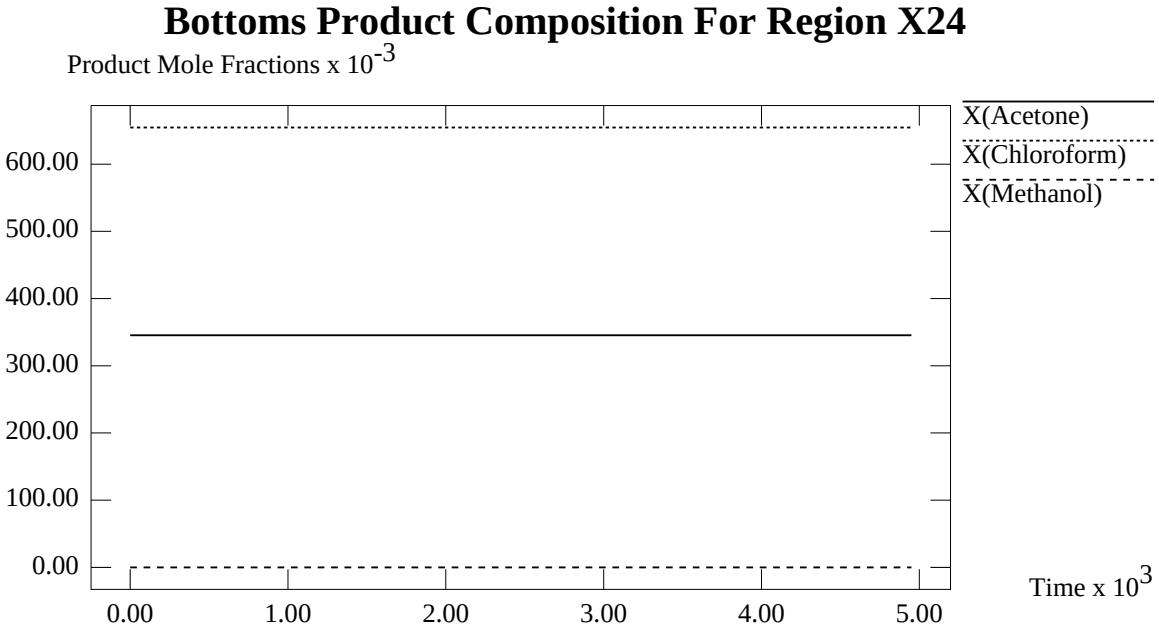

Figure 6-24: Graph of Bottoms Product Composition against Time

two products drawn at this point in time (namely AC and A), until the still pot composition finally enters the stable node of AC. At this point the alpha limit set is changed again to that of pure AC, which continues until the still pot runs dry (i.e., $\xi \to \infty$).

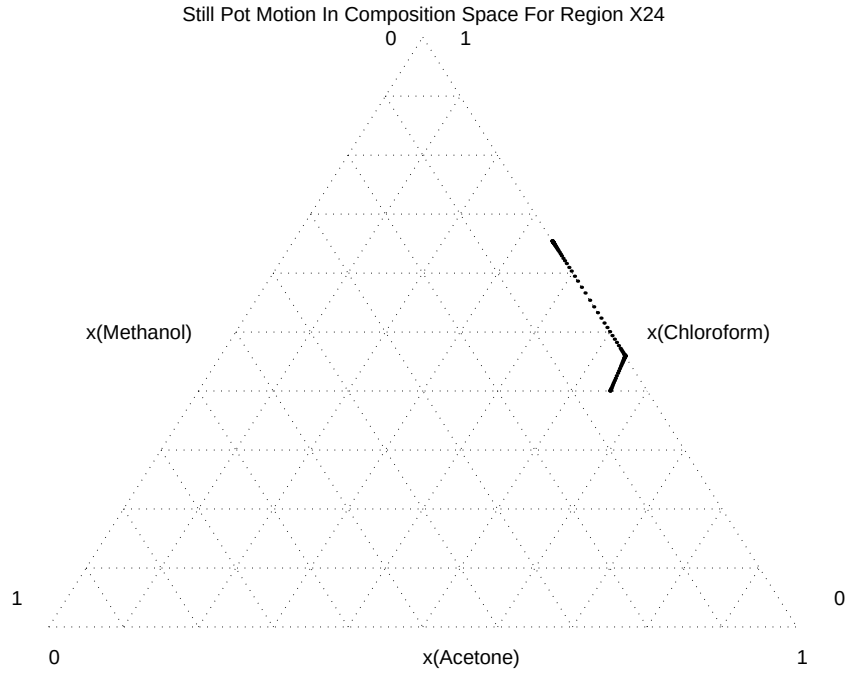

Figure 6-25: Plot of Still Pot Motion in Composition Space

6.4 A Comparison of Results in the Presence of Holdup in Trays

The purpose of this section is to show that as long as the molar holdup in each tray is not extensive, the assumption of negligible holdup does not affect the limiting results of the middle vessel column significantly.

A simulation was thus conducted in this spirit, to check that the results obtained for a column in which there is appreciable holdup, is indeed similar (if not equivalent) to a column in which holdup has been assumed to be negligible (as we had done so far in all our analyses). For an initial still pot composition starting in Region χ_{24}, a holdup of 0.1% of the entire charge in the column was assumed to be in each of

the 100 trays. This corresponded in total to 10% of the initial column charge being holdup in the trays.

Using the operating parameters developed in Section 6.3, simulations were conducted using a modified model of the middle vessel column, in which a molar holdup of 0.1 moles was introduced into each of the 100 trays (total holdup in the still pot of the column being 100 moles). An initial charge size of 110 moles with composition of ($X_A = 0.5498$, $X_B = 0.3939$, $X_C = 0.0563$) was chosen to represent the region χ_{24}. This was slightly different from the initial still pot composition was chosen to represent region χ_{24} in Section 6.3 which was given as ($X_A = 0.55$, $X_B = 0.40$, $X_C = 0.05$). However, upon initialization of the column profile, the charge of 110 moles of composition ($X_A = 0.5498$, $X_B = 0.3939$, $X_C = 0.0563$) resulted in a still pot with a holdup of 100 moles, and a composition of ($X_A = 0.55$, $X_B = 0.40$, $X_C = 0.05$). This then allows us to compare the movement of the still pot between the two cases of no holdup in the trays versus that of holdup in the trays, by starting the still pot composition at the same point.

As highlighted in Section 6.3, the expected product sequence for region χ_{24} is ([AM,AC], [A,AC], [AC,AC]), in the absence of holdup in the trays. Further, as illustrated in Figure 6-26, the distillate product cut sequence of the middle vessel column in the presence of significant holdup in trays, is exactly the same as that when there is no holdup in trays. The product sequence from the simulation with tray holdups was also (AM, A, AC), which was exactly as expected for the region in the presence of no holdups (which was illustrated in Figure 6-23). It should be noted, however, that in the presence of substantial holdup in trays, the transitions between cuts is not as sharp, but the qualitative behavior remains the same.

The bottoms product cut, on the other hand, was predicted to be invariant as AC, which again corresponded to the results obtained as shown in Figure 6-27, again exactly similar to Figure 6-24).

The resulting motion of the still pot composition in the composition simplex is also illustrated in Figures 6-28 through 6-30. Figure 6-28 illustrates the movement of the still pot composition (i.e., neglecting the holdup in the column) in composition

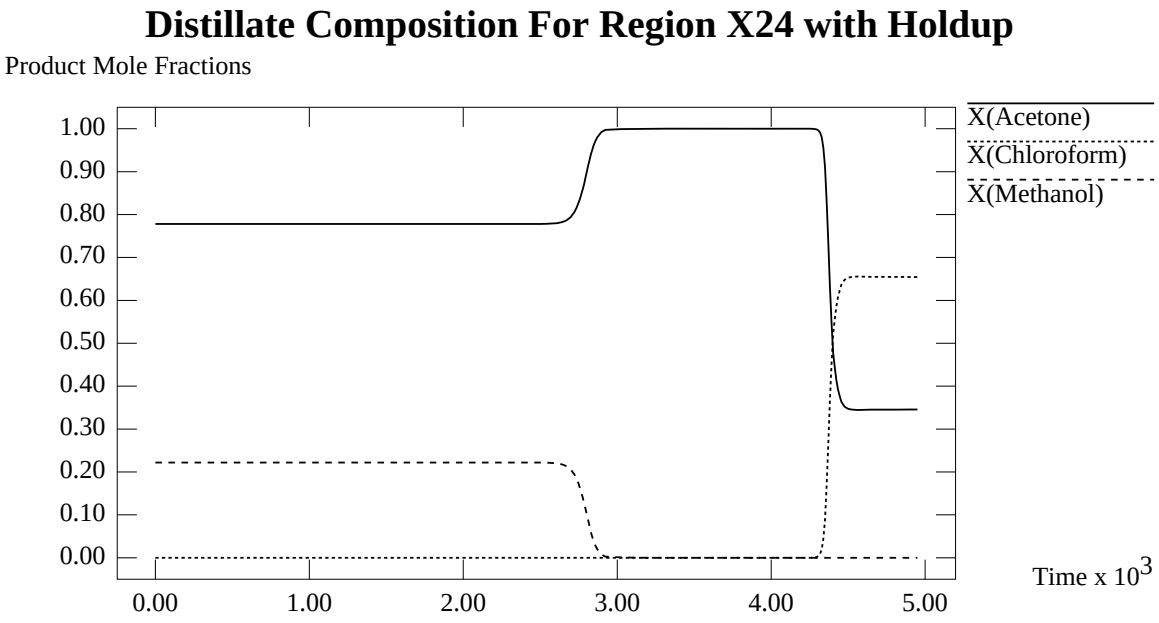

Figure 6-26: Graph of Distillate Product Composition against Time

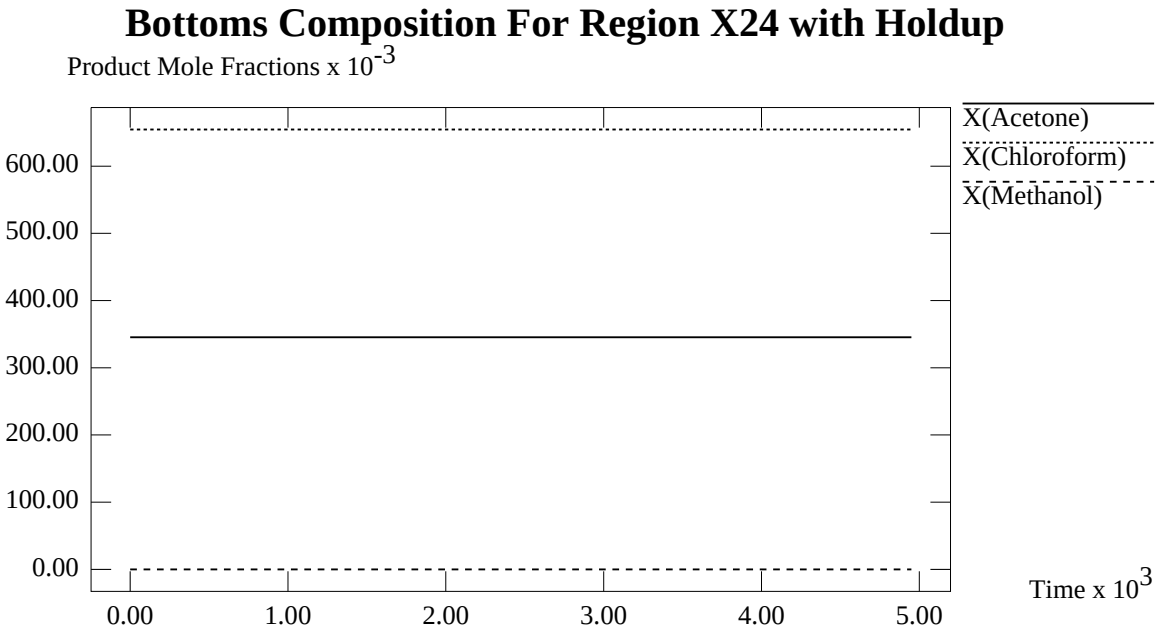

Figure 6-27: Graph of Bottoms Product Composition against Time

space. Figure 6-29 illustrates the movement of the net composition of the column (weighted average of all the holdups in the column), in composition space. They are not appreciably different from each other. Finally, Figure 6-30 plots the still pot composition motion in the case of no holdup (i.e., Figure 6-25), the still pot composition with holdup (i.e., Figure 6-28) and the total column composition with holdup (i.e., Figure 6-29) on the same plot. As we can see from Figure 6-30, there is no appreciable difference between the still pot composition paths for the two cases (of no holdup in trays vs holdup in trays).

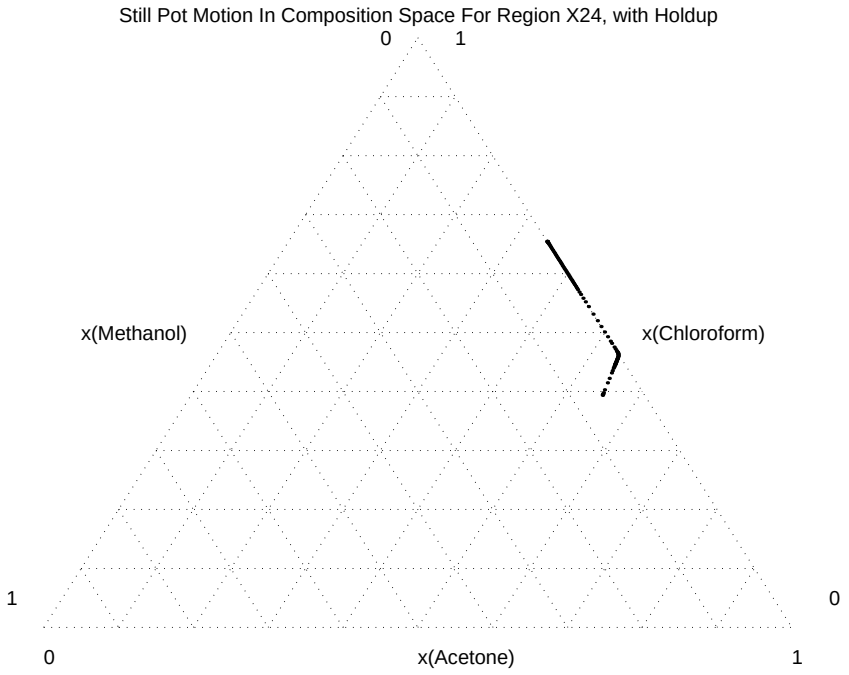

Figure 6-28: Plot of Still Pot Motion in Composition Space

From the results presented in this section, it thus seems reasonable to conclude that the assumption of negligible holdup in the columns is indeed valid as an approximation of a column in which holdup is not unreasonably large in each tray. The analysis associated with the limiting behavior of the middle vessel column (Chapters 4 and 5), thus remains applicable to columns where there are reasonable amounts of holdup in each of the trays in the column.

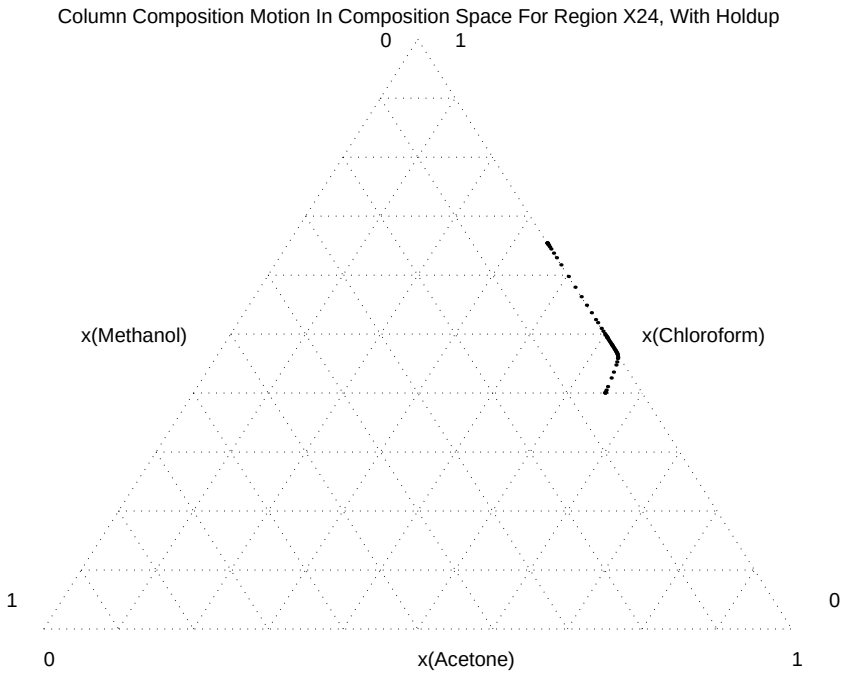

Figure 6-29: Plot of Total Holdup Motion in Composition Space

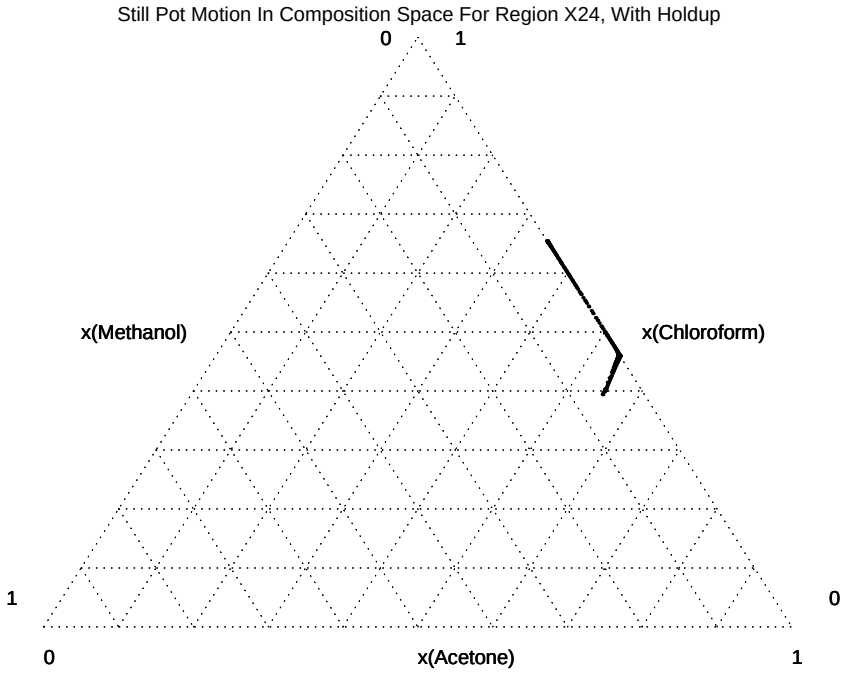

Figure 6-30: Combined Plot of Still Pot Motion and Total Holdup Motion in Composition Space, With and Without Holdup in Trays

Chapter 7

Azeotropic Batch Distillations with a Middle Vessel Column in the Presence of Curved Separatrices

Based on the analysis regarding the influence of curved separatrices on batch distillation regions in a middle vessel column (Chapter 5), a simulation was conducted for the separation of acetone, benzene and chloroform in a ternary mixture. The operating procedure for the middle vessel column was developed in Chapter 5. These ideas, in which an entrainer is added to the initial charge of the column for breaking the azeotropes, are *completely different* from that of adding an entrainer continuously over the course of the operation of the middle vessel column as suggested by Safrit *et al.* [35, 33]. These operating procedures were tested using the ABACUSS model of the middle vessel column, so as to validate the theory behind such an operating procedure. The results of the simulations are presented in this chapter.

This chapter is in five sections. The first section revisits the basic concepts explained in Chapter 5, which result in the plausible separation of a mixture of acetone, benzene and chloroform. The second section summarizes the operating policies in

quantitative terms. The third section presents the results of simulation using a quasi-static mode of operation with the addition of benzene as an entrainer. The fourth section compares and contrasts the pros and cons of adding an entrainer versus not adding an entrainer, for an original composition starting in region ν. Finally the fifth section compares the quasi-static mode of operation to that of a non-quasi-static mode of operation, in separating an original mixture corresponding to the azeotropic composition.

7.1 Separation of an Acetone, Benzene and Chloroform Mixture in a Middle Vessel Column

A separation scheme of the ternary system of Acetone (A), Benzene (B) and Chloroform (C) based on the theory developed in Chapter 5 was applied to the ABACUSS model of the middle vessel column.

Revisiting the operating sequence developed in Chapter 5, there were two modes of operation feasible: A) the recycle of an azeotropic cut to the next batch (or discarded as wasted) with no addition of benzene, and B) no/negligible recycle of azeotropic cuts, but with the addition of fresh benzene as an entrainer. The region of desired initial pot composition achieved via mixing for mode B, is given by σ as introduced in Chapter 5, and illustrated in Figure 7-1. By observing the location of the separatrix on the residue curves map, ρ was determined to be:

$$\begin{aligned} x_{benzene} &= 0.8 \ldots 1 \\ x_{chloroform} &= 0.2 \ldots 0 \\ x_{acetone} &\approx 0 \end{aligned} \tag{7.1}$$

This implies that the region σ is bounded by the A-B edge, the line segment defined as ρ on the B-C edge, and the line segment joining A to the composition point given by ($x_{acetone} = 0$, $x_{benzene} = 0.8$, $x_{chloroform} = 0.2$).

An original composition corresponding to that of the acetone-chloroform azeotrope

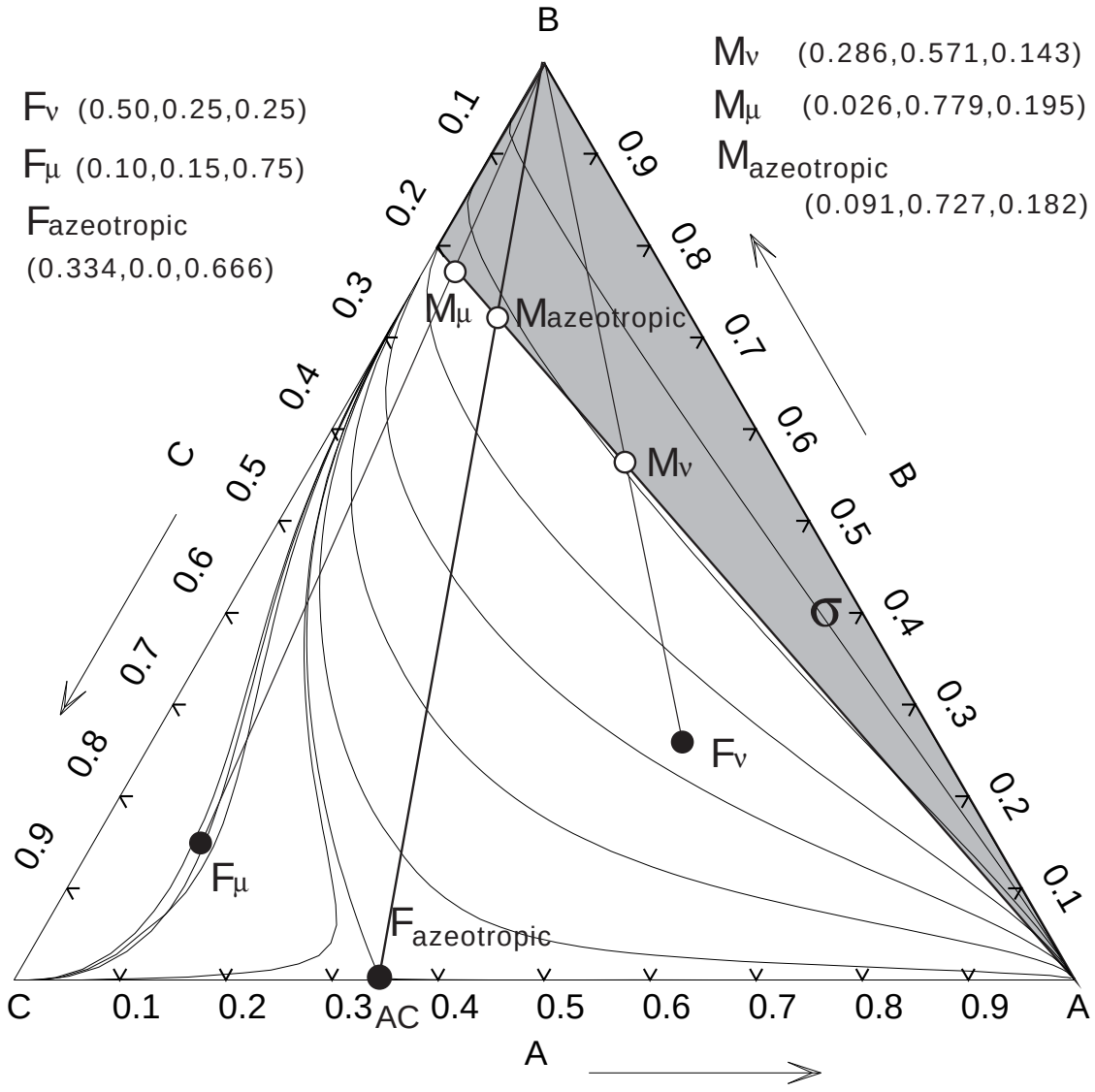

Figure 7-1: Initial Composition of Mixtures to be Separated, Before and After Benzene is Added as Entrainer to the Still Pot

$F_{azeotrope}$ was chosen to illustrate the applicability of mode B, but not mode A of operation, to an azeotropic mixture. To illustrate the applicability of mode B of operation to all regions of interest within the composition simplex, original charges F_μ and F_ν from each of the regions μ, ν were also chosen and operated under both mode B.

To compare and contrast the results of mode A versus mode B of operation (see Chapter 5, Section 5.2), the original charge of F_ν was operated under mode A (without mixing of benzene), and the results of the separation compared to that of F_ν operated under mode B.

Furthermore, it was determined in Chapter 5 that quasi-static operation of the column (after it crosses the separatrix) is superior, because purity is maintained (with the consistently high reflux ratio) while operation time was decreased. Hence, only operation of the middle vessel column with a quasi-static step was studied (i.e., with the use of the alternative steps listed in Section 5.2: step 5 instead of step 4 for Mode A, and step 6 rather than steps 4 and 5 for Mode B). The results for operating the column without a quasi-static step would just take a longer time, but the qualitative results remain the same: that it is possible to draw each of the 3 pure components as products.

7.2 Operating Parameters, Feed/Mixture Composition and Charge Sizes

In this section, the relevant operating parameters of the middle vessel column are categorized. As we are trying to replicate the limiting conditions of infinite reflux/reboil and infinite trays in the column, a large number of trays and an exceedingly large reflux/reboil ratio of 1000 would be used for the operating conditions of the column. It should be noted that when the column is operated as a stripper, reflux ratio in the rectifying section of the column is infinity, and conversely, the reboil ratio in the stripping section of the column is infinity when the column is operated as a rectifier.

Table 7.1: Operating Conditions for the Rectifier and Stripper Simulations

Operational Parameter	Numerical Value	Units
Vapor Flow Rate (Stripping)	10	Moles/Time
Liquid Flow Rate (Rectifying)	10	Moles/Time
Rectifying Product Flow Rate	0.01	Moles/Time
Stripping Product Flow Rate	0.01	Moles/Time
Resulting Reflux Ratio	1000	Dimensionless
Resulting Reboil Ratio	1000	Dimensionless
Number of Trays in the Rectifier Column	50	Dimensionless
Number of Trays in the Stripper Column	50	Dimensionless
Operating Pressure in Column	1	Bar

Operating conditions for each simulation were kept constant so as to ensure that the results could be comparable to each other. The pertinent operating parameters used are thus summarized in Table 7.1. The behavior of the column as $N \to \infty$ and the reflux/ratios $\to \infty$, was approximated by using a reflux/reboil ratio of 1000, and 100 trays in the column.

When the column is operated as a stripper ($\lambda = 0$), the rectifying product flow rate in the column is shut off, and the resulting reflux ratio is infinity. When the column is operated as a pure rectifier ($\lambda = 1$), the stripping product flow rate is also shut off, and the resulting reboil ratio is infinity. As before, the vapor-liquid equilibria relationships between the components are given by the NRTL activity coefficient model, and the vapor pressure of the components given by an extended Antoine equation from Aspen Plus.

In our attempt to produce product qualities of 99.9% or better, the following operating policy was employed in each of the simulations:

1. With the original charge of the mixture to be separated, an appropriate amount of benzene was added to the charge, such that the ratio of benzene to chloroform in the initial still pot composition is:

   Ratio of Benzene to Chloroform = 4 : 1

This corresponds to the still pot composition being on the edge of the region σ.

2. The middle vessel column is

   Operated at $\lambda = 1$

   (i.e., as a rectifier), until the following conditions are met:

   $x^D_{acetone} \leq 0.999$

   which corresponds to the event of the still pot composition reaching the separatrix, resulting in a degradation of product purity (from 100% purity), as the alpha limit set switches from that of pure acetone, to the azeotrope of AC.

3. The middle vessel column is then:

   Operated at $\lambda = 0$

   (i.e., as a stripper), until the following conditions are met:

   $x^M_{chloroform} \geq x^M_{benzene}$

   which corresponds to the point where pure chloroform should also be drawn from the column.

4. At this point, a distillate product flow rate of 0.01 $moles/time$ is reintroduced into the rectifying column, such that a reflux ratio of 1000 is again achieved in the rectifying section of the column, and such that benzene and chloroform will be exhausted in the still pot at the same point in time. This results in the column being:

   Operated at $\lambda = \frac{0.01}{0.01+0.01} = \frac{1}{2}$

   which is a quasi-static operation, until the following conditions are met:

   $x^D_{chloroform} < 0.999$ OR $x^B_{benzene} < 0.999$

which corresponds to the degradation of products as the column finally runs out of benzene and chloroform, and acetone starts becoming significant in either the distillate or bottoms product. Operation is ceased at this point. The resulting purity of all 3 components recovered were in the region of 100.0%.

It should be noted that the policy of drawing chloroform as near to the end of the operation as possible, is due to the following fact. Even though the separatrix hugs the B-C edge at the point in time when the still pot encounters the separatrix and stops drawing acetone, there remains some acetone in the still pot. While it is negligible initially when the quantity of benzene and chloroform is substantial, it no longer becomes negligible as the still pot boils down. If the column was operated in a quasi-static state immediately after the still pot composition crosses the separatrix, it would be forced back onto the separatrix after a short period of operation. When the still pot composition is forced back onto the separatrix, the net product drawn will have to be from a location that is tangent to the separatrix. As the separatrix approaches but not quite reaches the B-C edge, this would imply that pure chloroform and benzene can no longer be drawn in a quasi-static operation if this occurs. As such, this is avoided by moving the still pot composition towards the chloroform vertex (by drawing benzene in the stripping operation for a longer period of time), such that as the amount of acetone in the column becomes significant again, the still pot would move towards the acetone vertex within the region of μ, and encounter the separatrix only at a much later point in time. The point in time when the still pot composition encounters the separatrix again, is where the operation of the column is ceased.

Finally, it should thus be elucidated that if the stripper operation was allowed to continue until the still pot encounters the C-AC edge, followed by a rectifying operation to recover the chloroform, the amount of pure products recovered from the column will be maximized. However, this will result in a substantial increase in the processing time, which does not seem justifiable, given the minute quantities of A, B and C discarded as a result of using a quasi-static operation. This point is of importance, because should the chemicals to be separated prove extremely valuable, and time is not a concern, then a stripping operation, followed by a rectifying operation,

as enumerated below, would be the optimal policy. Steps 3 and 4 should then be subsituted as follows:

- The middle vessel column is then:

  Operated at $\lambda = 0$

  (i.e., as a stripper), until the the following conditions are met:

  $x^M_{benzene} \leq 0.001$

  which corresponds to the point where all pure benzene has been drawn from the column.

- At this point, the column is operated again as a rectifier, that is:

  Operated at $\lambda = 1$

  until the following conditions are met:

  $x^D_{chloroform} < 0.999$

  which corresponds to the degradation of products as the still pot composition encounters the azeotropic fixed point, and the azeotrope starts coming out of the rectifying section of the column. Operation is ceased at this point. Purity of all 3 components recovered are again in the region of 100.0%.

This operating policy will be simulated for the case of $F_{azeotrope}$ to illustrate that the time savings of the quasi-static operation largely outweighs the additional amount of products that can be recovered from the column as if the operating policy of a stripper followed by a rectifier was used instead.

7.3 Separation in the Middle Vessel Column Using Operation Mode B

As specified in Chapter 5 and Section 7.1, the use of Mode B of operation is preferred due to the time savings involved in operating the column such that both the rectifying

Table 7.2: Molar Amounts of Original Charge, Benzene Added, and Resultant Initial Still Pot Charge

Component	F_μ	F_ν	$F_{azeotrope}$
Original Charge of Acetone	10	50	33.4
Original Charge of Benzene	15	25	0.0
Original Charge of Chloroform	75	25	66.6
Amount of Benzene Added	285	75	266.4
Resulting Total Charge	385	175	366.4

Table 7.3: Compositions of Original Charge, and Initial Composition of Still Pot

Component	F_μ	F_ν	$F_{azeotrope}$
Original Charge Composition	(0.10,0.15,0.75)	(0.50,0.25,0.25)	(0.334,0.0,0.666)
Initial Still Pot Composition	(0.026,0.779,0.195)	(0.286,0.571,0.143)	(0.091,0.727,0.182)

and the stripping sections are simultaneously being utilized. The simulations were conducted for each of the 3 original charge compositions as illustrated in Figure 7-1; one point in region μ, given by F_μ, one point in region ν, given by F_ν, and lastly, a charge of the azeotrope AC, given by $F_{azeotrope}$ was separated in the column.

The original charges, the amount of benzene added to the charge, and the resultant total charge are summarized in Table 7.2. The original composition and resultant initial still pot compositions of each operation is summarized are Table 7.3.

7.3.1 Simulation For the Separation of $F_{azeotrope}$

In this section, the results of the simulation peformed for an initial charge with a composition corresponding to the azeotrope of AC. Total time required to separate the mixture was approximately $29,500$ units of time.

As expected, the purities of each of the cuts of acetone, benzene and chloroform were of purity $> 99.9\%$, as specified by the operating policy, and illustrated in Figures 7-2 and 7-3. Furthermore, Figure 7-2 shows the change in product composition

in the rectifying section, as the still pot composition crosses over from region ν to region μ. Due to the specified limiting conditions, the cut is extremely sharp, and this sharp cut helps in maintaining the purity of the products. It should be noted that this transition need not be so sharp, as the chloroform product is not drawn until much later, when the amount of benzene remaining in the column equals the amount of chloroform remaining in the column.

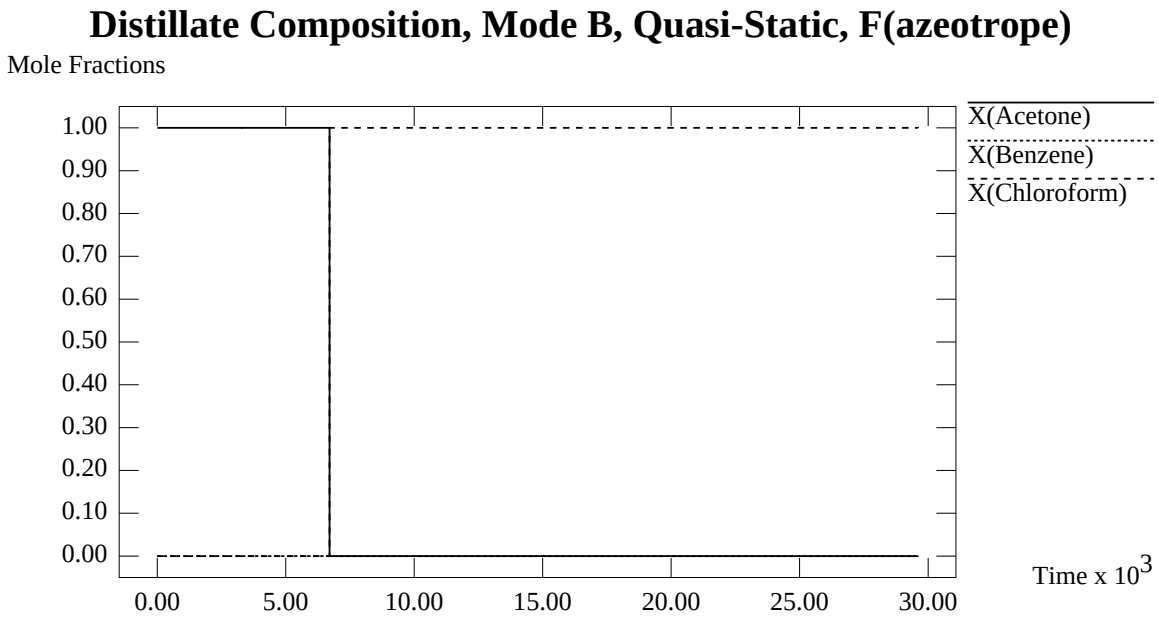

Figure 7-2: Distillate Composition For $F_{azeotrope}$

Next, the variation of the still pot composition during the operation is presented as a function of time (Figure 7-4) and within the composition simplex (Figure 7-5). As shown, in Figure 7-5, while operated as a rectifier, the initial still pot composition moves directly away from the acetone fixed point, encounters the separatrix near the B-C edge (in region ρ) and changes its operation to that of a stripper. The still pot composition than moves directly away from the fixed point of pure benzene, until the $x^M_{benzene} = x^M_{chloroform}$, at which point the "quasi-static" operation of the column begins. However, due to the presence of acetone in the column, the operation is not strictly quasi-static, as the acetone that is not drawn out of the column causes the still pot composition to move towards the acetone vertex. Finally, the still pot composition encounters the separatrix, and operation is ceased.

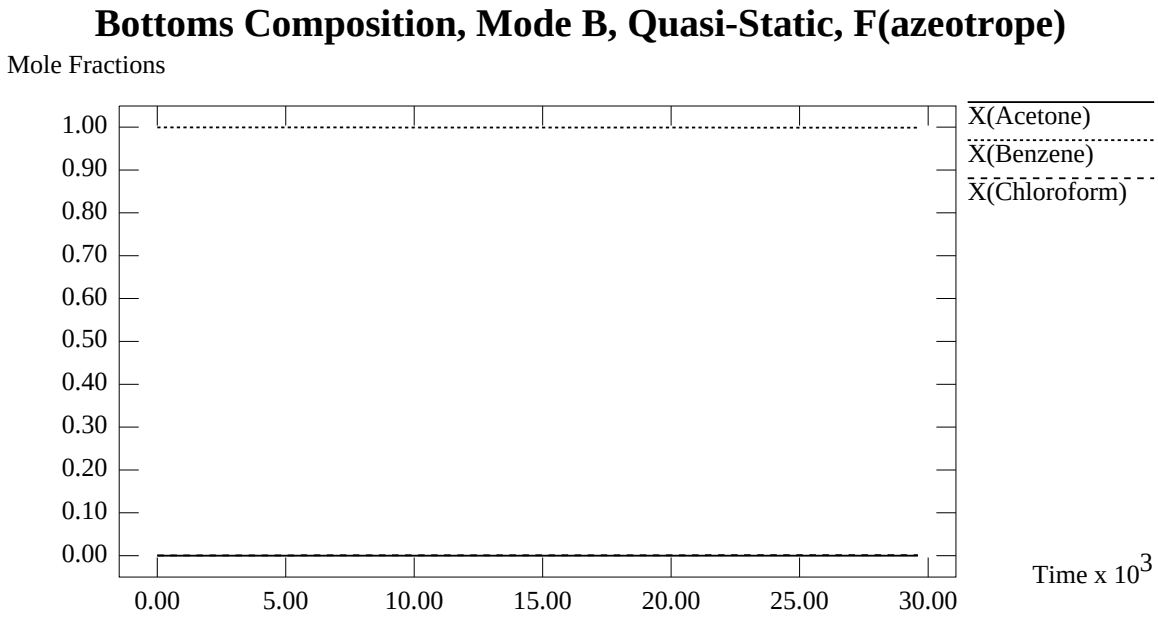

Figure 7-3: Bottoms Composition For $F_{azeotrope}$

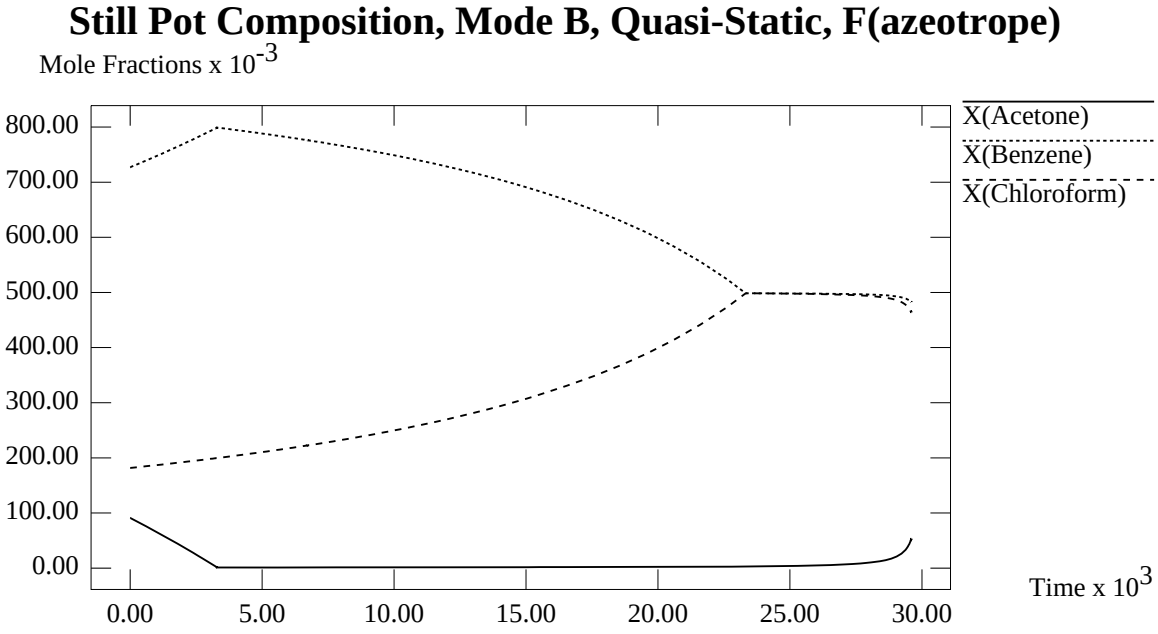

Figure 7-4: Still Pot Composition For $F_{azeotrope}$ as a Function of Time

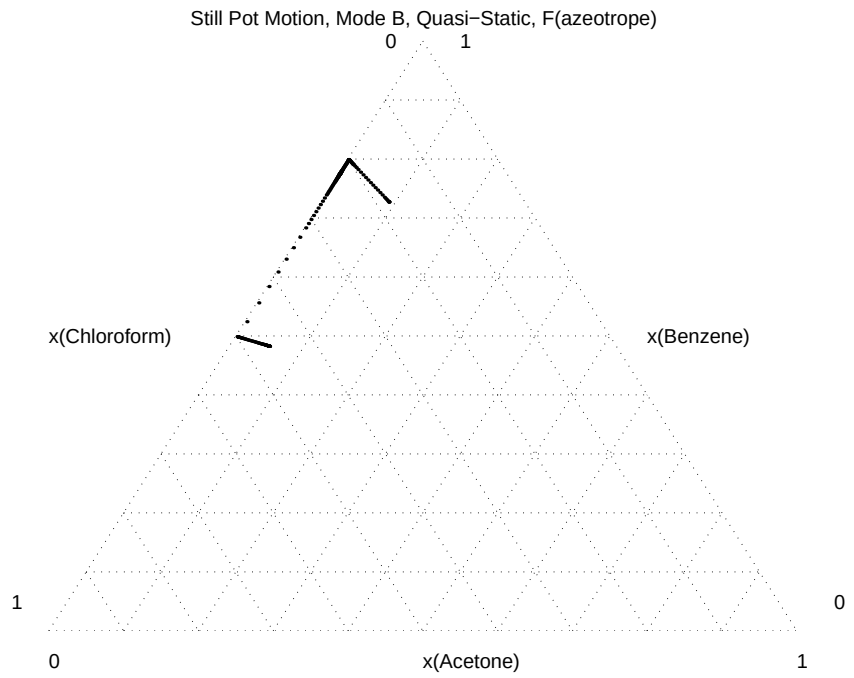

Figure 7-5: Still Pot Composition For $F_{azeotrope}$ in Composition Space

The corresponding holdup of the components in the still pot, and the accumulation of each of the distillate and bottoms cuts are illustrated in Figures 7-6 through 7-8. As shown in Figure 7-7, the two cuts of acetone, and chloroform drawn from the rectifying section of the column are sufficiently apart in time, that resolution of the cuts should not pose a problem. Even if the column was not limiting, and the cuts not as sharp as those simulated by our limiting column, complete separation should be possible. As expected, the bottoms cut is composed entirely of pure benzene as shown in Figure 7-8. At the end of the operation, only a trickle of a mixture of acetone, benzene and chloroform remain in the column as shown in Figure 7-6.

A summary of the inventory of each of the components at the end of the operation is presented in Table 7.4. As seen in Table 7.4, each of the cuts of acetone (distillate 1st cut), benzene (bottoms cut) and chloroform (distillate 2nd cut) had 100% purities. Only 1.20% of the acetone, and 5.08% of the chloroform were unrecoverable. 1.32% of the benzene added as entrainer was also discarded. This is negligible compared to the recovery of 98.8% of the acetone, and 94.2% of the chloroform that was charged as the azeotrope. 98.68% of the benzene introduced as entrainer was also recovered at

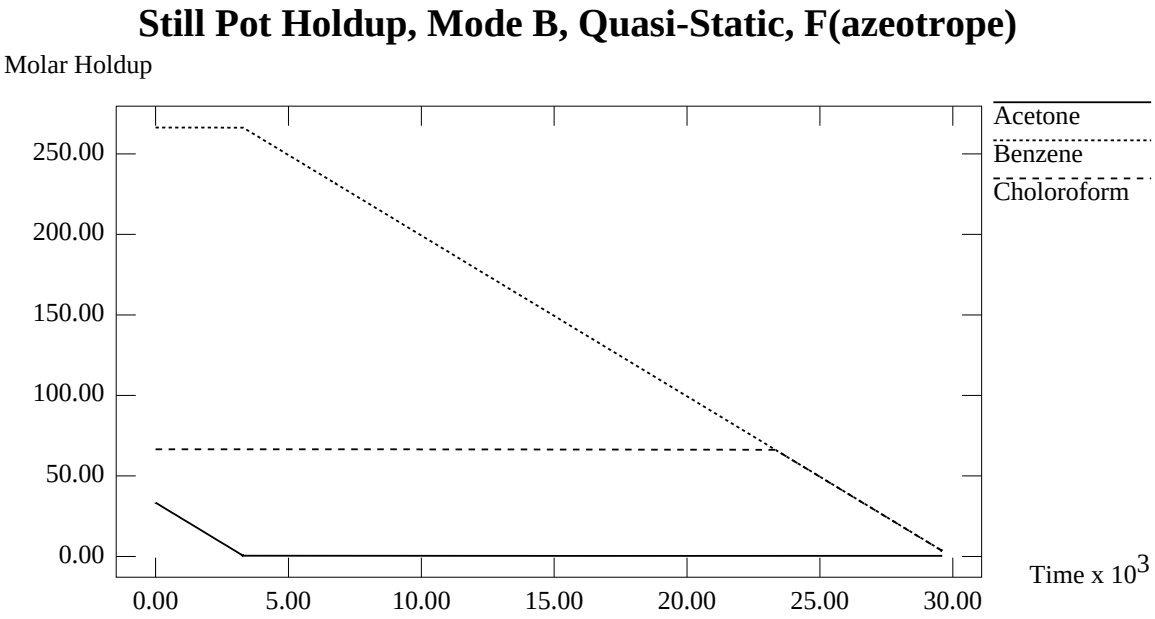

Figure 7-6: Still Pot Molar Holdup For $F_{azeotrope}$ as a Function of Time

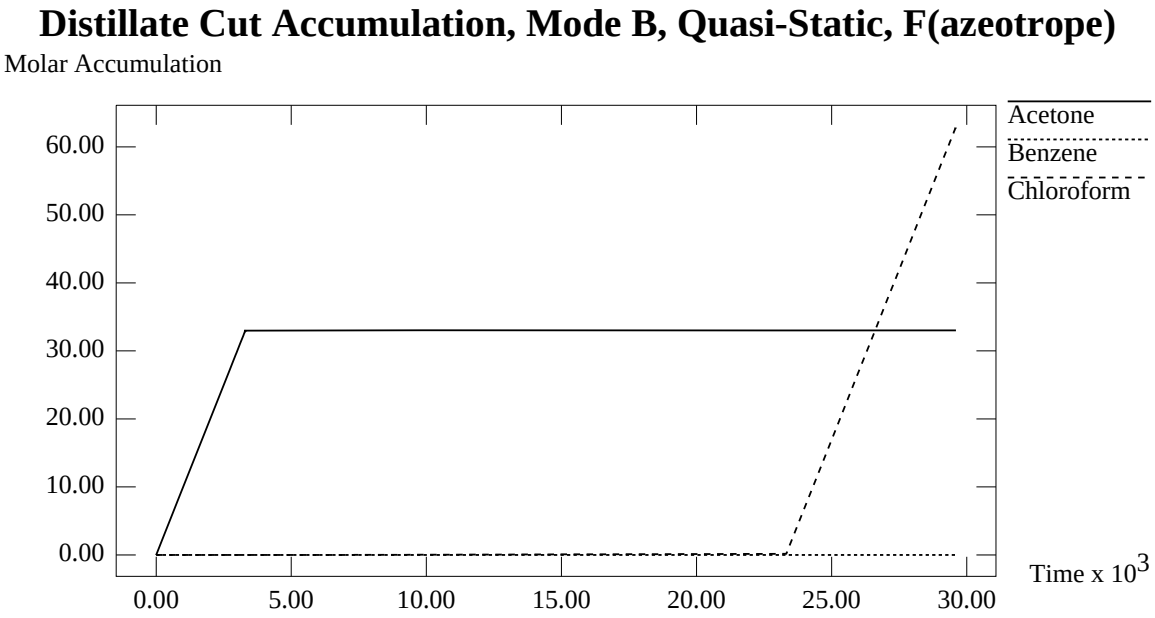

Figure 7-7: Distillate Molar Holdup For $F_{azeotrope}$ as a Function of Time

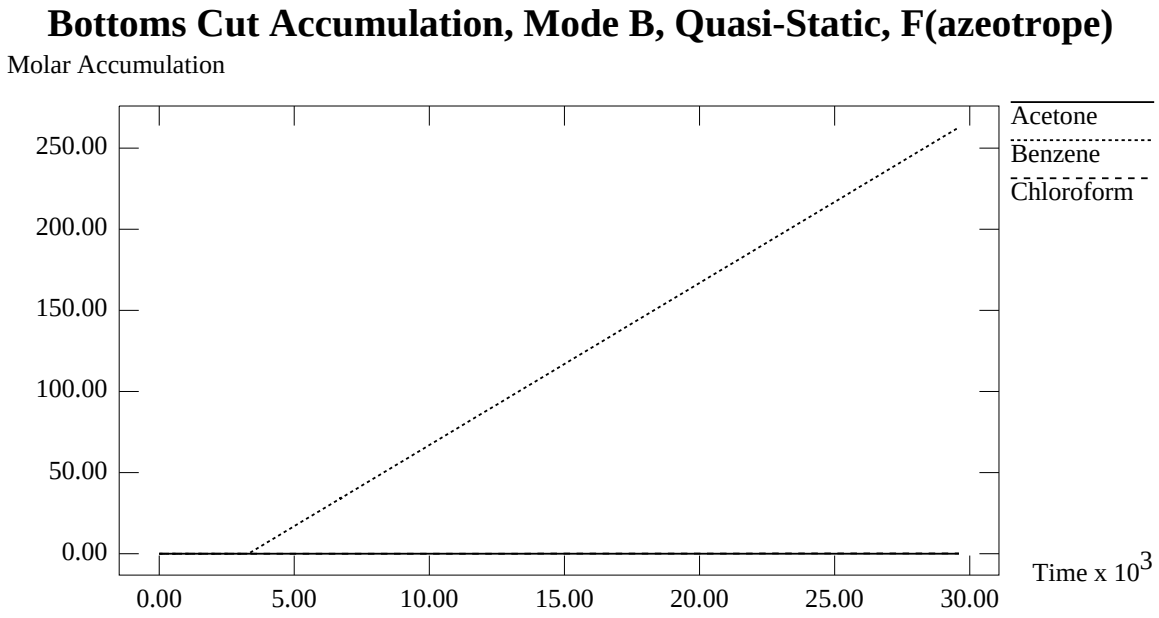

Figure 7-8: Bottoms Molar Holdup For $F_{azeotrope}$ as a Function of Time

100% purity, which means that it can be recycled for use in other parts of the plant, or resold at market value.

Finally, a plot of the middle vessel parameter as a function of time is also provided in Figure 7-9.

7.3.2 Simulation For the Separation of F_μ

In this section, the results of the simulation performed for an original charge lying within the composition space of the region μ, are presented. Total time required for the separation of this mixture was $31,000$ units of time.

As expected, the purities of each of the cuts of acetone, benzene and chloroform were again of purity $> 99.9\%$, as illustrated by Figures 7-10 and 7-11. Figure 7-10 also shows the change in product composition in the rectifying section, as the still pot composition crosses over from region ν to region μ.

Graphs of the still pot composition as a function of time and its path in the composition simplex, of the molar accumulation and holdups in each of the cuts and the still pot, and of the variation of λ with time, are all similar in nature to that for $F_{azeotrope}$, and as such are detailed in Appendix E. Of interest however, is the quality

Table 7.4: Final Inventory (Moles) of Components For $F_{azeotrope}$ using Mode B Operation

Component	Acetone	Benzene	Chloroform
Initial Still Pot	33.4	266.4	66.6
Final Still Pot	0.40	3.52	3.38
Percentage of Initial(%)	(1.20)	(1.32)	(5.08)
Distillate 1st Cut	33.0	0.0	0.0
Percentage of Initial(%)	(98.8)	(0.0)	(0.0)
Distillate 2nd Cut	0.0	0.0	63.22
Percentage of Initial(%)	(0.0)	(0.0)	(94.92)
Bottoms Cut	0.0	262.88	0.0
Percentage of Initial(%)	(0.0)	(98.68)	(0.0)

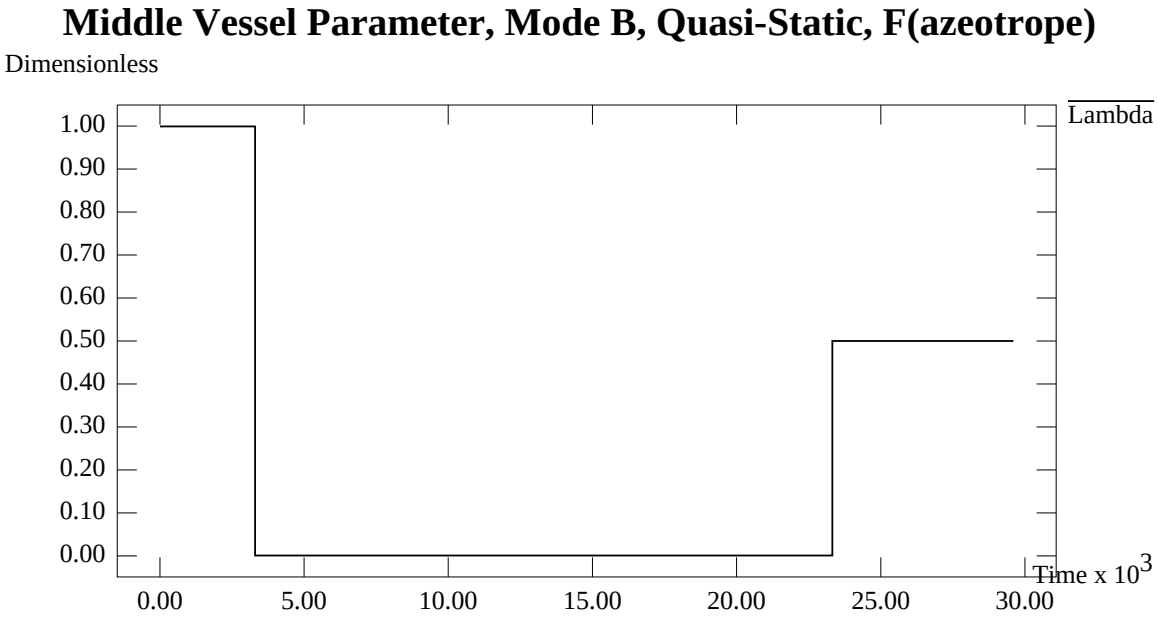

Figure 7-9: Middle Vessel Parameter, λ, For $F_{azeotrope}$ as a Function of Time

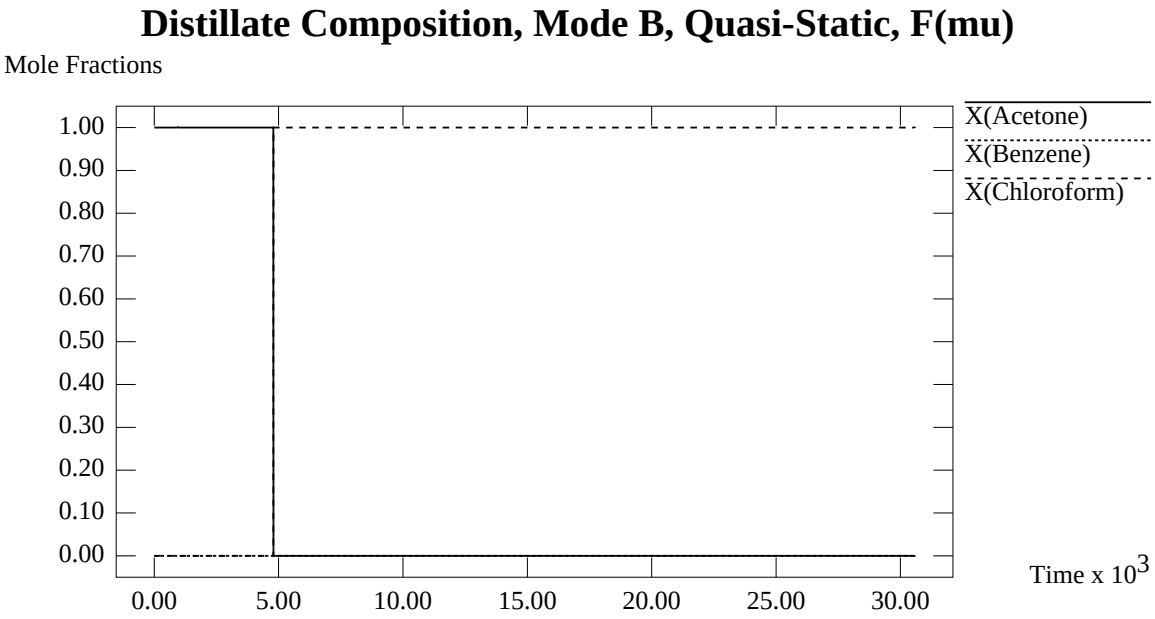

Figure 7-10: Distillate Composition For F_μ

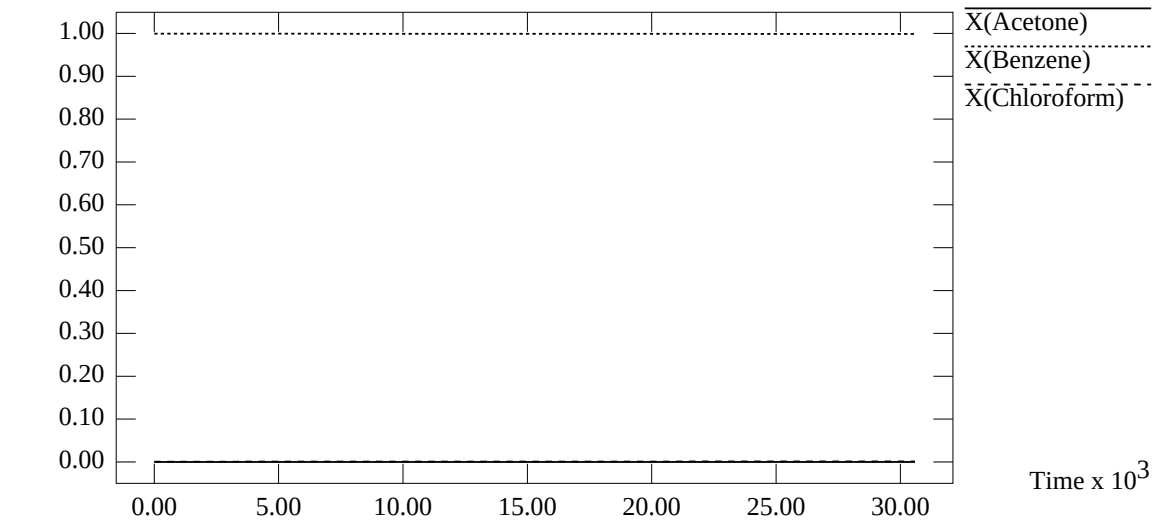

Figure 7-11: Bottoms Composition For F_μ

Table 7.5: Final Inventory (Moles) of Components For F_μ using Mode B Operation

Component	Acetone	Benzene	Chloroform
Initial Still Pot	10	300	75
Final Still Pot	(0.44)	(3.96)	(3.81)
Percentage of Initial(%)	(4.4)	(1.32)	(5.08)
Distillate 1st Cut	9.56	0.0	0.0
Percentage of Initial(%)	(95.6)	(0.0)	(0.0)
Distillate 2nd Cut	0.0	0.0	71.19
Percentage of Initial(%)	(0.0)	(0.0)	(94.92)
Bottoms Cut	0.0	296.04	0.0
Percentage of Initial(%)	(0.0)	(98.68)	(0.0)

of the separation with respect to the amount of acetone, benzene and chloroform recovered with respect to the initial amount of acetone, benzene and chloroform added. These information are summarized in Table 7.5.

As seen in Table 7.5, each of the cuts of acetone (distillate 1st cut), benzene (bottoms cut) and chloroform (distillate 2nd cut) are again of 100% purities. Only 4.4% of the acetone, and 5.08% of the chloroform were not recoverable. 1.32% of the benzene added as entrainer was also discarded. This is negligible compared to the recovery of 95.6% of the acetone, and 94.2% of the chloroform that was charged as the azeotrope. 98.68% of the benzene introduced as entrainer was also recovered at 100% purity, which means that it can be recycled for use in other parts of the plant, or resold at market value. The percentage of benzene and chloroform recovered are the same as that of $F_{azeotrope}$, because the operating policies separating benzene and chloroform (after most of the acetone was removed) were exactly the same. The percentage of acetone not recovered is larger in this case due to the larger initial charge of benzene and chloroform that was present in the still pot, which results in a larger amount of acetone retained in the still pot as the separatrix is encountered.

7.3.3 Simulation For the Separation of F_ν

In this section, the results of the simulation performed for an original charge lying within the composition space of the region ν, are presented. Total time required for

the separation of this mixture was $14,500$ units of time.

As expected, the purities of each of the cuts of acetone, benzene and chloroform were again of purity $> 99.9\%$, as illustrated by Figures 7-12 and 7-13. Figure 7-12 also shows the change in product composition in the rectifying section, as the still pot composition crosses over from region ν to region μ.

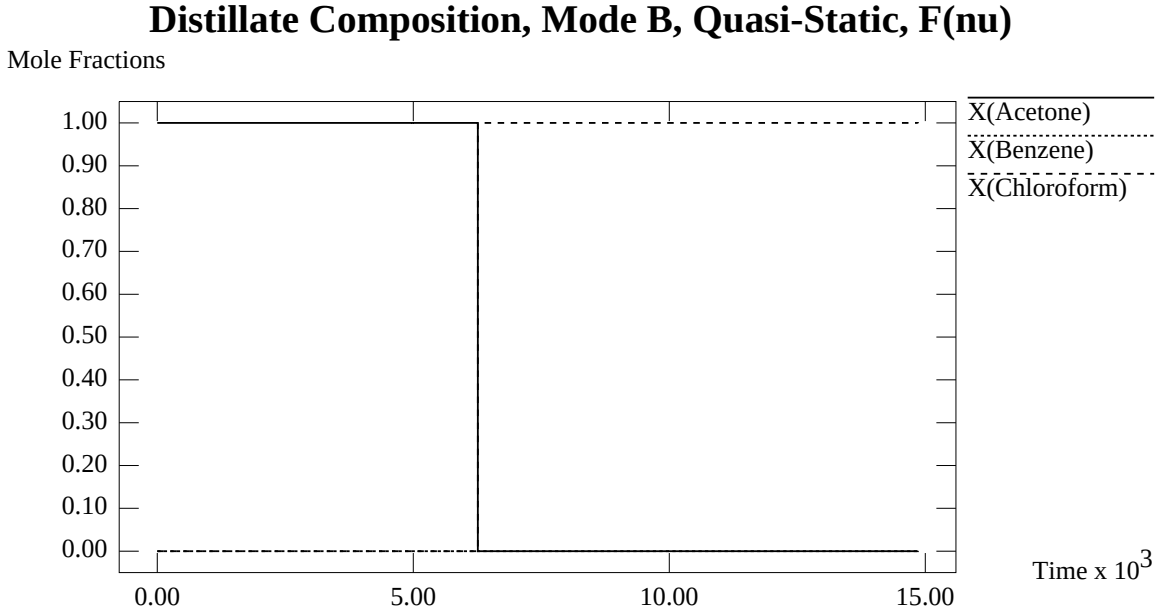

Figure 7-12: Distillate Composition For F_ν

Graphs of the still pot composition as a function of time and its path in the composition simplex, of the molar accumulation and holdups in each of the cuts and the still pot, and of the variation of λ with time, are again all similar in nature to that for $F_{azeotrope}$, and as such are detailed in Appendix E. Of interest however, is the quality of the separation with respect to the amount of acetone, benzene and chloroform recovered with respect to the initial amount of acetone, benzene and chloroform added. These data are summarized in Table 7.6.

As seen in Table 7.6, each of the cuts of acetone (distillate 1st cut), benzene (bottoms cut) and chloroform (distillate 2nd cut) are again of 100% purities. Only 0.3% of the acetone, and 5.08% of the chloroform were not recoverable. 1.32% of the benzene added as entrainer was also discarded. This is again negligible compared to the recovery of 95.6% of the acetone, and 94.2% of the chloroform that was charged

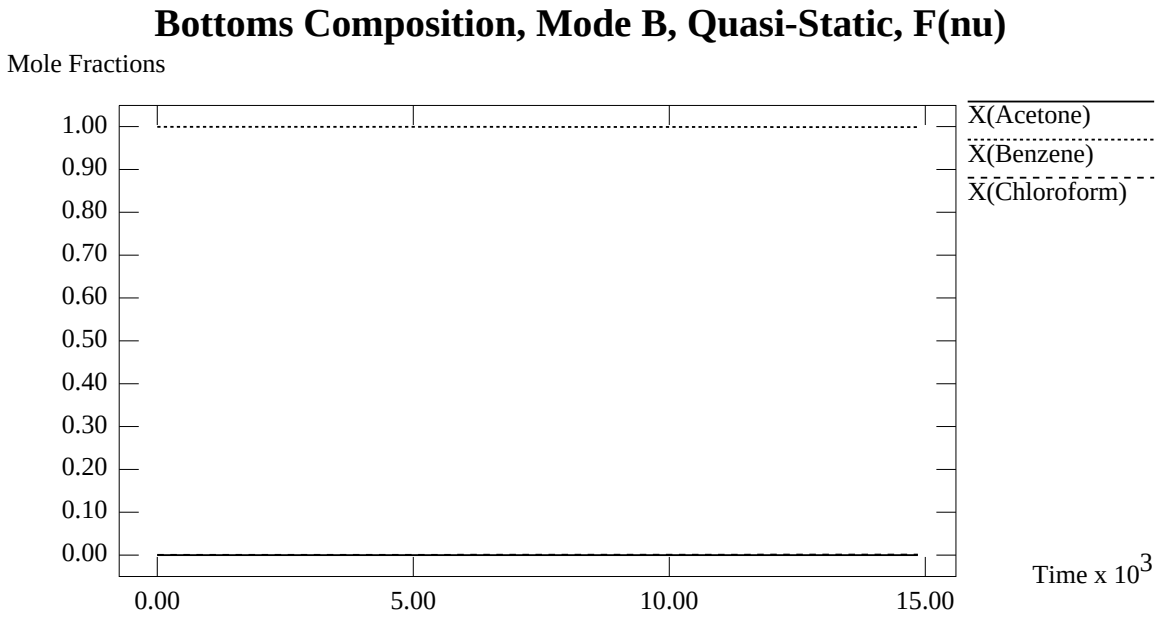

Figure 7-13: Bottoms Composition For F_ν

Table 7.6: Final Inventory (Moles) of Components For F_ν using Mode B Operation

Component	Acetone	Benzene	Chloroform
Initial Still Pot	50	100	25
Final Still Pot	0.15	1.32	1.27
Percentage of Initial(%)	(0.3)	(1.32)	(5.08)
Distillate 1st Cut	49.85	0.0	0.0
Percentage of Initial(%)	(99.7)	(0.0)	(0.0)
Distillate 2nd Cut	0.0	0.0	23.73
Percentage of Initial(%)	(0.0)	(0.0)	(94.92)
Bottoms Cut	0.0	98.68	0.0
Percentage of Initial(%)	(0.0)	(98.68)	(0.0)

as the azeotrope. 98.68% of the benzene introduced as entrainer was also recovered at 100% purity, which means that it can be recycled for use in other parts of the plant, or resold at market value. The percentage of benzene and chloroform recovered are again the same as that of $F_{azeotrope}$, for reasons as explained in the earlier subsection. The percentage of acetone not recovered is smaller in this case due to the smaller initial charge of benzene and chloroform that was present in the still pot, which allows a lower acetone content in the still pot before the separatrix is encountered.

7.4 A Comparison of Mode A of Operation vs Mode B of Operation

To highlight the differences between mode A of operation vs mode B of operation for an original mixture within the region ν, F_ν was also operated under mode A of operation. The results of that simulation are presented in this section, and compared to the results obtained in subsection 7.3.3.

The operating procedure for mode A to obtain product cuts with purity greater than 99.9%, is given as:

1. The middle vessel column is

   Operated at $\lambda = 1$

   (i.e., as a rectifier), until the following conditions are met:

   $x^D_{acetone} \leq 0.999$

   which corresponds to the event of the still pot composition reaching the separatrix, resulting in a degradation of product purity (from 100% purity), as the alpha limit set switches from that of pure acetone, to the azeotrope of AC.

2. The middle vessel column is then:

   Operated at $\lambda = 0$

(i.e., as a stripper), until the following conditions are met:

$$Mx^{M}_{benzene} \leq 0.01$$

which corresponds to the point where all the benzene has effectively been removed from the column, and the still pot composition is essentially a point on the A-AC edge.

3. At this point, a distillate product flow rate is reintroduced into the rectifying column, such that the operating λ in the column will be given by:

$$\text{Operated at } \lambda = \frac{x_A^{azeotrope} - x_A^M}{x_A^{azeotrope}}$$

which results in a quasi-static operation, drawing the azeotrope and chloroform in the appropriate proportions such that the still pot composition remains stationary, until the following conditions are met:

$$\sum_{B,D} (\text{Total Accumulation}) \geq 99$$

which corresponds to the still pot running dry, and operation is ceased at this point. The resulting purity of all 3 components recovered will all be in the region of 100.0%.

Following the above procedure, the results of the simulation performed for F_ν are presented. Total time required for the separation of this mixture was $10,000$ units of time. This was in comparison to the $14,500$ units of time required if mode B was used, a substantial time savings by mode A of up to $\frac{1}{3}$ of the time required by mode B.

As expected, the purities of each of the cuts of acetone, benzene and chloroform were again of purity $> 99.9\%$, as illustrated by Figures 7-14 and 7-15. Figure 7-14 shows the change in product composition in the rectifying section, as the still pot composition crosses over from region ν to region μ. Figure 7-15 shows the change over in the omega limit set from pure B to that of the azeotrope AC as the still pot composition encounters the A-AC edge.

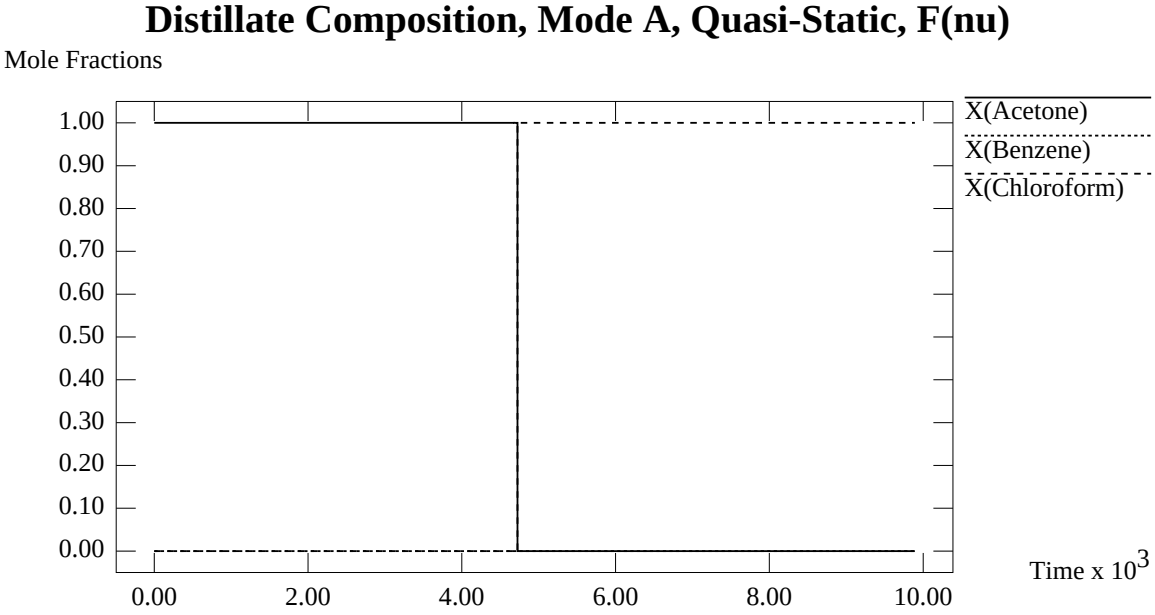

Figure 7-14: Distillate Composition For F_ν, Mode A

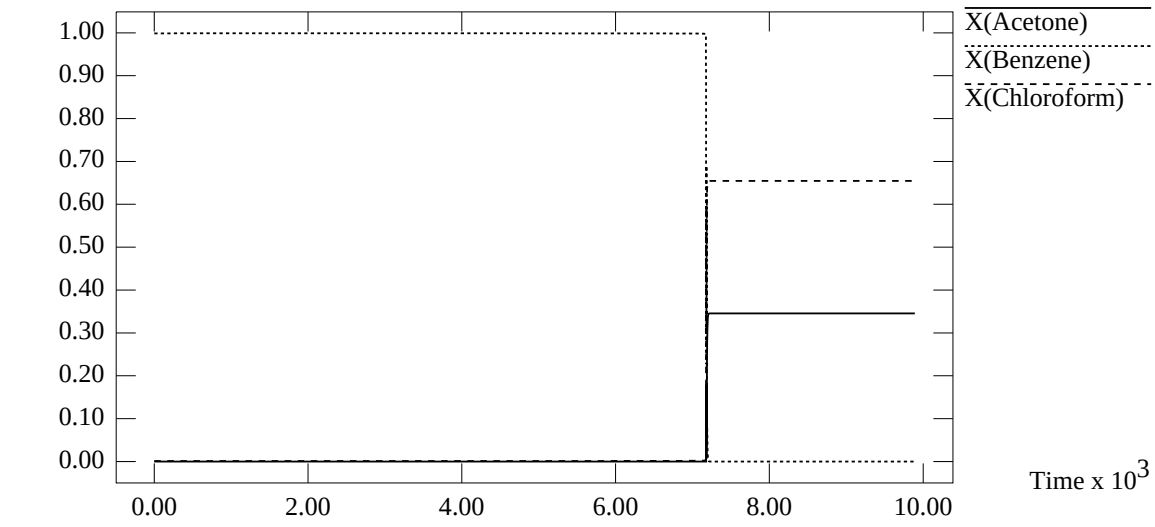

Figure 7-15: Bottoms Composition For F_ν, Mode A

The variation of the still pot composition during the operation is presented as a function of time (Figure 7-16) and within the composition simplex (Figure 7-17). As shown, in Figure 7-17, while operated as a rectifier, the initial still pot composition moves directly away from the acetone fixed point, encounters the separatrix near the B-C edge (in region ρ) and changes its operation to that of a stripper. The still pot composition than moves directly away from the fixed point of pure benzene, until the it encounters the A-AC edge, at which point the "quasi-static" operation of the column begins.

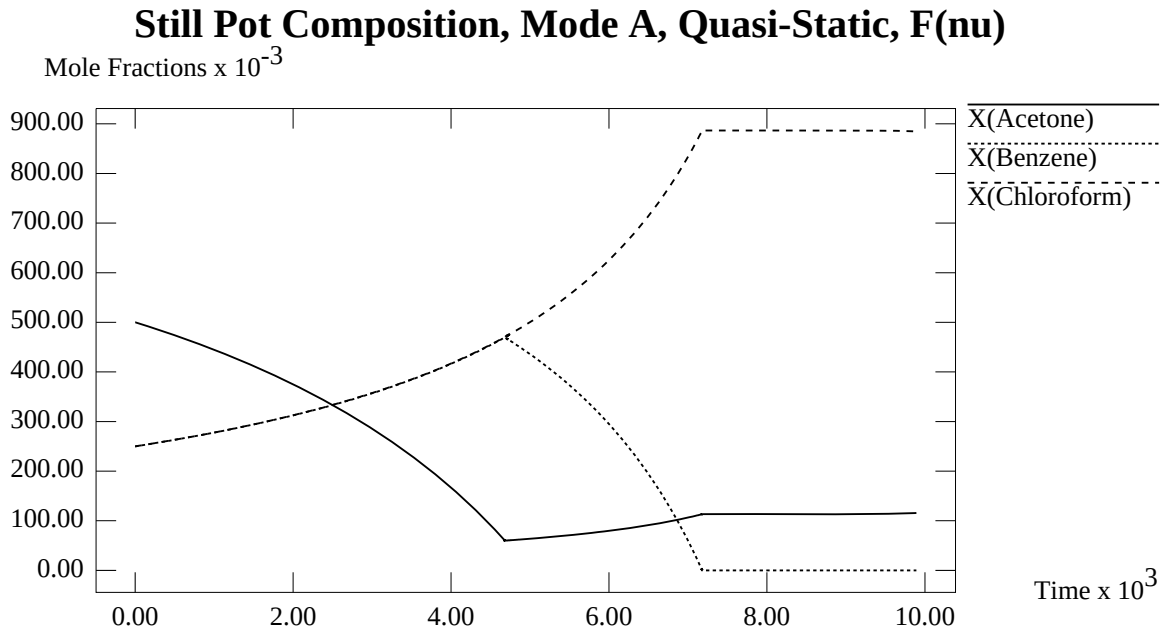

Figure 7-16: Still Pot Composition For $F_{azeotrope}$ as a Function of Time, Mode A

The corresponding holdup of the components in the still pot, and the accumulation of each of the distillate and bottoms cuts are illustrated in Figures 7-18 through 7-20. As shown in Figure 7-19, the two cuts of acetone, and chloroform drawn from the rectifying section of the column are sufficiently separated in time that resolution of the cuts should not pose a problem. As expected, the first bottoms cut is composed entirely of pure benzene as shown in Figure 7-20, while the second bottoms (azeotropic) cut, was sufficiently small and can be discarded without much lost or recycled to the next batch. At the end of the operation, only a trickle of a mixture of acetone, benzene and chloroform remain in the column as shown in Figure 7-18.

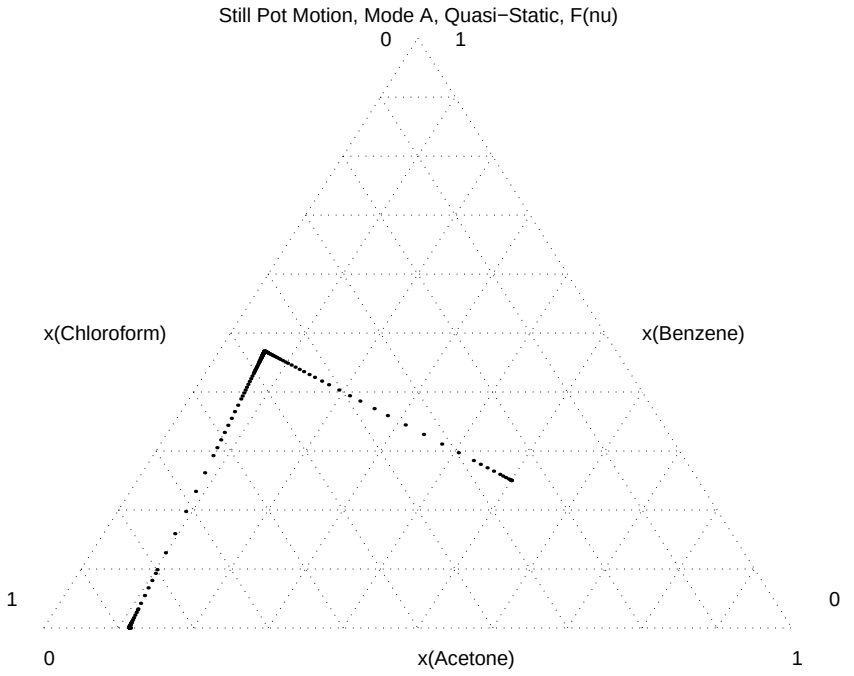

Figure 7-17: Still Pot Composition For F_ν in Composition Space, Mode A

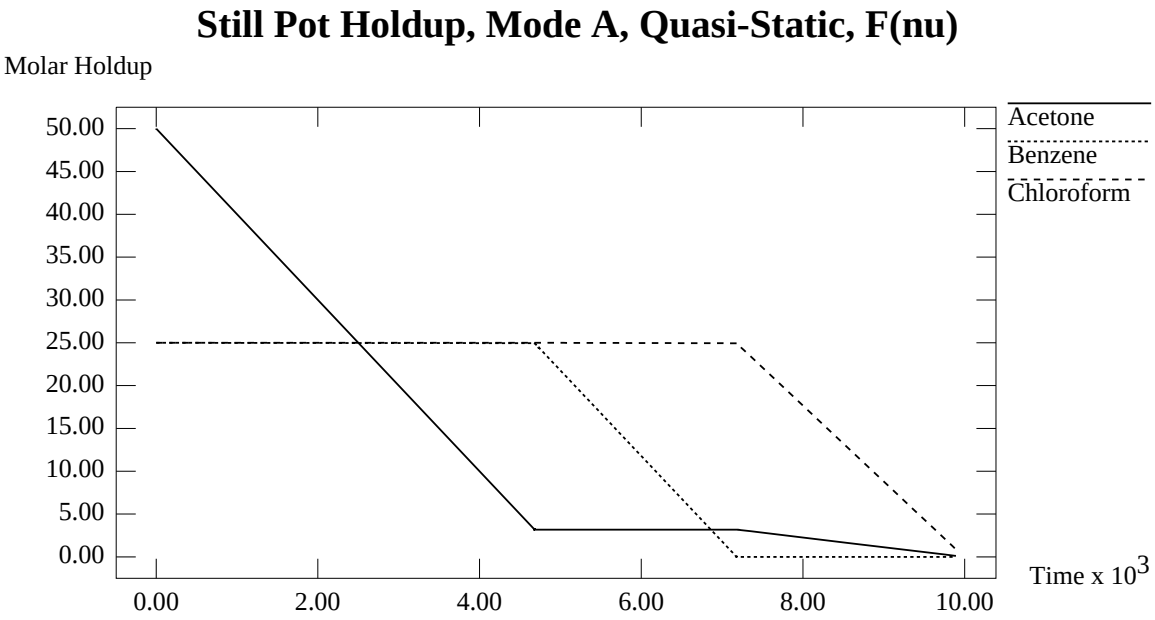

Figure 7-18: Still Pot Molar Holdup For F_ν as a Function of Time

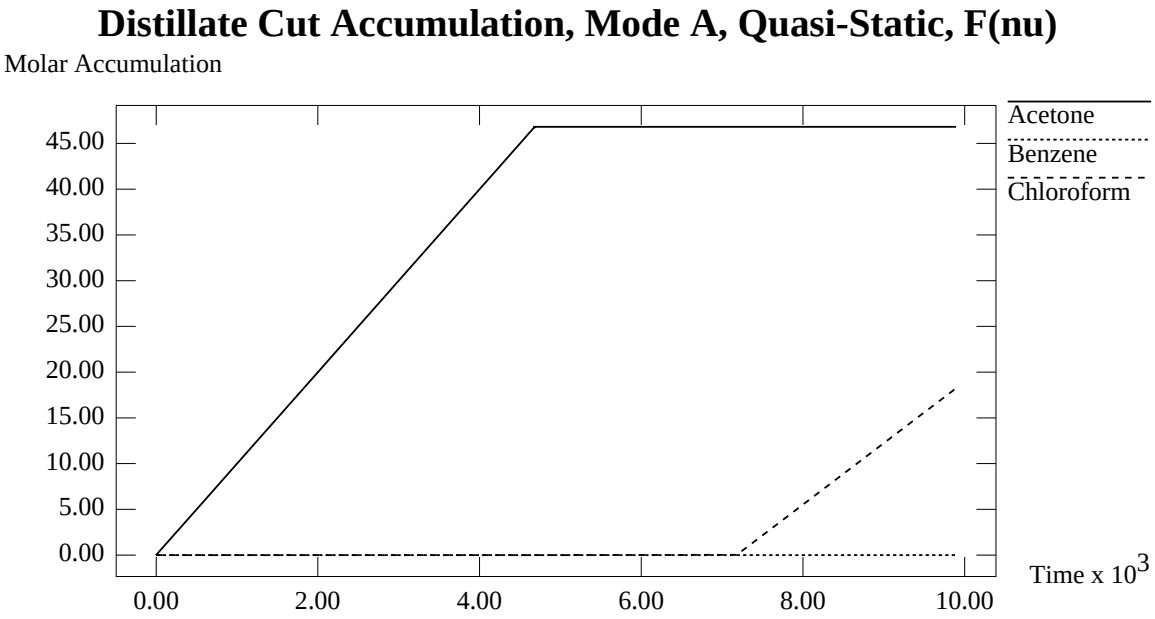

Figure 7-19: Distillate Molar Holdup For F_ν as a Function of Time

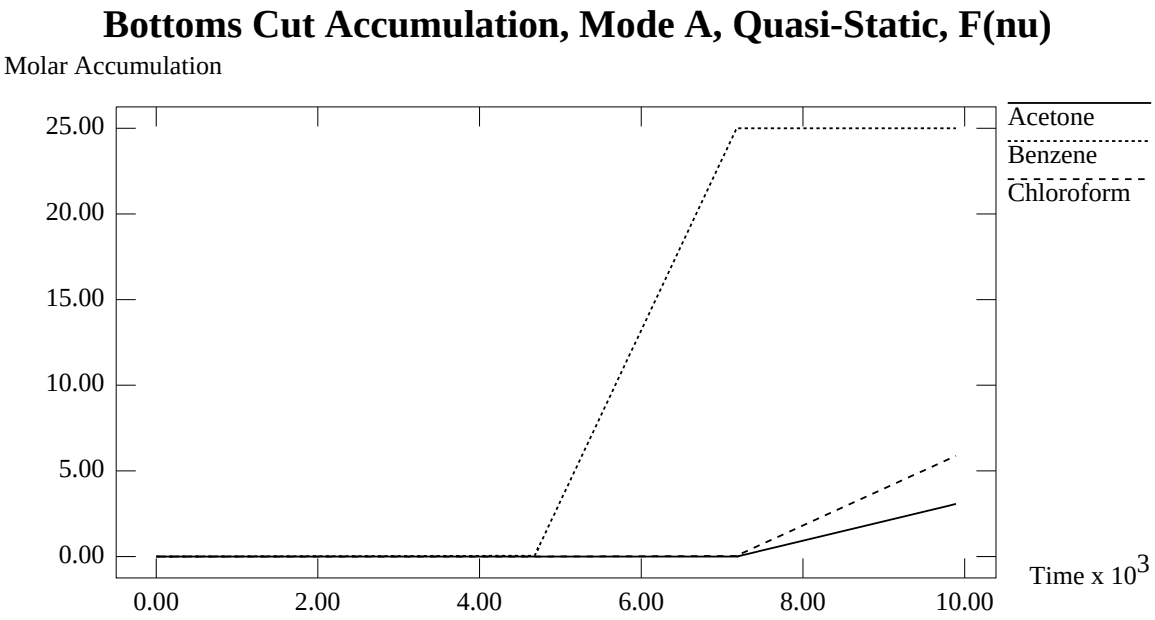

Figure 7-20: Bottoms Molar Holdup For F_ν as a Function of Time

Finally, a plot of the middle vessel parameter as a function of time is also provided in Figure 7-21, corresponding to the operation of the column as a rectifier ($\lambda = 1$) followed by a stripping operation ($\lambda = 0$) and finally another rectifying stage ($\lambda = 1$).

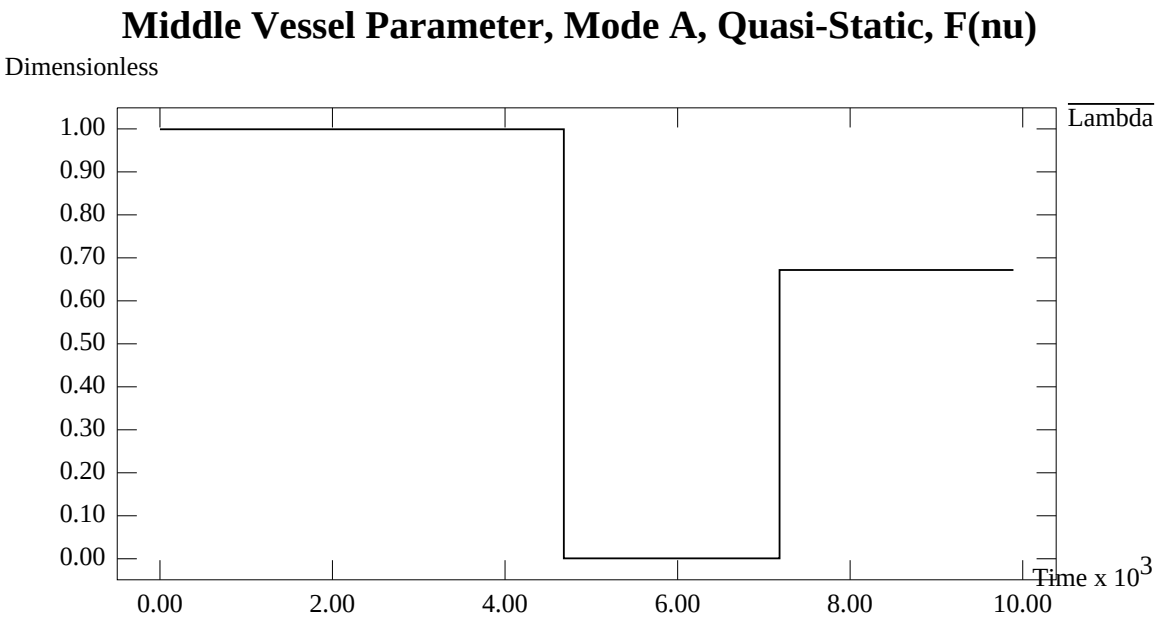

Figure 7-21: Middle Vessel Parameter, λ, For F_ν as a Function of Time

Also of interest is the quality and quantity of separation achieved with respect to the amount of acetone, benzene and chloroform recovered with respect to the initial amount of acetone, benzene and chloroform added. These data are summarized in Table 7.7.

As seen in Table 7.7, each of the cuts of acetone (distillate 1st cut), benzene (bottoms cut) and chloroform (distillate 2nd cut) are again of 100% purities. However up to as much as 7.26% of the acetone, and 27.04% of the chloroform were unrecoverable (lost in either the azeotropic cut, or as the residue in the still pot). None of the benzene added as entrainer was discarded, with 100% of the benzene obtained as a pure benzene cut, which can be recycled or resold. This is in relative large in comparison to the 0.3% of the acetone, and 5.08% of the chloroform lost in mode B. It should be noted however, that less of the benzene added (none) is lost when compared to the 1.32% of benzene lost in mode B.

Table 7.7: Final Inventory (Moles) of Components For F_ν using Mode A Operation

Component	Acetone	Benzene	Chloroform
Initial Still Pot	50	25	25
Final Still Pot	0.12	0.0	0.88
Percentage of Initial(%)	(0.24)	(0.0)	(3.54)
Distillate 1st Cut	46.81	0.0	0.0
Percentage of Initial(%)	(93.62)	(0.0)	(0.0)
Distillate 2nd Cut	0.0	0.0	18.24
Percentage of Initial(%)	(0.0)	(0.0)	(72.96)
Bottoms 1st Cut	0.0	25.00	0.0
Percentage of Initial(%)	(0.0)	(100.0)	(0.0)
Bottoms 2nd Cut	3.07	0.0	5.88
Percentage of Initial(%)	(7.14)	(0.0)	(23.52)

Thus, the use of a mode A operation of the middle vessel column results in a shorter separation time, but a larger portion of the original feed is discarded. Thus, a trade-off exists between a shorter separation time, versus a smaller portion of waste. Depending on the costs of operation, raw materials, and waste disposal, an appropriate trade-off can then be reached, in which perhaps less benzene is added (such that ratio of benzene to chloroform in the initial still pot composition is less than $4:1$), but a larger cut of the azeotrope is recycled, resulting in a moderate operating time.

7.5 Comparison of a Quasi-Static Operation for $F_{azeotrope}$ Versus a Non-Quasi-Static Operation

Lastly, this section explores the differences between a mode B operation with a quasi-static operation phase, as compared to one which does not have a quasi-static operation phase. The operating schedule for an operation which does not have a quasi-static phase was enumerated in Section 7.2. The results of the simulation are sumarized in this section, and compared to the results obtained for the quasi-static operation of $F_{azeotrope}$ in subsection 7.3.1.

Total time required to separate the mixture was approximately $36,500$ units of

time, about 7,000 units of time more with quasi-static operation, or up to 25% more time is required for the non-quasi-static operation of the column.

The purities of each of the cuts of acetone, benzene and chloroform were of purity $> 99.9\%$, as specified by the operating policy, and illustrated in Figures 7-22 and 7-23. It should be noted that the azeotropic cut appearing in the bottoms product (Figure 7-23) was not withdrawn from the column because the product flow rate at the bottom of the column was set to zero at that point in time (operated as a pure rectifier).

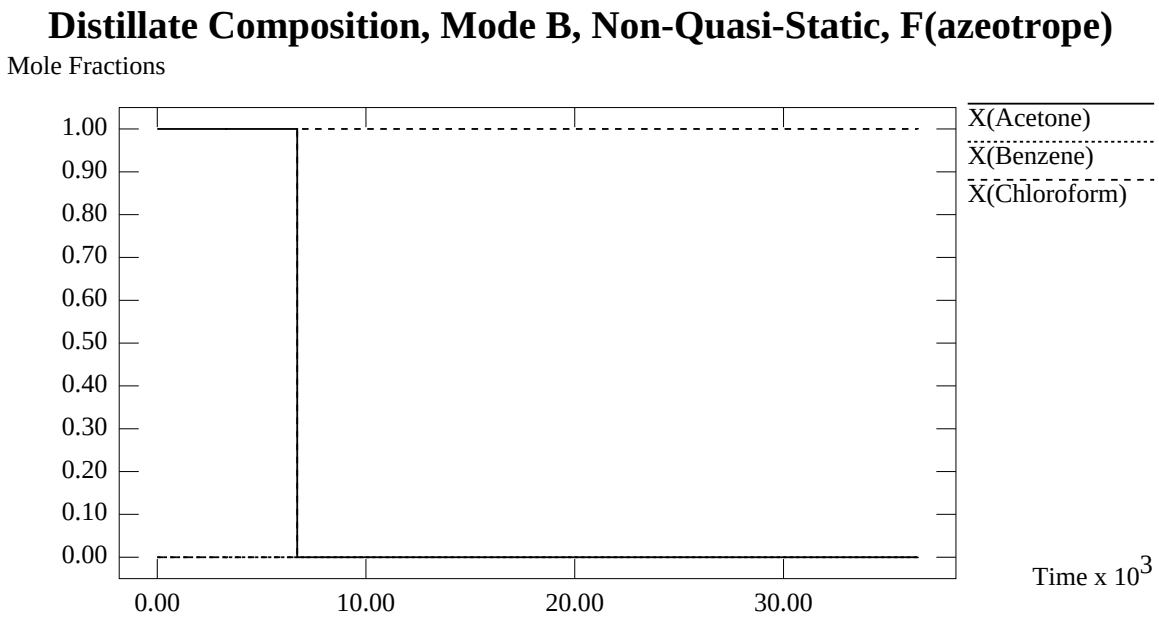

Figure 7-22: Distillate Composition For $F_{azeotrope}$, Non-Quasi-Static

Graphs of the still pot composition during the operation as a function of time and as its path within the composition simplex, are also illustrated in Figures 7-24 and 7-25.

Graphs of the molar accumulations in the cuts and the still pot, and of the operating λ are appended in Appendix E. They are extremely similar to that of the graphs obtained for $F_{azeotrope}$ operated under mode B of operation. Of greater interest are the benefits obtained from operating the column under non-quasi-static operation, which can be traded off against the 25% increase in operating time. This benefits come with a slight increase in the amount of pure products recovered from the separation. A

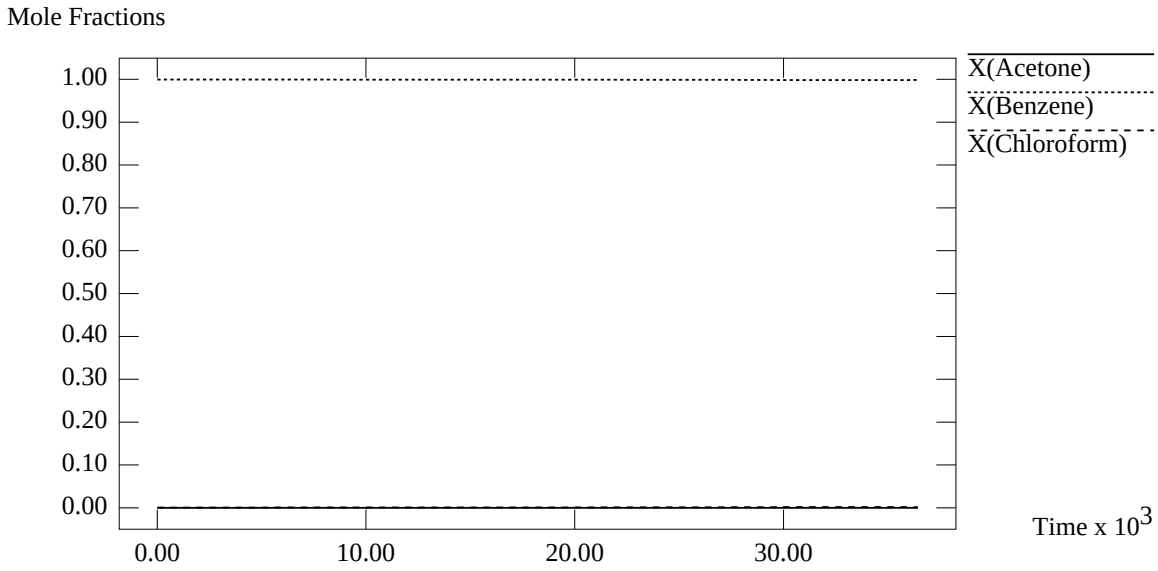

Figure 7-23: Bottoms Composition For $F_{azeotrope}$, Non-Quasi-Static

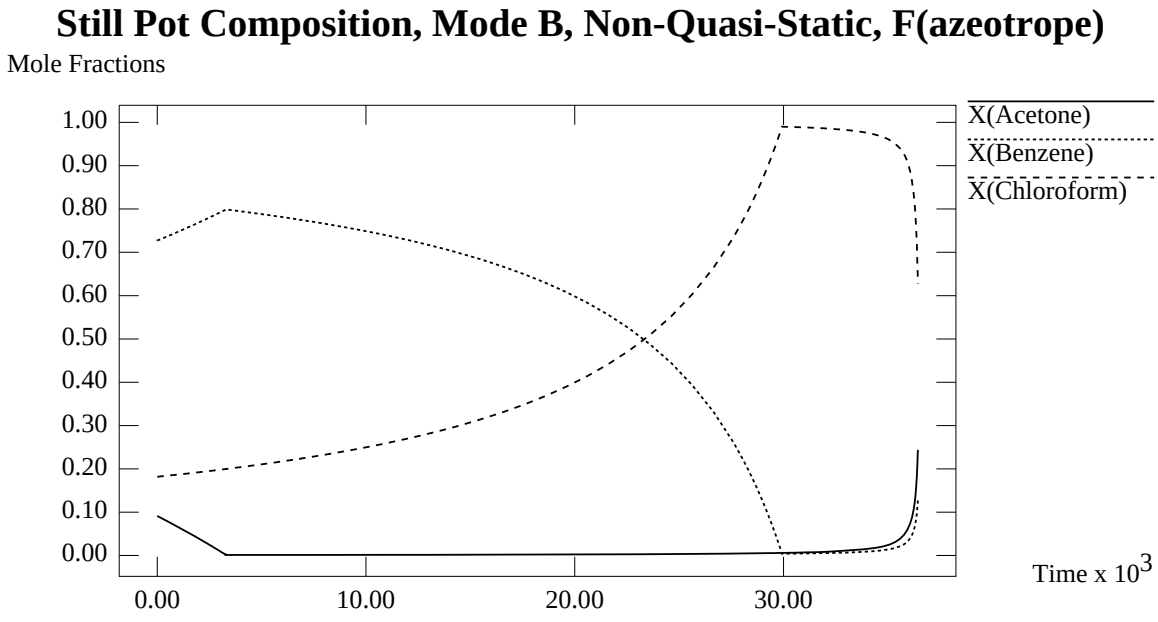

Figure 7-24: Still Pot Composition For $F_{azeotrope}$, Non-Quasi-Static

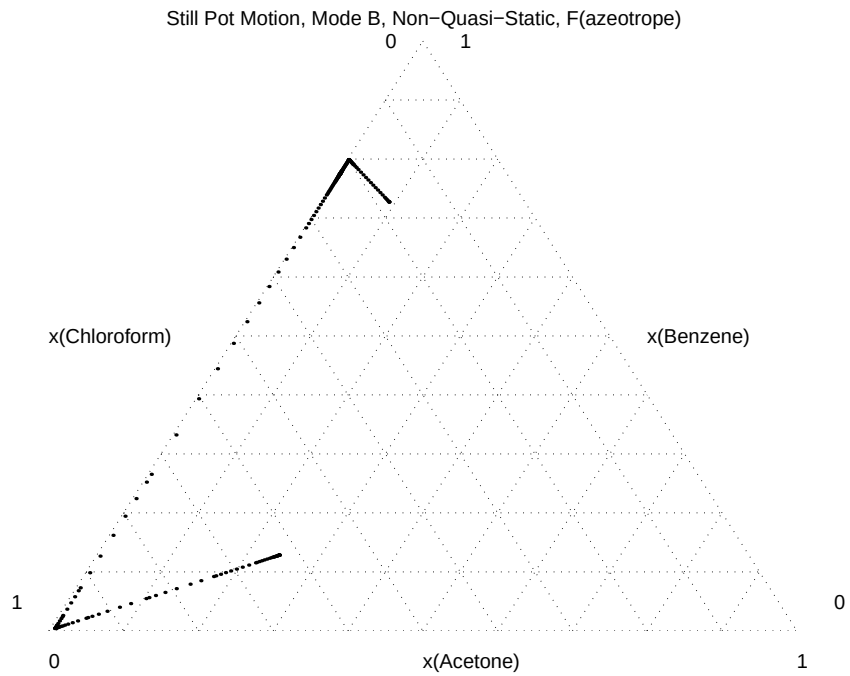

Figure 7-25: Still Pot Composition Motion For $F_{azeotrope}$, Non-Quasi-Static, in Composition Space

summary of the inventory at the end of the operation for each of the components is thus useful, and is presented in Table 7.8.

As seen in Table 7.8, each of the cuts of acetone (distillate 1st cut), benzene (bottoms cut) and chloroform (distillate 2nd cut) had 100% purities. A comparison of the amounts of acetone, benzene and chloroform lost in the two operation schemes (quasi-static, and non-quasi-static) are presented in Table 7.9.

As can be seen from the table the improvements in the amount of pure products obtained is in the order of magnitude of a few percent, as compared to the 25% increase in the operating time required. Unless the raw materials cost dominates the cost of the operation absolutely, there would seem to be no incentive to operate the column in a non-quasi-static mode, even if it improves the separation achievable slightly.

Table 7.8: Final Inventory (Moles) of Components For $F_{azeotrope}$ using Mode B Operation, Non-Quasi-Static

Component	Acetone	Benzene	Chloroform
Initial Still Pot	33.4	266.4	66.6
Final Still Pot	0.39	0.21	1.26
Percentage of Initial(%)	(1.17)	(0.08)	(1.89)
Distillate 1st Cut	33.02	0.0	0.0
Percentage of Initial(%)	(98.83)	(0.0)	(0.0)
Distillate 2nd Cut	0.0	0.0	65.34
Percentage of Initial(%)	(0.0)	(0.0)	(98.11)
Bottoms Cut	0.0	266.19	0.0
Percentage of Initial(%)	(0.0)	(99.92)	(0.0)

Table 7.9: Percentage of Acetone, Benzene and Chloroform Lost, Quasi-Static Operation versus Non-Quasi-Static Operation

Component	Acetone	Benzene	Chloroform
Percentage Lost Quasi-Static (%)	1.20	1.32	5.08
Percentage Lost Non-Quasi-Static (%)	1.17	0.08	1.26
Percentage Improvement (%)	0.03	1.24	3.82

Chapter 8

Conclusions

A mathematical model of a middle vessel batch distillation column was developed based on the simplifying assumptions of constant molar overflow, and quasi-steady state (or negligible holdup) on the trays of the column. Theory regarding the behavior of the middle vessel column based on a limiting analysis of the model (as number of trays in the column, ND and $NB \to \infty$, and reflux and reboil ratios R_d and $R_b \to \infty$) was also developed. This theory on the limiting behavior of the column was then tested out by simulating the middle vessel column in the ABACUSS simulation environment using the mathematical model developed.

A novel way of splitting azeotropes, specifically illustrated with the mixture of acetone, benzene, and chloroform (inverse-020 system) mixture, was also formulated. This served to illustrate that an understanding of the underlying theory behind the behavior of the middle vessel column would allow us to formulate effectively separations in the middle vessel column which would otherwise not be possible in traditional (stripper or rectifier) batch columns. Simulations were also conducted to verify this operational procedure suggested. All these species were recovered as pure cuts with purity greater than 99%.

However, more work on this subject is encouraged, as there is the possibility that novel separations and more novel columns can be formulated in the spirit of Stichlmair *et al.* [38] so as to increase the possibilities of separation which are not possible with the current array of separation equipment. In the light of this spirit, a few suggestions

are made regarding areas of further interest.

8.1 A Study of Multi-Vessel Columns

Having illustrated the increased flexibility of a middle vessel batch distillation column over that of a traditional stripper or a rectifier, it should be noted that this flexibility was afforded by the second product stream which is drawn from the column, and the fact that this stream is sufficiently different in composition from the first product stream drawn. This afforded a 2-dimensional vector cone in which the still pot is allowed to move, compared to the single direction in which a still pot composition must move when it is operated in a rectifier or stripper (which only draws a single product).

It is thus conceivable that a column which allows us to draw more than two sufficiently different product streams would afford a greater degree of freedom in the motion of the still pot composition. 3 product streams drawn mean 3 dimensions of possible motion, while n product streams drawn from the column mean n dimensions of possible motion. This usefulness of additional streams drawn from a distillation column is not novel. The drawing of split streams from a continuous distillation column to increase the variety of separation possible in the continuous column is a well documented process. Split streams can also be drawn from a middle vessel column with a corresponding increase in separation possibilities, which then leads to the conceptualization of the multi-vessel column, in which there exists multiple vessels located at intervals along the column (as suggested by Skogestad [37]), with products drawn from each of these vessels.

While the additional possibilities of still pot motion does not seem too exciting in a 3-component system where motion is restricted to the composition simplex plane given by $x_1+x_2+x_3 = 1$, it does offer additional possibilities of separation for mixtures with a larger number of components. For example, an n component mixture would have its motion restricted in an $n-1$ dimension composition simplex, and an $n-1$ dimension vector cone would allow the still pot composition to reach points in the

composition simplex which it otherwise would not be able to in a stripper, rectifier or for that matter in a middle vessel column. This thought experiment than leads us to elucidate the usefulness of multivessel columns in the separation of multi-component mixtures. In particular, an n-component mixture should be operated in a column with $n-1$ holdup trays, with a product stream drawn from each of the trays, to afford a total of $n-1$ product streams, with each stream substantially different from each other (i.e., there is no linear dependency of any of the vectors of motion given by $\mathbf{x}^{Column} - \mathbf{x}_i^P$, where $Column$ denotes the overall weighted average composition in the entire column, P denotes product, i denotes the tray from which it is drawn, with $i = 1 \ldots n-1$). Formulating this more formally, in the spirit of the still pot composition steering equations developed in Chapters 3 and 4, we obtain the following equation for the motion of the still pot as a function of the warped time τ.

Firstly, we define τ as follows:

$$d\tau = (\frac{\sum_{i=1}^{n-1} P_i}{M})dt \tag{8.1}$$

where P_i denotes the product flow rate from the i-th tray of the column, and M denotes the total molar holdup in the entire column. We also define the $n-1$ relevant parameters for the multi-vessel column as:

$$\begin{aligned}
\vartheta_1 &= \tfrac{P_1}{\sum_{i=1}^{n-1} P_i} \\
\vartheta_2 &= \tfrac{P_2}{\sum_{i=1}^{n-1} P_i} \\
&\vdots \\
\vartheta_{n-2} &= \tfrac{P_{n-2}}{\sum_{i=1}^{n-1} P_i} \\
\vartheta_{n-1} &= \tfrac{P_{n-1}}{\sum_{i=1}^{n-1} P_i}
\end{aligned} \tag{8.2}$$

such that by definition,

$$\sum_{i=1}^{n-1} \vartheta_i = 1 \tag{8.3}$$

The respective overall and component mole balances for the middle vessel column total holdup (i.e., of all the trays) would be given by a mass balance envelop around

the whole column. For the overall mole balance we obtain:

$$\frac{dM}{dt} = -\sum_{i=1}^{n-1} P_i \tag{8.4}$$

and consequently for the component mole balance around the whole column, we obtain:

$$\frac{dM\mathbf{x}^M}{dt} = -\sum_{i=1}^{n-1} \{P_i \mathbf{x}_i^P\} \tag{8.5}$$

Substituting equations (8.1), (8.2) and (8.4) into equation (8.5), the following equation is derived for the motion of the overall composition for the total holdup in a multi-vessel column (given by composition $\mathbf{x}^M$, with total molar holdup in the column M):

$$\frac{d\mathbf{x}^M}{dt} = \sum_{i=1}^{n-1} \vartheta_i (\mathbf{x}^M - \mathbf{x}_i^P) \tag{8.6}$$

Thus, the direction vectors of the possible motion for the total column holdup composition are given by the vectors $((\mathbf{x}^M - \mathbf{x}_i^P) \; \forall \; i = 1 \ldots n-1)$. It is this set of vectors which must *not be linearly dependent* in order for us to obtain a $n-1$ dimension vector cone of motion within a multi-vessel column separating a n component mixture. A detailed derivation of the above equations is provided in Appendix F.

Further detailed analysis of the behavior of the multi-vessel column based on the system of equations developed for the multi-vessel column (equations (8.1) through (8.6)) should be pursued. An understanding of the behavior of a multi-vessel column would allow us to better characterize its usefulness in separating multi-component mixtures.

8.2 Separation Possibilities at Finite Reflux Ratios

Most of the analysis conducted in this thesis was based on the limiting conditions of infinite reflux/reboil ratios, and infinite number of trays (R_d, $R_b \to \infty$; ND, $NB \to \infty$). However, as shown by Wahnschafft *et al* [39], it is often beneficial to operate a

column at finite reflux ratios as compared to infinite reflux ratios. This view has also been supported by Stichlmair [38] whose concern was with the dilution of entrainers at high reflux ratios. Laroche *et al.* [21] in their study of the feasible entrainers, also stated that at finite reflux ratios, it is possible for column profiles to cross the separatrices of residue curves, which normally serve as the boundary of distillation column profiles at infinite reflux and infinite trays in a ternary system. It is this crossing of the separatrices by the discrete column profiles at finite reflux/reboil ratios which result in a wider variety of separations affordable by distillation columns.

It is thus suggested that by using the mathematical model developed for the middle vessel column, studies of the behavior of the middle vessel column at finite reflux/reboil ratios should be conducted, so as to further characterize the behavior of the middle vessel column at low reflux ratios. Based on our analysis of the column profiles in a middle vessel column at low reflux/reboil ratios in Section 4.1, it was elucidated that the column profile in a middle vessel column behaves just like that of any other distillation column profile, and that at finite reflux ratios, the column profile is more curved than that of the residue curves. This increased curvature will offer an even greater variety of separations possible for azeotropic mixtures.

8.3 Optimal Control of a Middle Vessel Column

As stated in Chapter 3, the choice of an operating schedule for λ for a given separation process is an optimal control problem which depends very much on the objective function of the separation process. This has been studied somewhat by Safrit *et al.* [33] in the context of the optimal operation policy for a middle vessel column in the presence of an entrainer flow. However, much more work can be done in this realm if the use of the middle vessel column actually offers a wider selection of separations feasible within a single column.

The operation of the middle vessel column with constant product compositions but varying still pot composition (Section 5.4) also poses an open loop optimal control problem, for which an open loop optimal control policy can be devised with an

understanding of the behavior of the middle vessel column.

8.4 Feasible Entrainers For Separations in a Middle Vessel Column

Finally, as mentioned in Chapter 5, an analysis of the feasible entrainers for the separation of a given mixture in the middle vessel batch distillation column was beyond the scope of this thesis. It would thus be interesting, with this new understanding of the behavior for a middle vessel batch distillation column, to develop tools that could aid in the identification of suitable entrainers for a given azeotrope, (i.e., from their thermodynamic properties).

This would be useful because a "perfect entrainer" as defined in Section 5.5 would not exist for all azeotropes. Even if they do exist, it might not be desirable to mix this entrainer-azeotrope pair due to possible unfavorable side reactions, or the entrainer might be too expensive to use at an industrial scale. As such, an understanding of the feasible entrainers which allow the separation of azeotropes in a middle vessel batch distillation column would be invaluable in synthesizing an operational process for the separation of azeotropes into their pure components.

Development of these tools could also prove helpful in generating insights that would allow us to formulate operating procedures that can crack higher dimensional azeotropes.

Appendix A

Derivation of Middle Vessel Column Model Equations

Provided in this Appendix is the detailed derivation of the Middle Vessel Column Model equation (equation (3.7) and (3.8)) from the basic definition of warped time (equation (3.5)), the component mass balance equation obtained for the middle vessel column (equation (3.4)), and the overall mass balance for the middle vessel column (equation (3.2)).

Starting with the equation for component mass balance,

$$\frac{dM\mathbf{x}^M}{dt} = -(D\mathbf{x}^D + B\mathbf{x}^B) \tag{A.1}$$

differentiate the LHS by parts to obtain,

$$\mathbf{x}^M \frac{dM}{dt} + M\frac{d\mathbf{x}^M}{dt} = -(D\mathbf{x}^D + B\mathbf{x}^B) \tag{A.2}$$

We also have the overall mass balance equation given as,

$$\frac{dM}{dt} = -(D + B) \tag{A.3}$$

Substituting equation (A.3) into equation (A.2), the following expression is obtained,

$$-\mathbf{x}^M(D+B)+M\frac{d\mathbf{x}^M}{dt}=-(D\mathbf{x}^D+B\mathbf{x}^B) \tag{A.4}$$

or

$$M\frac{d\mathbf{x}^M}{dt}=(D+B)\mathbf{x}^M-(D\mathbf{x}^D+B\mathbf{x}^B) \tag{A.5}$$

But, from the definition of warped time,

$$d\xi=(\frac{D+B}{M})dt \tag{A.6}$$

which can be rearranged to obtain,

$$1=(\frac{D+B}{M})\frac{dt}{d\xi} \tag{A.7}$$

Multiplying the LHS of equation (A.5) by equation (A.7) which equals unity, the RHS is unchanged, and we obtain,

$$M\frac{d\mathbf{x}^M}{dt}(\frac{D+B}{M})\frac{dt}{d\xi}=(D+B)\mathbf{x}^M-(D\mathbf{x}^D+B\mathbf{x}^B) \tag{A.8}$$

from which M and dt can be cancelled to give,

$$(D+B)\frac{d\mathbf{x}^M}{d\xi}=(D+B)\mathbf{x}^M-(D\mathbf{x}^D+B\mathbf{x}^B) \tag{A.9}$$

Dividing equation (A.9) by $(D+B)$,

$$\frac{d\mathbf{x}^M}{d\xi}=\mathbf{x}^M-(\frac{D}{D+B}\mathbf{x}^D+\frac{B}{D+B}\mathbf{x}^B) \tag{A.10}$$

and remembering the definition of the middle vessel column parameter λ, as being,

$$\lambda=\frac{D}{D+B} \tag{A.11}$$

λ is then substituted into equation (A.10) to give,

$$\frac{d\mathbf{x}^M}{d\xi} = \mathbf{x}^M - \lambda\mathbf{x}^D - (1-\lambda)\mathbf{x}^B \tag{A.12}$$

which is equivalent to equation (3.7) in Chapter 3.

The derivation of the definition of warped time as given by equation (3.8) in Chapter 3 is also presented as follows. From the overall mass balance equation as given by equation (A.3), we obtain,

$$dM = -(D+B)dt \tag{A.13}$$

Equation (A.13) can then be substitued into our definition of the dimensionless warped time given by equation (A.6) to obtain

$$d\xi = \frac{dM}{M} \tag{A.14}$$

but

$$\frac{d}{dM}ln(M) = \frac{1}{M} \tag{A.15}$$

which implies that

$$d[ln(M)] = \frac{dM}{M} \tag{A.16}$$

and substituting equation (A.16) into equation (A.14), we obtain,

$$d\xi = d[ln(M)] \tag{A.17}$$

which is exactly equation (3.8) in Chapter 3.

Appendix B

Residue Curve Maps for the A-C-M and A-B-C Systems

In this Appendix, the residue curve map for the two ternary systems studied extensively in this thesis are provided. They are that of the acetone, chloroform, methanol system and the acetone, benzene, chloroform system. Relevant vapor-liquid equilibrium data and parameters used for the NRTL Activity Coefficient Model and the Extended Antoine Vapor Pressure Models are obtained from Aspen Plus.

B.1 Residue Curve Maps for Ternary System of Acetone, Chloroform and Methanol

In this section, the residue curve map for the Acetone, Chloroform, and Methanol system, is presented in Figure B-1. There are a total of 4 azeotropes exhibited by this system, with the compositions calculated with the NRTL model and the Extended Antoine Equation given in Table B.1. This is relatively similar to the experimental data available on the composition of these corresponding azeotropes as documented in Table B.2.

The experimental values for the composition of the azeotropes was calculated based on the weight percentage composition of these azeotropes reported by Hors-

Table B.1: Calculated Composition of Fixed Points in the Acetone, Chloroform and Methanol System and their Characteristic Behavior

Components Label	$x_{Acetone}$	$x_{Chloroform}$	$x_{Methanol}$	Characteristic Behavior
A	1.0	0.0	0.0	Saddle Point
C	0.0	1.0	0.0	Saddle Point
M	0.0	0.0	1.0	Stable Node
AC	0.3455	0.6545	0.0	Stable Node
AM	0.7780	0.0	0.2220	Unstable Node
CM	0.0	0.6579	0.3421	Unstable Node
ACM	0.3396	0.2322	0.4282	Saddle Point

Table B.2: Experimental Values for the Composition of Azeotropes in the Acetone, Chloroform and Methanol System

Azeotrope Label	$x_{Acetone}$	$x_{Chloroform}$	$x_{Methanol}$
AC	0.3400-0.3607	0.6600-0.6393	0.0
AM	0.7605-0.8018	0.0	0.2395-0.1982
CM	0.0	0.6500-0.6605	0.3500-0.3395
ACM	0.3175	0.2414	0.4411

ley, Dow Chemical Company [19, 20]. Weight percent of chloroform in the acetone-chloroform azeotrope was found to range between 78.5% and 80.0%. Weight percent of chloroform in the chloroform-methanol azeotrope was found to range between 87.4% and 87.9% Weight percent of methanol in the acetone-methanol azeotrope was found to range between 12% and 14.8%. Finally, the ternary azeotrope of acetone-chloroform-methanol was reported to be 47 $wt\%$ chloroform, 23 $wt\%$ methanol and 30 $wt\%$ acetone. The above data was translated into mole fractions, and are summarized in Table B.2.

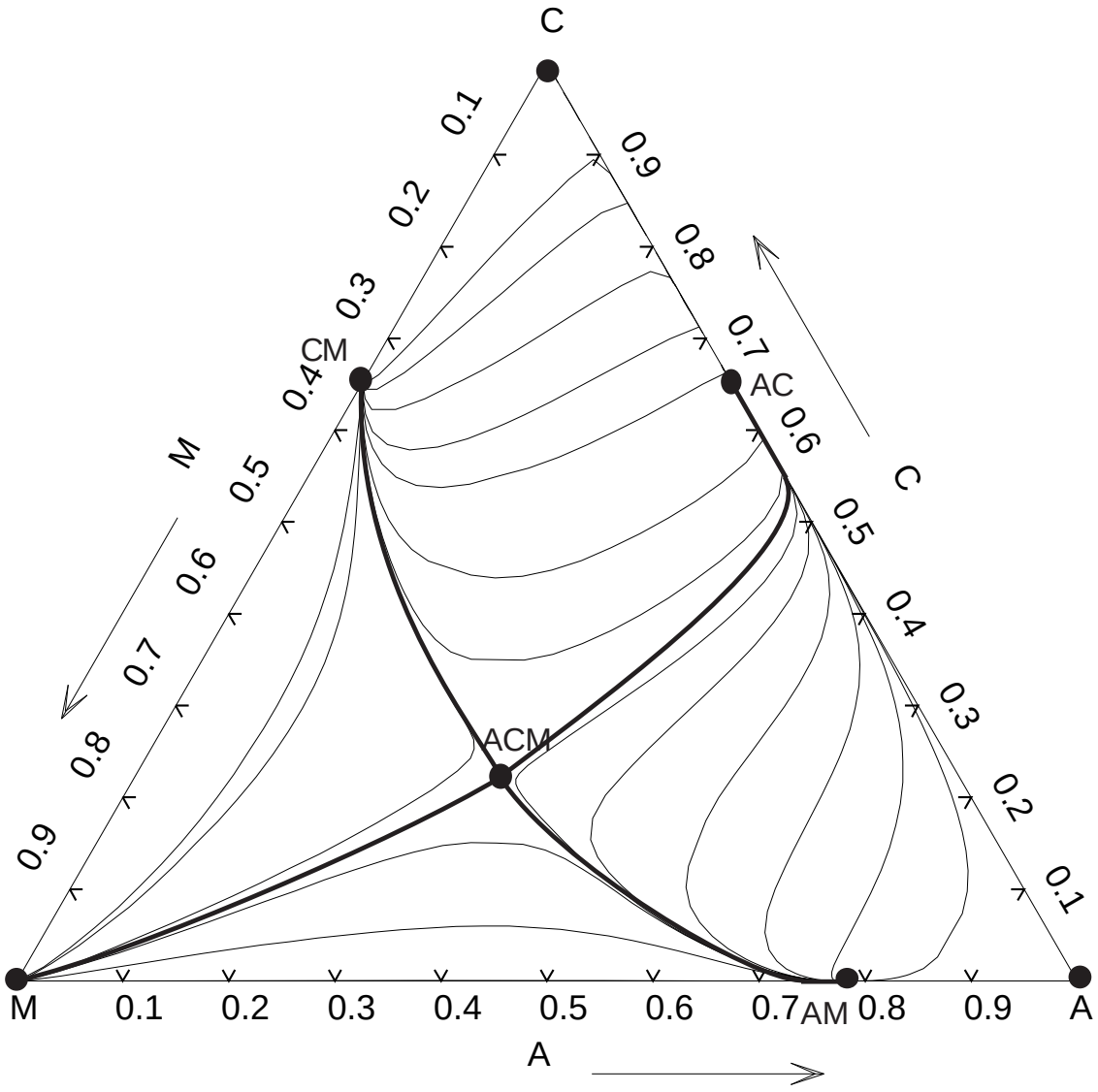

Figure B-1: Residue Curve Map for Acetone Chloroform Methanol System

Table B.3: Characteristic Behavior of Fixed Points in the Acetone, Benzene and Chloroform System

Components Label	$x_{Acetone}$	$x_{Benzene}$	$x_{Chloroform}$	Characteristic Behavior
A	1.0	0.0	0.0	Unstable Node
B	0.0	1.0	0.0	Stable Node
C	0.0	0.0	1.0	Unstable Node
AC	0.3455	0.6545	0.0	Saddle Point

B.2 Residue Curve Maps for Ternary System of Acetone, Benzene and Chloroform

In this section, the residue curve map for the Acetone, Benzene, and Chloroform system, is presented in Figure B-2. There is only one azeotrope exhibited by the ternary system of acetone, benzene and chloroform, which is given by the binary mixture of acetone and chloroform. The composition of the azeotrope was calculated to be (0.3455, 0.0, 0.6545). This is in close agreement with the experimental values obtained for the composition of the acetone-chloroform azeotrope, which was found to range between (0.3400, 0.0, 0.6600) and (0.3607, 0.0, 0.6393). The characteristic behavior of each of the fixed points in the A-B-C system are summarized in Table B.3.

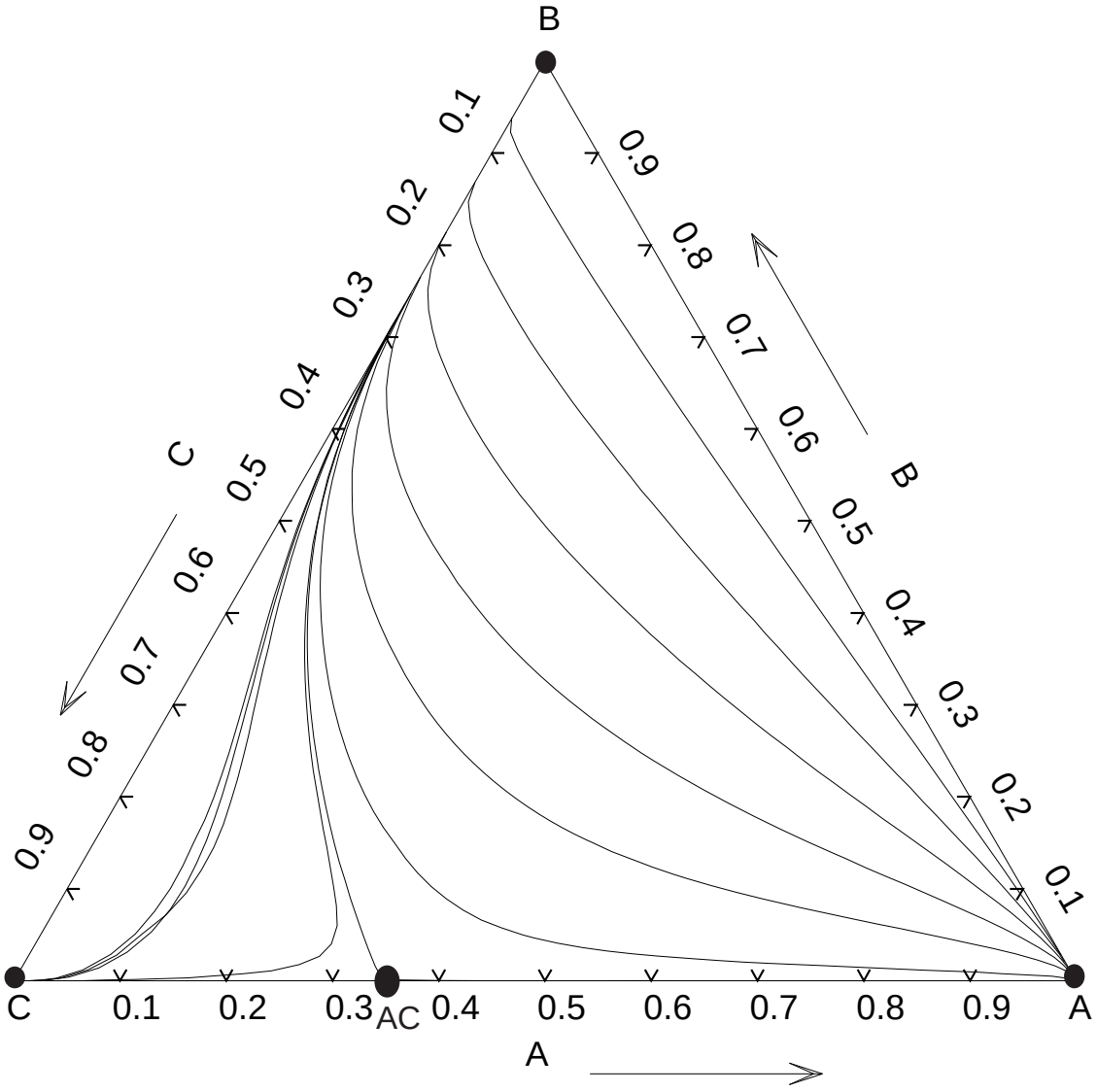

Figure B-2: Residue Curve Map for Acetone Benzene Chloroform System

Appendix C

Derivation of Model Equations For Middle Vessel Column in the Presence of Entrainers

Provided in this Appendix is the detailed derivation of the equations for the middle vessel column operated with an entrainer, using an operating policy suggested by Safrit and Westerberg [35, 33]. As presented in equations (4.28) and (4.29), these equations which define the direction of still pot motion in the middle vessel entrainer column are derived from the definition of warped time given by equation (4.25), and the component mass balance equation obtained for the middle vessel entrainer column (equation (4.24)), and the overall mass balance for the column.

Starting with the equation for component mass balance,

$$\frac{dH\,x_s}{dt} = -Dx_d - Bx_b + Ex_e \tag{C.1}$$

we differentiate the LHS by parts to obtain,

$$x_s\frac{dH}{dt} + H\frac{dx_s}{dt} = -Dx_d - Bx_b + Ex_e \tag{C.2}$$

But, the overall mass balance equation is given as,

$$\frac{dH}{dt} = -D - B + E \tag{C.3}$$

Hence, substituting equation (C.3) into equation (C.2), the following expression is obtained,

$$x_s(-D - B + E) + H\frac{dx_s}{dt} = -Dx_d - Bx_b + Ex_e \tag{C.4}$$

or equivalently,

$$H\frac{dx_s}{dt} = (D + B - E)x_s - Dx_d - Bx_b + Ex_e \tag{C.5}$$

But, from the definition of warped time ζ for the middle vessel entrainer column as given in Chapter 4,

$$d\zeta = (\frac{D + B - E}{H})dt \tag{C.6}$$

which can be rearranged to obtain,

$$1 = (\frac{D + B - E}{H})\frac{dt}{d\zeta} \tag{C.7}$$

Multiplying the LHS of equation (C.5) by equation (C.7) which equals unity, the RHS is unchanged, and we obtain the following equation,

$$H\frac{dx_s}{dt}(\frac{D + B - E}{H})\frac{dt}{d\zeta} = (D + B - E)x_s - Dx_d - Bx_b + Ex_e \tag{C.8}$$

from which H and dt are cancelled,

$$(D + B - E)\frac{dx_s}{d\zeta} = (D + B - E)x_s - Dx_d - Bx_b + Ex_e \tag{C.9}$$

Dividing equation (C.9) by $(D + B - E)$,

$$\frac{dx_s}{d\zeta} = x_s - \frac{D}{D + B - E}x_d - \frac{B}{D + B - E}x_b + \frac{E}{D + B - E}x_e \tag{C.10}$$

The definition of the middle vessel column parameters in the presence of the entrainer, was defined in Chapter 4 by equation (4.26) as,

$$\begin{aligned} \theta_1 &= \tfrac{D}{D+B-E} \\ \theta_2 &= \tfrac{B}{D+B-E} \\ \theta_3 &= -\tfrac{E}{D+B-E} < 0 \end{aligned} \tag{C.11}$$

θ_1, θ_2 and θ_3, are then substituted into equation (C.10) to give,

$$\frac{dx_s}{d\zeta} = x_s - \theta_1 x_d - \theta_2 x_b - \theta_3 x_e \tag{C.12}$$

which is equivalent to equation (4.28) in Chapter 4.

We can also obtain an alternate definition of warped time as follows. From the overall mass balance equation as given by equation (C.3), we obtain,

$$dH = (-D - B + E)dt \tag{C.13}$$

Equation (C.13) can then be substitued into our definition of the dimensionless warped time given by equation (C.6) to obtain

$$d\zeta = \frac{dH}{H} \tag{C.14}$$

but

$$\frac{d}{dH} ln(H) = \frac{1}{H} \tag{C.15}$$

which implies that

$$d[ln(H)] = \frac{dH}{H} \tag{C.16}$$

and substituting equation (C.16) into equation (C.14), we obtain,

$$d\zeta = d[ln(H)] \tag{C.17}$$

which gives a definition of warped time different from that of equation (C.6).

Appendix D

Detailed Simulation Results of the 3-Component Mixture of Acetone, Chloroform, and Methanol

In this appendix, the detailed simulation results for each of the middle vessel batch distillation regions χ_1 through χ_{24} for the Acetone, Chloroform and Methanol system studied in Chapter 6 are presented. Also categorized are the results for each of the rectifying batch distillation regions (Y_1 through Y_6) and each of the stripping batch distillation regions (Z_1 through Z_6). These results include the graphs of distillate and bottoms product composition against time, the graphs of middle vessel composition against time, plots of the still pot composition motion on a ternary composition diagram, and graphs of accumulation for each of the components in each of the 3 locations (still pot, distillate cut, and bottoms cut) as a function of time. The behavior of the middle vessel column product cuts and still pot composition motion for the initial compositions starting in each of the 24 middle vessel regions are similar to those explained in Chapter 6. Hence, they will not be explained in detail. Similarly, the results obtained for the simulation of the middle vessel as a stripper and a rectifier (regions Y_i and Z_i) are also similar to those explained in Chapter 6 and can also be easily understood based on the work of Van Dongen and Doherty [15] and Bernot *et al.* [5, 6]. However, the results are presented as follows for ease of reference.

Table D.1: Product Sequences for Regions Y_i for $i = 1..6$, in a Batch Rectifier for the A-C-M Mixture, Straight Line Boundaries

Region	First Cut	Second Cut	Third Cut
Y_1	CM	C	AC
Y_2	CM	ACM	AC
Y_3	CM	ACM	M
Y_4	AM	ACM	M
Y_5	AM	ACM	AC
Y_6	AM	A	AC

D.1 Product Sequences Expected For Each Stripper and Rectifier Batch Distillation Region in the Presence of Straight Line Boundaries

Summarized in Table D.1 and Table D.2 are the expected product sequences for each of the regions Y_1 through Y_6 in a rectifier configuration in the presence of straight line boundaries. Also summarized in Table D.2 are the expected product sequences for each of the regions Z_1 through Z_6 in a stripper configuration in the presence of straight line boundaries. A, C, M indicate pure products acetone, chloroform and methanol respectively. AC, AM, and CM indicate the binary azeotropes acetone-chloroform, acetone-methanol, and chloroform-methanol respectively. Finally, ACM represents the ternary azeotrope of acetone-chloroform-methanol. The composition for each of these azeotropes are categorized in detail within Appendix B.

As was noted in Chapter 6, due to the presence of highly curved boundaries in the Acetone-Chloroform-Methanol system, the product cuts which result does not correspond exactly to the sequence enumerated in Tables D.1 and D.2. This happens particularly when the still pot composition encounters a middle vessel batch distillation boundary in the region of a curved separatrix of the simple distillation residue curve map, and is forced to trace a route along this middle vessel batch distillation boundary (as explained in Chapter 6). For example, the resulting composition for the expected ACM cut thus tends not to be the ACM azeotrope composition, but rather

Table D.2: Product Sequences for Regions Z_i for $i = 1..6$, in a Batch Stripper for the A-C-M Mixture, Straight Line Boundaries

Region	First Cut	Second Cut	Third Cut
Z_1	AC	C	CM
Z_2	AC	ACM	CM
Z_3	M	ACM	CM
Z_4	M	ACM	M
Z_5	AC	ACM	AM
Z_6	AC	A	AM

some varying ternary mixture composition which allows the mass balance around the column to be satisfied while the still pot composition traces out a route along the middle vessel batch distillation boundary.

D.2 Simulation Results From ABACUSS Model of Various Initial Still Pot Composition in Each of the 6 Rectifying and Stripping Regions

Summarized in this section are the results of the simulations obtained for initial still pot compositions in each of the 6 stripping and rectifying regions enumerated for the Acetone-Chloroform-Methanol system. It should be noted the behavior of a composition point anywhere in each of the 6 regions is indicative of the behavior of any of the composition points in that region. Thus, simulations were conducted for one initial still pot composition in each of the regions. The initial still pot composition chosen for each region are summarized in Table D.3.

Operating conditions for each simulation were kept constant so as to ensure that the results could be comparable to each other. The pertinent operating parameters used are thus summarized in Table D.4. The behavior of the column as $N \to \infty$ and the reflux/ratios $\to \infty$, was modelled by using a reflux/reboil ratio of 1000, and up

Table D.3: Initial Still Pot Compositions Chosen for Each of the Regions Y_1/Z_1 through Y_6/Z_6

Region	Acetone	Chloroform	Methanol
Y_1/Z_1	0.10	0.80	0.10
Y_2/Z_2	0.25	0.50	0.25
Y_3/Z_3	0.10	0.30	0.60
Y_4/Z_4	0.35	0.10	0.55
Y_5/Z_5	0.50	0.25	0.25
Y_6/Z_6	0.70	0.20	0.10

Table D.4: Operating Conditions for the Rectifier and Stripper Simulations, (Infinite Reflux/Reboil, Infinite Number of Trays)

Operational Parameter	Numerical Value	Units
Initial Still Pot Holdup	100	Moles
Vapor Flow Rate (Stripping Section)	10	Moles/Time
Liquid Flow Rate (Rectifying Section)	10	Moles/Time
Distillate Product Flow Rate	0.01	Moles/Time
Bottoms Product Flow Rate	0.01	Moles/Time
Resulting Reflux Ratio	1000	Dimensionless
Resulting Reboil Ratio	1000	Dimensionless
Number of Trays in the Rectifying Section	50	Dimensionless
Number of Trays in the Stripping Section	50	Dimensionless
Operating Pressure in Column	1	Bar

to 50 trays in the column.

In the graphs that follow, the results of the simulation for each of the regions are presented categorically, classified according to the region. Product composition as a function of time, the still pot motion in the composition space, and the accumulation of components as a function of time are provided for each initial composition for each of the 12 regions enumerated (6 stripper regions and 6 rectifier regions).

D.2.1 Simulation Results for Region Y_1

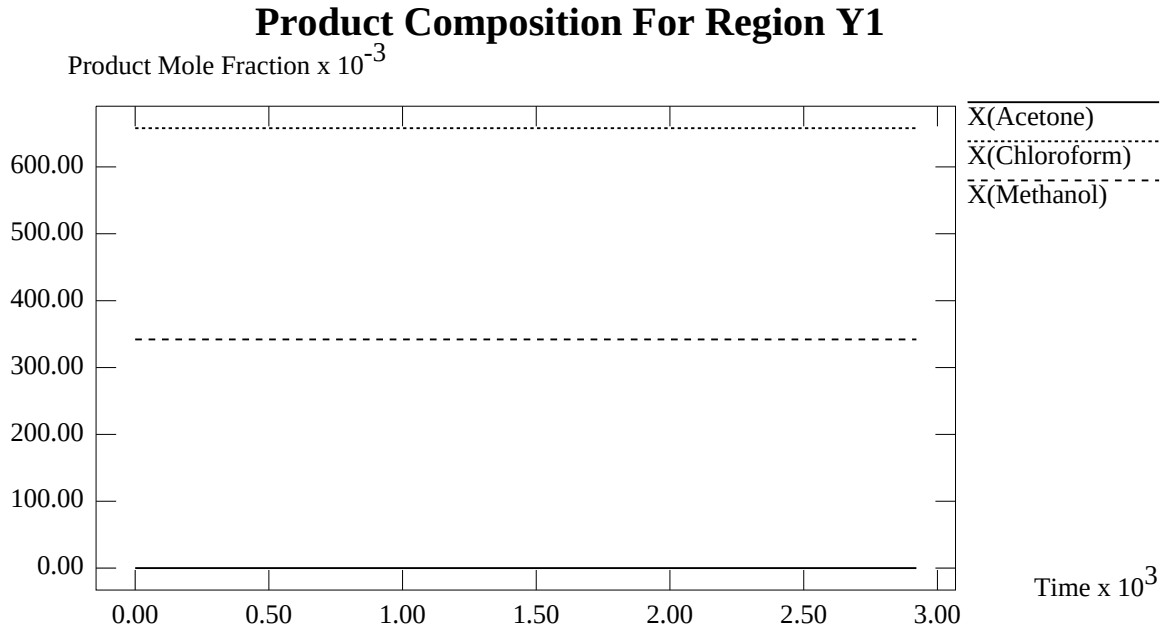

Figure D-1: Graph of Product Composition against Time

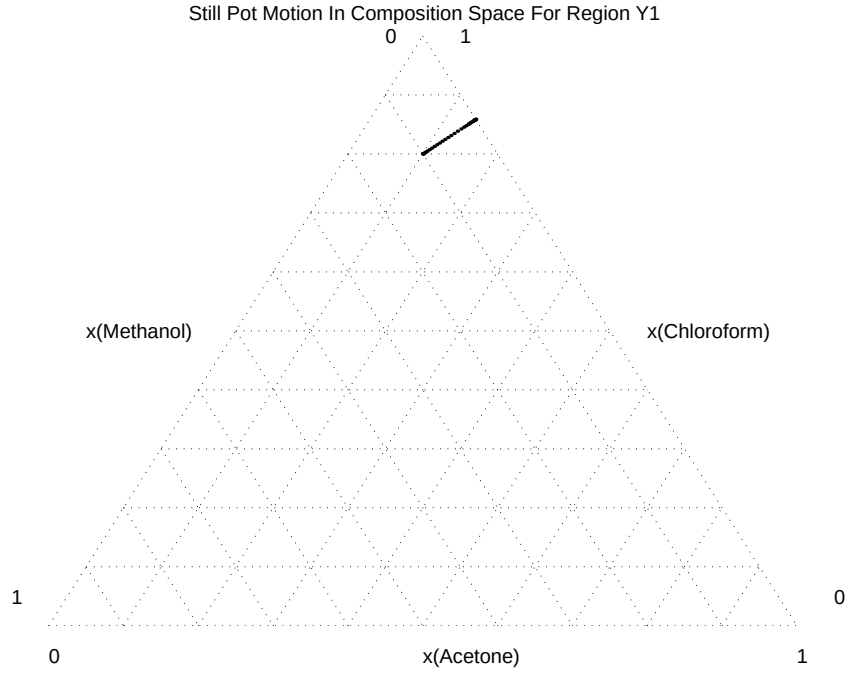

Figure D-2: Plot of Still Pot Motion in Composition Space

D.2.2 Simulation Results for Region Y_2

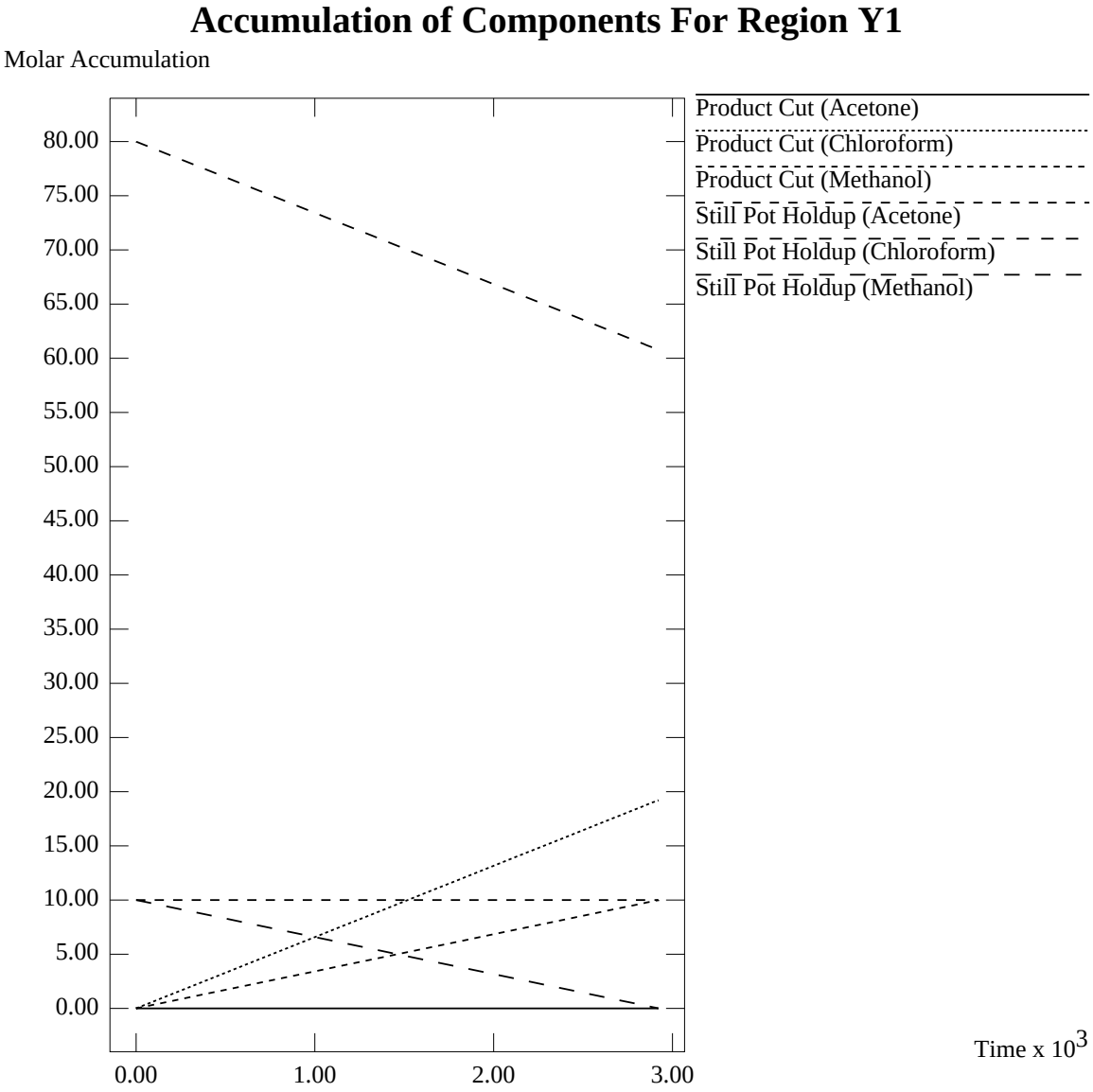

Figure D-3: Graph of Accumulation of Each Component against Time

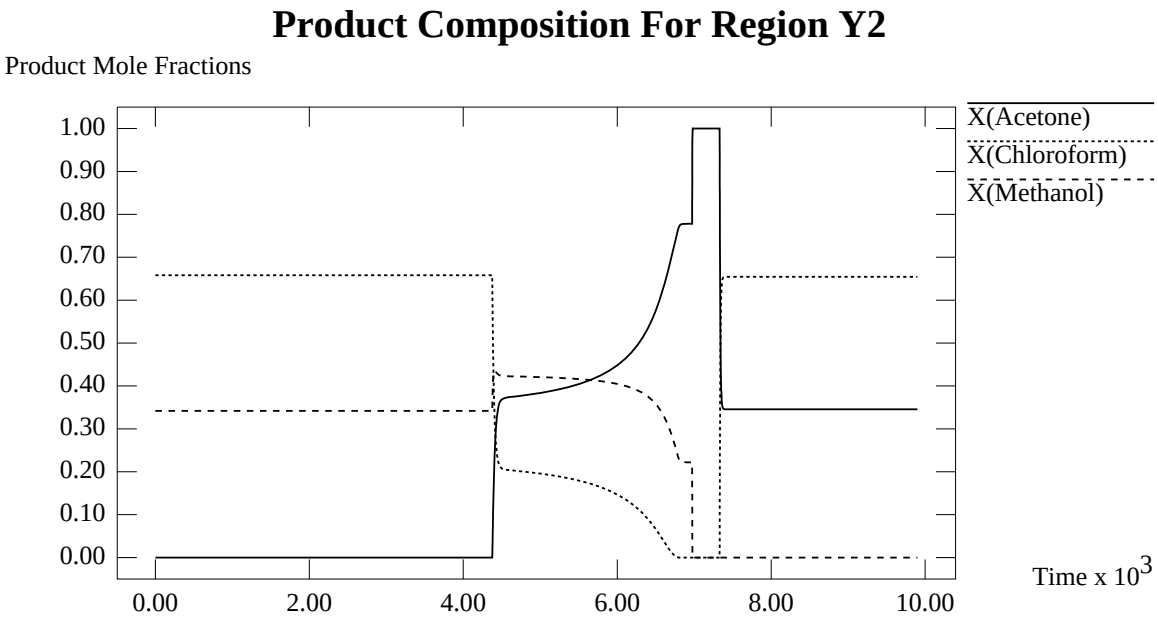

Figure D-4: Graph of Product Composition against Time

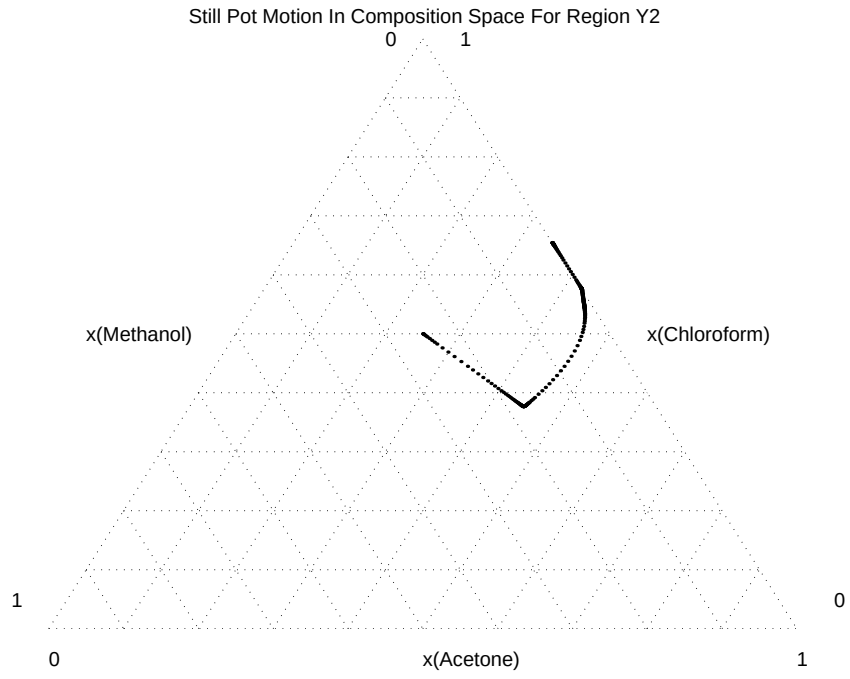

Figure D-5: Plot of Still Pot Motion in Composition Space

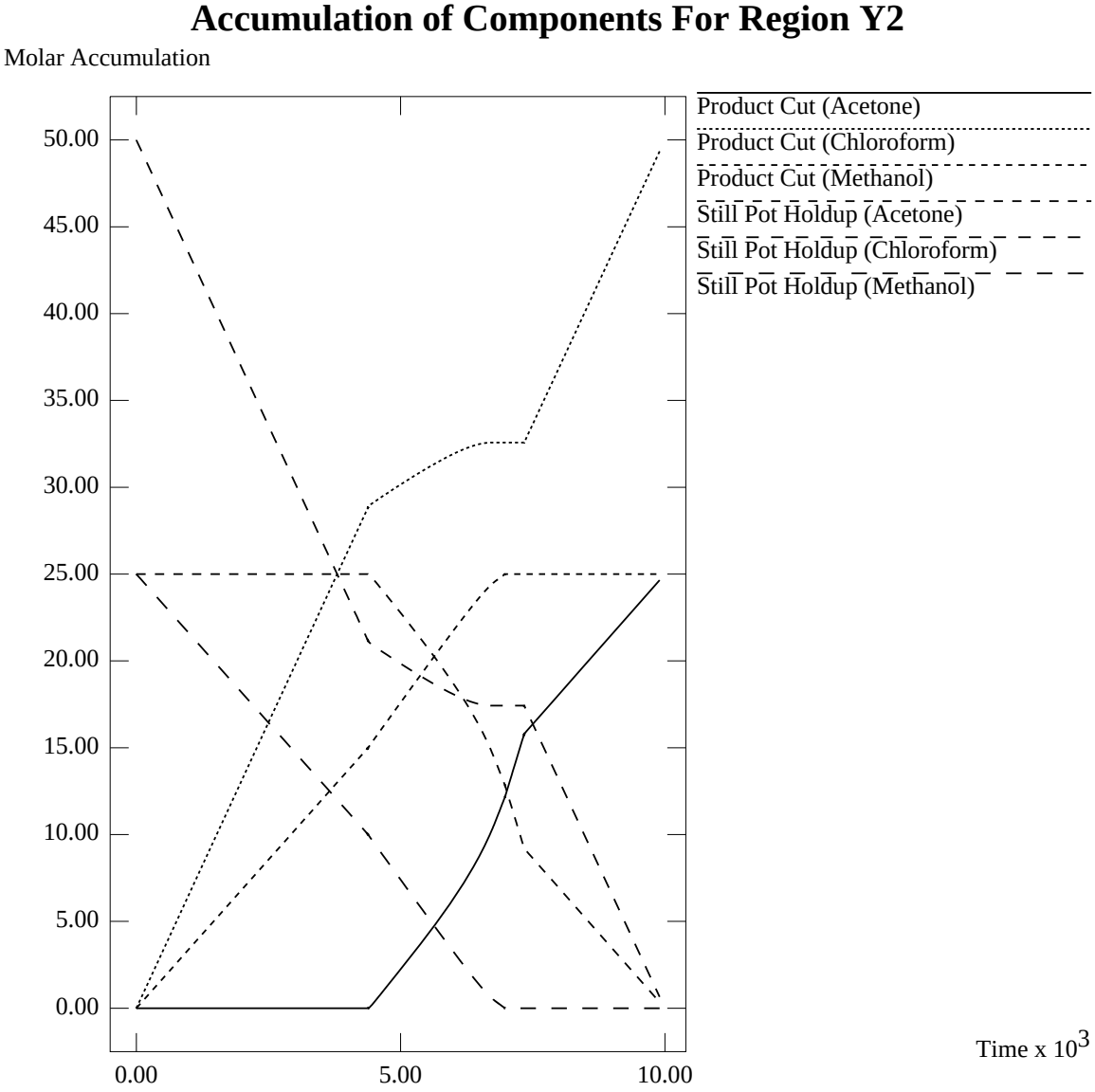

Figure D-6: Graph of Accumulation of Each Component against Time

D.2.3 Simulation Results for Region Y_3

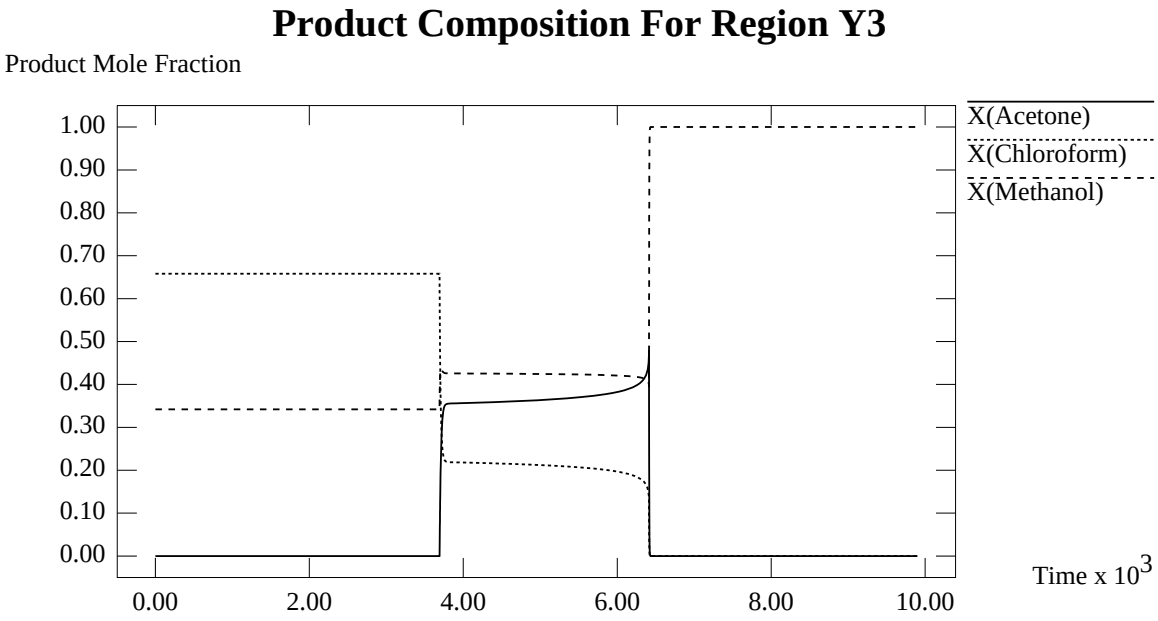

Figure D-7: Graph of Product Composition against Time

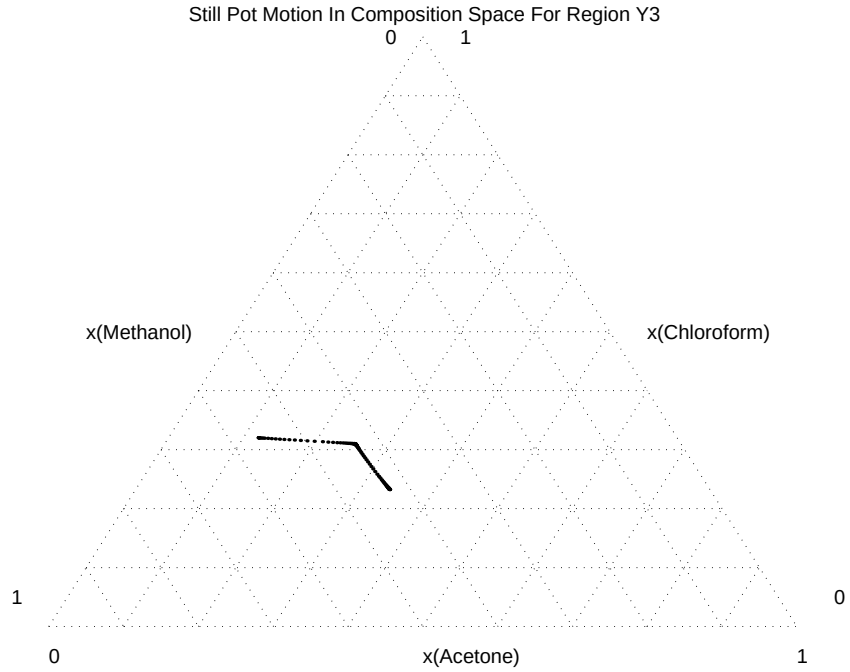

Figure D-8: Plot of Still Pot Motion in Composition Space

D.2.4 Simulation Results for Region Y_4

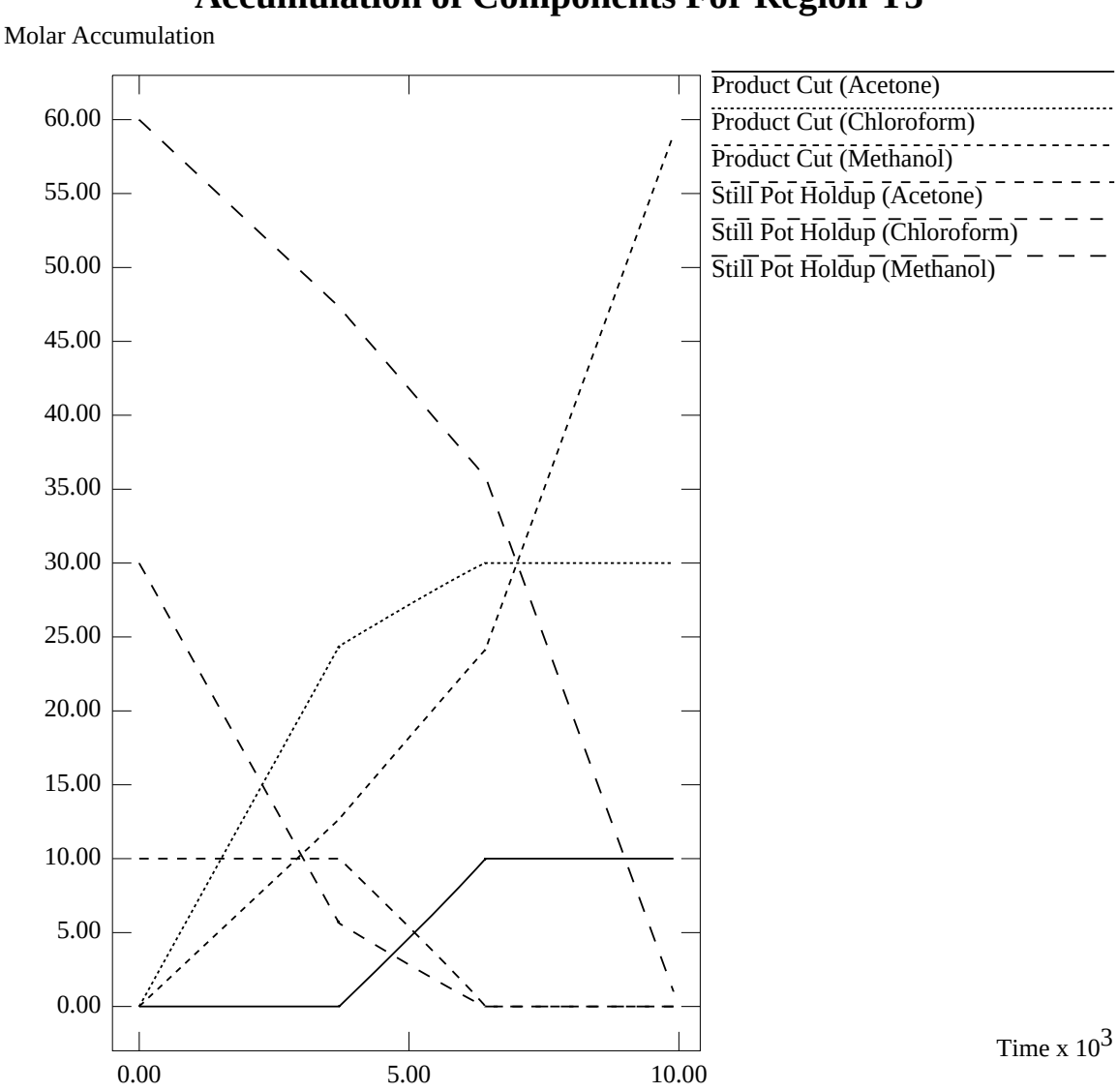

Figure D-9: Graph of Accumulation of Each Component against Time

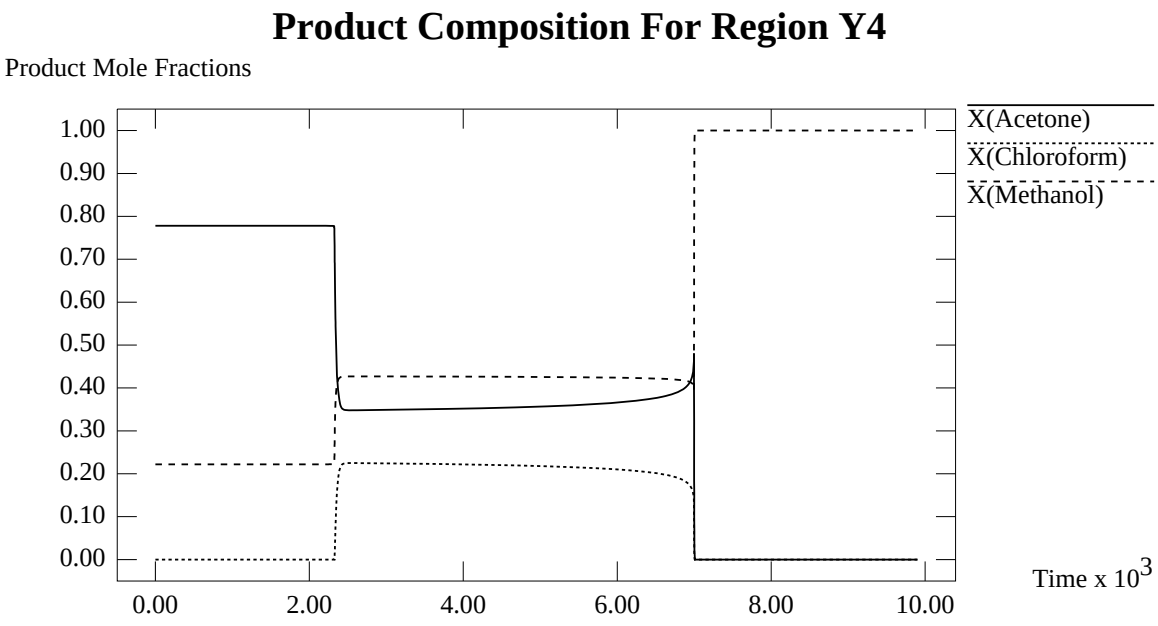

Figure D-10: Graph of Product Composition against Time

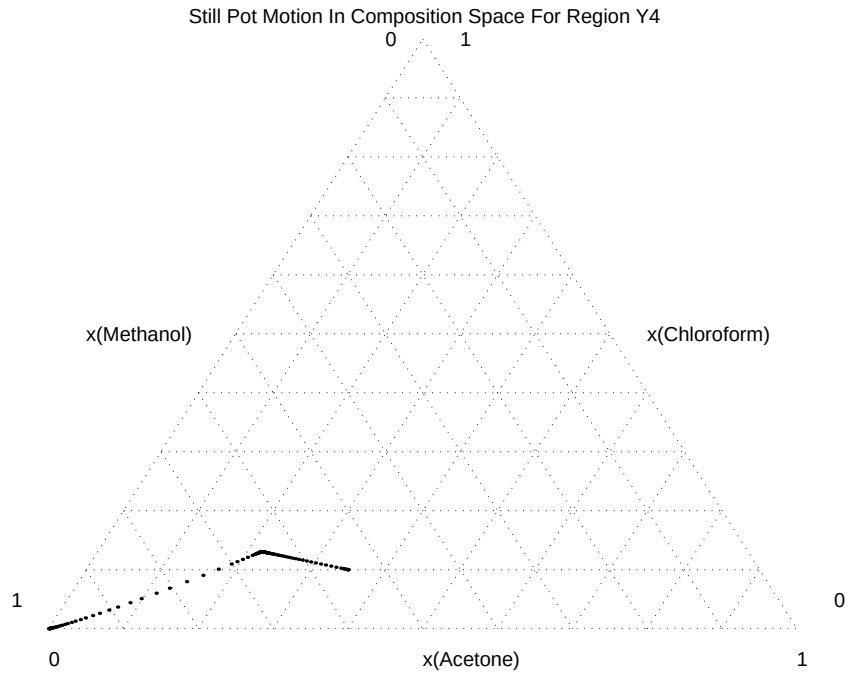

Figure D-11: Plot of Still Pot Motion in Composition Space

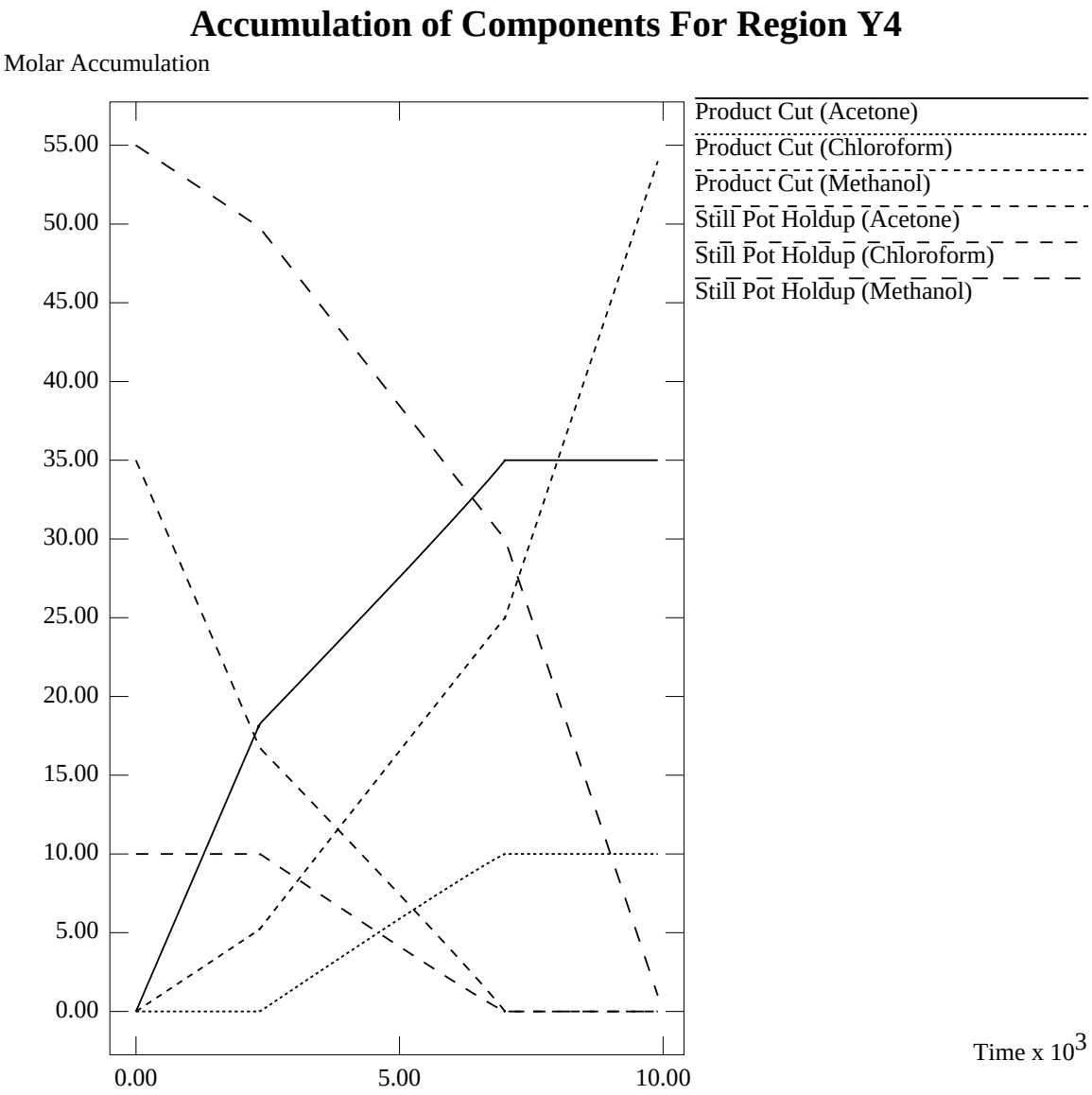

Figure D-12: Graph of Accumulation of Each Component against Time

D.2.5 Simulation Results for Region Y_5

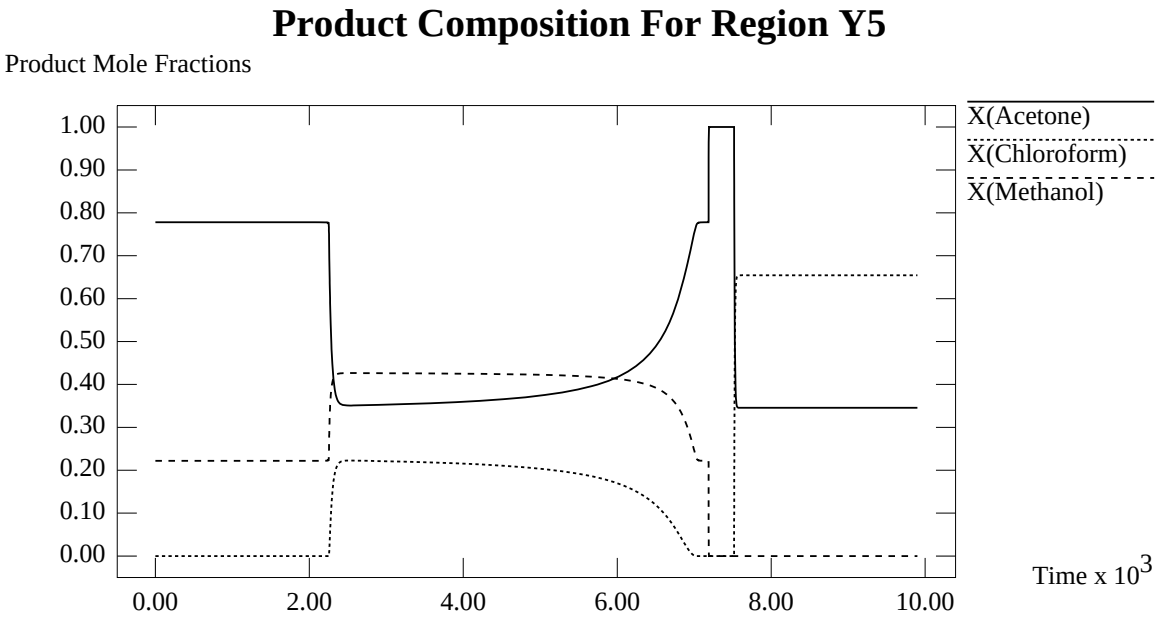

Figure D-13: Graph of Product Composition against Time

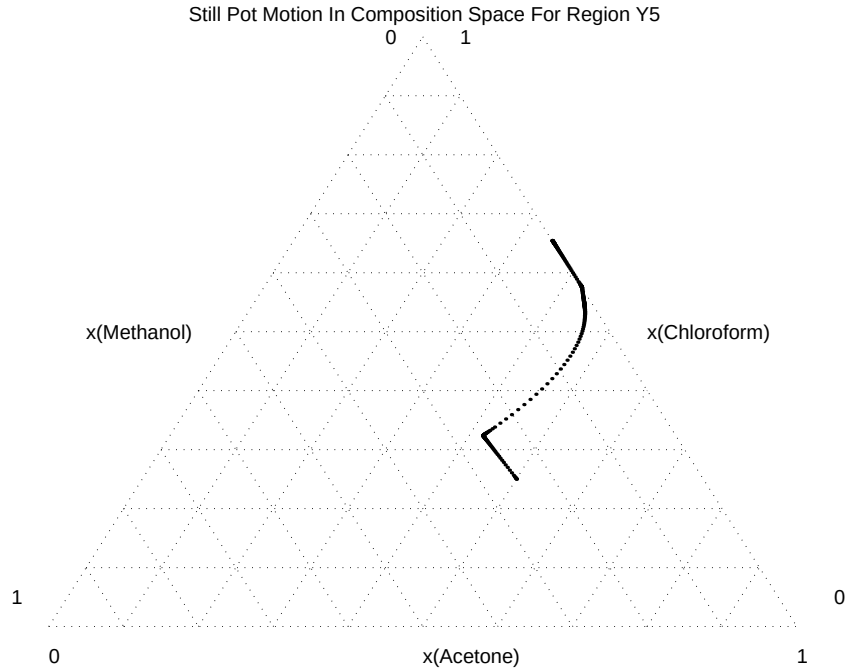

Figure D-14: Plot of Still Pot Motion in Composition Space

D.2.6 Simulation Results for Region Y_6

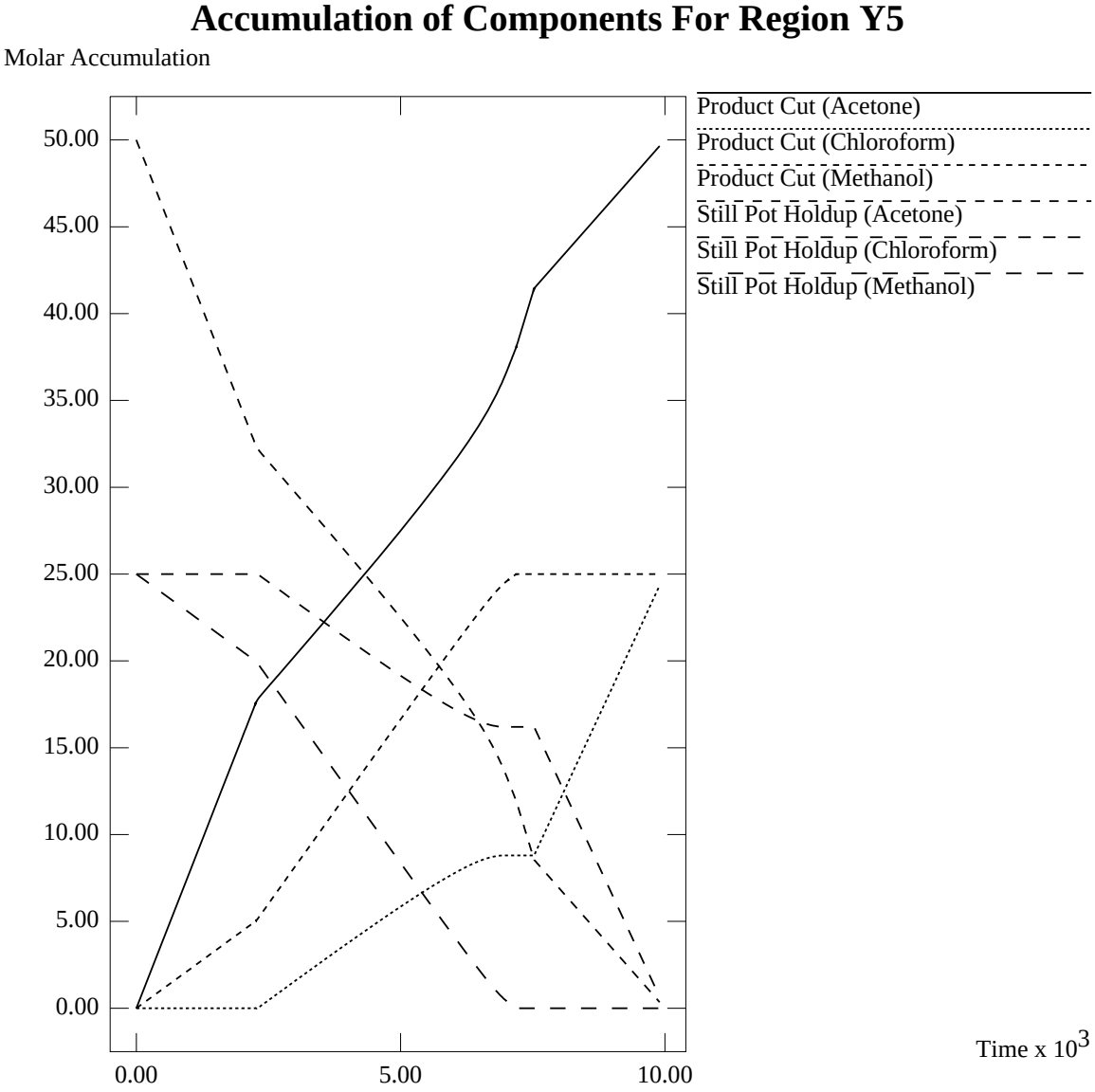

Figure D-15: Graph of Accumulation of Each Component against Time

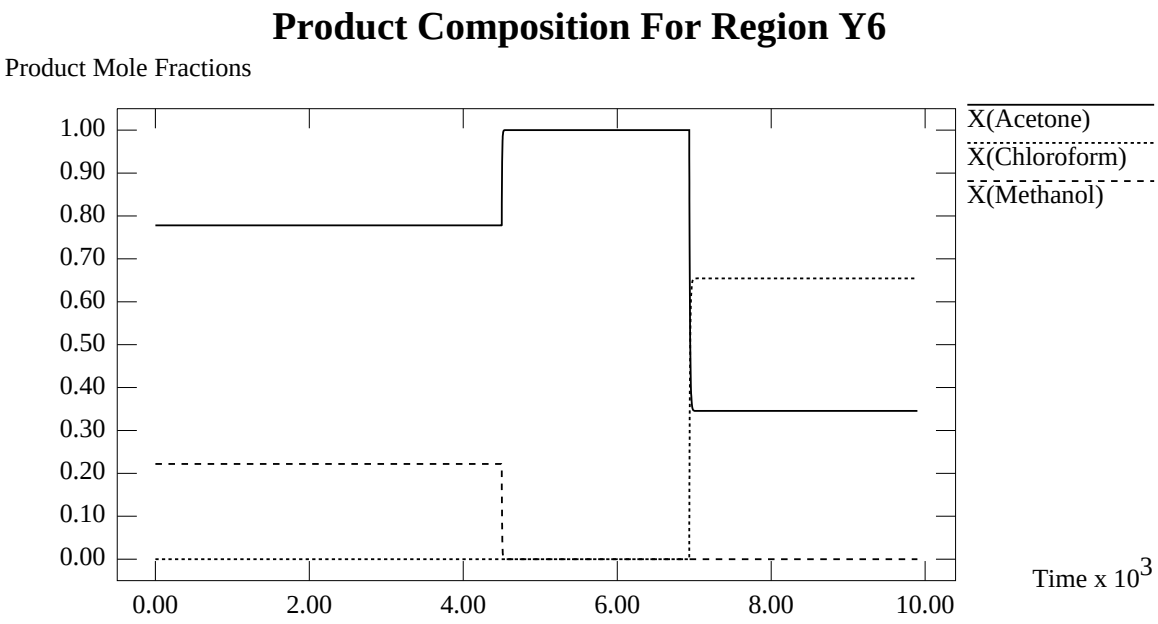

Figure D-16: Graph of Product Composition against Time

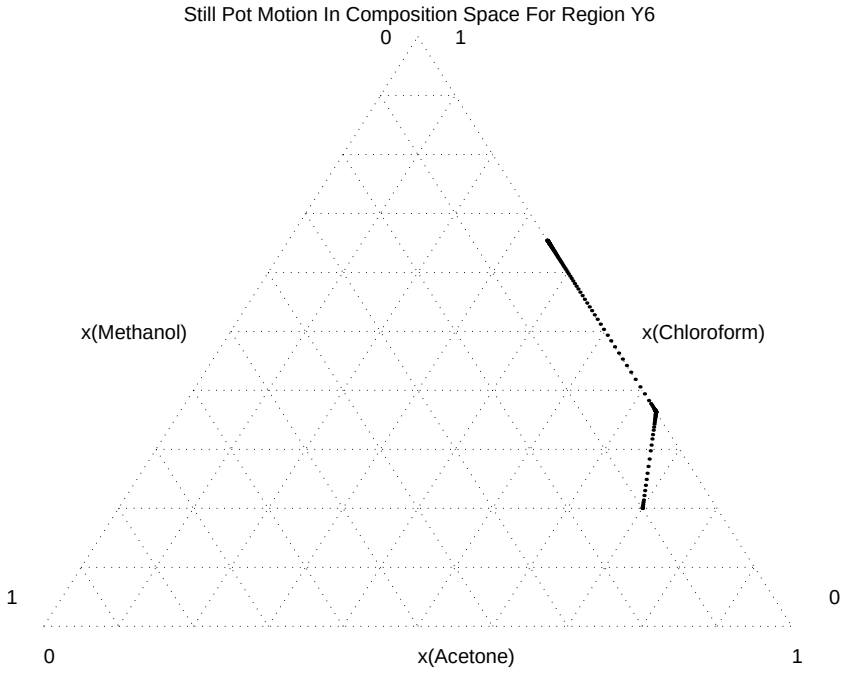

Figure D-17: Plot of Still Pot Motion in Composition Space

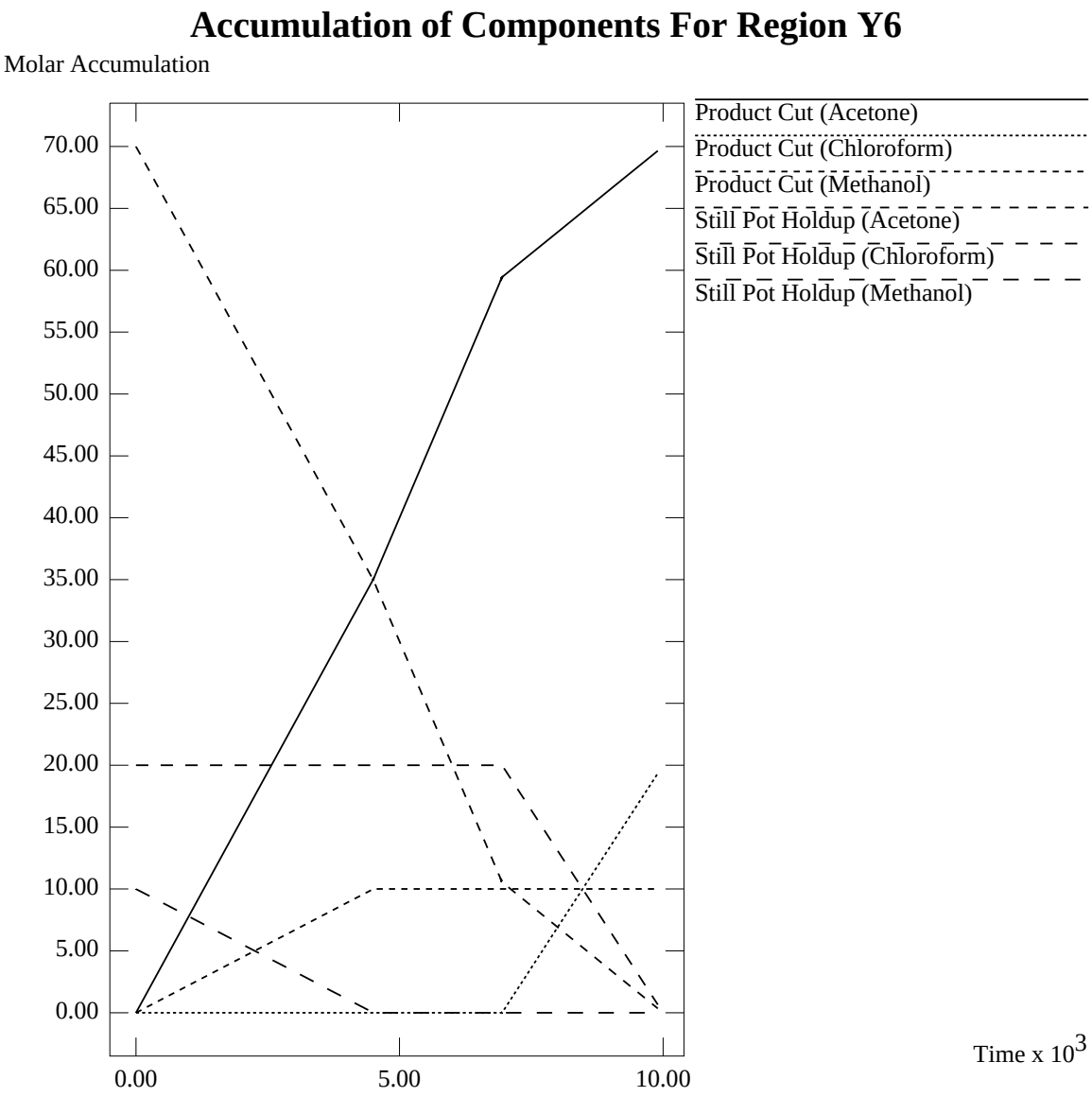

Figure D-18: Graph of Accumulation of Each Component against Time

D.2.7 Simulation Results for Region Z_1

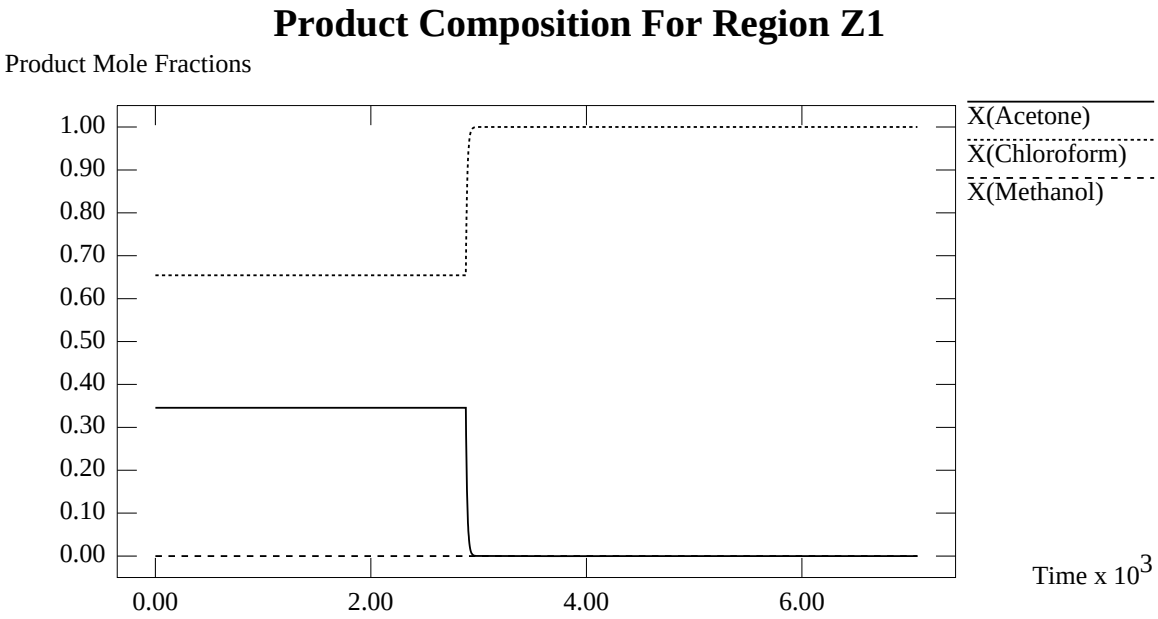

Figure D-19: Graph of Product Composition against Time

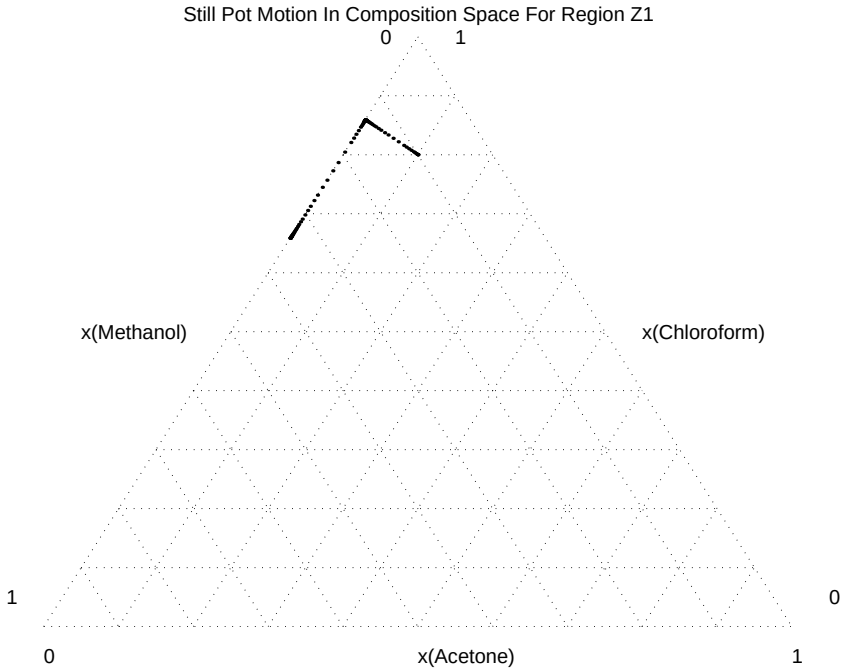

Figure D-20: Plot of Still Pot Motion in Composition Space

D.2.8 Simulation Results for Region Z_2

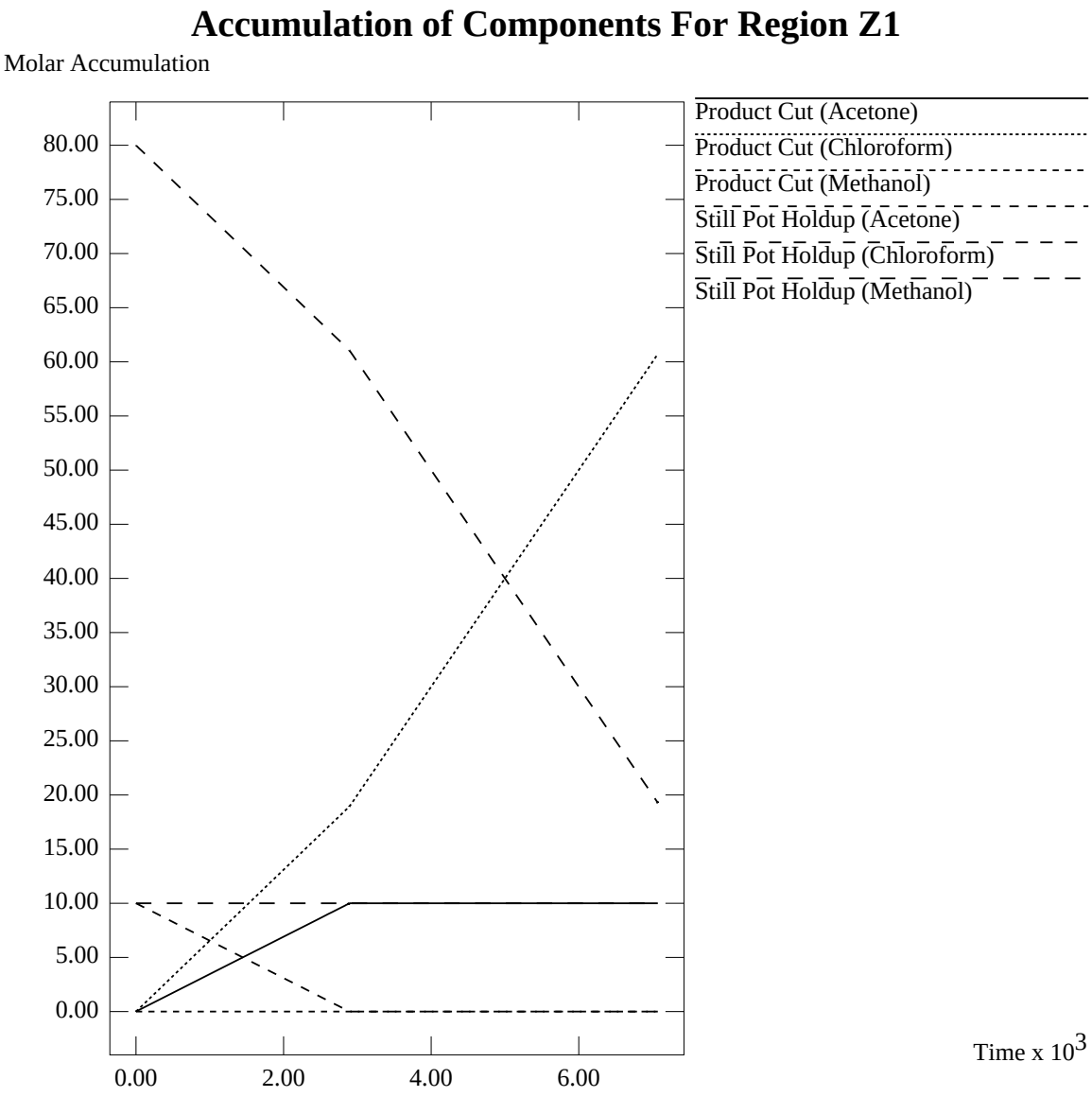

Figure D-21: Graph of Accumulation of Each Component against Time

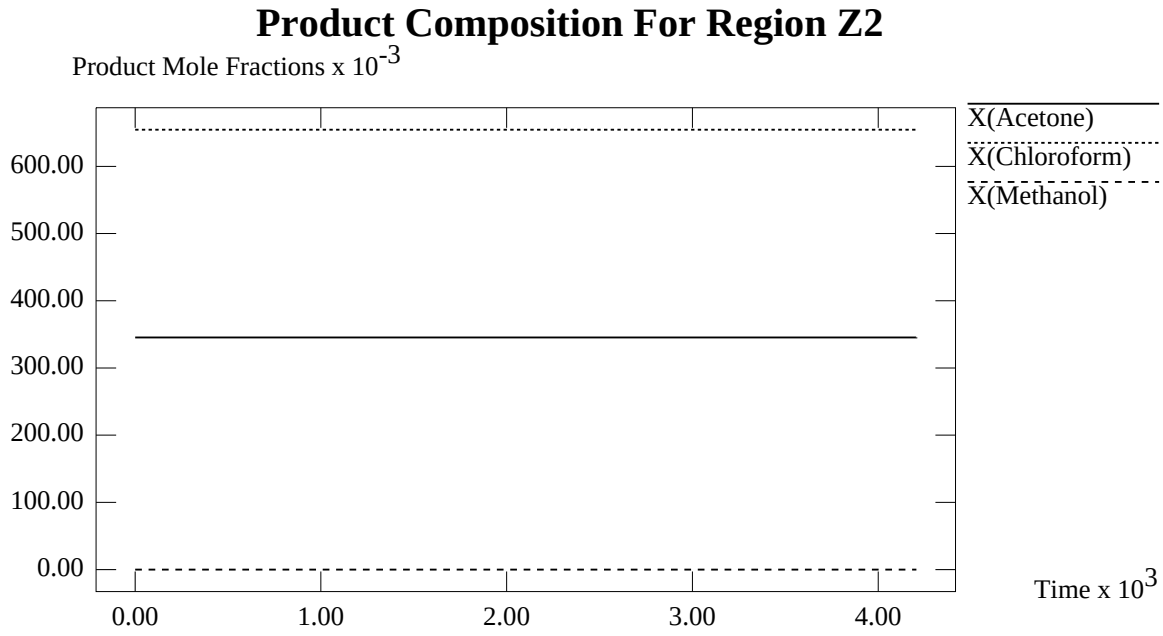

Figure D-22: Graph of Product Composition against Time

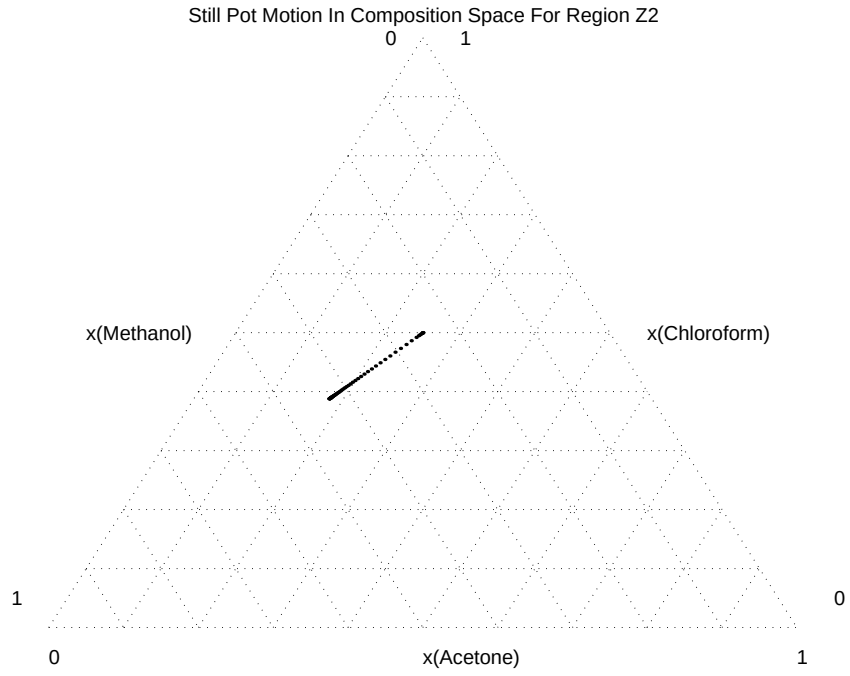

Figure D-23: Plot of Still Pot Motion in Composition Space

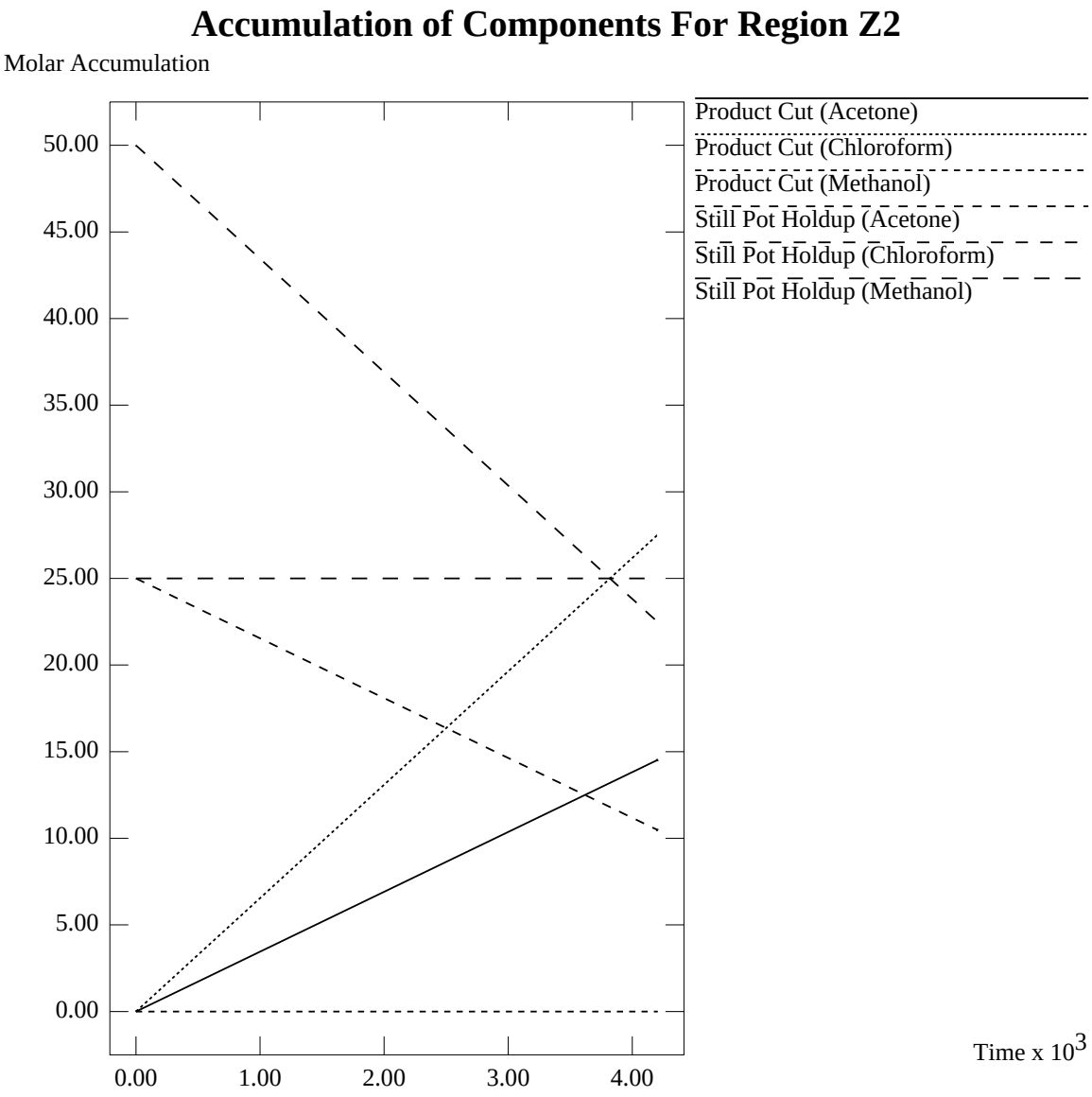

Figure D-24: Graph of Accumulation of Each Component against Time

D.2.9 Simulation Results for Region Z_3

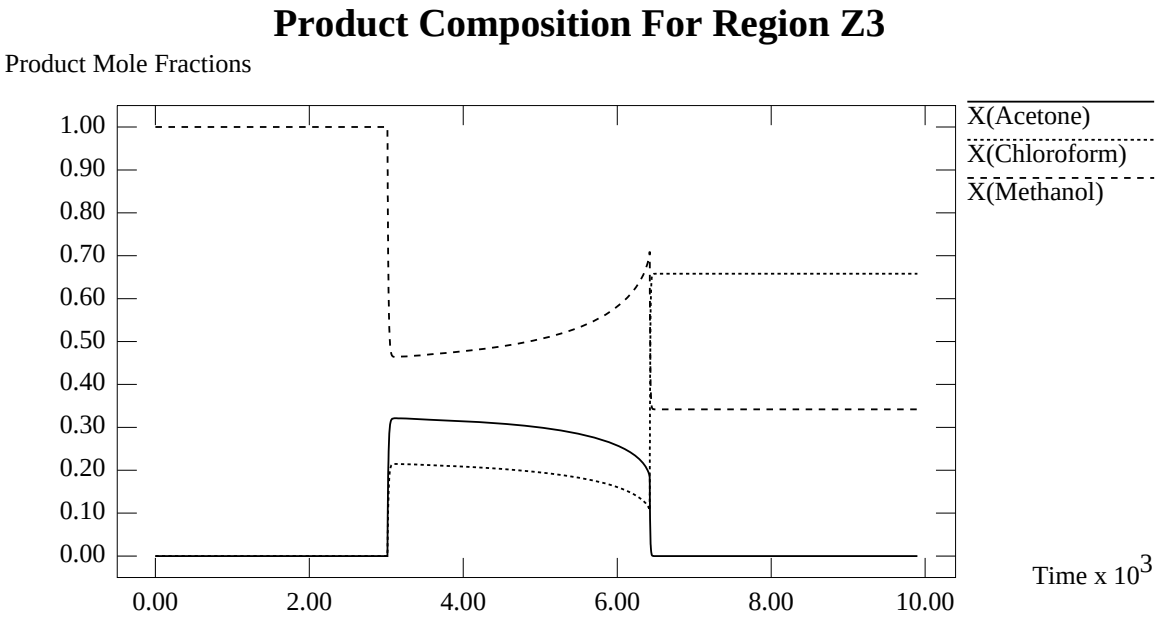

Figure D-25: Graph of Product Composition against Time

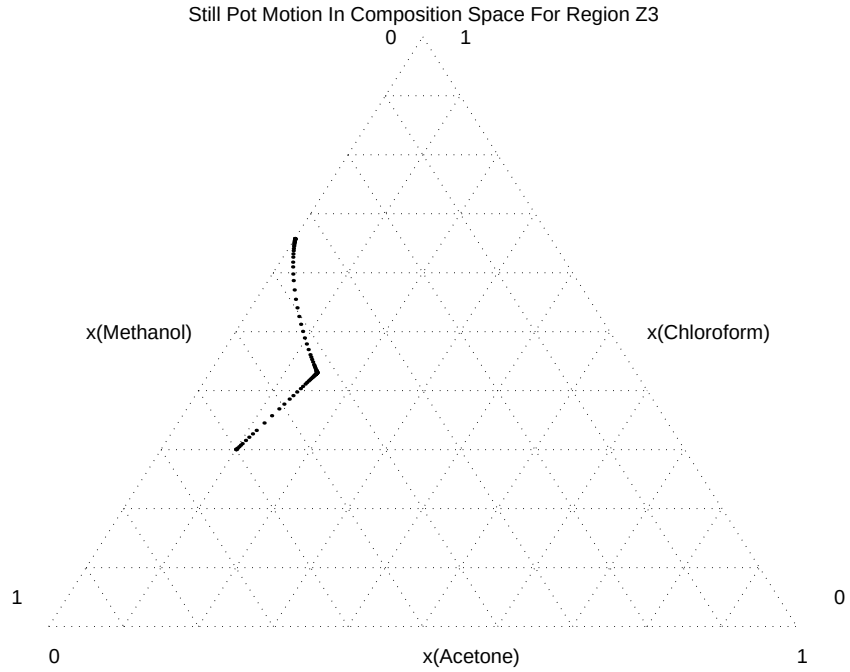

Figure D-26: Plot of Still Pot Motion in Composition Space

D.2.10 Simulation Results for Region Z_4

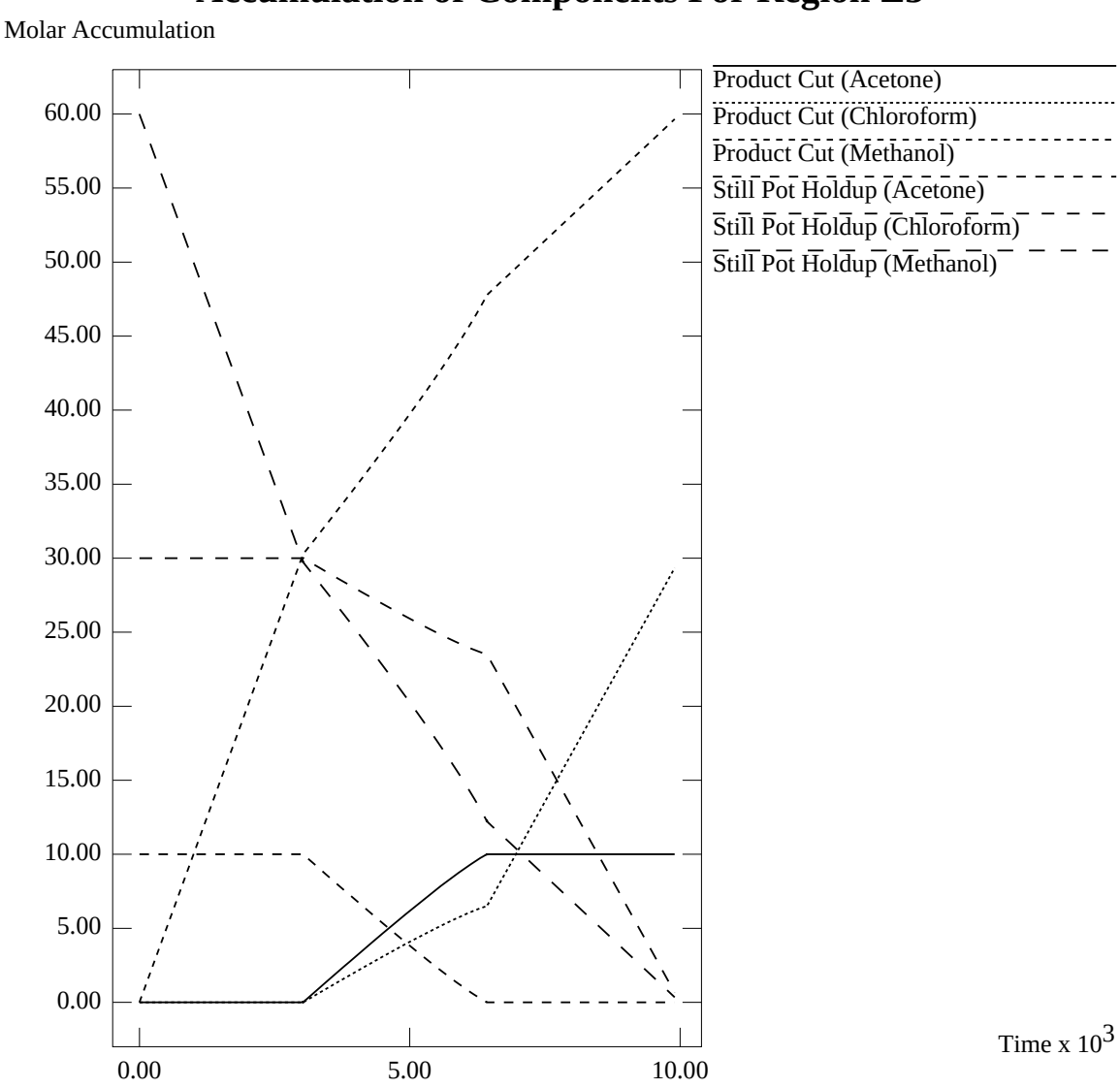

Figure D-27: Graph of Accumulation of Each Component against Time

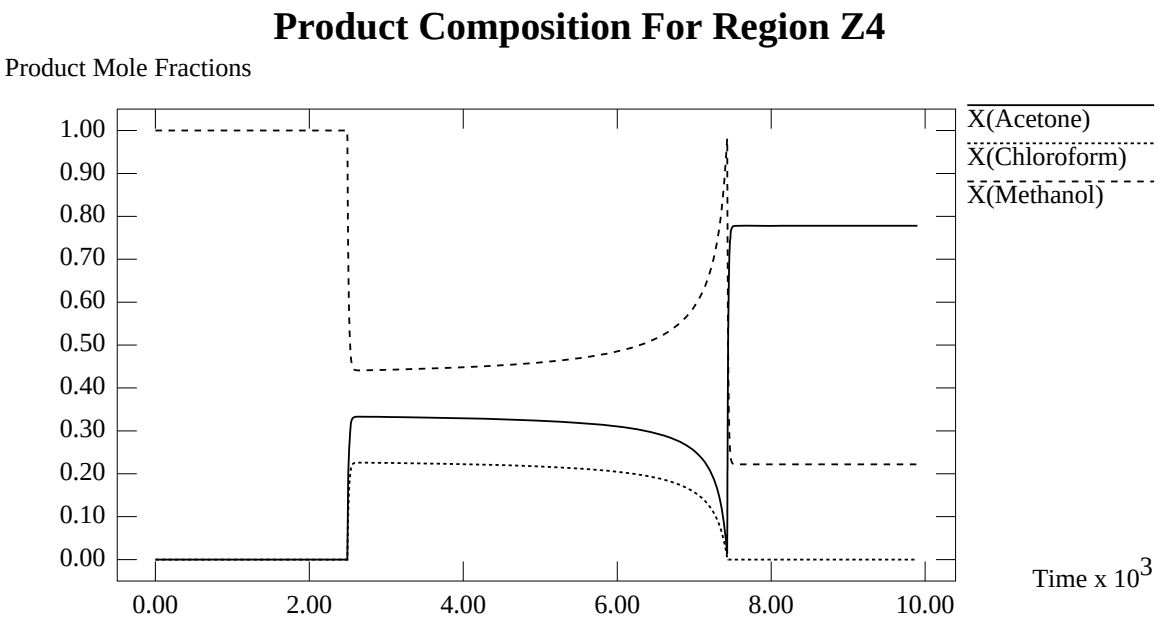

Figure D-28: Graph of Product Composition against Time

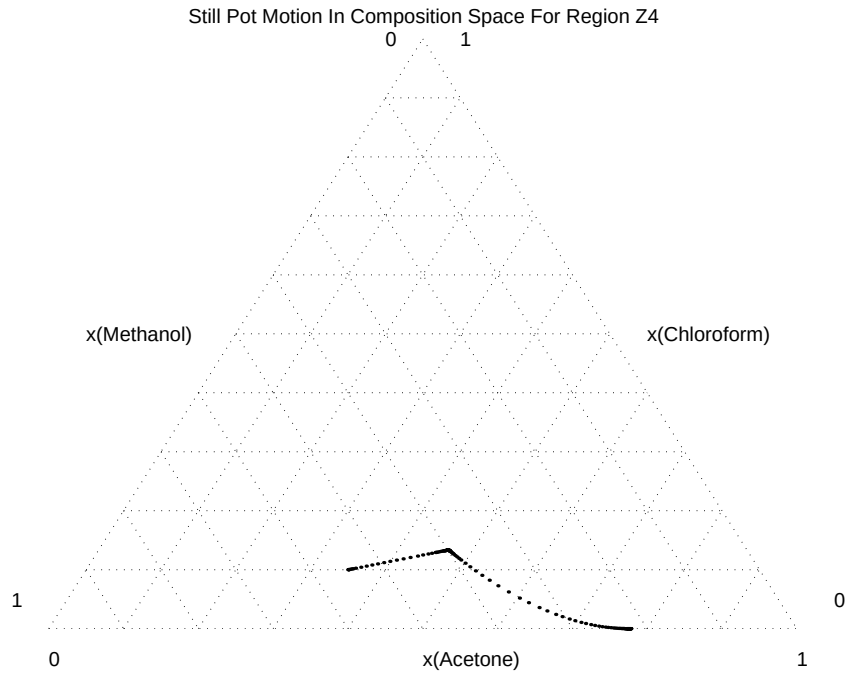

Figure D-29: Plot of Still Pot Motion in Composition Space

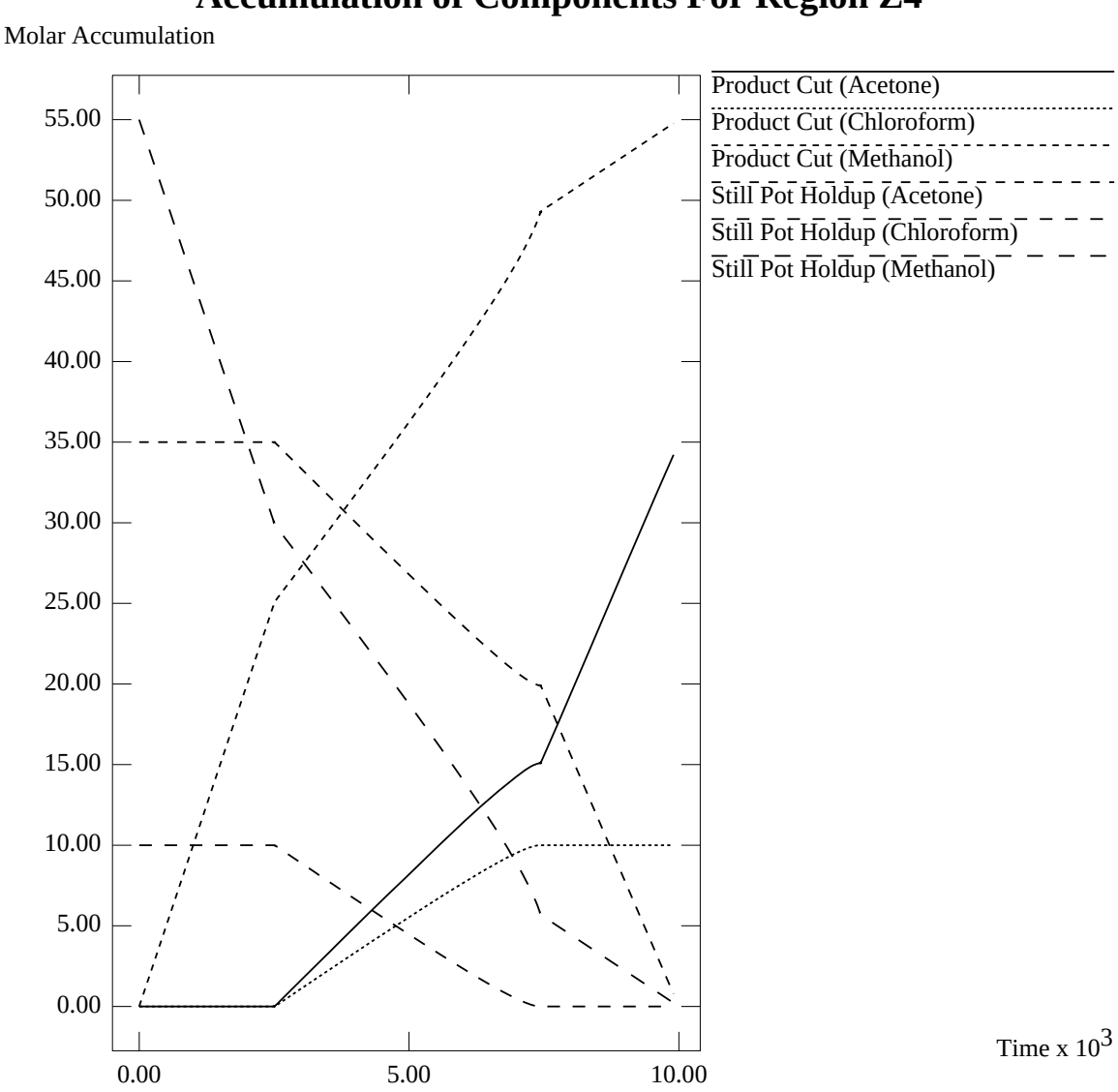

Figure D-30: Graph of Accumulation of Each Component against Time

D.2.11 Simulation Results for Region Z_5

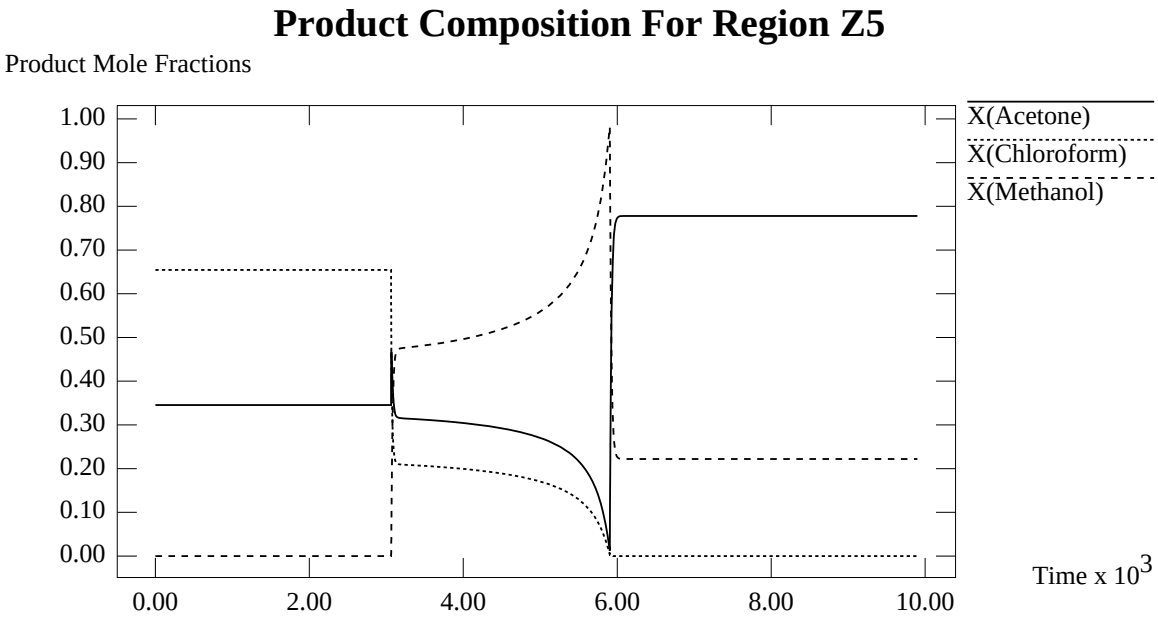

Figure D-31: Graph of Product Composition against Time

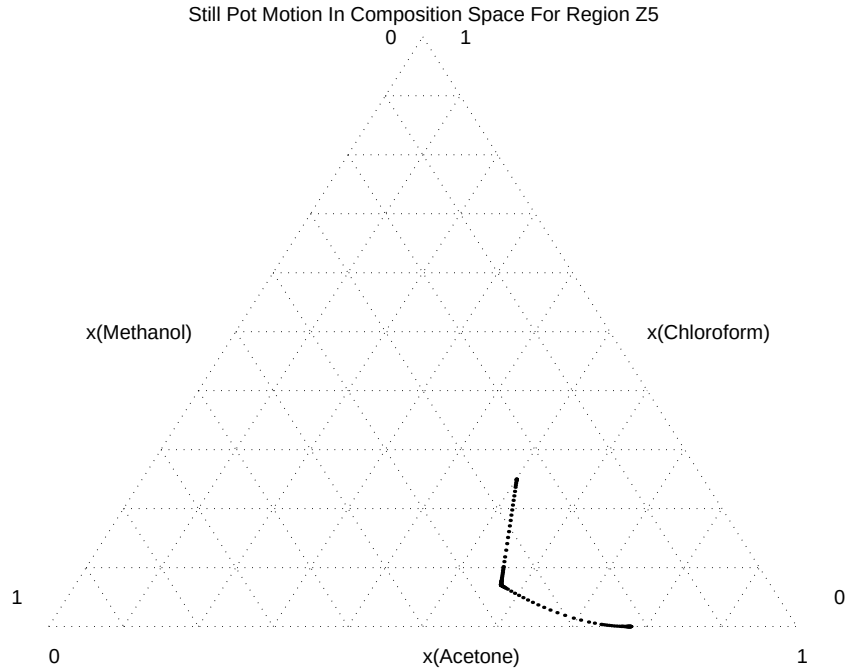

Figure D-32: Plot of Still Pot Motion in Composition Space

D.2.12 Simulation Results for Region Z_6

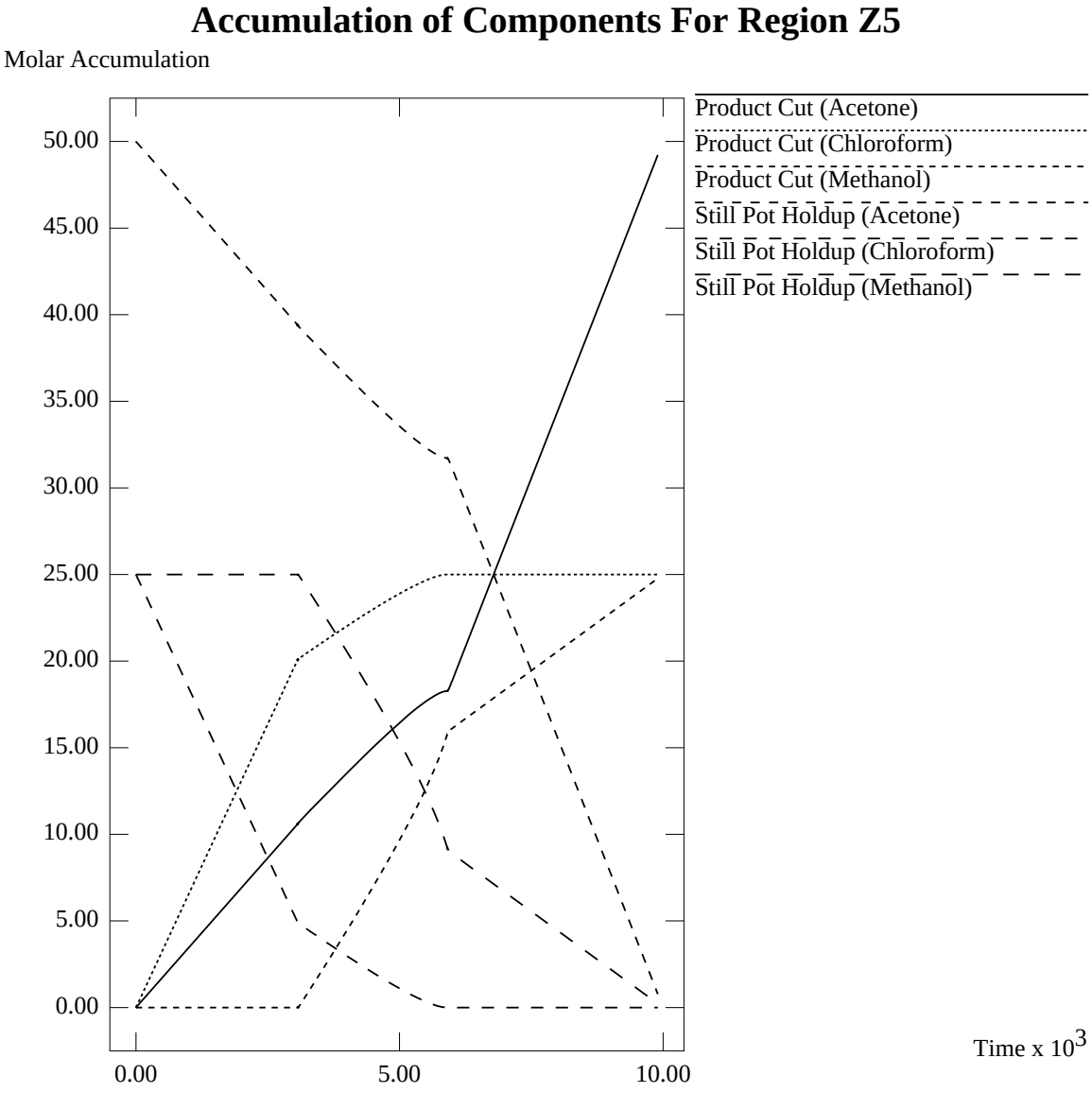

Figure D-33: Graph of Accumulation of Each Component against Time

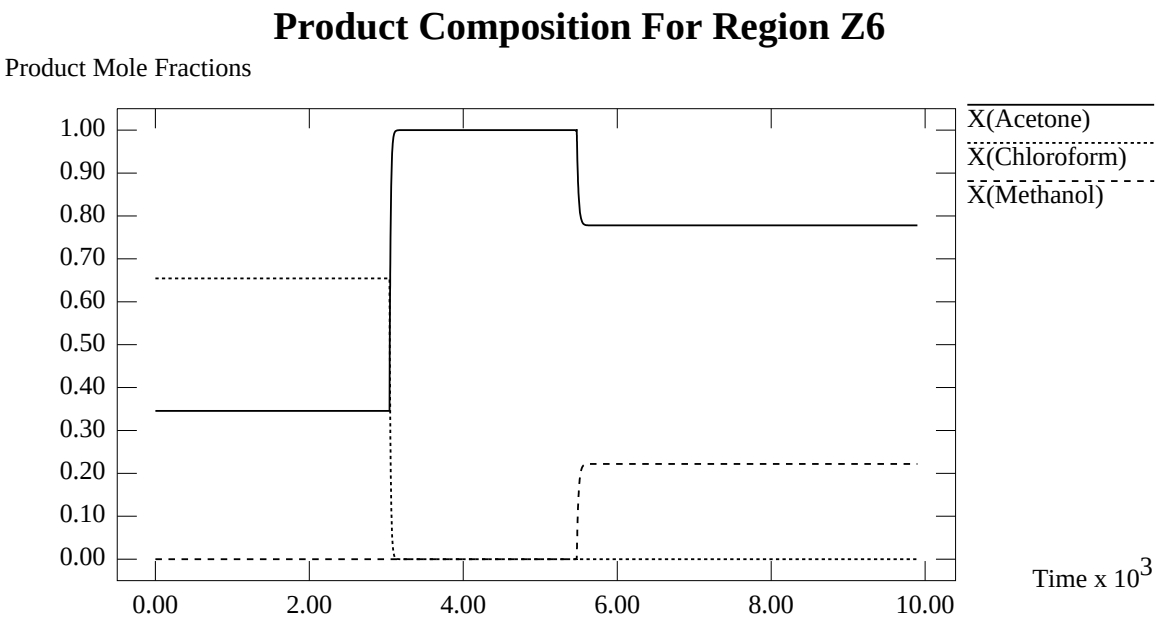

Figure D-34: Graph of Product Composition against Time

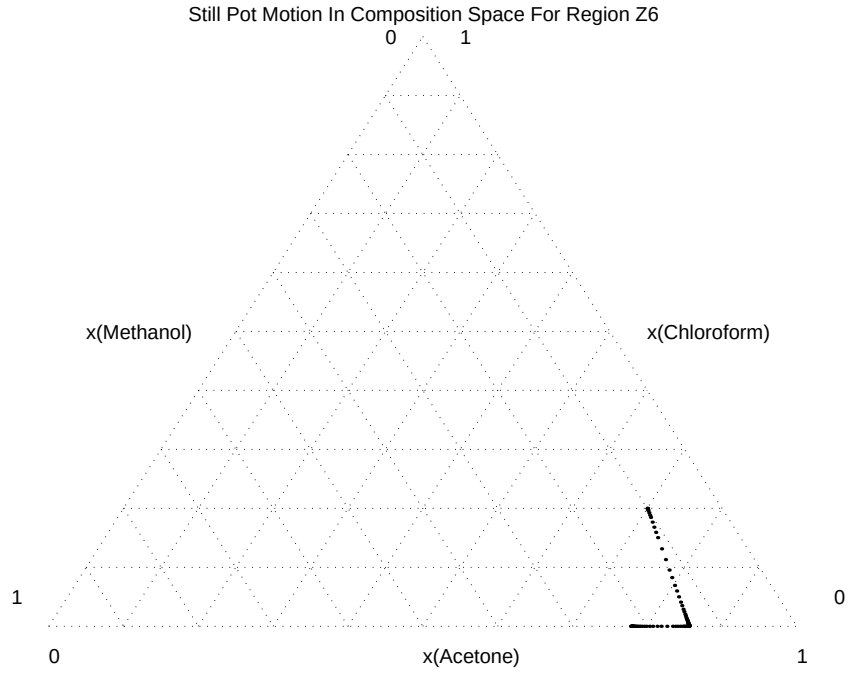

Figure D-35: Plot of Still Pot Motion in Composition Space

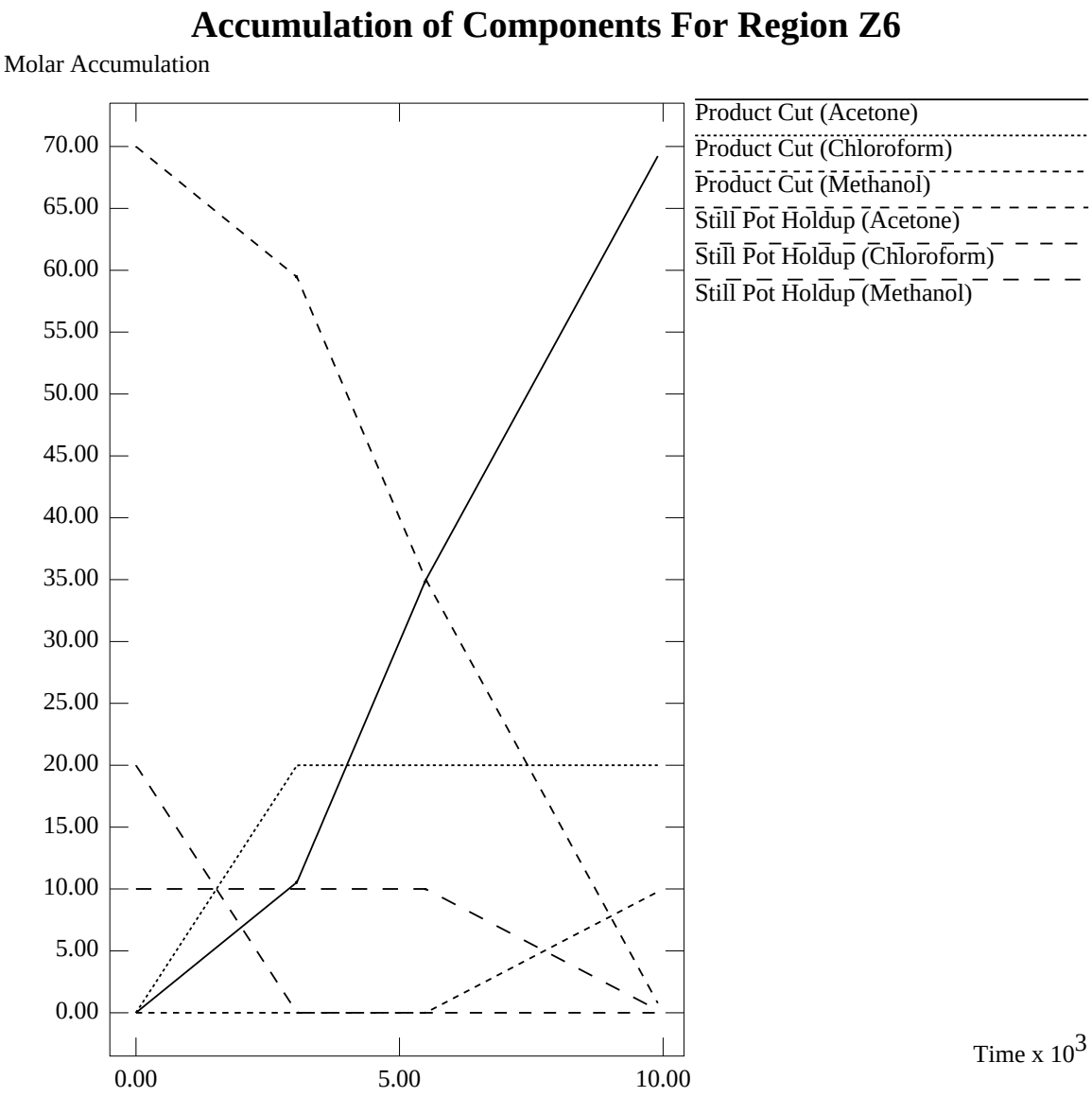

Figure D-36: Graph of Accumulation of Each Component against Time

D.3 Product Sequences Expected For Each Middle Vessel Batch Distillation Region in the Presence of Straight Line Boundaries

Summarized in Table D.5 are the expected product sequences for each of the regions χ_1 through chi_{24} for the ternary system of Acetone, Chloroform and Methanol studied in Chapter 6. As defined earlier, the first term in the square bracket indicates the distillate product drawn from the middle vessel column, while the second term indicates the bottoms product drawn from the middle vessel column. A, C, M indicate pure products acetone, chloroform and methanol respectively. AC, AM, and CM indicate the binary azeotropes acetone-chloroform, acetone-methanol, and chloroform-methanol respectively. Finally, ACM represents the ternary azeotrope of acetone-chloroform-methanol. The composition for each of these azeotropes are categorized in detail within Appendix B.

Due to the extreme stiffness of the system of equations describing the dynamic model of the middle vessel column between product cuts, the simulations for regions X9 through X13 failed during the numerical integration of the model equations. However, the results for regions X9 through X13 prior to the simulation failures are presented. These results also correspond to the expected behavior of a middle vessel column.

As was noted in Chapter 6, due to the presence of highly curved boundaries in the Acetone-Chloroform-Methanol system, the product cuts which result from the operation of the middle vessel column at $\lambda = \frac{1}{2}$ does not correspond exactly to the sequence enumerated in Table D.5. This happens particularly when the still pot composition encounters a middle vessel batch distillation boundary that is a curved stable or unstable separatrix of the simple distillation residue curve map, and is forced to trace a route along this middle vessel batch distillation boundary (as explained in Chapter 6). For example, the resulting composition for the expected ACM cut thus tends not to be the ACM azeotrope composition, but rather some varying ternary

Table D.5: Product Sequences Expected For Each Region χ_1 through χ_{24} in the Presence of Straight Line Boundaries, $\lambda = \frac{1}{2}$

Region	First Cut	Second Cut	Third Cut
χ_1	$[CM,M]$	$[ACM,M]$	$[M,M]$
χ_2	$[CM,M]$	$[ACM,M]$	$[ACM,ACM]$
χ_3	$[CM,M]$	$[CM,ACM]$	$[ACM,ACM]$
χ_4	$[CM,M]$	$[CM,ACM]$	$[CM,CM]$
χ_5	$[AM,M]$	$[ACM,M]$	$[M,M]$
χ_6	$[AM,M]$	$[ACM,M]$	$[ACM,ACM]$
χ_7	$[AM,M]$	$[AM,ACM]$	$[ACM,ACM]$
χ_8	$[AM,M]$	$[AM,ACM]$	$[AM,AM]$
χ_9	$[CM,AC]$	$[CM,C]$	$[CM,CM]$
χ_{10}	$[CM,AC]$	$[CM,C]$	$[C,C]$
χ_{11}	$[CM,AC]$	$[C,AC]$	$[C,C]$
χ_{12}	$[CM,AC]$	$[C,AC]$	$[AC,AC]$
χ_{13}	$[CM,AC]$	$[CM,ACM]$	$[CM,CM]$
χ_{14}	$[CM,AC]$	$[CM,ACM]$	$[ACM,ACM]$
χ_{15}	$[CM,AC]$	$[ACM,AC]$	$[AC,AC]$
χ_{16}	$[CM,AC]$	$[ACM,AC]$	$[ACM,ACM]$
χ_{17}	$[AM,AC]$	$[ACM,AC]$	$[ACM,ACM]$
χ_{18}	$[AM,AC]$	$[ACM,AC]$	$[AC,AC]$
χ_{19}	$[AM,AC]$	$[AM,ACM]$	$[ACM,ACM]$
χ_{20}	$[AM,AC]$	$[AM,ACM]$	$[AM,AM]$
χ_{21}	$[AM,AC]$	$[AM,A]$	$[AM,AM]$
χ_{22}	$[AM,AC]$	$[AM,A]$	$[A,A]$
χ_{23}	$[AM,AC]$	$[A,AC]$	$[A,A]$
χ_{24}	$[AM,AC]$	$[A,AC]$	$[AC,AC]$

mixture composition which allows the mass balance around the column to be satisfied while the still pot composition traces out a route along the middle vessel batch distillation boundary. At times, this mixture might even involve a pure component as the separatrices are so curved that they are tangential to the composition simplex edges as the separatrix approaches the fixed points. Based on the limiting analysis developed in Chapter 5 in the presence of curved separatrices, the resulting product sequence, in the presence of the curved separatrices, is enumerated in Table D.6 for each of the regions χ_1 through χ_{24}. In Table D.6, a suffix of "mix" following the indicated product composition indicates a mixture that is close to, but not quite the expected composition; a direct result of the curvature of the middle vessel batch distillation boundaries. As indicated in Chapter 6, these middle vessel batch distillation boundaries correspond to the operation of the column at $\lambda = \frac{1}{2}$, and is a hybrid mix of the batch distillation boundaries for the stripper and the rectifier.

D.4 Simulation Results From ABACUSS Model of Various Initial Still Pot Composition in Each of the 24 Middle Vessel Regions

Summarized in this section are the results of the simulations obtained for initial still pot compositions in each of the 24 middle vessel regions enumerated for the Acetone-Chloroform-Methanol system. It should be noted the behavior of a composition point anywhere in each of the 24 regions is indicative of the behavior of any of the composition points in that region. Thus, simulations were conducted for one initial still pot composition in each of the regions. The initial still pot composition chosen for each region are summarized in Table D.7.

Operating conditions for each simulation were kept constant so as to ensure that the results could be comparable to each other. The pertinent operating parameters used are thus summarized in Table D.8. The behavior of the column as $NS \to \infty$ and the reflux and reboil ratios $\to \infty$, was modelled by using a reflux/reboil ratio of

Table D.6: Product Sequences Expected For Each Region χ_1 through χ_{24} in the Presence of Curved Boundaries, $\lambda = \frac{1}{2}$

Region	First Cut	Second Cut	Third Cut
χ_1	$[CM,M]$	$[ACM\text{-mix},M]$	$[M,M]$
χ_2	$[CM,M]$	$[ACM\text{-mix},M]$	$[ACM,ACM]$
χ_3	$[CM,M]$	$[CM,ACM\text{-mix}]$	$[ACM,ACM]$
χ_4	$[CM,M]$	$[CM,ACM\text{-mix}]$	$[CM,CM]$
χ_5	$[AM,M]$	$[ACM\text{-mix},M]$	$[M,M]$
χ_6	$[AM,M]$	$[ACM\text{-mix},M]$	$[ACM,ACM]$
χ_7	$[AM,M]$	$[AM,ACM\text{-mix}]$	$[ACM,ACM]$
χ_8	$[AM,M]$	$[AM,ACM\text{-mix}]$	$[AM,AM]$
χ_9	$[CM,AC]$	$[CM,C]$	$[CM,CM]$
χ_{10}	$[CM,AC]$	$[CM,C]$	$[C,C]$
χ_{11}	$[CM,AC]$	$[C,AC]$	$[C,C]$
χ_{12}	$[CM,AC]$	$[C,AC]$	$[AC,AC]$
χ_{13}	$[CM,AC]$	$[CM,ACM\text{-mix}]$	$[CM,CM]$
χ_{14}	$[CM,AC]$	$[CM,ACM\text{-mix}]$	$[ACM,ACM]$
χ_{15}	$[CM,AC]$	$[ACM\text{-mix},AC]$	$[AC,AC]$
χ_{16}	$[CM,AC]$	$[ACM\text{-mix},AC]$	$[ACM,ACM]$
χ_{17}	$[AM,AC]$	$[ACM\text{-mix},AC]$	$[ACM,ACM]$
χ_{18}	$[AM,AC]$	$[ACM\text{-mix},AC]$	$[AC,AC]$
χ_{19}	$[AM,AC]$	$[AM,ACM\text{-mix}]$	$[ACM,ACM]$
χ_{20}	$[AM,AC]$	$[AM,ACM\text{-mix}]$	$[AM,AM]$
χ_{21}	$[AM,AC]$	$[AM,A]$	$[AM,AM]$
χ_{22}	$[AM,AC]$	$[AM,A]$	$[A,A]$
χ_{23}	$[AM,AC]$	$[A,AC]$	$[A,A]$
χ_{24}	$[AM,AC]$	$[A,AC]$	$[AC,AC]$

Table D.7: Initial Still Pot Compositions Chosen for Each of the Middle Vessel Regions χ_1 through χ_{24}

Region	Acetone	Chloroform	Methanol
χ_1	0.05	0.22	0.73
χ_2	0.13	0.25	0.62
χ_3	0.12	0.32	0.56
χ_4	0.05	0.43	0.52
χ_5	0.20	0.05	0.75
χ_6	0.35	0.08	0.57
χ_7	0.40	0.10	0.50
χ_8	0.55	0.03	0.42
χ_9	0.10	0.70	0.20
χ_{10}	0.09	0.78	0.13
χ_{11}	0.12	0.80	0.08
χ_{12}	0.22	0.70	0.08
χ_{13}	0.15	0.58	0.27
χ_{14}	0.20	0.50	0.30
χ_{15}	0.35	0.55	0.10
χ_{16}	0.28	0.50	0.22
χ_{17}	0.49	0.33	0.18
χ_{18}	0.53	0.37	0.10
χ_{19}	0.50	0.25	0.25
χ_{20}	0.60	0.22	0.18
χ_{21}	0.71	0.12	0.17
χ_{22}	0.78	0.15	0.07
χ_{23}	0.70	0.25	0.05
χ_{24}	0.55	0.40	0.05

Table D.8: Operating Conditions for the Middle Vessel Column Simulations, (Infinite Reflux/Reboil, Infinite Number of Trays)

Operational Parameter	Numerical Value	Units
Initial Still Pot Holdup	100	Moles
Vapor Flow Rate in Column	10	Moles/Time
Liquid Flow Rate in Column	10	Moles/Time
Distillate Product Flow Rate	0.01	Moles/Time
Bottoms Product Flow Rate	0.01	Moles/Time
Resulting Reflux Ratio	1000	Dimensionless
Resulting Reboil Ratio	1000	Dimensionless
Number of Trays in the Rectifying Section of Column	50	Dimensionless
Number of Trays in the Stripping Section of Column	50	Dimensionless
Operating Pressure in Column	1	Bar

1000, and up to 100 trays in the entire column.

In the graphs that follow, the results of the simulation for each of the regions are presented categorically, classified according to the region. The distillate product composition as a function of time, bottoms product composition as a function of time, still pot composition as a function of time, the still pot motion in the composition space, and the accumulation of components as a function of time are provided for each initial composition for each of the 24 regions enumerated.

D.4.1 Simulation Results for Region χ_1

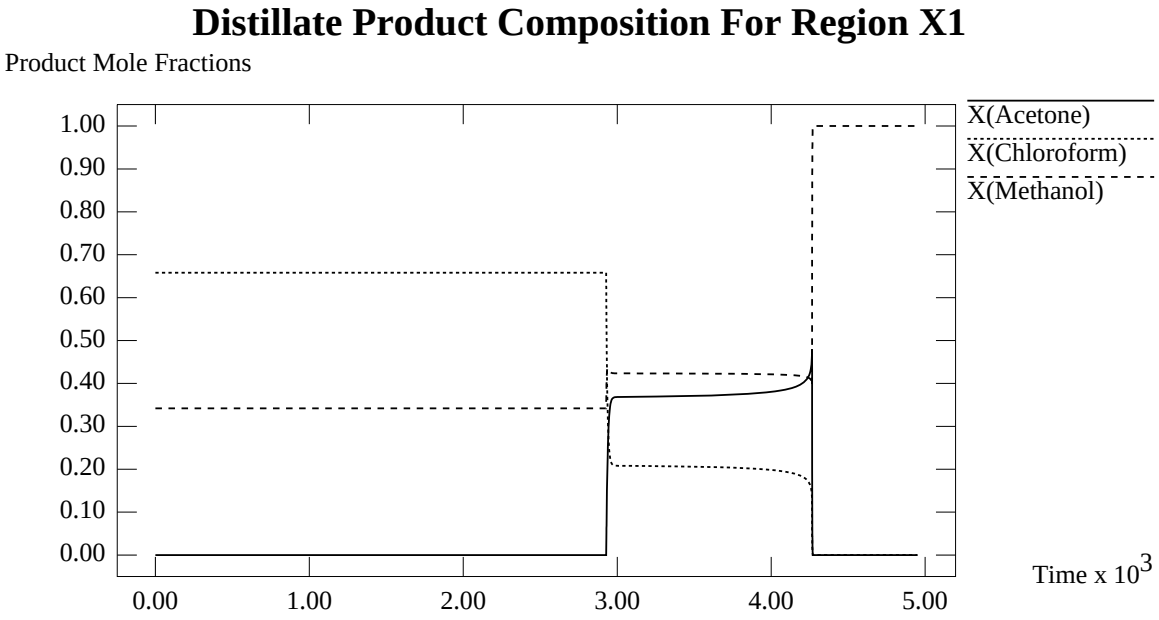

Figure D-37: Graph of Distillate Product Composition against Time

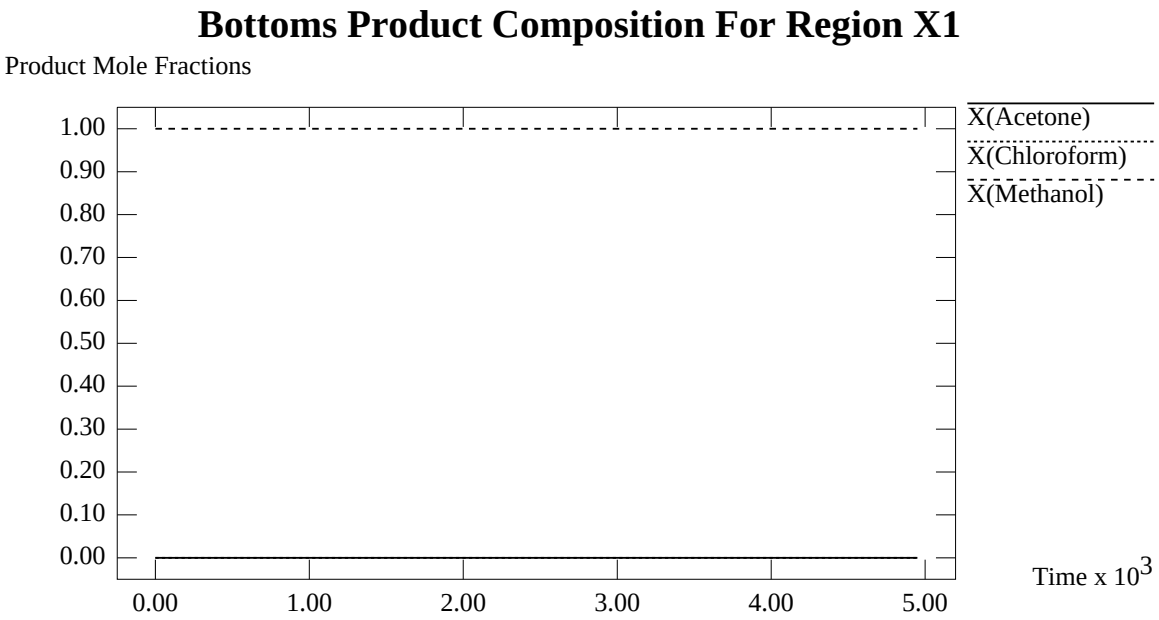

Figure D-38: Graph of Bottoms Product Composition against Time

D.4.2 Simulation Results for Region χ_2

D.4.3 Simulation Results for Region χ_3

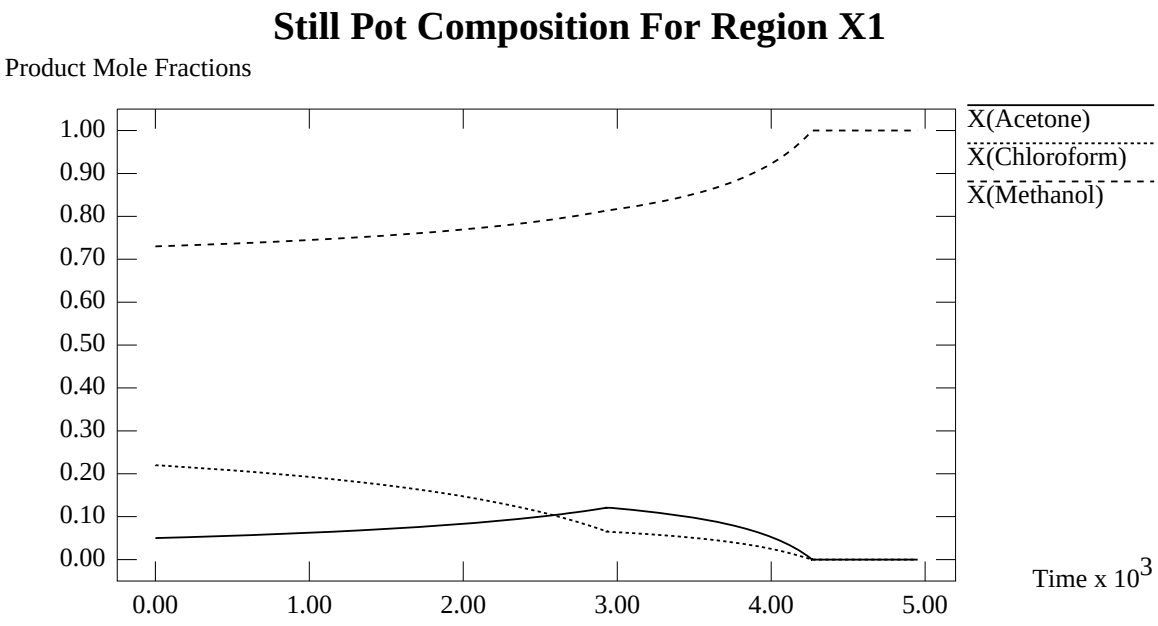

Figure D-39: Graph of Still Pot Composition against Time

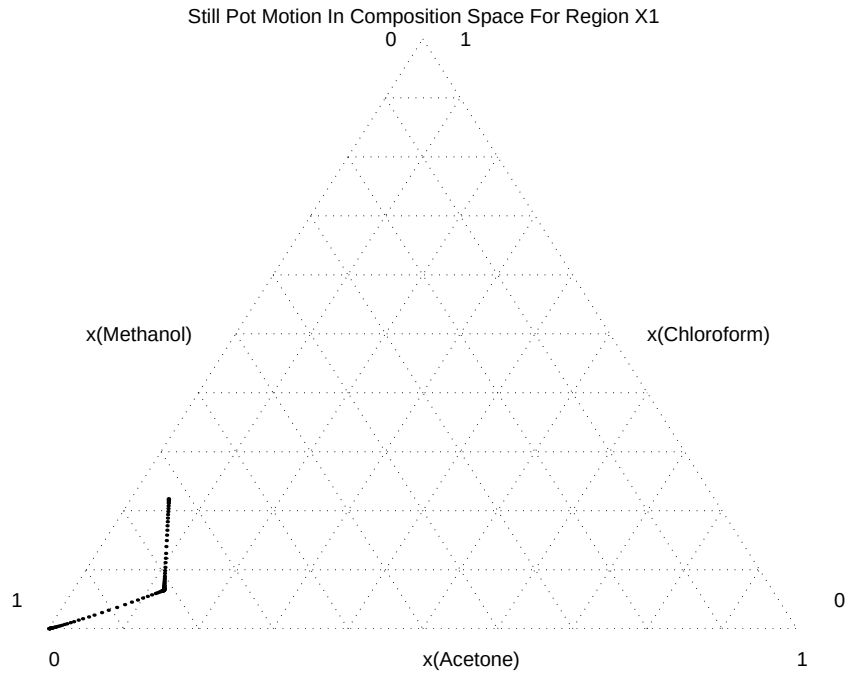

Figure D-40: Plot of Still Pot Motion in Composition Space

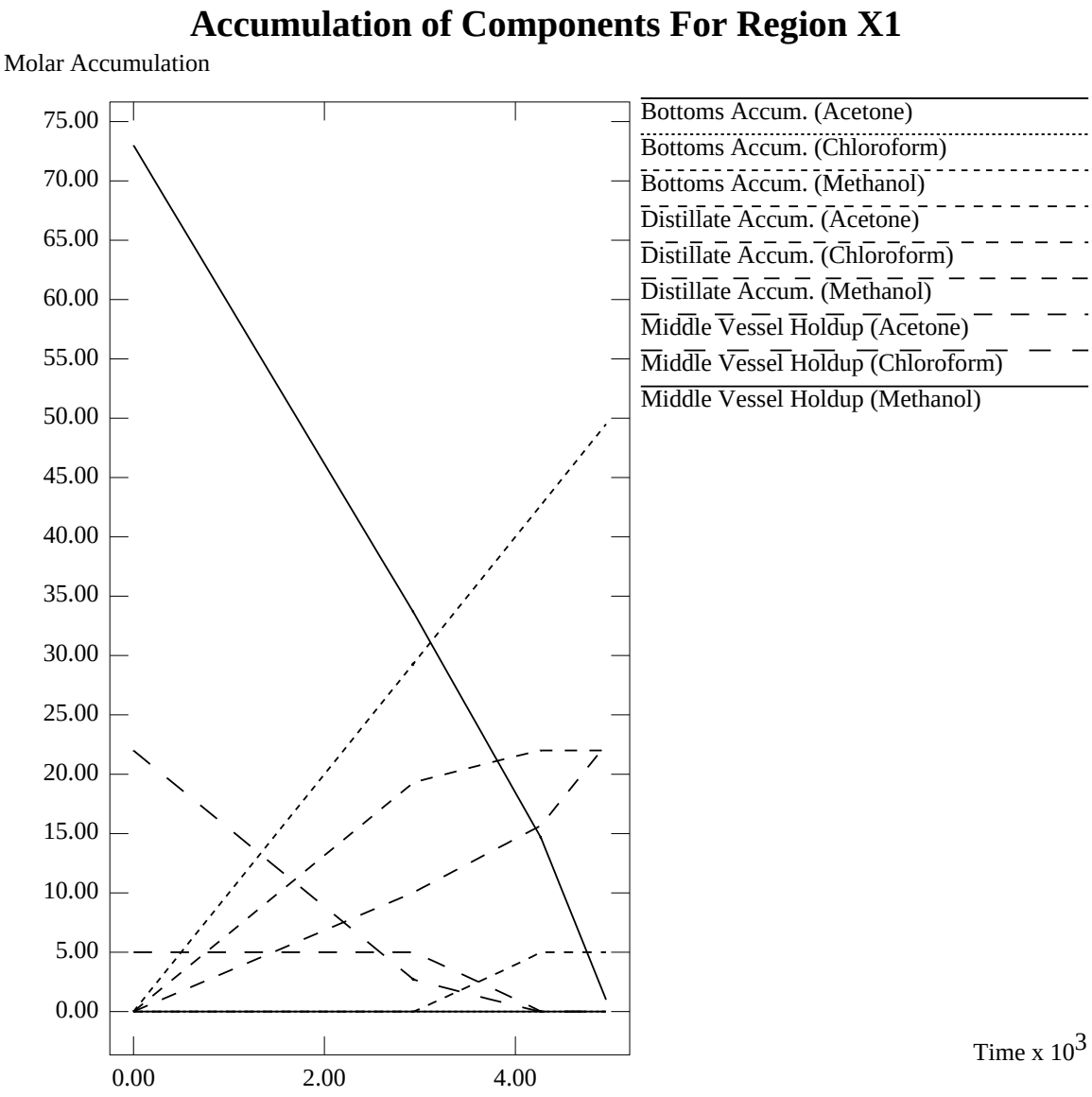

Figure D-41: Graph of Accumulation of Each Component against Time

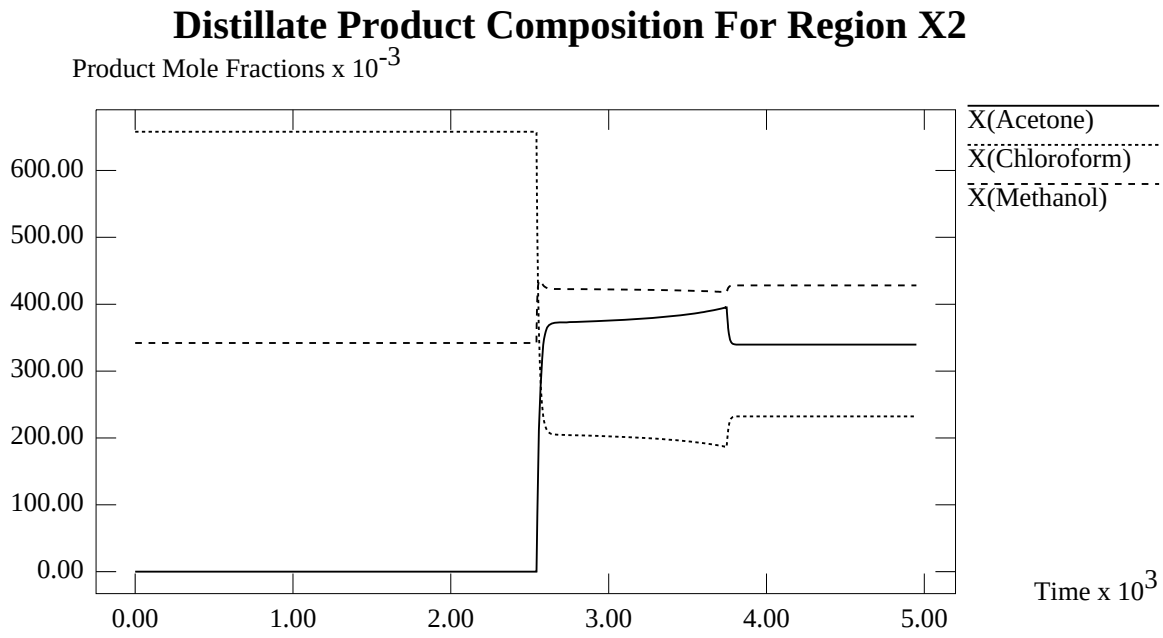

Figure D-42: Graph of Distillate Product Composition against Time

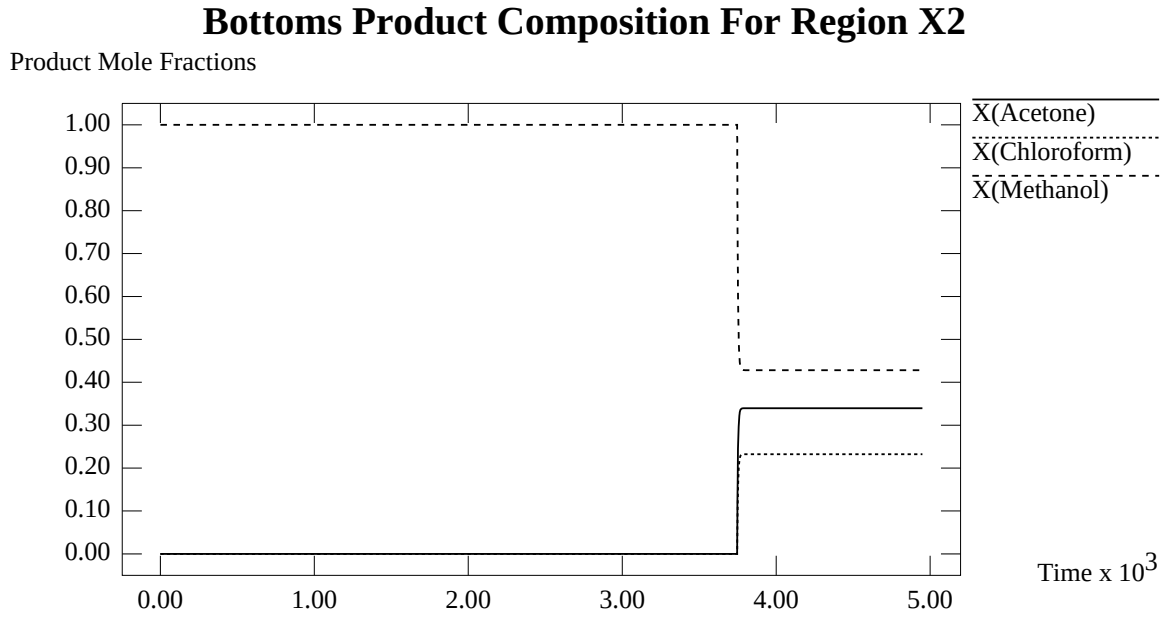

Figure D-43: Graph of Bottoms Product Composition against Time

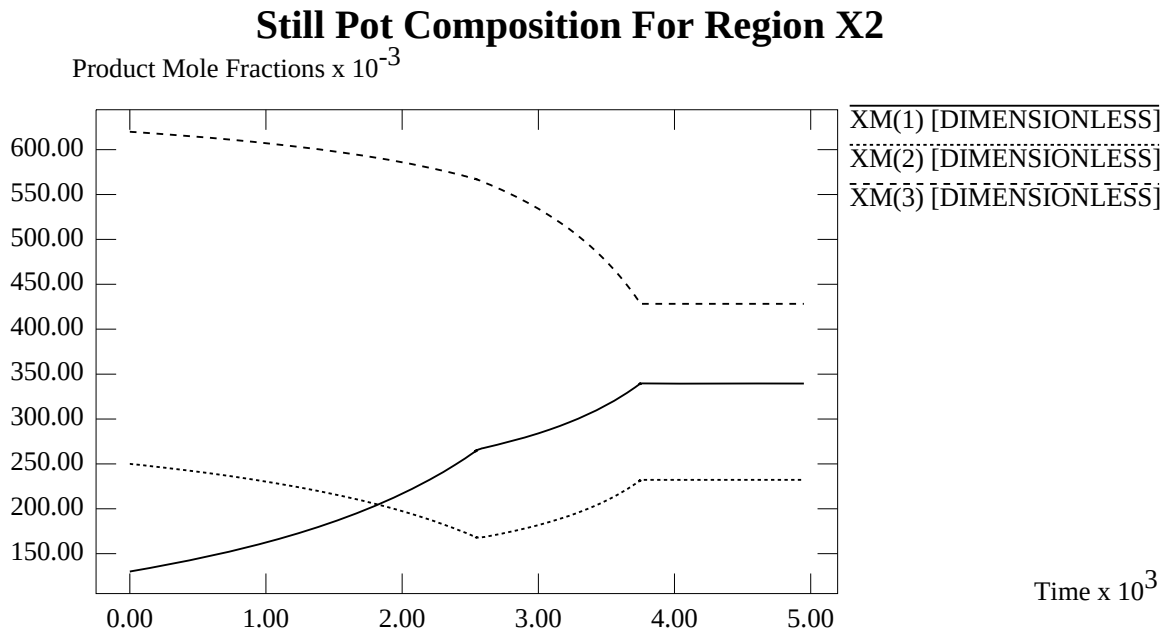

Figure D-44: Graph of Still Pot Composition against Time

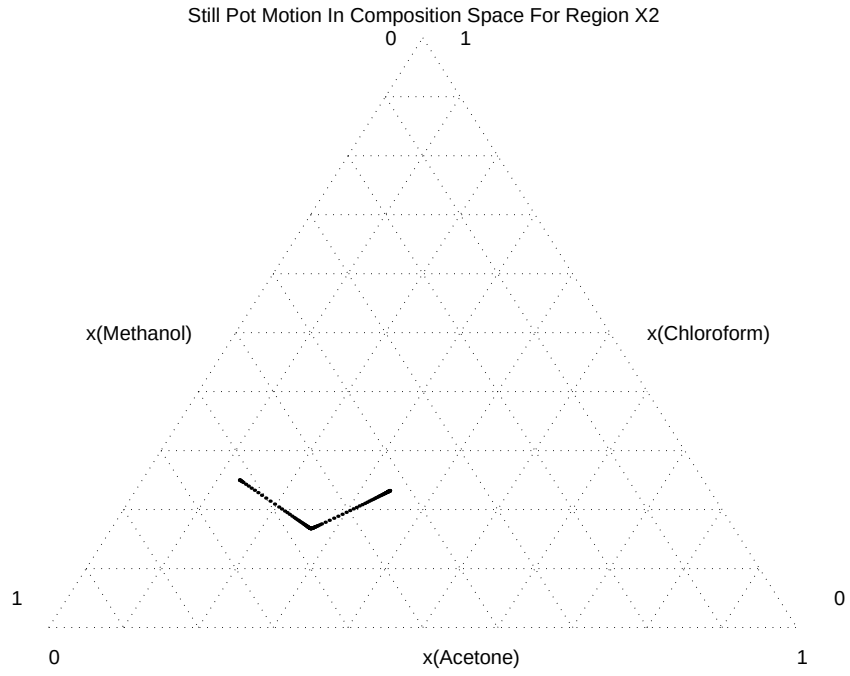

Figure D-45: Plot of Still Pot Motion in Composition Space

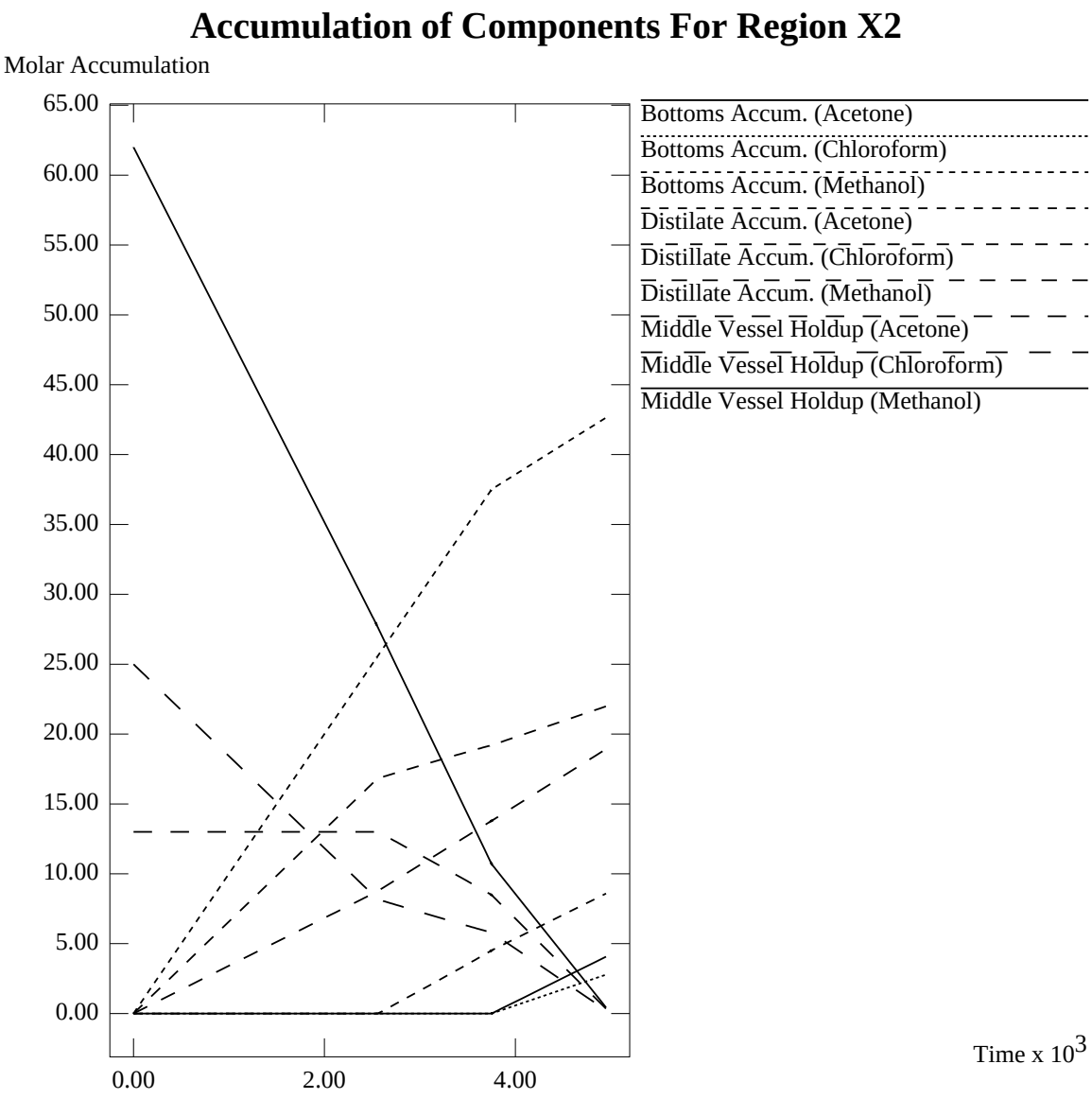

Figure D-46: Graph of Accumulation of Each Component against Time

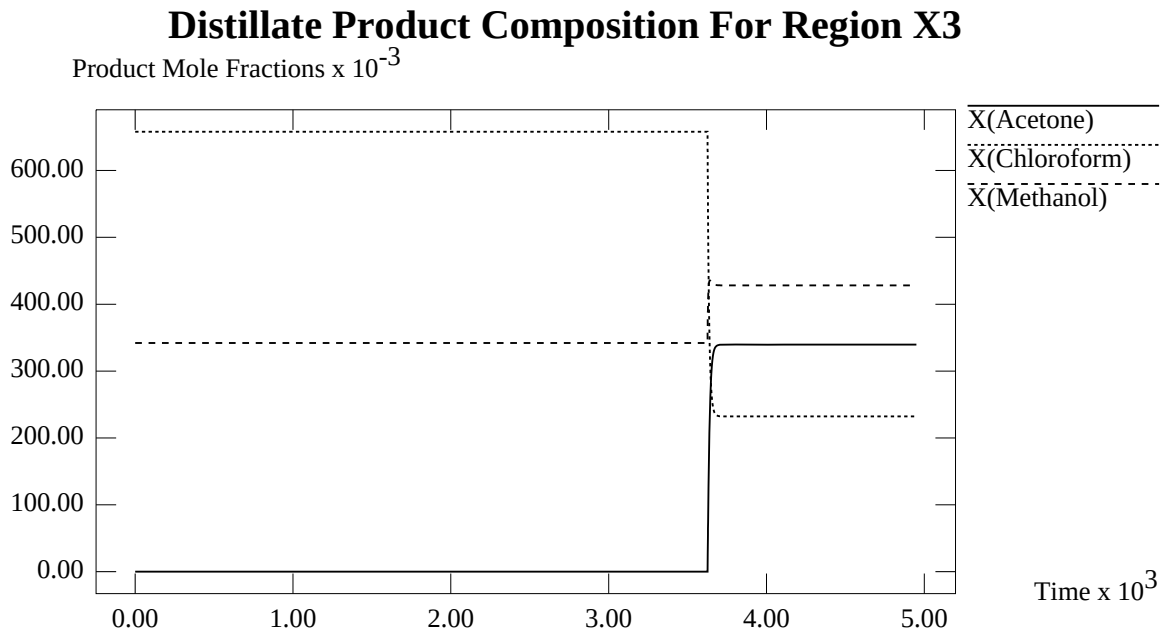

Figure D-47: Graph of Distillate Product Composition against Time

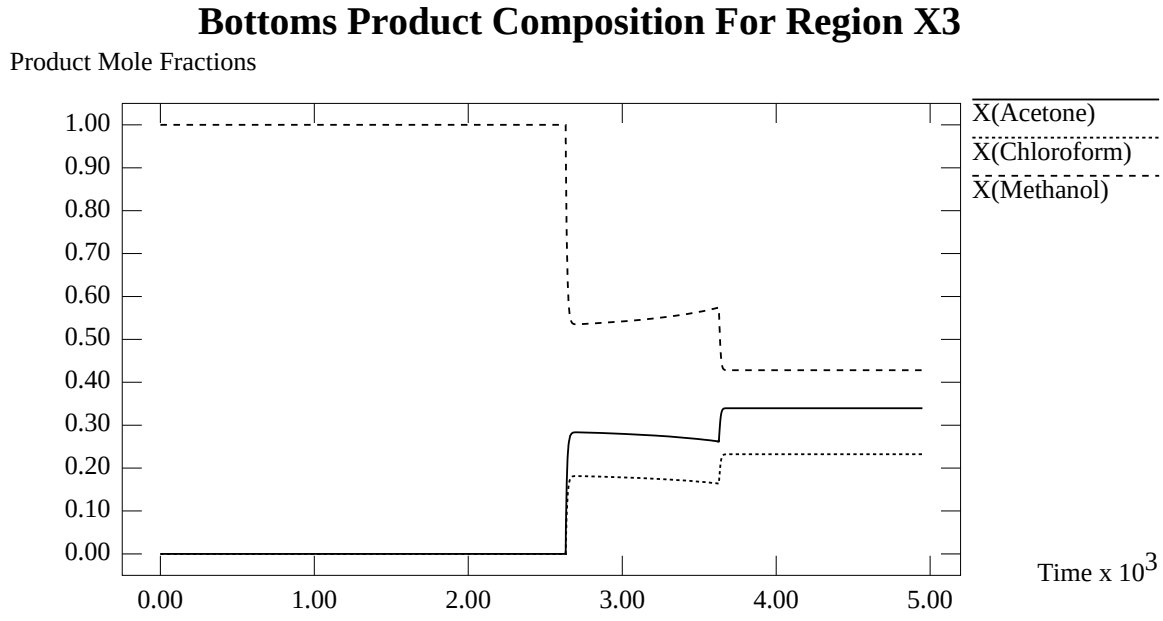

Figure D-48: Graph of Bottoms Product Composition against Time

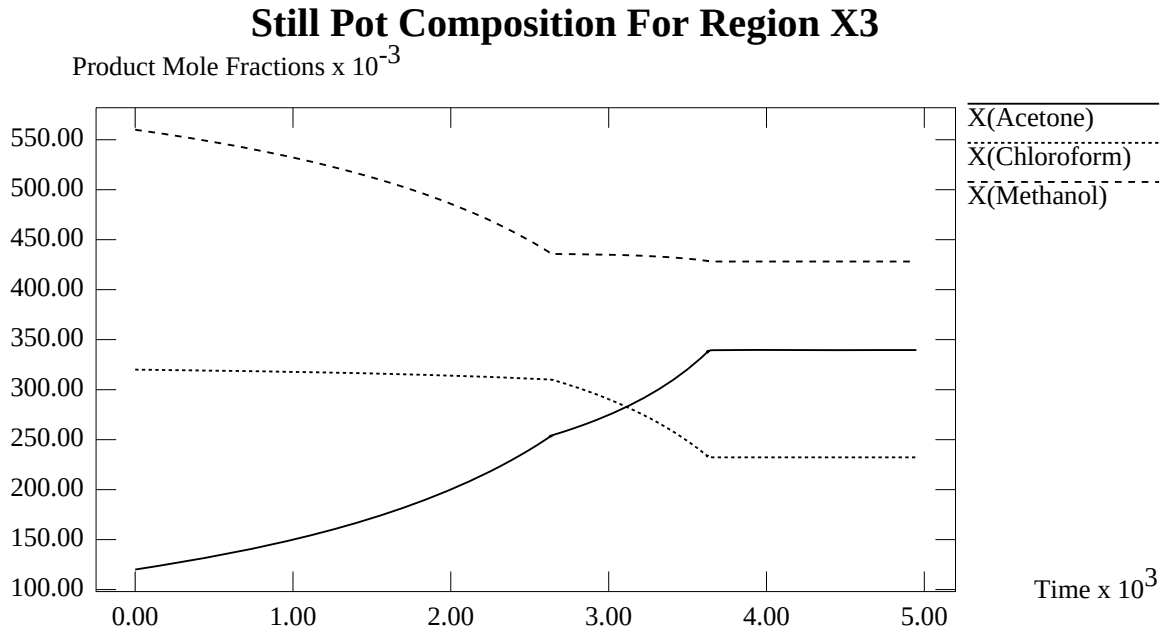

Figure D-49: Graph of Still Pot Composition against Time

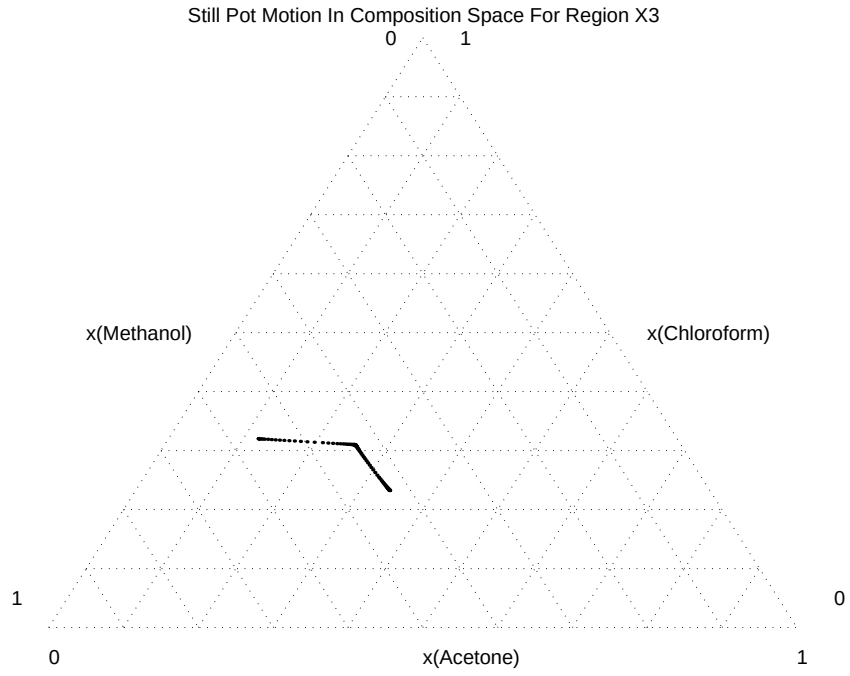

Figure D-50: Plot of Still Pot Motion in Composition Space

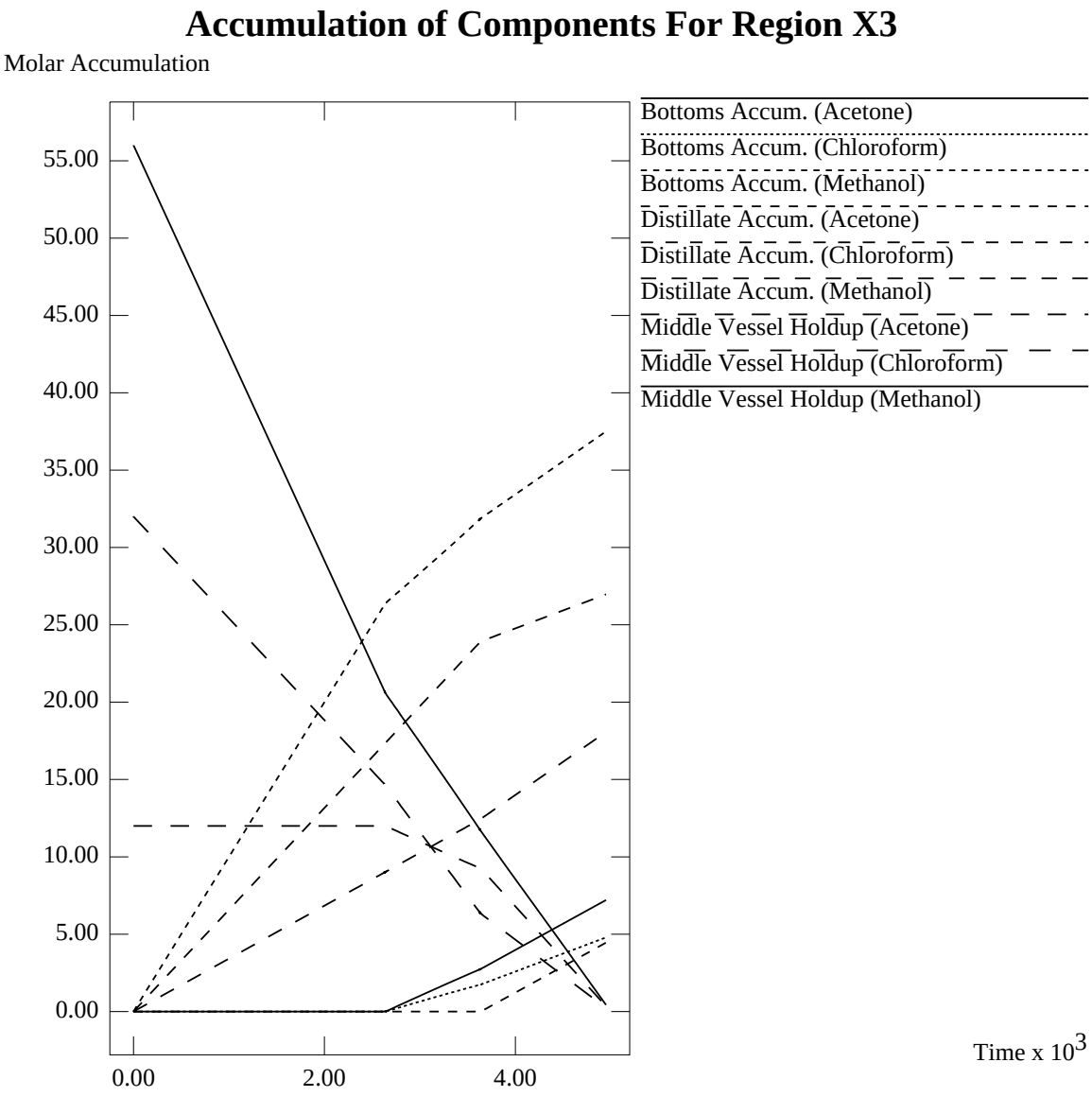

Figure D-51: Graph of Accumulation of Each Component against Time

D.4.4 Simulation Results for Region χ_4

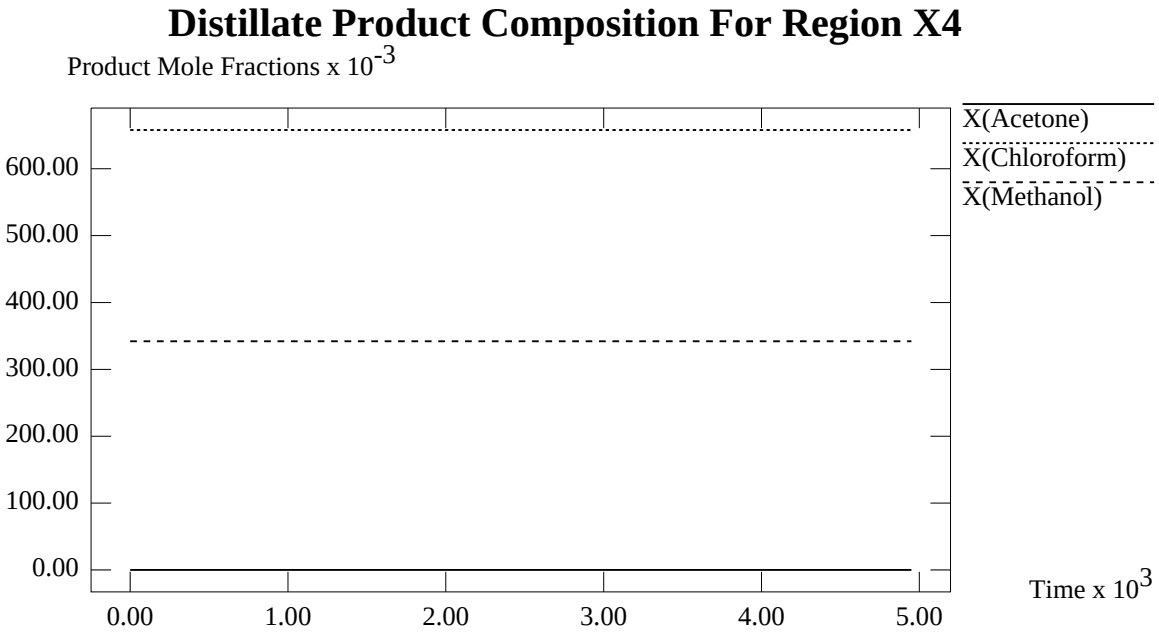

Figure D-52: Graph of Distillate Product Composition against Time

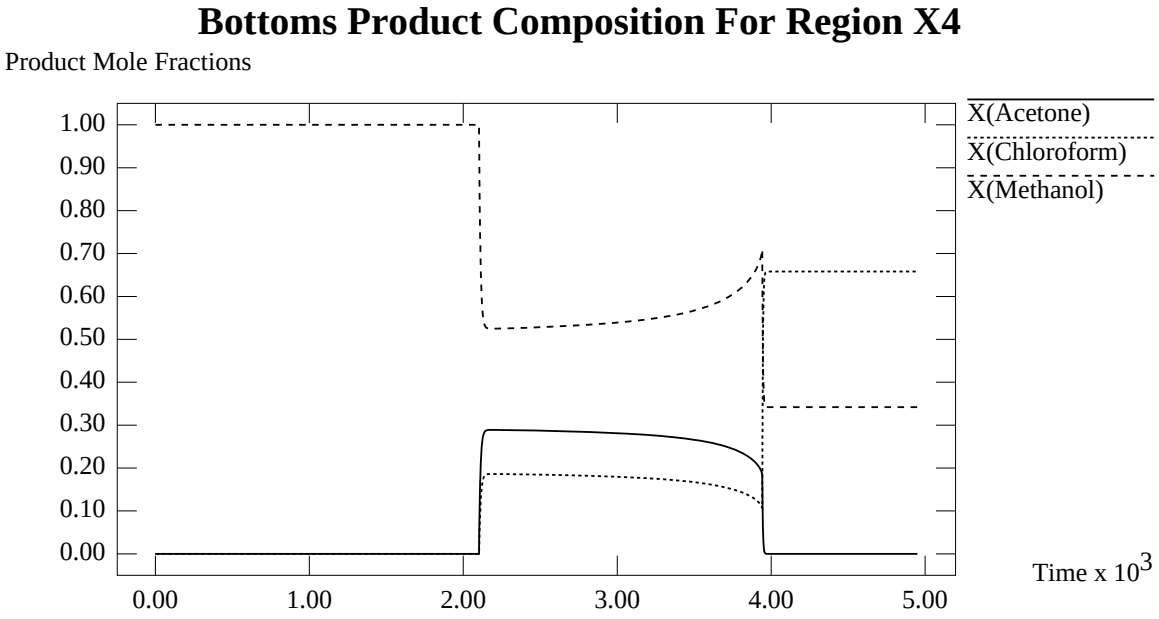

Figure D-53: Graph of Bottoms Product Composition against Time

D.4.5 Simulation Results for Region χ_5

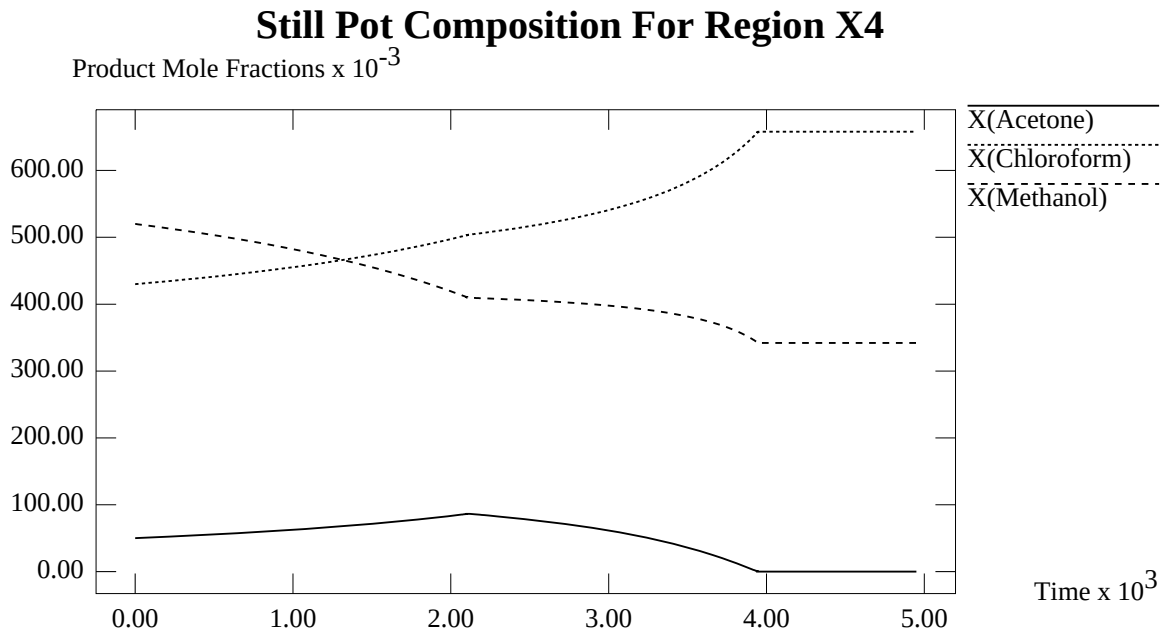

Figure D-54: Graph of Still Pot Composition against Time

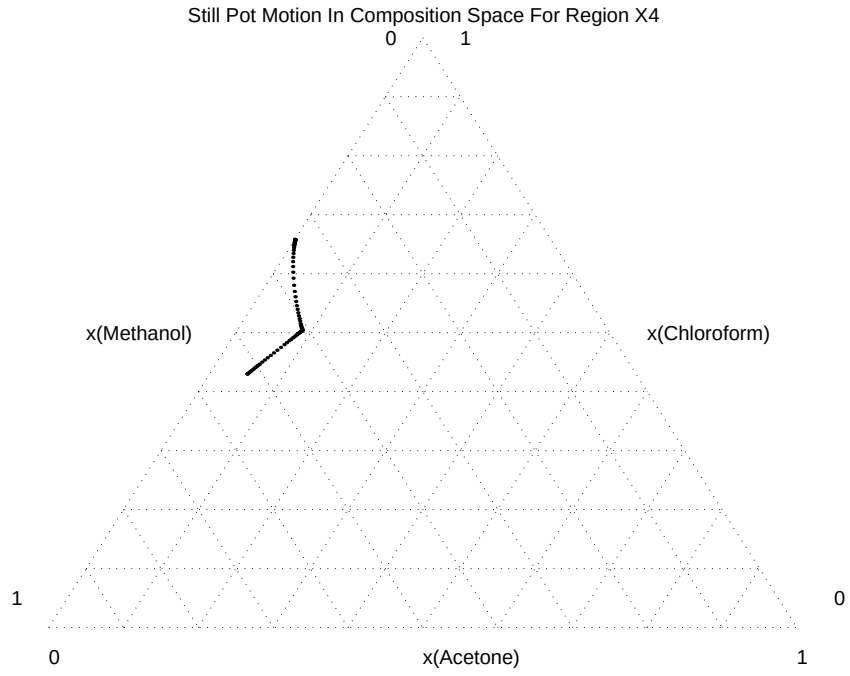

Figure D-55: Plot of Still Pot Motion in Composition Space

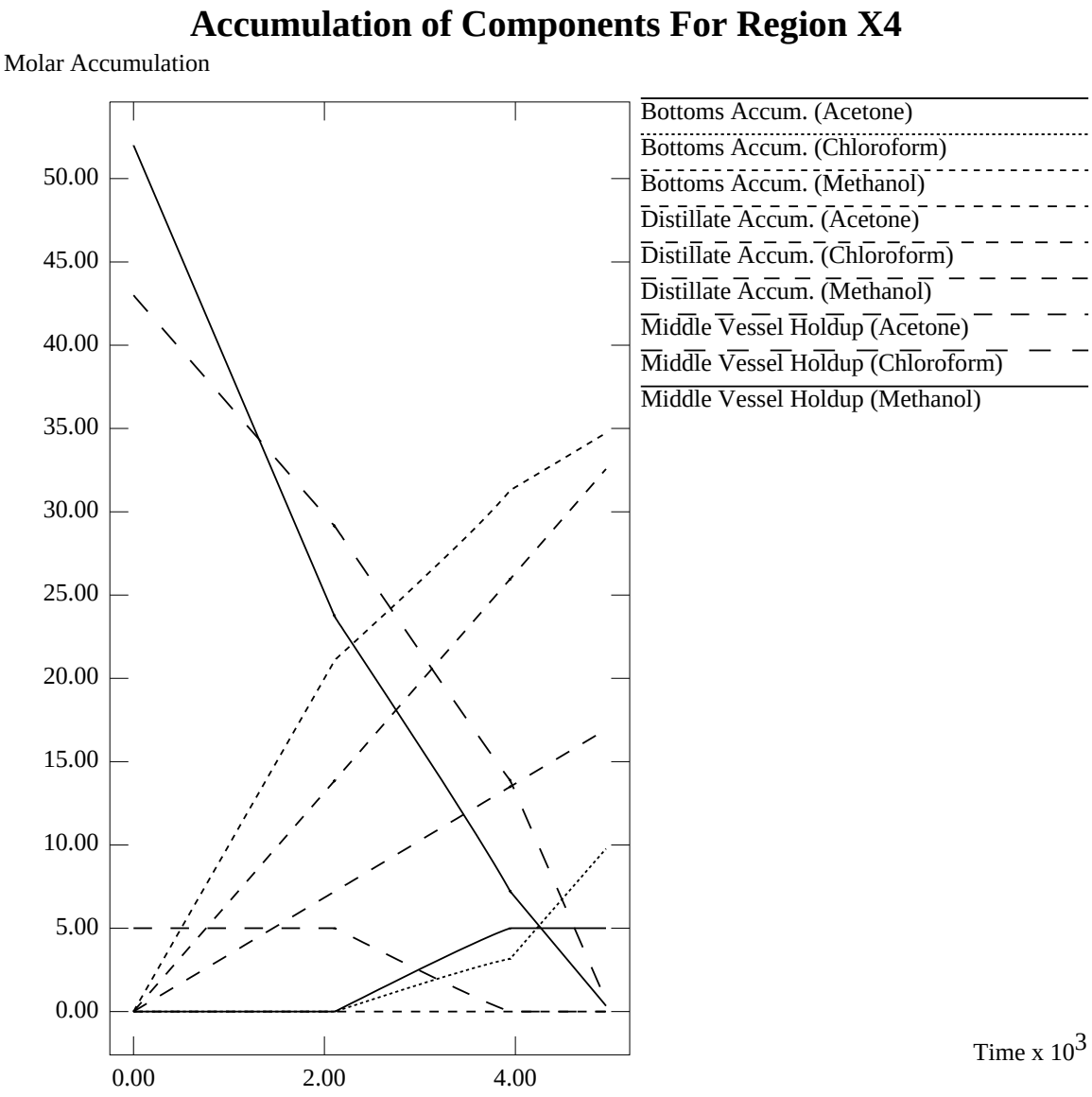

Figure D-56: Graph of Accumulation of Each Component against Time

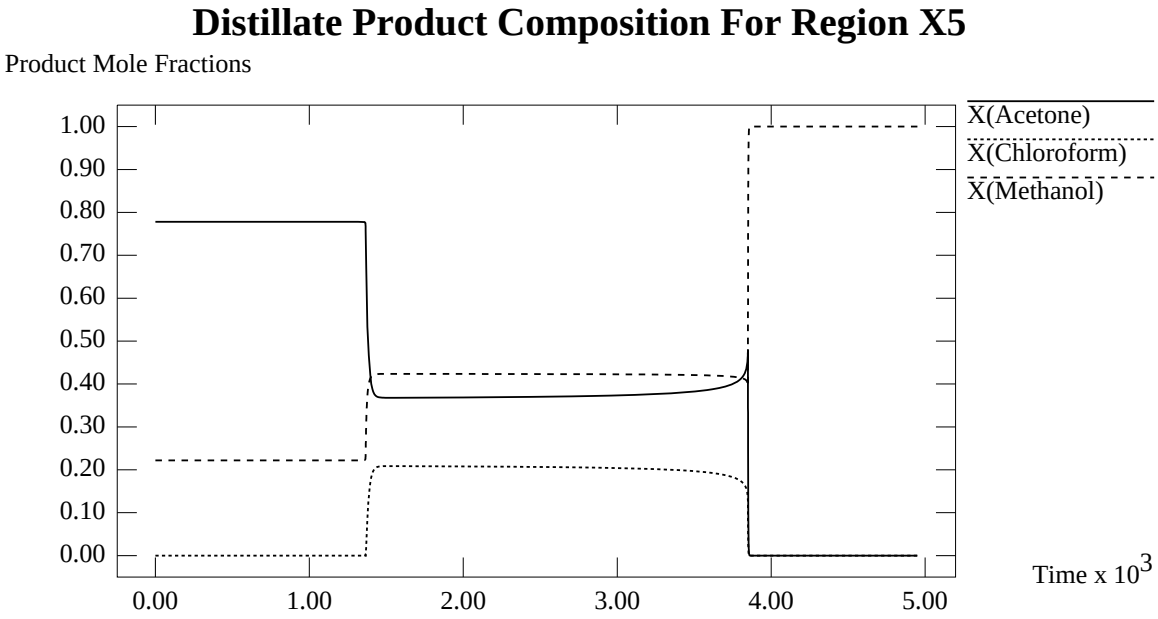

Figure D-57: Graph of Distillate Product Composition against Time

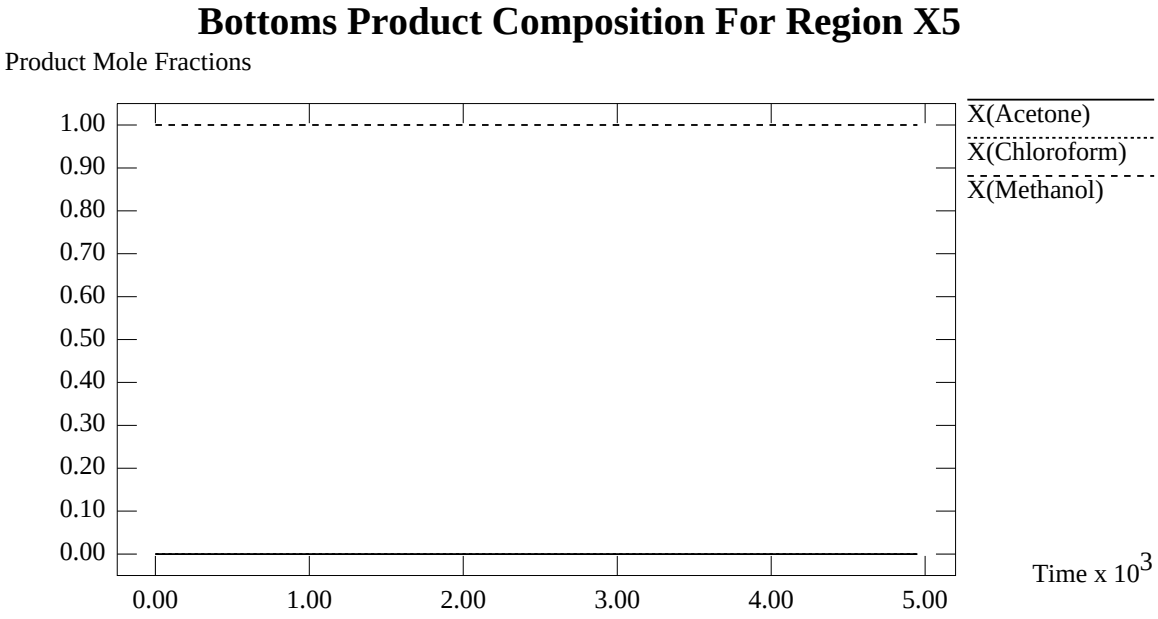

Figure D-58: Graph of Bottoms Product Composition against Time

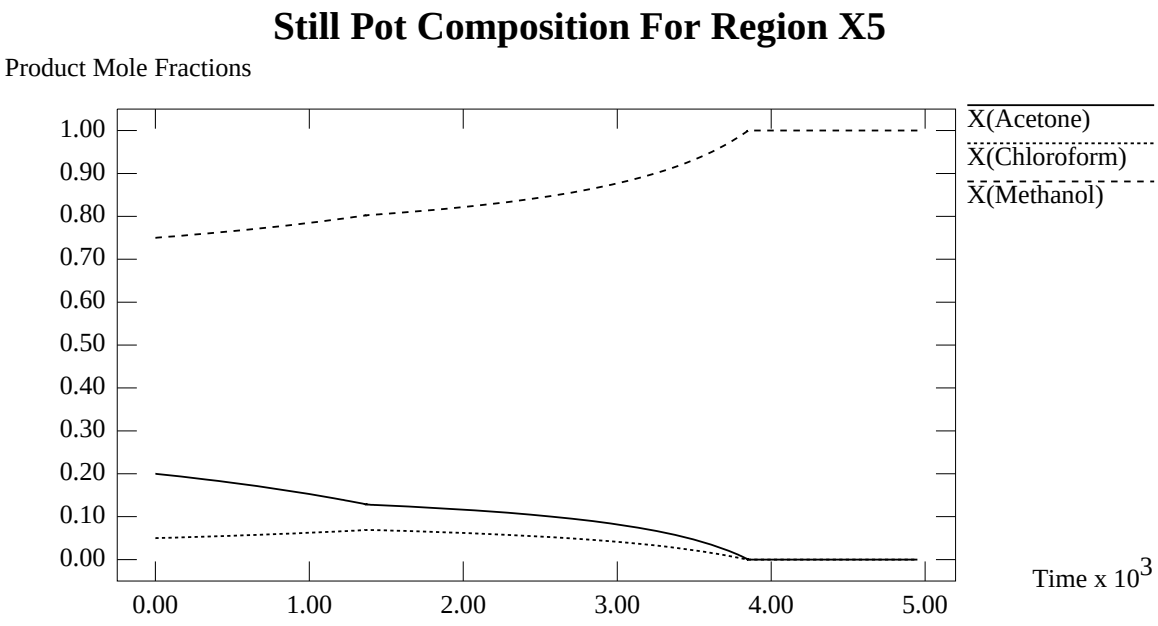

Figure D-59: Graph of Still Pot Composition against Time

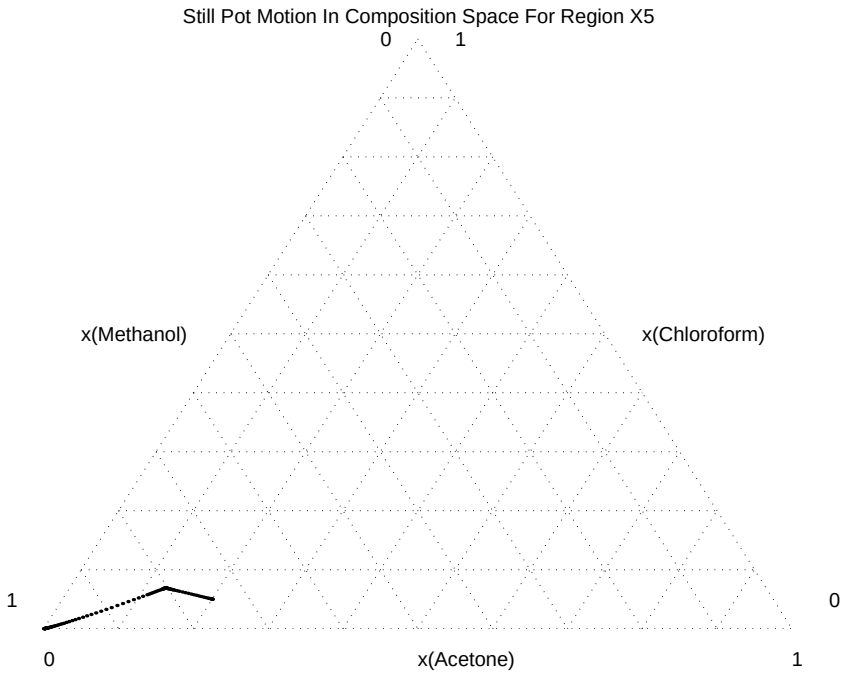

Figure D-60: Plot of Still Pot Motion in Composition Space

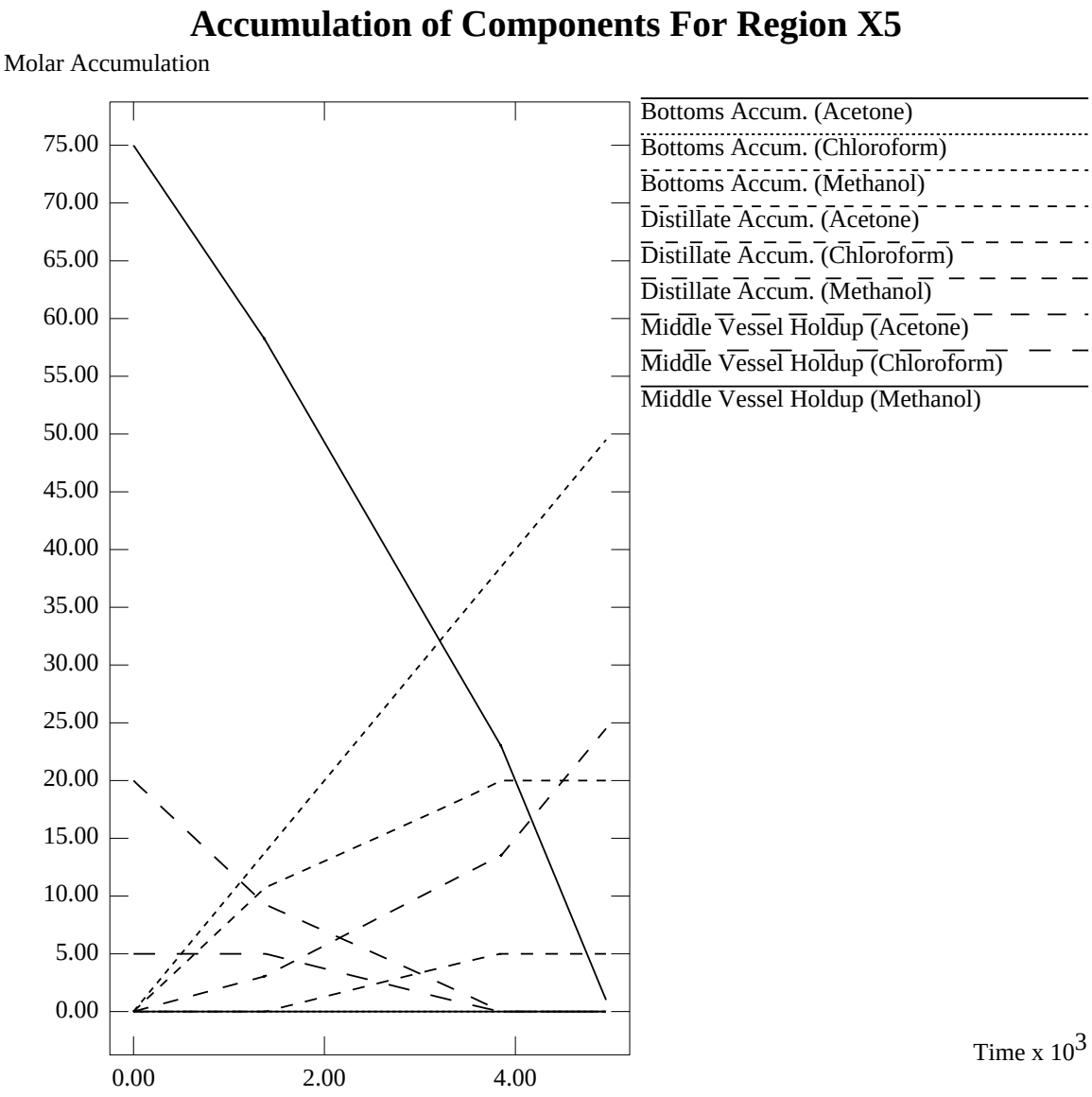

Figure D-61: Graph of Accumulation of Each Component against Time

D.4.6 Simulation Results for Region χ_6

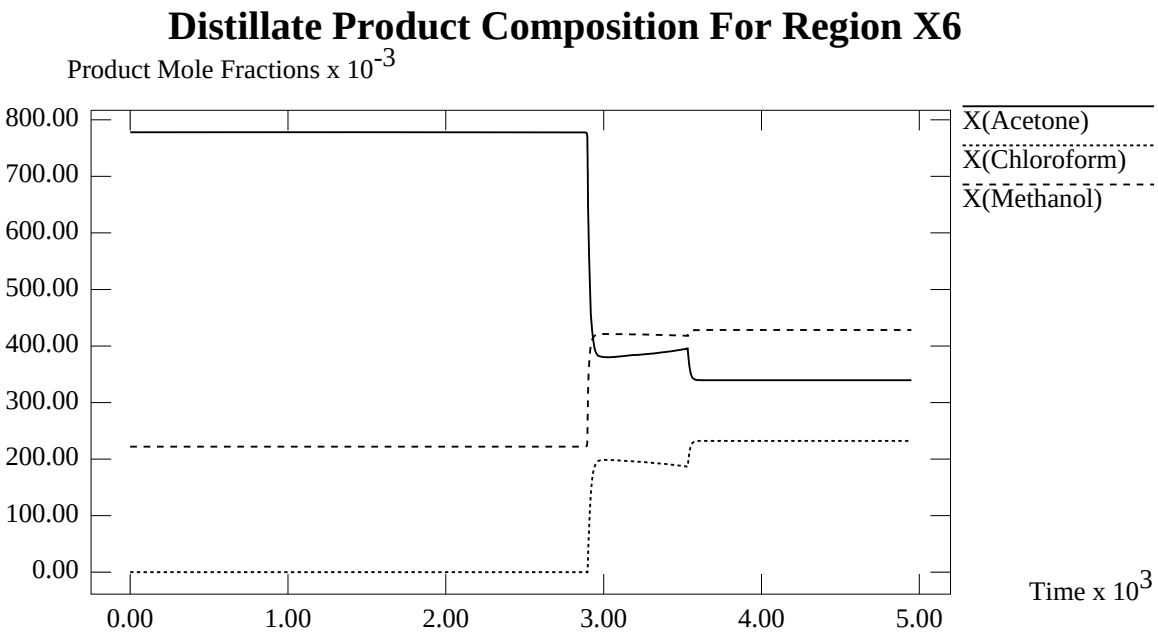

Figure D-62: Graph of Distillate Product Composition against Time

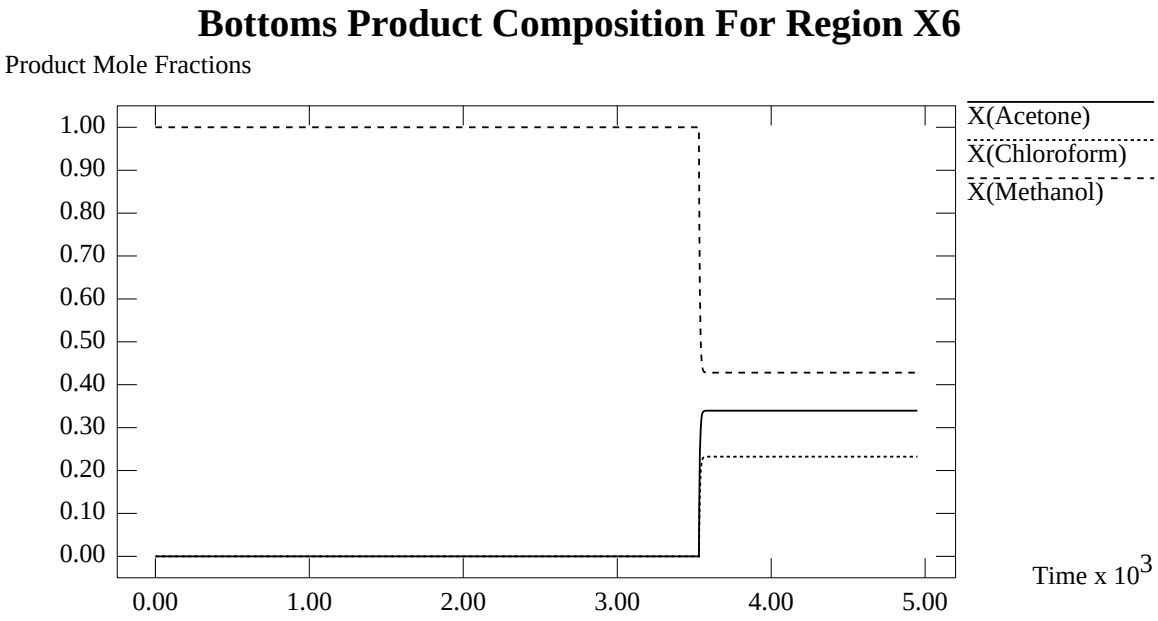

Figure D-63: Graph of Bottoms Product Composition against Time

D.4.7 Simulation Results for Region χ_7

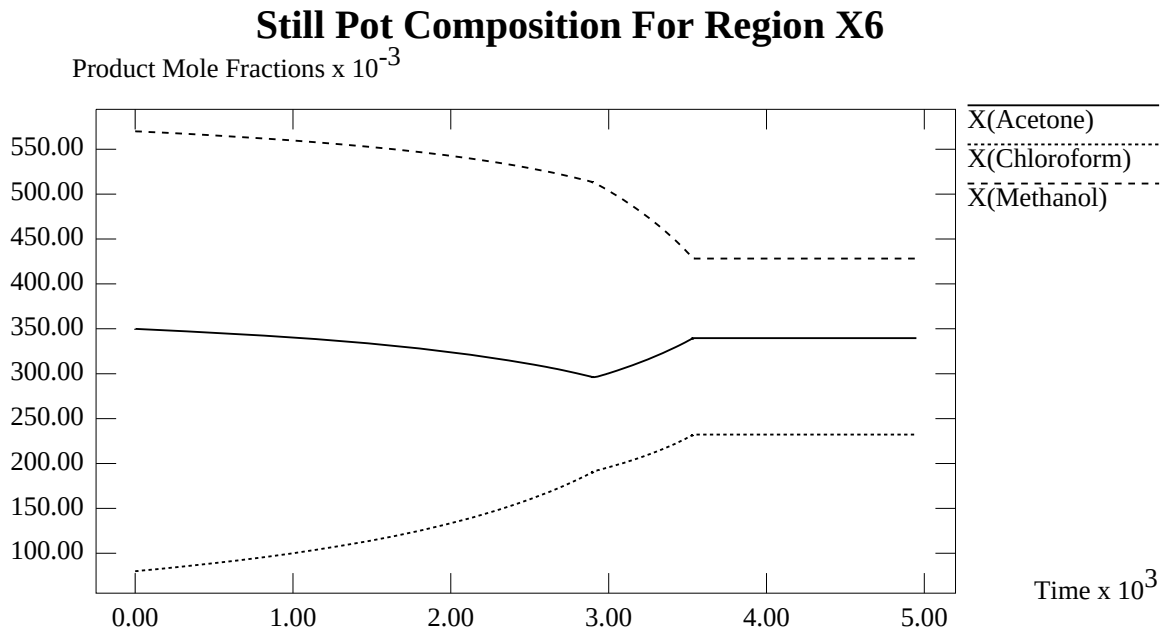

Figure D-64: Graph of Still Pot Composition against Time

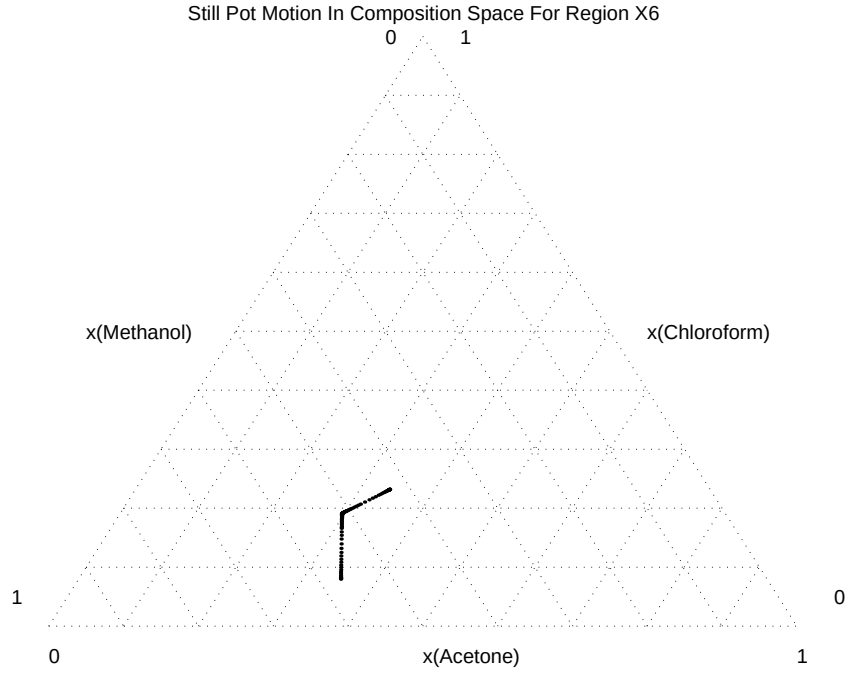

Figure D-65: Plot of Still Pot Motion in Composition Space

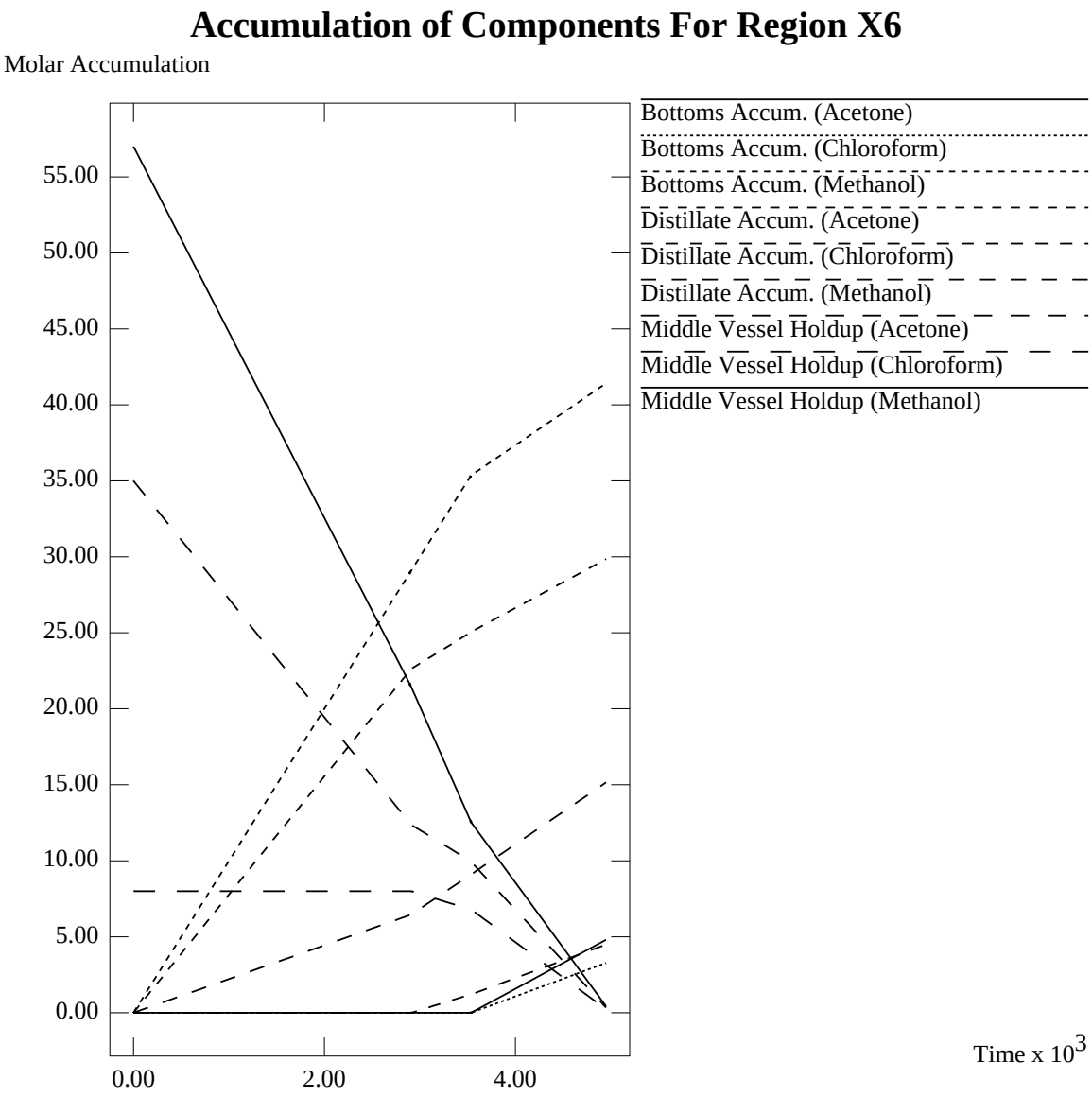

Figure D-66: Graph of Accumulation of Each Component against Time

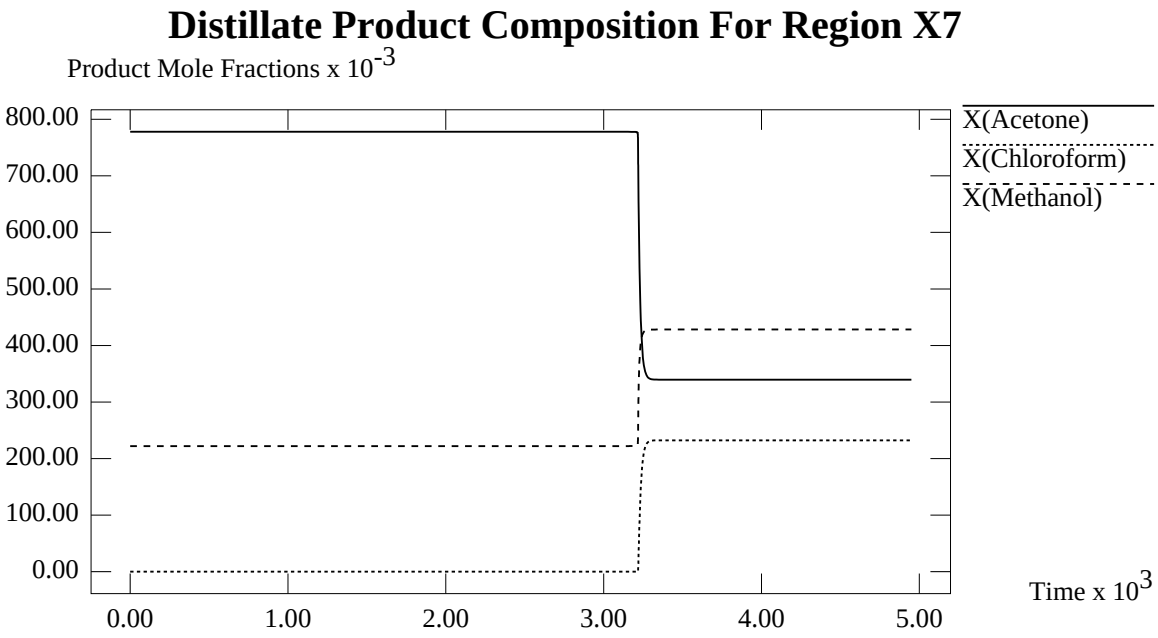

Figure D-67: Graph of Distillate Product Composition against Time

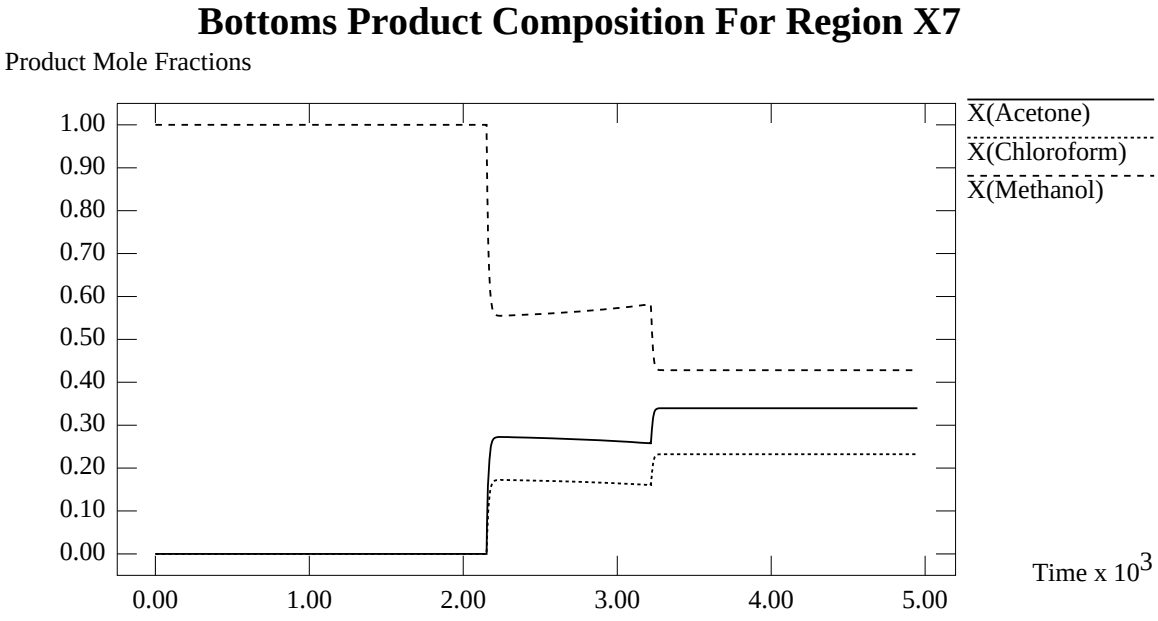

Figure D-68: Graph of Bottoms Product Composition against Time

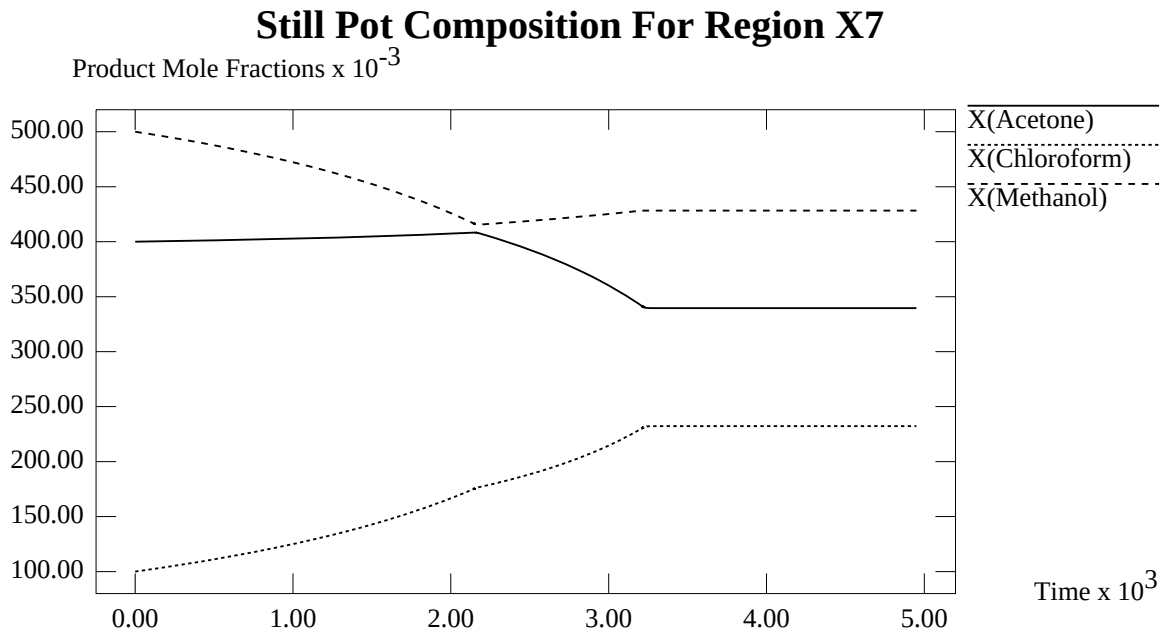

Figure D-69: Graph of Still Pot Composition against Time

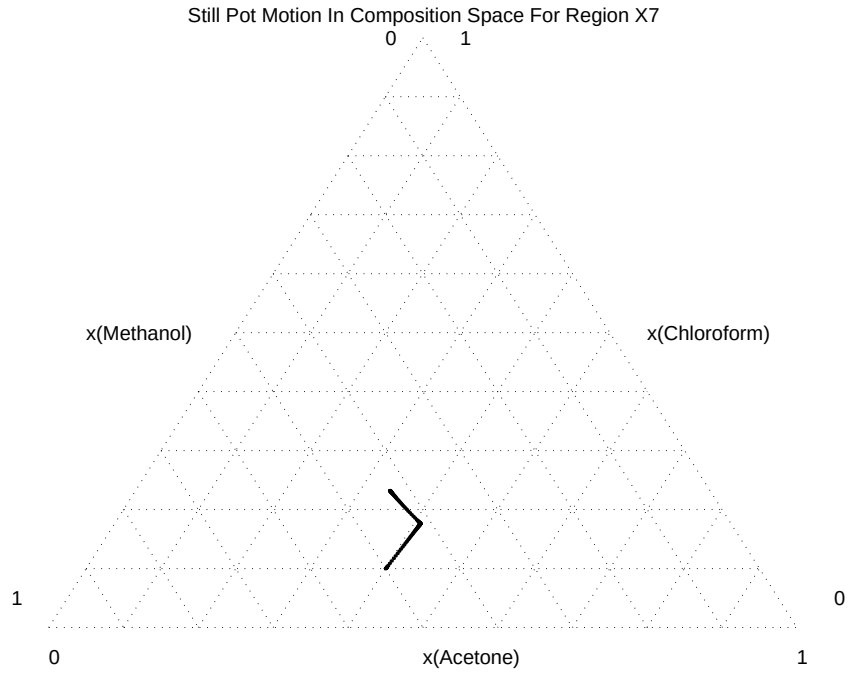

Figure D-70: Plot of Still Pot Motion in Composition Space

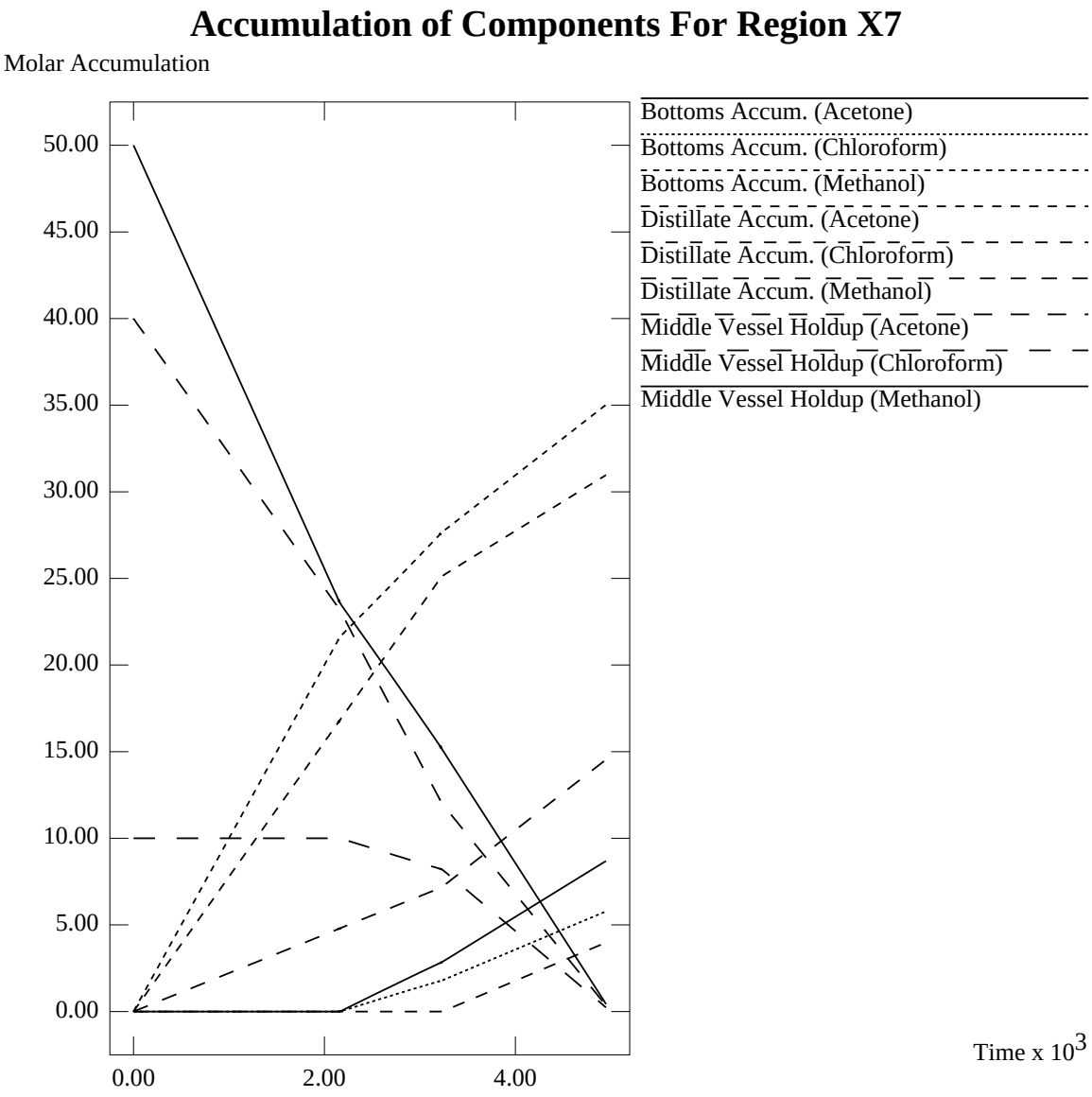

Figure D-71: Graph of Accumulation of Each Component against Time

D.4.8 Simulation Results for Region χ_8

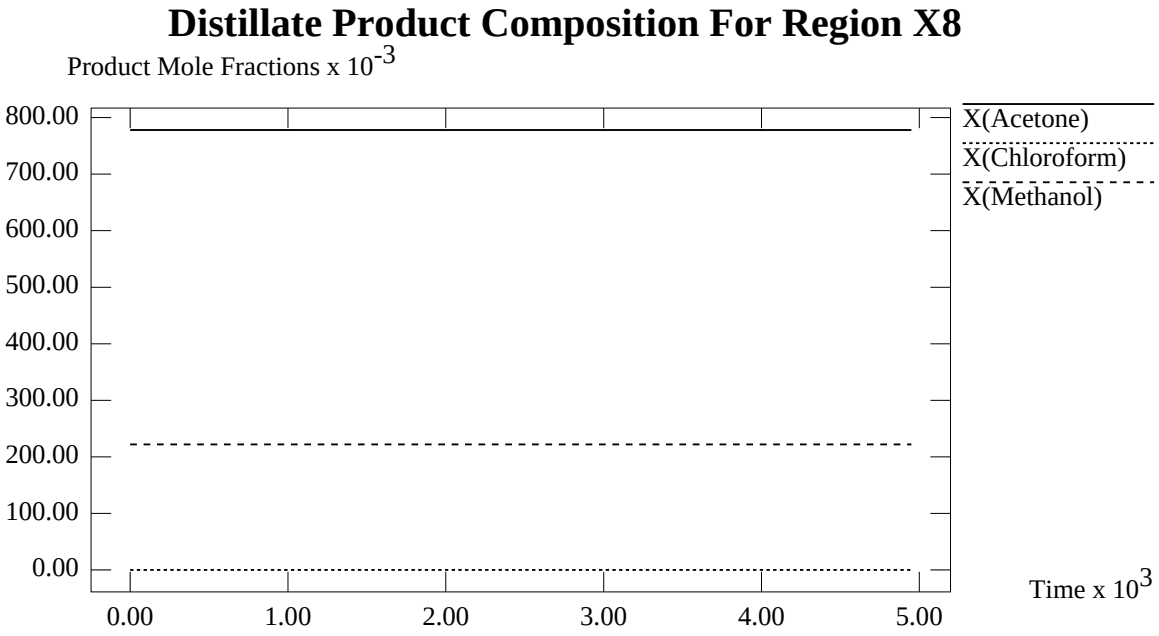

Figure D-72: Graph of Distillate Product Composition against Time

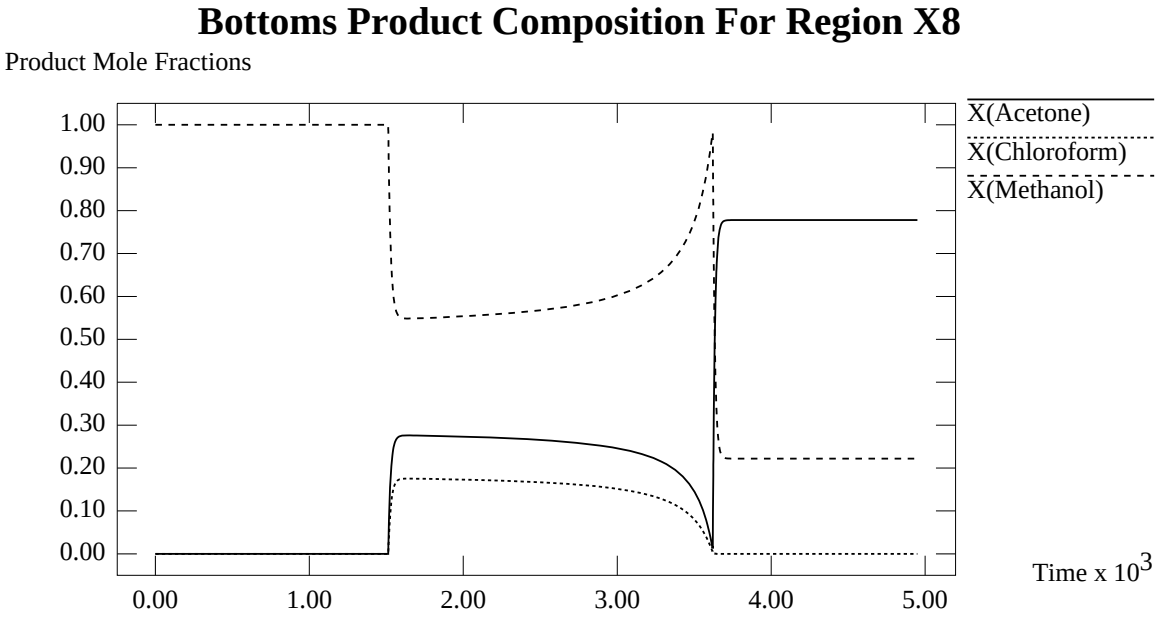

Figure D-73: Graph of Bottoms Product Composition against Time

D.4.9 Simulation Results for Region χ_9

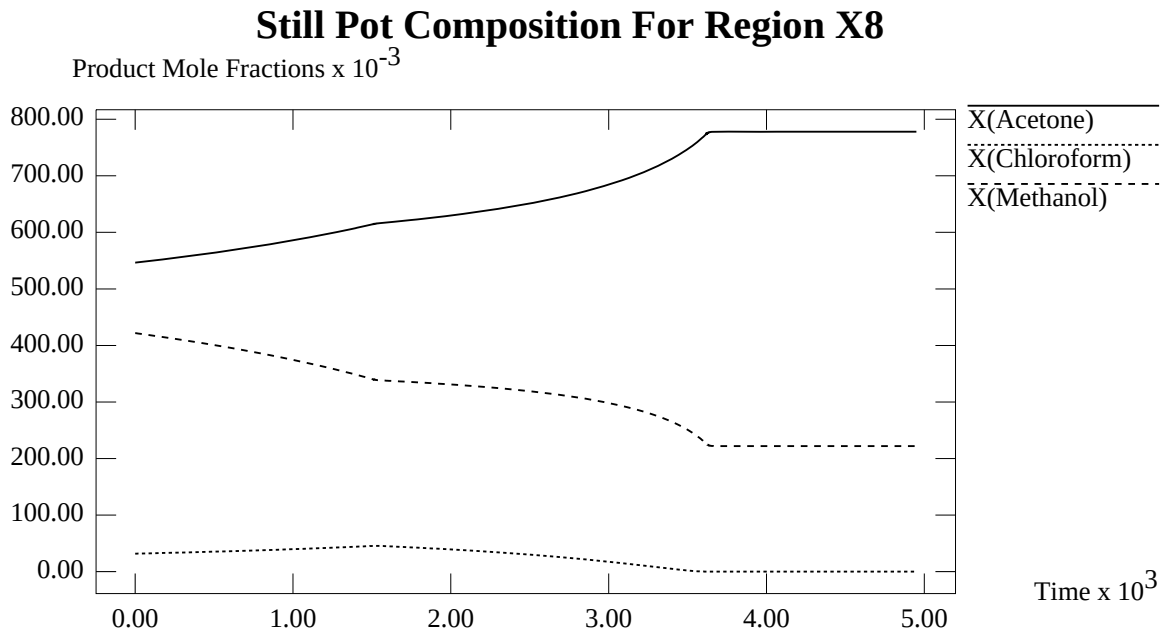

Figure D-74: Graph of Still Pot Composition against Time

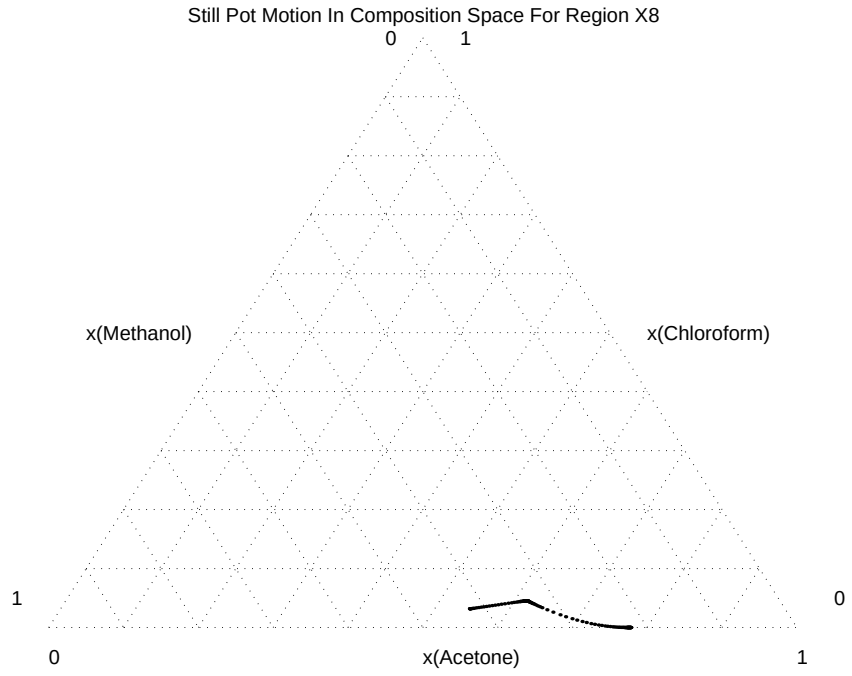

Figure D-75: Plot of Still Pot Motion in Composition Space

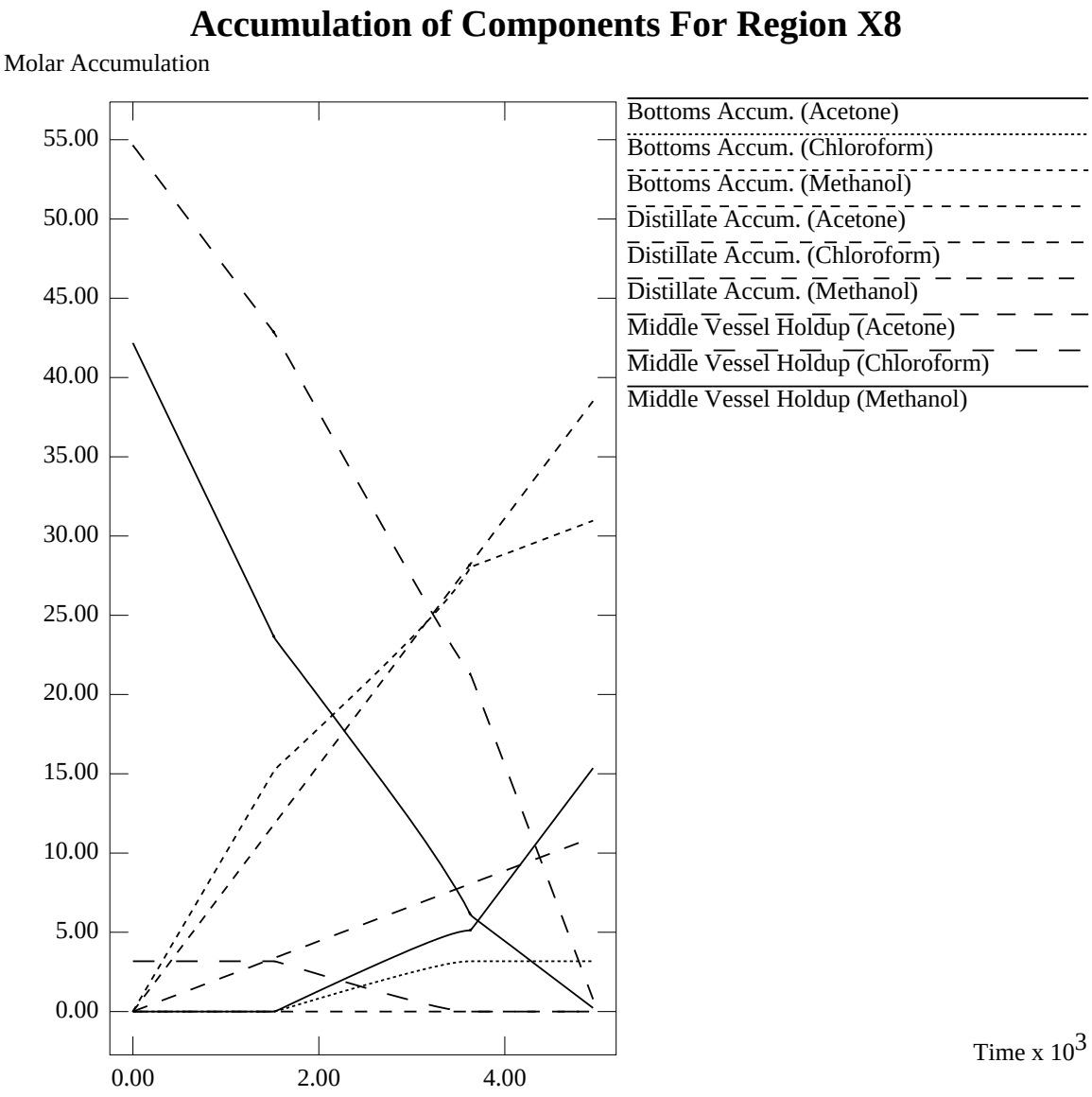

Figure D-76: Graph of Accumulation of Each Component against Time

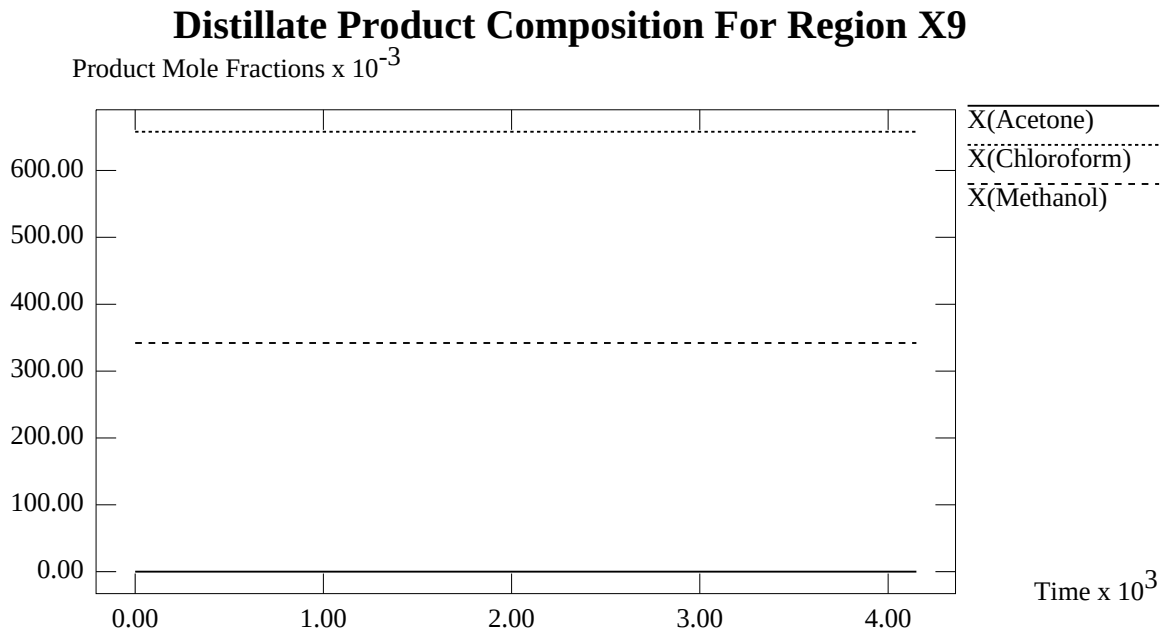

Figure D-77: Graph of Distillate Product Composition against Time

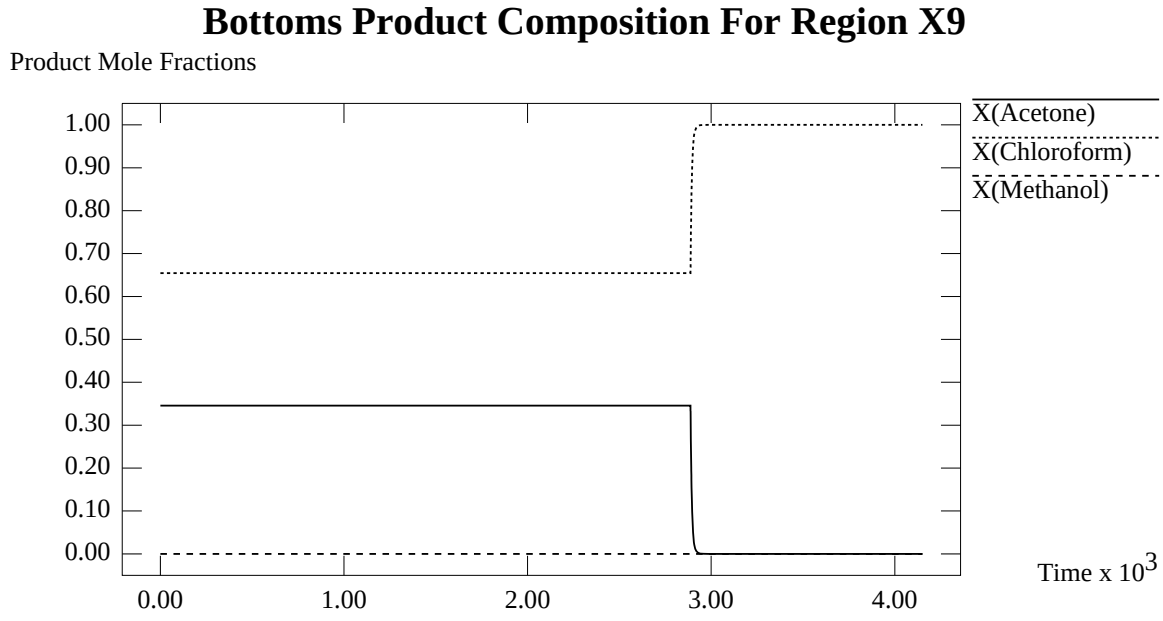

Figure D-78: Graph of Bottoms Product Composition against Time

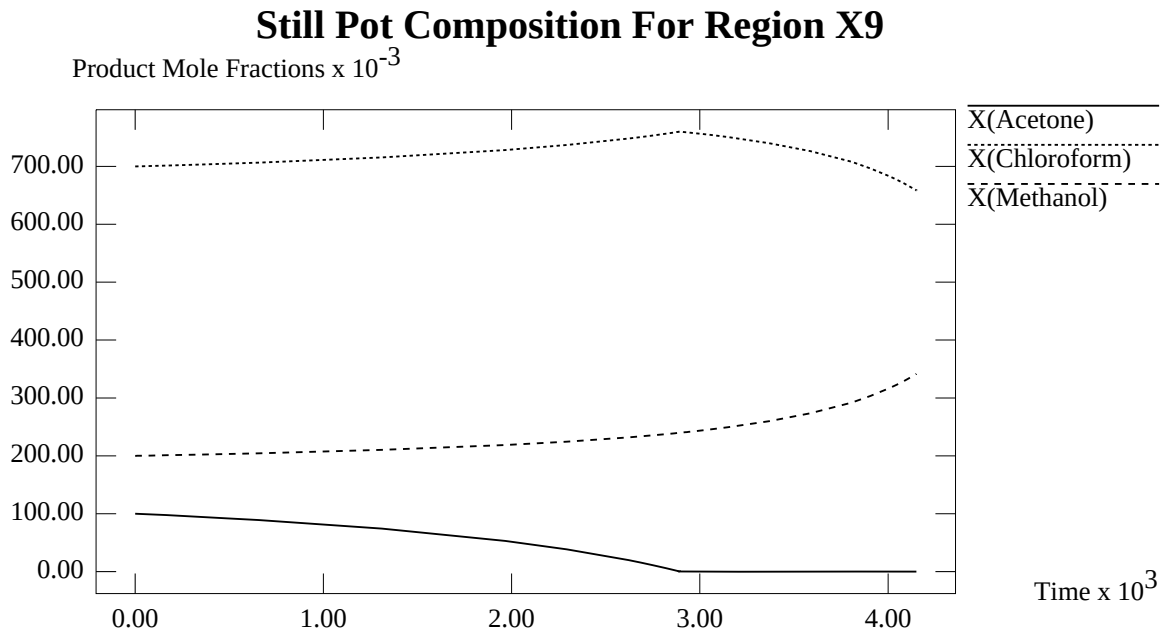

Figure D-79: Graph of Still Pot Composition against Time

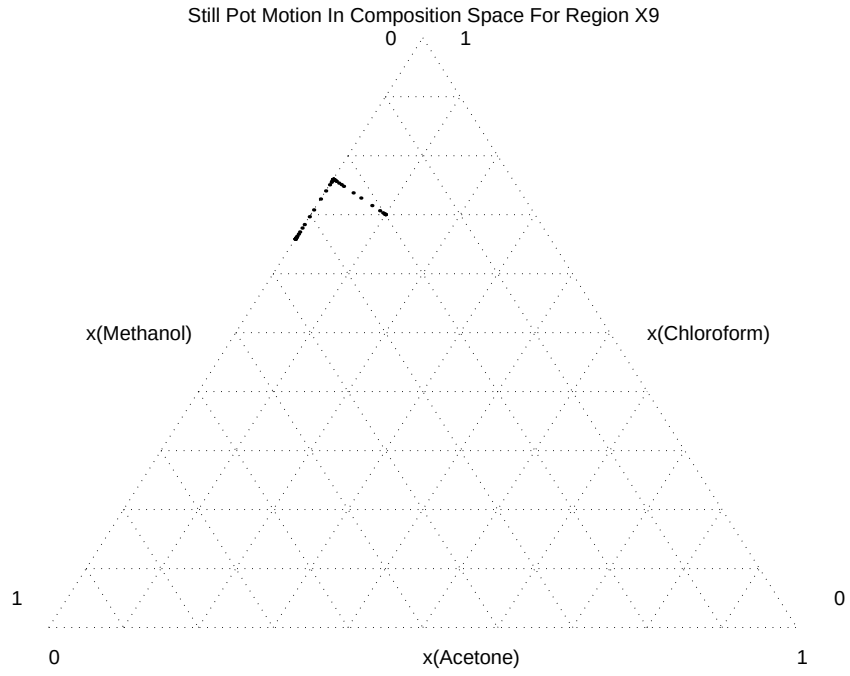

Figure D-80: Plot of Still Pot Motion in Composition Space

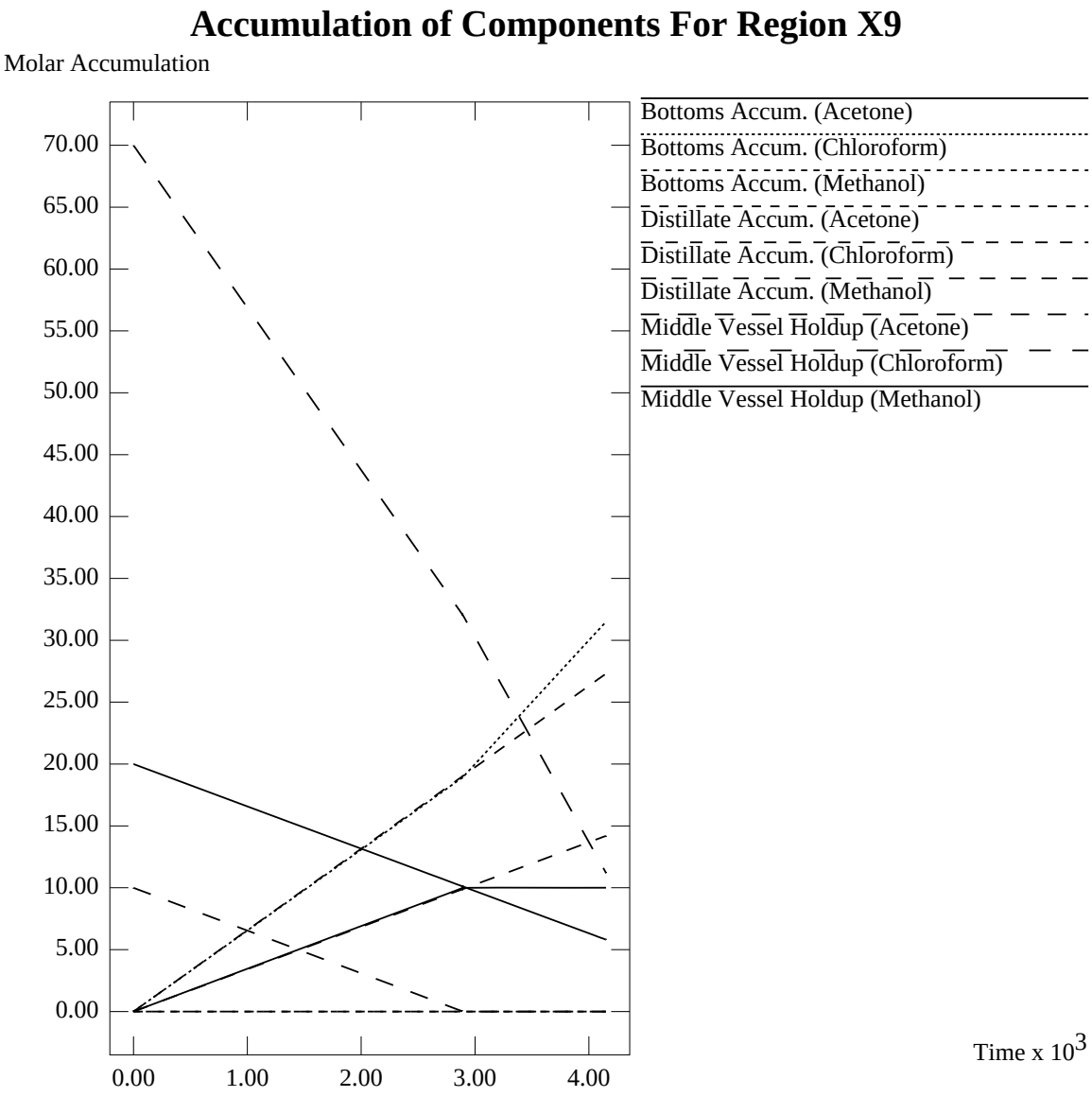

Figure D-81: Graph of Accumulation of Each Component against Time

D.4.10 Simulation Results for Region χ_{10}

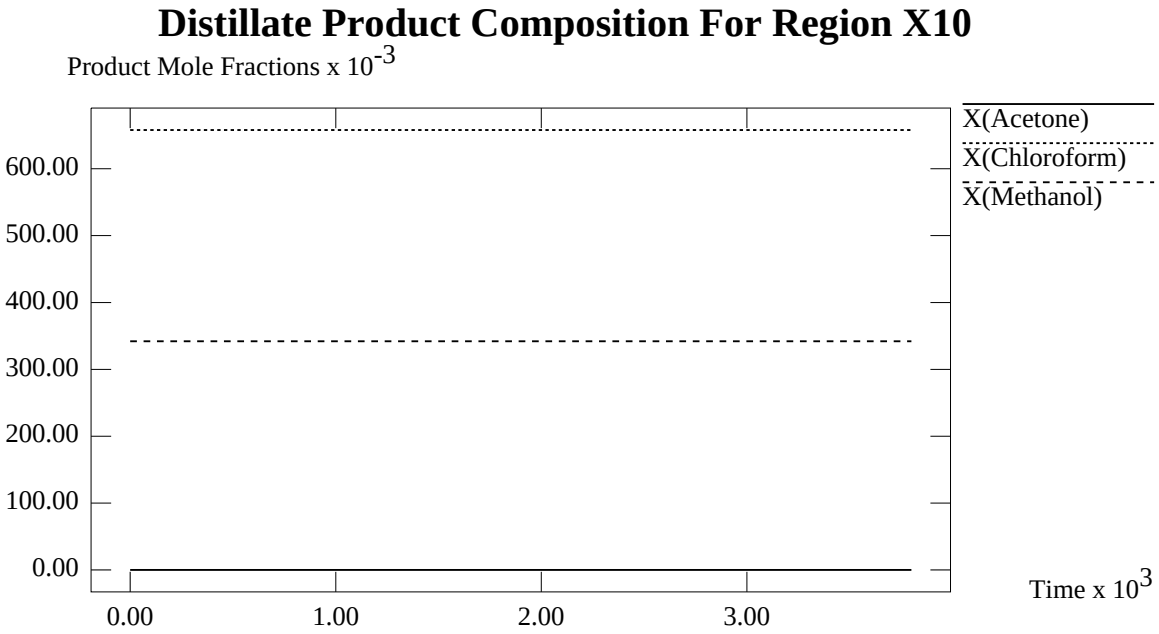

Figure D-82: Graph of Distillate Product Composition against Time

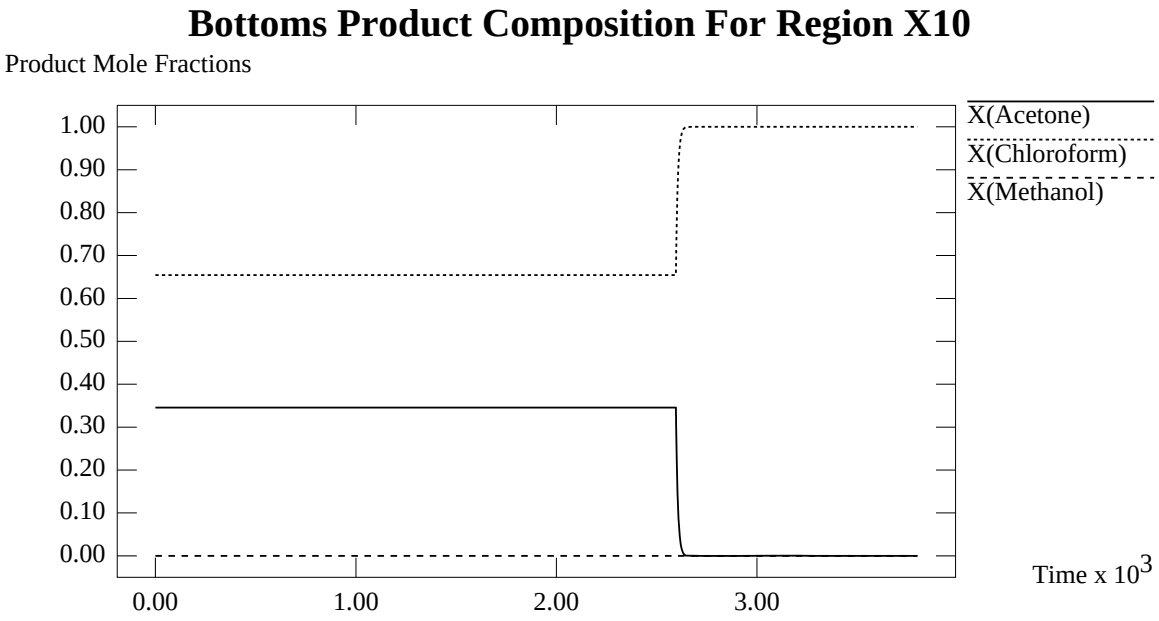

Figure D-83: Graph of Bottoms Product Composition against Time

D.4.11 Simulation Results for Region χ_{11}

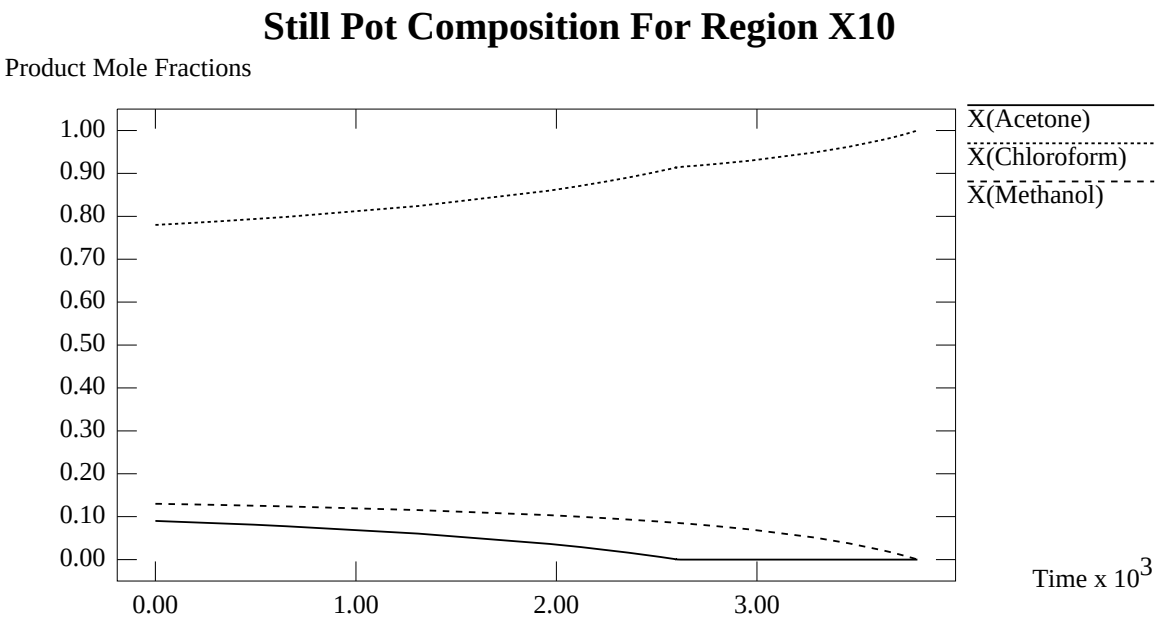

Figure D-84: Graph of Still Pot Composition against Time

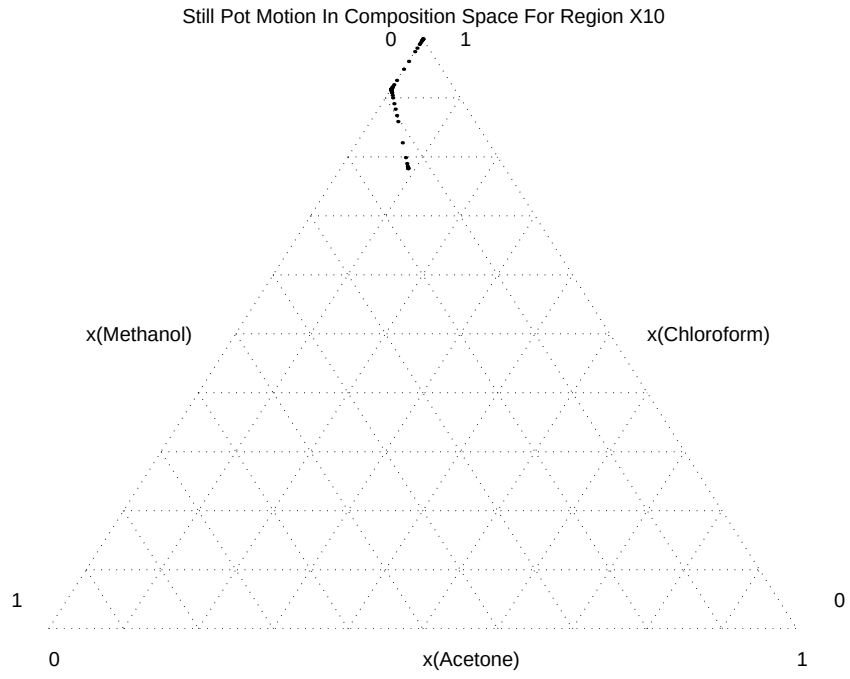

Figure D-85: Plot of Still Pot Motion in Composition Space

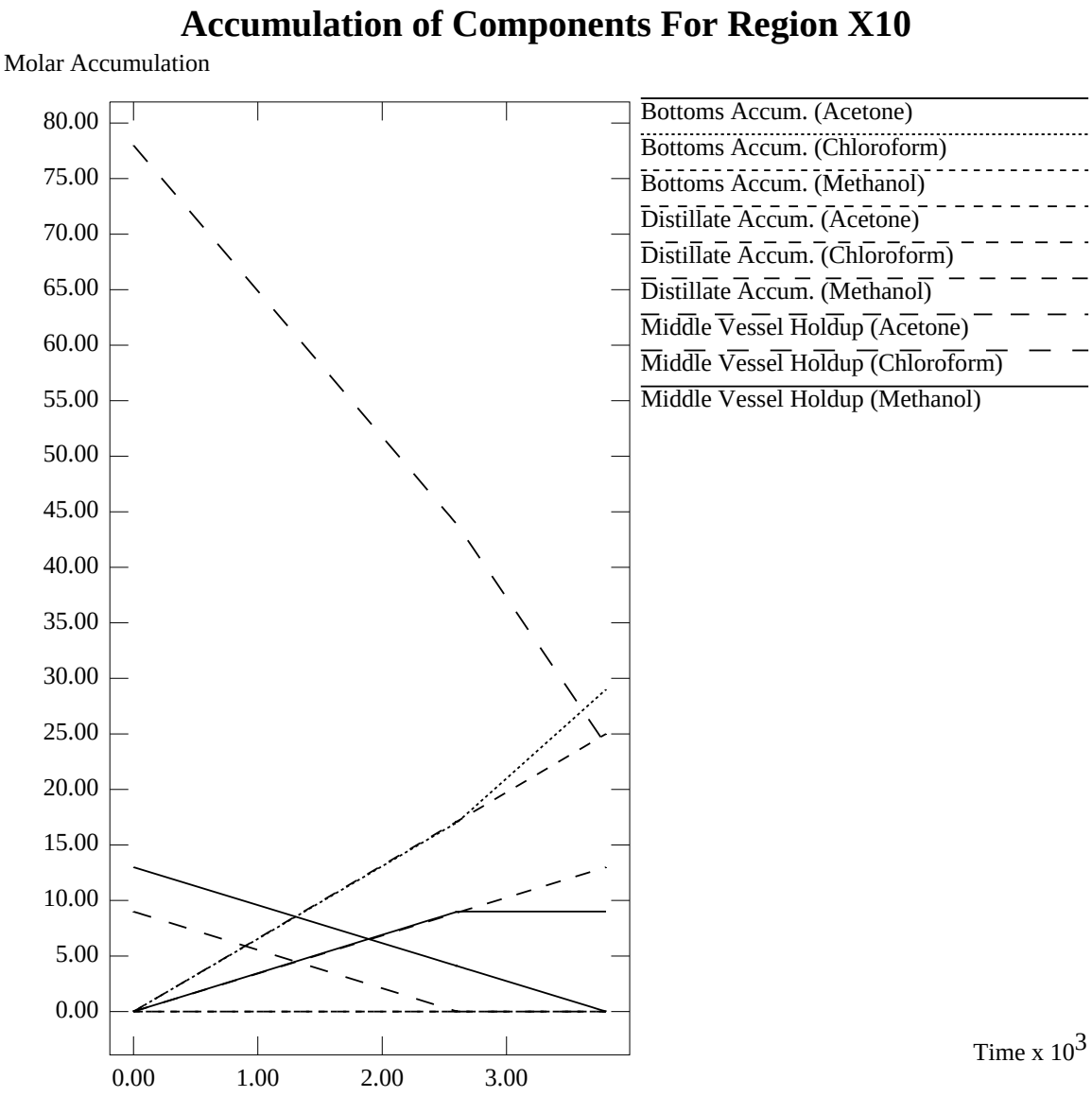

Figure D-86: Graph of Accumulation of Each Component against Time

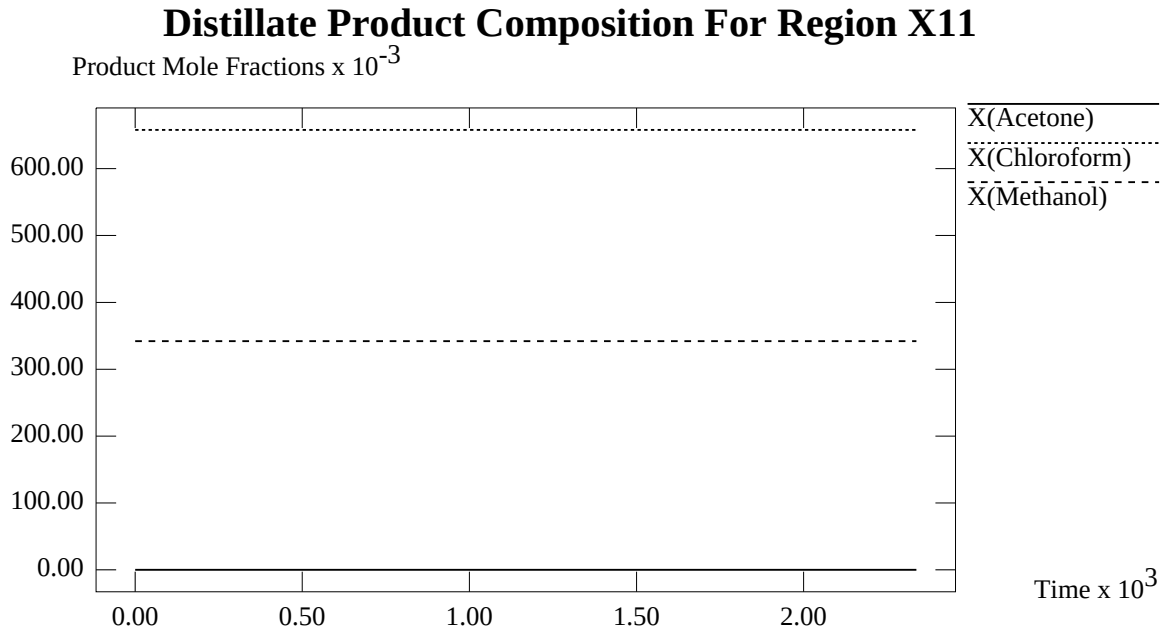

Figure D-87: Graph of Distillate Product Composition against Time

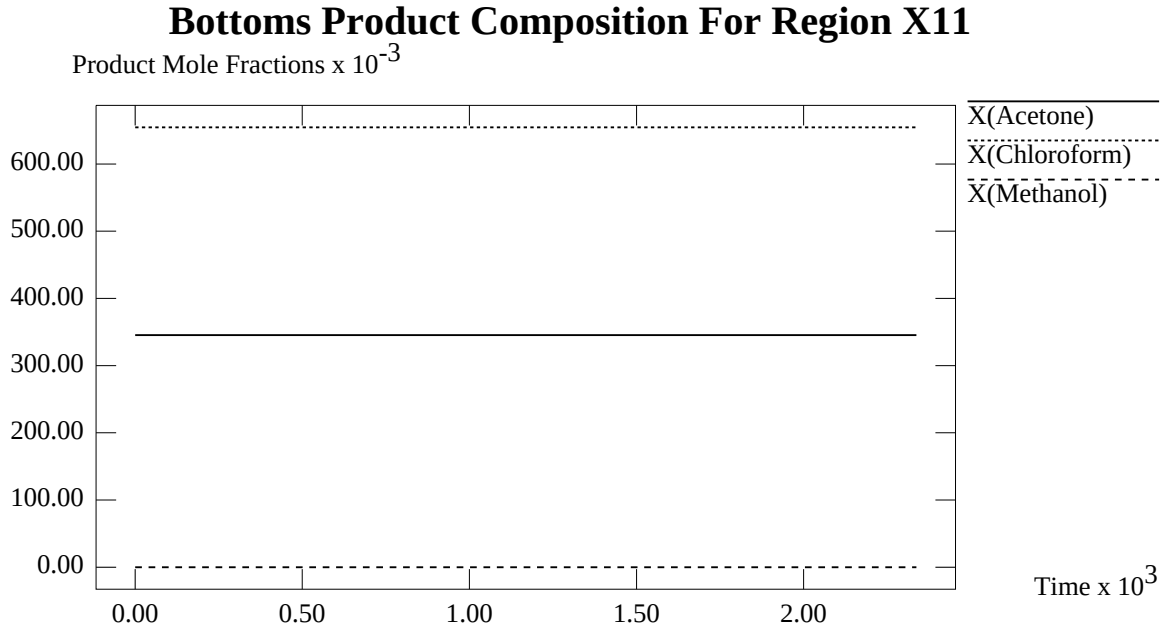

Figure D-88: Graph of Bottoms Product Composition against Time

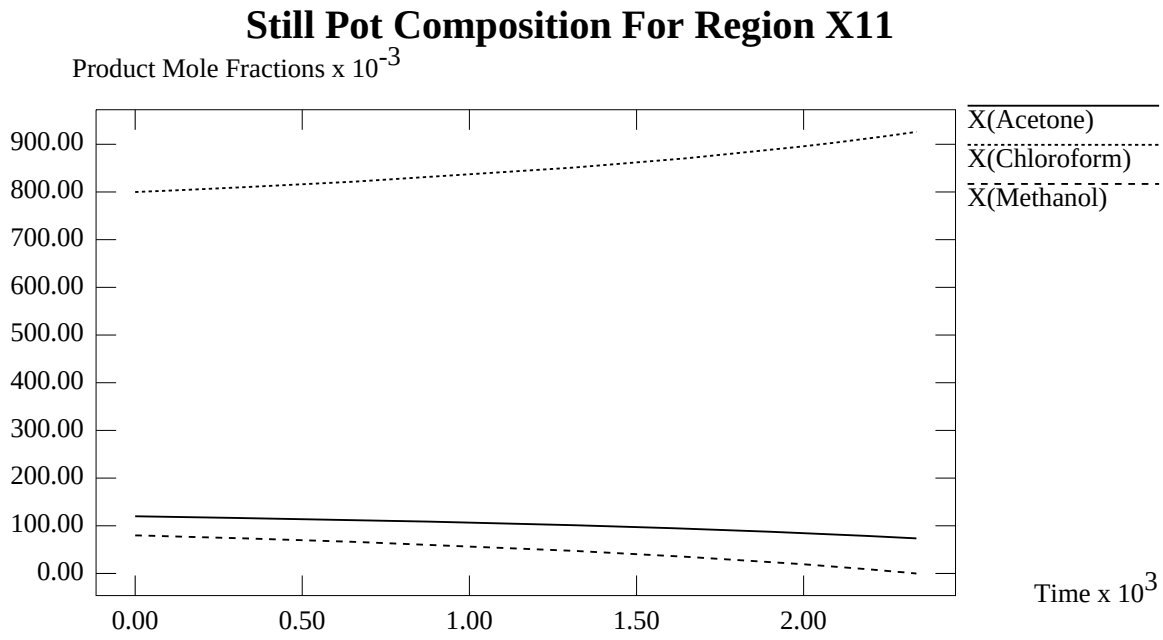

Figure D-89: Graph of Still Pot Composition against Time

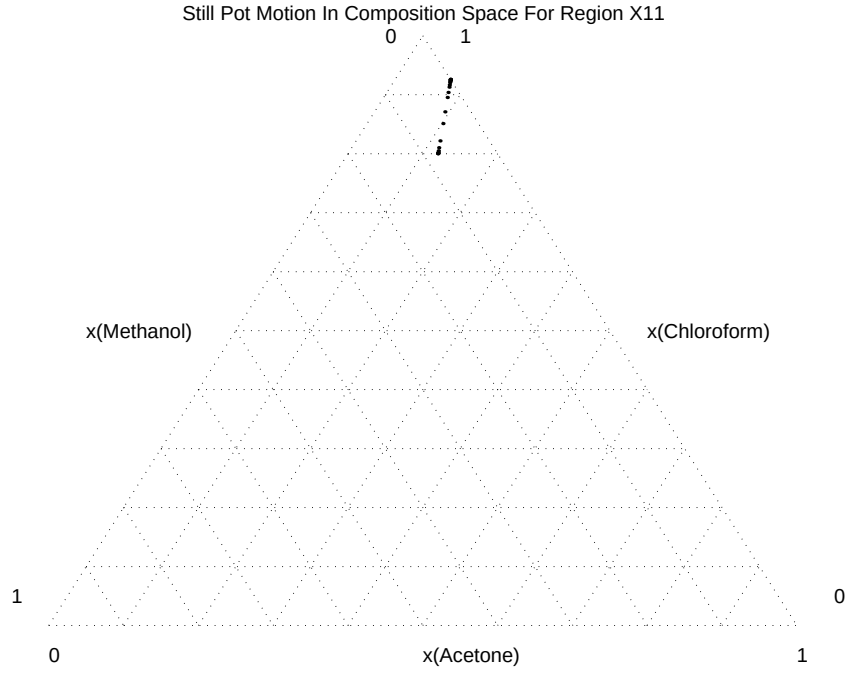

Figure D-90: Plot of Still Pot Motion in Composition Space

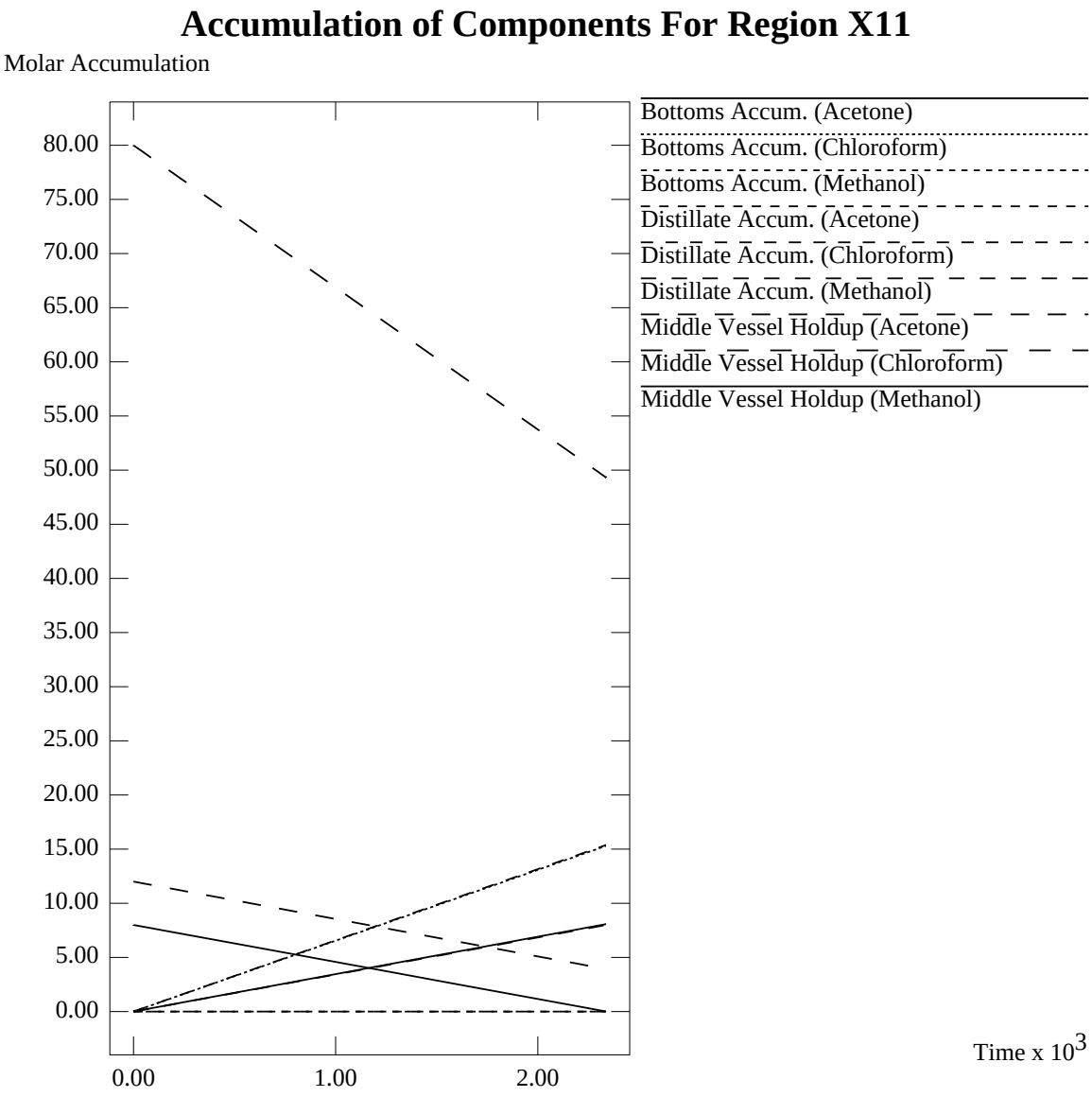

Figure D-91: Graph of Accumulation of Each Component against Time

D.4.12 Simulation Results for Region χ_{12}

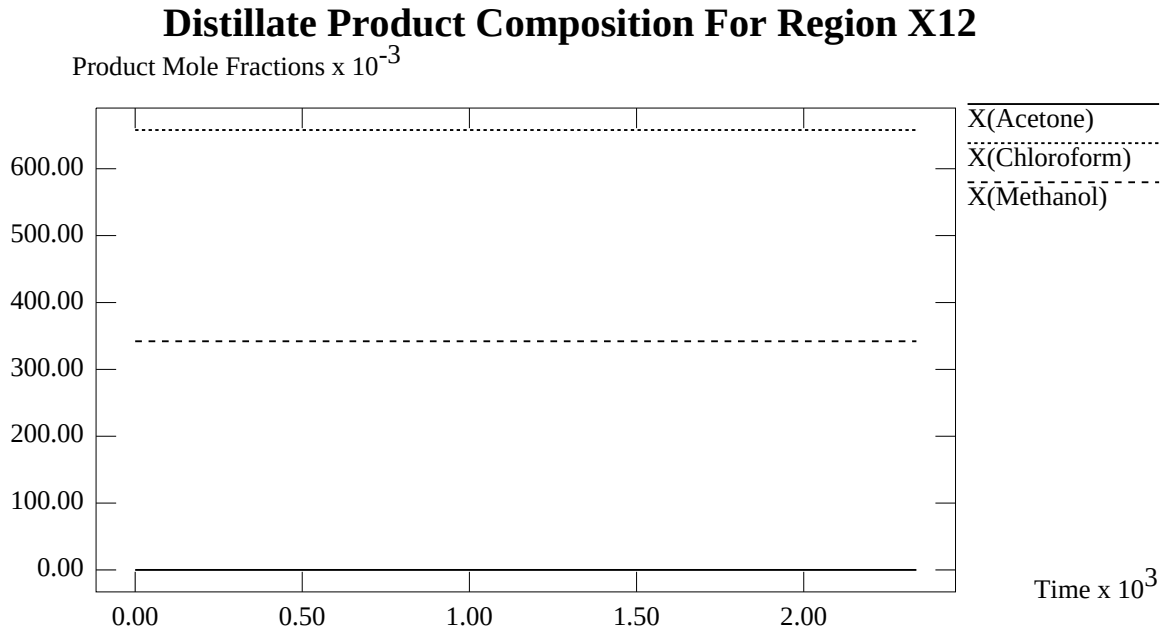

Figure D-92: Graph of Distillate Product Composition against Time

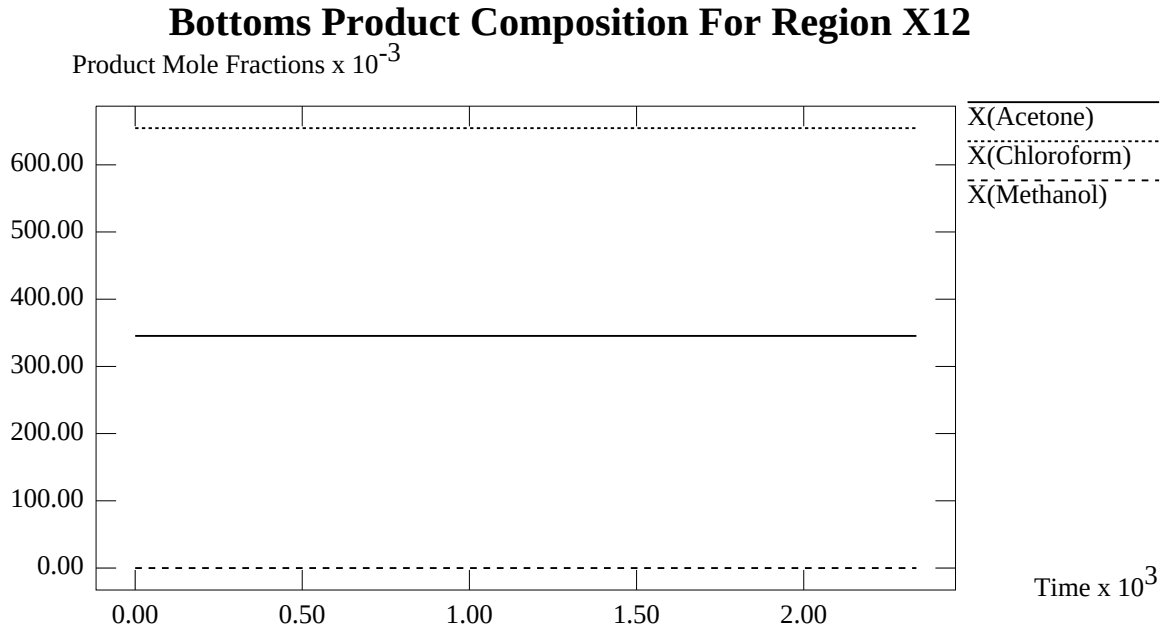

Figure D-93: Graph of Bottoms Product Composition against Time

D.4.13 Simulation Results for Region χ_{13}

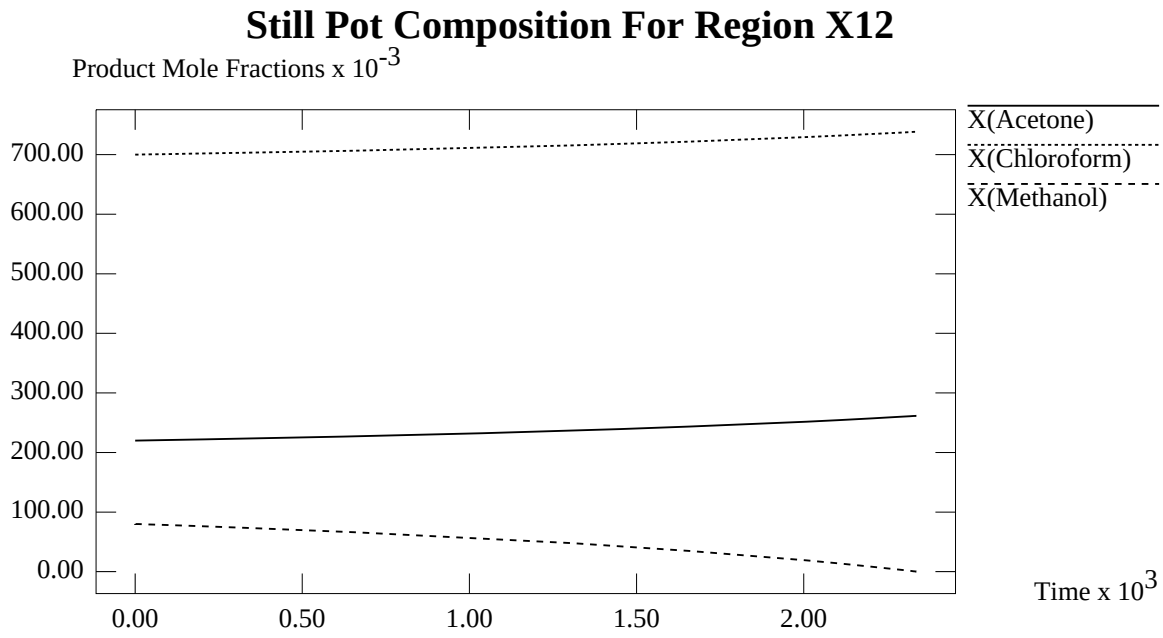

Figure D-94: Graph of Still Pot Composition against Time

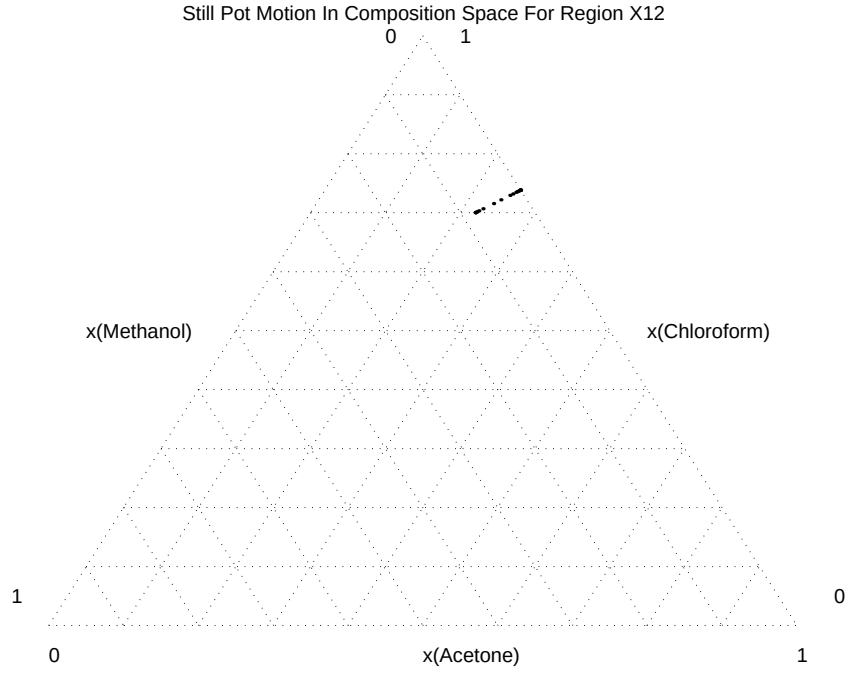

Figure D-95: Plot of Still Pot Motion in Composition Space

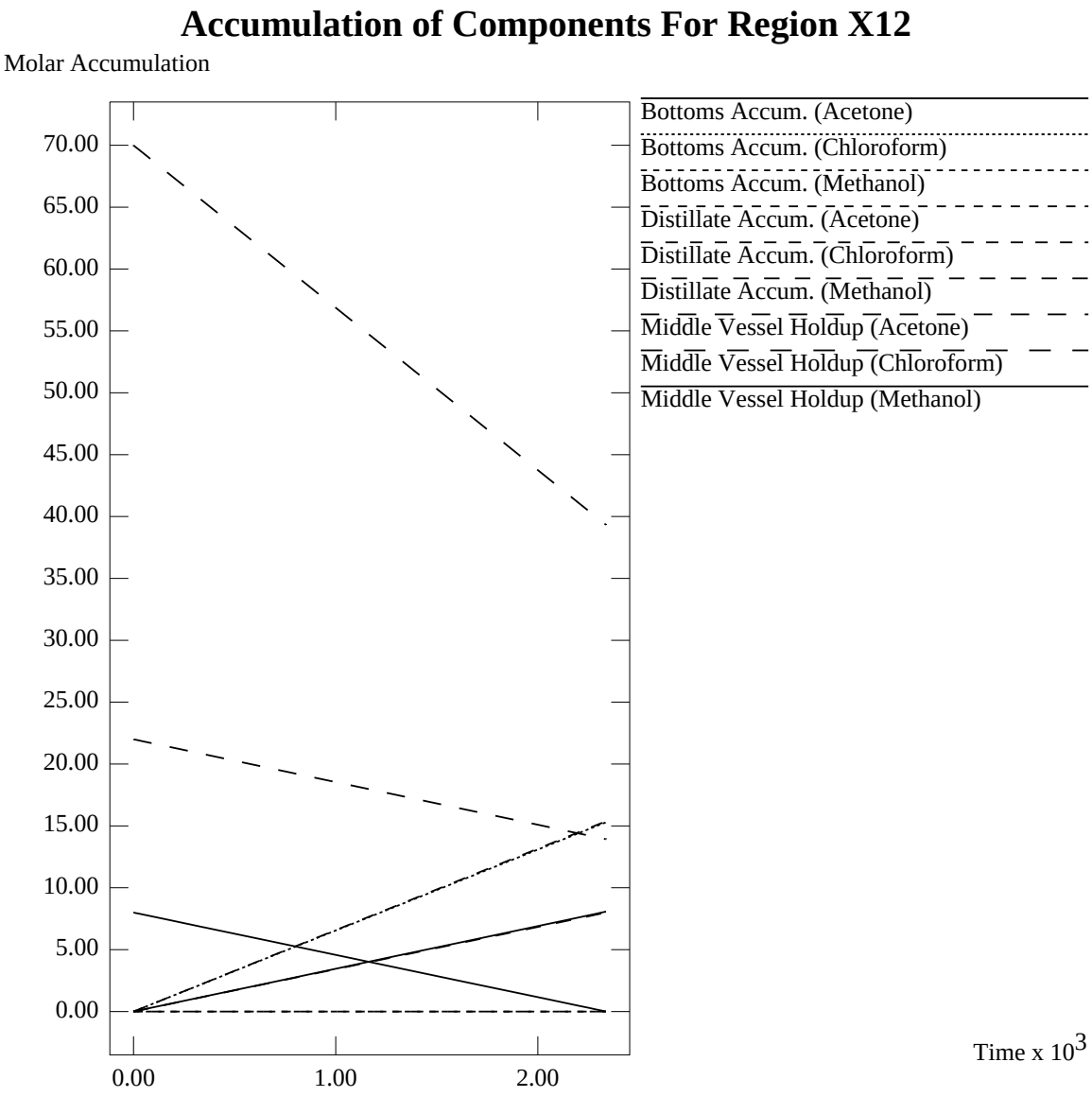

Figure D-96: Graph of Accumulation of Each Component against Time

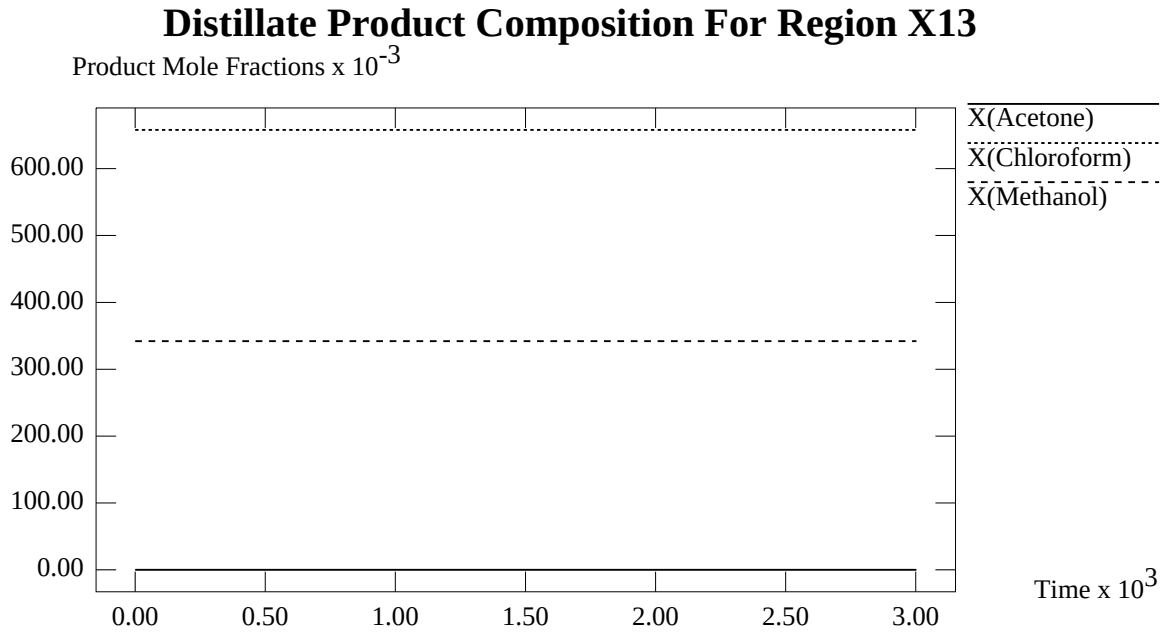

Figure D-97: Graph of Distillate Product Composition against Time

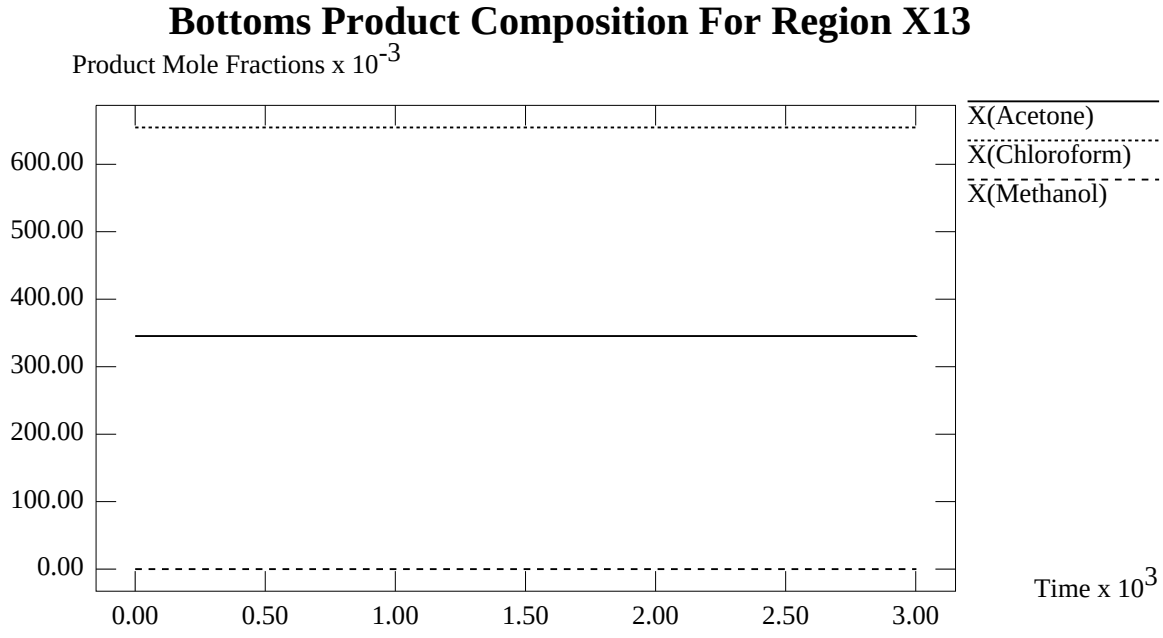

Figure D-98: Graph of Bottoms Product Composition against Time

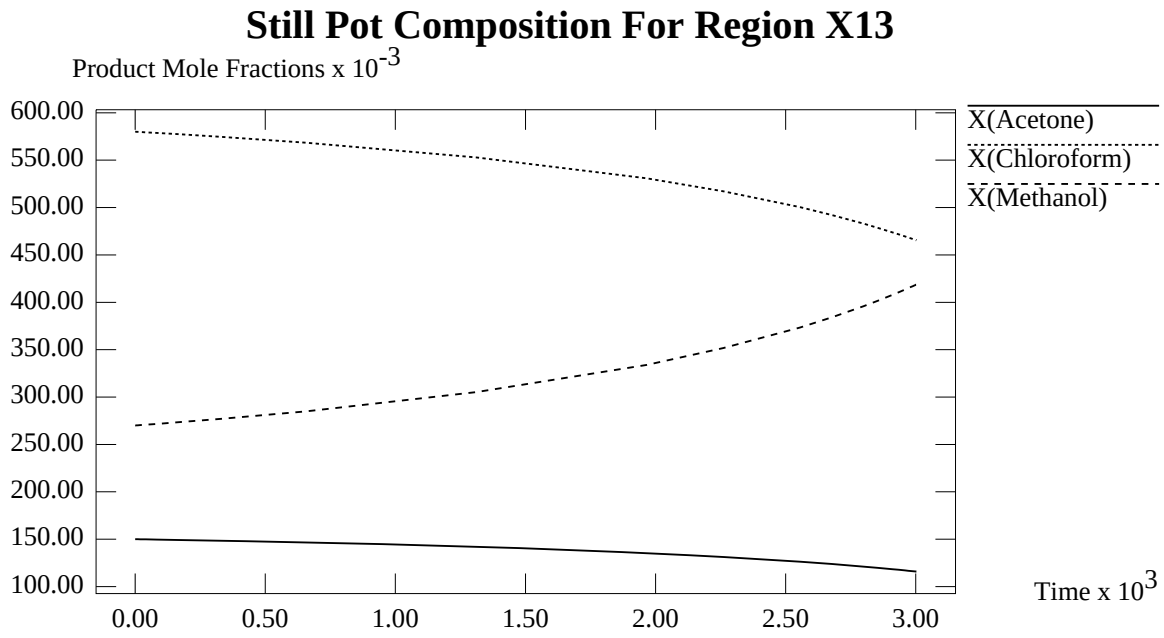

Figure D-99: Graph of Still Pot Composition against Time

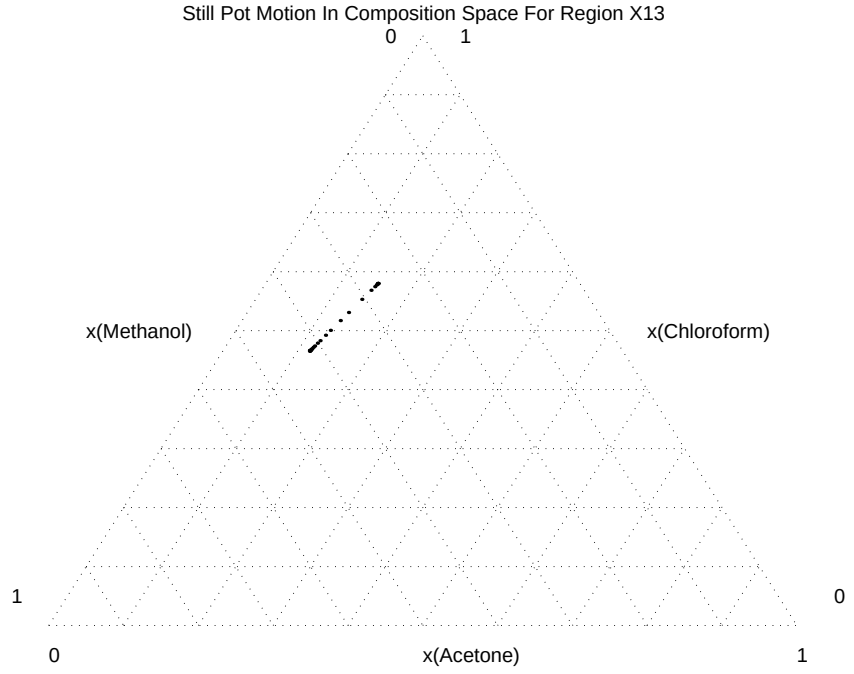

Figure D-100: Plot of Still Pot Motion in Composition Space

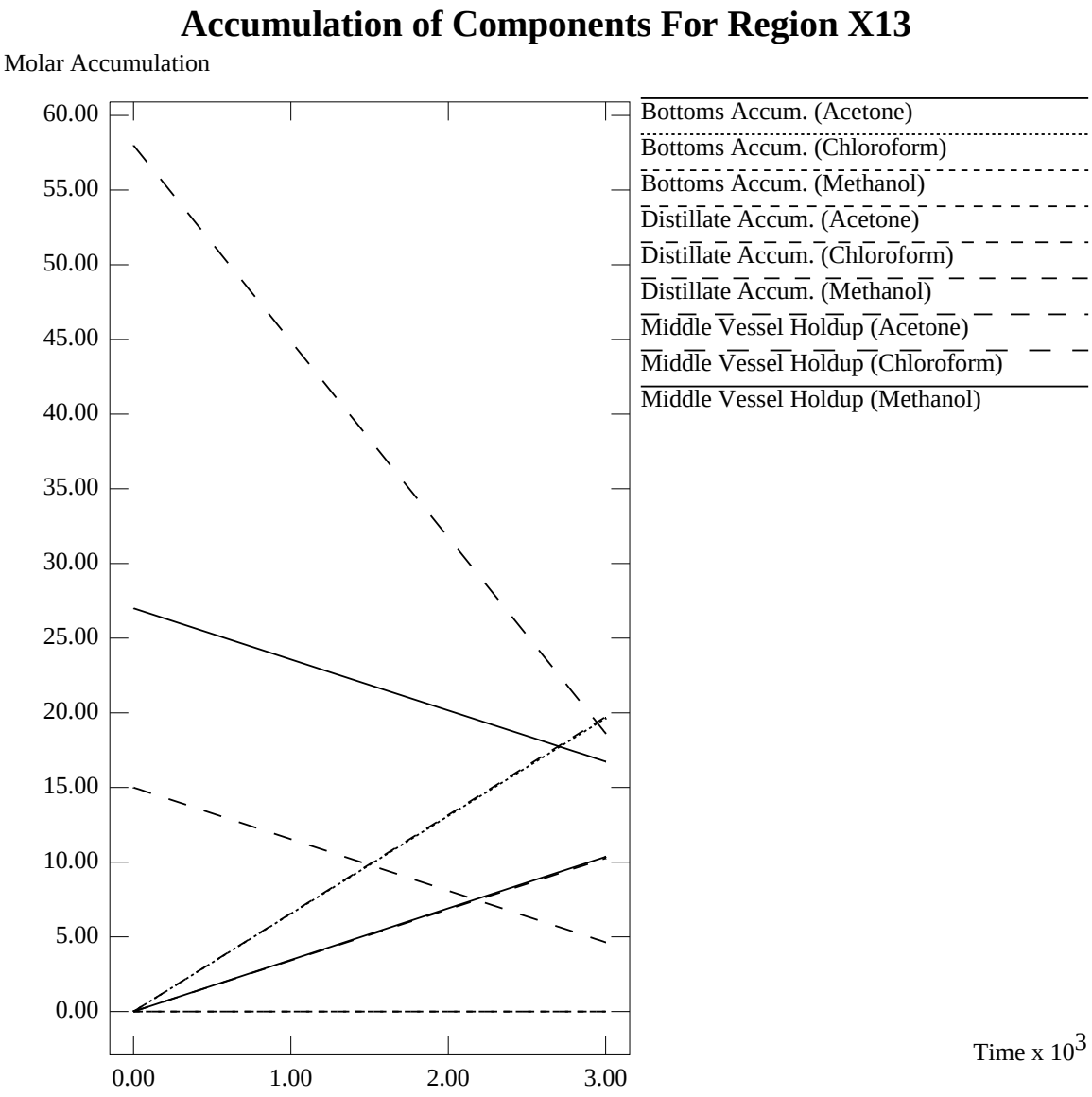

Figure D-101: Graph of Accumulation of Each Component against Time

D.4.14 Simulation Results for Region χ_{14}

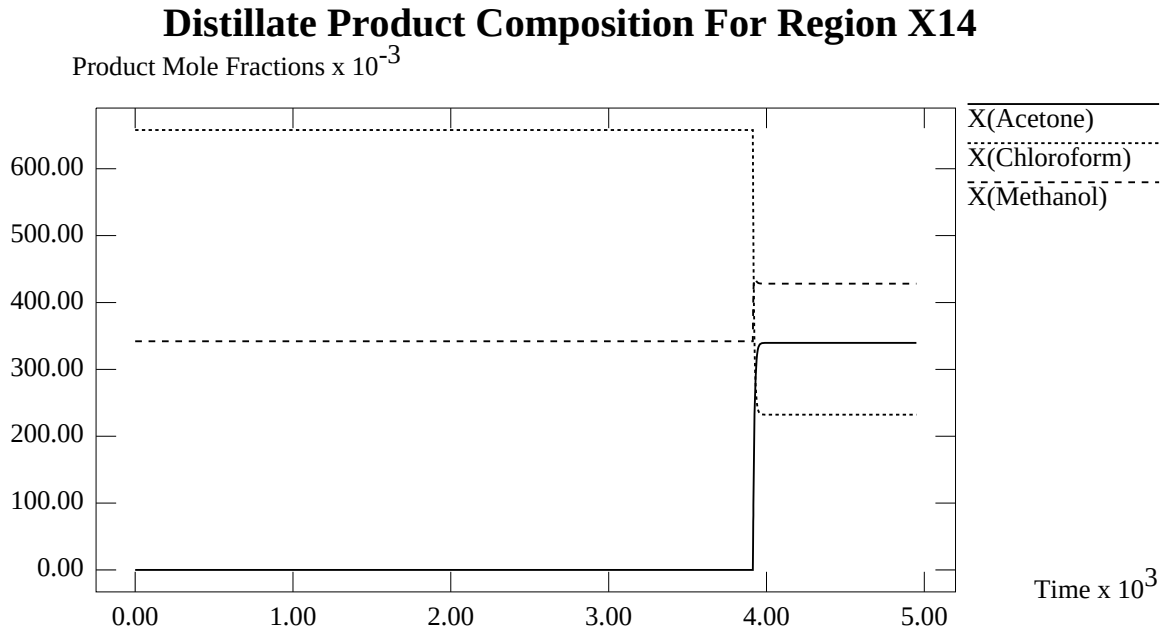

Figure D-102: Graph of Distillate Product Composition against Time

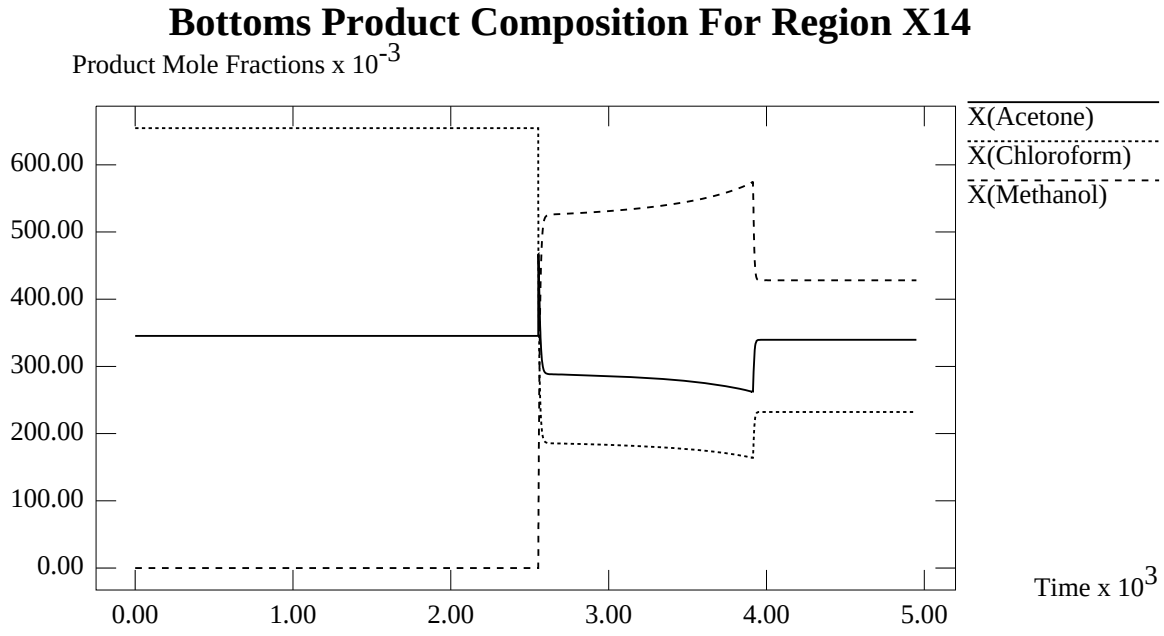

Figure D-103: Graph of Bottoms Product Composition against Time

D.4.15 Simulation Results for Region χ_{15}

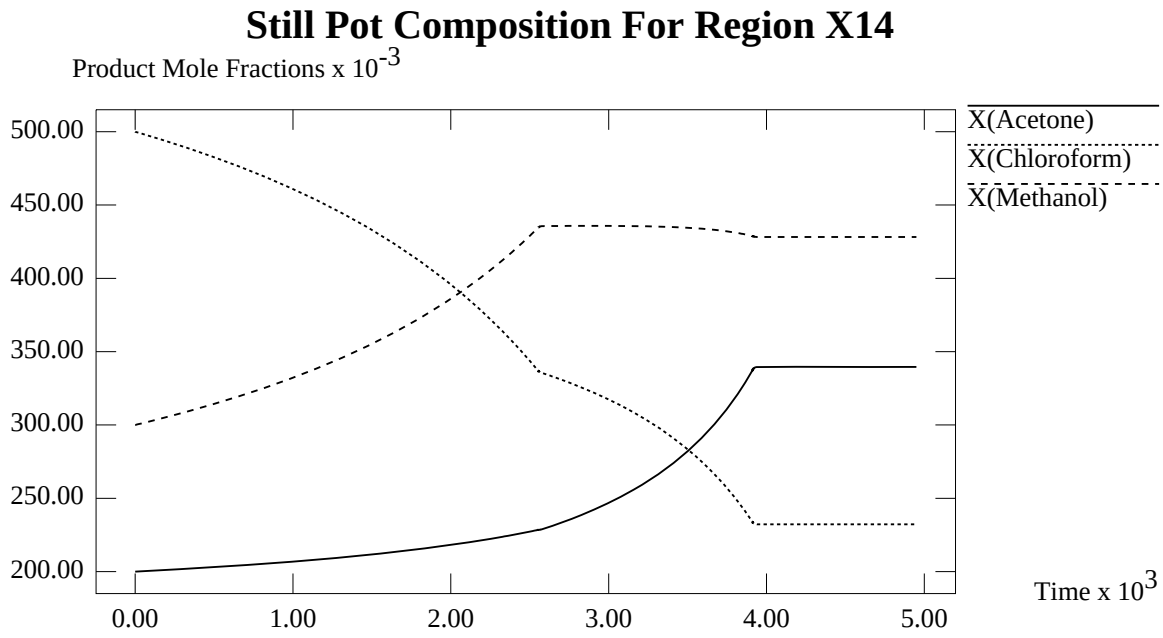

Figure D-104: Graph of Still Pot Composition against Time

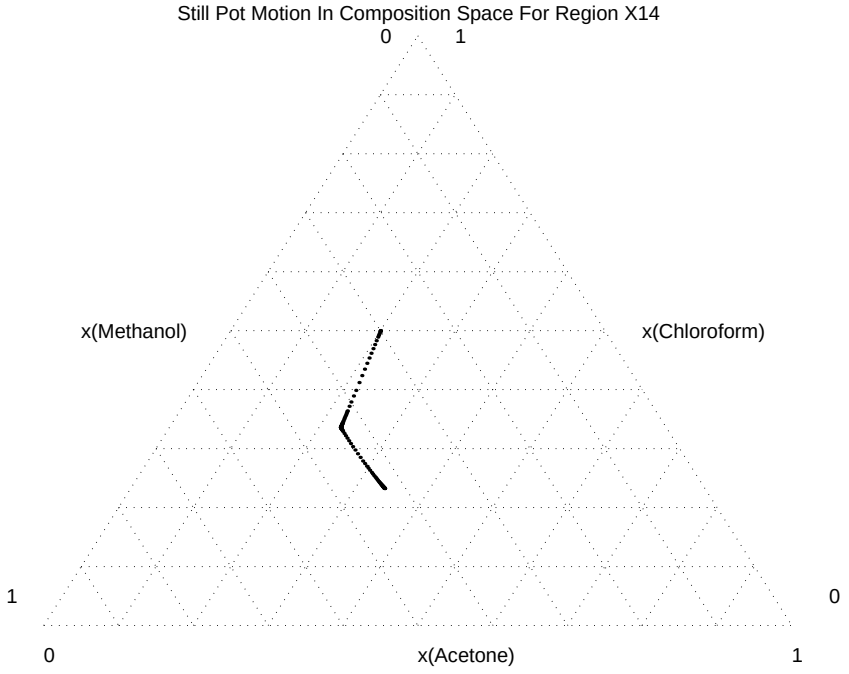

Figure D-105: Plot of Still Pot Motion in Composition Space

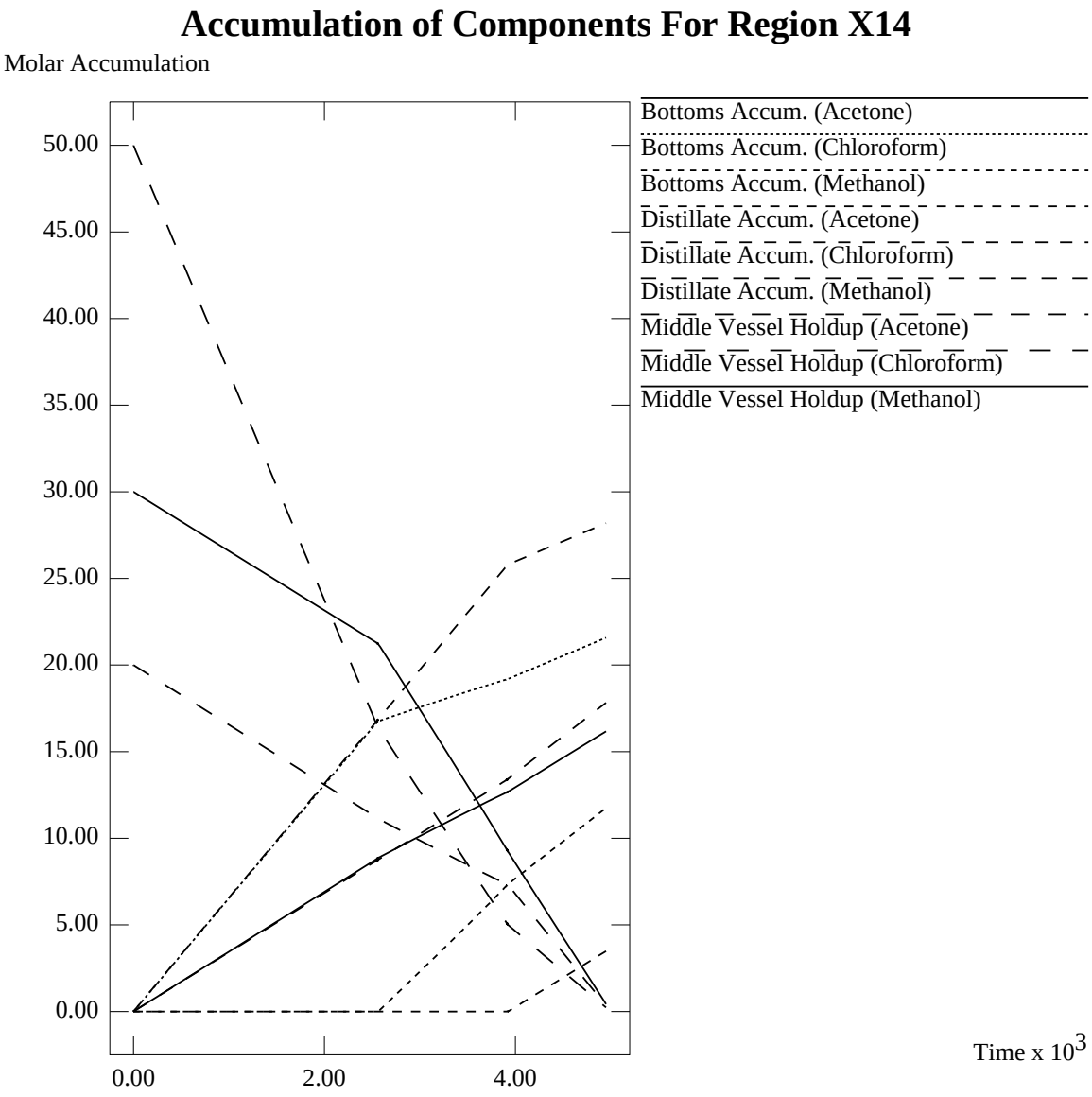

Figure D-106: Graph of Accumulation of Each Component against Time

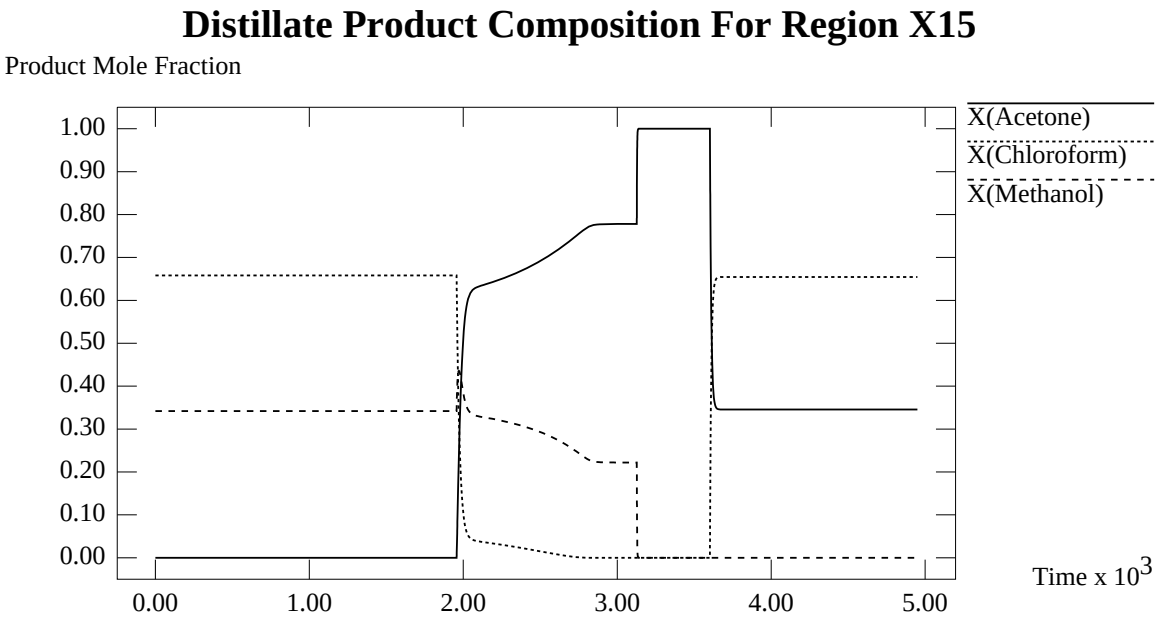

Figure D-107: Graph of Distillate Product Composition against Time

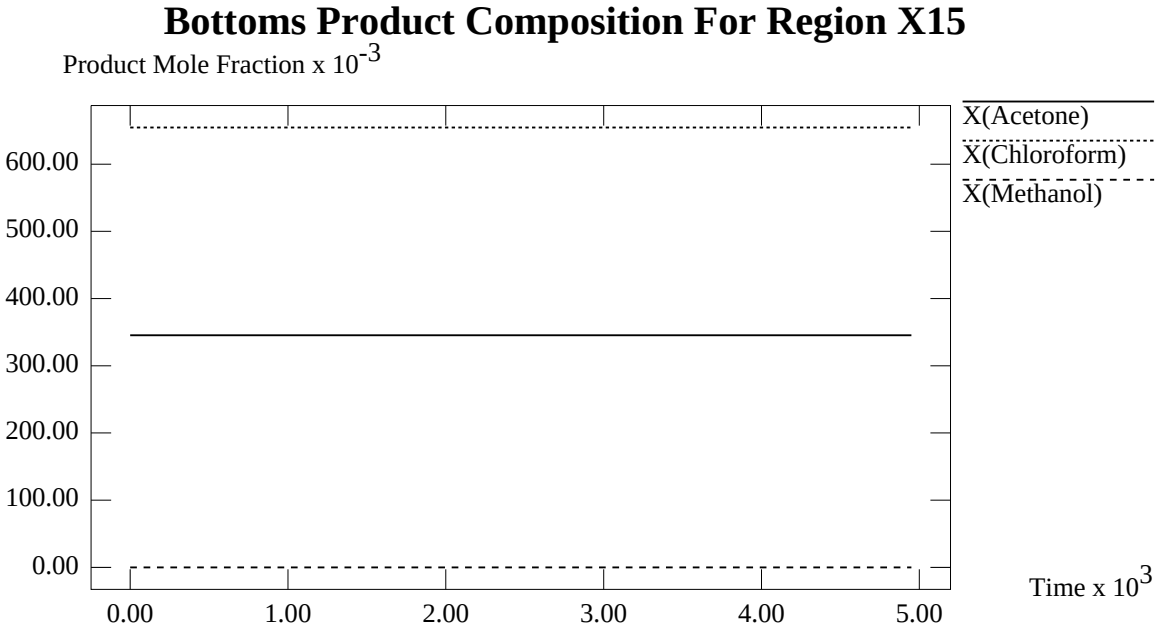

Figure D-108: Graph of Bottoms Product Composition against Time

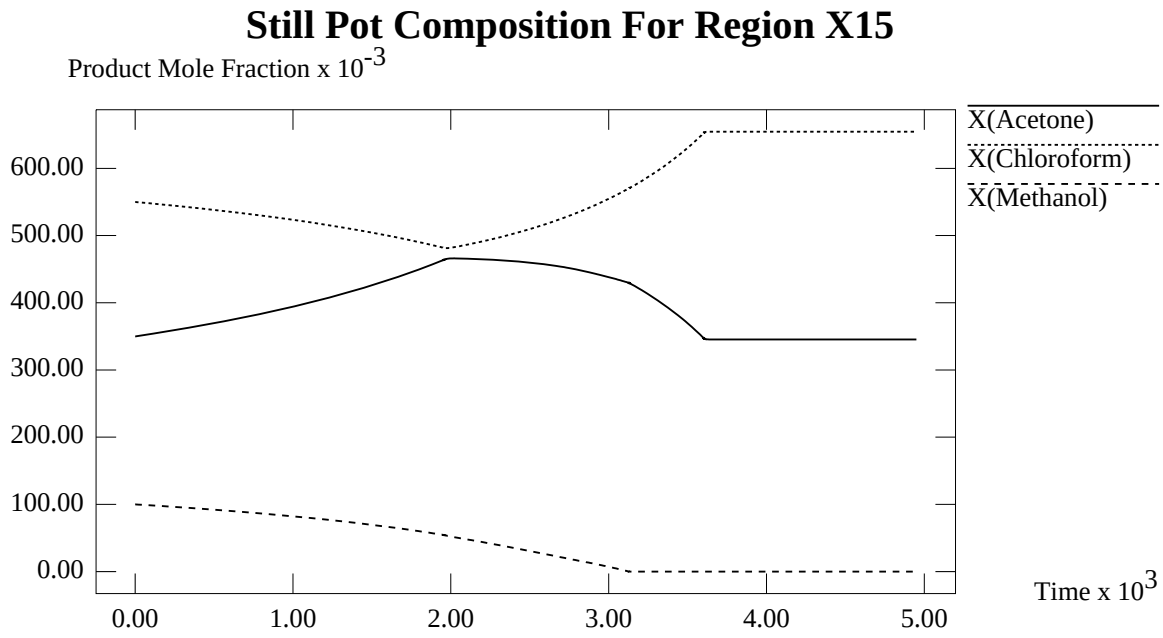

Figure D-109: Graph of Still Pot Composition against Time

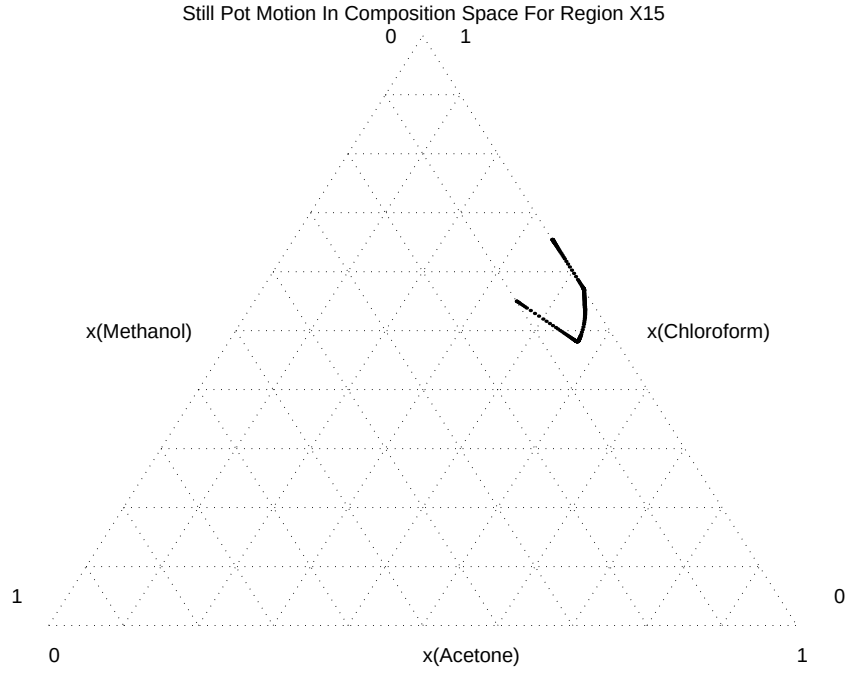

Figure D-110: Plot of Still Pot Motion in Composition Space

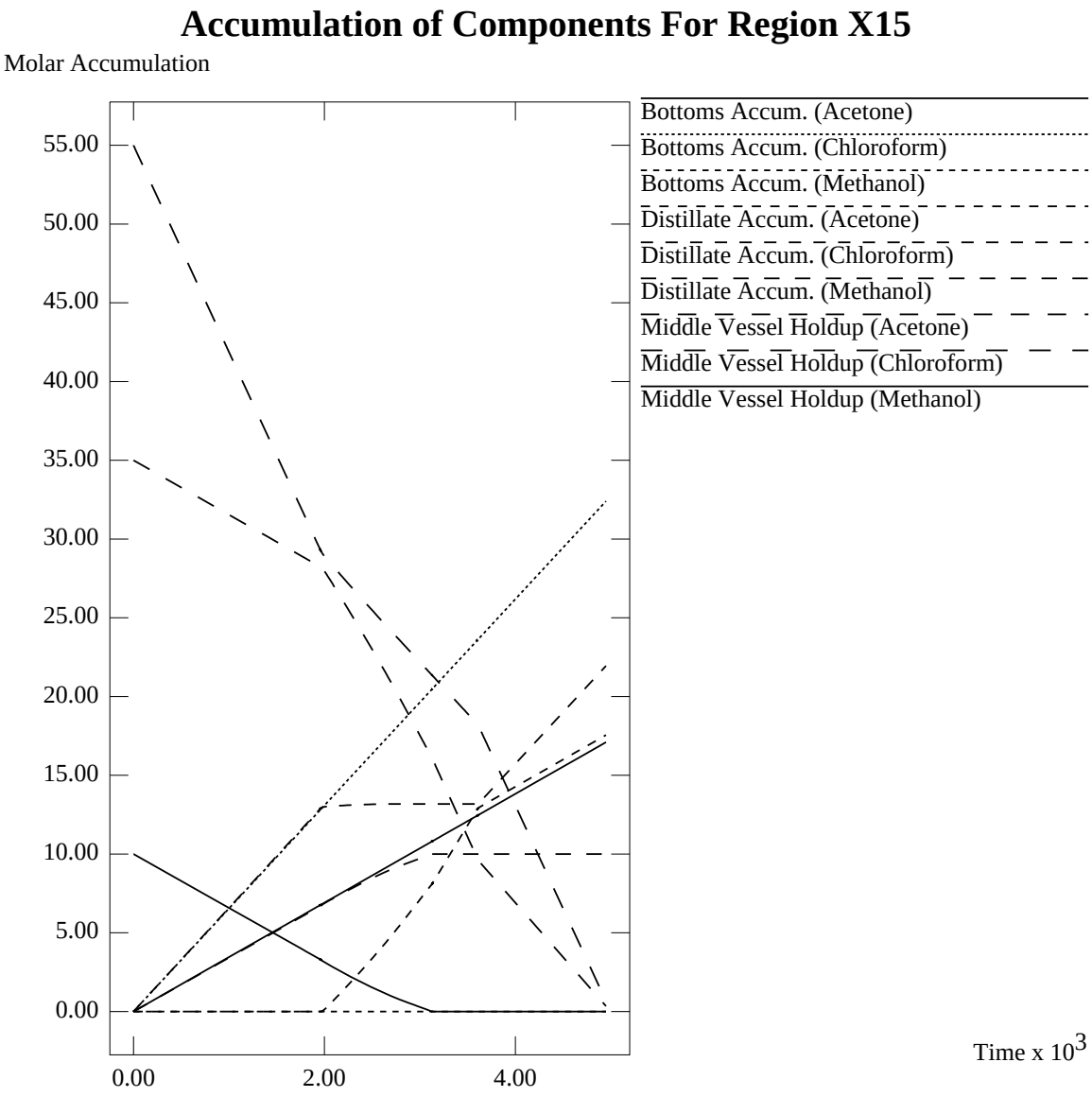

Figure D-111: Graph of Accumulation of Each Component against Time

D.4.16 Simulation Results for Region χ_{16}

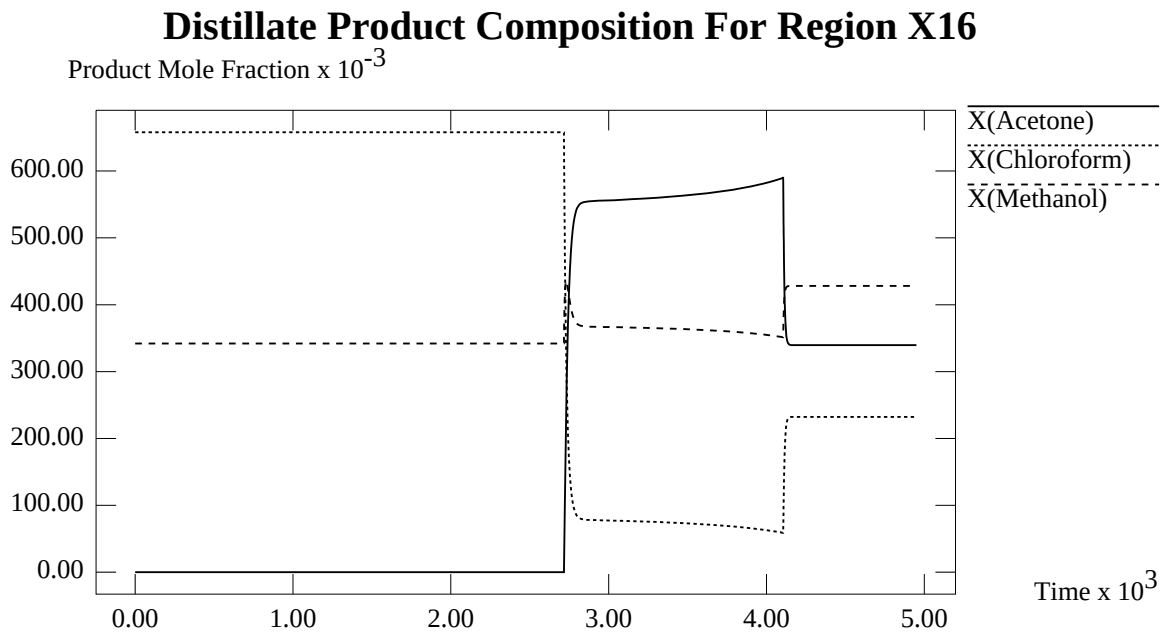

Figure D-112: Graph of Distillate Product Composition against Time

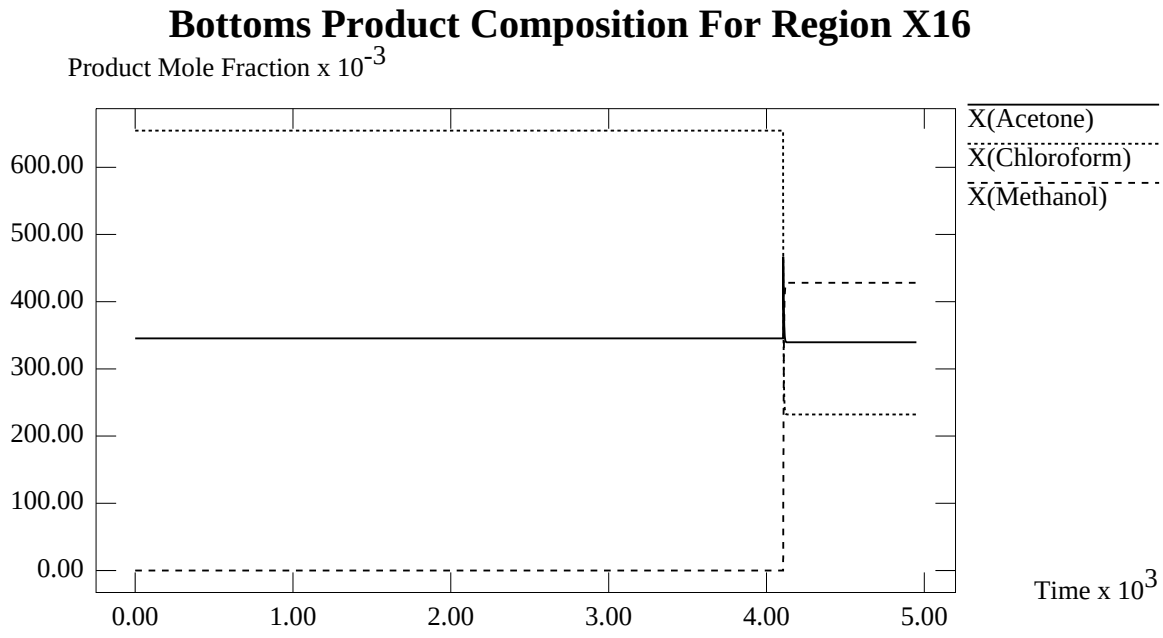

Figure D-113: Graph of Bottoms Product Composition against Time

D.4.17 Simulation Results for Region χ_{17}

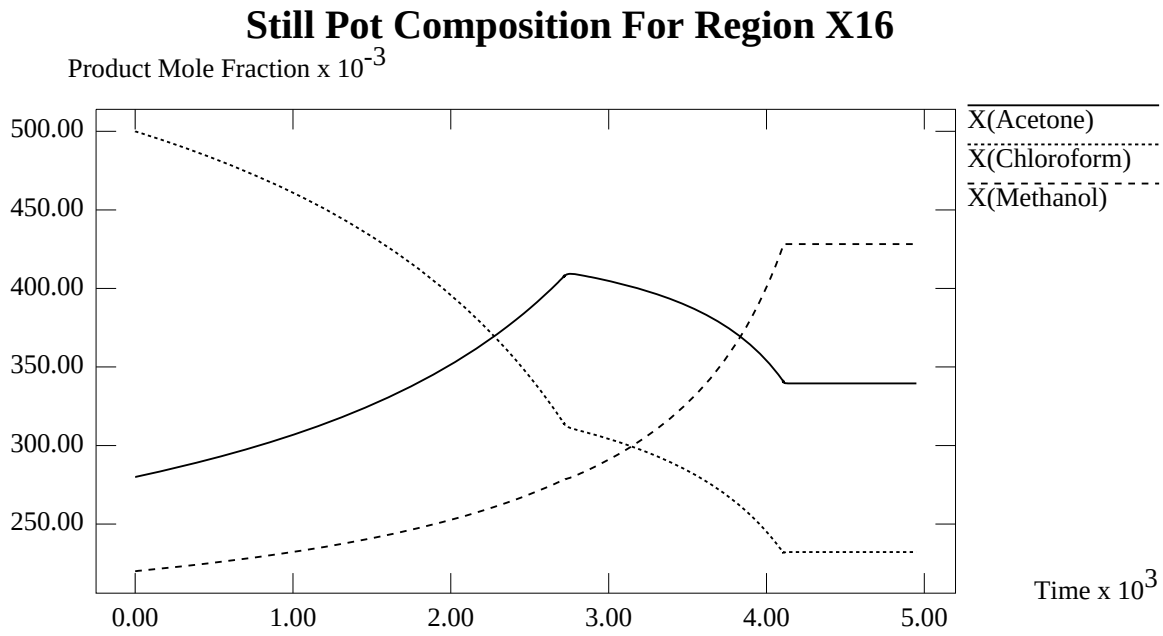

Figure D-114: Graph of Still Pot Composition against Time

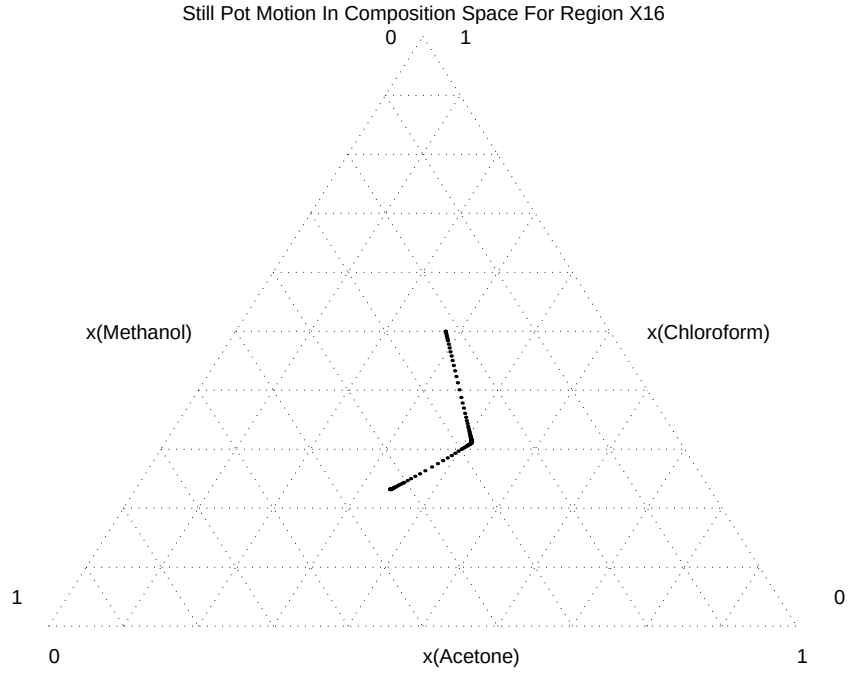

Figure D-115: Plot of Still Pot Motion in Composition Space

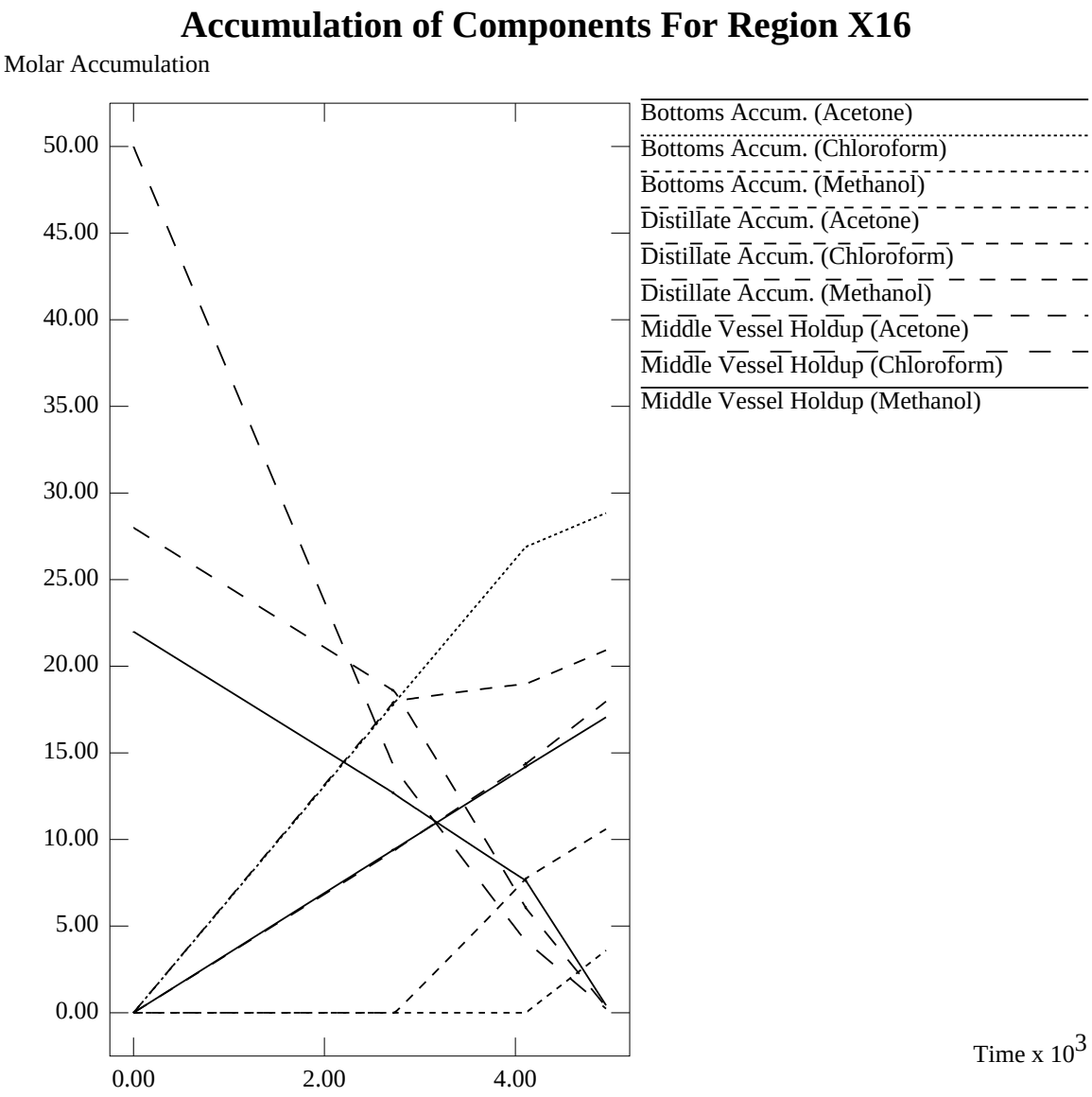

Figure D-116: Graph of Accumulation of Each Component against Time

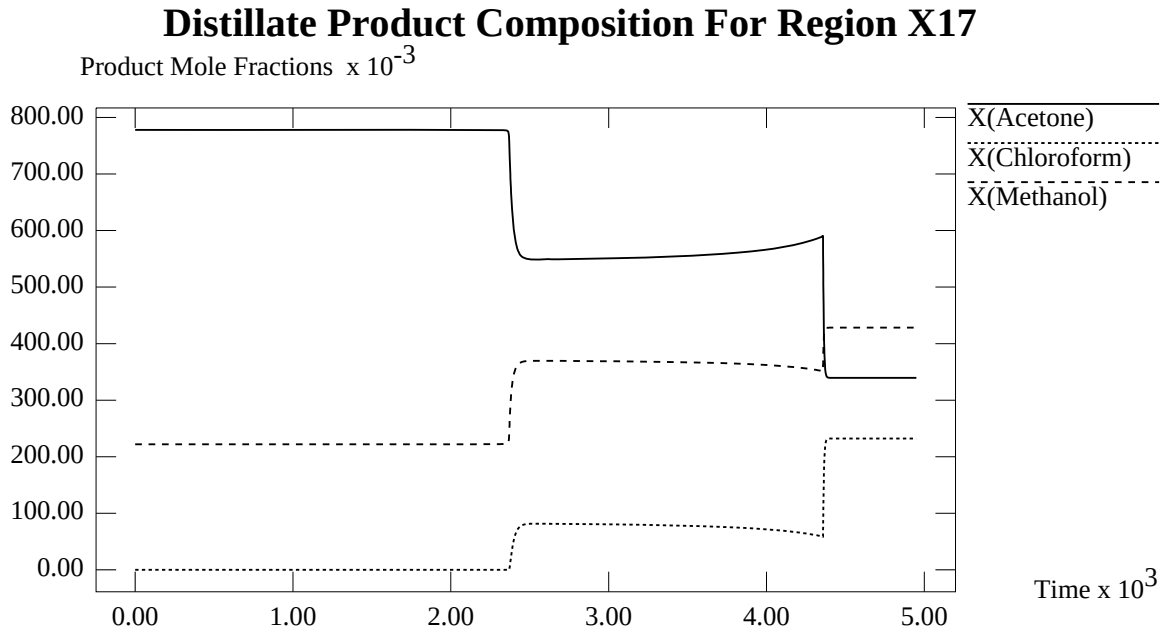

Figure D-117: Graph of Distillate Product Composition against Time

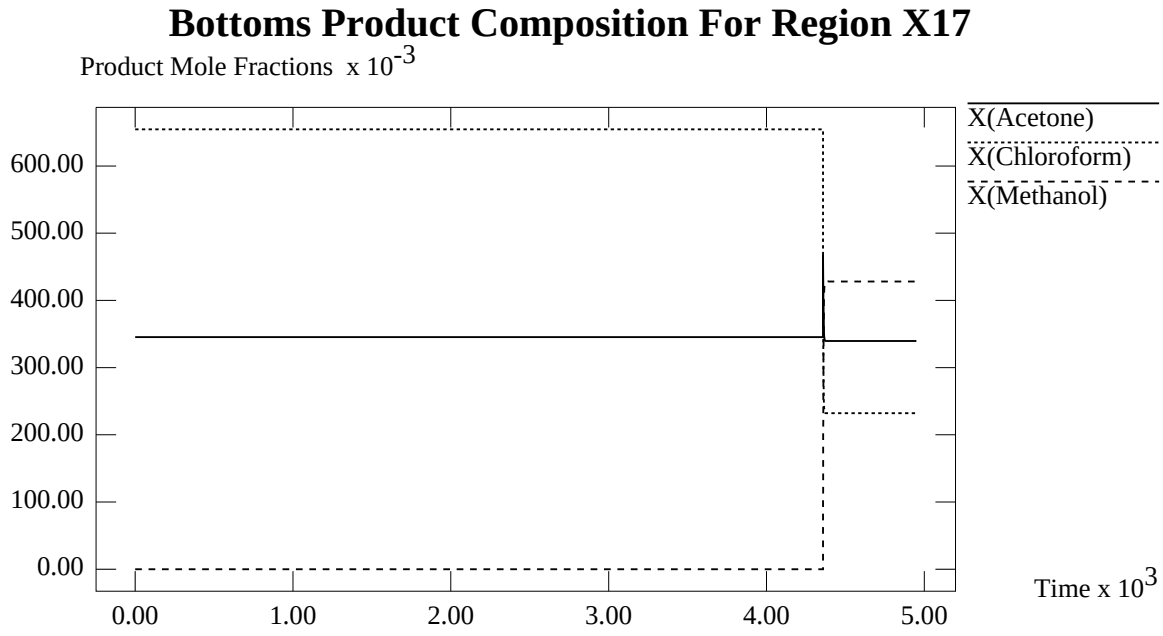

Figure D-118: Graph of Bottoms Product Composition against Time

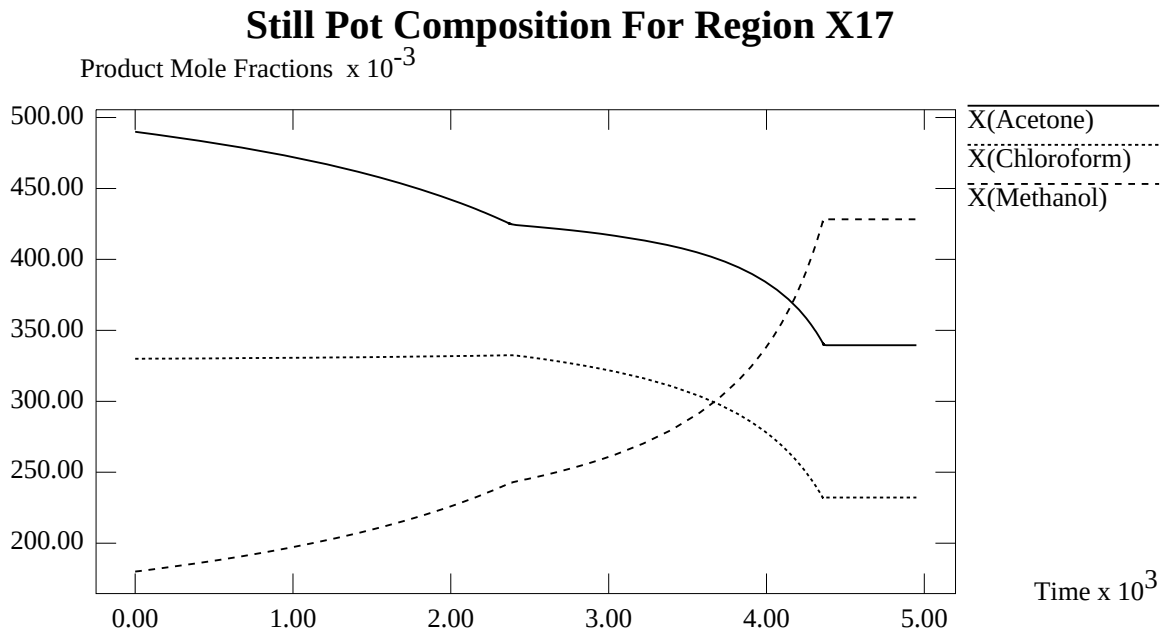

Figure D-119: Graph of Still Pot Composition against Time

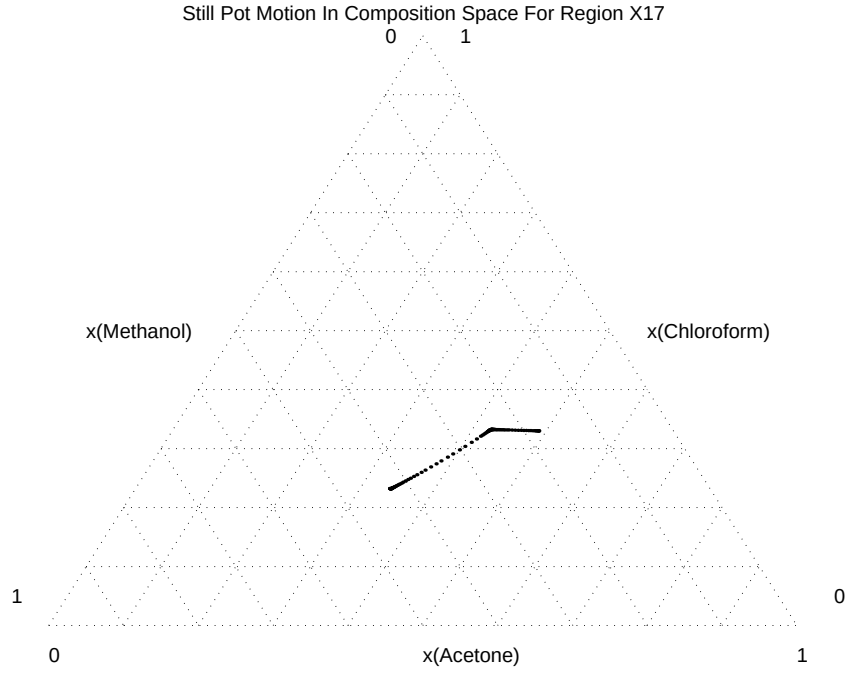

Figure D-120: Plot of Still Pot Motion in Composition Space

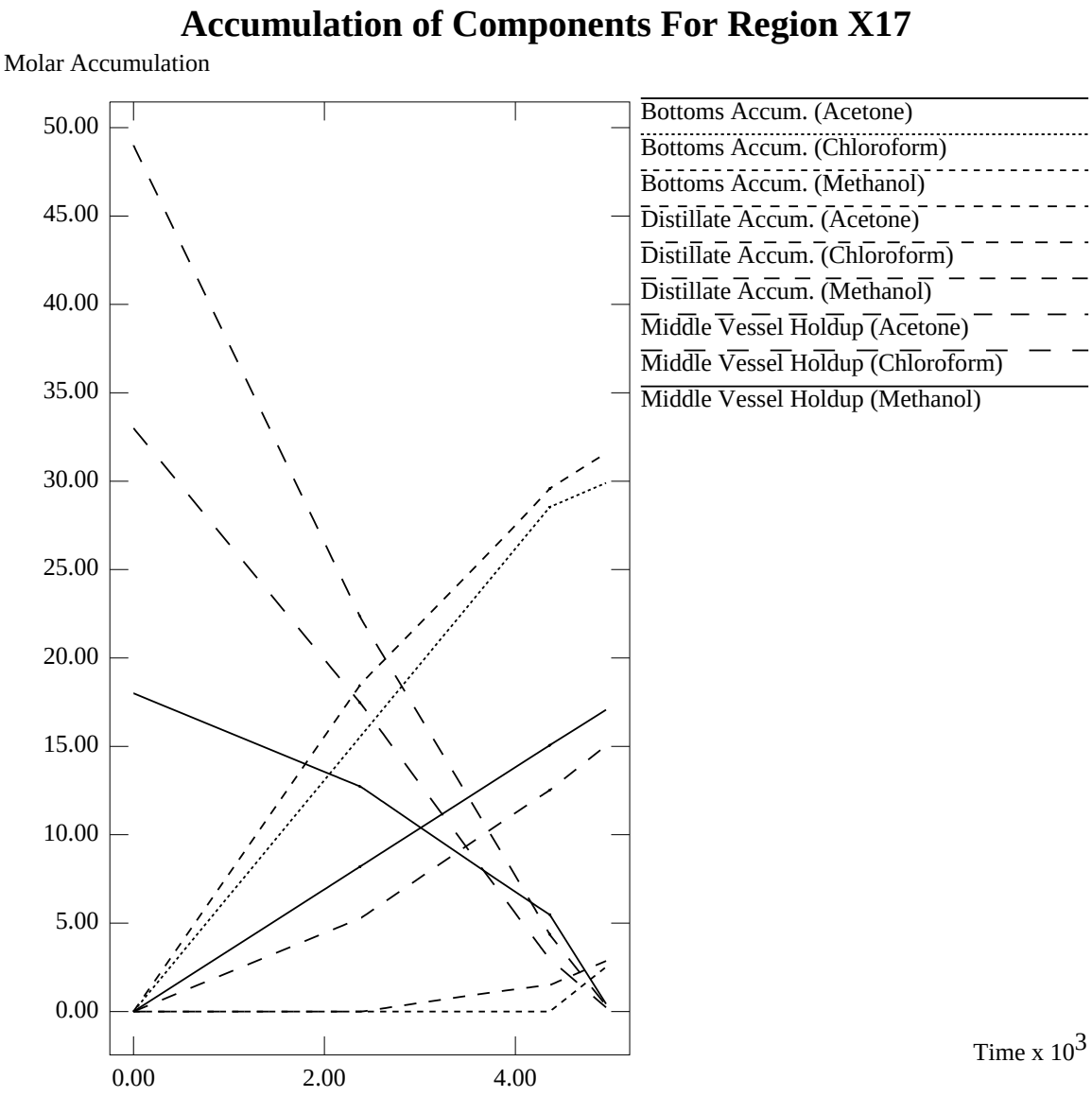

Figure D-121: Graph of Accumulation of Each Component against Time

D.4.18 Simulation Results for Region χ_{18}

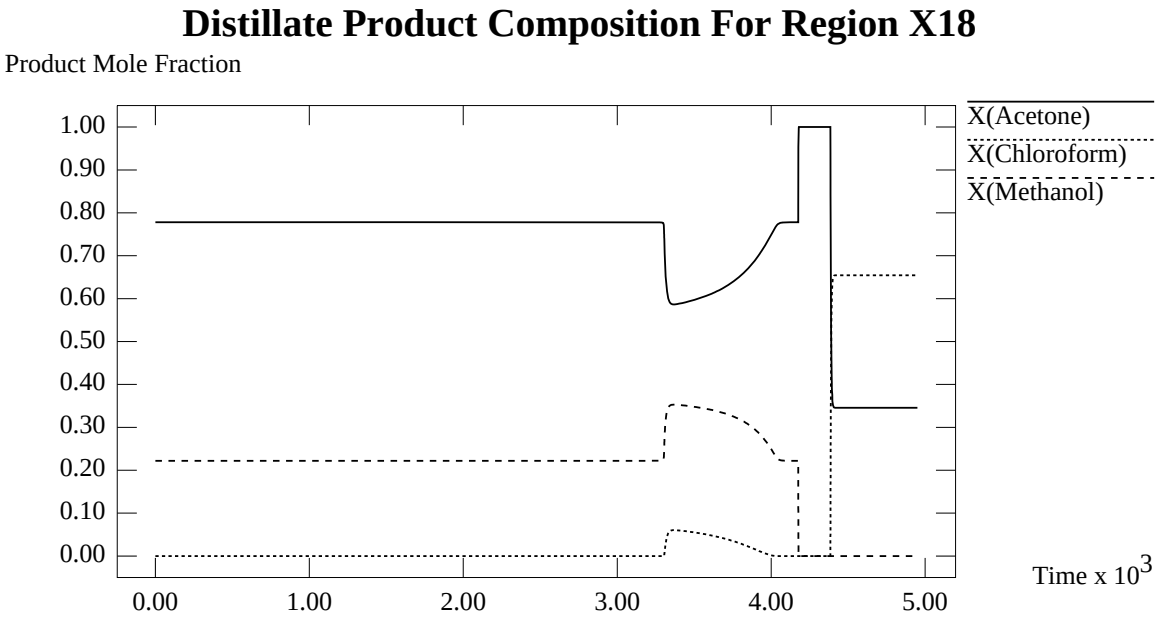

Figure D-122: Graph of Distillate Product Composition against Time

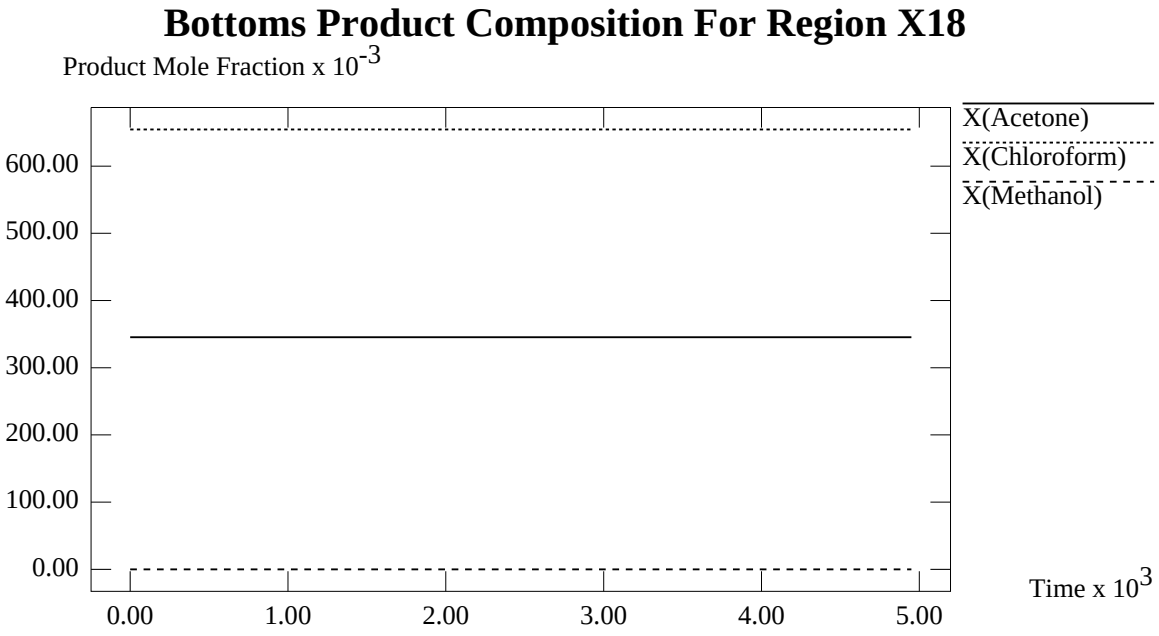

Figure D-123: Graph of Bottoms Product Composition against Time

D.4.19 Simulation Results for Region χ_{19}

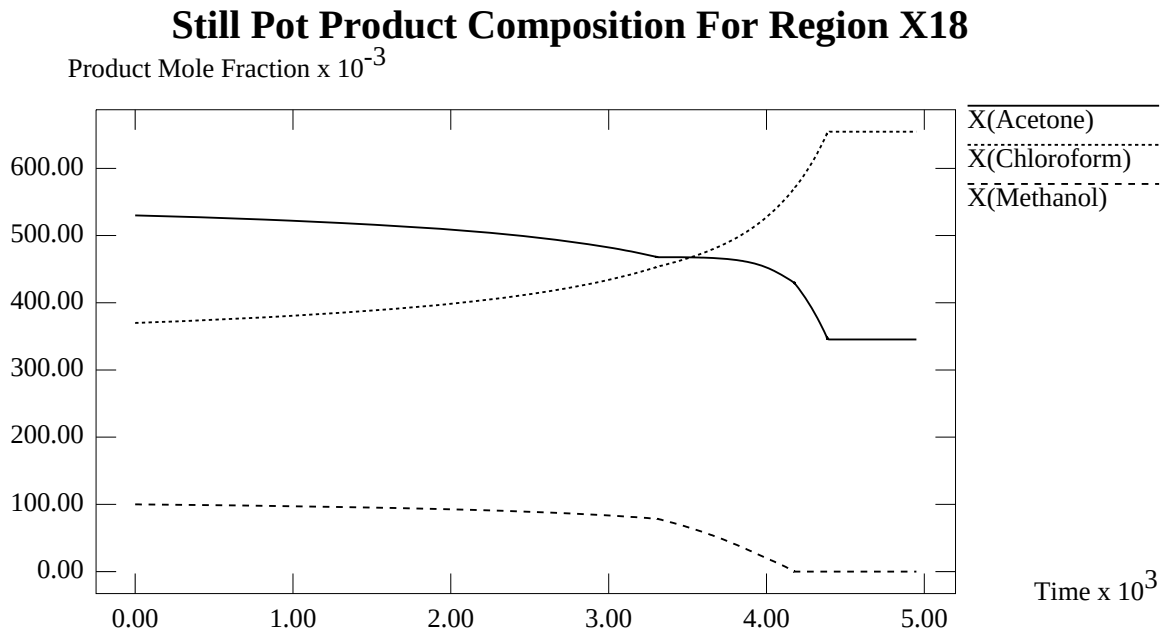

Figure D-124: Graph of Still Pot Composition against Time

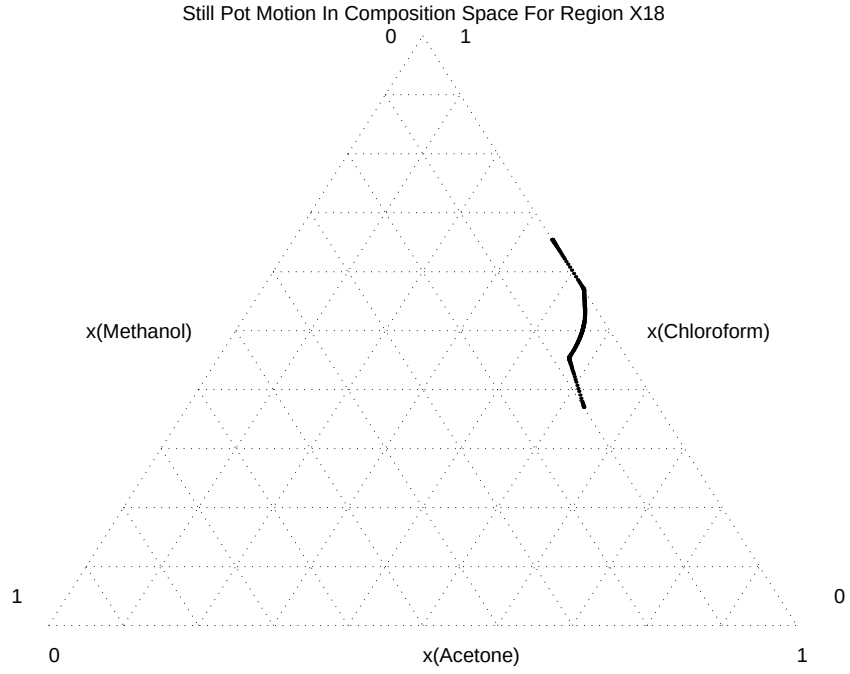

Figure D-125: Plot of Still Pot Motion in Composition Space

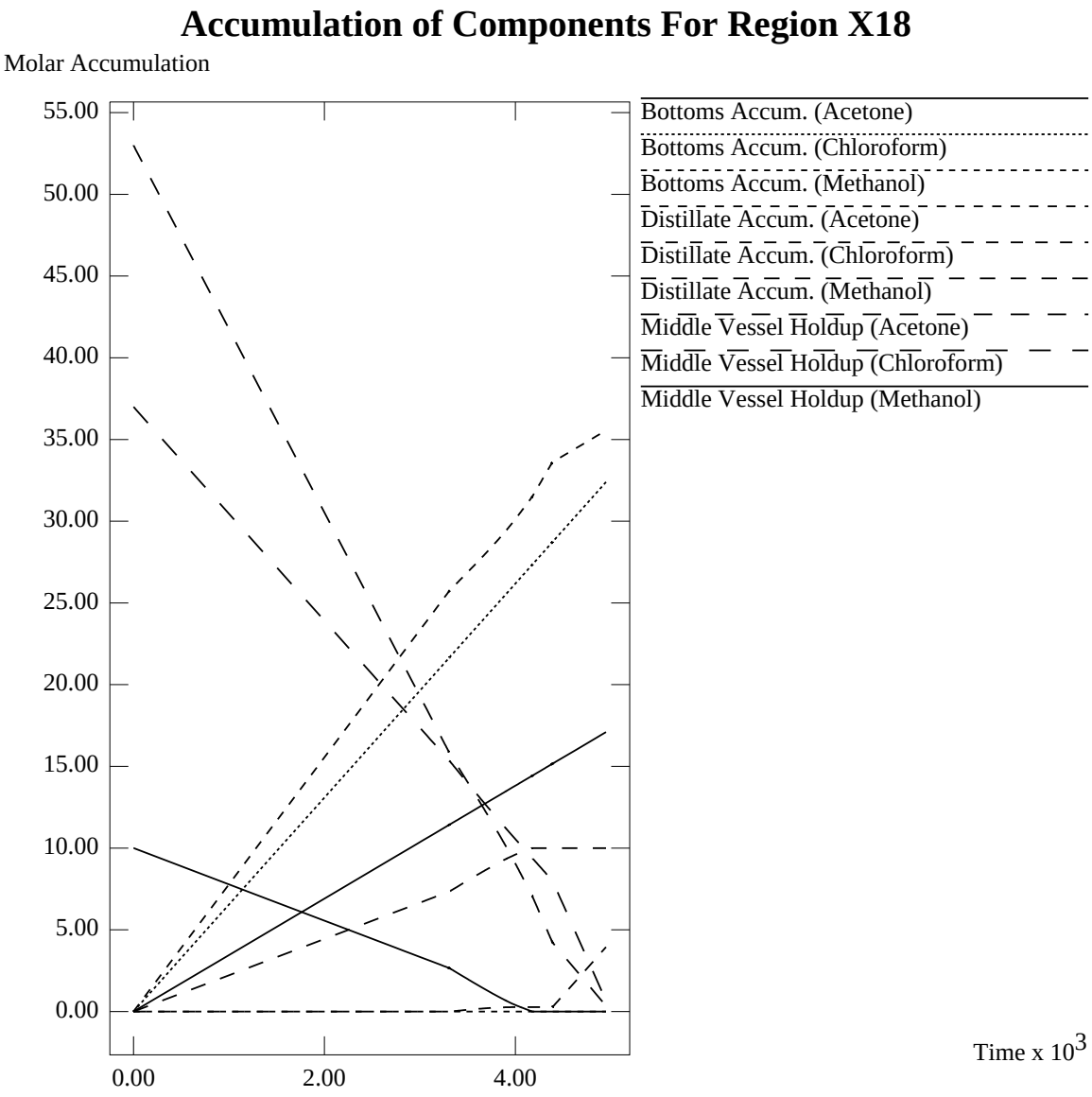

Figure D-126: Graph of Accumulation of Each Component against Time

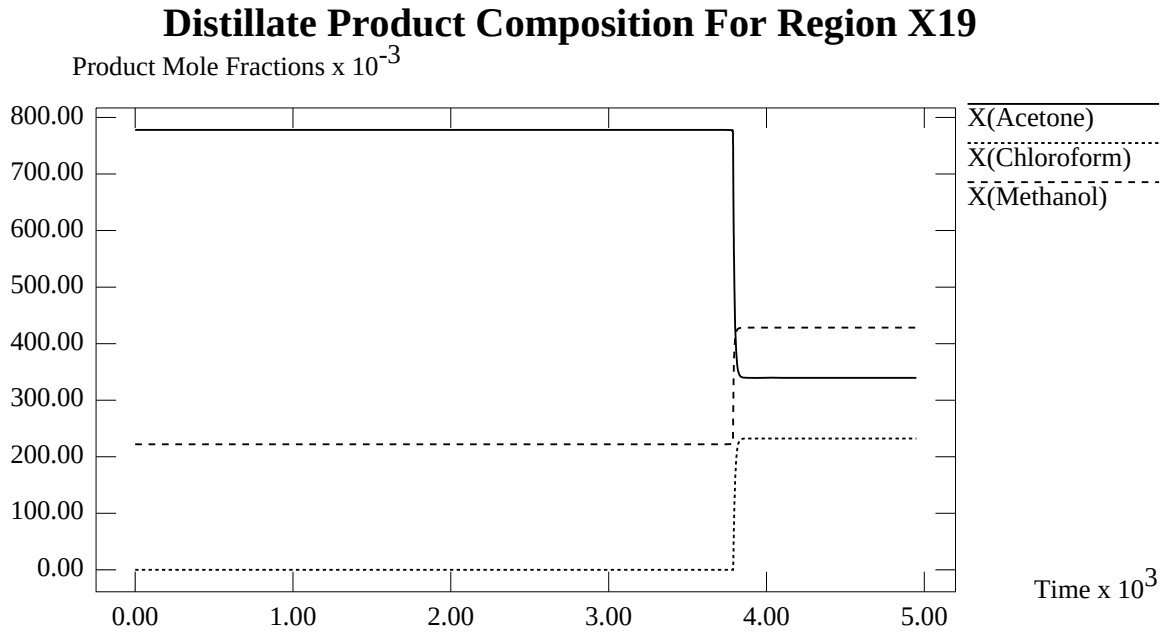

Figure D-127: Graph of Distillate Product Composition against Time

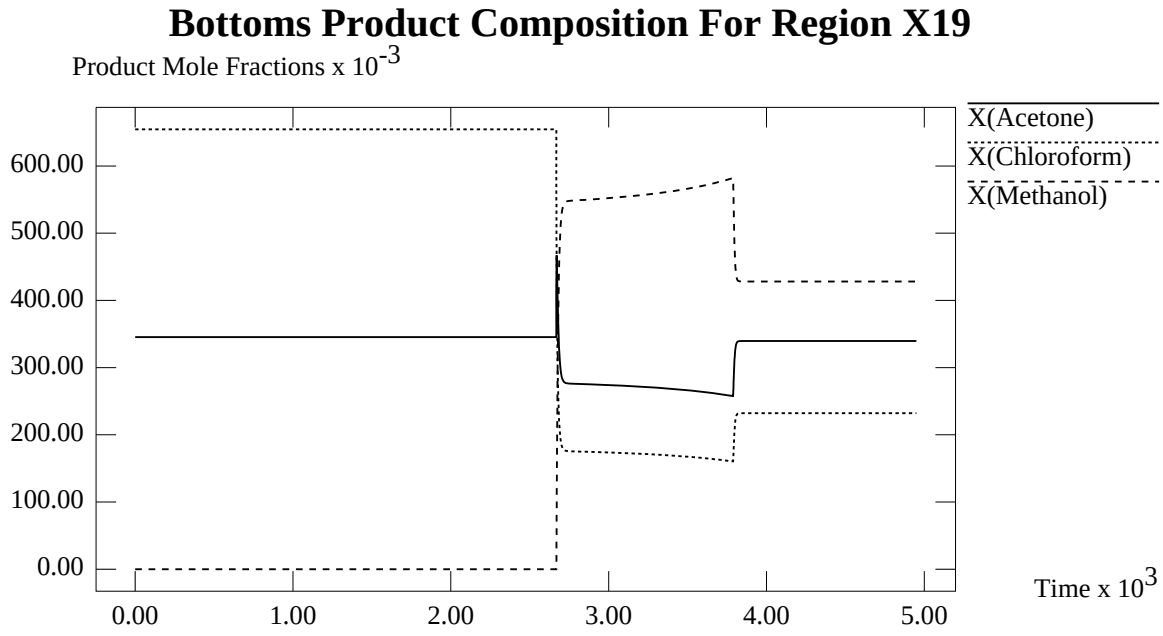

Figure D-128: Graph of Bottoms Product Composition against Time

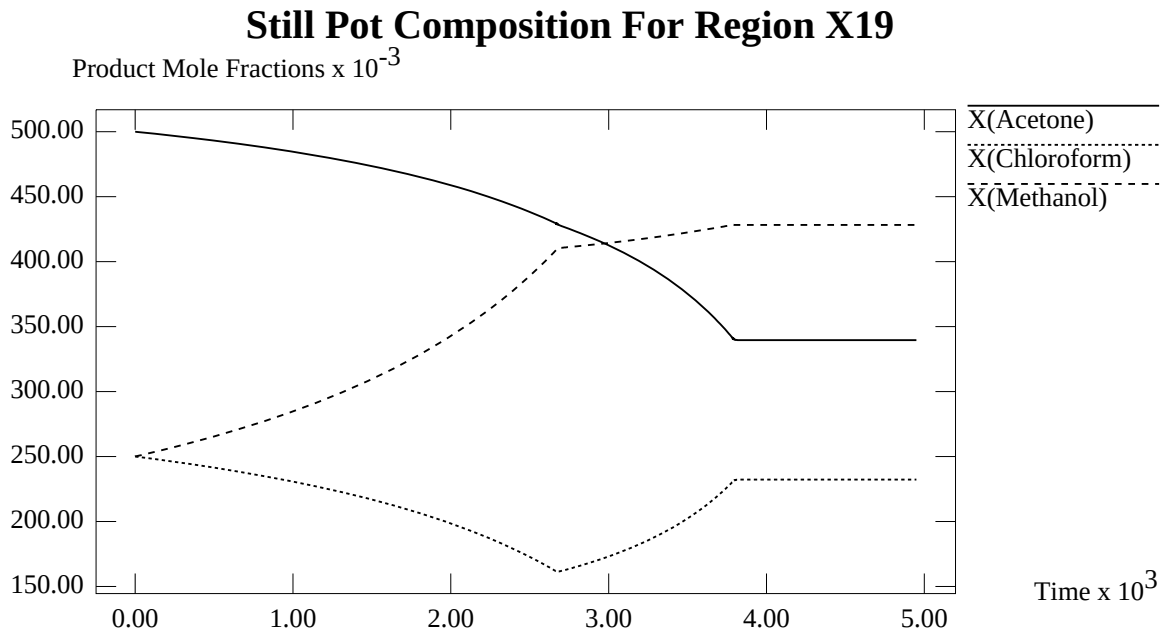

Figure D-129: Graph of Still Pot Composition against Time

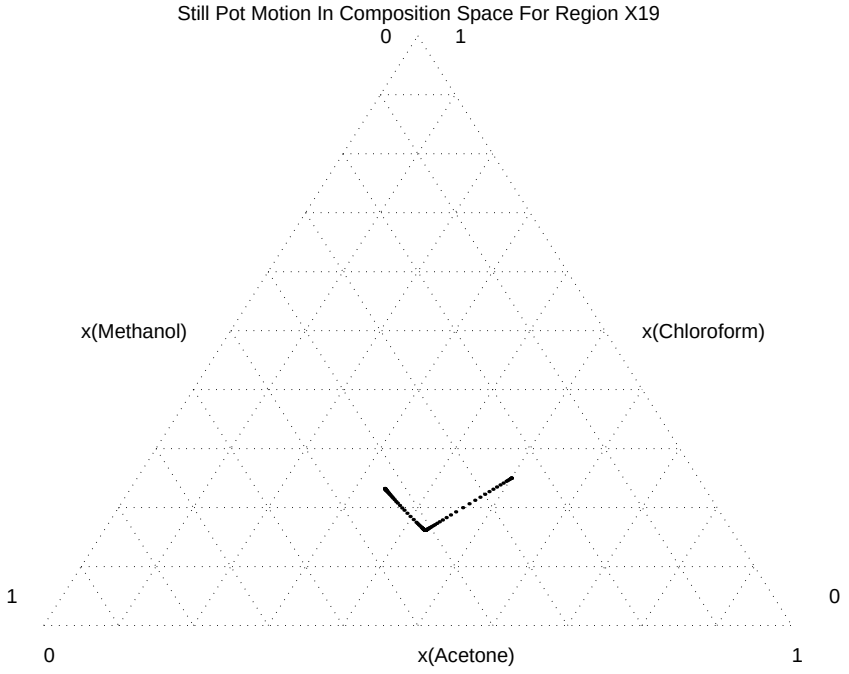

Figure D-130: Plot of Still Pot Motion in Composition Space

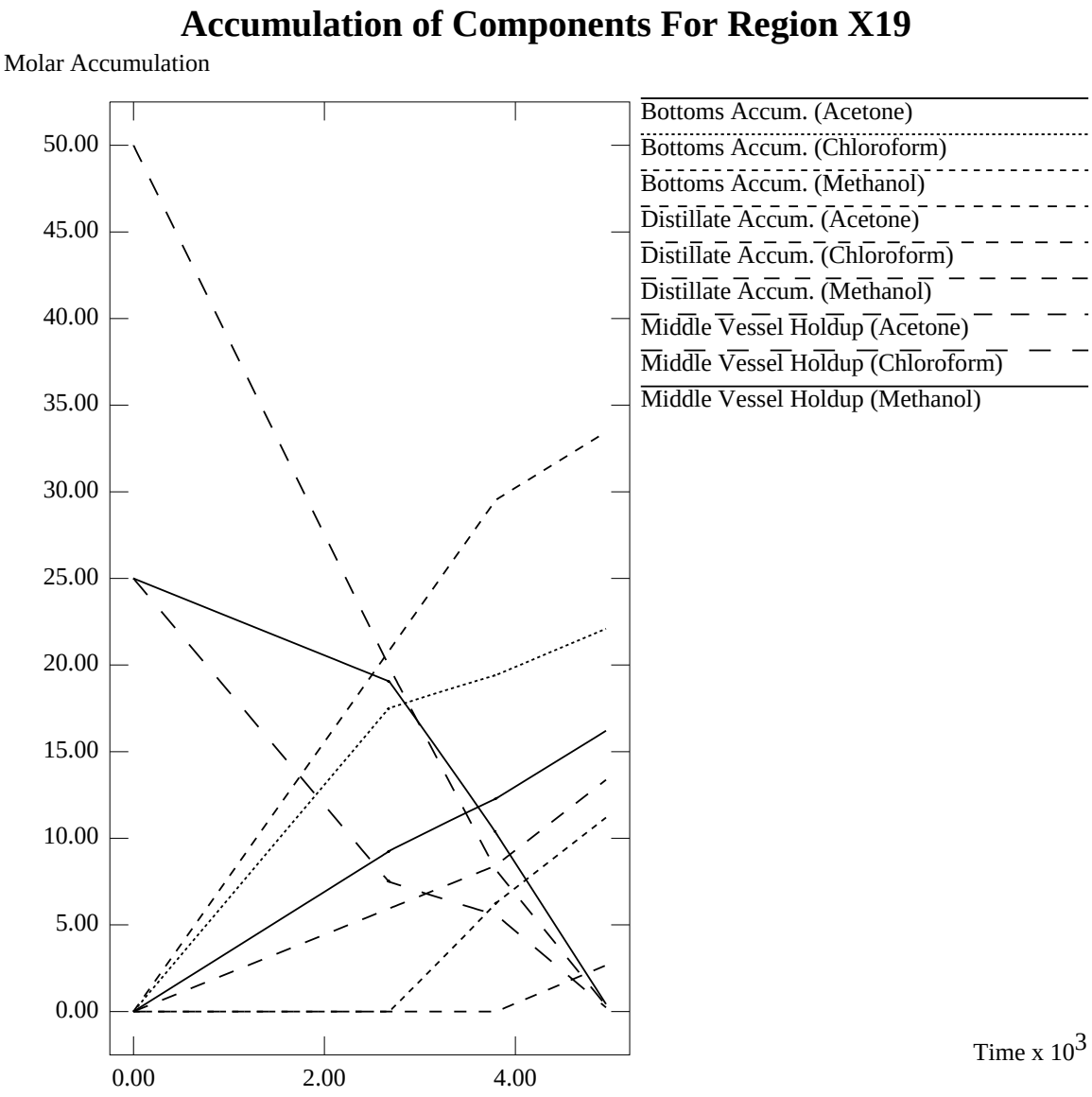

Figure D-131: Graph of Accumulation of Each Component against Time

D.4.20 Simulation Results for Region χ_{20}

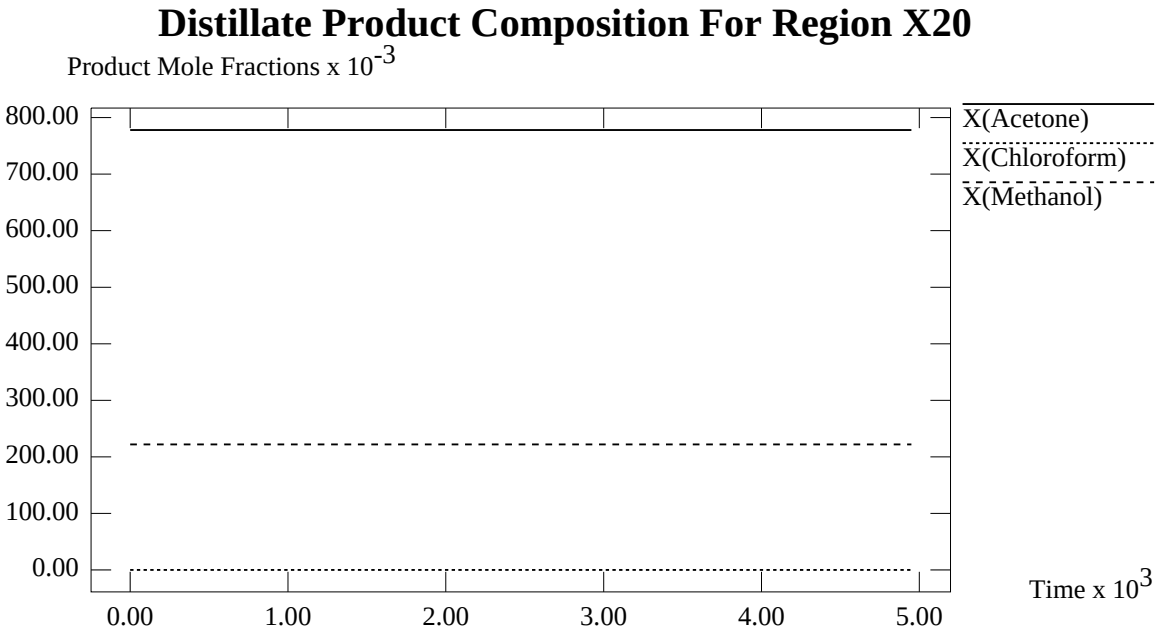

Figure D-132: Graph of Distillate Product Composition against Time

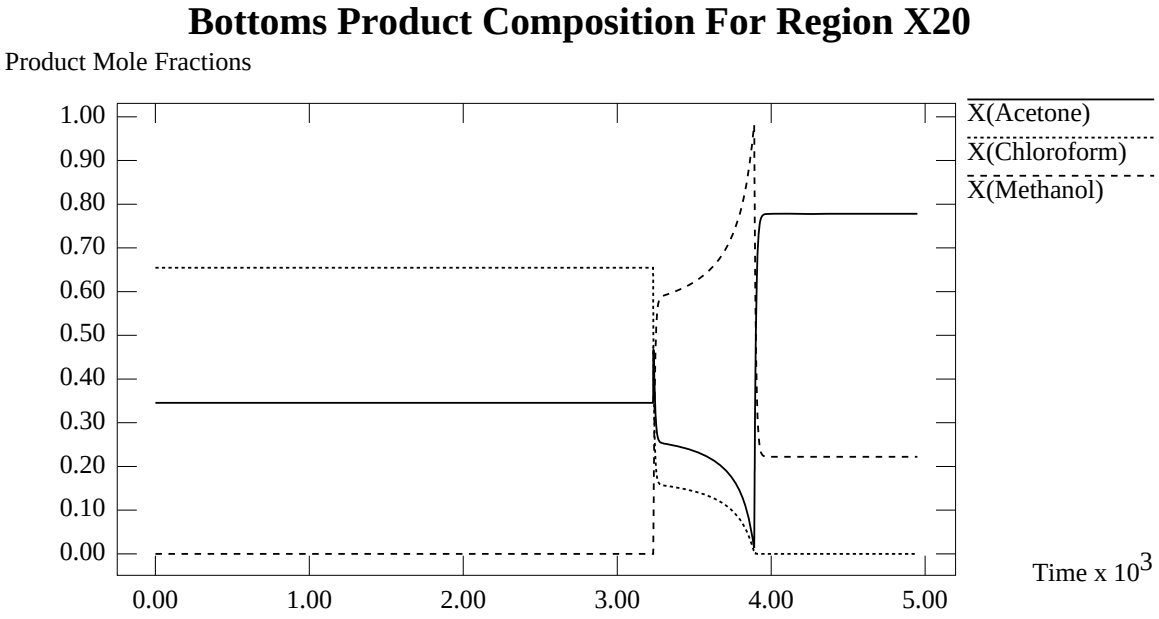

Figure D-133: Graph of Bottoms Product Composition against Time

D.4.21 Simulation Results for Region χ_{21}

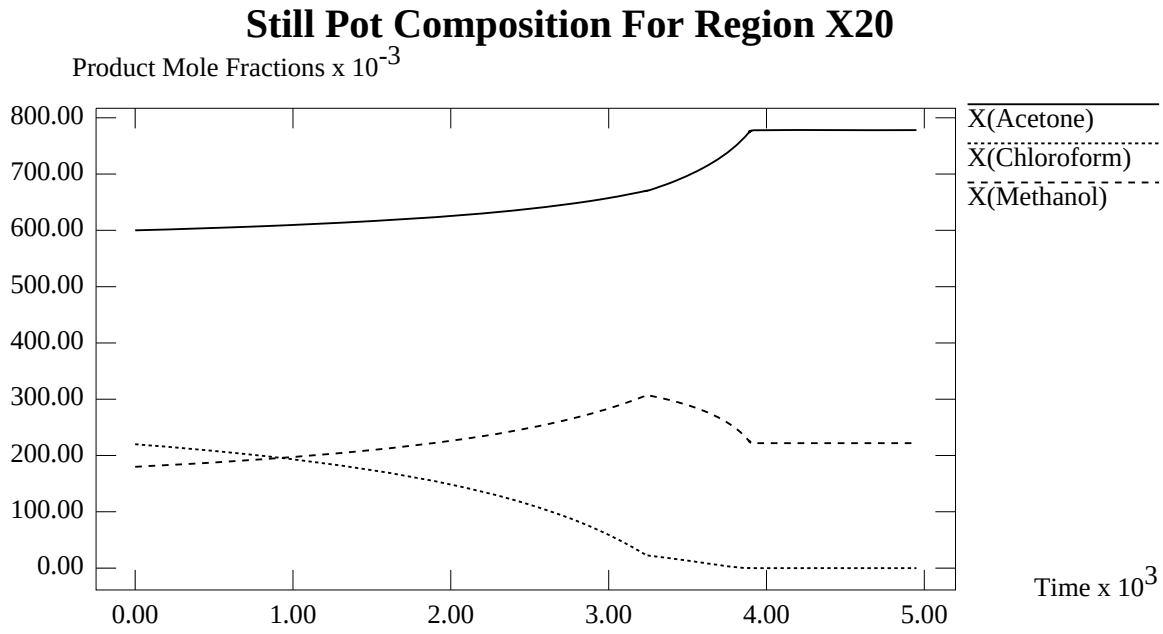

Figure D-134: Graph of Still Pot Composition against Time

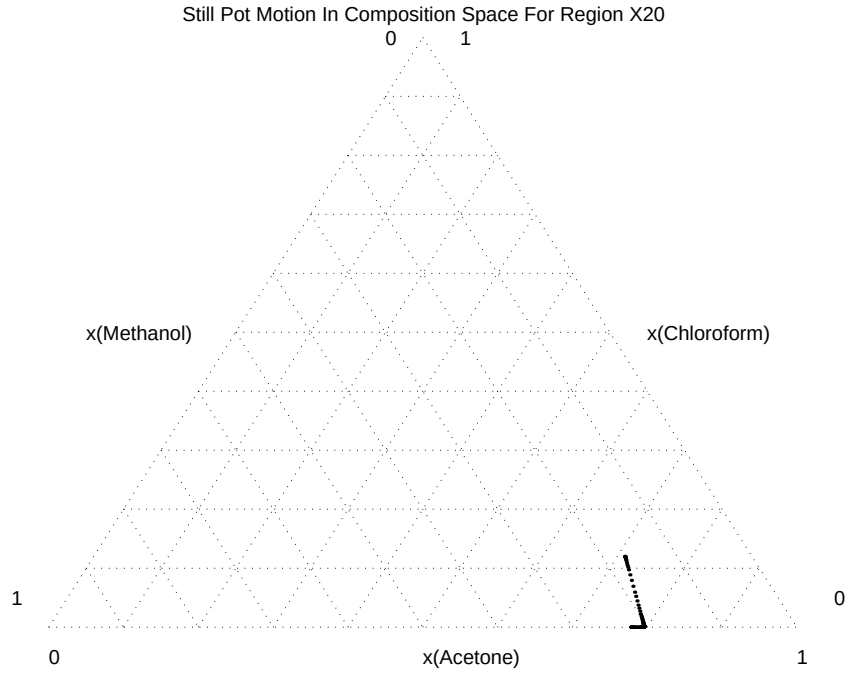

Figure D-135: Plot of Still Pot Motion in Composition Space

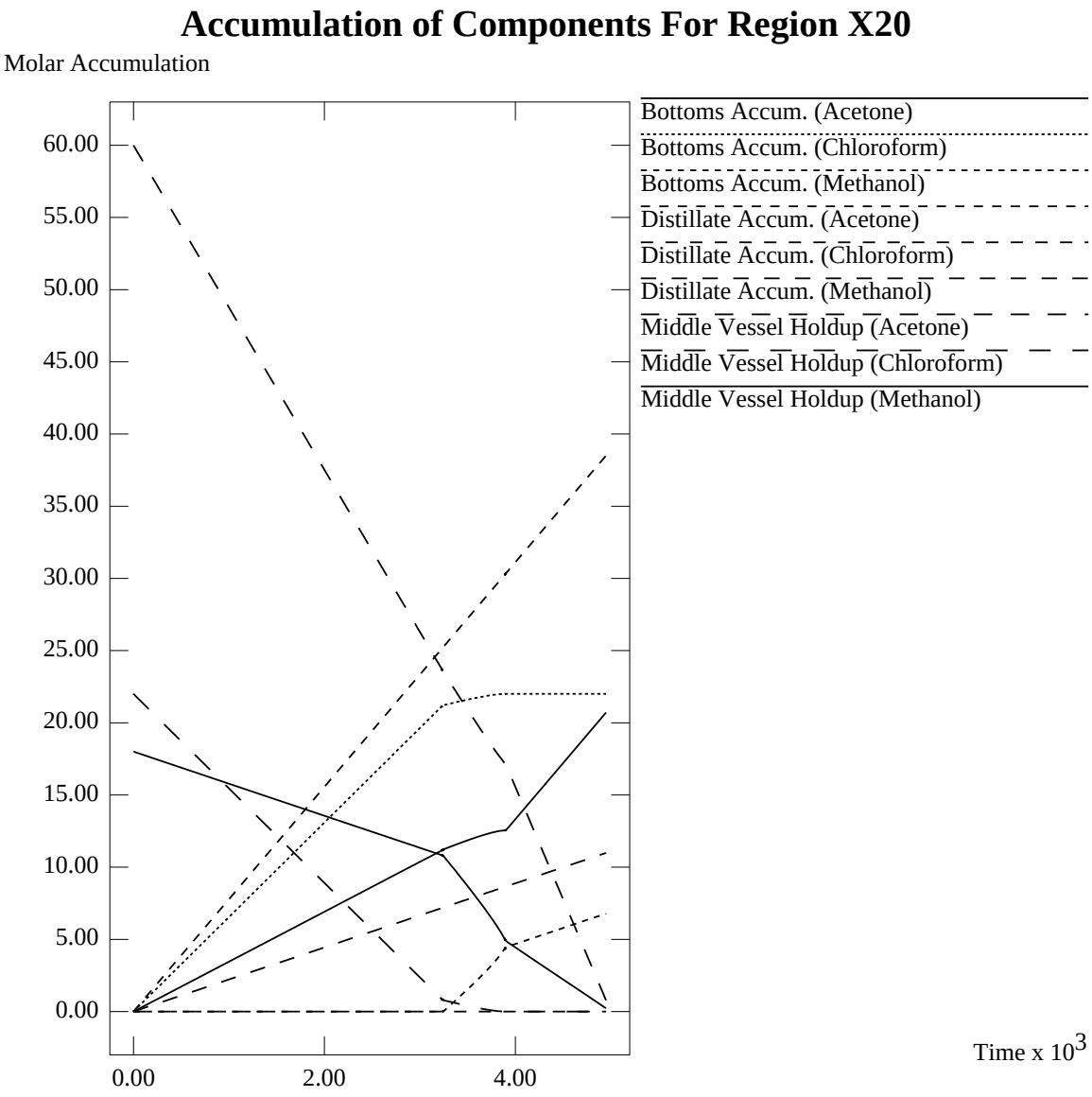

Figure D-136: Graph of Accumulation of Each Component against Time

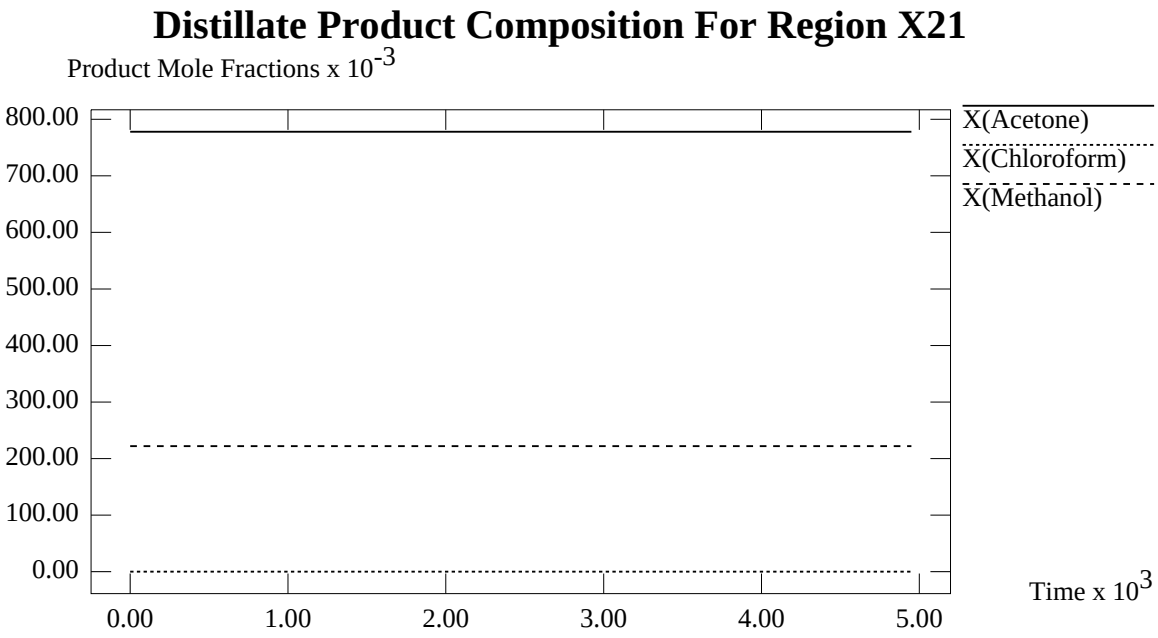

Figure D-137: Graph of Distillate Product Composition against Time

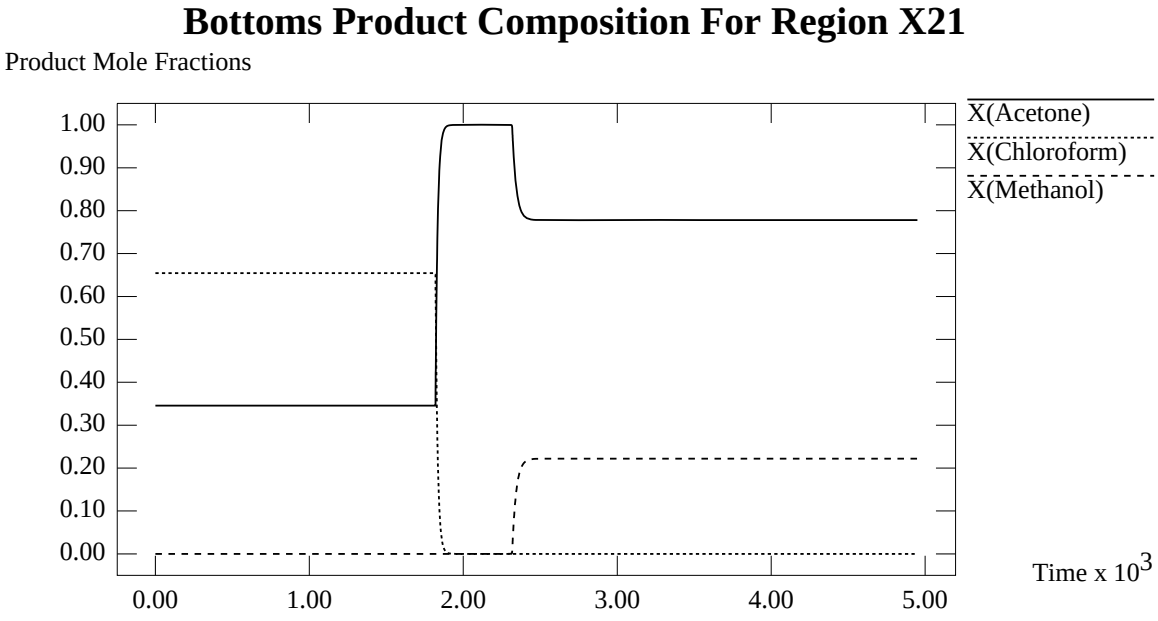

Figure D-138: Graph of Bottoms Product Composition against Time

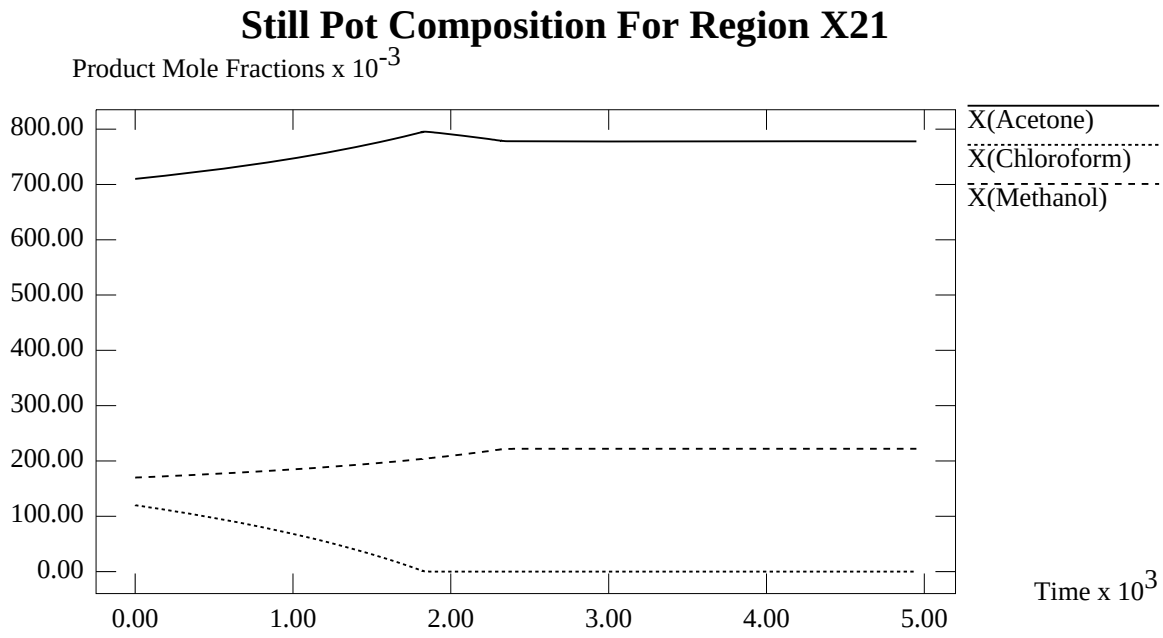

Figure D-139: Graph of Still Pot Composition against Time

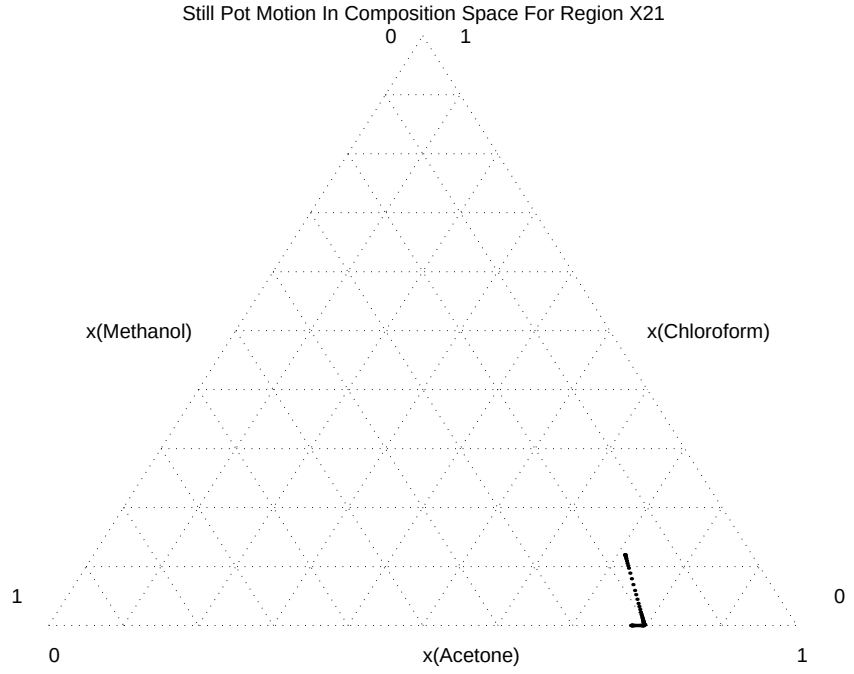

Figure D-140: Plot of Still Pot Motion in Composition Space

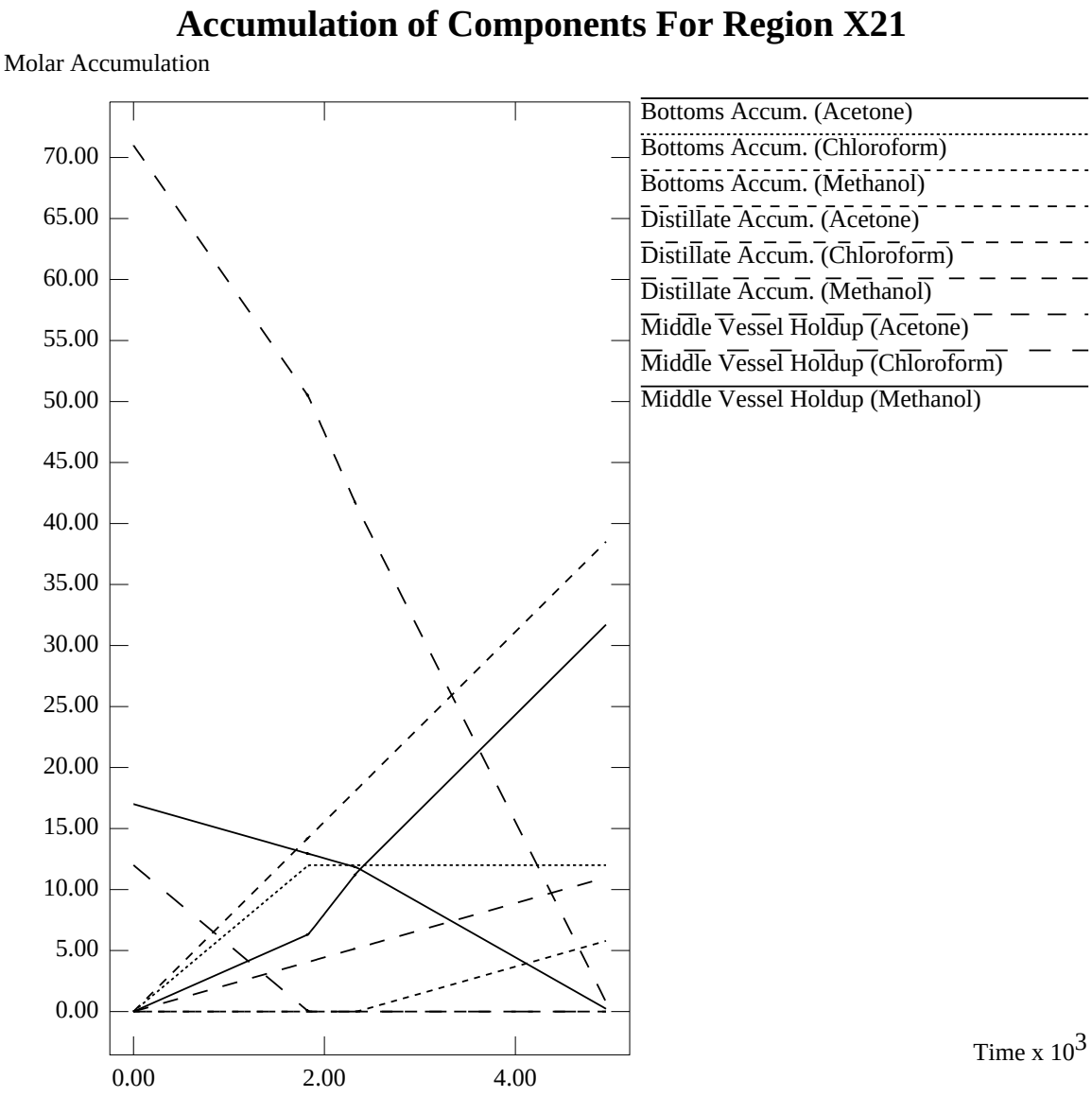

Figure D-141: Graph of Accumulation of Each Component against Time

D.4.22 Simulation Results for Region χ_{22}

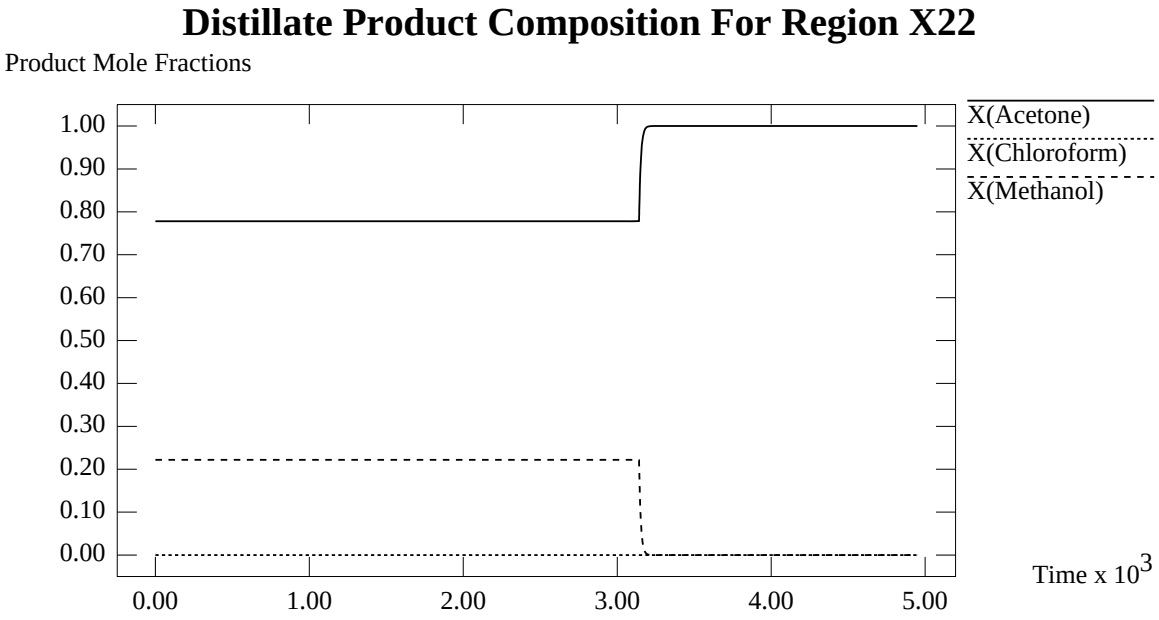

Figure D-142: Graph of Distillate Product Composition against Time

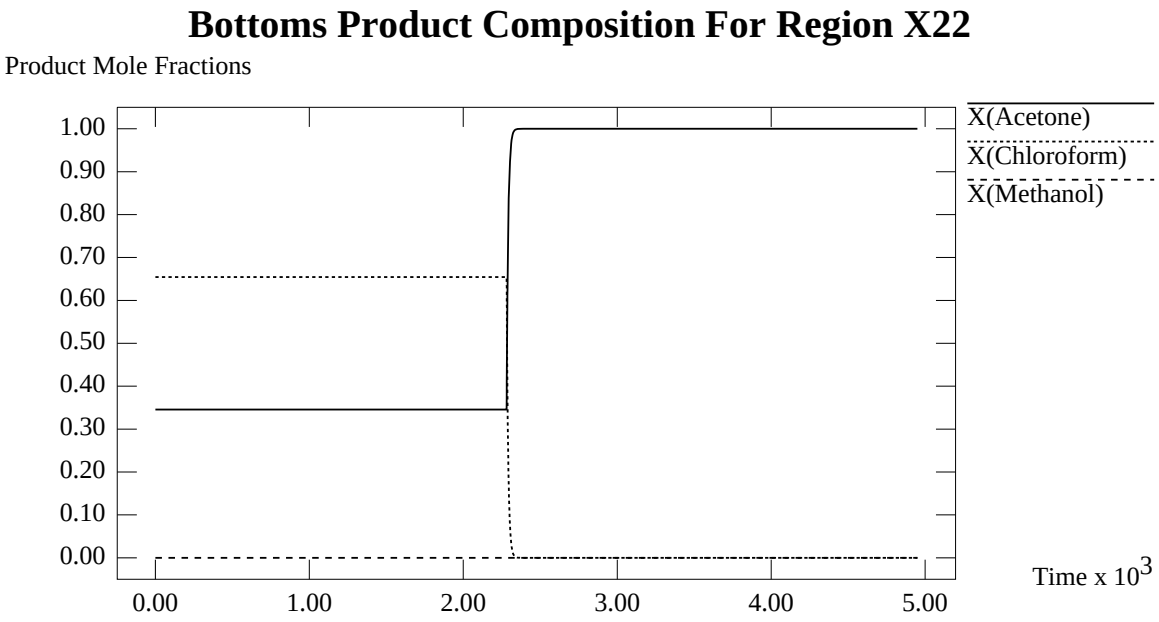

Figure D-143: Graph of Bottoms Product Composition against Time

D.4.23 Simulation Results for Region χ_{23}

D.4.24 Simulation Results for Region χ_{24}

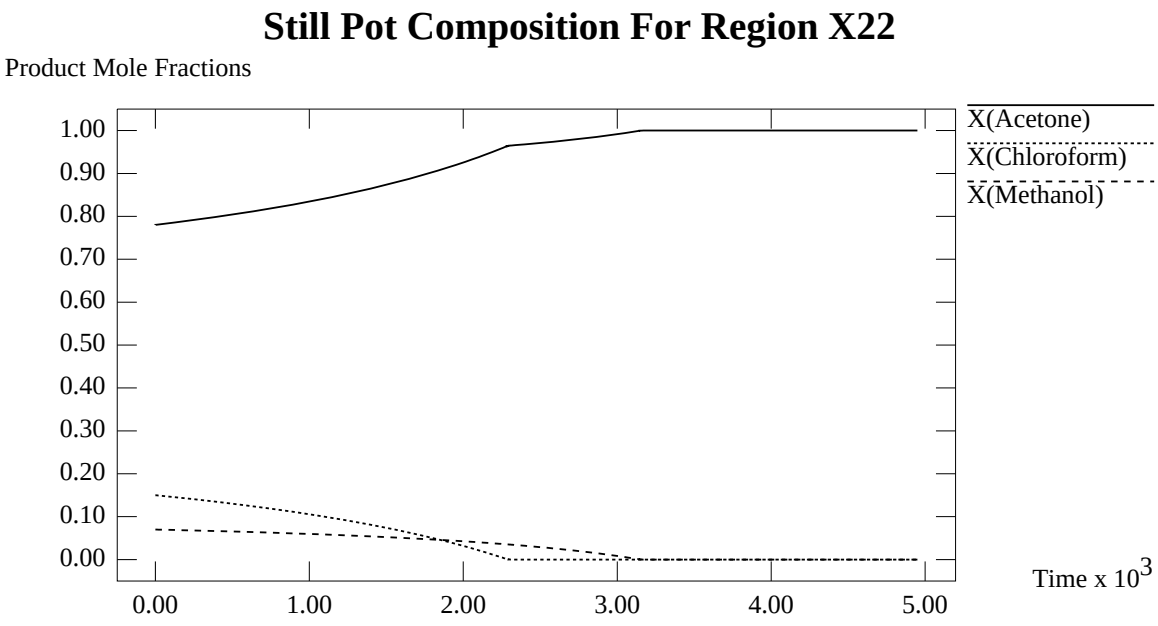

Figure D-144: Graph of Still Pot Composition against Time

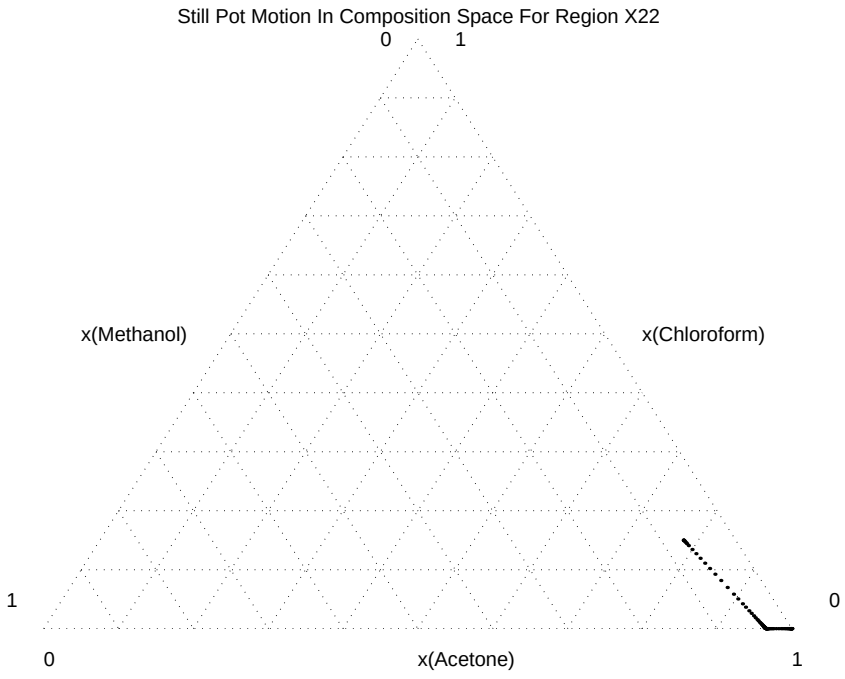

Figure D-145: Plot of Still Pot Motion in Composition Space

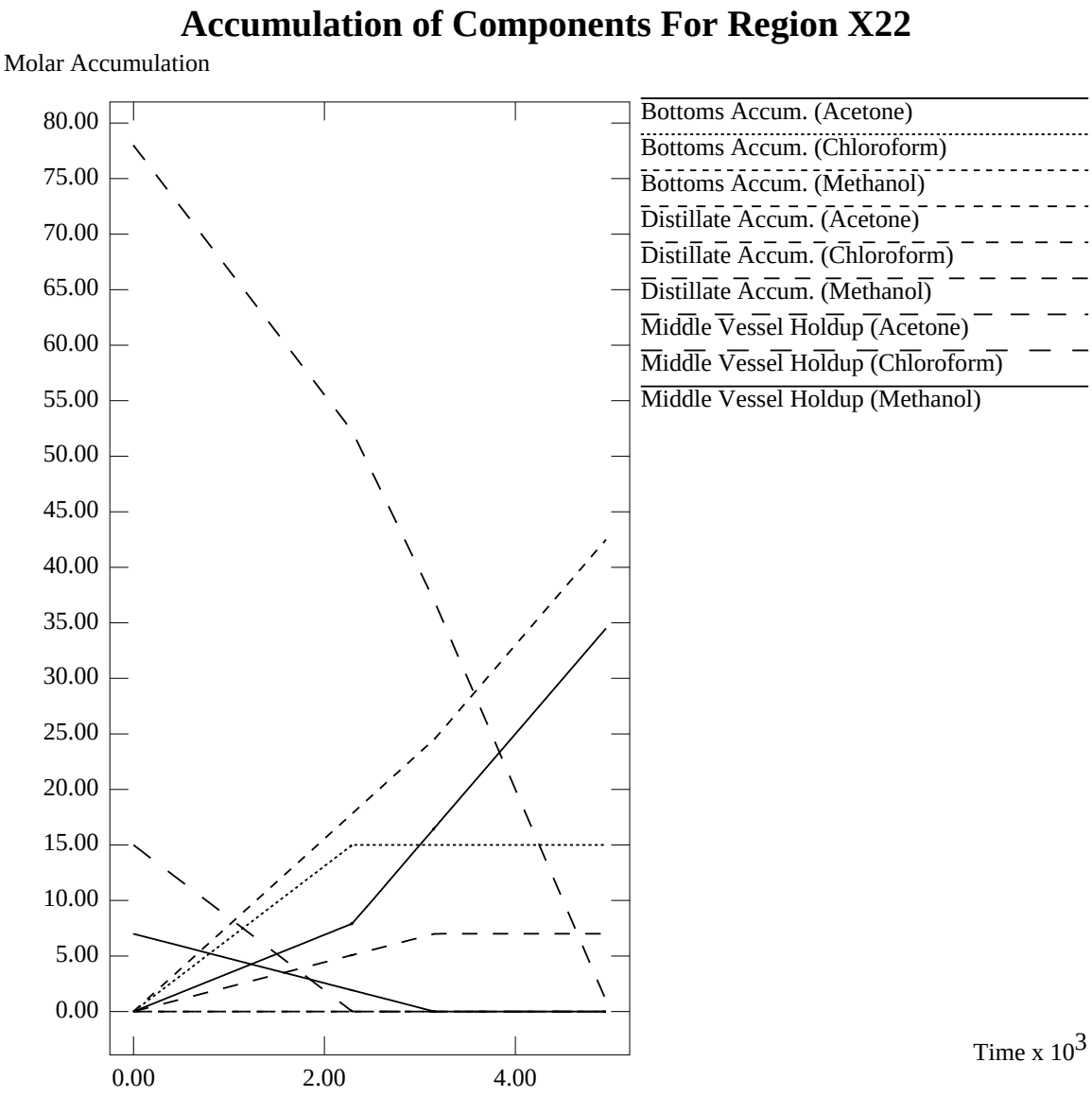

Figure D-146: Graph of Accumulation of Each Component against Time

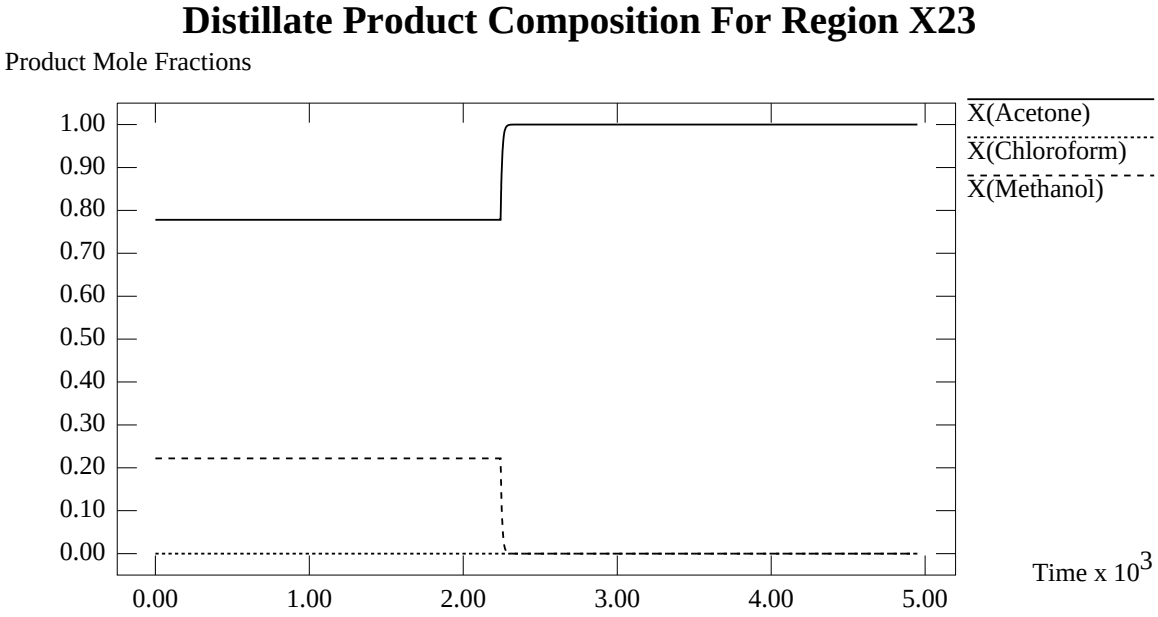

Figure D-147: Graph of Distillate Product Composition against Time

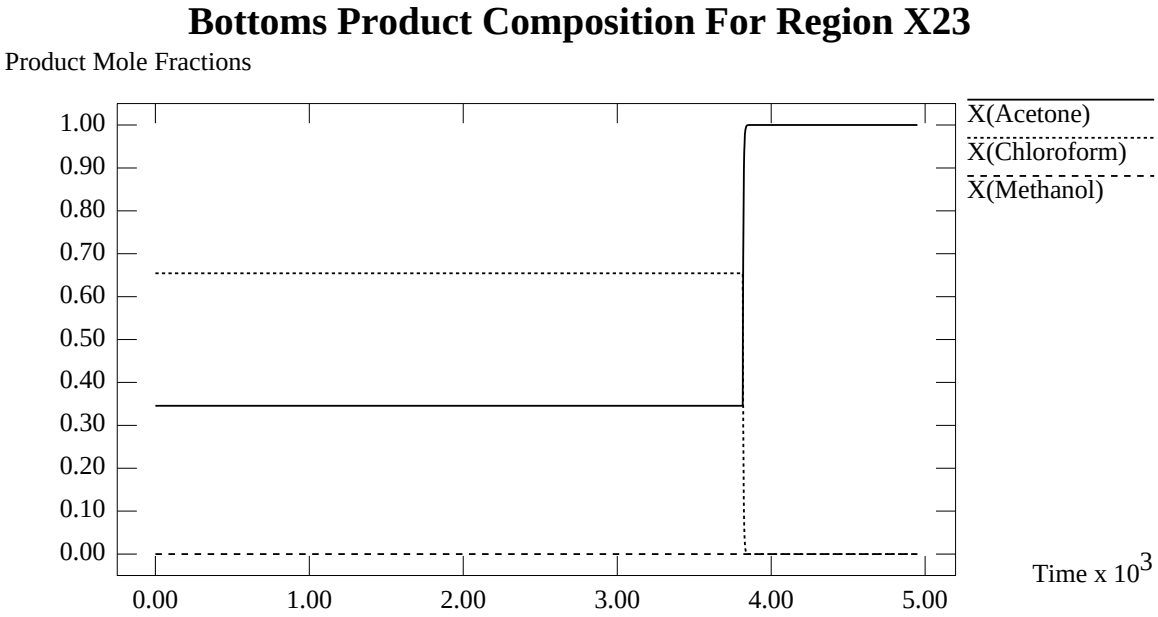

Figure D-148: Graph of Bottoms Product Composition against Time

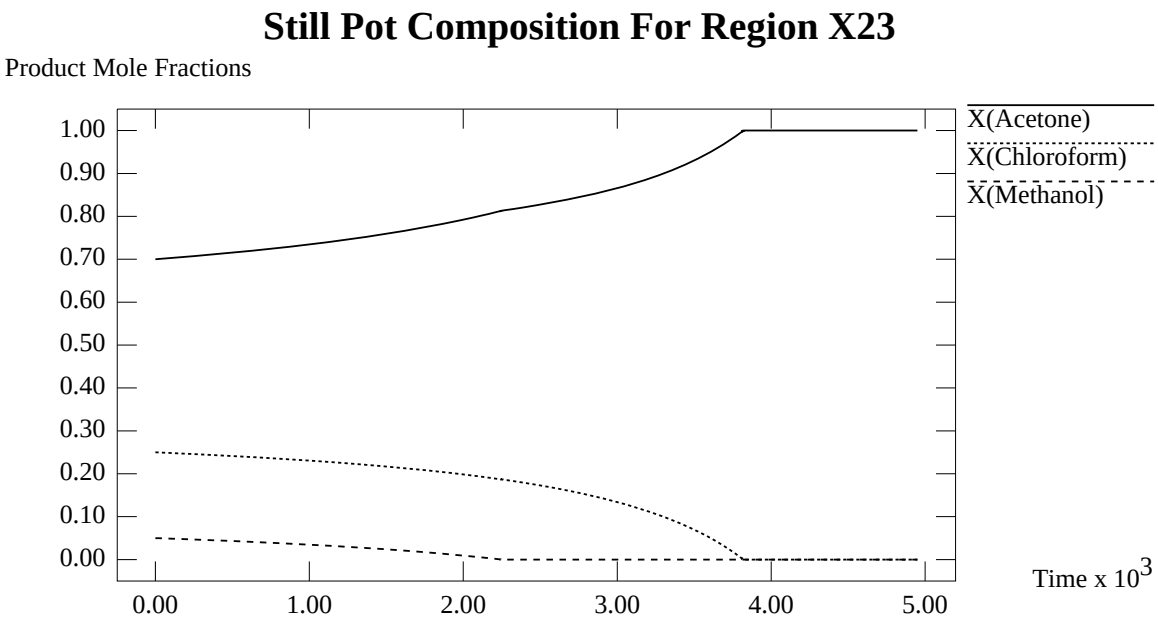

Figure D-149: Graph of Still Pot Composition against Time

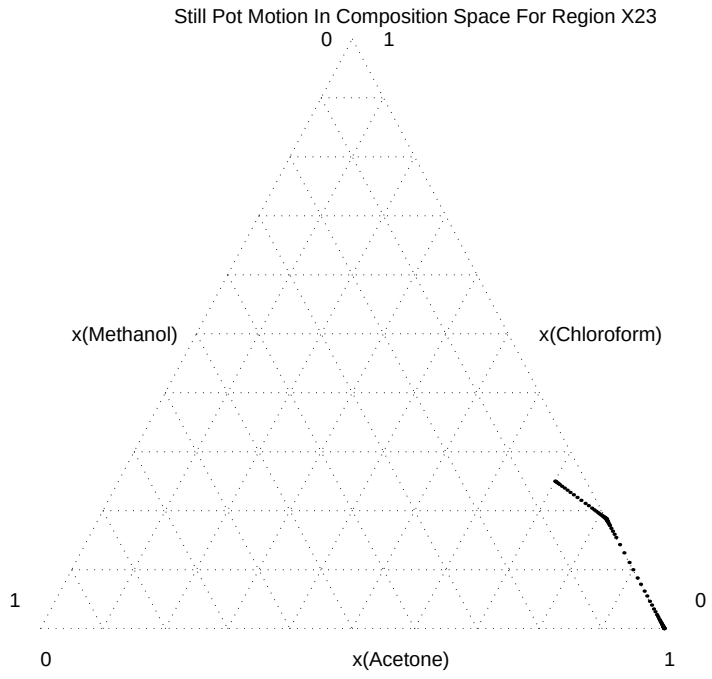

Figure D-150: Plot of Still Pot Motion in Composition Space

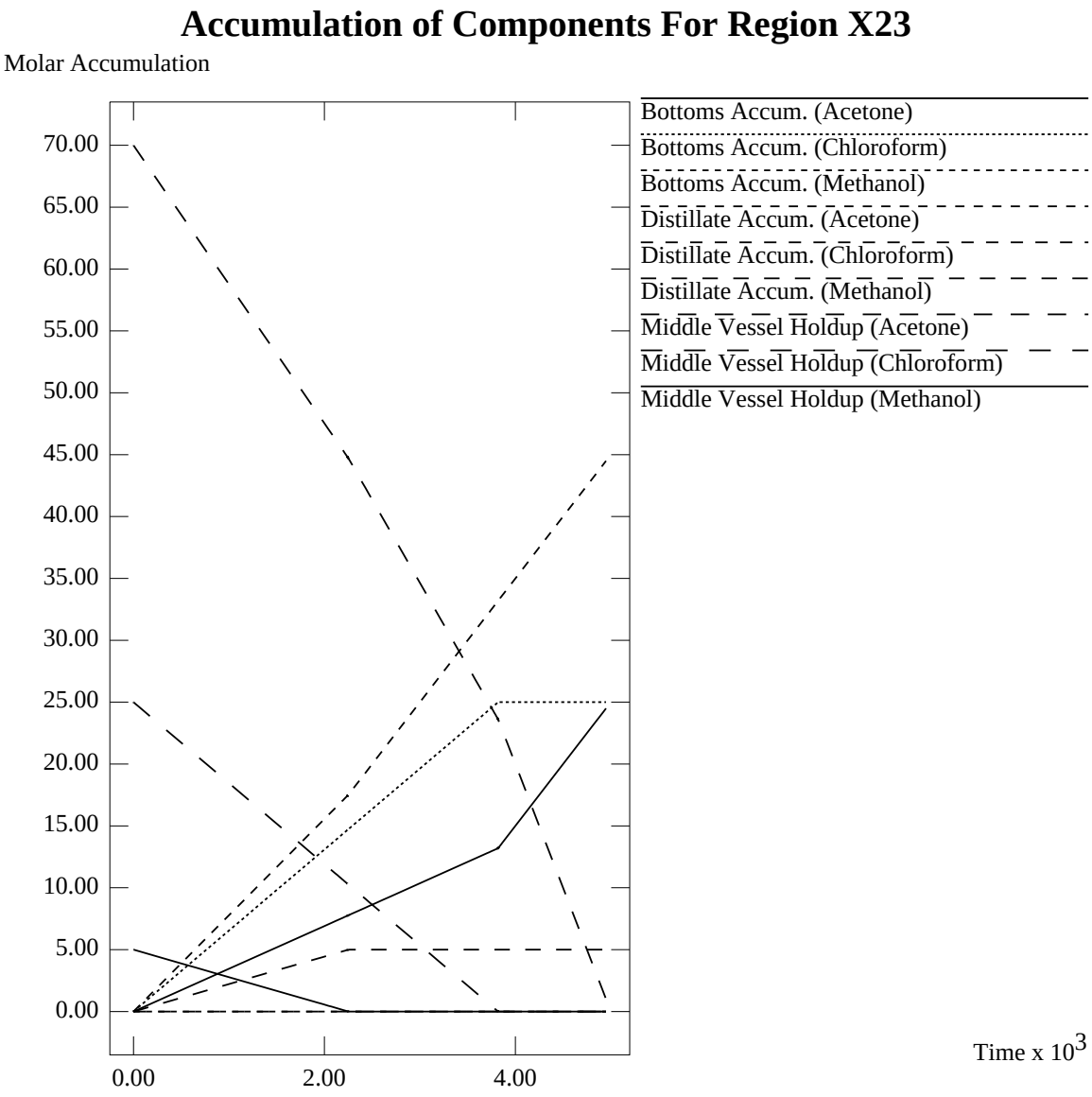

Figure D-151: Graph of Accumulation of Each Component against Time

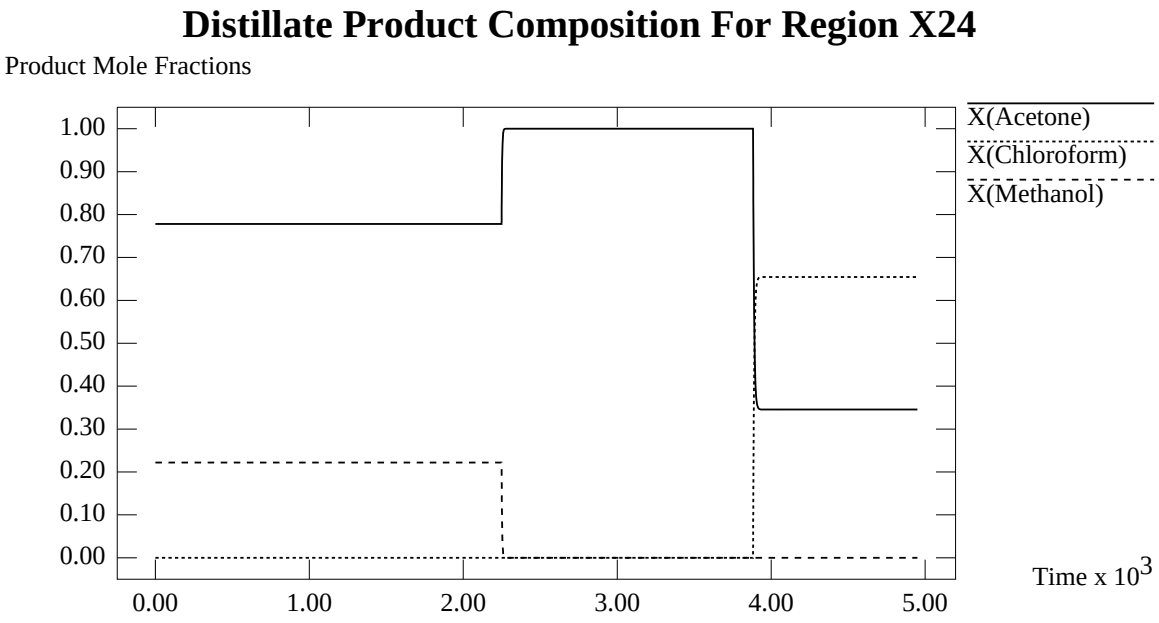

Figure D-152: Graph of Distillate Product Composition against Time

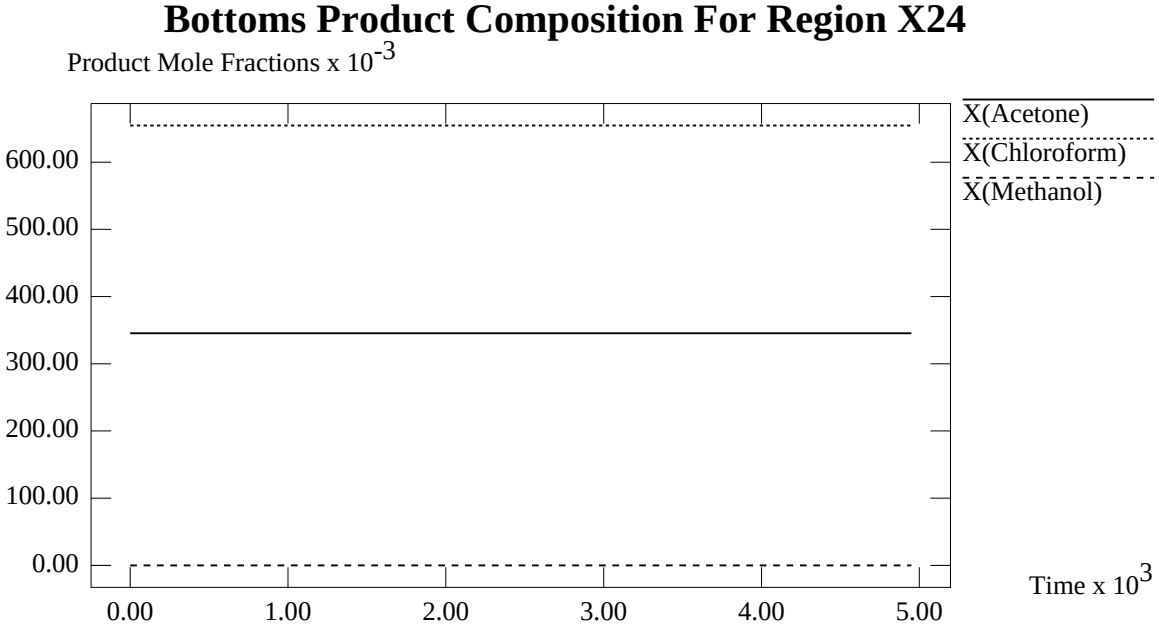

Figure D-153: Graph of Bottoms Product Composition against Time

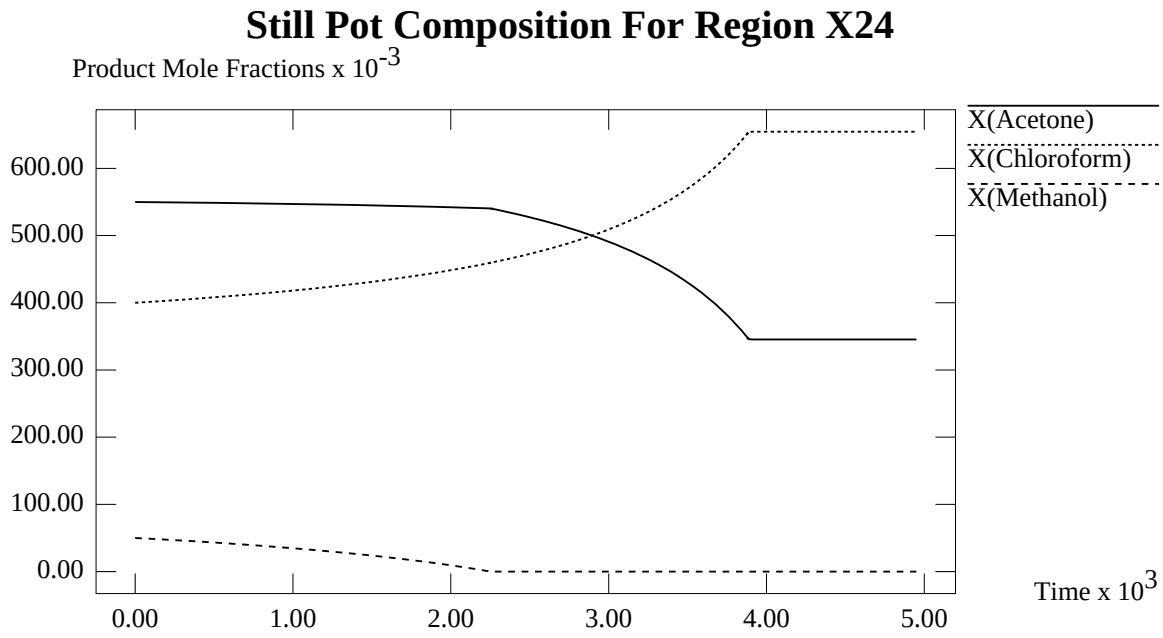

Figure D-154: Graph of Still Pot Composition against Time

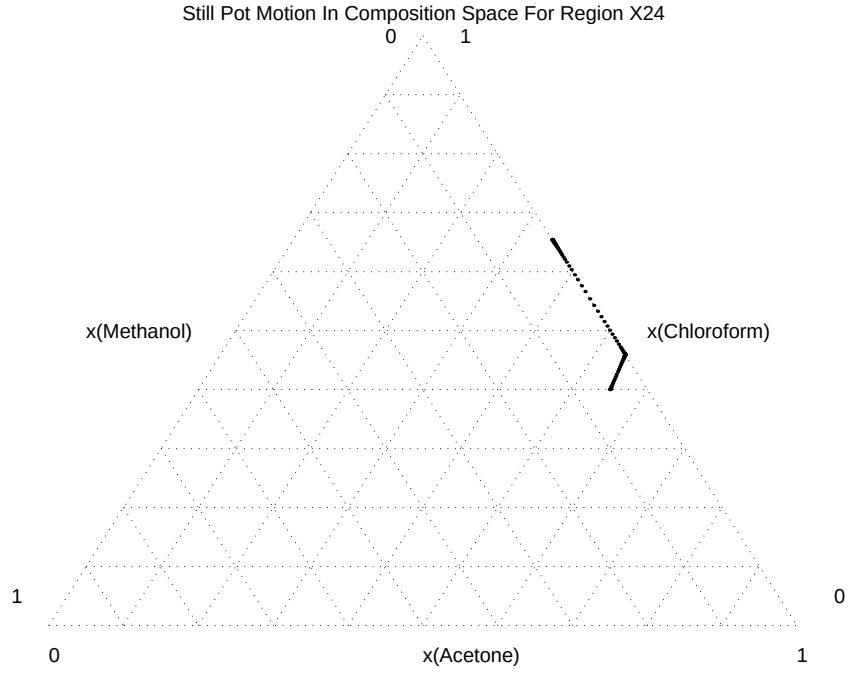

Figure D-155: Plot of Still Pot Motion in Composition Space

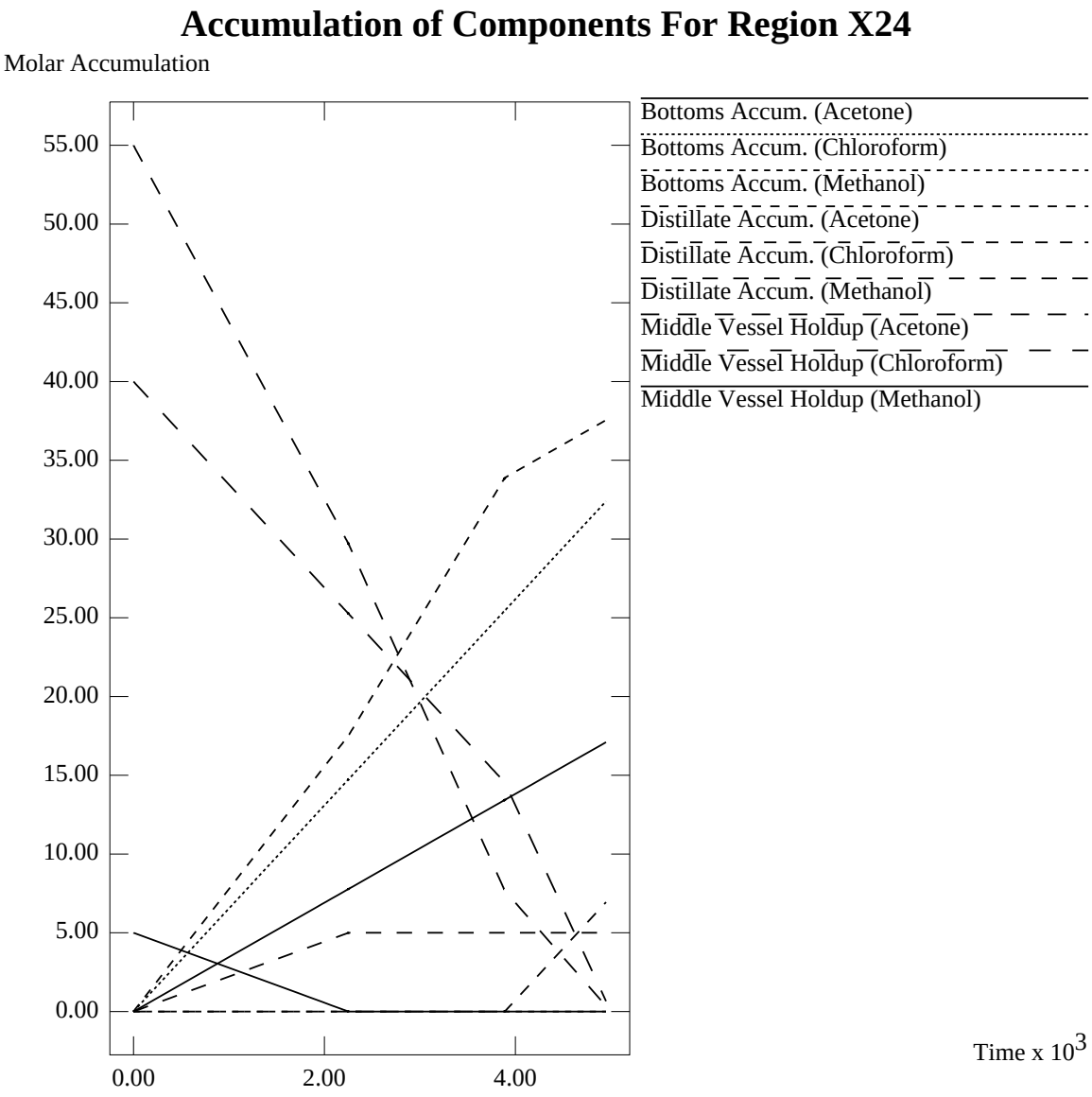

Figure D-156: Graph of Accumulation of Each Component against Time

Appendix E

Detailed Simulation Results of the 3-Component Mixture of Acetone, Chloroform, and Methanol

In this appendix, the detailed simulation results for the separation of the acetone-benzene-chloroform mixtures ($F_{azeotrope}$, F_{μ}, and F_{ν}) are detailed.

Operating conditions for each simulation were kept constant so as to ensure that the results could be comparable to each other. The pertinent operating parameters used are thus summarized in Table E.1. The behavior of the column as $N \rightarrow \infty$ and the reflux/ratios $\rightarrow \infty$, was modelled by using a reflux/reboil ratio of 1000, and up to 50 trays in the column.

E.1 Simulation Results For The Separation of F_{μ}, F_{ν}, and $F_{azeotrope}$ Using Mode B of Operation

In the graphs that follow, the results of the simulation for each of the original compositions are presented categorically. Product composition as a function of time, the still pot motion as a function of time and in the composition space, and the accumulation of components as a function of time and the variation of λ as a function of

Table E.1: Operating Conditions for the Rectifier and Stripper Simulations, (Infinite Reflux/Reboil, Infinite Number of Trays)

Operational Parameter	Numerical Value	Units
Initial Still Pot Holdup	100	Moles
Vapor Flow Rate (Stripping)	10	*Moles/Time*
Liquid Flow Rate (Rectifying)	10	*Moles/Time*
Distillate Product Flow Rate	0.01	*Moles/Time*
Bottoms Product Flow Rate	0.01	*Moles/Time*
Resulting Reflux Ratio	1000	Dimensionless
Resulting Reboil Ratio	1000	Dimensionless
Number of Trays in the Rectifier Column	50	Dimensionless
Number of Trays in the Stripper Column	50	Dimensionless
Operating Pressure in Column	1	Bar

time are provided for each initial composition.

E.1.1 Simulation Results for $F_{azeotrope}$, Mode B, Quasi-Static

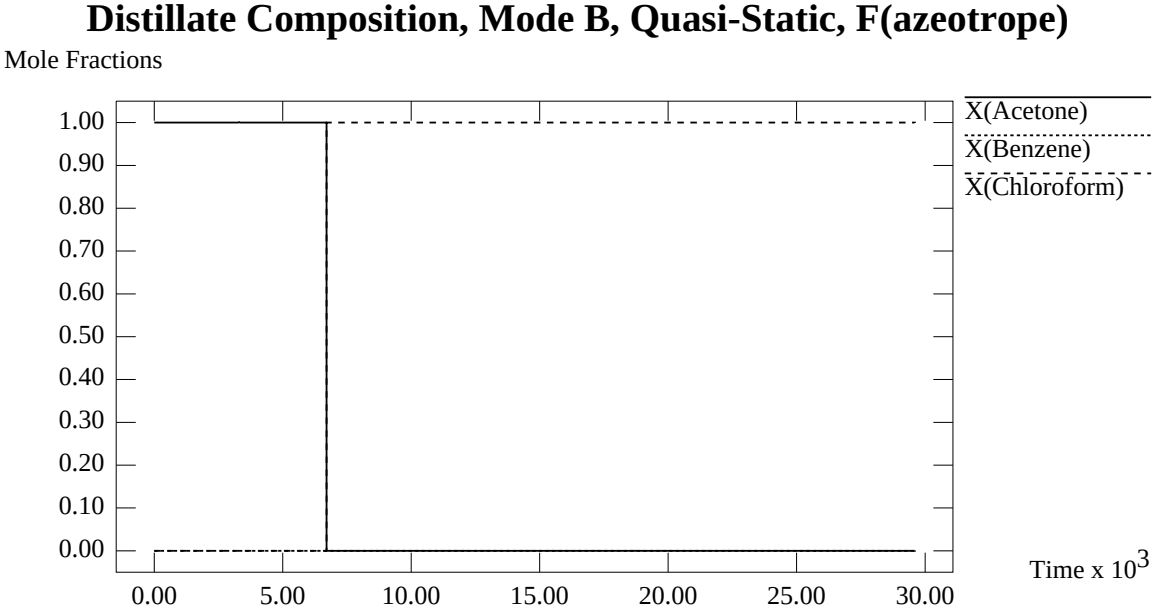

Figure E-1: Distillate Composition For $F_{azeotrope}$

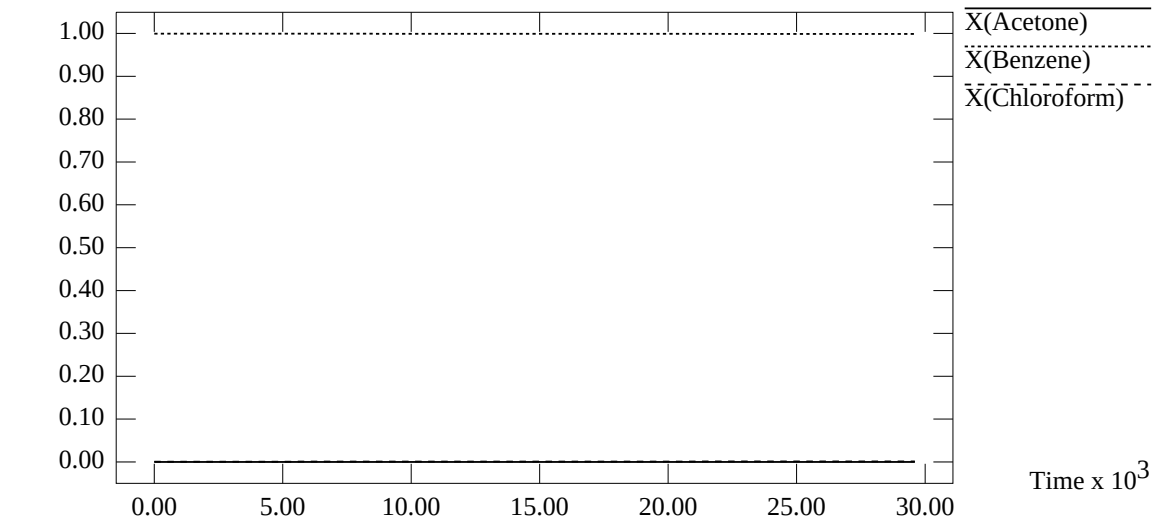

Figure E-2: Bottoms Composition For $F_{azeotrope}$

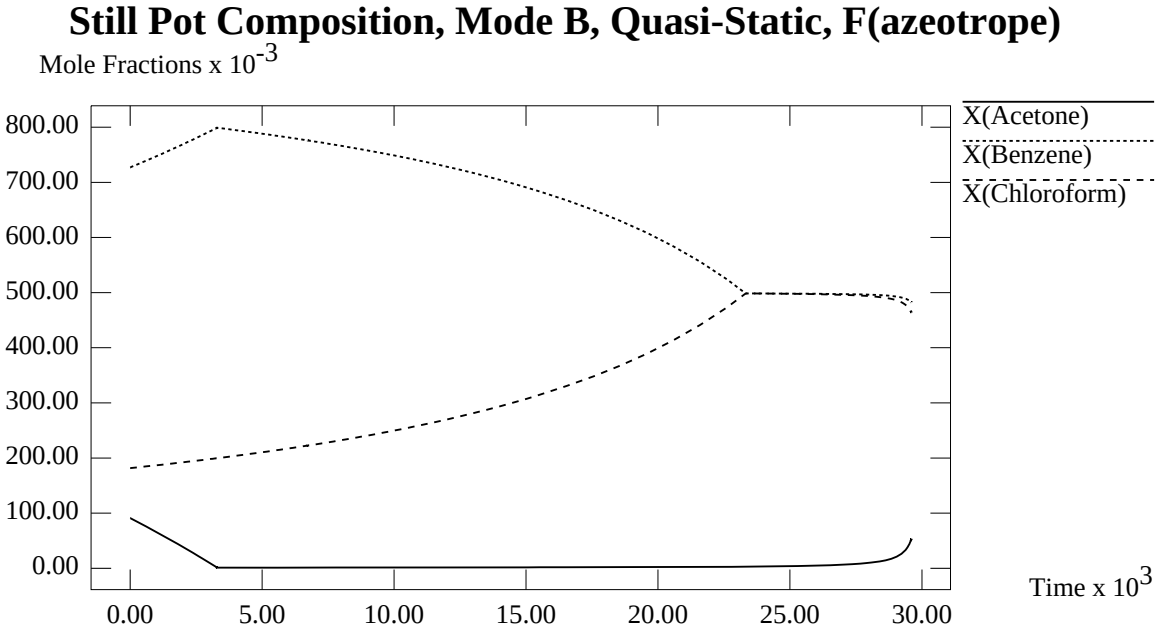

Figure E-3: Still Pot Composition For $F_{azeotrope}$ as a Function of Time

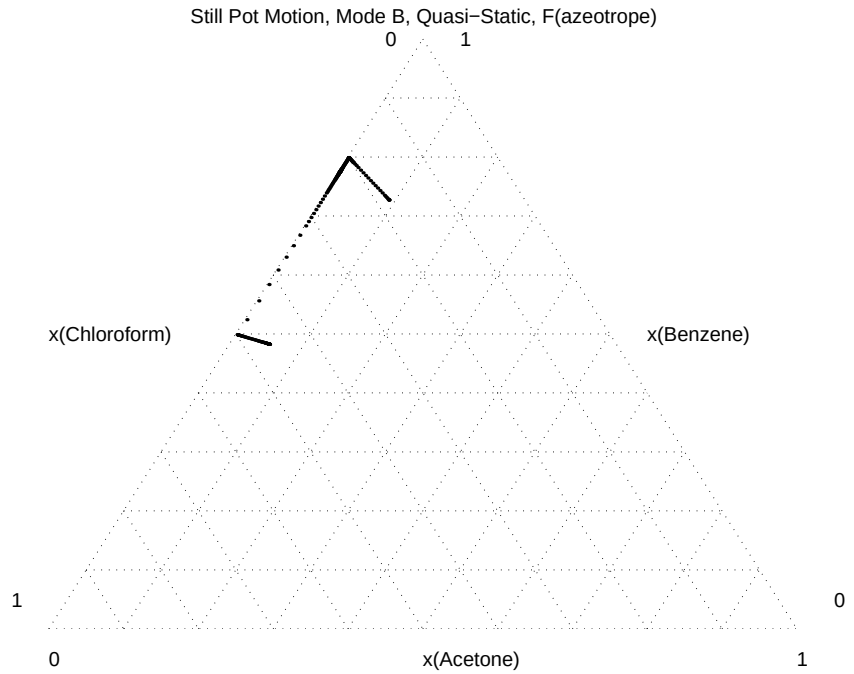

Figure E-4: Still Pot Composition For $F_{azeotrope}$ in Composition Space

E.1.2 Simulation Results for F_μ, Mode B, Quasi-Static

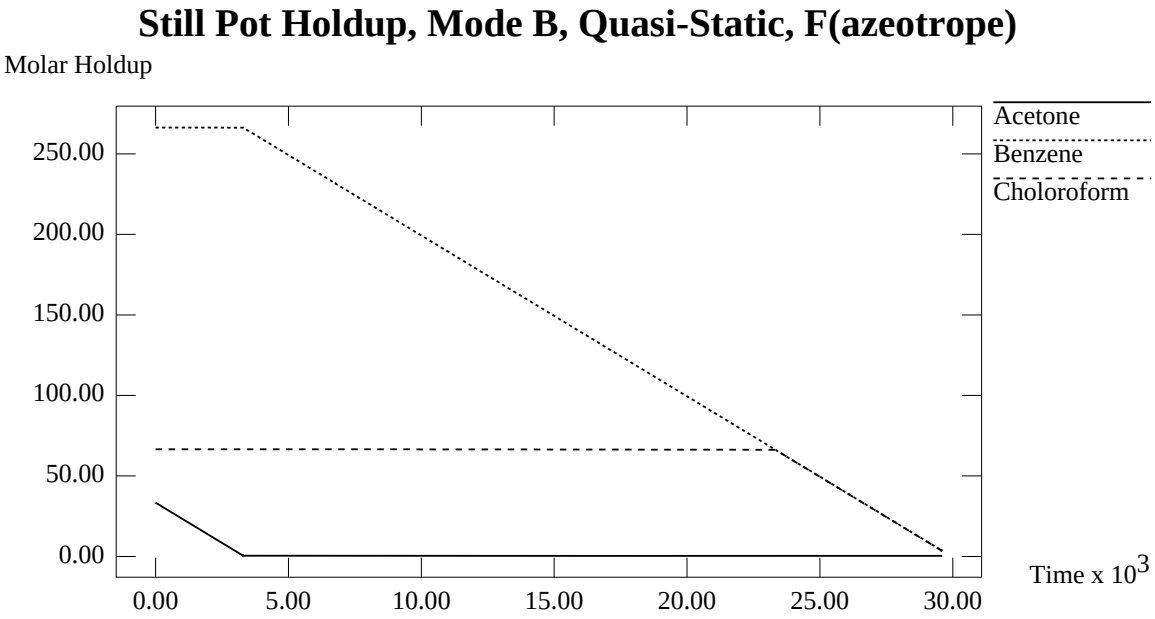

Figure E-5: Still Pot Molar Holdup For $F_{azeotrope}$ as a Function of Time

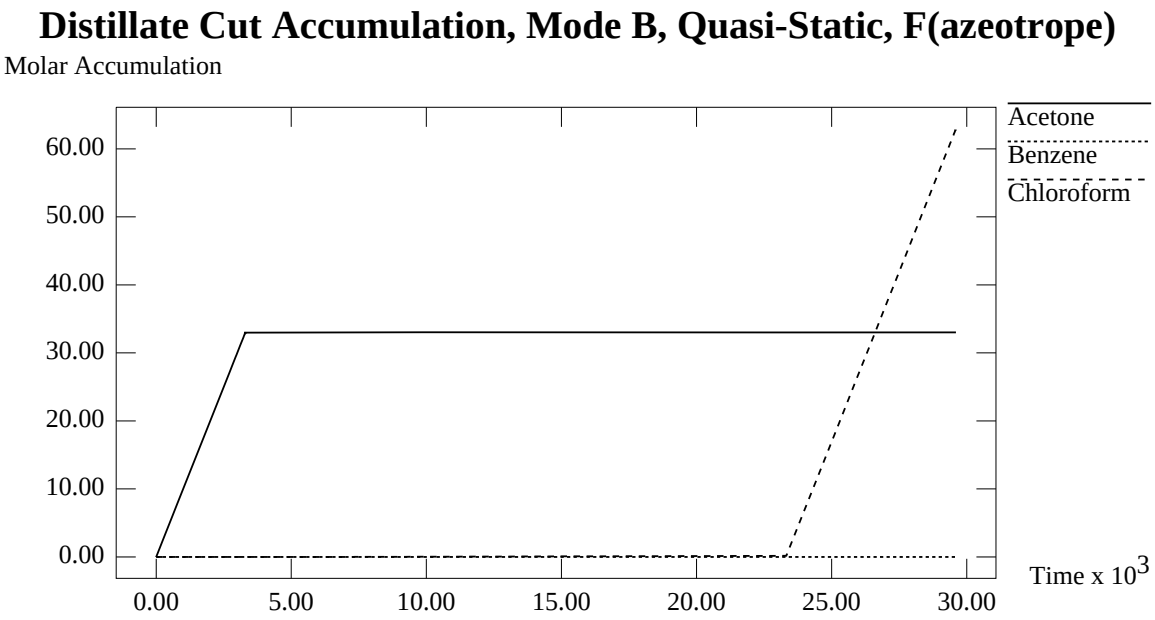

Figure E-6: Distillate Molar Holdup For $F_{azeotrope}$ as a Function of Time

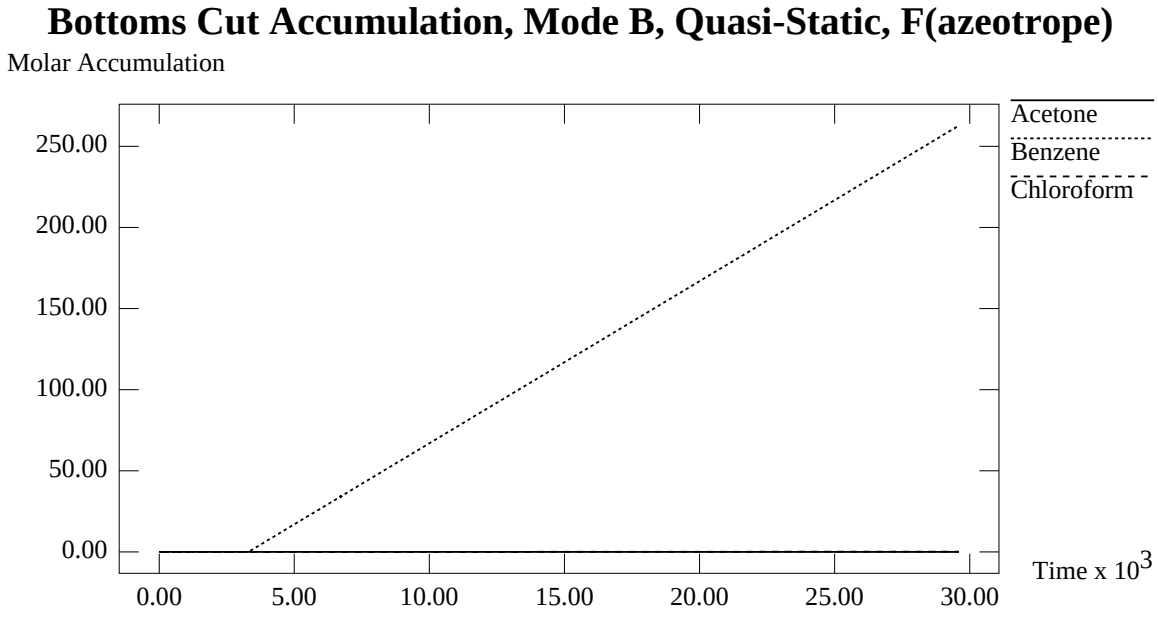

Figure E-7: Bottoms Molar Holdup For $F_{azeotrope}$ as a Function of Time

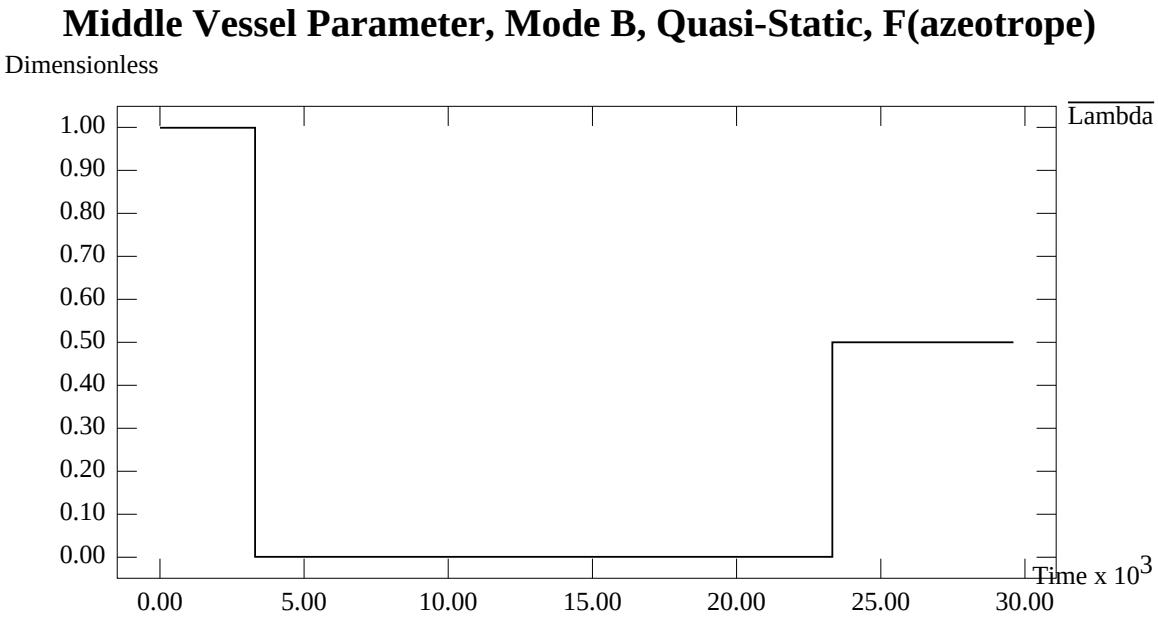

Figure E-8: Middle Vessel Parameter, λ, For $F_{azeotrope}$ as a Function of Time

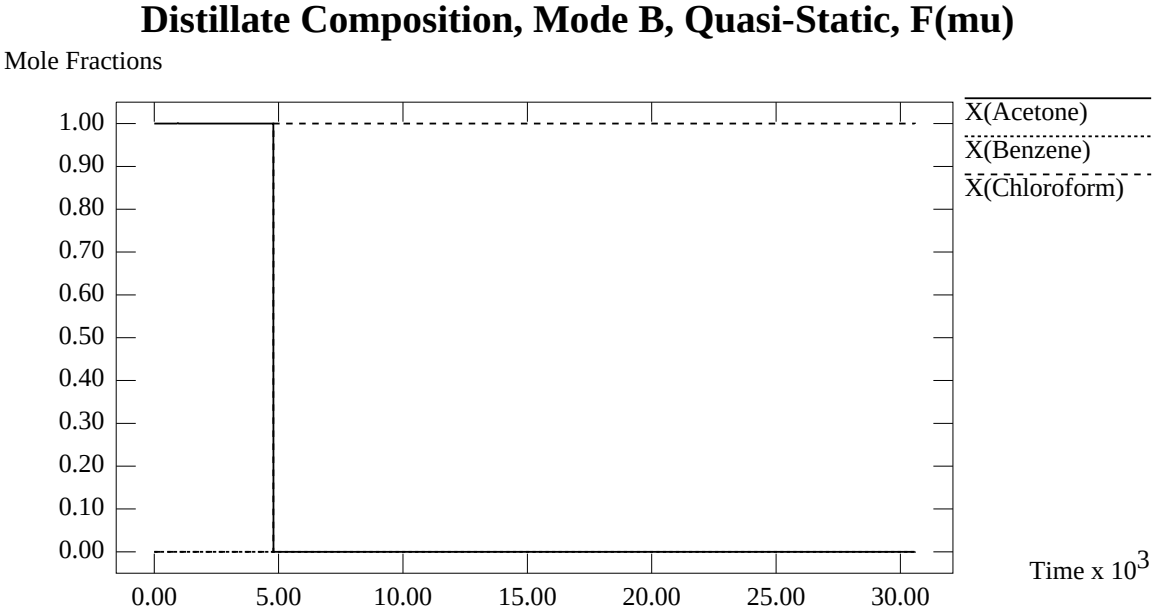

Figure E-9: Distillate Composition For F_μ

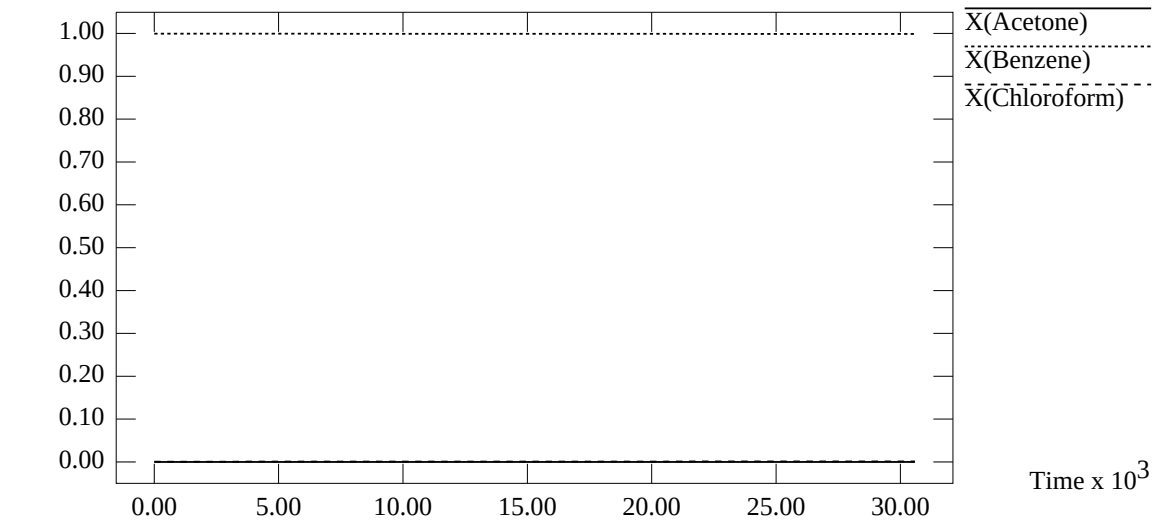

Figure E-10: Bottoms Composition For F_μ

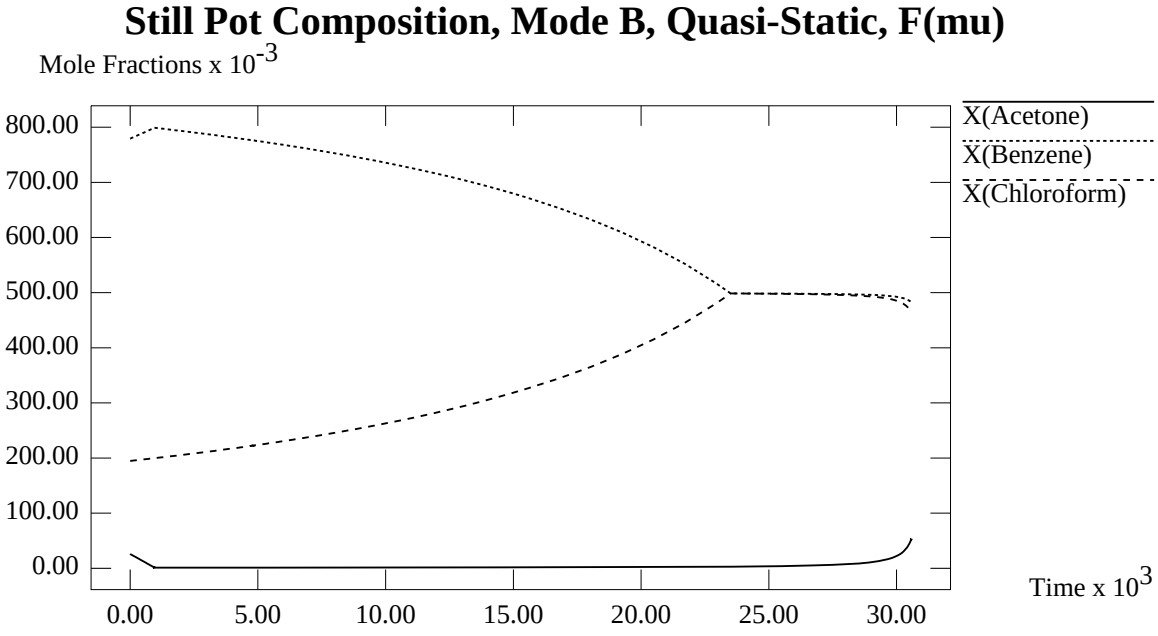

Figure E-11: Still Pot Composition For F_μ as a Function of Time

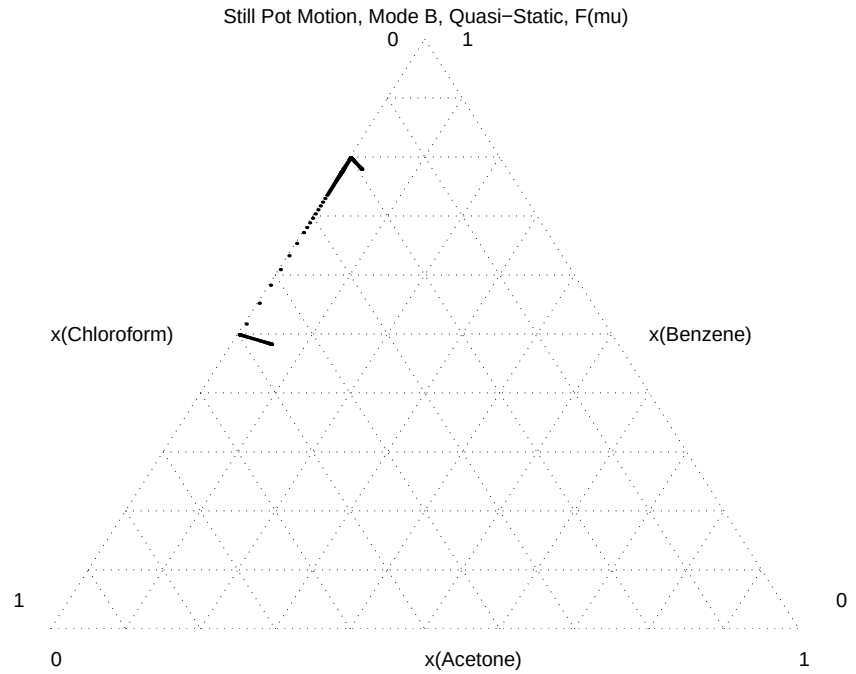

Figure E-12: Still Pot Composition For F_μ in Composition Space

E.1.3 Simulation Results for F_ν, Mode B, Quasi-Static

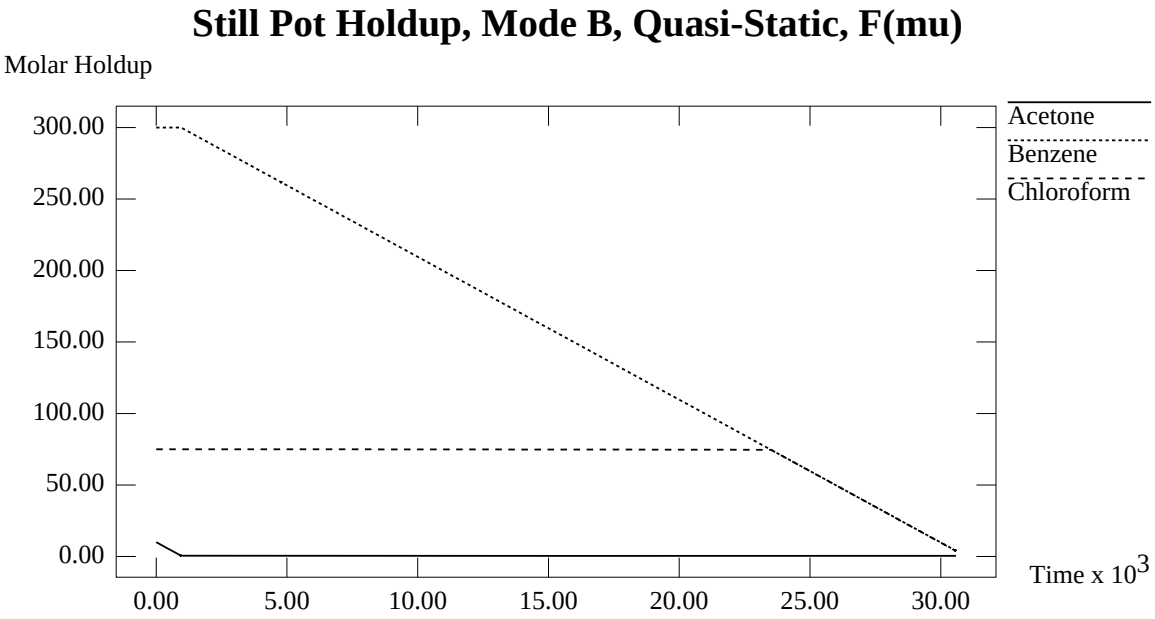

Figure E-13: Still Pot Molar Holdup For F_μ as a Function of Time

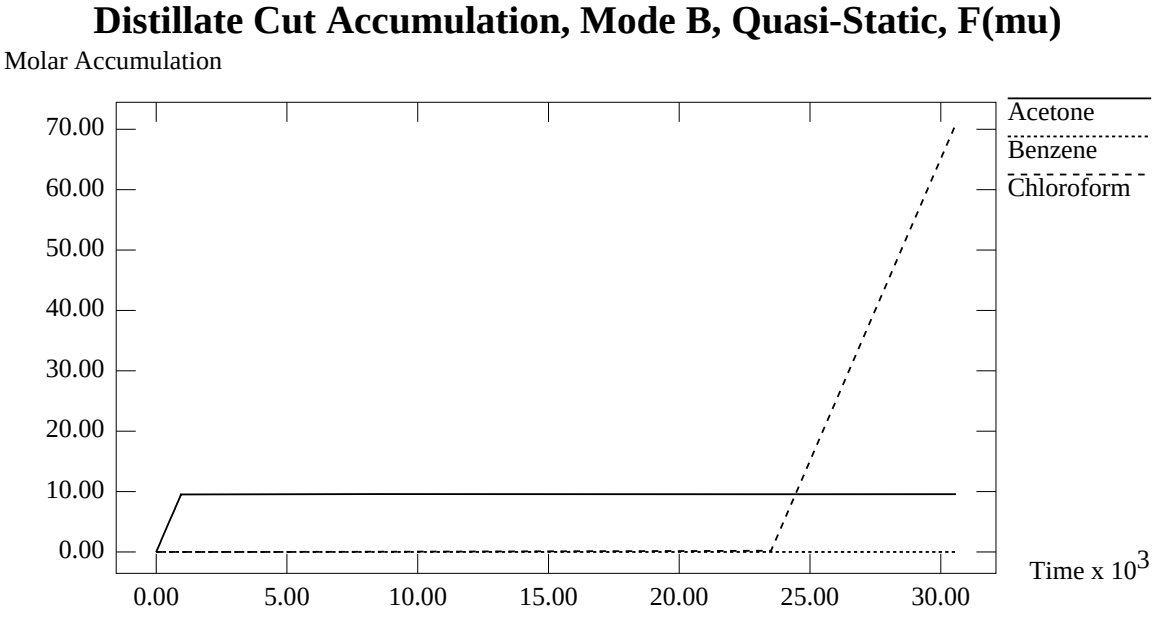

Figure E-14: Distillate Molar Holdup For F_μ as a Function of Time

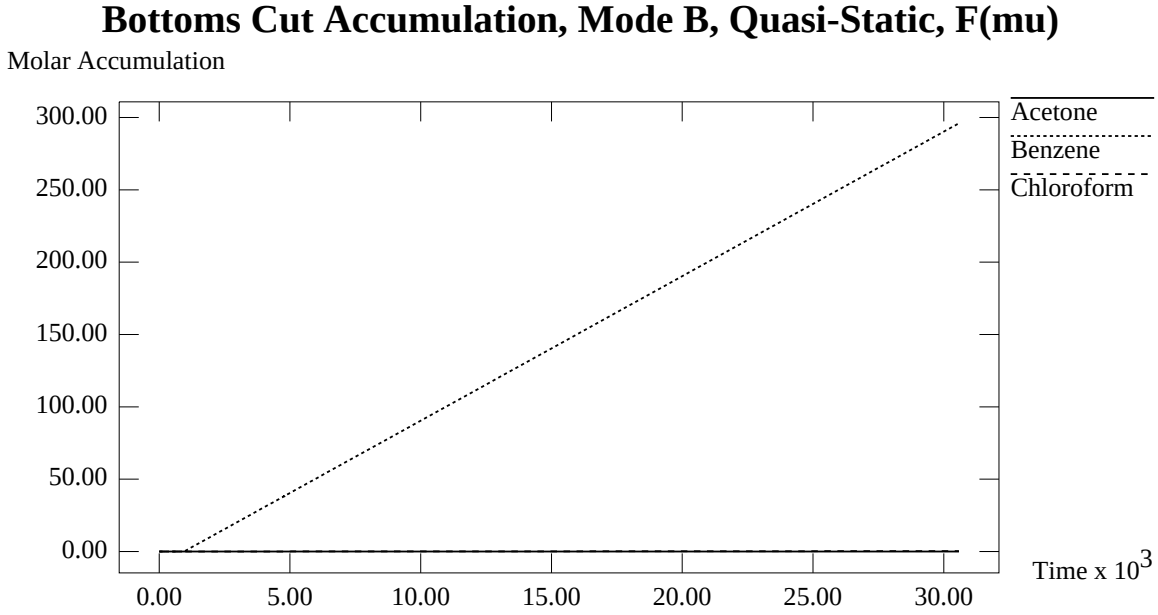

Figure E-15: Bottoms Molar Holdup For F_μ as a Function of Time

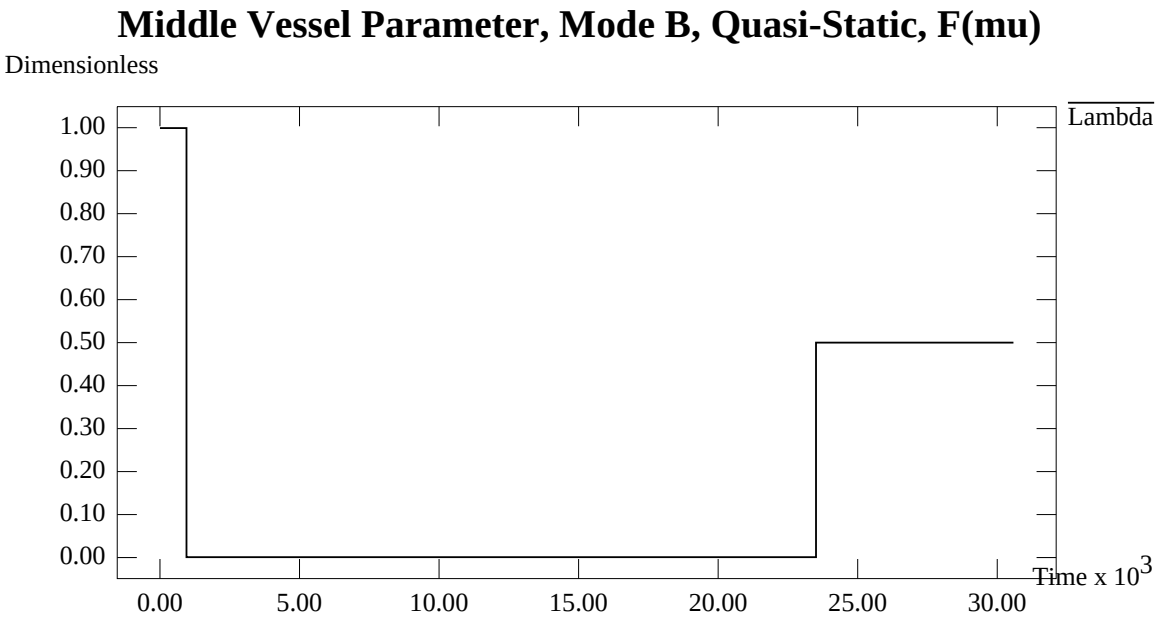

Figure E-16: Middle Vessel Parameter, λ, For F_μ as a Function of Time

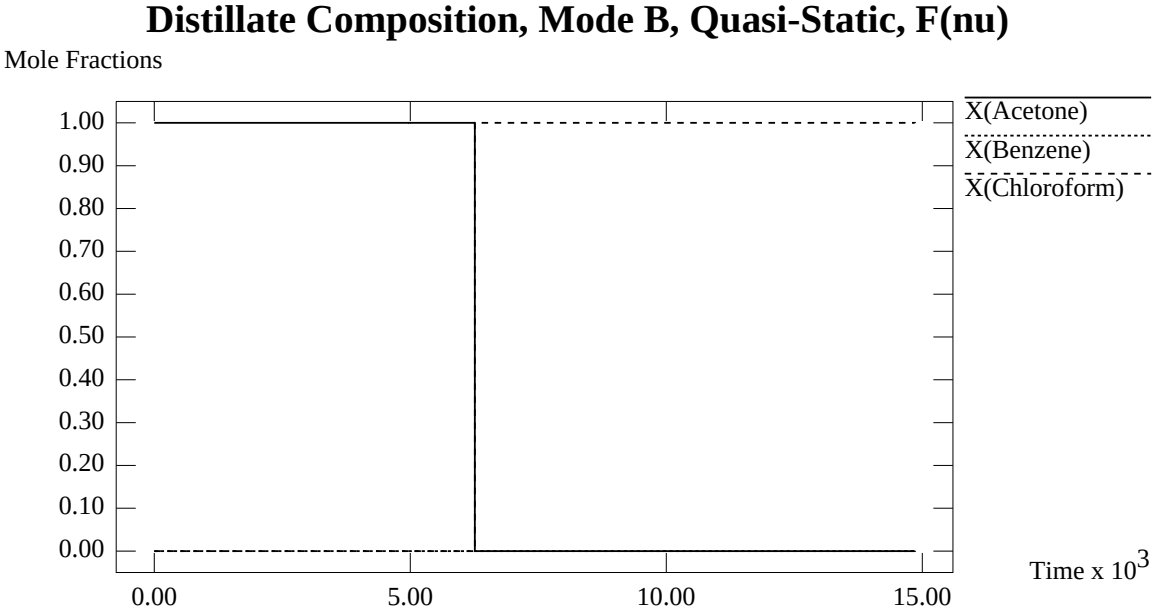

Figure E-17: Distillate Composition For F_ν

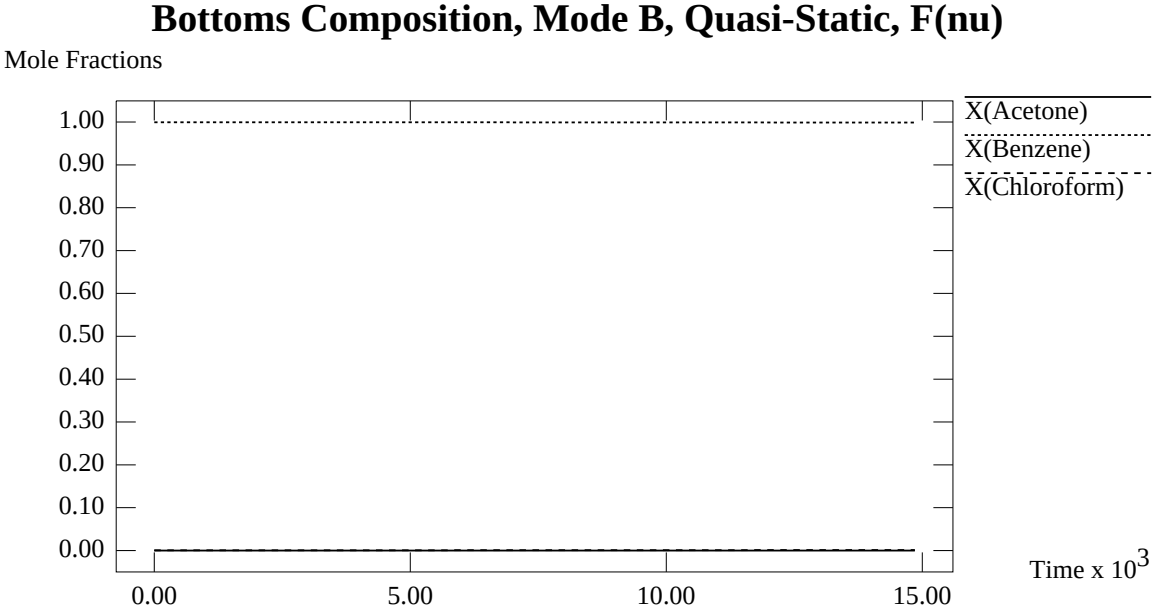

Figure E-18: Bottoms Composition For F_ν

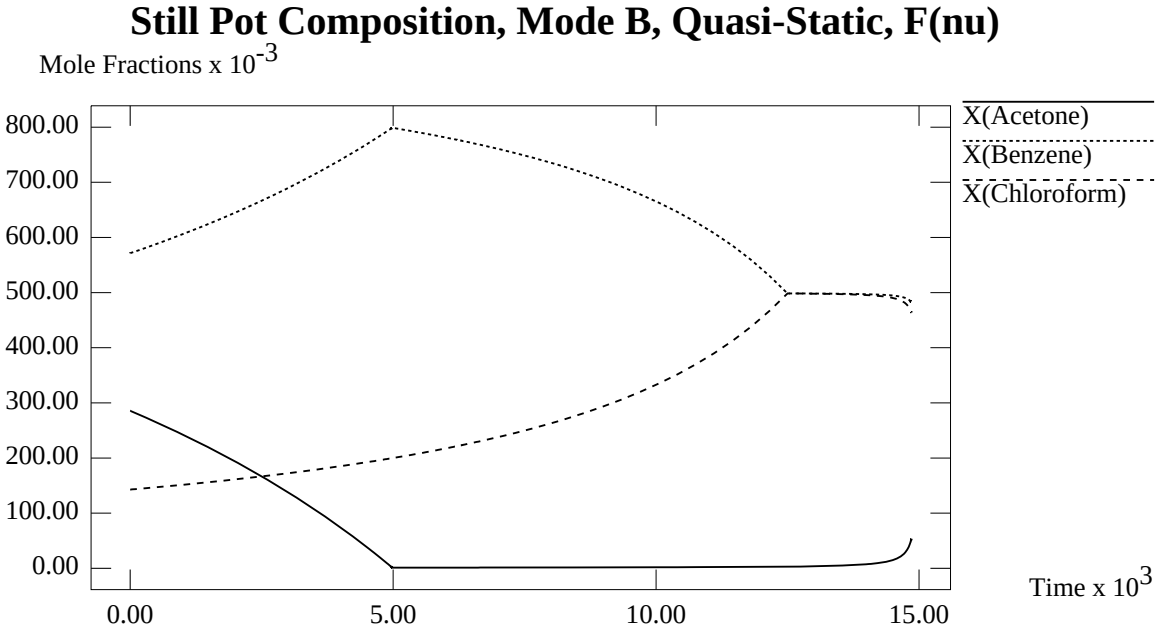

Figure E-19: Still Pot Composition For F_ν as a Function of Time

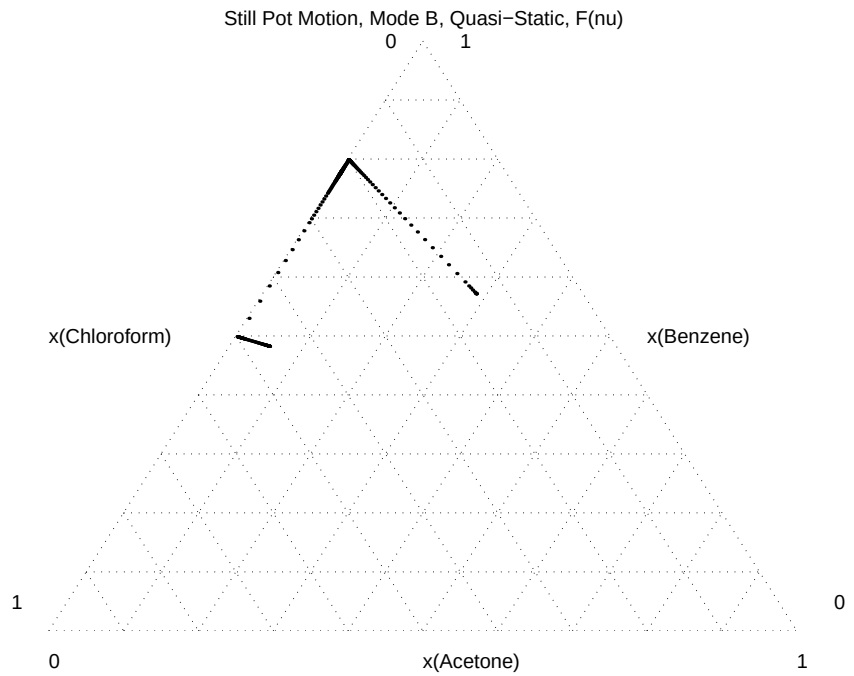

Figure E-20: Still Pot Composition For F_ν in Composition Space

E.2 Simulation Results For The Separation of F_ν using Mode A, Quasi-Static Operation

In the graphs that follow, the results of the simulation for F_ν operated with quasi-static operation at the last cut, are presented categorically. Product composition as a function of time, the still pot motion as a function of time and in the composition space, and the accumulation of components as a function of time and the variation of λ as a function of time are provided.

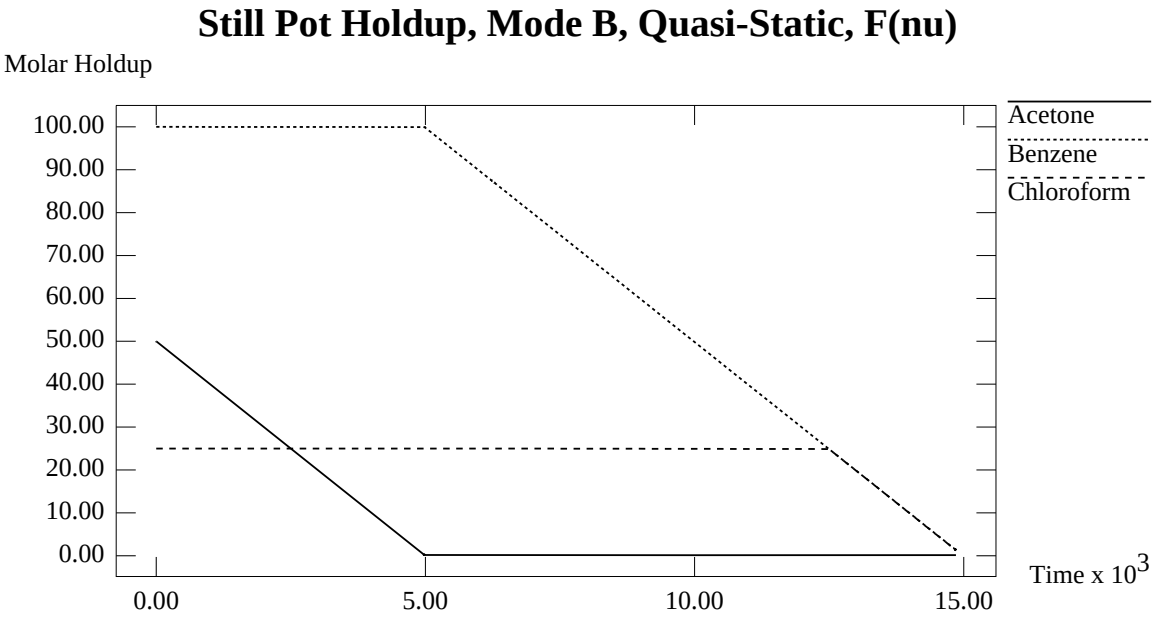

Figure E-21: Still Pot Molar Holdup For F_ν as a Function of Time

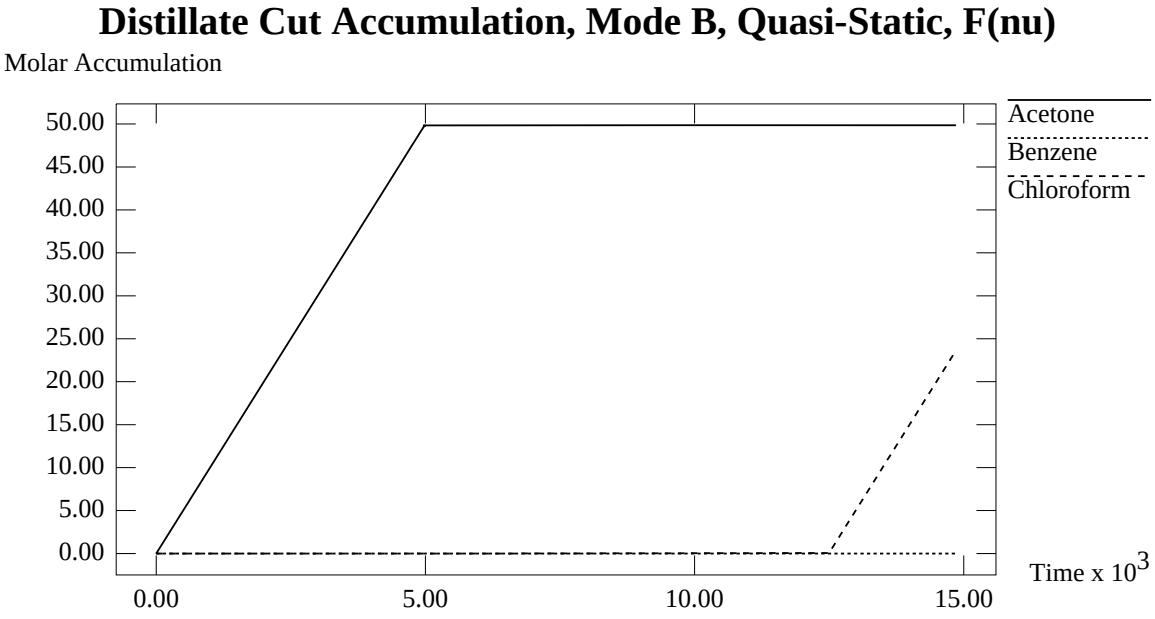

Figure E-22: Distillate Molar Holdup For F_ν as a Function of Time

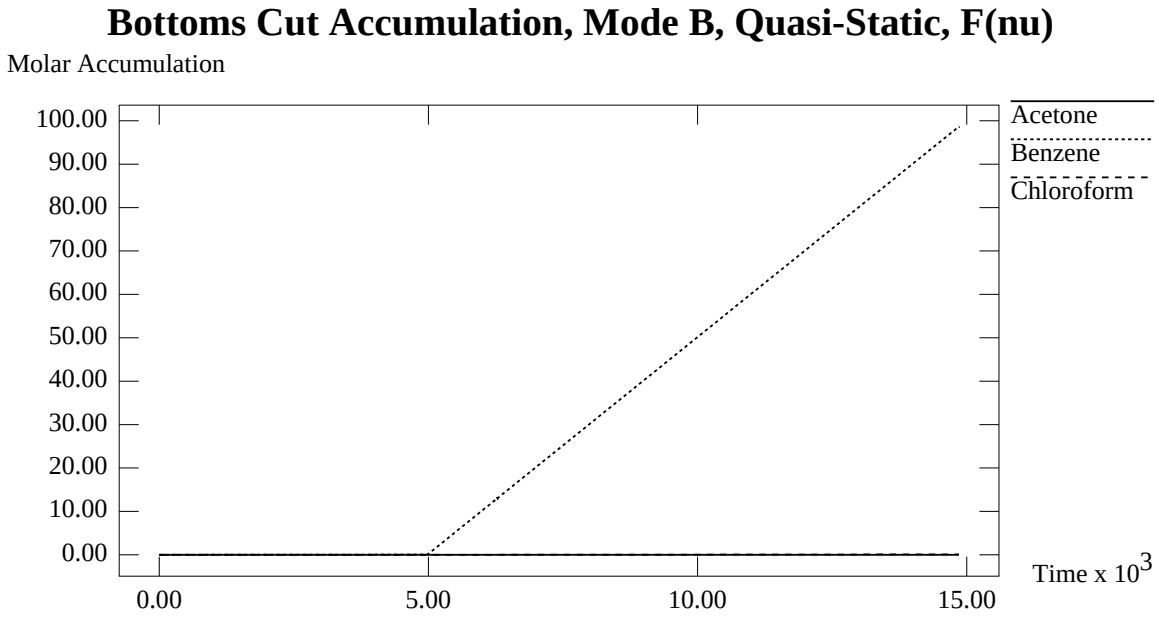

Figure E-23: Bottoms Molar Holdup For F_ν as a Function of Time

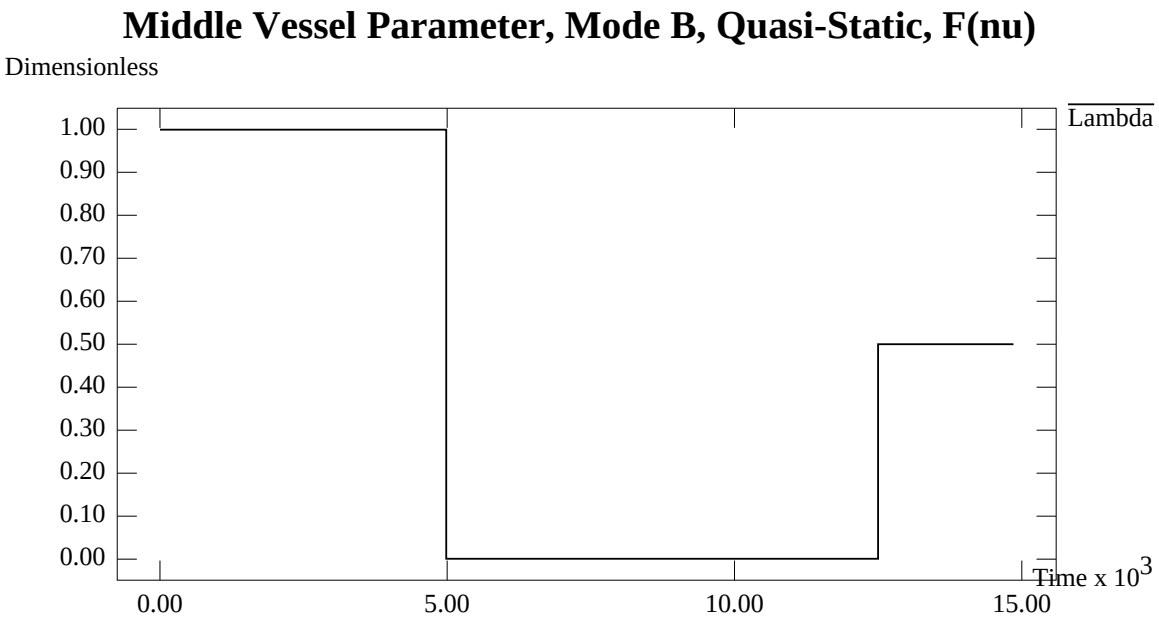

Figure E-24: Middle Vessel Parameter, λ, For F_ν as a Function of Time

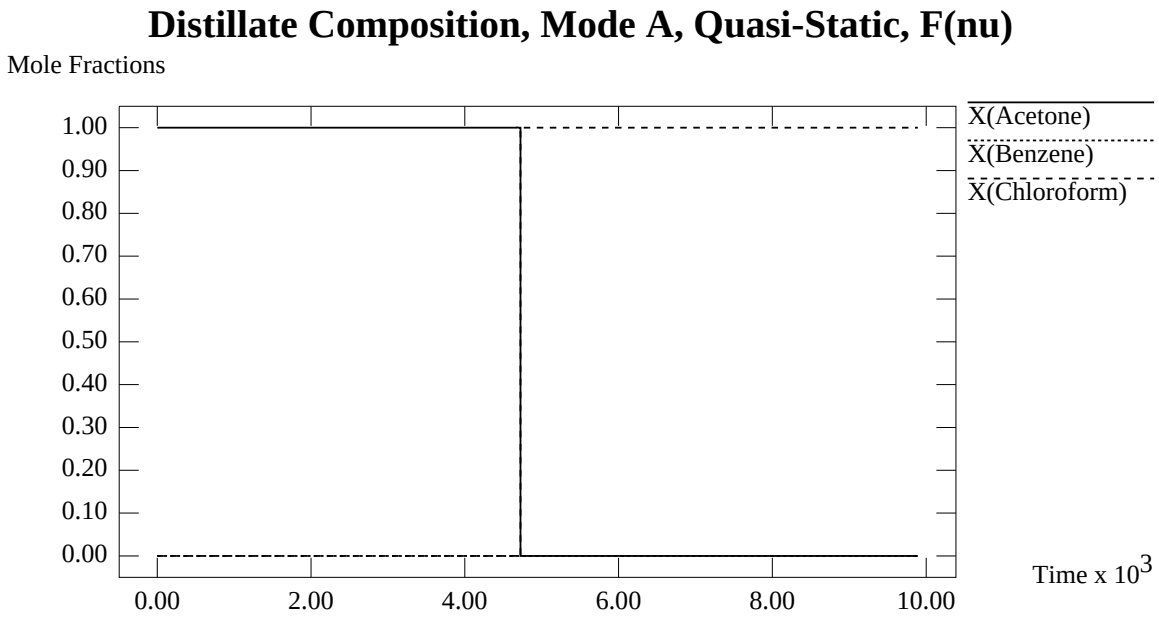

Figure E-25: Distillate Composition For F_ν, Mode A

E.3 Simulation Results For Breaking $F_{azeotrope}$ using Mode B, Non-Quasi-Static Operation

In the graphs that follow, the results of the simulation for $F_{azeotrope}$ operated with non-quasi-static operations are presented categorically. Product composition as a function of time, the still pot motion as a function of time and in the composition space, and the accumulation of components as a function of time and the variation of λ as a function of time are provided.

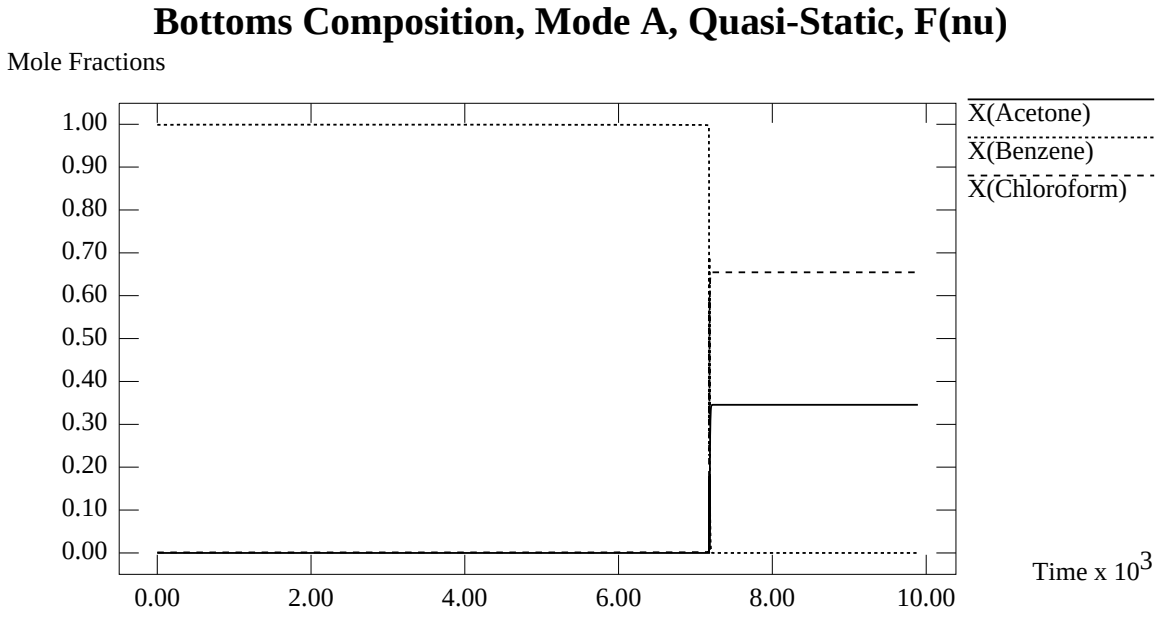

Figure E-26: Bottoms Composition For F_ν, Mode A

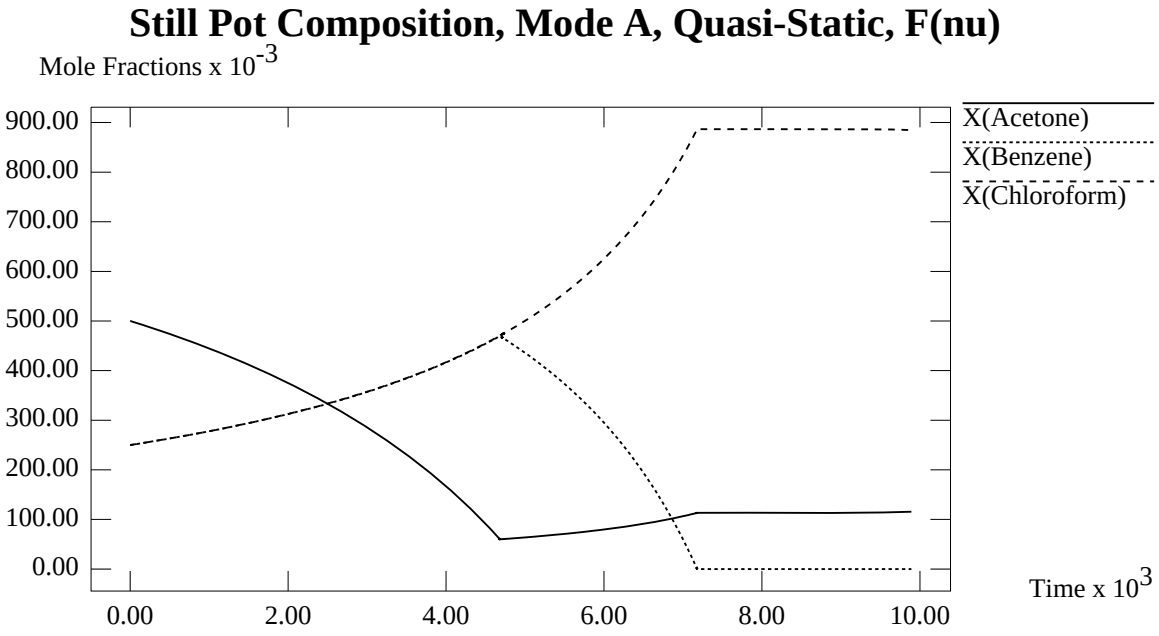

Figure E-27: Still Pot Composition For F_ν as a Function of Time, Mode A

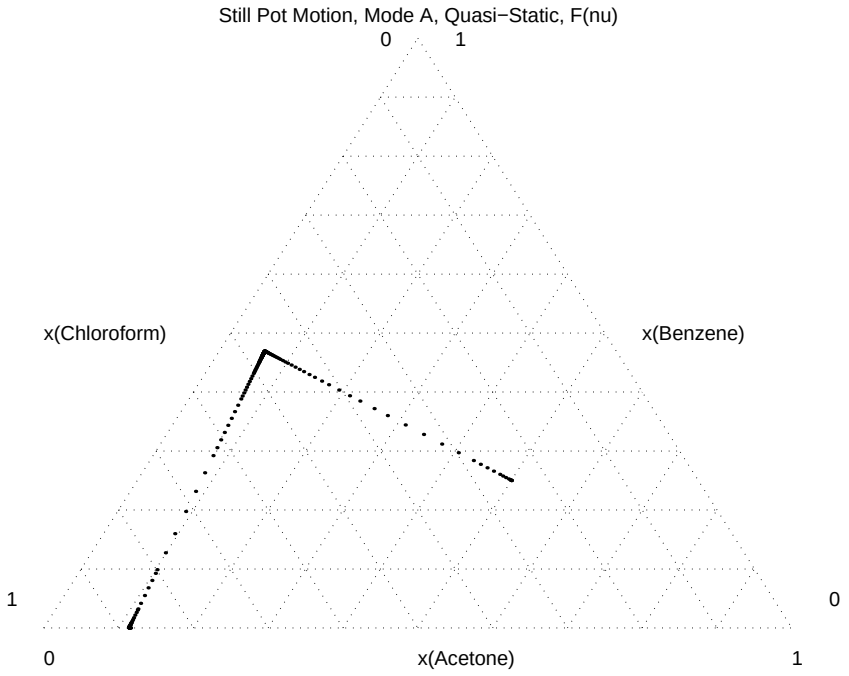

Figure E-28: Still Pot Composition For F_ν in Composition Space, Mode A

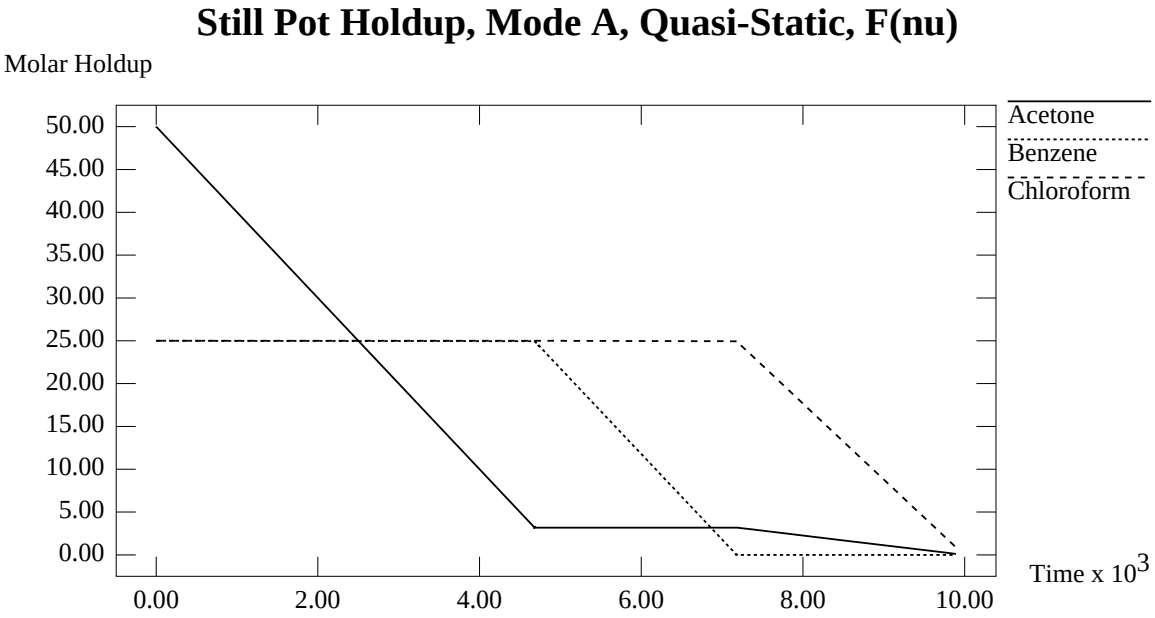

Figure E-29: Still Pot Molar Holdup For F_ν as a Function of Time, Mode A

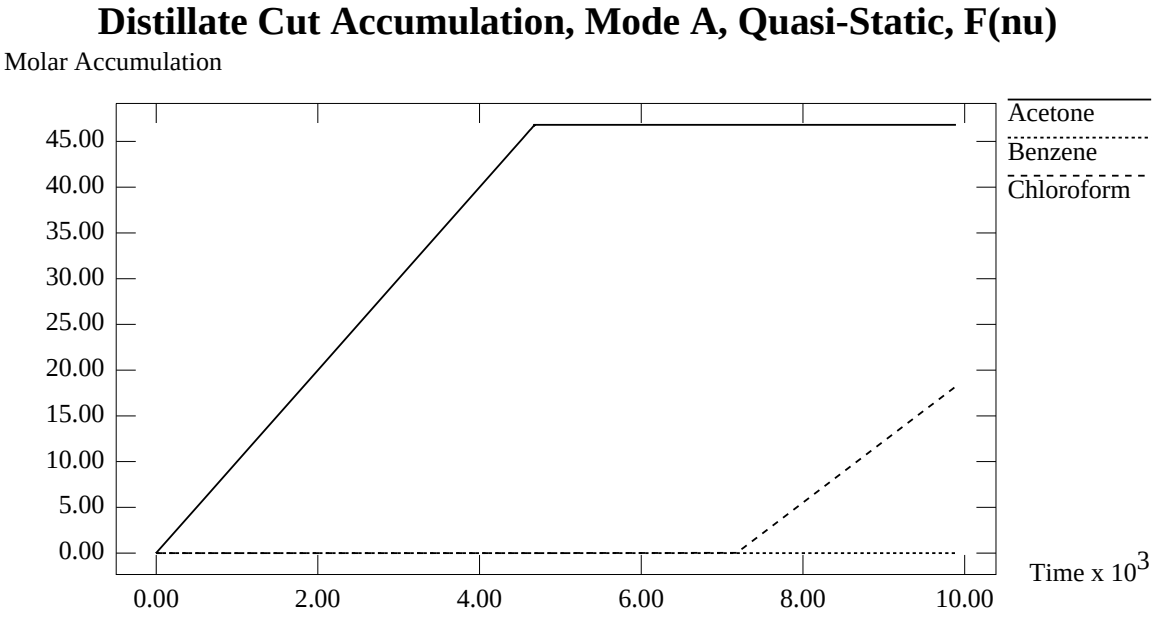

Figure E-30: Distillate Molar Holdup For F_ν as a Function of Time, Mode A

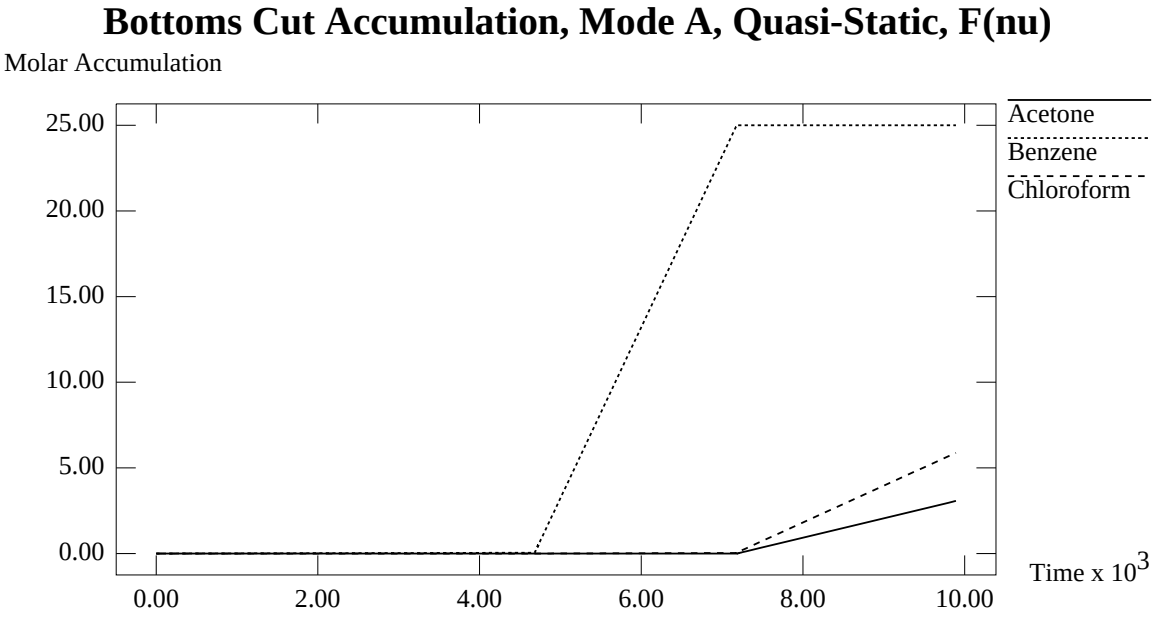

Figure E-31: Bottoms Molar Holdup For F_ν as a Function of Time, Mode A

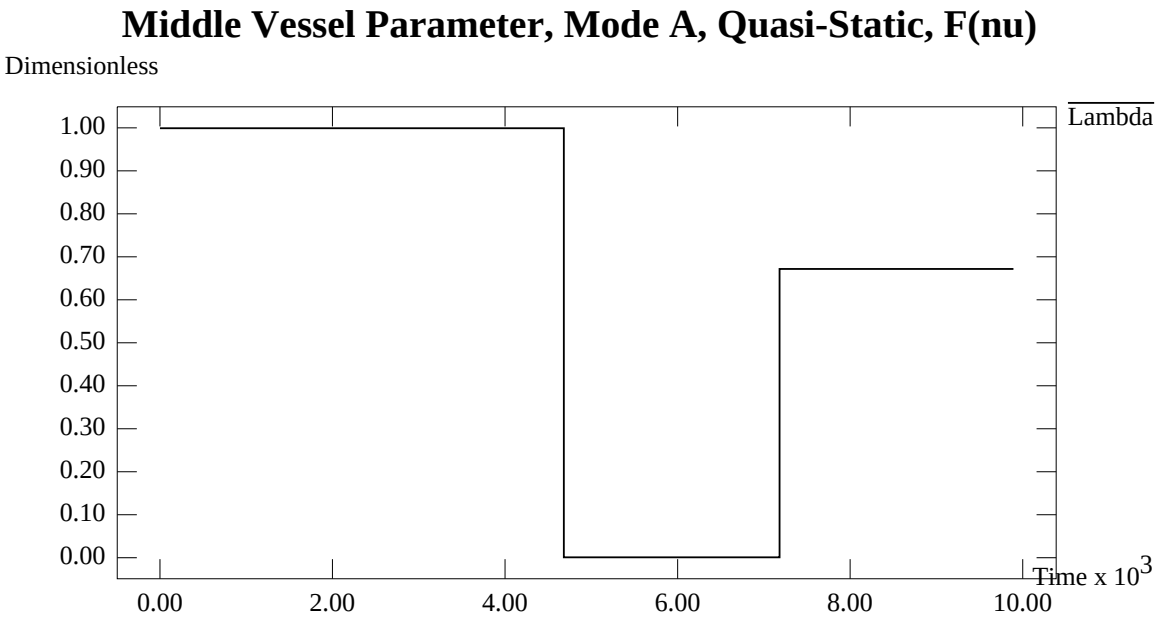

Figure E-32: Middle Vessel Parameter, λ, For F_ν as a Function of Time, Mode A

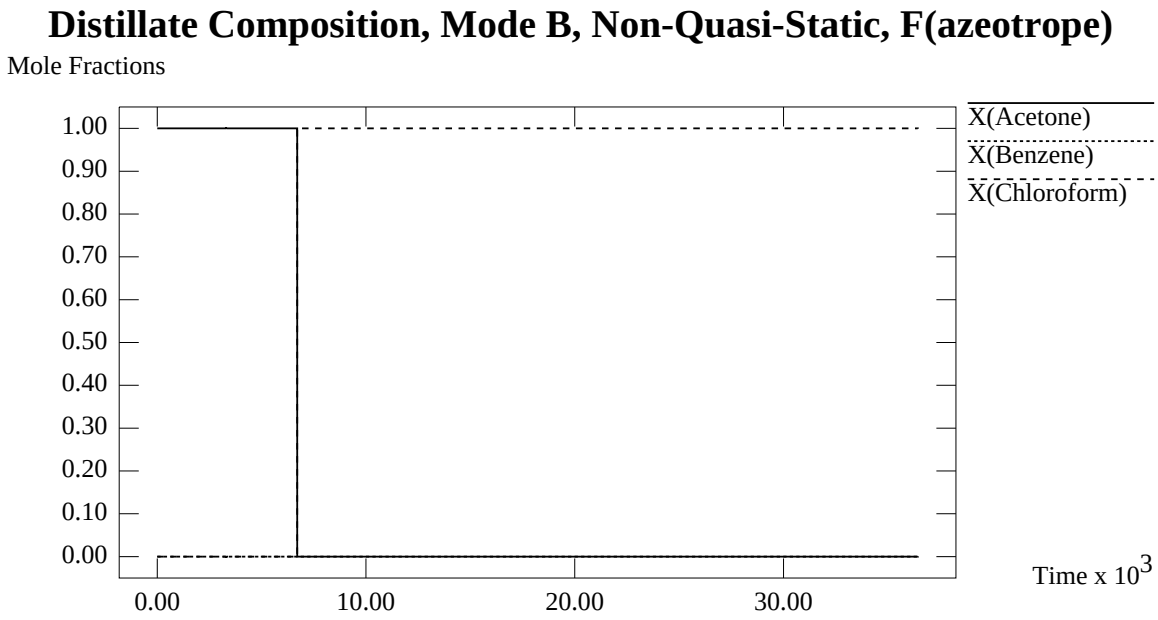

Figure E-33: Distillate Composition For $F_{azeotrope}$, Non-Quasi-Static

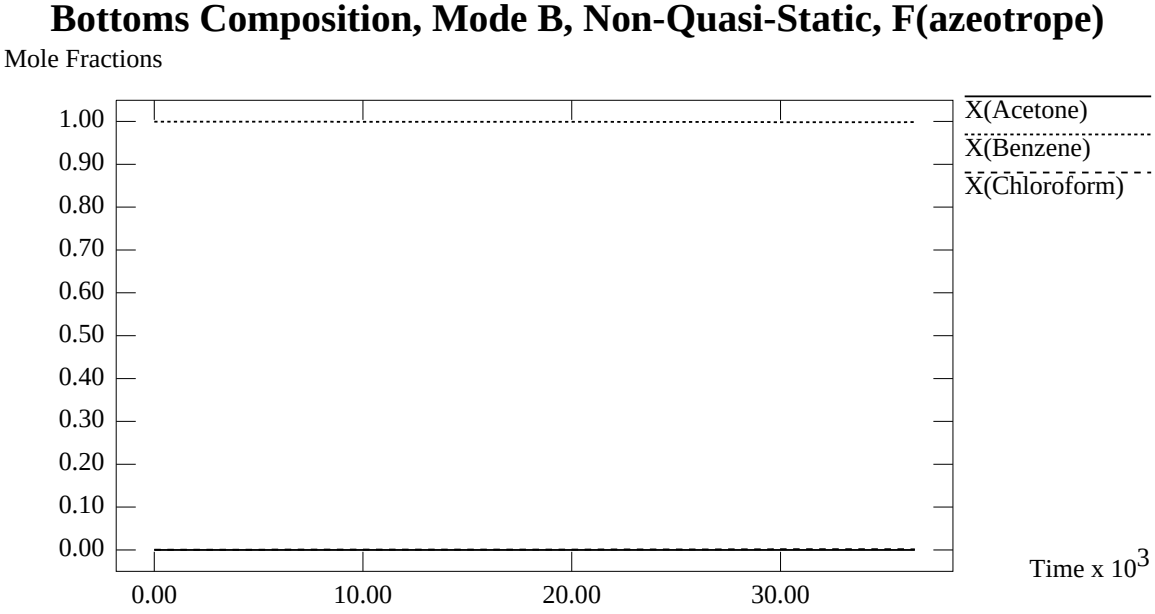

Figure E-34: Bottoms Composition For $F_{azeotrope}$, Non-Quasi-Static

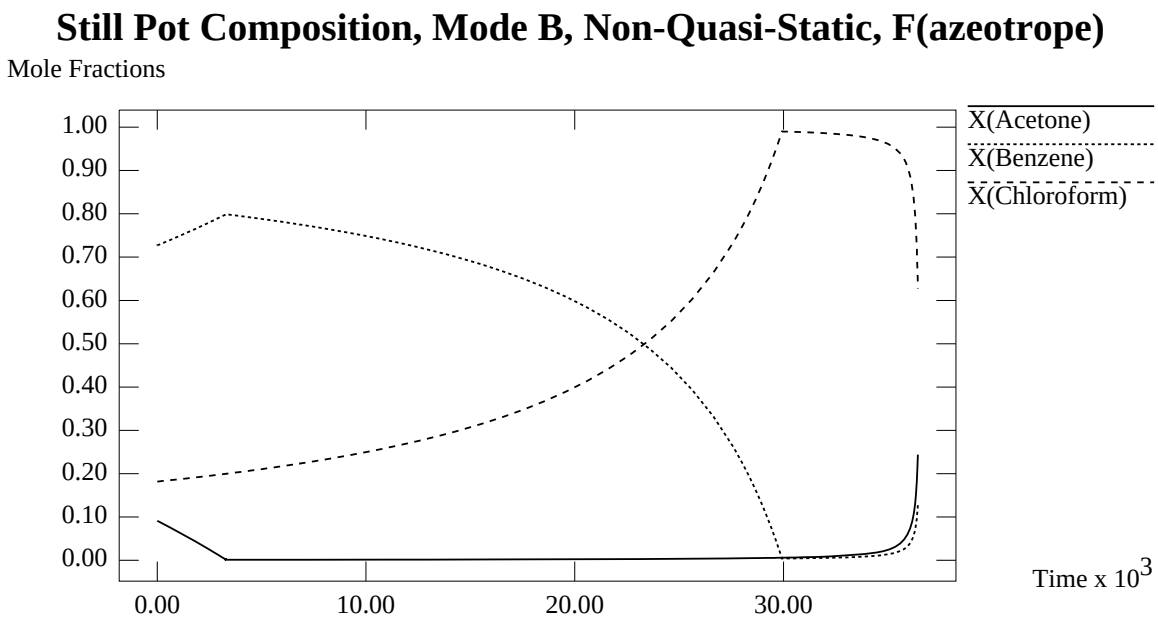

Figure E-35: Still Pot Composition For $F_{azeotrope}$ as a Function of Time, Non-Quasi-Static

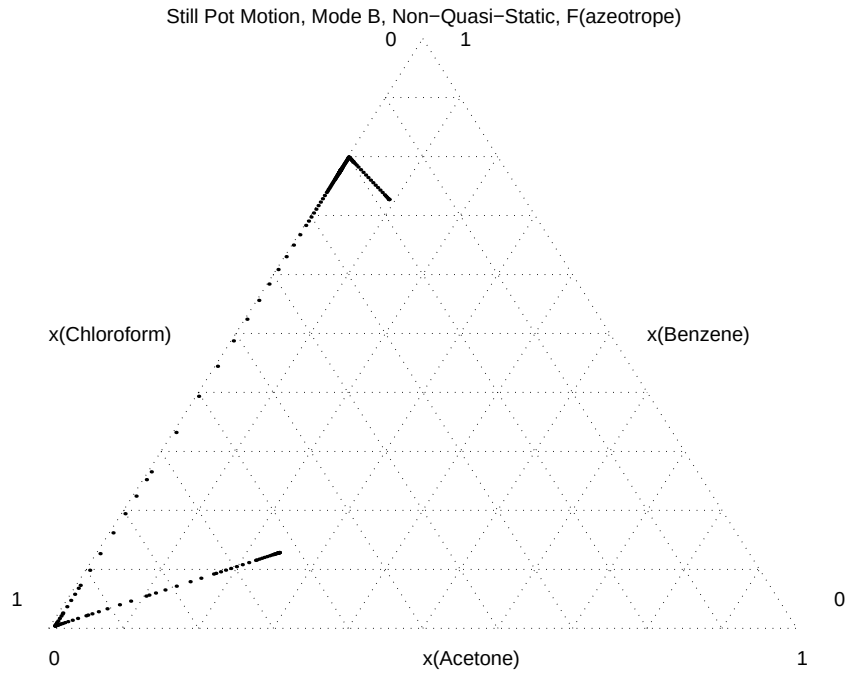

Figure E-36: Still Pot Composition For $F_{azeotrope}$ in Composition Space, Non-Quasi-Static

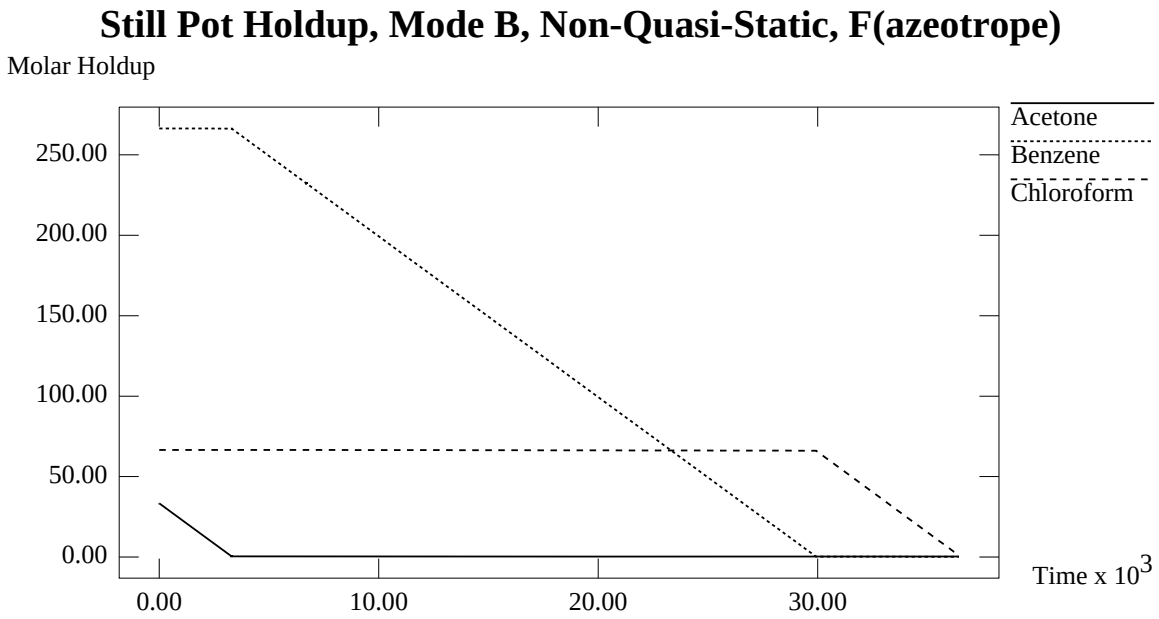

Figure E-37: Still Pot Molar Holdup For $F_{azeotrope}$ as a Function of Time, Non-Quasi-Static

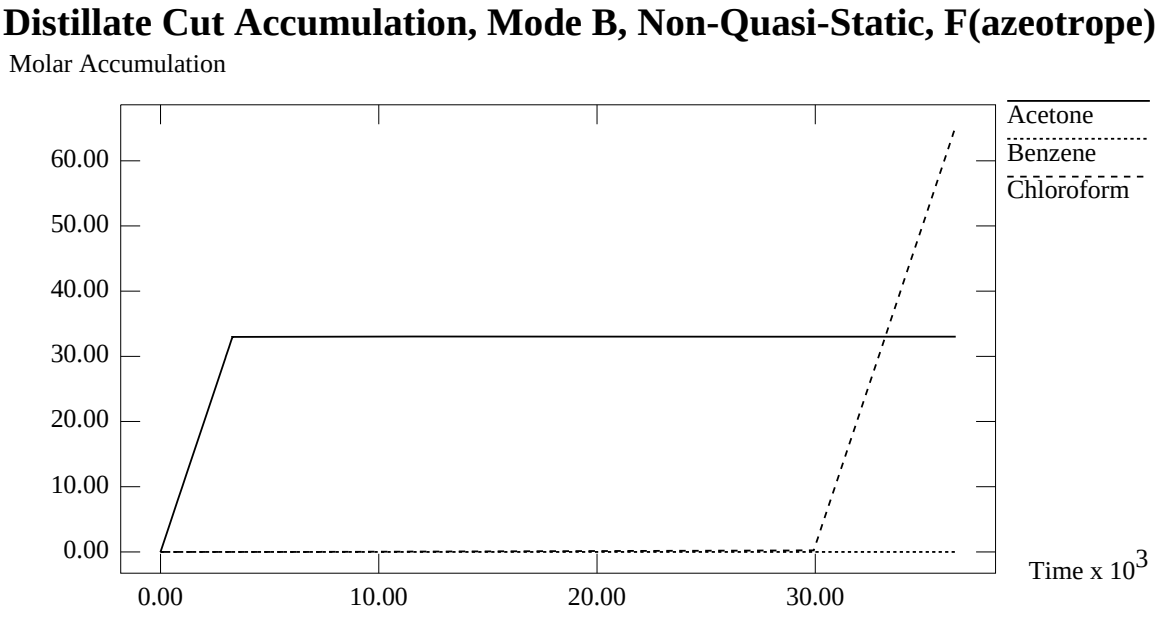

Figure E-38: Distillate Molar Holdup For $F_{azeotrope}$ as a Function of Time, Non-Quasi-Static

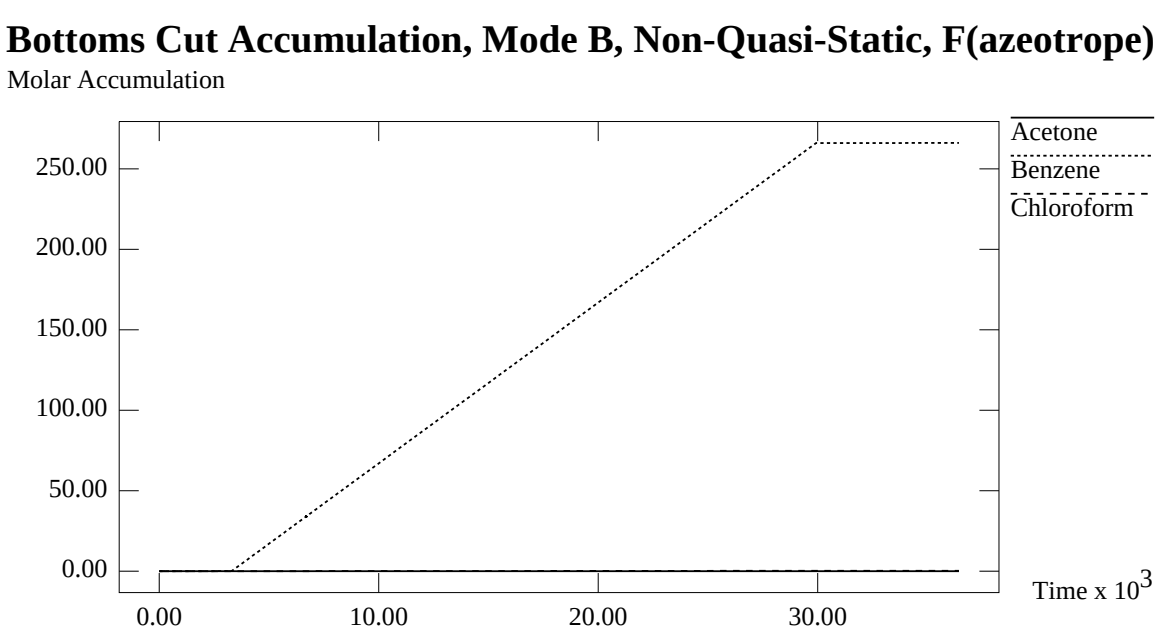

Figure E-39: Bottoms Molar Holdup For $F_{azeotrope}$ as a Function of Time, Non-Quasi-Static

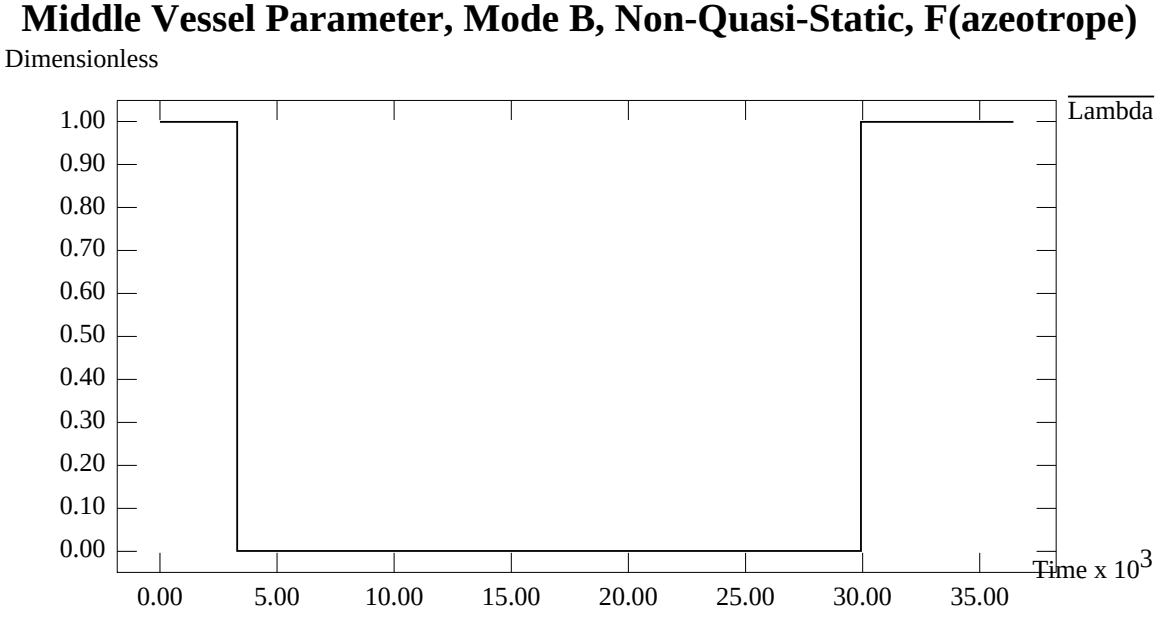

Figure E-40: Middle Vessel Parameter, λ, For $F_{azeotrope}$ as a Function of Time, Non-Quasi-Static

Appendix F

Derivation of Model Equations For the Multi-Vessel Column

Provided in this Appendix is the detailed derivation of the equations for the multi-vessel column as introduced in Chapter 8. As presented in Chapter 8, equation (8.6), which define the direction of motion for the total column composition, was derived from the definition of warped time τ given by equation (8.1), the definition of the multi-vessel column parameters ϑ_1 through ϑ_{n-1} (equation (8.2)), the component mass balance equations (equation (8.5)), and the overall mass balance equation (equation (8.4)).

Starting with the equation for component mass balance,

$$\frac{dM\mathbf{x}^M}{dt} = -\sum_{i=1}^{n-1}\{P_i\mathbf{x}_i^P\} \tag{F.1}$$

we differentiate the LHS by parts to obtain,

$$\mathbf{x}^M\frac{dM}{dt} + M\frac{d\mathbf{x}^M}{dt} = -\sum_{i=1}^{n-1}\{P_i\mathbf{x}_i^P\} \tag{F.2}$$

But, the overall mass balance equation is given as,

$$\frac{dM}{dt} = -\sum_{i=1}^{n-1} P_i \tag{F.3}$$

Hence, substituting equation (F.3) into equation (F.1), the following expression is obtained,

$$\mathbf{x}^M(-\sum_{i=1}^{n-1} P_i) + M\frac{d\mathbf{x}^M}{dt} = -\sum_{i=1}^{n-1}\{P_i\mathbf{x}_i^P\} \tag{F.4}$$

or equivalently,

$$\begin{aligned} M\tfrac{d\mathbf{x}^M}{dt} &= \mathbf{x}^M(\textstyle\sum_{i=1}^{n-1} P_i) - \sum_{i=1}^{n-1}\{P_i\mathbf{x}_i^P\} \\ &= \textstyle\sum_{i=1}^{n-1} P_i(\mathbf{x}^M - \mathbf{x}_i^P) \end{aligned} \tag{F.5}$$

But, from the definition of warped time τ for the middle vessel entrainer column as given in Chapter 8,

$$d\tau = (\frac{\sum_{i=1}^{n-1} P_i}{M})dt \tag{F.6}$$

which can be rearranged to obtain,

$$1 = (\frac{\sum_{i=1}^{n-1} P_i}{M})\frac{dt}{d\tau} \tag{F.7}$$

Multiplying the LHS of equation (F.5) by equation (F.7) which equals unity, the RHS is unchanged, and we obtain the following equation,

$$(\frac{\sum_{i=1}^{n-1} P_i}{M})\frac{dt}{d\tau}M\frac{d\mathbf{x}^M}{dt} = \sum_{i=1}^{n-1} P_i(\mathbf{x}^M - \mathbf{x}_i^P) \tag{F.8}$$

from which M and dt are cancelled,

$$\sum_{i=1}^{n-1} P_i\frac{d\mathbf{x}^M}{d\tau} = \sum_{i=1}^{n-1} P_i(\mathbf{x}^M - \mathbf{x}_i^P) \tag{F.9}$$

Dividing equation (F.9) by $(\sum_{i=1}^{n-1} P_i)$,

$$\frac{d\mathbf{x}^M}{d\tau} = \frac{\sum_{i=1}^{n-1} P_i(\mathbf{x}^M - \mathbf{x}_i^P)}{\sum_{i=1}^{n-1} P_i} \tag{F.10}$$

The definition of the multi-vessel column parameters were defined in Chapter 8 by

equation (8.2) as,

$$\begin{aligned}
\vartheta_1 &= \tfrac{P_1}{\sum_{i=1}^{n-1} P_i} \\
\vartheta_2 &= \tfrac{P_2}{\sum_{i=1}^{n-1} P_i} \\
&\vdots \\
\vartheta_{n-2} &= \tfrac{P_{n-2}}{\sum_{i=1}^{n-1} P_i} \\
\vartheta_{n-1} &= \tfrac{P_{n-1}}{\sum_{i=1}^{n-1} P_i}
\end{aligned} \tag{F.11}$$

ϑ_1 through ϑ_{n-1} are then substituted into equation (F.10) to give,

$$\frac{d\mathbf{x}^M}{dt} = \sum_{i=1}^{n-1} \vartheta_i (\mathbf{x}^M - \mathbf{x}_i^P) \tag{F.12}$$

which is equation (8.6) in Chapter 8.

We can also obtain an alternate definition of warped time as follows. From the overall mass balance equation as given by equation (F.3), we obtain,

$$dM = -(\sum_{i=1}^{n-1} P_i)dt \tag{F.13}$$

Equation (F.13) can then be substitued into our definition of the dimensionless warped time given by equation (F.6) to obtain

$$d\tau = \frac{dM}{M} \tag{F.14}$$

but

$$\frac{d}{dM} ln(M) = \frac{1}{M} \tag{F.15}$$

which implies that

$$d[ln(M)] = \frac{dM}{M} \tag{F.16}$$

and substituting equation (F.16) into equation (F.14), we obtain,

$$d\tau = d[ln(M)] \tag{F.17}$$

which gives a definition of warped time different from that of equation (F.6).

Appendix G

Sample ABACUSS Input Files for the Middle Vessel Column Model

In this Appendix, sample code of the ABACUSS input files used for the modelling of the middle vessel column is presented. There are a total of 7 files, which are as follows:

1. Declare.ABACUSS: Declares all the variables and their bounds and declares the models to be used in the simulation, and their nesting structure. This is a generic files used for all simulations conducted in ABACUSS involving thermodynamic models.

2. ExAntoine1.ABACUSS: Defines the form of the extended Antoine equation used for calculating the vapor pressure of each individual component. This extended Antoine equation is based on equations obtained from Aspen Plus.

3. NRTL.ABACUSS: Defines the form of the NRTL equation used for calculating liquid-liquid interactions as characterized by activity coefficients. The general form of the equation is again based on equations from Asepn Plus.

4. NI_VLE.ABACUSS: Defines the VlE behavior of the components, based on an activity-coefficient type model of vapor-liquid equilibrium.

5. Column.ABACUSS: Model of the middle vessel column is defined in this file. Nested within the column model, are VLE relationships for each tray in the column.

6. FSNR_ABC.ABACUSS: Flowsheet for the separation of the ABC mixture. Defines the parameters used, and the number of trays, location of the middle vessel column, and any other relevant parameters.

7. ABCSepBazeotrope.ABACUSS: Simulation file, in which all degrees of freedom in the model are accounted for by defining values for certain variables. Lists the initial conditions for the solution of differential equations. States the operating schedule for the simulation.

G.1 Declare.ABACUSS

```
#=================================================================
#
# %h Declarations of Variable and Stream types for ABACUSS
#    Modifications:
#     Russell Allgor : March 14, 1994
#      - changed the lower bound on Fraction to -1E-12 (old value 0)
#      - this was done to allow ABACUSS to integrate along a bound
#     Berit Ahmad : March 30, 1994
#      - added stream type of Column_Stream for streams between
#        trays in a column %
#
#
# Language: ABACUSS
# Purpose:  Establishes variable types for use in ABACUSS models to
#           provide uniformity for modeling activities.
#
```

```
# Date: February 23, 1994
#
# Creator: Russell Allgor
#          Copyright October 1994
#          MIT .
#
#====================================================================
DECLARE

  TYPE                 # Default   Min     Max   UNITS
      Concentration    = 0    : -1e-6 : 1E5    unit = "mol/m^3"
      Energy           = 0    : -1E20 : 1E20   unit = "GJ"
      EnergyFlowRate   = 0    : -1E20 : 1E20   unit = "GJ/s"
      MolarEnthalpy    = 1    : -1E15 : 1E15   unit = "GJ/mol"
      LiquidMolarVolume= 20   :  1e-9 : 2000   unit = "cm3/mol"
      VaporMolarVolume = .0224: 1e-9  : 12     unit = "m3/mol"
      MassFlowRate     = 1    : 0     : 1E6    unit = "g/s"
      KgMassFlowRate   = 1    : 0     : 1E6    unit = "kg/s"
      MolarVolume      = .01  : 1e-9  : 12     unit = "m^3/mol"
      Fraction         = .5   : -1E-3 : 1.001  unit = "dimensionless"
      MolarFlowRate    = 0    : -1e-2 : 1001   unit = "mol/s"
      Length        = .5   : -1E-2 : 1000   unit = "m"
      MolarHoldup      = 1    : -1e-3 : 1E7    unit = "mol"
      PositiveValue    = .75  : 0     : 1E15   unit = "dimensionless"
      Pressure         = 1.013: 0     : 1000   unit = "bar"
      Power            = 0    : -1E20 : 1E20   unit = "GJ/s"
      ReactionRate     = 0    : -1e-4 : 1E9    unit = "mol/m3/s"
      ReducedQuantity  = .5   :  0    : 10     unit = "dimensionless"
      SmallValue       = .02  : -10   : 10     unit = "dimensionless"
      Temperature      = 336  :  50   : 2000   unit = "K"
```

```
      Value            = 1    : -1e10 : 1e10   unit = "dimensionless"
      Paramvalue       = 1    : -1e4  : 1e4    unit = "dimensionless"
      Velocity         = 2    : -1e5  : 1e5    unit = "m/s"
      Volume           = 1    : 1e-9  : 10000  unit = "m^3"
      PosValue        = 1    : 1e-40 : 1e40   unit = "dimensionless"
#=================================================================


  STREAM
         Process_Stream     IS     Fraction,
                                   MolarFlowRate,
                                   Pressure,
                                   Temperature,
                                   MolarEnthalpy

         Column_Stream     IS Fraction,
                                 MolarFlowRate,
                                 MolarEnthalpy

         Column_Vapor_Stream   IS     Fraction,
                                      MolarFlowRate,
                                      Pressure,
                                      VaporMolarVolume,
                                      MolarEnthalpy

     Pure_Stream       IS      MolarFlowRate,
                                   Pressure,
                                   Temperature,
                                   MolarEnthalpy
END  # Declarations
```

G.2 ExAntoine1.ABACUSS

```
MODEL ExtendedAntoine1
#=================================================================%h
#-----------------------------------------------------------------
# File:      ExAntoine1.ABACUSS
# Property : Vapor Pressure
# MODEL Extended-Antoine1 - Extended Antoine Vapor Pressure Model
#
# Purpose : Find vapor pressure of all the components in the mixture.
#      Equation used is from AspenPlus User Guide Appendices,
#     p.E-4.
#
# Created by Berit Ahmad and Russell Allgor
# Date : August 1993
# %
# Copyright August 1993 MIT
#=================================================================%h
#  Modifications:
#     Sarwat Khattak: Feb. 16, 1995
#      - Equation now written so that the exp. is multiplied by
#        1e-5 instead of taking the log of Pvap*1e5.
#
#-----------------------------------------------------------------%
#=================================================================
# PARAMETERS:
#
#  ANTOINE(NC:9) Coefficients for the extended Antoine
```

```
# Equation. These coefficients provide the
# Pressure in Pascal, therefore a conversion
# factor is included in this model to predict
# pressures in bar. The parameters
# can be found in AspenPlus.
#
#  NC Number of components. [dimensionless]
#
#=====================================================================
# VARIABLES:
#
# Vapor_Pressure Array(NC) of Pressure [bars]
#
# Temp Temperature [K]
#
#=====================================================================
# DEGREES OF FREEDOM:
#
# Number of variables: NC + 1
# Number of equations:     NC
# Degrees of freedom :      1
#
#=====================================================================

  PARAMETER
   NC           AS INTEGER
   ANTOINE       AS ARRAY(NC,9) of Real

  VARIABLE
   Vapor_Pressure AS ARRAY(NC) of Pressure
```

```
   Temp           AS Temperature
Z               AS ARRAY(NC) of Fraction
#internal variable given
   #as x in equation in book
  EQUATION

For I := 1 TO NC DO
#Choose one of 2 possible forms of expressing vapor pressure.
        #============================================================
        Vapor_Pressure(I) = 1e-5 *EXP( ANTOINE(I,1)
                       + ANTOINE(I,2)/(Temp + ANTOINE(I,3))
                           + ANTOINE(I,4)*Temp
+ ANTOINE(I,5)*log(Temp)
                     + ANTOINE(I,6)*Temp^ANTOINE(I,7));
#============================================================
      # LOG(Vapor_Pressure(I)*1e5) =  ANTOINE(I,1)
      #                 + ANTOINE(I,2)/(Temp + ANTOINE(I,3))
     #                 + ANTOINE(I,4)*Temp
# + ANTOINE(I,5)*log(Temp)
     #                 + ANTOINE(I,6)*Temp^ANTOINE(I,7);
    #============================================================
   Z(i)= 1;
END #FOR

END # MODEL ExtendedAntoine1

MODEL VaporPressure INHERITS ExtendedAntoine1
END # VaporPressure
```

G.3 NRTL.ABACUSS

```
MODEL NRTL

#=====================================================================
#                          Activity Coefficient Model
#
# File:    NRTL.ABACUSS
# Purpose: Solves for activity coefficients for components of liquid
#    mixtures using the Non-Random Two-Liquid model.
#
# Created by Weiyang Cheong
# Date: August 1997
# %
# Copyright August 1997 MIT
#
#=====================================================================
# %h Activity Coefficient: NRTL Equation
#    Modifications: Who, When, What %
#=====================================================================
# BACKGROUND/REFERENCES:
#
#   This model assumes the form of the NRTL used in its
#   implementation in Aspen Plus (see AspenPlus User Guide
#   Appendices Model GMRENON).
#
#=====================================================================
# ASSUMPTIONS:
#   1. Model predicts liquid/liquid phase splitting.
#
```

```
#=======================================================================
# PARAMETER:
#
# NC Number of components [dimensionless]
#
# NRTL_A ARRAY(NC,NC) of REAL  [dimensionless]
#  refers to parameters
# a_ij & a_ji
#
# NRTL_B ARRAY(NC,NC) of REAL  [K]
# refers to parameters
# b_ij & b_ji
#
# NRTL_C ARRAY(NC,NC) of REAL [dimensionless]
# refers to parameters
# c_ij & c_ji
#
# NRTL_D ARRAY(NC,NC) of REAL [K]
# refers to parameters
# d_ij & d_ji
#
# NRTL_E ARRAY(NC,NC) of REAL [K]
# refers to parameters
# e_ij & e_ji
#
# NRTL_F ARRAY(NC,NC) of REAL [K]
# refers to parameters
# f_ij & f_ji
#
# Note: NRTL_E and NRTL_F are usually null matrices, due to e,
```

```
# f parameters being zero. Hence, model might not include NRTL_E
# and NRTL_F.
#-----------------------------------------------------------------
# DATA:
# The binary interaction parameters (NRTL_A(i,j) through
# NRTL_F(i,j)) can be obtained directly from Aspen Plus, or
# calculated from experimental data. AspenPlus can also be
# used to estimate these parameters via VLE/LLE regression.
#
#=================================================================
# VARIABLES:
#
# Gamma ARRAY (NC) of PositiveValue   [dimensionless]
# Activity Coefficient.
#
# G ARRAY(NC,NC) of PositiveValue [dimensionless]
# Internal variable.
#
# Tau ARRAY(NC,NC) of Value [dimensionless]
# Internal variable.
#
# Alpha ARRAY(NC,NC) of Value [dimensionless]
# Internal variable.
#
# Temp Temperature [K]
#
# x ARRAY(NC) of Fraction [dimensionless]
# Liquid Mole Fraction.
#
# Var1 ARRAY(NC) of Value [dimensionless]
```

```
# Temporary Variable.
#
# Var2 ARRAY(NC) of Value [dimensionless]
# Temporary Variable.
#
#===============================================================
# EQUATIONS:
#
# The NRTL equation is employed in the following form
# (AspenPlus):
#
# LOG(Gamma(I)) =
# (SUM(J:=1..NC) (x(J)*Tau(J,I)*G(J,I)))/
# (SUM(J:=1..NC) (x(J)*G(J,I)))
# + (SUM(J:=1..NC) ( ((x(J)*G(I,J))/
# (SUM(K:=1..NC) x(K)*G(K,J)))*
# (Tau(I,J) - (SUM(M:=1..NC) (x(M)*Tau(M,J)*G(M,J)))/
# (SUM(K:=1..NC)(x(J)*G(K,J))))));
#
# or LOG(Gamma(I))= SIGMA(x()*Tau(,I)*G(,I))/SIGMA(x()*G(,I))
# + SIGMA(J)(((x()*G(I,))/(SIGMA(x()*G(,J))))*
# (Tau(I,) - SIGMA(x()*Tau(,J)*G(,J))/SIGMA(x()*G(,J))));
#
# where G(I,J) = EXP( -alpha(I,J)*Tau(I,J))
#
# Tau(I,J) = NRTL_A(I,J) + NRTL_B(I,J)/Temp
#
# or# Tau(I,J) = NRTL_A(I,J) + NRTL_B(I,J)/Temp
# + NRTL_E(I,J)*LOG(Temp) + NRTL_F(I,J)*Temp
# (see explanation in the parameters section)
```

```
#
# Alpha(I,J) = NRTL_C(I,J) + NRTL_D(I,J)*(Temp-273.15)
#
# Tau(I,I) = 0
#
# G(I,I) =  1
#
# NRTL_A(I,J) != NRTL_A(J,I)
#
# NRTL_B(I,J) != NRTL_B(J,I)
#
# NRTL_C(I,J) = NRTL_C(J,I)
#
# NRTL_D(I,J) = NRTL_D(J,I)
#
# or with introduction of the temporary variables
#
# Var1(I) =  SUM(K:=1..NC) (x(K)*G(K,I))
# =  SIGMA(x()*G(,I))
#
# Var2(I) =  SUM(K:=1..NC) (x(K)*Tau(K,I)*G(K,I))
# = SIGMA(x()*Tau(,J)*G(,I))
#
# equation simplifies to:
#
# LOG(GAMMA(I)) = (Var2(I))/(Var1(I))
# +SUM(J:=1..NC)
# ((x(J)*G(I,J)/Var1(J))*(Tau(I,J) - Var2(J)/Var1(J)));
#
# or LOG(GAMMA(I)) = (Var2(I)/Var1(I)) +
```

```
# SIGMA( (x()*G(I,)/Var1())*(Tau(I,) - Var2()/Var1()));
#
#
#=================================================================
#  Presently, no function to perform double summations exists.
#  Temporary variables have been defined instead, which aid in
#  double summation.
#=================================================================
# DEGREES OF FREEDOM:
#
# Number of variables: 10NC + 1
# Number of equations:      9NC
# Degrees of freedom :   NC + 1
#
#=================================================================

  PARAMETER

NC AS INTEGER
NRTL_A AS ARRAY(NC,NC) of REAL
NRTL_B AS ARRAY(NC,NC) of REAL
NRTL_C AS ARRAY(NC,NC) of REAL
NRTL_D AS ARRAY(NC,NC) of REAL
# NRTL_E AS ARRAY(NC,NC) of REAL
# NRTL_F AS ARRAY(NC,NC) of REAL


  VARIABLE

Gamma AS ARRAY (NC)  of  PosValue
```

```
G AS ARRAY(NC,NC) of PosValue
Tau AS ARRAY(NC,NC) of Value
Alpha AS ARRAY(NC,NC) of Value
Temp AS Temperature
x AS ARRAY(NC) of Fraction
Var1 AS ARRAY(NC) of Value
Var2 AS ARRAY(NC) of Value


  EQUATION

FOR I:=1 to NC DO

FOR J:=1 to NC DO

  Tau(I,J) = (NRTL_A(I,J)) + (NRTL_B(I,J)/Temp);

#-------------------------------------------------------------------
# or   Tau(I,J) = NRTL_A(I,J) + NRTL_B(I,J)/Temp
#       + NRTL_E(I,J)*LOG(Temp)
#         + NRTL_F)I,J)*Temp;
# if using NRTL_E and NRTL_F
#-------------------------------------------------------------------

  Alpha(I,J) = NRTL_C(I,J)+NRTL_D(I,J)*(Temp-273.15);

  G(I,J) = EXP(-(Alpha(I,J)*Tau(I,J)));

END #For J
```

```
END #For I

FOR I:=1 to NC DO

Var1(I) = SIGMA(x()*G(,I));

Var2(I) = SIGMA(x()*Tau(,I)*G(,I));

END #For I

FOR I:=1 to NC DO

#-------------------------------------------------------------------
# Form 1
# LOG(Gamma(I))= Var2(I)/Var1(I) +
# SIGMA(((x()*G(I,))/
# Var1())*(Tau(I,) - (Var2()/Var1())));
#
#-------------------------------------------------------------------
# Form 2
Gamma(I) = EXP( Var2(I)/Var1(I) +
SIGMA(((x()*G(I,))/Var1())*(Tau(I,)
- (Var2()/Var1())));
#
#-------------------------------------------------------------------
END #For I

END # NRTL model

MODEL ActivityCoefficient INHERITS NRTL
```

```
END # ActivityCoefficient
```

G.4 NI_VLE.ABACUSS

```
MODEL NonIdeal_VLE

#=====================================================================
#               Model for Vapor Liquid Equilibrium
#
# File :    NI_VLE.ABACUSS
# Purpose : Relate x (liquid phase mole fractions) and y (vapor
#     phase mole fractions for a liquid/gas equilibrium
#           mixture.
#
# Created by Russell Allgor and Sarwat Khattak
# Date :  September 15, 1994
#
# Copyright February 1994 MIT
#=====================================================================
# %h Vapor-Liquid Equilibrium: NonIdeal_VLE
#    Modifications: Who, When, What %
#
#=====================================================================
# Assumptions:
#   1. The vapor phase is an ideal gas.
#   2. The liquid phase is modeled using Activity Coefficients.
#   3. The pressure dependence on liquid phase fugacity has been
#      ignored (Poynting Correction, Poynting Factor = 1).
#   4. The liquid phase pure component fugacities are equal to the
#      component's vapor pressure.  Won't work well for components
```

```
#      above their critical points since the vapor pressure is not
#      valid in this region.
#
#=======================================================================
# UNITS:
#
# VaporPressure  Thermodynamic Model to calculate vapor
# pressures of components at the given
# temperature.
#
# ActivityCoefficient Thermodynamic Model to calculate
# the activity coefficients of the
# components at a given
# temperature and mole fraction.
#
#=======================================================================
# PARAMETERS:
#
# NC Number of components [dimensionless]
#
#=======================================================================
# VARIABLES:
#
# Press Pressure    [Pa]
#
# Temp Temperature    [K]
#
# x  ARRAY(NC) of Liquid Mole Fraction     [dimensionless]
#
# y ARRAY(NC) of Vapor Mole Fraction      [dimensionless]
```

```
#
# Gammma ARRAY(NC) of Activity Coefficient > 0 [dimensionless]
#
#
#=================================================================
# EQUATIONS:
#
#     Y * PRESS  = X * PVAP.VAPOR_PRESSURE * ACTIVITYCOEFF.GAMMA;
#
# Partial Pressure = Gas Mole Fraction*Total Pressure =
# Liquid Mole Fraction*Activity Coefficient
# *Vapor Pressure,Pure Component
#
#=================================================================
# DEGREES OF FREEDOM:
#
# Number of Variables: 2NC + 2
#   Number of Equations:         NC
# Degrees of Freedom :     NC + 2
#
#=================================================================

  PARAMETER

     NC           AS Integer

  UNIT

     Pvap           AS VaporPressure
     ActivityCoeff  AS ActivityCoefficient
```

```
  VARIABLE

     Press  AS Pressure
     Temp   AS Temperature
     x           AS ARRAY(NC) of Fraction
     y          AS ARRAY(NC) of Fraction

  EQUATION

# Equate Fugacities: Ideal Vapor|Liquid modeled using Activity Coeff

y * Press  = x * Pvap.Vapor_Pressure * ActivityCoeff.Gamma;

# Pass variables to submodels

x         = ActivityCoeff.x;
     Temp      = ActivityCoeff.Temp;
     Temp      = Pvap.Temp;



END # MODEL Nonideal_VLE



MODEL VLE INHERITS NonIdeal_VLE
END # VLE
```

G.5 Column.ABACUSS

```
MODEL Column
```

```
#=====================================================================
# BATCH DISTILLATION MIDDLE VESSEL COLUMN
#  based on Bernot's model (Bernot et al. 1990)
# File: Column.ABACUSS
#
# Modified from Code by Berit S. Ahmad
#  Created by: Weiyang Cheong
#  Date:       April, 1997
#
#=====================================================================
# MODIFICATIONS: Who, When, What
#
#=====================================================================
# ASSUMPTIONS/HINTS:
# - holdup on stages and in condenser are negligible
# - no heat effects
# - constant molar overflow
# - quasi-steady state in column
# - Trays are numbered from bottom to top, 1 being the bottoms
#   product NS+1 being the top/distillate product. M being the
#   middle vessel, where 1 < M < NS+1, which makes NS trays total
#   + holdup pot M.
#=====================================================================
# UNITS:
#
# VLE Vapor-Liquid-Equilibrium Model to calculate the
#               liquid and vapor mole fractions in equilibrium with
# each other in a given tray. May not detect
# liquid-liquid phase splits.
```

```
#
#=================================================================
# PARAMETERS:
#
#    NC number of components [dimensionless]
#
#    NS   number of equilibrium stages [dimensionless]
#
# M position of Middle Vessel [dimensionless]
#
#=================================================================
# VARIABLES:
#
# moleholdup  ARRAY(NC) of Molar Holdup in Mid Vessel [mole]
#
# totalholdup Total Molar Holdup in Mid Vessel [mole]
#
# mold ARRAY(NC) of original mole holdup [mole]
#
# mnew ARRAY(NC) of new mole holdup [mole]
#
# x ARRAY(NS+1,NC) of Liquid Mole [dimensionless]
# Fraction in each Tray, of each Component
#
# y ARRAY(NS+1,NC) of Vapor Mole  [dimensionless]
# Fraction in each Tray, of each Component
#
# xd ARRAY(NC) of Distillate Composition [dimensionless]
#
# xb ARRAY(NC) of Bottoms Composition    [dimensionless]
```

```
#
# xm ARRAY(NC) of Midvessel Liquid Comp. [dimensionless]
#
# ym ARRAY(NC) of Midvessel Vapor Comp.  [dimensionless]
#
# temp ARRAY(NS+1) of Temperature in each Tray [K]
#
# press Pressure in the whole Column [bar]
#
# LD LD=Liquid Rate in Top Section [mole/time]
#
# VB VB=Vapor Rate in Bottom Section [mole/time]
#
# D Distillate Flow Rate [mole/time]
#
# B Bottoms Flow Rate [mole/time]
#
# DOld Old (Original) Distillate Flow Rate [mole/time]
#
# BOld Old (Original) Bottoms Flow Rate [mole/time]
#
# DNew New Distillate Flow Rate [mole/time]
#
# BNew New Bottoms Flow Rate [mole/time]
#
# DNone Zero Distillate Flow Rate [mole/time]
#
# BNone Zero Bottoms Flow Rate [mole/time]
#
# P Middle Column Parameter=D/(D+B),0<P<1 [dimensionless]
```

```
#
# accumulationd ARRAY(NC) of Molar Holdup in [mole]
# Distillate Collected
#
# accumulationb ARRAY(NC) of Molar Holdup in [mole]
# Bottoms Product Withdrawn
#
#=================================================================
# EQUATIONS:
#
#     Equations employed to represent the column are as follows:
#
# Phase equilibrium for each tray, as obtained
# from VLE model, for NS+1 trays. Each VLE model
# contains NC equation, 1 model per tray. [(NS+1)*NC]
#
# FOR i:= 1 to NS+1 DO
#         y(i,)     = VLE(i).y ;
#         x(i,)     = VLE(i).x ;
#         temp(i)   = VLE(i).temp ;
#         press     = VLE(i).press ;
#
# Constitutive Equations, sum of vapor mole fractions = 1,
# defines Temp(NS+1) of tray given pressure. [NS+1]
#
#          SIGMA(y(i,)) = 1;
#
# END# FOR loop, VLE for each tray, 1 through NS+1
#
#
```

```
# Composition of Middle Vessel, as defined by moleholdup
# and total holdup. Identity equation for defining x(M,).
# [NC]
#
#   moleholdup = totalholdup*x(M, );
#
#
# Molebalance equation in the middle vessel.
# Use one or other alternative equations. [1]
#   # $totalholdup = D + B ; #or
# totalholdup = sigma(moleholdup());
#
#
# Composition change in Middle Vessel given by:
# $moleholdup = -VD(M)*y(M,)+LD(M+1)*x(M+1,)
# -LB(M)*x(M,)+VB(M-1)*y(M-1,);
# where VD is vapor rate in column above middle vessel
#   LD is liquid rate in column above middle vessel
#   VB is vapor rate in column below middle vessel
#   LB is liquid rate in column below the middle vessel
# [NC]
#
# $moleholdup  = -(LD+D)*y(M,)+(LD)*x(M+1,)
# -(VB+B)*x(M,)+(VB)*y(M-1,) ;
#
#
# Midvessel Column Parameter Definition, 0<P<1.
# Value of P determines the mix of products obtained. [1]
#
# P=D/(D+B) ;
```

```
#
#
# Middle Vessel Composition, identity equations,
# for ease of plotting purposes. [2NC]
#
# FOR i := 1 to NC DO
#         xm(i) = x(M,i) ;
# ym(i) = y(M,i) ;
# End #For
#
#
# Reboiler equation for bottoms tray (1) output.
# Total reboiler configuration, bottoms x(1,) is drawn off,
# the rest completely boiled off back into the column.
# No extra stage of equilibrium in the reboiler,to
# maintain symmetry of the configuration (wrt Condenser).
# [NC]
#
# Equation simplified from the following mass balance equation:
#
#  -x(1,)*(VB+B) -y(1,)*VB +x(2,)*(VB+B) +x(1,)*VB = 0 ;
#
#
# Condenser equation for top tray (NS+1) output.
# Total condenser configuration, distillate x(NS+1,) drawn off,
# the rest totally condensed and refluxed into the column.
# [NC]
#
# Equation simplified from the following mass balance equation:
#
```

```
#  -x(NS+1,)*LD -y(NS+1,)*(LD+D) +y(NS+1,)*LD +y(NS,)*(LD+D) = 0 ;
#
#
# Composition change on each tray, mass balance equations
# giving stage by stage operating lines.
# For Trays below the middle vessel. [(M-1-1)*NC]
#
# Simplified from orginal mass balance equation:
#  -x(i,)*(VB+B) -y(i,)*VB +x(i+1,)*(VB+B) +y(i-1,)*VB = 0 ;
#
# FOR i:= 2 to M-1 DO
#   -x(i,)*(VB+B) -y(i,)*VB +x(i+1,)*(VB+B) +y(i-1,)*VB = 0 ;
# END #For
#
#
# For Trays above the middle vessel. [(NS-M)*NC]
#
# Simplified from orginal mass balance equation:
#  -x(i,)*LD -y(i,)*(LD+D) +x(i+1,)*LD +y(i-1,)*(LD+D) = 0 ;
#
# FOR i:= M+1 to NS DO
#   -x(i,)*LD -y(i,)*(LD+D) +x(i+1,)*LD +y(i-1,)*(LD+D) = 0 ;
# END #For
#
# Condenser composition profile; identity equations
# for ease of plotting. Distillate drawn off as vapor. [NC]
#
# For i:=1 to NC DO
# xd(i) = y(NS+1,i) ;
#
```

```
# Accumulation of the product cuts drawn from distillate.
# Moles of each component accumulated. [NC]
#
# $accumulationd(i) = xd(i)*D ;
# END #For
#
#
# Reboiler composition profile; identity equations
# for ease of plotting. Bottoms drawn off as liquid. [NC]
#
# For i:=1 to NC DO
# xb(i) = x(1,i) ;
#
# Accumulation of the product cuts drawn from bottoms.
# Moles of each component accumulated. [NC]
#
# $accumulationb(i) = xb(i)*B ;
# END #For
#
#
#=================================================================
# DEGREES OF FREEDOM:
#
# Number of variables: 2NS*NC + 9NC + NS + 8
# Number of equations: 2NS*NC + 9NC + NS + 3
# Degrees of freedom :       5
#    (LD, VB, D, B, Press)
#
#=================================================================
```

```
  PARAMETER

    NC as INTEGER
   NS as INTEGER
M as INTEGER

  UNIT

   VLE as ARRAY(NS+1) of VLE

  VARIABLE

moleholdup as ARRAY(NC) of MolarHoldup
  totalholdup as MolarHoldup
    x as ARRAY(NS+1,NC) of Fraction
    y as ARRAY(NS+1,NC) of Fraction
     xd as ARRAY(NC) of Fraction
    xb as ARRAY(NC) of Fraction
    xm as ARRAY(NC) of Fraction
    ym as ARRAY(NC) of Fraction
    mold as ARRAY(NC) of Fraction
    mnew as ARRAY(NC) of Fraction
    temp as ARRAY(NS+1) of Temperature
    press as Pressure
    LD as PositiveValue
    VB as PositiveValue
    D as PositiveValue
     B as PositiveValue
    DOld as PositiveValue
```

```
     BOld as PositiveValue
DNew as PositiveValue
     BNew as PositiveValue
DNone as PositiveValue
     BNone as PositiveValue
    P as PositiveValue
  accumulationd as ARRAY(NC) of MolarHoldup
  accumulationb as ARRAY(NC) of MolarHoldup
Lambda1 as PositiveValue
Lambda2 as PositiveValue



  EQUATION

FOR i:= 1 to NS+1 DO
         y(i,)     = VLE(i).y ;
         x(i,)     = VLE(i).x ;
         temp(i)   = VLE(i).temp ;
         press     = VLE(i).press ;

          SIGMA(y(i,)) = 1 ;
END #For

   moleholdup = totalholdup*x(M, ) ;
totalholdup = sigma(moleholdup()) ;

$moleholdup = -(LD+D)*y(M,)+LD*x(M+1,)
-(VB+B)*x(M,)+VB*y(M-1,);
```

```
P = D/(D+B) ;

       FOR i := 1 to NC DO
         xm(i) = x(M,i) ;
ym(i) = y(M,i) ;
        End #For


-x(1,)*(VB+B) - y(1,)*VB + x(2,)*(VB+B) + x(1,)*VB = 0 ;
-x(NS+1,)*LD - y(NS+1,)*(LD+D) + y(NS+1,)*LD + y(NS,)*(LD+D) = 0 ;


FOR i:= 2 to M-1 DO
  -x(i,)*(VB+B) -  y(i,)*VB + x(i+1,)*(VB+B) + y(i-1,)*VB = 0 ;
END #For


FOR i:= M+1 to NS DO
  -x(i,)*LD -  y(i,)*(LD+D) + x(i+1,)*LD + y(i-1,)*(LD+D) = 0 ;
END #For


FOR i:=1 to NC DO
xd(i) = y(NS+1,i) ;
$accumulationd(i) = xd(i)*D ;
END #For


FOR i:=1 to NC DO
```

```
xb(i) = x(1,i) ;
$accumulationb(i) = xb(i)*B ;
END #For

END # Batch Model Column
```

G.6 FSNR_ABC.ABACUSS

```
MODEL flowsheet

#=====================================================================
# Thermodynamic Data and Column Parameters for 3 Component
#       Systems Acetone, Benzene, Chloroform, ExAntoine1, NRTL.
#
# File :     FSNR_ABC.ABACUSS
# Purpose :  Flowsheet for the Middle Vessel Column, defining
# the relevant parameters required for the column,
# and the thermodynamic data required for each of
# the components present in the column.
#
# Created by Cheong Wei Yang, modified from code by Berit S. Ahmad.
# Date :  July 31, 1997
#
# Copyright July 1997 MIT
#=====================================================================
# %h Thermodynamic Data/Column Parameters,Acetone,Benzene,Chloroform
#    Modifications: Who, When, What %
#
#=====================================================================
# Assumptions:
```

```
#
#=====================================================================
# UNITS:
#
# Column Bernot-type model of a Middle Vessel column
# for simulation of its behavior.
#
#=====================================================================
# PARAMETERS:
#
# NC Number of components [dimensionless]
#
# M  Middle Vessel Position [dimensionless]
#
# NS    Number of Trays in Column [dimensionless]
#
# COMPONENT1  Component Name as Index = 1 [dimensionless]
#
# COMPONENT2     Component Name as Index = 2 [dimensionless]
#
# COMPONENT3  Component Name as Index = 3 [dimensionless]
#
# COMPONENT4     Component Name as Index = 4 [dimensionless]
#
# ANTOINE ARRAY(NC,9) for extended antoine, [dimensionless]
# Aspen model, 9 constants #or
#
# ANTOINE ARRAY(NC,6) for ex-antoine, Reid,  [dimensionless]
# Prausnitz, Pollig, 6 constants #or
#
```

```
# ANTOINE ARRAY(NC,3) for simple antoine model, [dimensionless]
# 3 contants.
#
# NRTL_A  ARRAY(NC,NC), NRTL Parameters, a(ij) [dimensionless]
#
# NRTL_B  ARRAY(NC,NC), NRTL Parameters, b(ij) [K]
#
# NRTL_C  ARRAY(NC,NC), NRTL Parameters, c(ij) [dimensionless]
#
# NRTL_D  ARRAY(NC,NC), NRTL Parameters, d(ij) [K]
#
# NRTL_E  ARRAY(NC,NC), NRTL Parameters, e(ij) [dimensionless]
#
# NRTL_F  ARRAY(NC,NC), NRTL Parameters, f(ij) [1/K]
#
#
#
#=====================================================================
# VARIABLES:
#
#=====================================================================
# EQUATIONS:
#
#=====================================================================
# DEGREES OF FREEDOM:
#
#=====================================================================

  PARAMETER
```

```
NC as Integer
NS as Integer
M as Integer
ACETONE as Integer
BENZENE as Integer
CHLOROFORM as Integer
ANTOINE as ARRAY(NC,9) of REAL
NRTL_A as ARRAY(NC,NC) of REAL
NRTL_B as ARRAY(NC,NC) of REAL
NRTL_C as ARRAY(NC,NC) of REAL
NRTL_D as ARRAY(NC,NC) of REAL
# NRTL_E as ARRAY(NC,NC) of REAL
# NRTL_F as ARRAY(NC,NC) of REAL

  UNIT

Column as Column

  SET

NS := 100;
NC := 3;
M := 51;


# Component: Acetone -
ACETONE := 1;
ANTOINE(ACETONE,) :=
[69.0060,-5599.60,0.0,0.0,-7.0985,6.2237e-6,2.00,178.450,508.200] ;
```

```
# Component: Benzene -
BENZENE := 2;
ANTOINE(BENZENE,) :=
[83.9180,-6517.70,0.0,0.0,-9.34530,7.11820e-6,2.00,278.680,562.160] ;

# Component: Chloroform -
CHLOROFORM := 3;
ANTOINE(CHLOROFORM,) :=
[146.430,-7792.30,0.0,0.0,-20.6140,2.4578e-2,1.00,207.150,536.400] ;

 NRTL_A(ACETONE,) := [    0.0, -0.1015,  0.9646];
 NRTL_A(BENZENE,)    := [ 0.4224,     0.0,     0.0];
 NRTL_A(CHLOROFORM,) := [ 0.5382,     0.0,     0.0];

 NRTL_B(ACETONE,) := [     0.0,  306.066, -590.026];
 NRTL_B(BENZENE,)    := [-239.901,      0.0, -375.431];
 NRTL_B(CHLOROFORM,) := [-106.422,  313.011,      0.0];

 NRTL_C(ACETONE,) := [ 0.00, 0.30, 0.30];
 NRTL_C(BENZENE,)    := [ 0.30, 0.00, 0.47];
 NRTL_C(CHLOROFORM,) := [ 0.30, 0.47, 0.00];

 NRTL_D(ACETONE,) := [ 0.0, 0.0, 0.0];
 NRTL_D(BENZENE,)    := [ 0.0, 0.0, 0.0];
 NRTL_D(CHLOROFORM,) := [ 0.0, 0.0, 0.0];

END # flowsheet
```

G.7 ABCSepBazeotrope.ABACUSS

```
SIMULATION separate

#=====================================================================
# Simulation File for Middle Vessel Column, 3 Component System
#
# File :     ABCSepBazeotrope.ABACUSS
# Purpose :  Simulation for the Middle Vessel Column, defining the
# relevant initial conditions required for the 3NC
# differential equations in the column (NC for molar
# holdup, NC for each of accumulation in the distillate
# and bottoms). Also provided are the values of the 5
# variables, allowed by the 5 degrees of freedom in the
# equations for the column. Preset Values are provided
# to ease convergence of initialization calculations.
#
# This file was created for the separation of an initial charge with
# an azeotropic composition (acetone-chloroform), to which entrainer:
# Benzene was added to allow complete separation of azeotrope into
# pure components.
#
# Created by Cheong Wei Yang, modified from code by Berit S. Ahmad.
# Date :  May 10, 1998
#
# Copyright May 1998 MIT
#=====================================================================
# %h Simulation, Middle Vessel, 3 component, ABC, ExAntoine1, NRTL,
#    100 Trays, M = 51
#    Modifications: Who, When, What %
#
#=====================================================================
```

```
# Assumptions:
#
#=====================================================================
# UNITS:
#
# Flowsheet Bernot-type model of a Middle Vessel column
# for simulation of its behavior, with
# parameters fully defined by FS files.
#
#=====================================================================
# INPUT:
#
# Define in the input section, the values of the 5 variables which
# have to be defined in the column model, to create a fully specified
# column.
#
#
# press :=  1 ; Pressure in bars. Default at Atmospheric Pressure.
#
# LD    := 10 ; Rectifying Section Liquid Rate. Use approx 10 for a
# still pot of 100. Vary D to vary Rd.
#
# VB    := 10 ; Stripping Section Vapor Rate. Use approx 10 for a
# still pot of 100. Vary B to vary Rb.
#
# D :=  0.01 ; Distillate Withdrawal Rate.
# B :=  0.01 ; Bottoms Withdrawal Rate.
#
# Coupled together, D,B defines the Middle Vessel
# Parameter, P, and also defines the rate at which
```

```
# the simulation will be completed, given the initial
# total molar holdup in the middle vessel.
#
#=====================================================================
# PRESET:
#
# Initial Preset values to aid the convergence of initialization
# calculations. The initial middle column composition is defined by
# the moleholdup in the initial section, hence it is totally defined
# and included in the inital preset section. With the middle vessel
# compostion initialized, the rest of the variables involved in the
# calculation can be initialized by running the simulation at the
# correct number of trays, but a very low reflux rate, and with the
# Schedule section commented out. Save/preset at the ABACUSS prompt.
# Obtain preset values from ABACUSS.sav, and paste into file.
#
# COLUMN.COLUMN.XM(i) := moleholdup(i)/totalmoleholdup ;
#     := moleholdup(i)/100 ;
#
#=====================================================================
# INITIAL:
#
# Initial Conditions for the 3NC differential equations are provided.
#
# Specify initial moleholdups, total should add up to 100.
# Initial moleholdup when completely specified defines initial
# middle vessel composition, as given in the preset section.
#
# moleholdup(i) = value i ; [NC]
#
```

```
# Initial accumulation, in bottoms (accumulationb)
# and distillate (accumulationd) both set to 0 at time = 0.
#
# accumulationb(i) = 0 ; [NC]
#
# accumulationd(i) = 0 ; [NC]
#
#
#=====================================================================
# SCHEDULE:
#
# Delineates the end condition of the simulation, and the operating
# schedule throughout the operation of the column. Use of homotopy
# continuation in ensuring that calculations reinitialize after
# a switch in parameters in the middle of the operation.
#
# Comment out the Schedule section when doing a initialization
# calculation to obtain the presets for the Column.
#
#=====================================================================

  UNIT
column AS flowsheet

  INPUT
WITHIN column.column DO
press :=  1 ;
VB      :=  10 ;
LD :=  10 ;
D :=  0.01 ;
```

```
B :=  0.01 ;
DOld :=  0.01 ;
BOld :=  0.01 ;
DNew :=  0.01 ;
BNew :=  0.01 ;
DNone :=  0.0000 ;
BNone :=  0.0000 ;
Lambda1 :=  0 ;
Lambda2 :=  0 ;

mold(1) := 33.41 ;
mold(2) := 0 ;
mold(3) := 66.59 ;

mnew(1) := 33.41 ;
mnew(2) := 266.36 ;
mnew(3) := 66.59 ;

END #Within Loop


PRESET

##############################
# Variable Values for PRESET #
##############################
(Preset Values are Entered Here)


  INITIAL
```

```
WITHIN column.column DO

moleholdup = Lambda1*mnew + (1-Lambda1)*mold ;

accumulationb(1) = 0 ;
accumulationb(2) = 0 ;
accumulationb(3) = 0 ;

accumulationd(1) = 0 ;
accumulationd(2) = 0 ;
accumulationd(3) = 0 ;

END #Within Loop


  SCHEDULE
      SEQUENCE
WHILE Column.Column.Lambda1 < 0.99 DO
    PARALLEL
      RESET
        Column.Column.Lambda1 := OLD(Column.Column.Lambda1) + 0.1;
      END #Reset
      REINITIAL
        column.column.moleholdup
      WITH
        WITHIN Column.Column DO
  moleholdup = Lambda1*mnew + (1-Lambda1)*mold ;
        END #Within
      END #Reinitial
           END #Parellel
```

```
END #While



WHILE Column.Column.Lambda2 < 1 DO
    PARALLEL
      RESET
        Column.Column.Lambda2 := OLD(Column.Column.Lambda2) + 0.1;
      END #Reset
      RESET
WITHIN Column.Column DO
        B := OLD(BOld)*((OLD(BNone)/OLD(BOld))^OLD(Lambda2));
END #Within
      END #Reset
           END #Parellel
END #While

Continue Until
Column.Column.XD(1) < 0.999

RESET
  Column.Column.Lambda2 := 0;
END # Reset

WHILE Column.Column.Lambda2 < 1 DO
    PARALLEL
      RESET
        Column.Column.Lambda2 := OLD(Column.Column.Lambda2) + 0.1;
      END #Reset
      RESET
WITHIN Column.Column DO
```

```
        B := OLD(BNone)*((OLD(BOld)/OLD(BNone))^OLD(Lambda2));
END #Within
      END #Reset
            END #Parellel
END #While

RESET
  Column.Column.Lambda2 := 0;
END # Reset

WHILE Column.Column.Lambda2 < 1 DO
    PARALLEL
      RESET
        Column.Column.Lambda2 := OLD(Column.Column.Lambda2) + 0.1;
      END #Reset
      RESET
WITHIN Column.Column DO
        D := OLD(DOld)*((OLD(DNone)/OLD(DOld))^OLD(Lambda2));
END #Within
      END #Reset
            END #Parellel
END #While

Continue Until
        Column.Column.XB(2) < 0.999

RESET
  Column.Column.Lambda2 := 0;
END # Reset
```

```
WHILE Column.Column.Lambda2 < 1 DO
    PARALLEL
      RESET
        Column.Column.Lambda2 := OLD(Column.Column.Lambda2) + 0.1;
      END #Reset
      RESET
       WITHIN Column.Column DO
        D := OLD(DNone)*((OLD(DOld)/OLD(DNone))^OLD(Lambda2));
END #Within
      END #Reset
            END #Parellel
END #While

RESET
  Column.Column.Lambda2 := 0;
END # Reset

WHILE Column.Column.Lambda2 < 1 DO
    PARALLEL
      RESET
        Column.Column.Lambda2 := OLD(Column.Column.Lambda2) + 0.1;
      END #Reset
      RESET
       WITHIN Column.Column DO
        B := OLD(BOld)*((OLD(BNone)/OLD(BOld))^OLD(Lambda2));
END #Within
      END #Reset
            END #Parellel
END #While
```

```
Continue Until
Column.Column.XD(3) < 0.999



END #sequence


END #separate
```

Bibliography

[1] B. S. Ahmad and P. I. Barton. Homogeneous multicomponent azeotropic batch distillation. *AIChE Journal*, 42(12):3419–3433, December 1996.

[2] L. V. Baburina, V. M. Platonov, and M. G. Slin'ko. Classification of vapor-liquid phase diagrams for homoazeotropic systems. *Theoretical Foundations of Chemical Engineering*, 22:390–396, 1988.

[3] M. Barolo, G. B. Guarise, N. Ribon, S. A. Rienzi, and A. Trotta. Some issues in the design and operation of a batch distillation column with a middle vessel. *Computers Chemical Engineering*, 20:S37–S42, 1996.

[4] M. Barolo, G. B. Guarise, S. A. Rienzi, A. Trotta, and S. Macchietto. Running batch distillation in a column with a middle vessel. *Industrial Engineering Chemical Research*, 35(12):4612–4618, December 1996.

[5] C. Bernot, M. F. Doherty, and M. F. Malone. Patterns of composition change in multicomponent batch distillation. *Chemical Engineering Science*, 45(5):1207–1221, May 1990.

[6] C. Bernot, M. F. Doherty, and M. F. Malone. Feasibility and separation sequencing in multicomponent batch distillation. *Chemical Engineering Science*, 46(5):1311–1326, 1991.

[7] A. G. Davidyan, V. N. Kiva, G. A. Meski, and M. Morari. Batch distillation in a column with a middle vessel. *Chemical Engineering Science*, 49(18):3033–3051, September 1994.

[8] G. G. Devyatikh and M. F. Churbanov. Methods of high purification. *Znanie*, 1976.

[9] U. M. Diwekar. *Batch Distillation: Simulation, Optimal Design and Control.* Taylor-Francis, Washington, DC, 1995.

[10] M. F. Doherty. The presynthesis problem for homogeneous azeotropic distillations has a unique explicit solution. *Chemical Engineering Science*, 40:1885–1889, 1985.

[11] M. F. Doherty and G. A. Caldarola. Design and synthesis of homogeneous azeotropic distillations. 3. the sequencing of columns for azeotropic and extractive distillations. *Industrial Engineering Chemistry Fundamentals*, 24(4):474–485, April 1985.

[12] M. F. Doherty and J. D. Perkins. On the dynamics of distillation processes i: The simple distillation of multicomponent non-reacting homogeneous liquid mixtures. *Chemical Engineering Science*, 33:281–301, 1978.

[13] M. F. Doherty and J. D. Perkins. On the dynamics of distillation processes ii: The simple distillation of model solutions. *Chemical Engineering Science*, 33:569–578, 1978.

[14] D. B. Van Dongen and M. F. Doherty. On the dynamics of distillation processes v: The topology of the boiling surface and its relation to azeotropic distillation. *Chemical Engineering Science*, 39(5):883–892, May 1984.

[15] D. B. Van Dongen and M. F. Doherty. On the dynamics of distillation processes vi: Batch distillation. *Chemical Engineering Science*, 40(11):2087–2093, November 1985.

[16] R. H. Ewell and L. M. Welch. Rectification in ternary systems containing binary azeotropes. *Industrial and Engineering Chemistry*, 37:1224–1231, 1945.

[17] S. Hasebe, T. Kurooka, B. B. A. Aziz, I. Hashimoto, and T. Watanabe. Simultaneous separation of light and heavy impurities by a complex batch distllation column. *Journal of Chemical Engineering Japan*, 29(6):1000–1006, June 1996.

[18] S. Hasebe, M. Noda, and I. Hashimoto. Optimal operation policy for multi-effect batch distillation system. *Computers Chemical Engineering*, 21:S1221–S1226, 1997.

[19] L.H. Horsley. *Azeotropic Data.* American Chemical Society, Washington D.C., 1952.

[20] L.H. Horsley. *Azeotropic Data.* American Chemical Society, Washington D.C., 1962.

[21] L. Laroche, N. Bekiaris, H. W. Andersen, and M. Morari. Homogeneous azeotropic distillation: Separability and flowsheet synthesis. *Industrial Engineering Chemistry Research*, 31(9):2190–2209, September 1992.

[22] W. L. Luyben. Multicomponent batch distillation. 1. ternary sytems with slop recycle. *Industrial Engineering Chemistry Research*, 27:642–647, 1988.

[23] Y. I. Malenko. Physiochemical analysis of fractional distillation diagrams i: Theoretical basis method. *Russian Journal of Physical Chemistry*, 44:824–826, 1970.

[24] Y. I. Malenko. Physiochemical analysis of fractional distillation diagrams ii: Quarternary systems. *Russian Journal of Physical Chemistry*, 44:916–919, 1970.

[25] Y. I. Malenko. Physiochemical analysis of fractional distillation diagrams iii: Multicomponent (n-component) systems. *Russian Journal of Physical Chemistry*, 44:920–922, 1970.

[26] H. Matsuyama and H. Nishimura. Topological and thermodynamic classification of ternary vapor-liquid equilibria. *Journal of Chemical Engineering of Japan*, 10(3):181–187, March 1977.

[27] G. A. Meski and M. Morari. Design and operation of a batch distillation column with a middle vessel. *Computers Chemical Engineering*, 19:S597–S602, 1995.

[28] F. B. Petlyuk. Structure of concentration space and synthesis of schemes for separating azeotropic mixtures. *Theoretical Foundations of Chemical Engineering*, 11:1–7, 1975.

[29] F. B. Petlyuk, V. Y. Kievskii, and L. A. Serafimov. Method for the isolation of the regions of the rectification of polyazeotropic mixtures using an electronic computer. *Theoretical Foundations of Chemical Engineering*, 11:1–7, 1975.

[30] W. Reinders and Miss C.H. De Minjer. Vapor liquid equilibrium in ternary systems. *Recl. Trans. Chim.*, 59:207–230, 1940.

[31] C. S. Robinson and E. R. Gilliland. *Elements of Fractional Distillation*. McGraw-Hill, New York, fourth edition, 1950.

[32] B. T. Safrit and A. W. Westerberg. Algorithm for generating the distllation regions for azeotropic multicomponent mixtures. *Industrial Engineering Chemistry Research*, 36(5):1827–1840, May 1997.

[33] B. T. Safrit and A. W. Westerberg. Improved operational policies for batch extractive distillation columns. *Industrial Engineering Chemistry Research*, 36(2):436–443, February 1997.

[34] B. T. Safrit and A. W. Westerberg. Synthesis of azeotropic batch distillation separation systems. *Industrial Engineering Chemistry Research*, 36(5):1841–1854, May 1997.

[35] B. T. Safrit, A. W. Westerberg, U. Diwekar, and O. M. Wahnschafft. Extending continuous conventional and extractive distillation feasibility insights to batch distillation. *Industrial Engineering Chemistry Research*, 34(10):3257–3264, October 1995.

[36] L. A. Serafimov, F. B. Petlyuk, and I. B. Aleksandrov. The number of trajectory clusters representing continuous rectification of azeotropic multicomponent mixtures. *Theoretical Foundations of Chemical Engineering*, 8:847–850, 1974.

[37] S. Skogestad, B. Wittgens, R. Litto, and E. Sørensen. Multivessel batch distillation. *AIChE Journal*, 43(4):971–978, April 1997.

[38] J. Stichlmair, J. R. Fair, and J. L. Bravo. Separation of azeotropic mixtures via enhanced distillation. *Chemical Engineering Progress*, 85(1):63–69, January 1989.

[39] O. M. Wahnschafft, J. W. Koehler, E. Blass, and A. W. Westerberg. The product composition regions of single-feed azeotropic distillation columns. *Industrial Engineering Chemistry Research*, 31(10):2345–2362, October 1992.

[40] O. M. Wahnschafft, JP. Le Rudulier, and A. W. Westerberg. A problem decomposition approach for the synthesis of complex separation processes with recycles. *Industrial Engineering Chemistry Research*, 32(6):1121–1141, June 1993.

[41] S. Widagdo and W.D. Seider. Journal review: Azeotropic distillation. *AIChE Journal*, 42(1):96–130, January 1996.

[42] B. Wittgens, R. Litto, E. Sørensen, and S. Skogestad. Total reflux operation of multivessel batch distillation. *Computers Chemical Engineering*, 20:S1041–S1046, 1996.